

# UNCLASSIFIED

AD NUMBER
AD921137
NEW LIMITATION CHANGE
TO Approved for public release, distribution unlimited
FROM Distribution authorized to U.S. Gov't. agencies only; Test and Evaluation; APR 1974. Other requests shall be referred to Eustis Directorate, U.S. Army Air Mobility Research and Development Lab., Fort Eustis, VA 23604.
AUTHORITY
Eustis Directorate, U.S. Army Air Mobility Research and Development Lab. ltr dtd 18 Nov 1975

THIS PAGE IS UNCLASSIFIED

AD921137

AD

# USAAMRDL TECHNICAL REPORT 74-15

## 10:1 PRESSURE RATIO SINGLE-STAGE CENTRIFUGAL COMPRESSOR PROGRAM

By

William J. McAnally, III

April 1974

**EUSTIS DIRECTORATE  
U. S. ARMY AIR MOBILITY RESEARCH AND DEVELOPMENT LABORATORY  
FORT EUSTIS, VIRGINIA**

**CONTRACT DAAJ02-70-C-0006  
PRATT & WHITNEY AIRCRAFT DIVISION  
UNITED AIRCRAFT CORPORATION  
FLORIDA RESEARCH AND DEVELOPMENT CENTER  
WEST PALM BEACH, FLORIDA**

Distribution limited to U. S. Government agencies only, test and evaluation, April 1974. Other requests for this document must be referred to the Eustis Directorate, U. S. Army Air Mobility Research and Development Laboratory, Fort Eustis, Virginia 23604.



**D D C  
RECEIVED  
AUG 2 1974  
D**

#### DISCLAIMERS

The findings in this report are not to be construed as an official Department of the Army position unless so designated by other authorized documents.

When Government drawings, specifications, or other data are used for any purpose other than in connection with a definitely related Government procurement operation, the United States Government thereby incurs no responsibility nor any obligation whatsoever; and the fact that the Government may have formulated, furnished, or in any way supplied the said drawings, specifications, or other data is not to be regarded by implication or otherwise as in any manner licensing the holder or any other person or corporation, or conveying any rights or permission, to manufacture, use, or sell any patented invention that may in any way be related thereto.

Trade names cited in this report do not constitute an official endorsement or approval of the use of such commercial hardware or software.

#### DISPOSITION INSTRUCTIONS

Destroy this report when no longer needed. Do not return it to the originator.



DEPARTMENT OF THE ARMY  
U. S. ARMY AIR MOBILITY RESEARCH & DEVELOPMENT LABORATORY  
EUSTIS DIRECTORATE  
FORT EUSTIS, VIRGINIA 23604

The objective of this contractual effort was to conduct the preliminary design, detail design, fabrication, test, and evaluation of a single-stage, high-pressure-ratio centrifugal compressor. The performance targets stated herein were derived from potential performance indicated by tests of earlier compressors and are in no way felt to be the ultimate in performance for this type of compressor.

This report was prepared by Pratt & Whitney Aircraft Division of United Aircraft Corporation, Florida Research and Development Center, under the terms of Contract DAAJ02-70-C-0006. It describes the design approach, test equipment and procedures, instrumentation, and results of tests of the compressor. The details of the aerodynamic design are presented in a separate volume as Appendix II to this report.

This report has been reviewed by technical personnel of this directorate. The conclusions contained herein are concurred in by this directorate and will be considered in any future research programs. The U.S. Army project engineer for this effort was Mr. Robert A. Langworthy, Technology Applications Division.



Task 1G162203D14413  
Contract DAAJ02-70-C-0006  
USAMRDL Technical Report 74-15  
April 1974

10:1 PRESSURE RATIO  
SINGLE-STAGE CENTRIFUGAL COMPRESSOR PROGRAM

Final Report

By

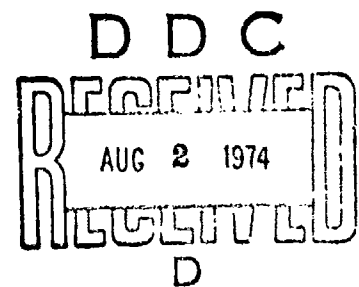
William J. McAnally, III

Prepared By

Pratt & Whitney Aircraft Division  
United Aircraft Corporation  
Florida Research and Development Center  
West Palm Beach, Florida

for

EUSTIS DIRECTORATE  
U. S. ARMY AIR MOBILITY RESEARCH  
AND DEVELOPMENT LABORATORY  
FORT EUSTIS, VIRGINIA



Distribution limited to U. S. Government agencies only;  
test and evaluation; April 1974. Other requests for this  
document must be referred to the Eustis Directorate,  
U.S. Army Air Mobility Research and Development  
Laboratory, Fort Eustis, Virginia 23604.

### SUMMARY

The objective of this program was to design, fabricate and test a 2-to-5 lb/sec airflow single-stage centrifugal compressor that could be incorporated in a future Army advanced technology gas turbine engine. The design speed performance goals were to exceed 75% efficiency at 10:1 pressure ratio. Since gas turbine engines for Army aircraft applications operate under part-power conditions a majority of the time, an off-design performance goal of 80% efficiency at 8:1 pressure ratio was established.

In the design of the compressor, parametric studies were conducted to select an overall design consistent with optimum compressor performance at both performance goals. These studies defined the compressor inlet corrected flow rate, impeller inlet hub and tip radii, corrected impeller rotational speed, and inlet prewhirl. Airflow selection and the selection of the hub radius were influenced by the decision to design a compressor that could be used in a small turboshaft engine with a concentric shaft front drive.

The tip radius was selected after determining the effect on axial Mach number, inducer tip relative Mach number, and inlet choke flow margin. The effect of inlet guide vane losses, inlet shock losses, diffuser losses, and shroud friction heating were parametrically evaluated analytically before selecting an IGV prewhirl and rotor speed to provide optimum overall compressor performance. A remote inducer design was selected over an integral inducer-impeller configuration so that the inducer could be designed using transonic axial-flow compressor technology. The work split between the inducer and impeller was selected so that the relative Mach number into the impeller would be subsonic. A pipe diffuser was selected over vane island and cascade diffusers, because it has the lowest demonstrated losses over the largest range of Mach number and because P&W<sup>TM</sup> has substantial experience in designing and fabricating this type of diffuser.

Demonstrated total-to-static performance was as high as 79.6% efficiency at 8.192:1 pressure ratio and 73.8% efficiency at 10.03:1 pressure ratio. Performance adjusted for increased losses from a damaged diffuser (10.15:1 pressure ratio and 75.9% efficiency) indicates that the basic compressor design would surpass the minimum 10:1 pressure ratio program goal. A composite overall performance map for the compressor is presented in Figure 1. Evaluation of component performance data revealed that excessive losses occurred in the inducer above 95% of design speed and that a redesign of this component could produce an additional performance improvement at 10:1 pressure ratio.

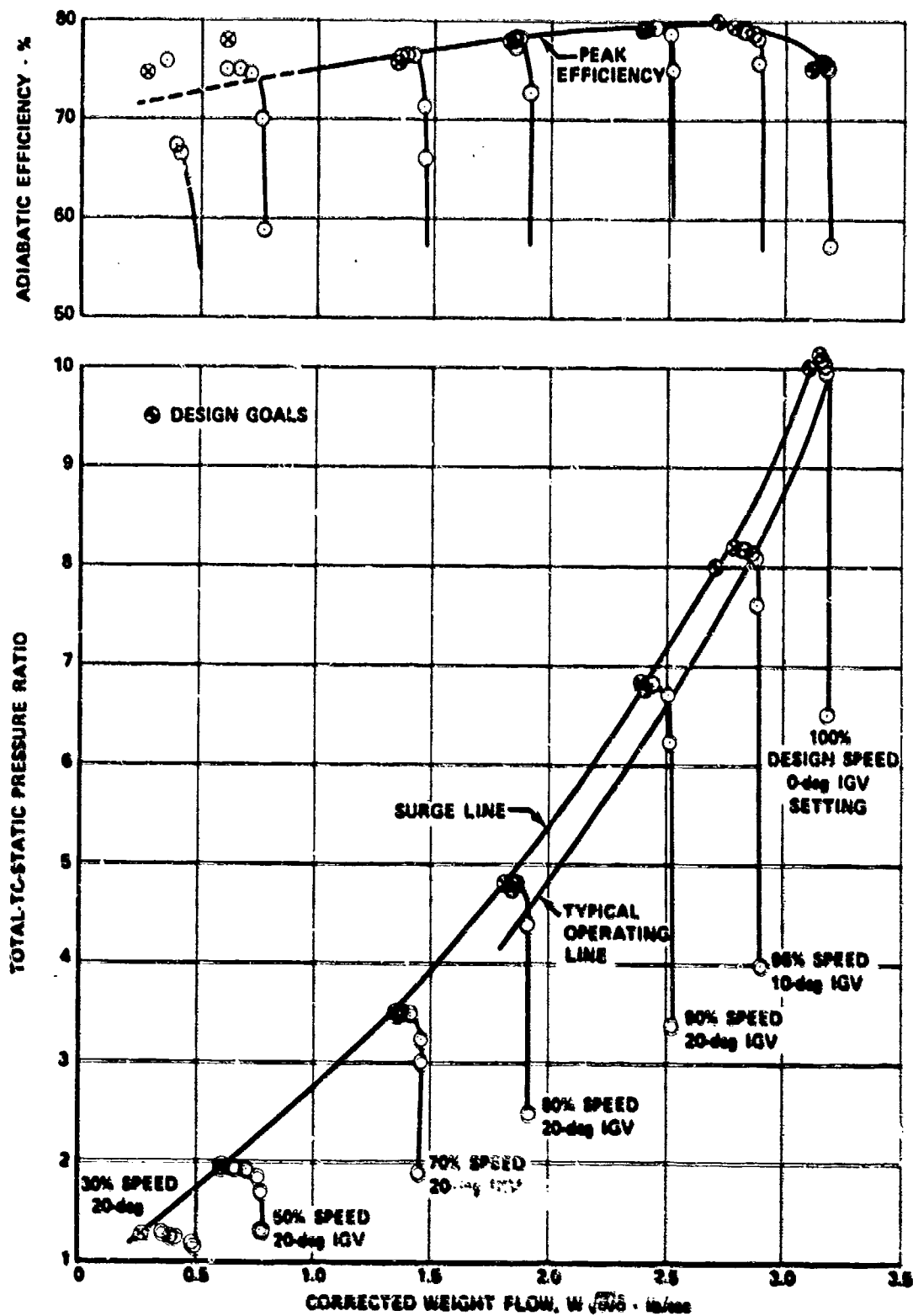


Figure 1. Composite 10:1 Overall Performance Map.

## TABLE OF CONTENTS

	<u>Page</u>
SUMMARY . . . . .	iii
LIST OF ILLUSTRATIONS . . . . .	vi
LIST OF TABLES . . . . .	xxv
LIST OF SYMBOLS . . . . .	xxxii
INTRODUCTION . . . . .	1
DESIGN APPROACH . . . . .	3
Aerodynamic Design . . . . .	3
Mechanical Design . . . . .	6
Mechanical Redesign . . . . .	16
TEST EQUIPMENT . . . . .	21
Compressor Test Rig . . . . .	21
Test Facilities . . . . .	21
INSTRUMENTATION . . . . .	28
PROCEDURES . . . . .	
Test Procedures . . . . .	44
Data Reduction Procedures . . . . .	49
Validation of Test Data . . . . .	56
RESULTS AND DISCUSSION . . . . .	64
Overall Performance . . . . .	64
Component Performance . . . . .	73
High-Frequency Response Data . . . . .	127
CONCLUSIONS . . . . .	130
RECOMMENDATIONS . . . . .	131
APPENDIX I - Overall Performance Tabulations . . . . .	132
APPENDIX II - Aerodynamic Design (Classified Confidential - under separate cover)	
DISTRIBUTION . . . . .	395

## LIST OF ILLUSTRATIONS

<u>Figure</u>		<u>Page</u>
1	Composite 10:1 Overall Performance Map .....	iv
2	10:1 Pressure Ratio Centrifugal Compressor Stage .....	3
3	10:1 Pressure Ratio Centrifugal Impeller and Remote Inducer .....	4
4	Initial Design of 10.0:1 Pressure Ratio Centrifugal Compressor and P&WA <sup>TM</sup> Drive Turbine .....	7
5	Inducer Vibration Analysis. ....	8
6	Impeller and Inducer Attachment .....	9
7	Tip Clearance Probe Installation. ....	10
8	Initial Compressor Drive and Bearing Support Design .....	11
9	Bearing Designs .....	12
10	Compressor and Turbine Rotor Assembly. ....	14
11	Initial Rotor Configuration Predicted Front Bearing Loads .....	14
12	Initial Rotor Configuration Predicted Rear Bearing Loads .....	15
13	Predicted Ball Bearing Minimum Thrust Load Requirements .....	15
14	Impeller Shaft Attachment Modification .....	16
15	Redesigned 10:1 Pressure Ratio Centrifugal Compressor and P&WA <sup>TM</sup> Drive Turbine. ....	27
16	Redesigned Rotor Assembly .....	18
17	Redesigned Rotor Assembly Predicted Front Bearing Load vs Speed .....	19
18	Redesigned Rotor Assembly Predicted Rear Bearing Load vs Speed .....	20

# LIST OF ILLUSTRATIONS (Continued)

<u>Figure</u>		<u>Page</u>
19	Front Bearing Compartment Carbon Face Seal . . . . .	20
20	Compressor Test Rig Nonrotating Components . . . . .	22
21	Impeller Spin Tooling . . . . .	22
22	Impeller Installation in Diffuser Case . . . . .	23
23	Redesigned Rotor Assembly Components . . . . .	23
24	Assembled and Fully Instrumented Compressor Rig . . . . .	24
25	P&WA <sup>TM</sup> FRDC High-Speed Compressor Test Stand . . . . .	25
26	Particle Separator With Integral Fast-Acting Shutoff Valve . . . . .	26
27	Compressor Rig Installed in B-2 Test Facility . . . . .	27
28	Compressor Instrumentation Station Locations . . . . .	28
29	Inlet Orifice Installation . . . . .	29
30	Diffuser Exit Total Pressure Rakes . . . . .	30
31	Location of Diffuser Exit Total Pressure Rakes . . . . .	31
32	Placement of Total Pressure Probes in Diffuser Exit Plane Station . . . . .	32
33	Collector Instrumentation Locations . . . . .	34
34	Axial Locations of Inlet and Inducer Instrumentation . . . . .	36
35	Construction of Traverse Cobra Probes . . . . .	37
36	Location of Impeller Shroud Static Pressure Taps . . . . .	37
37	Impeller Tip Static Pressure Passage . . . . .	38
38	Impeller Exit Cobra Probe Installation . . . . .	39
39	Impeller Exit Total Temperature Probe Construction . . . . .	40

# LIST OF ILLUSTRATIONS (Continued)

<u>Figure</u>		<u>Page</u>
40	Location of Diffuser Static Pressure Instrumentation . . .	42
41	High-Frequency Response Kulites . . . . .	43
42	Maximum Front Bearing 1E Acceleration, Build No. 3 . . . . .	45
43	Impeller Tip Axial Shroud Clearance, Build No. 2 . . . . .	46
44	Clearance Probe Measurements, Build No. 3 . . . . .	46
45	Shroud Clearance Measurements, Build No. 6 . . . . .	47
46	Inlet Guide Vane Exit Flow Correspondence, Build No. 6 . . . . .	61
47	Inducer Exit Integrated Flow Correspondence, Build No. 6 . . . . .	61
48	Impeller Exit Integrated Flow Correspondence, Build No. 6 . . . . .	62
49	Overall Performance, Build No. 2 Shakedown Test . . . . .	65
50	High-Speed Centrifugal Compressor Flow Characteristics . . . . .	65
51	Diffuser Loss Characteristic, Build No. 2 Shakedown Test . . . . .	66
52	Diffuser Throat Blockage Characteristic, Build No. 2 Shakedown Test . . . . .	66
53	Overall Performance, Build No. 3, 10-deg IGV . . . . .	67
54	Overall Performance, Build No. 3, 0-deg IGV . . . . .	68
55	Build No. 3 Overall Performance, 20-deg IGV . . . . .	69
56	Build No. 6 Overall Performance . . . . .	71
57	Composite Overall Performance Map . . . . .	72
58	Component Efficiency Representation . . . . .	74

# LIST OF ILLUSTRATIONS (Continued)

<u>Figure</u>		<u>Page</u>
59	IGV Turning vs Setting, Build No. 6 . . . . .	75
60	IGV Exit Vortex Distribution, 10-deg IGV . . . . .	75
61	Inlet Section Total Pressure Loss Characteristics . . . . .	76
62	IGV Circumferential Traverse, Build No. 6, 100% Speed, 10-deg IGV, 50% Span . . . . .	77
63	IGV Exit Radial Traverse, Build No. 6, 100% Speed, 10-deg IGV, Near Stall . . . . .	78
64	Build No. 6, Inlet Guide Vane Losses at Approximately 0.46 Mach Number. . . . .	79
65	Inducer Inlet Conditions, 100% Speed, 10-deg IGV . . . . .	81
66	Inducer Inlet Conditions, 101% Speed, -4-deg IGV . . . . .	82
67	Inducer Inlet Conditions, Build No. 3, 95% Speed, 10-deg IGV, Near Stall . . . . .	83
68	Inducer Performance, Build No. 6 . . . . .	84
69	Inducer Exit Traverse, Build No. 6, 101% Speed, -4-deg IGV, Wide Open Discharge . . . . .	85
70	Inducer Exit Traverse, Build No. 6, 100% Speed, 10-deg IGV . . . . .	86
71	Inducer Exit Traverse, Build No. 6, 95% Speed, 10-deg IGV, Near Stall . . . . .	88
72	Inducer Losses . . . . .	89
73	Impeller Inlet Conditions, 100% Design Speed, 10-deg IGV . . . . .	90
74	Inducer Exit Air Angle Profile, 100% Design Speed, 10-deg IGV . . . . .	90
75	Impeller Inlet Conditions, 101% Speed, -4-deg IGV . . . . .	91
76	Inducer Exit Air Angle Profile, 101% Speed, -4-deg IGV . . . . .	91



# LIST OF ILLUSTRATIONS (Continued)

<u>Figure</u>		<u>Page</u>
77	IGV Exit Static Pressure Profile, 100% Speed, 10-deg IGV .....	93
78	Inducer Exit Static Pressure Profile, 100% Speed, 10-deg IGV .....	93
79	Impeller Inlet Conditions, 100% Speed, 10-deg IGV .....	94
80	Inducer Exit Air Angle Profile, 100% Speed, 10-deg IGV .....	
81	Choke Point Flow as a Function of Rotor Speed, Build No. 3 .....	95
82	Build No. 6 Choke Point Flow as a Function of Rotor Speed .....	95
83	Build No. 6 Impeller Performance Derived From Traverse Data .....	97
84	Inducer-Impeller Performance Derived From Traverse Data .....	98
85	Build No. 3 Impeller Performance Map Derived From Internal Flow Analysis .....	99
86	Build No. 6 Inducer-Impeller Performance Map Derived From Internal Analysis .....	100
87	Build No. 2 Impeller Efficiency-Incidence Characteristic .....	101
88	Build No. 6 Inducer-Impeller Efficiency- Incidence Characteristic .....	102
89	Effect of Prewhirl on Inducer-Impeller Per- formance Near 10:1 Pressure Ratio .....	104
90	Effect of Prewhirl on Inducer-Impeller Performance Near 5:1 Pressure Ratio .....	104
91	Impeller Exit Slip Factor .....	105
92	Impeller Exit Discharge Coefficient .....	105

# LIST OF ILLUSTRATIONS (Continued)

<u>Figure</u>		<u>Page</u>
93	Impeller Exit Traverse, Build No. 6, 101% Speed, -4-deg IGV, Near Stall . . . . .	106
94	Impeller Exit Traverse, Build No. 3, 95% Speed, 10-deg IGV, Near Stall . . . . .	107
95	Impeller Exit Traverse, Build No. 6, 95% Speed, 10-deg IGV, Near Stall . . . . .	108
96	Normalized Radial Velocity Distribution, Build No. 6, 101% Speed, -4-deg IGV . . . . .	109
97	Normalized Radial Velocity Distribution, Build No. 3, 95% Speed, 10-deg IGV . . . . .	109
98	Normalized Radial Velocity Distribution, Build No. 6, 95% $N/\sqrt{\theta}$ Design, 10-deg IGV . . . . .	110
99	Discharge Velocity Ratio Comparisons . . . . .	111
100	Stall Transient Data at 1 Scan/sec and Continuous Scan. . . . .	112
101	Static Pressure Variation Along Impeller Shroud, 95% Speed, Near Stall, 10-deg IGV . . . . .	113
102	Diffuser Static Pressure Profile: Build No. 3, 95% Speed, 10-deg IGV . . . . .	114
103	Diffuser Static Pressure Profile: Build No. 3, 100% Speed, 10-deg IGV, Near Stall. . . . .	115
104	Diffuser Gapwise Static Pressure Distributions Along the Tangency Radius: Build No. 3, 10-deg IGV Setting . . . . .	115
105	Diffuser Shroud Static Pressure Contours: Build No. 3, 100% Speed, 10-deg IGV. . . . .	116
106	Diffuser Throat Static Pressure Distribution: Build No. 3, 95% Speed, 10-deg IGV . . . . .	117
107	Damaged Diffuser Pipe Leading Edges . . . . .	118
108	Typical Undamaged Diffuser Pipe Leading Edge . . . . .	119

# LIST OF ILLUSTRATIONS (Continued)

<u>Figure</u>		<u>Page</u>
109	Post-Test Condition of Diffuser .....	119
110	Diffuser Static Pressure Profile: Build No. 6, 95% Speed, 10-deg IGV, Near Stall .....	120
111	Diffuser Static Pressure Profile: Build No. 6, 100% Speed, 10-deg IGV, Near Stall .....	120
112	Diffuser Static Pressure Profile: Build No. 6, 101% Speed, -4-deg IGV. ....	121
113	Diffuser Exit Mach Number Profile: Build No. 3, 95% Speed, $N/\sqrt{\theta}$ 10-deg IGV, Near Stall .....	122
114	Diffuser Exit Mach Number Profile: Build No. 6, 95% Speed, 10-deg IGV, Near Stall .....	122
115	Diffuser Exit Mach Number Profile: Build No. 6, 100% Speed, 10-deg IGV, Near Stall .....	123
116	Diffuser Exit Mach Number Profile: Build No. 6, 101% Speed, -4-deg IGV, Near Stall .....	123
117	Diffuser Exit Mach Number Profile: Build No. 6, 101% Speed, -4-deg IGV, Wide Open Discharge .....	124
118	Diffuser Losses vs Corrected Weight Flow, Near Stall .....	125
119	Diffuser Losses vs Impeller Exit Mach Number, Near Stall .....	125
120	Diffuser Dump Losses Near Stall. ....	126
121	Diffuser Static Pressure Rise Coefficient vs Corrected Weight Flow .....	126
122	High-Frequency Response Data at 70% Speed. ....	128
123	High-Frequency Response Data at 78% Speed. ....	129
124	IGV Exit Radial Traverse, Build No. 6, 101% Speed, 0-deg IGV, Near Stall .....	140
125	IGV Circumferential Traverse, Build No. 6, 101% Speed, 0-deg IGV, 10% Span .....	141

# LIST OF ILLUSTRATIONS (Continued)

<u>Figure</u>		<u>Page</u>
126	IGV Circumferential Traverse, Build No. 6, 101% Speed, 0-deg IGV, 30% Span.....	142
127	IGV Circumferential Traverse, Build No. 6, 101% Speed, 0-deg IGV, 50% Span.....	143
128	IGV Circumferential Traverse, Build No. 6, 101% Speed, 0-deg IGV, 70% Span.....	144
129	IGV Circumferential Traverse, Build No. 6, 101% Speed, 0-deg IGV, 90% Span.....	145
130	IGV Exit Radial Traverse, Build No. 6, 101% Speed, -4-deg IGV.....	146
131	IGV Circumferential Traverse, Build No. 6, 101% Speed, -4-deg IGV, 10% Span.....	147
132	IGV Circumferential Traverse, Build No. 6, 101% Speed, -4-deg IGV, 30% Span.....	148
133	IGV Circumferential Traverse, Build No. 6, 101% Speed, -4-deg IGV, 50% Span.....	149
134	IGV Circumferential Traverse, Build No. 6, 101% Speed, -4-deg IGV, 70% Span.....	150
135	IGV Circumferential Traverse, Build No. 6, 101% Speed, -4-deg IGV, 90% Span.....	151
136	IGV Exit Radial Traverse, Build No. 6, 101% Speed, -5-deg IGV.....	152
137	IGV Exit Radial Traverse, Build No. 6, 100% Speed, 10-deg IGV, Near Stall.....	153
138	IGV Circumferential Traverse, Build No. 6, 100% Speed, 10-deg IGV, 10% Span.....	154
139	IGV Circumferential Traverse, Build No. 6, 100% Speed, 10-deg IGV, 30% Span.....	155
140	IGV Circumferential Traverse, Build No. 6, 100% Speed, 10-deg IGV, 50% Span.....	156
141	IGV Circumferential Traverse, Build No. 6, 100% Speed, 10-deg IGV, 70% Span.....	157

# LIST OF ILLUSTRATIONS (Continued)

<u>Figure</u>		<u>Page</u>
142	IGV Circumferential Traverse, Build No. 6, 100% Speed, 10-deg IGV, 90% Span .....	158
143	IGV Circumferential Traverse, Build No. 3, 70% Speed, 10-deg IGV, 10% Span .....	159
144	IGV Circumferential Traverse, Build No. 3, 70% Speed, 10-deg IGV, 30% Span .....	160
145	IGV Circumferential Traverse, Build No. 3, 70% Speed, 10-deg IGV, 50% Span .....	161
146	IGV Circumferential Traverse, Build No. 3, 70% Speed, 10-deg IGV, 70% Span .....	162
147	IGV Circumferential Traverse, Build No. 3, 70% Speed, 10-deg IGV, 90% Span .....	163
148	IGV Exit Radial Traverse, Build No. 6, 70% Speed, 10-deg IGV, Near Stall .....	164
149	IGV Circumferential Traverse, Build No. 6, 70% Speed, 10-deg IGV, 10% Span .....	165
150	IGV Circumferential Traverse, Build No. 6, 70% Speed, 10-deg IGV, 30% Span .....	166
151	IGV Circumferential Traverse, Build No. 6, 70% Speed, 10-deg IGV, 50% Span .....	167
152	IGV Circumferential Traverse, Build No. 6, 70% Speed, 10-deg IGV, 70% Span .....	168
153	Inducer Exit Traverse, Build No. 6, 101% Speed, 5-deg IGV, Wide Open Discharge .....	169
154	Inducer Exit Traverse, Build No. 6, 101% Speed, 5-deg IGV, Near Stall .....	170
155	Inducer Exit Traverse, Build No. 6, 101% Speed, 0-deg IGV, Wide Open Discharge .....	171
156	Inducer Exit Traverse, Build No. 6, 101% Speed, 0-deg IGV, Near Stall .....	172
157	Inducer Exit Traverse, Build No. 6, 101% Speed, -4-deg IGV, Wide Open Discharge .....	173

# LIST OF ILLUSTRATIONS (Continued)

<u>Figure</u>		<u>Page</u>
158	Inducer Exit Traverse, Build No. 6, 101% Speed, -4-deg IGV, Near Stall . . . . .	174
159	Inducer Exit With Coolant, Build No. 6, 101% Speed, -4-deg IGV, Near Stall . . . . .	175
160	Inducer Exit Traverse, Build No. 6, 101% Speed, -5-deg IGV . . . . .	176
161	Inducer Exit Traverse, Build No. 6, 100% Speed, 10-deg IGV . . . . .	177
162	Inducer Exit Traverse, Build No. 6, 95% Speed, 15-deg IGV, Wide Open Discharge. . . . .	178
163	Inducer Exit Traverse, Build No. 6, 95% Speed, 15-deg IGV, Near Stall . . . . .	179
164	Inducer Exit Traverse, Build No. 3, 95% Speed, 10-deg IGV, Wide Open Discharge. . . . .	179
165	Inducer Exit Traverse, Build No. 3, 95% Speed, 10-deg IGV, Near Stall . . . . .	180
166	Inducer Exit Traverse, Build No. 3, 95% Speed, 10-deg IGV, Below Near Stall. . . . .	180
167	Inducer Exit Traverse, Build No. 6, 95% Speed, 10-deg IGV, Wide Open Discharge. . . . .	181
168	Inducer Exit Traverse, Build No. 6, 95% Speed, 10-deg IGV, Near Stall . . . . .	182
169	Inducer Exit Traverse, Build No. 6, 95% Speed, 10-deg IGV, Wide Open Discharge. . . . .	183
170	Inducer Exit Traverse, Build No. 6, 95% Speed, 10-deg IGV, Near Stall . . . . .	184
171	Inducer Exit Traverse, Build No. 6, 85% Speed, 30-deg IGV, Near Stall . . . . .	185
172	Inducer Exit Traverse, Build No. 6, 85% Speed, 20-deg IGV, Near Stall . . . . .	186
173	Inducer Exit Traverse, Build No. 6, 70% Speed, 30-deg IGV, Near Stall . . . . .	187

# LIST OF ILLUSTRATIONS (Continued)

<u>Figure</u>		<u>Page</u>
174	Inducer Exit Traverse, Build No. 6, 70% Speed, 20-deg IGV, Near Stall . . . . .	188
175	Impeller Exit Traverse, Build No. 6, 101% Speed, 5-deg IGV, Near Stall . . . . .	189
176	Impeller Exit Traverse, Build No. 6, 101% Speed, 0-deg IGV, Near Stall . . . . .	190
177	Impeller Exit Traverse, Build No. 6, 101% Speed, -4-deg IGV, Near Stall . . . . .	191
178	Impeller Exit Traverse With Flange Coolant, Build No. 6, 101% Speed, -4-deg IGV . . . . .	192
179	Impeller Exit Traverse, Build No. 6, 101% Speed, -5-deg IGV . . . . .	193
180	Impeller Exit Traverse, Build No. 6, 101% Speed, -5-deg IGV . . . . .	193
181	Impeller Exit Traverse, Build No. 6, 95% Speed, 15-deg IGV . . . . .	194
182	Impeller Exit Traverse, Build No. 3, 95% Speed, 10-deg IGV, Wide Open Discharge . . . . .	195
183	Impeller Exit Traverse, Build No. 3, 95% Speed, 10-deg IGV, Near Stall . . . . .	196
184	Impeller Exit Traverse, Build No. 3, 95% Speed, 10-deg IGV, Below Near Stall . . . . .	197
185	Impeller Exit Traverse, Build No. 6, 95% Speed, 10-deg IGV, Wide Open Discharge . . . . .	198
186	Impeller Exit Traverse, Build No. 6, 95% Speed, 10-deg IGV . . . . .	199
187	Impeller Exit Traverse, Build No. 6, 95% Speed, 10-deg IGV, Near Stall . . . . .	200
188	Impeller Exit Traverse, Build No. 6, 85% Speed, 30-deg IGV . . . . .	201
189	Impeller Exit Traverse, Build No. 6, 85% Speed, 20-deg IGV, Near Stall . . . . .	202

# LIST OF ILLUSTRATIONS (Continued)

<u>Figure</u>		<u>Page</u>
190	Impeller Exit Traverse, Build No. 3, 70% Speed, 20-deg IGV, Wide Open Discharge . . . . .	203
191	Impeller Exit Traverse, Build No. 3, 70% Speed, 20-deg IGV, Near Stall . . . . .	204
192	Impeller Exit Traverse, Build No. 3, 70% Speed, 20-deg IGV, Below Near Stall. . . . .	205
193	Impeller Exit Traverse, Build No. 3, 70% Speed, 10-deg IGV, Wide Open Discharge. . . . .	206
194	Impeller Exit Traverse, Build No. 3, 70% Speed, 10-deg IGV, Near Stall . . . . .	207
195	Impeller Exit Traverse, Build No. 3, 70% Speed, 10-deg IGV, Below Near Stall. . . . .	208
196	Impeller Exit Traverse, Build No. 3, 70% Speed, 0-deg IGV, Wide Open Discharge . . . . .	209
197	Impeller Exit Traverse, Build No. 3, 70% Speed, 0-deg IGV, Near Stall . . . . .	210
198	Impeller Exit Traverse, Build No. 3, 70% Speed, 0-deg IGV, Below Near Stall . . . . .	211
199	Impeller Exit Traverse, Build No. 6, 70% Speed, 30-deg IGV . . . . .	212
200	Impeller Exit Traverse, Build No. 6, 70% Speed, 20-deg IGV . . . . .	213
201	Impeller Exit Traverse, Build No. 3, 30% Speed, 20-deg IGV, Wide Open Discharge. . . . .	214
202	Impeller Exit Traverse, Build No. 3, 30% Speed, 20-deg IGV, Near Stall . . . . .	215
203	Impeller Exit Traverse, Build No. 3, 30% Speed, 20-deg IGV, Below Near Stall. . . . .	216
204	Impeller Exit Traverse, Build No. 3, 30% Speed, 10-deg IGV, Wide Open Discharge. . . . .	217
205	Impeller Exit Traverse, Build No. 3, 30% Speed, 10-deg IGV, Near Stall . . . . .	218



# LIST OF ILLUSTRATIONS (Continued)

<u>Figure</u>		<u>Page</u>
206	Impeller Exit Traverse, Build No. 3, 30% Speed, 10-deg IGV, Below Near Stall .....	219
207	Impeller Exit Traverse, Build No. 3, 30% Speed, 10-deg IGV, Below Near Stall .....	220
208	Impeller Exit Traverse, Build No. 3, 30% Speed, 0-deg IGV, Wide Open Discharge .....	221
209	Impeller Exit Traverse, Build No. 3, 30% Speed, 0-deg IGV, Near Stall .....	222
210	Impeller Exit Traverse, Build No. 3, 30% Speed, 0-deg IGV, Below Near Stall .....	223
211	Impeller Exit Temperature Traverse, Build No. 6, 101% Speed, 5-deg IGV .....	224
212	Impeller Exit Temperature Traverse, Build No. 6, 101% Speed, 0-deg IGV .....	225
213	Impeller Exit Traverse With Coolant, Build No. 6, 101% Speed, -4-deg IGV .....	226
214	Impeller Exit Traverse With Coolant, Build No. 6, 101% Speed, -4-deg IGV .....	227
215	Impeller Exit Temperature Traverse, Build No. 6, 101% Speed, -4-deg IGV .....	228
216	Impeller Exit Temperature Traverse, Build No. 6, 94.5% Speed, 15-deg IGV .....	229
217	Impeller Exit Temperature Traverse, Build No. 6, 94.5% Speed, 10-deg IGV .....	230
218	Impeller Exit Temperature Traverse, Build No. 6, 95% Speed, 10-deg IGV, Wide Open Discharge .....	231
219	Impeller Exit Temperature Traverse, Build No. 6, 95% Speed, 10-deg IGV .....	232
220	Static Pressure Profile Along Flow Path, Build No. 3, 100% Speed, 10-deg IGV, Near Stall .....	316

# LIST OF ILLUSTRATIONS (Continued)

<u>Figure</u>		<u>Page</u>
221	Static Pressure Profile Along Flow Path, Build No. 3, 95% Speed, 20-deg IGV, Near Stall . . . . .	316
222	Static Pressure Profile Along Flow Path, Build No. 3, 95% Speed, 10-deg IGV, Wide Open Discharge . . . . .	317
223	Static Pressure Profile Along Flow Path, Build No. 3, 95% Speed, 10-deg IGV, Near Stall . . . . .	317
224	Static Pressure Profile Along Flow Path, Build No. 3, 95% Speed, 0-deg IGV, Near Stall . . . . .	318
225	Static Pressure Profile Along Flow Path, Build No. 3, 70% Speed, 10-deg IGV, Near Stall . . . . .	318
226	Static Pressure Profile Along Flow Path, Build No. 6, 101% Speed, -4-deg IGV, Wide Open Discharge . . . . .	319
227	Static Pressure Profile Along Flow Path, Build No. 6, 100% Speed, 10-deg IGV, Near Stall . . . . .	319
228	Static Pressure Profile Along Flow Path, Build No. 6, 101% Speed, -4-deg IGV, Near Stall . . . . .	320
229	Static Pressure Profile Along Flow Path, Build No. 6, 95% Speed, 10-deg IGV, Near Stall . . . . .	320
230	Static Pressure Variation Along Impeller Shroud, Build No. 3, 100% Speed, 10-deg IGV, Near Stall . . . . .	321
231	Static Pressure Variation Along Impeller Shroud, Build No. 3, 95% Speed, 20-deg IGV, Near Stall . . . . .	321
232	Static Pressure Variation Along Impeller Shroud, Build No. 3, 95% Speed, 10-deg IGV, Wide Open Discharge . . . . .	322
233	Static Pressure Variation Along Impeller Shroud, Build No. 3, 95% Speed, 10-deg IGV, Near Stall . . . . .	322
234	Static Pressure Variation Along Impeller Shroud, Build No. 3, 95% Speed, 0-deg IGV, Near Stall . . . . .	323
235	Static Pressure Variation Along Impeller Shroud, Build No. 3, 70% Speed, 10-deg IGV, Near Stall . . . . .	323

# LIST OF ILLUSTRATIONS (Continued)

<u>Figure</u>		<u>Page</u>
236	Static Pressure Variation Along Impeller Shroud, Build No. 6, 101% Speed, -4-deg IGV, Wide Open Discharge . . . . .	324
237	Static Pressure Variation Along Impeller Shroud, Build No. 6, 101% Speed, -4-deg IGV, Near Stall . . . . .	324
238	Static Pressure Variation Along Impeller Shroud, Build No. 6, 100% Speed, 10-deg IGV, Near Stall . . . . .	325
239	Static Pressure Variation Along Impeller Shroud, Build No. 6, 95% Speed, 10-deg IGV, Near Stall . . . . .	325
240	Diffuser Static Pressure Profile, Build No. 3, 95% Speed, Near Stall . . . . .	326
241	Diffuser Static Pressure Profile, Build No. 3, 10-deg IGV, Near Stall . . . . .	326
242	High-Frequency Response Data, 70% Speed, Steady-State, PTIDK1 . . . . .	328
243	High-Frequency Response Data, 70% Speed, Steady-State, PSDVK1 . . . . .	329
244	High-Frequency Response Data, 70% Speed, Steady-State, PSDVK2 . . . . .	330
245	High-Frequency Response Data, 70% Speed, Steady-State, PSDEK1 . . . . .	331
246	High-Frequency Response Data, 70% Speed, Stall Transient, Time 406, PTIDK1 . . . . .	332
247	High-Frequency Response Data, 70% Speed, Stall Transient, Time 426, PTIDK1 . . . . .	333
248	High-Frequency Response Data, 70% Speed, Stall Transient, Time 434 PTIDK1 . . . . .	334
249	High-Frequency Response Data, 70% Speed, Stall Transient, Time 436, PTIDK1 . . . . .	335
250	High-Frequency Response Data, 70% Speed, Time 438, PTIDK1 . . . . .	336

# LIST OF ILLUSTRATIONS (Continued)

<u>Figure</u>		<u>Page</u>
251	High-Frequency Response Data, 70% Speed, Stalled, Time 440, PTIDK1 .....	337
252	High-Frequency Response Data, 70% Speed, Stall Transient, Time 406, PSDVK1 .....	338
253	High-Frequency Response Data, 70% Speed, Stall Transient, Time 426, PSDVK1 .....	339
254	High-Frequency Response Data, 70% Speed, Stall Transient, Time 434, PSDVK1 .....	340
255	High-Frequency Response Data, 70% Speed, Stall Transient, Time 436, PSDVK1 .....	341
256	High-Frequency Response Data, 70% Speed, Stalled, Time 438, PSDVK1 .....	342
257	High-Frequency Response Data, 70% Speed, Stalled, Time 440, PSDVK1 .....	343
258	High-Frequency Response Data, 70% Speed, Stall Transient, Time 406, PSDVK2 .....	344
259	High-Frequency Response Data, 70% Speed, Stall Transient, Time 426, PSDVK2 .....	345
260	High-Frequency Response Data, 70% Speed, Stall Transient, Time 434, PSDVK2 .....	346
261	High-Frequency Response Data, 70% Speed, Stall Transient, Time 436, PSDVK2 .....	347
262	High-Frequency Response Data, 70% Speed, Stalled, Time 438, PSDVK2 .....	348
263	High-Frequency Response Data, 70% Speed, Stalled, Time 440, PSDVK2 .....	349
264	High-Frequency Response Data, 76% Speed, Stall Transient, Time 406, PSDEK1 .....	350
265	High-Frequency Response Data, 76% Speed, Stall Transient, Time 426, PSDEK1 .....	351

# LIST OF ILLUSTRATIONS (Continued)

<u>Figure</u>		<u>Page</u>
266	High-Frequency Response Data, 70% Speed, Stall Transient, Time 434, PSDEK1 .....	352
267	High-Frequency Response Data, 70% Speed, Stall Transient, Time 436, PSDEK1 .....	353
268	High-Frequency Response Data, 70% Speed, Stalled, Time 438, PSDEK1 .....	354
269	High-Frequency Response Data, 70% Speed, Stalled, Time 440, PSDEK1 .....	355
270	High-Frequency Response Data, 78% Speed, Steady-State, PTIDK1 .....	356
271	High-Frequency Response Data, 78% Speed, Steady-State, PSDVK1 .....	357
272	High-Frequency Response Data, 78% Speed, Steady-State, PSDVK2 .....	358
273	High-Frequency Response Data, 78% Speed, Steady-State, PSDEK1 .....	359
274	High-Frequency Response Data, 78% Speed, Stall Transient, Time 533, PTIDK1 .....	360
275	High-Frequency Response Data, 78% Speed, Stall Transient, Time 533, PTIDK1 .....	361
276	High-Frequency Response Data, 78% Speed, Stall Transient, Time 561, PTIDK1 .....	362
277	High-Frequency Response Data, 78% Speed, Stall Transient, Time 563, PTIDK1 .....	363
278	High-Frequency Response Data, 78% Speed, Stalled, Time 565, PTIDK1 .....	364
279	High-Frequency Response Data, 78% Speed, Stalled, Time 567, PTIDK1 .....	365
280	High-Frequency Response Data, 78% Speed, Stall Transient, Time 533, PSDVK1 .....	366

# LIST OF ILLUSTRATIONS (Continued)

<u>Figure</u>		<u>Page</u>
281	High-Frequency Response Data, 78% Speed, Stall Transient, Time 553, PSDVK1 .....	367
282	High-Frequency Response Data, 78% Speed, Stall Transient, Time 561, PSDVK1 .....	368
283	High-Frequency Response Data, 78% Speed, Stall Transient, Time 563, PSDVK1 .....	369
284	High-Frequency Response Data, 78% Speed, Stalled, Time 565, PSDVK1 .....	370
285	High-Frequency Response Data, 78% Speed, Stalled, Time 567, PSDVK1 .....	371
286	High-Frequency Response Data, 78% Speed, Stall Transient, Time 533, PSDVK2 .....	372
287	High-Frequency Response Data, 78% Speed, Stall Transient, Time 553, PSDVK2 .....	373
288	High-Frequency Response Data, 78% Speed, Stall Transient, Time 561, PSDVK2 .....	374
289	High-Frequency Response Data, 78% Speed, Stall Transient, Time 563, PSDVK2 .....	375
290	High-Frequency Response Data, 78% Speed, Stalled, Time 565, PSDVK2 .....	376
291	High-Frequency Response Data, 78% Speed, Stalled, Time 567, PSDVK2 .....	377
292	High-Frequency Response Data, 78% Speed, Stall Transient, Time 533, PSDEK1 .....	378
293	High-Frequency Response Data, 78% Speed, Stall Transient, Time 553, PSDEK1 .....	379
294	High-Frequency Response Data, 78% Speed, Stall Transient, Time 561, PSDEK1 .....	380
295	High-Frequency Response Data, 78% Speed, Stall Transient, Time 563, PSDEK1 .....	381

# LIST OF ILLUSTRATIONS (Continued)

<u>Figure</u>		<u>Page</u>
296	High-Frequency Response Data, 78% Speed, Stall Transient, Time 565, PSDEK1 .....	382
297	High-Frequency Response Data, 78% Speed, Stalled, Time 567, PSDEK1 .....	383
298	Stall Transient Data, 101% Speed, 5-deg IGV, ISPS Rate .....	385
299	Stall Transient Data, 101% Speed, 5-deg IGV, Maximum Rate .....	386
300	Stall Transient Data, 101% Speed, 0-deg IGV, ISPS Rate .....	387
301	Stall Transient Data, 101% Speed, 0-deg IGV, Maximum Rate .....	388
302	Stall Transient Data, 101% Speed, -4-deg IGV, ISPS Rate .....	389
303	Stall Transient Data, 101% Speed, -4-deg IGV, Maximum Rate .....	390
304	Stall Transient Data, 94.5% Speed, 15-deg IGV, ISPS Rate .....	391
305	Stall Transient Data, 94.5% Speed, 15-deg IGV, Maximum Rate .....	392
306	Stall Transient Data, 95% Speed, 10-deg IGV, ISPS Rate .....	393
307	Stall Transient Data, 95% Speed, 10-deg IGV, Maximum Rate .....	394

# LIST OF TABLES

<u>Table</u>		<u>Page</u>
I	Single-Stage Centrifugal Compressor Design Summary . . . .	5
II	Bearing Features . . . . .	13
III	Test Facility Safety Systems . . . . .	26
IV	Compressor Instrumentation Stations . . . . .	28
V	Compressor Component Performance Instrumentation Summary . . . . .	35
VI	High-Frequency Response Probe Locations . . . . .	41
VII	Data Summary . . . . .	48
VIII	Estimate of Instrumentation Accuracy . . . . .	57
IX	Typical Printout for a Near-Stall, Steady-State Point at 101% Design Speed and -4-deg Inlet Guide Vane Setting . .	59
X	Traverse Data - Internal Flow Analysis Performance Comparison . . . . .	63
XI	Inlet Guide Vane Circumferential Traverse Data - 100% Speed, 10-deg IGV Setting . . . . .	80
XII	Inducer Exit Traverse Data, 101% Speed, -4-deg IGV Setting . . . . .	87
XIII	Inducer Exit Traverse Data, 100% Speed, 10-deg IGV Setting . . . . .	87
XIV	Overall Performance Tabulation - Build No. 3, 0-deg Prewirl . . . . .	133
XV	Overall Performance Tabulation - Build No. 3, 10-deg Prewirl . . . . .	134
XVI	Overall Performance Tabulation - Build No. 3, 20-deg Prewirl . . . . .	135
XVII	Overall Performance Tabulation - Build No. 6 . . . . .	137
XVIII	Inlet Guide Vane Performance Printout, 70% Speed, 10-deg IGV, Near Stall, Build No. 3 . . . . .	234



# LIST OF TABLES (Continued)

<u>Table</u>		<u>Page</u>
XIX	Inlet Guide Vane Performance Printout, 90% Speed, 10-deg IGV, Near Stall, Build No. 3 . . . . .	235
XX	Inlet Guide Vane Performance Printout, 85% Speed, 20-deg IGV, Near Stall, Build No. 6 . . . . .	236
XXI	Inlet Guide Vane Performance Printout, 85% Speed, 30-deg IGV, Near Stall, Build No. 6 . . . . .	237
XXII	Inlet Guide Vane Performance Printout, 8/1 Speed, 10-deg IGV, Near Stall, Build No. 6 . . . . .	238
XXIII	Inlet Guide Vane Performance Printout, 8/1 Speed, 15-deg IGV, Near Stall, Build No. 6 . . . . .	239
XXIV	Inlet Guide Vane Performance Printout, 101% Speed, 5-deg IGV, Below Near Stall, Build No. 6 . . . . .	240
XXV	Inlet Guide Vane Performance Printout, 95% Speed, 10-deg IGV, Near Stall, Build No. 6 . . . . .	241
XXVI	Inlet Guide Vane Performance Printout, 100% Speed, 10-deg IGV, Near Stall, Build No. 6 . . . . .	242
XXVII	Inlet Guide Vane Performance Printout, 101% Speed, -4-deg IGV, Near Stall, Build No. 6 . . . . .	243
XXVIII	Inlet Guide Vane Performance Printout, 101% Speed, 0-deg IGV, Near Stall, Build No. 6 . . . . .	244
XXIX	Inlet Guide Vane Performance Printout, 101% Speed, 5-deg IGV, Near Stall, Build No. 6 . . . . .	245
XXX	10/1 Centrifugal Compressor, Impeller Traverse, 30 Percent Speed, WDCV, Run 3.06, IGV = 0 deg Flow Rate = 0.494, Speed = 19700.0 . . . . .	247
XXXI	10/1 Centrifugal Compressor, Impeller Traverse, 30 Percent Speed, Below Near Stall, Run 3.06, IGV Setting = 0 deg, Flow Rate = 0.302, Speed = 19420.0 . . . . .	248
XXXII	10/1 Centrifugal Compressor, Impeller Traverse, 30 Percent Speed, Near Stall, Run 3.06, IGV Setting = 0 deg, Flow Rate = 0.253, Speed = 19537.0 . . . . .	249

# LIST OF TABLES (Continued)

<u>Table</u>		<u>Page</u>
XXXIII	10/1 Centrifugal Compressor, Impeller Traverse, 30 Percent Speed, WDCV, Run 3.05, IGV Setting = 10 deg, Flow Rate = 0.432, Speed = 19798.0 . . . .	250
XXXIV	10/1 Centrifugal Compressor, Impeller Traverse, 30 Percent Speed, Knee, Run 3.06, IGV Setting = 10 deg, Flow Rate = 0.337, Speed = 19877.0 . . . . .	251
XXXV	10/1 Centrifugal Compressor, Impeller Traverse, 30 Percent Speed, Below Near Stall, Run 3.05, IGV Setting = 10 deg, Flow Rate = 0.246, Speed = 19647.0 . . . .	252
XXXVI	10/1 Centrifugal Compressor, Impeller Traverse, 30 Percent Speed, Near Stall, Run 3.05, IGV Setting = 10 deg, Flow Rate = 0.223, Speed = 19422.0 . . . . .	253
XXXVII	10/1 Centrifugal Compressor, Impeller Traverse, 30 Percent Speed, WDCV, Run 3.06, IGV Setting = 20 deg, Flow Rate = 0.494, Speed = 19874.0 . . . . .	254
XXXVIII	10/1 Centrifugal Compressor, Impeller Traverse, 30 Percent Speed, Below Near Stall, Run 3.06, IGV Setting = 20 deg, Flow Rate = 0.358, Speed = 19912.0 . . . .	255
XXXIX	10/1 Centrifugal Compressor, Impeller Traverse, 30 Percent Speed, Near Stall, Run 3.06, IGV Setting = 20 deg, Flow Rate = 0.269, Speed = 19458.0 . . . .	256
XL	10/1 Centrifugal Compressor, Impeller Traverse, 70 Percent Speed, Wide Open Discharge, Run 3.07, IGV Turning = 0 deg, Flow Rate = 1.454, Speed = 45557.0 . . . .	257
XLI	10/1 Centrifugal Compressor, Impeller Traverse, 70 Percent Speed, Below Near Stall, Run 3.07, IGV Turning = 0 deg, Flow Rate = 1.464, Speed = 45712.0 . . . .	258
XLII	10/1 Centrifugal Compressor, Impeller Traverse, 70 Percent Speed, Near Stall, Run 3.07, IGV Turning = 0 deg, Flow Rate = 1.452, Speed = 45542.0 . . . .	259
XLIII	10/1 Centrifugal Compressor, Impeller Traverse, 70 Percent Speed, Wide Open Discharge, Run 3.07, IGV Turning = 10 deg, Flow Rate = 1.463, Speed = 45806.0 . . . . .	260

# LIST OF TABLES (Continued)

<u>Table</u>		<u>Page</u>
XLIV	10/1 Centrifugal Compressor, Impeller Traverse, 70 Percent Speed, Below Near Stall, Run 3.07, IGV Turning = 10 deg, Flow Rate = 1.460, Speed = 45883.0 . . .	261
XLV	10/1 Centrifugal Compressor, Impeller Traverse, 70 Percent Speed, Near Stall, Run 3.07, IGV Turning = 10 deg, Flow Rate = 1.462, Speed = 45771.0 . . .	262
XLVI	10/1 Centrifugal Compressor, Impeller Traverse, 70 Percent Speed, Wide Open Discharge, Run 3.07, IGV Turning = 20 deg, Flow Rate = 1.448, Speed = 45574.0 . . .	263
XLVII	10/1 Centrifugal Compressor, Impeller Traverse, 70 Percent Speed, Below Near Stall, Run 3.07, IGV Turning = 20 deg, Flow Rate = 1.459, Speed = 45699.0 . . .	264
XLVIII	10/1 Centrifugal Compressor, Impeller Traverse, 70 Percent Speed, Near Stall, Run 3.07, IGV Turning = 20 deg, Flow Rate = 1.458, Speed = 45913.0 . . .	265
XLIX	10/1 Centrifugal Compressor, Impeller Exit Traverse, 90 Percent Speed, Near Stall, Run 3.08, IGV Turning = 0 deg, Flow Rate = 2.604, Speed = 58529.6 . . .	266
L	10/1 Centrifugal Compressor, Inducer and Impeller Traverse, 8/1 Line, Wide Open Discharge, Run 3.09, IGV Turning = 10 deg, Flow Rate = 2.898, Speed = 61877.0 . . . . .	268
LI	10/1 Centrifugal Compressor, Inducer Traverse, 8/1 Line, Below Near Stall, Run 3.09, IGV Turning = 10 deg, Flow Rate = 2.902, Speed = 61921.0 . . . . .	270
LII	10/1 Centrifugal Compressor, Impeller Traverse, 8/1 Line, Below Near Stall, Run 3.09, IGV Turning = 10 deg, Flow Rate = 2.902, Speed = 61904.0 . . . . .	271
LIII	10/1 Centrifugal Compressor, Inducer Traverse, 8/1 Line, Near Stall, Run 3.09, IGV Turning = 10 deg, Flow Rate = 2.818, Speed = 62035.0 . . . . .	272
LIV	10/1 Centrifugal Compressor, Impeller Traverse, 8/1 Line, Near Stall, Run 3.09, IGV Turning = 10 deg, Flow Rate = 2.895, Speed = 62126.0 . . . . .	273

# LIST OF TABLES (Continued)

<u>Table</u>		<u>Page</u>
LV	10/1 Centrifugal Compressor, Inducer and Impeller Traverse, 70 Percent Speed, Near Stall, 20 deg IGV Turning, Build 6, Flow Rate = 1.279, Speed = 45548.9 . . . . .	274
LVI	10/1 Centrifugal Compressor, Inducer and Impeller Traverse, 70 Percent Speed, Near Stall, 30 deg IGV Turning, Build 6, Flow Rate = 1.242, Speed = 45528.7 . . . . .	276
LVII	10/1 Centrifugal Compressor, Inducer and Impeller Traverse, 85 Percent Speed, Near Stall, 20 deg IGV Turning, Build 6, Flow Rate = 2.125, Speed = 55663.1 . . . .	278
LVIII	10/1 Centrifugal Compressor, Inducer and Impeller Traverse, 85 Percent Speed, Near Stall, 30 deg IGV Turning, Build 6, Flow Rate = 2.071, Speed 55505.1 . . . .	280
LIX	10/1 Centrifugal Compressor, Inducer Traverse, 8/1 Speedline, WOD, 10 deg IGV Turning, Build 6, Flow Rate = 2.823, Speed = 61657.2 . . . . .	282
LX	10/1 Centrifugal Compressor, Inducer and Impeller Traverse, 8/1 Speedline, Near Stall, 10 deg IGV Turning, Build 6, Flow Rate = 2.796, Speed = 61819.2 . . .	283
LXI	10/1 Centrifugal Compressor, Inducer Traverse, 8/1 Speedline, WOD, 15 deg IGV Turning, Build 6, Flow Rate = 2.807, Speed = 61605.6 . . . . .	285
LXII	10/1 Centrifugal Compressor, Inducer and Impeller Traverse, 8/1 Speedline, Near Stall, 15 deg IGV Turning, Build 6, Flow Rate = 2.787, Speed = 61700.7 . . . .	286
LXIII	10/1 Centrifugal Compressor, Inducer and Impeller Traverse, 95 Percent Speed, WOD, 10 deg IGV Turning, Build 6, Flow Rate = 2.885, Speed = 62114.1 . . . . .	288
LXIV	10/1 Centrifugal Compressor, Inducer and Impeller Traverse, 95 Percent Speed, Near Stall, 10 deg IGV Turning, Build 6, Flow Rate = 2.877, Speed = 62138.8 . . .	290
LXV	10/1 Centrifugal Compressor, Inducer Traverse, 100 Percent Speed, Near Stall, 10 deg IGV Turning, Build 6, Flow Rate = 3.058, Speed = 65238.1 . . . . .	292

# LIST OF TABLES (Continued)

<u>Table</u>		<u>Page</u>
LXVI	10/1 Centrifugal Compressor, Inducer Traverse, 101 Percent Speed, WOD, -4 deg IGV Turning, Build 6, Flow Rate = 3.214, Speed = 65934.3 . . . . .	293
LXVII	10/1 Centrifugal Compressor, Inducer and Impeller Traverse, 101 Percent Speed, Near Stall, -4 deg IGV Turning, Build 6, Flow Rate = 3.209, Speed = 65987.7 . . .	294
LXVIII	10/1 Centrifugal Compressor, Inducer and Impeller Traverse, 101 Percent Speed, Near Stall, -4 deg IGV, With Coolant, Build 6, Flow Rate = 3.214, Speed = 65779.6 . . .	296
LXIX	10/1 Centrifugal Compressor, Inducer Traverse, 101 Percent Speed, WOD, 0 deg IGV Turning, Build 6, Flow Rate = 3.192, Speed = 65834.8 . . . . .	298
LXX	10/1 Centrifugal Compressor, Inducer and Impeller Traverse, 101 Percent Speed, Near Stall, 0 deg IGV Turning, Build 6, Flow Rate = 3.185, Speed = 65952.8 . . .	299
LXXI	10/1 Centrifugal Compressor, Inducer Traverse, 101 Percent Speed, WOD, 5 deg IGV Turning, Build 6, Flow Rate = 3.150, Speed = 65974.5 . . . . .	301
LXXII	10/1 Centrifugal Compressor, Inducer and Impeller Traverse, 101 Percent Speed, Near Stall, 5 deg IGV Turning, Build 6, Flow Rate = 3.142, Speed = 66122.6 . . .	302
LXXIII	10/1 Centrifugal Compressor, Inducer Traverse, 100 Percent Speed, Near Stall, 10 deg IGV Turning, Build 6, Flow Rate = 3.058, Speed = 65238.1 . . . . .	304
LXXIV	10/1 Centrifugal Compressor, Inducer and Impeller Traverse, 101 Percent Speed, Near Stall, -4 deg IGV Turning, Build 6, Flow Rate = 3.209, Speed = 65987.7 . . .	305
LXXV	10/1 Centrifugal Compressor, Impeller Traverse, 8/1 Speedline, Near Stall, 10 deg IGV Turning, Build 6, Flow Rate = 2.796, Speed = 61819.2 . . . . .	307
LXXVI	10/1 Centrifugal Compressor, Impeller Traverse, 8/1 Speedline, Near Stall, 15 deg IGV Turning, Build 6, Flow Rate = 2.787, Speed = 61700.7 . . . . .	308

# LIST OF TABLES (Continued)

<u>Table</u>		<u>Page</u>
LXXVII	10/1 Centrifugal Compressor, Impeller Traverse, 95 Percent Speed, WOD, 10 deg IGV Turning, Build 6, Flow Rate = 2.885, Speed = 62114.1 . . . . .	309
LXXVIII	10/1 Centrifugal Compressor, Impeller Traverse, 95 Percent Speed, Near Stall, 10 deg IGV Turning, Build 6, Flow Rate = 2.877, Speed = 62138.8 . . . . .	310
LXXIX	10/1 Centrifugal Compressor, Impeller Traverse, 101 Percent Speed, Near Stall, -4 deg IGV Turning, Build 6, Flow Rate = 3.209, Speed = 65987.7 . . . . .	311
LXXX	10/1 Centrifugal Compressor, Impeller Traverse, 101 Percent Speed, Near Stall, -4 deg IGV, With Coolant, Build 6, Flow Rate = 3.214, Speed = 65779.6 . . . . .	312
LXXXI	10/1 Centrifugal Compressor, Impeller Traverse, 101 Percent Speed, Near Stall, 0 deg IGV Turning, Build 6, Flow Rate = 3.185, Speed = 65952.8 . . . . .	313
LXXXII	10/1 Centrifugal Compressor, Impeller Traverse, 101 Percent Speed, Near Stall, 5 deg IGV Turning, Build 6, Flow Rate = 3.142, Speed = 66122.6 . . . . .	314

# LIST OF SYMBOLS

A	cross-sectional area, in. <sup>2</sup>
A*	throat area, in. <sup>2</sup>
a	speed of sound, ft/sec
B*	throat blockage
C <sub>d</sub>	inlet flow coefficient
C <sub>d</sub> *	diffuser discharge coefficient
C <sub>p</sub>	pressure recovery coefficient
c	uncertainty of an individual sensor
G	gravitational constant = 32.174, lb <sub>m</sub> -ft/lb <sub>f</sub> -sec <sup>2</sup>
h	enthalpy/unit mass
i	incidence, deg
K	$f \text{ (Mach number)} = M \sqrt{\frac{\gamma G}{R}} \left(1 + \frac{\gamma-1}{2} M^2\right)^{\frac{\gamma+1}{2(\gamma-1)}}$
M	relative Mach number
M <sub>0</sub>	absolute Mach number
N	rotor speed, rpm
n	Number of sensors
P	static pressure, psia
P <sub>r</sub>	pressure ratio
P <sub>t</sub>	total pressure, psia
R	gas constant = 53.345, ft-lb <sub>f</sub> /lb <sub>m</sub> -°R
T	total temperature, °R
T <sub>r</sub>	temperature ratio
T <sub>s</sub>	static temperature, °R

### LIST OF SYMBOLS (Continued)

U	rotor speed, ft/sec
u	overall uncertainty
V	absolute velocity, ft/sec
W	relative velocity, ft/sec
w	weight flow, lb/sec
$\alpha$	absolute air angle, deg
$\beta$	relative air angle, deg
$\beta^+$	leading edge metal angle, deg
$\gamma$	ratio of specific heats
$\delta$	$P_0/14.694$
$\epsilon$	diffuser effectiveness
$\eta$	adiabatic efficiency
$\theta$	$T_0/518.688$

### SUBSCRIPTS

act	actual
cal	calculated
cor	corrected to standard day inlet conditions
i	ideal
m	axial component
rel	relative
s	strut
t-s	total to static
u	tangential component



### LIST OF SYMBOLS (Continued)

v	vane
o	plenum
1	IGV exit instrumentation station
1.5	inducer exit instrumentation station
2	impeller exit instrumentation station
3	collector

### SUPERSCRIPTS

( $\bar{\phantom{x}}$ )	mass averaged
( $\ast$ )	sonic (throat) condition

## INTRODUCTION

High-pressure ratio, single-stage centrifugal compressors offer the possibility of providing rugged, relatively erosion-resistant and low-cost compression systems for advanced gas turbine engines of the 2-to-5-lb/sec airflow class. If good efficiency can be obtained at high pressure ratios, this type of compressor will be more useful than the multistage axial flow compressors now used in small military aircraft engines. The objective of this five-phase program was to design, fabricate, and test a high pressure ratio centrifugal compressor with the following minimum goals:

1. Pressure ratio of 10.0:1 and corresponding adiabatic efficiency of 75% at design speed and flow.
2. Pressure ratio of 8.0:1 and corresponding adiabatic efficiency of 80% at a speed and flow condition less than that of the design point.

The five program phases are (1) initial compressor design, (2) fabrication and assembly of the test hardware, (3) test of the initial configuration, (4) evaluation of the test data, and (5) compressor modification to include fabrication and assembly of new hardware, test, and data evaluation.

This report contains information pertaining to all phases of the program. It includes two appendixes. Appendix I contains tabulated and plotted data not necessary to the general text. Appendix II (separately bound) contains the detailed aerodynamic design and is classified CONFIDENTIAL.

The two test phases of the program were completed during six test periods over a 3-year span. The progress of the contract experimental program was interrupted to permit redesign and modification of the test rig to achieve its rated rpm. The following chronological sequence of the tests conducted during this program will aid in understanding the design and data described in this report. Each successive configuration of either the test stage or rig is identified by a build number.

- Build No. 1: The initial build of the rig was tested to approximately 70% of the design speed. The impeller rubbed the shroud and the run program was terminated.
- Build No. 2: The second build contained modifications to prevent the impeller from contacting the shroud. This build was tested to approximately 85% of design speed, where testing was terminated due to high rig vibration levels. Performance data from this test were evaluated and permitted a minor aerodynamic redesign to be completed. As a result of the redesign, the diffuser was resized to match the inducer-impeller characteristic.
- Build No. 3: The vibrations encountered in Build No. 2 were diagnosed as a critical speed problem, and the rotor system and impeller attachment were stiffened to increase the critical

speed out, hopefully, of the running range. While these modifications improved the rig operating envelope, high vibrations were again encountered at design speed. The entire test program was completed, with the exception of the design speed testing and special instrumentation tests. It was determined that the prediction of rig critical speed was relatively inaccurate for the overhung rotor configuration. It was further determined that a straddle-mounted bearing system (impeller between bearings) would be capable of running at higher speeds without failure, and the rig was re-designed accordingly, including rerouting the inlet flow path around the new front bearing compartment.

- Build No. 4:** This build was tested as a checkout for the redesigned rig bearing system; however, testing was terminated by an impeller-to-shroud rub, which occurred at approximately 85% speed. Silver scraped from the shroud during the rub caused damage to the diffuser entrance region during this test. Data obtained during this test indicated the presence of potential heat transfer into the inlet and also through the cases. The inlet and inlet plenum were insulated and a thermal dam was machined between the inducer and impeller shrouds to eliminate these problems.
- Build No. 5:** The rig was modified to include a thermal dam to limit the heat transfer between the inducer and impeller shrouds, and the clearances were modified to prevent rubbing between impeller and shroud. The rig mechanical redesign was successfully checked out to design speed.
- Build No. 6:** This build concluded the contract test program, as all phases of the modified test plan that concentrated on obtaining data near design speed were successfully completed. Stable rig operation was demonstrated at speeds as high as 72,000 rpm (112% of design speed).

The aerodynamic and performance data in this report primarily result from the tests of Builds No. 2, 3, and 6. The only change in aerodynamic hardware from Build No. 2 to Build No. 3 consisted of removal of 0.020 in. of the impeller exit diameter to prevent contact with the diffuser shroud during testing. The Build No. 6 impeller did not have this 0.020 in. of material removed and thus was identical to the original design. Build No. 6 did have a new inlet bellmouth and a converging inlet with two additional inlet struts due to the new rig mechanical arrangement required to achieve design speed. The inlet guide vanes and inducer were unchanged from the original design, and the diffuser was repaired as much as possible, but still contained damage in the entrance region due to the Build No. 4 impeller-to-shroud rub.

## DESIGN APPROACH

### AERODYNAMIC DESIGN

The aerodynamic design is completely described in a separate volume as Appendix II to this report and is classified **CONFIDENTIAL**. A brief summary of the design of the stage, shown in Figure 2, is presented herein. The design consists of variable inlet guide vanes, an impeller with a remote inducer, and a pipe diffuser.

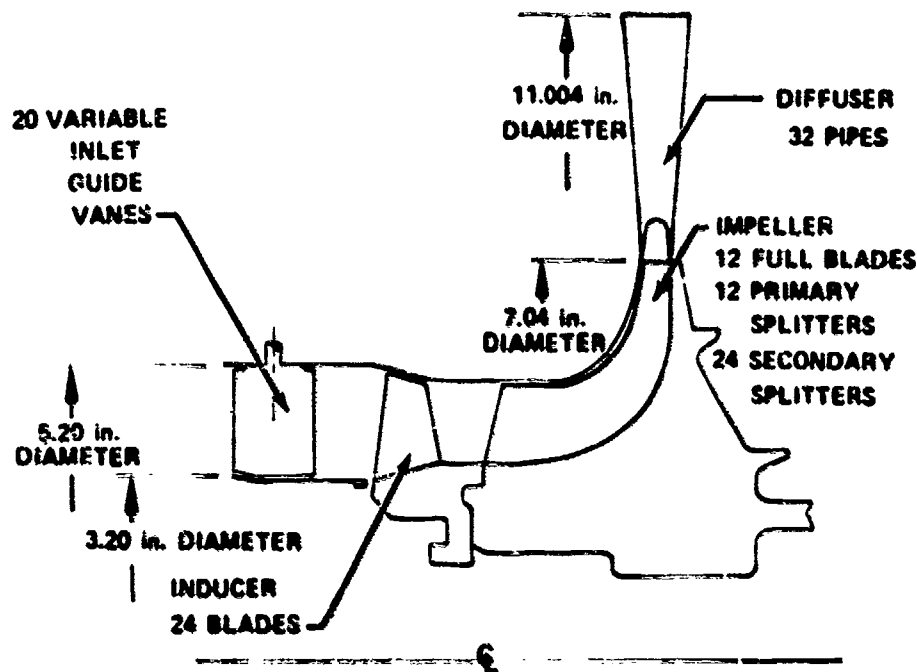


Figure 2. 10:1 Pressure Ratio Centrifugal Compressor Stage.

The objective of the program was to design a 2-to-5-lb/sec airflow single-stage centrifugal compressor that could be incorporated in a future Army advanced technology gas turbine engine. The design speed performance goals were to exceed 75% efficiency at 10:1 pressure ratio. Since gas turbine engines for Army aircraft applications operate under part-power conditions a majority of the time, an off-design performance goal of 80% efficiency at 8:1 pressure ratio was established.

In the design of the compressor, parametric studies were conducted to select an overall design consistent with optimum compressor performance at both performance goals. These studies defined the compressor inlet corrected flow rate, impeller inlet hub and tip radii, corrected impeller rotational speed, and inlet prewhirl. Airflow selection and the selection of the hub radius were influenced by the decision to design a compressor that could be used in a small turboshaft engine with a concentric shaft front drive. This configuration required a larger inlet hub radius than that normally associated with research impellers but it was felt that the loss in potential performance was not significant.

The tip radius was selected after determining the effect on axial Mach number, inducer tip relative Mach number, and inlet choke flow margin. The effect of inlet guide vane losses, inlet shock losses, diffuser losses, and shroud friction heating were parametrically evaluated before selecting IGV prewhirl and rotor speed to provide the optimum overall compressor performance.

A remote inducer design was selected over an integral inducer-impeller configuration so that the inducer could be designed using transonic axial-flow compressor technology. The work split between the inducer and impeller was selected so that the relative Mach number into the impeller would be subsonic with no more than a 1.6:1 inducer pressure ratio. The resultant 10:1 pressure ratio impeller with remote inducer is shown in Figure 3.



Figure 3. 10:1 Pressure Ratio Centrifugal Impeller and Remote Inducer.

Two inducer configurations were evaluated with respect to their potential for application to the single-stage compressor. A pipe diffuser was selected over vane radial and cascade diffusers, because it has the lowest losses over the largest range of Mach number and because P&WA<sup>TM</sup> has had substantial experience in designing and fabricating this type of diffuser.

A tabulation of pertinent compressor design information is presented in Table I.

TABLE I. SINGLE-STAGE CENTRIFUGAL COMPRESSOR DESIGN SUMMARY

Compressor Overall		
Pressure Ratio		10:1*
Adiabatic Efficiency, %		75
Flow rate, lb/sec		3.1
Rotor Speed, rpm		65,300
Specific Speed		80
Inlet		
4 Struts		NACA 400 Series
20 Inlet Guide Vanes		NACA 63 Series
Nominal Guide Vane Setting, deg		10
Specific Flow, lb/ft <sup>2</sup> /sec		34
Hub Radius, in.		1.6
Tip Radius, in.		2.6
Inducer		
Remote Arrangement		
24-Transonic Blades		
Hub-Tip Ratio		0.615
Nominal Pressure Ratio		1.57:1
Nominal Efficiency, %		87.6
Impeller		
Nominal Pressure Ratio		7.34:1
Nominal Efficiency, %		82.8
Exit Flow Angle, deg		19.5
Exit Tip Radius, in.		3.52
Exit Blade Height, in.		0.230
Nominal Operating Clearance		0.005
Diffuser		
32-Passage Conical Pipe Type		
Vaneless Space Radius Ratio, in.		1.10
Throat Radius		0.11
Straightening Section		L/d = 0.5
Cone Geometry, deg		3 to 5
Nominal Loss ( $\Delta P_t/P_t$ )		0.12
Pressure Recovery Coefficient		0.789

\*Unless otherwise specified, pressure ratio is the ratio of discharge static (plenum) pressure to inlet stagnation pressure. Efficiency is also specified using this pressure ratio.

## MECHANICAL DESIGN

Although the objectives of this program were primarily aerodynamic, the mechanical aspects of the test compressor, drive turbine, and the test facility exerted a large influence on the course of the program. As is the case with all high-speed rotating machinery, design emphasis was placed on the evaluation of blade and disk stress limits, determination of rotor critical speeds, and calculation of bearing loads. Tests using the original compressor-drive turbine configuration, described in the Introduction section, uncovered serious limitations to the safe rig operating envelope and necessitated a substantial redesign of the rig rotor system. Although the design and development of the high-speed drive turbine was not part of the scope of the work of this contract, the contract compressor stage was directly mounted on the drive turbine rotor and their system dynamics were integral. Consequently, a discussion of the drive turbine design and its subsequent redesign are included in this section. The mechanical design of the 10:1 pressure ratio centrifugal stage is discussed in the following paragraphs. A schematic drawing of the initial drive turbine and compressor test hardware design is provided in Figure 4. The design featured an axial flow inlet, variable inlet guide vanes, overhung spline drive inducer and impeller, and a double radial inflow drive turbine.

### Inlet

The inlet section was required to support the inlet centerbody, house the variable inlet guide vanes, and provide lubricating oil to the front bearing and instrumentation routing channels. It was fabricated from aluminum weldments. The thickness of the four supporting struts was determined by the size of the oil supply line. An analysis indicated that the oil flow requirement could be accomplished with a 1/8-in. OD tube. Therefore, a conservative maximum thickness of 1/4-in. strut was selected.

With 4 struts and 20 inlet guide vanes, it was appropriate to place every 5th guide vane in line with a strut. All of the guide vanes were connected to a synchronizing ring, which allowed variable positioning of the vanes from zero to 30 deg of pre-whirl. An actuator was used to position the vanes. The actuation linkage was designed with close tolerances wherever feasible to keep alignment errors to a minimum. The calculated maximum misalignment of an individual vane was  $\pm 1.5$  deg from the nominal angle. Sealing of leakage flow around each vane was accomplished with an O-ring on each vane shaft. Contouring of the vane hub and tip provided a clearance of 0.005 to 0.015 in. at all positions of actuation.

### Inducer

In the mechanical design of the inducer, a thin conical splined shaft was used to transmit torque from the drive shaft. The design of the remote inducer permitted it to be readily modified to a close-coupled inducer configuration at a later date. A stress analysis of the AISI Ti-6Al-4V inducer disk showed the maximum effective disk stress to be just under 35,000 psi, which gave a burst margin of 106%. An analysis of the 1.04 aspect ratio blade natural frequencies indicated that there were no bending or torsional modes within the intended operating range (Figure 5).

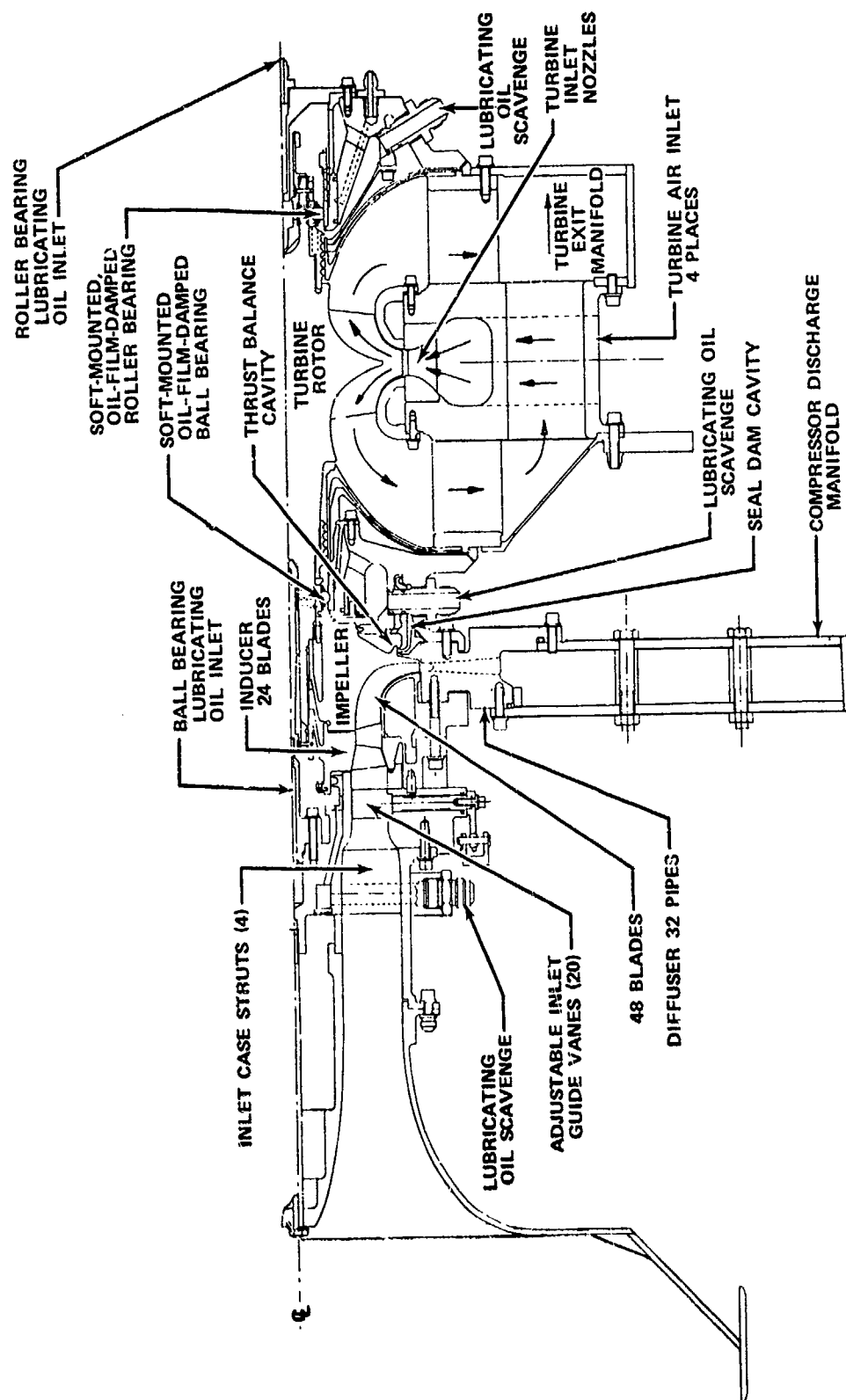


Figure 4. Initial Design of 10.0:1 Pressure Ratio Centrifugal Compressor and P&WA™ Drive Turbine.



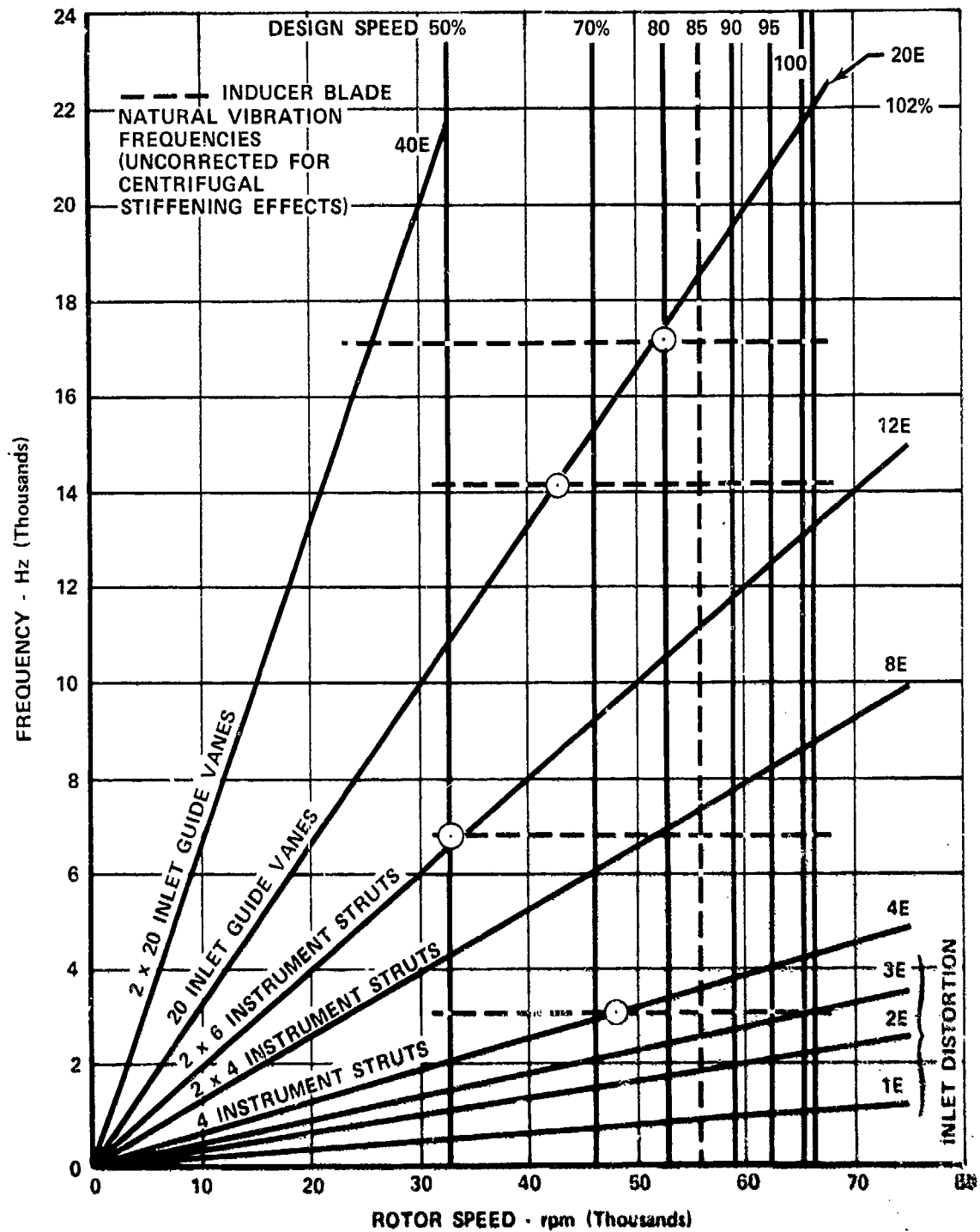


Figure 5. Inducer Vibration Analysis.

### Impeller

The impeller attachment design also employed a thin conical splined shaft to transmit torque and had a press fit on the drive shaft for alignment. The impeller and inducer were mated with an interference (snap) fit, as shown in Figure 6. Stress analysis of the impeller disk at 72,000 rpm showed maximum predicted bore effective stress of 133,000 psi. Using AISI Ti-6Al-2Sn-4Zr-6Mo material, with a 0.2% yield strength of 153,000 psi, at the maximum predicted bore temperature of 220°F, the disk stresses are within acceptable limits. A calculated burst speed of 98,900 rpm results in an adequate burst margin of 37.2%. A stress analysis of the impeller blades predicted maximum blade stresses at about 75% of the local yield stress (loss of strength due to increased temperature taken into account).

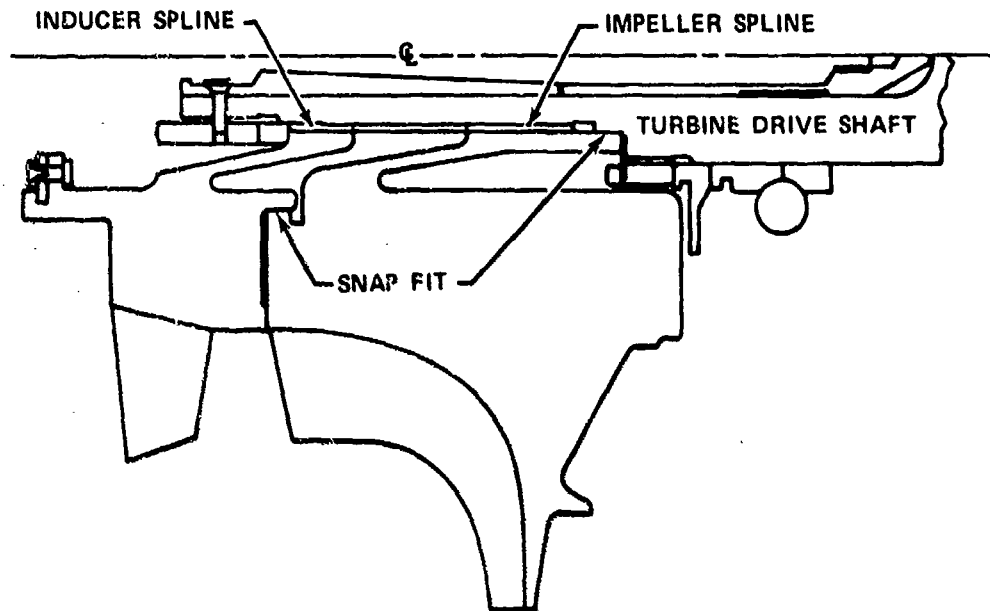


Figure 6. Impeller and Inducer Attachment.

### Shrouds and Diffuser

Aerodynamic design of the inducer had the tip diameter converge from the leading to the trailing edges. This convergence resulted in a separate inducer and impeller to allow assembly. The aerodynamic design of the impeller and inducer also required operation with very small shroud clearances, on the order of 0.005 in. To minimize the consequences of rubbing a titanium blade on a stainless steel shroud, both impeller and inducer shrouds were plated with a thin layer of silver, 0.005 to 0.007 in. thick, which provided a relatively soft rub surface. Positioning of the shrouds relative to the impeller-inducer was accomplished by means of shim selection at assembly.

Stainless Steel 410 was selected for making the 32-passage pipe diffuser because its low coefficient of thermal expansion approaches that of the titanium impeller. The insides of the diffuser pipes were nickel plated to minimize corrosion. The

alignment of the diffuser inlet with respect to the impeller blade exit was designed to be adjusted at assembly with shims.

To define running clearances and diffuser-impeller alignment, mechanical clearance probes were designed to experimentally measure the running tip clearance (Figure 7). The projection of the replaceable aluminum wire into the clearance space was measured during assembly. On the test stand, rotor rpm was increased by increments, and after each increment, the probes were removed and the length of wire was measured to determine clearance as a function of rotor speed. The clearance thus determined is the net result of any impeller movement and shroud and diffuser thermal growth.

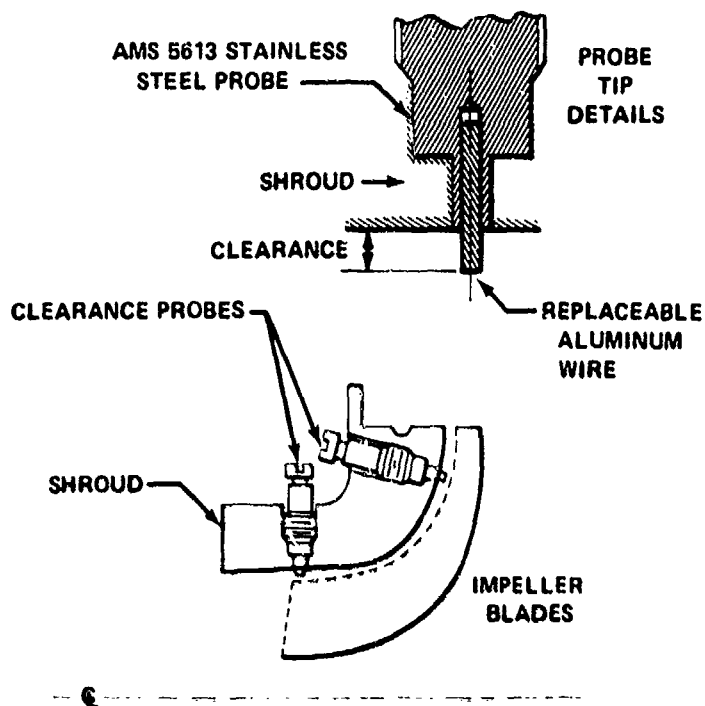


Figure 7. Tip Clearance Probe Installation.

#### Bearings and Seals

The bearing support for the compressor and drive turbine consisted of two 35-mm rolling element bearings straddle mounted on either side of the turbine rotor. The compressor splined drive shaft was overhung beyond the front bearing, as shown in Figure 8.

The forward bearing, which also functions as a thrust bearing and, hence, positions the impeller, is a split-inner-race ball bearing that can accommodate transient thrust reversals. The rear bearing is a straight-through-outer-ring roller bearing that can accommodate axial thermal growth. At the design speed of 63,300 rpm, the bearing DN (bore diameter in mm x rpm) is 2.28 million. Selecting a smaller bearing diameter would force more severe limitations on potential

front-drive capability in an engine application. It would also reduce the allowable thrust load range of the ball bearing (between skid and fatigue limits) to a point where precise thrust balance control would be required. The bearing material, M50 alloy steel (PWA<sup>TM</sup> 725), was selected as the best available alloy for both bearings. Bearing cross sections are shown in Figure 9, and pertinent design parameters are listed in Table II. Both bearings have one-piece, inner-land-riding cages that are machined from AMS 6414 steel and silver plated. Wide cage lands ensure adequate cage journal support area. Lubricating oil is supplied from within the shaft to ensure adequate inner race cooling and positive oil distribution within the bearings. Total oil flows are 7 and 4 lb/min, respectively, for the ball and roller bearings.

Ball bearing raceway curvatures for the compressor rig were selected to limit Hertz stress and to keep spin-to-roll ratio (heat generation) to reasonable levels. The inner race curvature was increased somewhat above the optimum fatigue life value to reduce potential cage problems and heat generation. The higher curvature tends to provide lower cage loading and wear by restricting contact angle variation due to misalignment or excessive radial load. To provide additional margin in this respect, it was desirable to restrict radial loads on the ball bearing to no more than one third of the thrust load. Within this framework, the design analysis indicated that a complement of 15 balls with 5/16 in. diameter would provide the maximum fatigue life.

The compressor rig roller bearing was designed to support radial loads (predicted from rotor dynamic analysis) up to 150 lb in excess of 150 hr with proper balance, alignment, and lubrication. This resulted in a complement of fourteen 7.5- by 7.5-mm rollers.

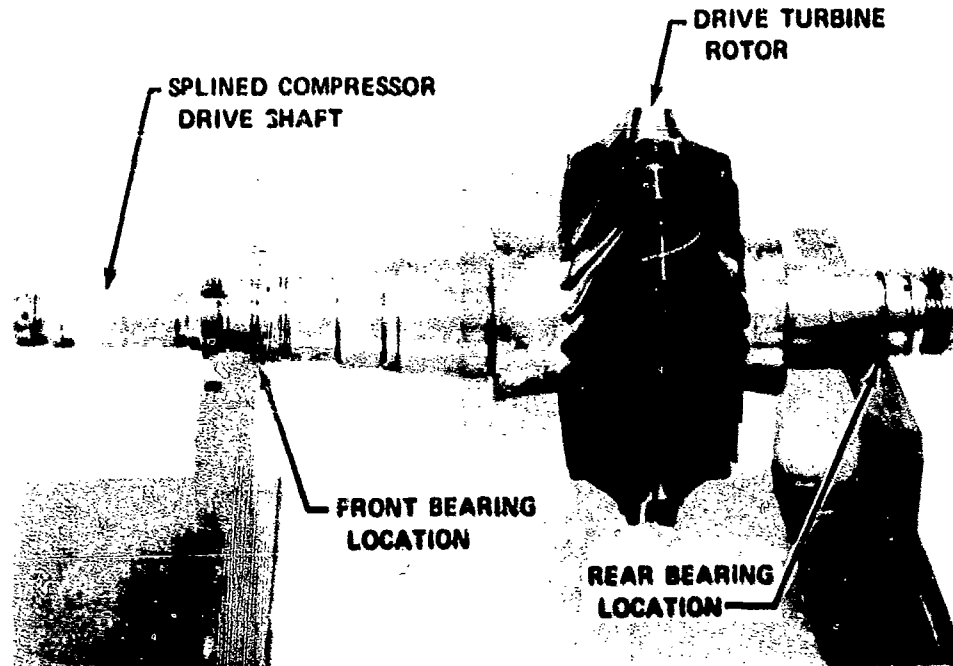


Figure 3. Initial Compressor Drive and Bearing Support Design.

BORE SIZE, mm: 35  
 OIL: MIL-L-23699  
 INLET TEMPERATURE, °F: 150

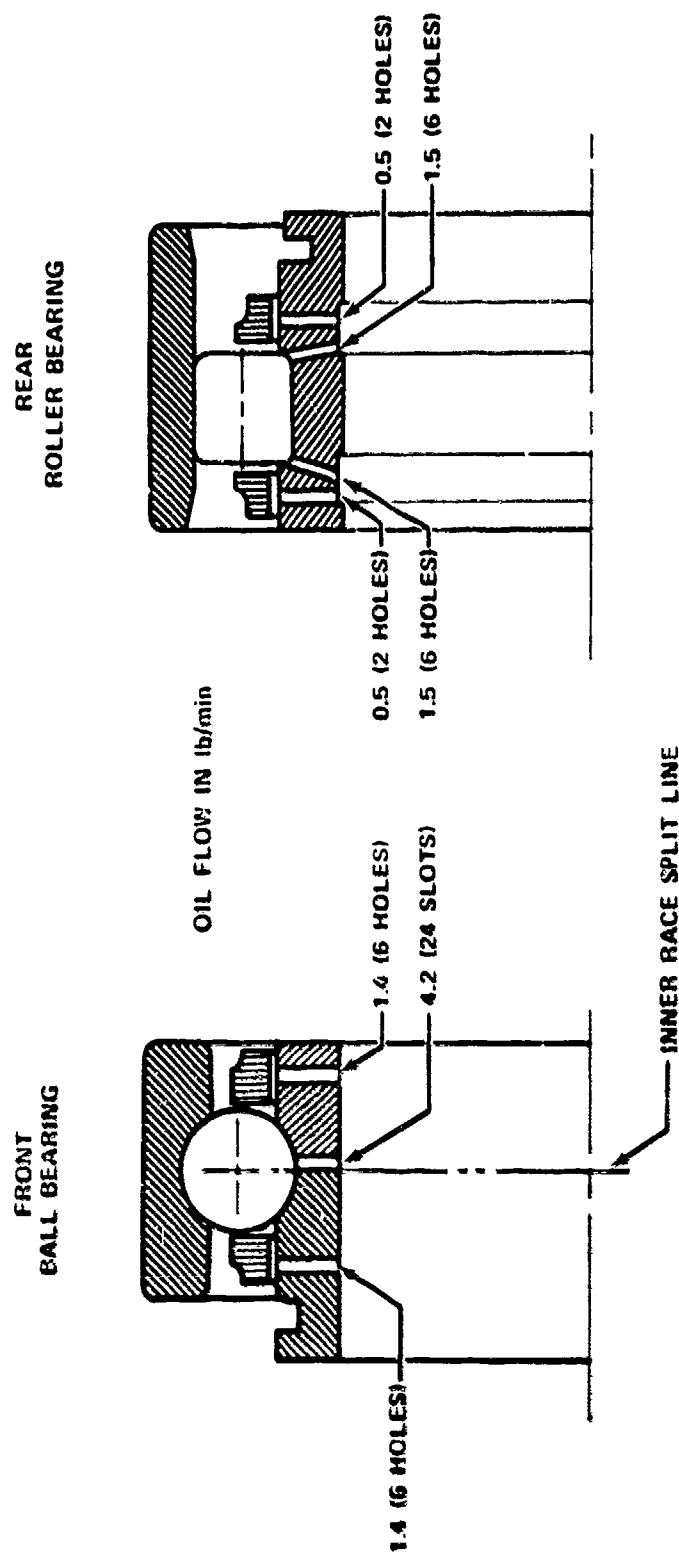


Figure 9. Bearing Designs.

TABLE II. BEARING FEATURES<sup>(1)</sup>

	Ball	Roller
Nominal bore size, mm	35	35
OD, in.	2.4408	2.4408
ID, in.	1.3779	1.3779
Number of elements	15	14
Element size	5/16 in.	7.5 x 7.5 mm <sup>(2)</sup>
Pitch circle diameter, in.	1.9095	1.9095
Outer raceway curvature, % <sup>(3)</sup>	52	-
Inner raceway curvature, % <sup>(3)</sup>	56	-
Contact angle, deg	25	-
<sup>(1)</sup> Room temperature		
<sup>(2)</sup> 10-in. radius crown		
<sup>(3)</sup> (radius of curvature/ball diameter) x 100		

Due to the high centrifugal loading, the rollers were designed with more than normal crown drop to reduce the tendency for end loading and wear.

#### Rotor Dynamics

A vibrational analysis of the compressor and turbine rotor assembly, shown in Figure 10, indicated acceptable bearing loads and rotor deflections. The bounce and pitch modes (11,000 and 25,000 rpm, respectively) of the rotor were in the lower end of the operating speed range and their response would be readily damped by the oil film dampers at the ball and roller bearing supports. Calculation of the first bending mode rotor critical speed showed it was well out of the running range. Dynamic response calculations of bearing loads are shown in Figures 11 and 12 for a 0.1 oz-in. unbalance at the front and rear bearings, respectively.

#### Thrust Balance

An external system was incorporated to supply gaseous nitrogen on the rear face of the compressor impeller to maintain a minimum thrust load on the ball bearing. Calculated load as a function of speed required to prevent the ball bearing from skidding is shown in Figure 13. The 240 lb required at design speed was well below the maximum recommended ball bearing thrust load capacity of 400 lb. Labyrinth-type knife edge seals were used to contain the nitrogen in the thrust balance cavity. In addition, a seal dam cavity between the impeller tip backface and the thrust balance cavity was incorporated that minimized flow between the impeller tip backface and the thrust balance cavity.

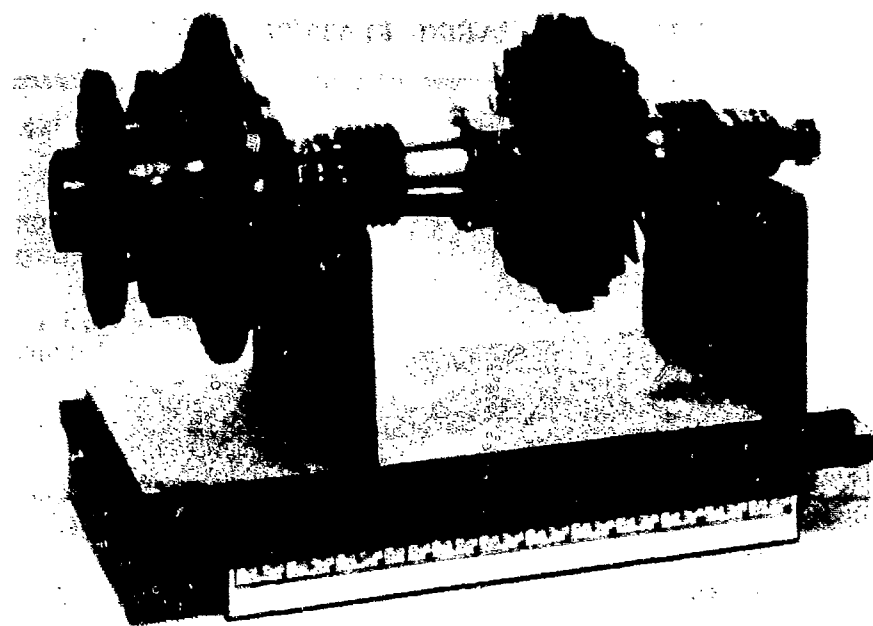


Figure 10. Compressor and Turbine Rotor Assembly.

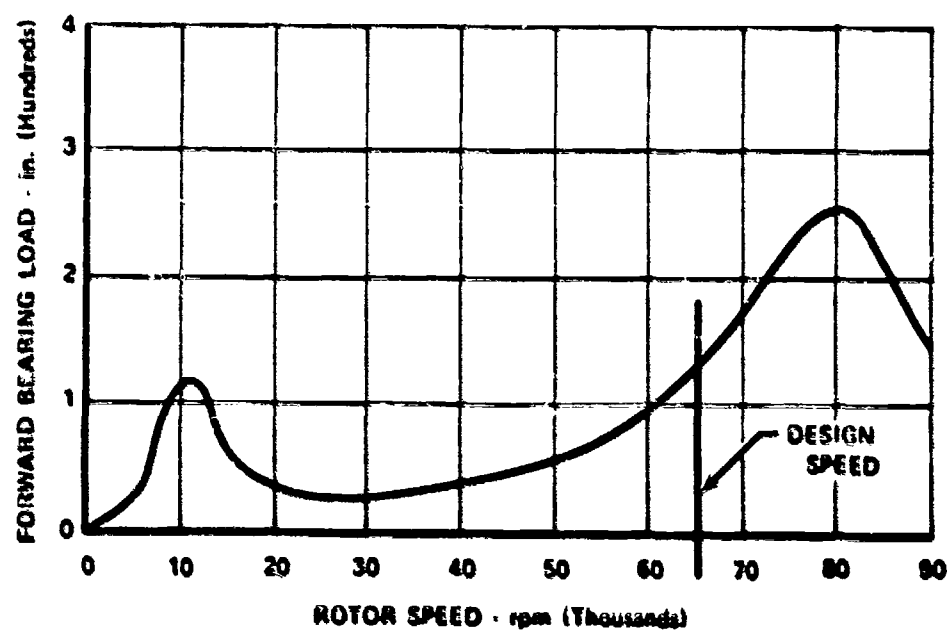


Figure 11. Initial Rotor Configuration Predicted Front Bearing Loads.

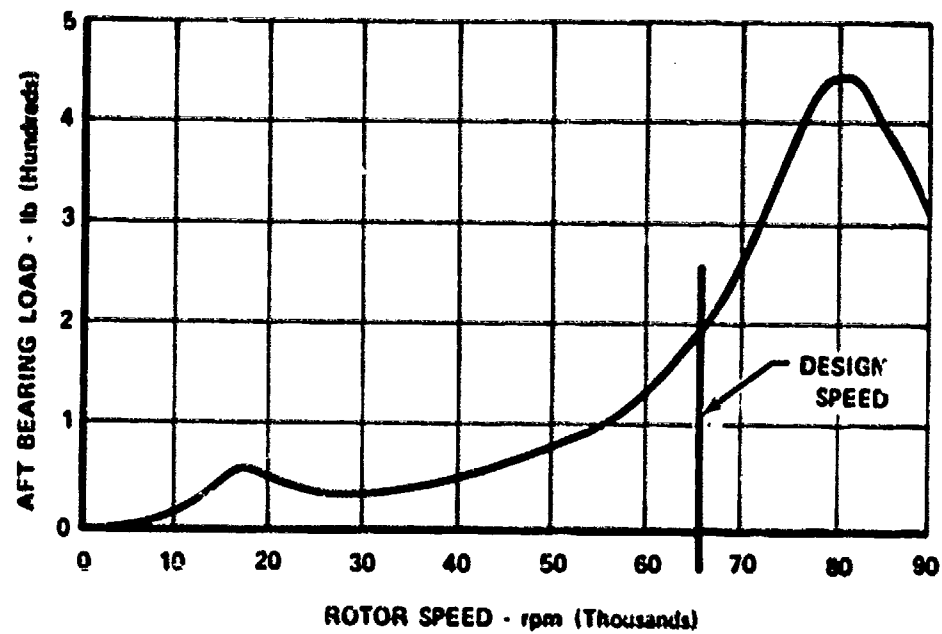


Figure 12. Initial Rotor Configuration Predicted Rear Bearing Loads.

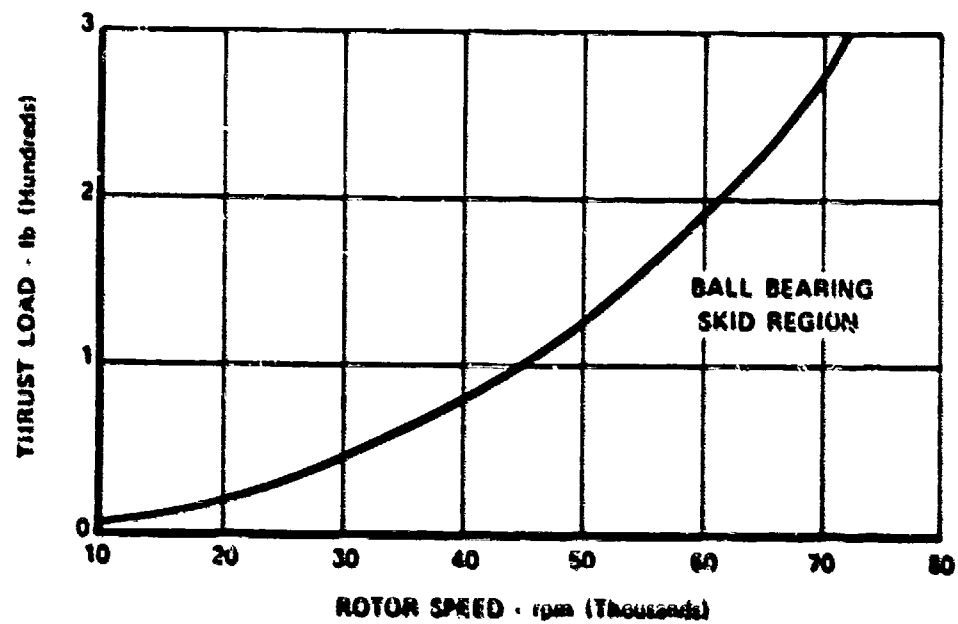


Figure 13. Predicted Ball Bearing Minimum Thrust Load Requirements.



### Modifications

The impeller attachment scheme was stiffened when high rotor vibrations in Build No. 2 limited maximum speed to 58,000 rpm. The impeller bore diameter was increased to permit insertion of a cylindrical spacer, shown in Figure 14. The cylindrical spacer added stiffness at the impeller-shaft attachment point due to the larger diameter in the impeller region. A spacer was also added between the inducer and impeller. This spacer, in conjunction with the impeller cylindrical spacer, permitted the axial load to be transmitted from the front of the inducer, through the impeller, to the drive shaft in a more direct fashion. Further action was taken to prevent a rub from occurring in the event rotor vibrations were not corrected. The impeller exit diameter was reduced 0.020 in. to prevent the impeller tip from rubbing the diffuser vaneless space.

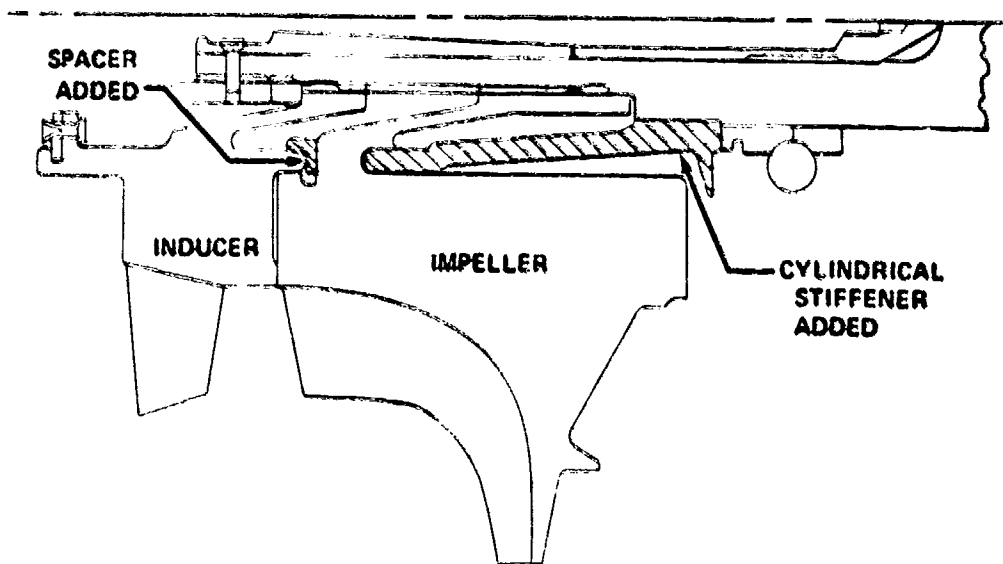


Figure 14. Impeller Shaft Attachment Modification.

The impeller attachment modifications increased the maximum allowable rotor speed to slightly in excess of design speed (63,300 rpm). However, during Build No. 3, high vibrations at or near design speed caused the front bearing to fail after 3.1 hr of operation at 95 to 100% of design speed. Rapid shutdown procedures prevented any damage to the compressor, but it was decided not to resume testing until after the rotor assembly was completely redesigned for increased dynamic stability.

### MECHANICAL REDESIGN

The approach taken in the mechanical redesign of the compressor/turbine rotor assembly was to significantly increase critical speed margin and to increase the front bearing radial load capacity to ensure continuous operation at design speeds and above. The redesigned test hardware, shown in Figure 15, features tandem ball and roller bearings, a carbon face seal at the front of the impeller, and a CTRVIC<sup>®</sup> coupling to join the impeller and drive turbine.



### Inlet

Placing two bearings and a carbon seal in front of the impeller required the flow path to be changed from a parallel flow inlet to a converging configuration, to provide the additional space needed for the bearing compartment and seal support. The increased supply of oil needed for lubricating the two bearings and cooling the carbon seal plate, and additional scavenge and breather requirements could not be accommodated in the four original inlet struts. Two additional struts were incorporated for a total of six equally spaced struts. By terminating the flow path convergence at the inlet guide vanes, it was possible to use the same 20 inlet guide vanes that were used in the original inlet.

### Inducer

In the redesign of the rotor assembly, the attachment of the inducer was changed to eliminate the spline. Friction was used to drive the inducer and was transmitted by the tiebolt and the radial inducer-impeller interface. The axial tiebolt load at room temperature was 18,500 lb. A stress analysis of the redesigned inducer disk indicated maximum effective stress to be 96,900 psi. This was equivalent to a burst margin of 49%, which, although less than the original design, was still more than adequate. The inducer remote spacing was maintained.

### Impeller

The attachment of the impeller to the drive turbine was redesigned to use a CURVIC coupling for maintaining rotor assembly concentricity and transmitting the torque from the drive turbine. The redesigned rotor assembly is shown in Figure 16. The forward end of the original drive turbine was modified for a CURVIC coupling. A CURVIC spacer was used to separate the turbine and impeller. The use of a tiebolt to hold the rotor assembly together required changing the original impeller bore geometry. A stress analysis showed the redesigned impeller maximum bore stresses to be 120,000 psi, which was nearly the same as the original impeller design and provided an adequate burst margin of 41%.

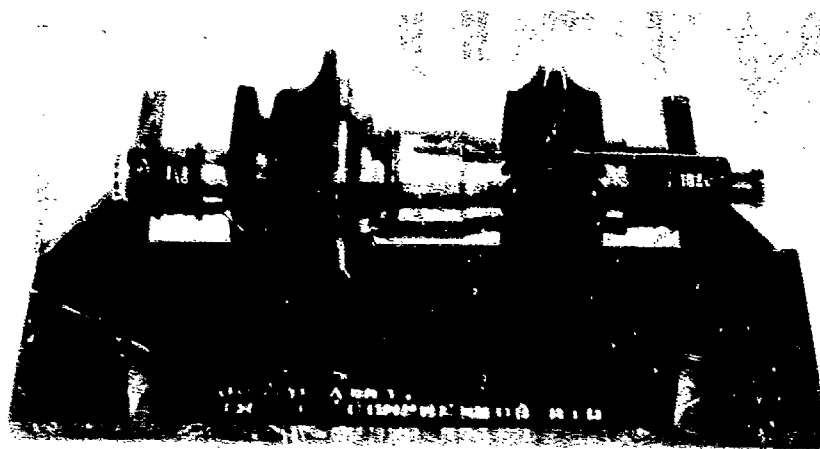


Figure 16. Redesigned Rotor Assembly.

## Bearings and Seals

A dual front-bearing configuration was selected to provide a substantial increase in radial load capacity over the original design. This dual arrangement located a "floating" ball thrust bearing adjacent to a roller bearing, which allowed the roller bearing to carry all the radial load and the ball bearing all the thrust load. The rear bearing compartment (turbine end) was the same as the original design.

Both the front and rear bearings were the same as the original designs and were soft mounted on oil-film-damped supports, with lubrication provided through the inner races as before.

A vibration analysis of the redesigned rotor assembly predicted substantially lower bearing unbalance loads at design speed compared to the loads predicted for the initial design, as shown in Figures 17 and 18 for the front and rear bearings, respectively.

A carbon face seal was incorporated in the redesigned inlet case to eliminate air and oil leakage to and from the forward bearing compartment and inlet flow path. The seal nosepiece was graphitic carbon, and the seal runner was AMS 6322 alloy steel, with a flame-sprayed coating of chrome-carbide to improve wear characteristics. The seal runner was cooled by flowing oil through small radial holes. Secondary sealing was accomplished by a bellows, which was damped at the OD to reduce bellows fatigue problems. The face seal cross section is shown in Figure 19.

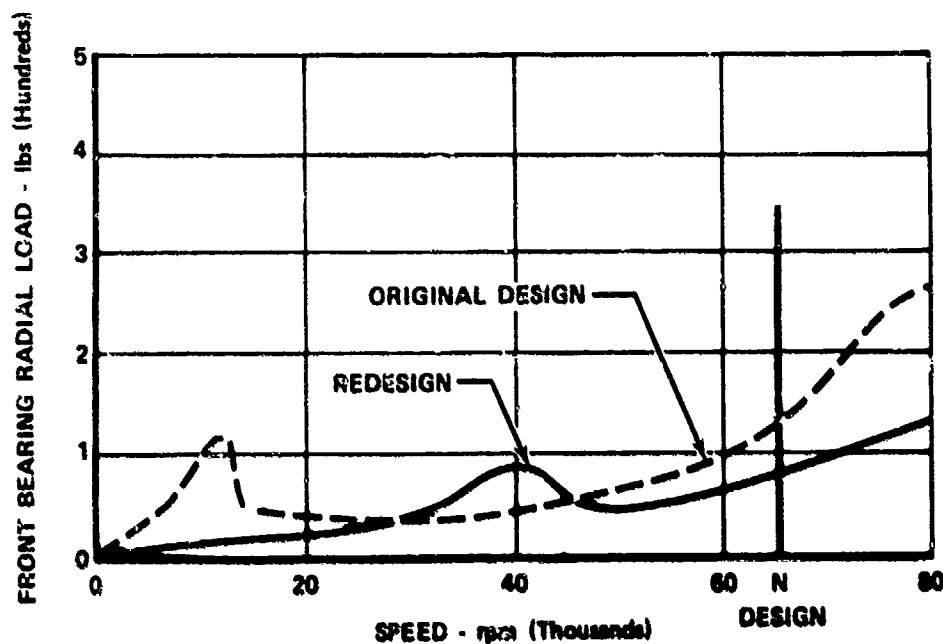


Figure 17. Redesigned Rotor Assembly Predicted Front Bearing Load vs Speed.

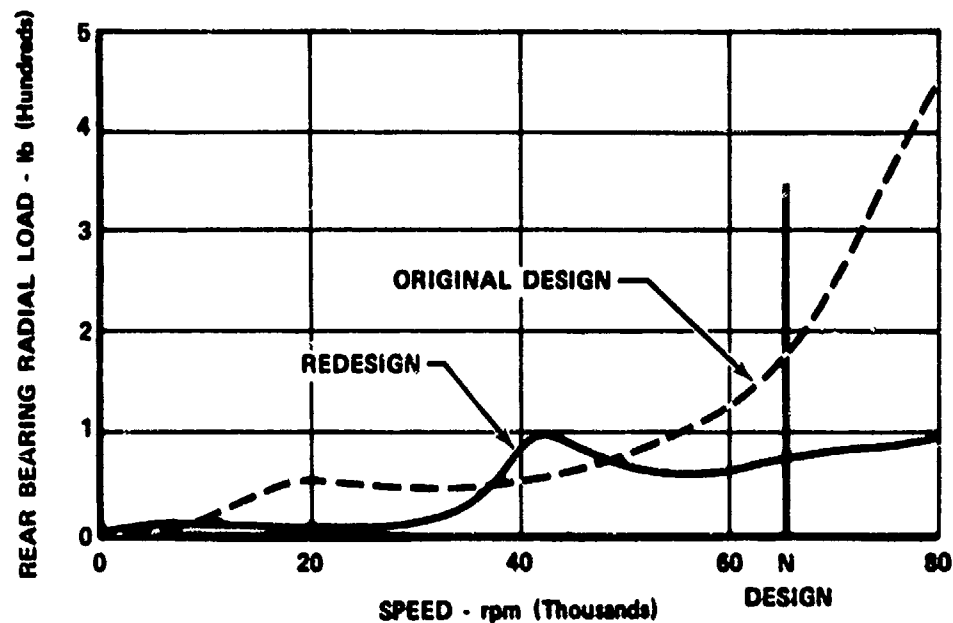


Figure 18. Redesigned Rotor Assembly Predicted Rear Bearing Load vs Speed.

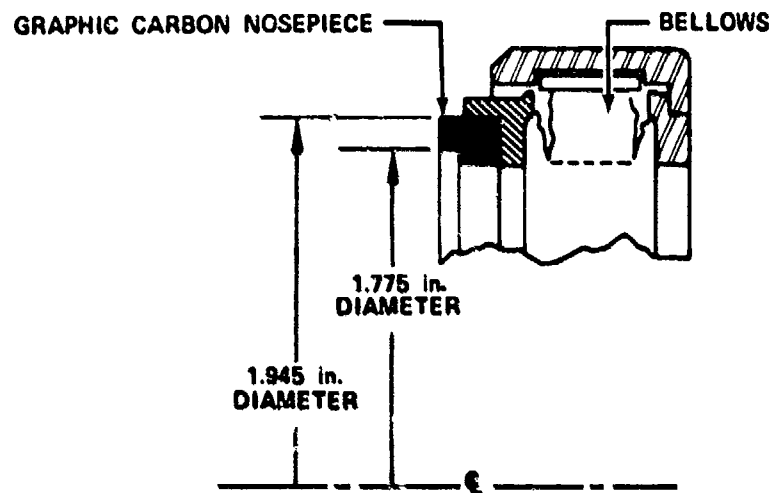


Figure 19. Front Bearing Compartment Carbon Face Seal.

Although the seal rubbing speeds (520 to 530 ft/sec) were higher than current engine experience, seal requirements in terms of differential pressure (less than 10 psi) and temperature (250°F) were relatively modest. A seal pressure balance was selected to reduce the contribution of pressure-area forces on the seal face to minimize the wear rate.

The dual ball and roller bearing arrangement and the carbon face seal performed satisfactorily in subsequent tests in the compressor rig, and provided new experience with high-speed bearing and seal designs of this type.

## TEST EQUIPMENT

### COMPRESSOR TEST RIG

The major nonrotating components of the compressor test rig are shown in Figure 20. They consist of the bellmouth inlet, inlet case, inlet guide vanes, inducer shroud, impeller shroud, diffuser, and diffuser collector. Prior to assembling the impeller in the cases, it was first spin tested with the tooling shown in Figure 21 to 73,000 rpm (112% of design speed) to verify its mechanical integrity.

Installation of the impeller into the diffuser in its original spline-drive configuration is shown in Figure 22. When the impeller attachment geometry was changed from the original spline-drive configuration to a CURVIC coupling, the impeller and drive turbine became an integral rotor assembly. The components used to build up the redesigned rotor assembly are shown in Figure 23. The inducer, impeller, spacer, and turbine were held together with a tiebolt. A "Z" brace was used in the assembly to support the middle of the tiebolt and increase its critical speed to well beyond the design operating range.

During the assembly of the compressor rig, particular attention was given to balancing operations. Rotor components such as the inducer, impeller, and turbine were individually balanced by material removal. Then the rotor was assembled out of the cases, concentricities were checked for less than 0.001-in. runout, and the assembly was balanced to less than 0.0003-oz-in. unbalance, again by material removal from the impeller and turbine. This method put an unbalance in the impeller and turbine as components; however, the correction plane was near the true plane of unbalance, since these two components were the heaviest in the rotor assembly. Final balance of the rotor assembly in the compressor and turbine cases was accomplished within 0.0012 oz-in. unbalance with rivets and pins on each end of the rotor assembly.

The assembled and fully instrumented compressor rig and drive turbine are shown in Figure 24. The compressor rig and drive turbine were installed in a combination shipping and mount stand for ease of installation in the test stand.

### TEST FACILITIES

A schematic of the B-2 test stand high-speed compressor test facility is shown in Figure 25. The drive turbine was powered by compressor bleed air from a P&WA™ J-75 slave engine. Drive turbine supply air was controlled by two pneumatic valves, one of which was used as vernier control. Since the drive turbine was a radial inflow-type and particles in the supply air tend to erode the blade tips, a particle separator was installed downstream of the drive turbine control valves. The design of the particle separator (Figure 26) was a derivative of the semi-reverse flow separator, designed and tested under Army Contract DAAJ02-70-C-0003. The separator center body was free to move and act as an emergency shutdown valve. Safety systems built into the test facilities included a rapid shutdown and an abort system. These systems operated automatically when preset conditions were encountered. Table III summarizes the initiating actions required to activate the safety controls and the actions taken.

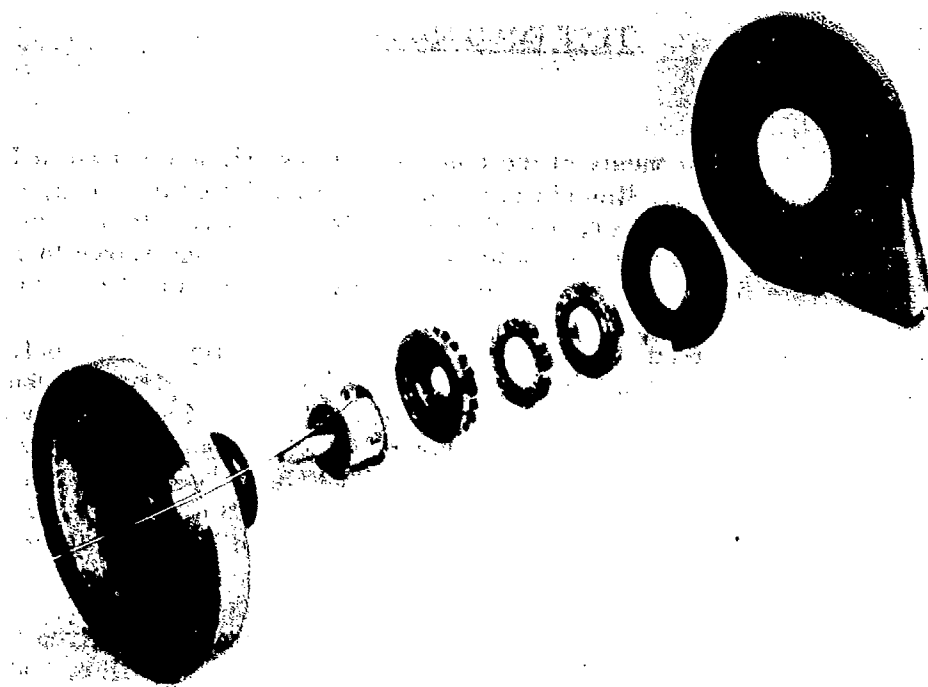


Figure 20. Compressor Test Rig Nonrotating Components.

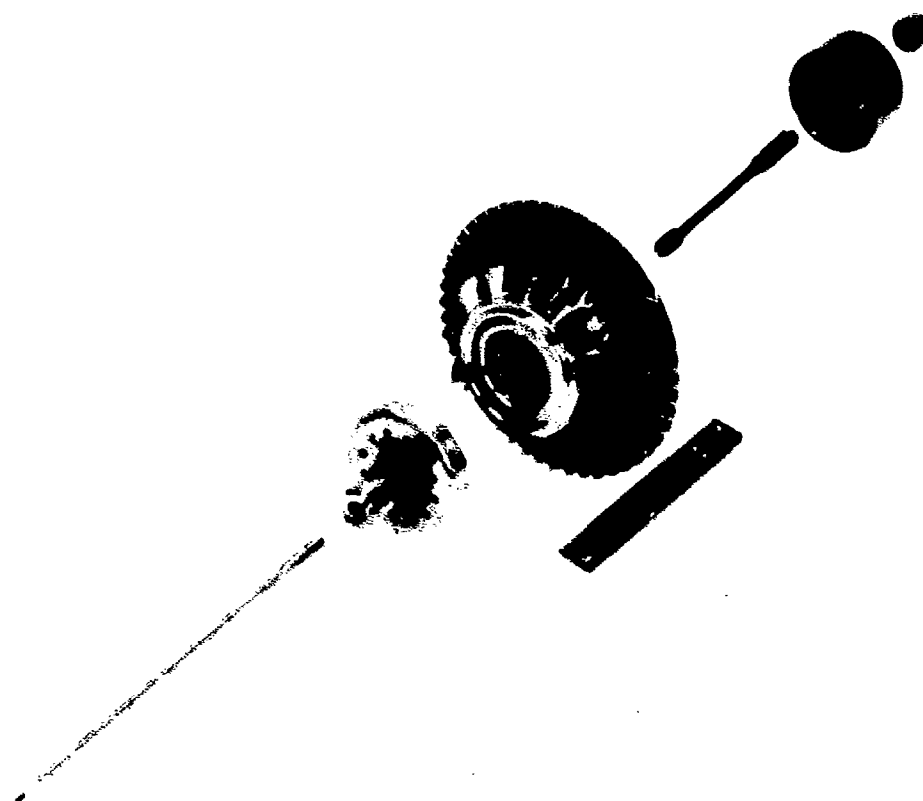


Figure 21. Impeller Spin Tooling.



Figure 22. Impeller Installation in Diffuser Case.

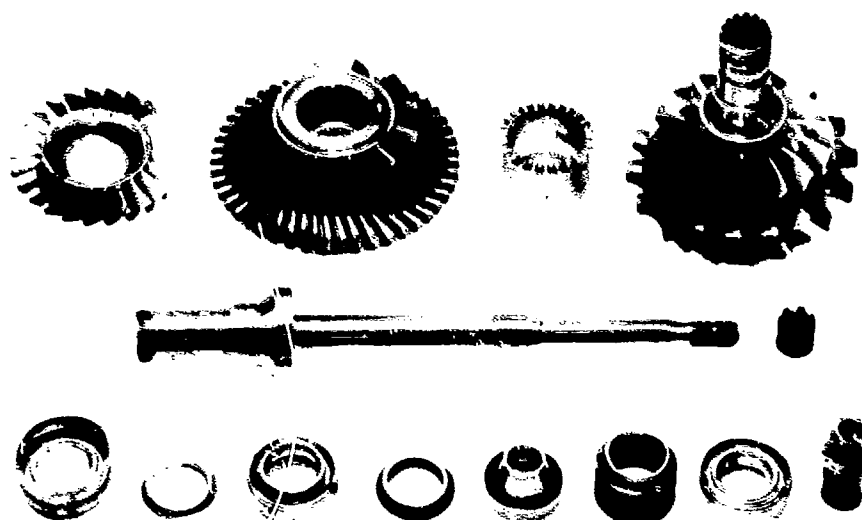


Figure 23. Redesigned Rotor Assembly Components.



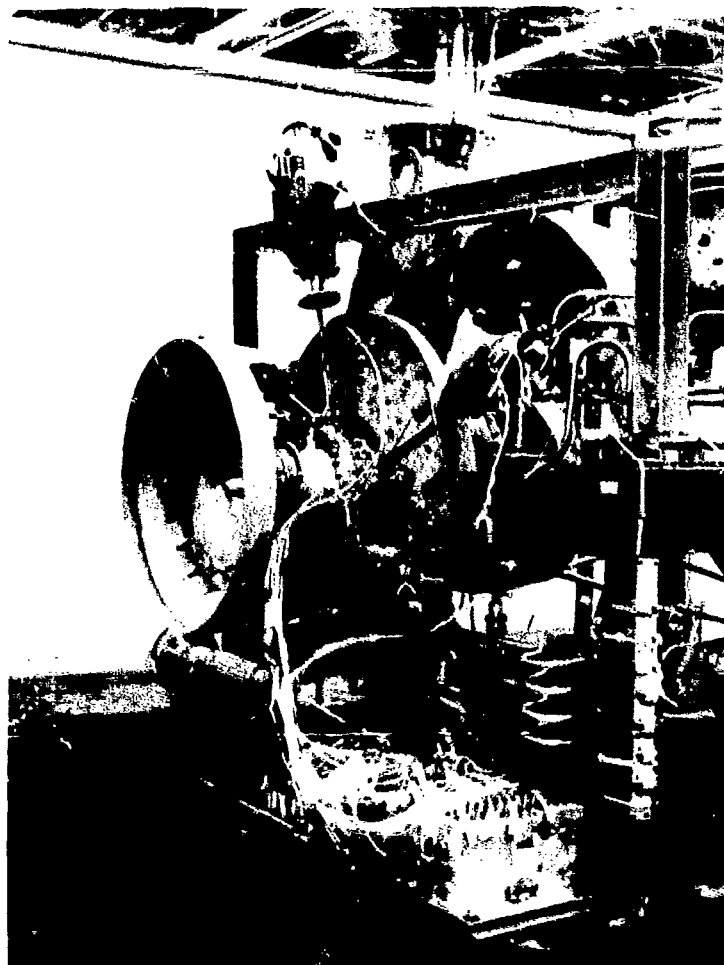


Figure 24. Assembled and Fully Instrumented Compressor Rig.

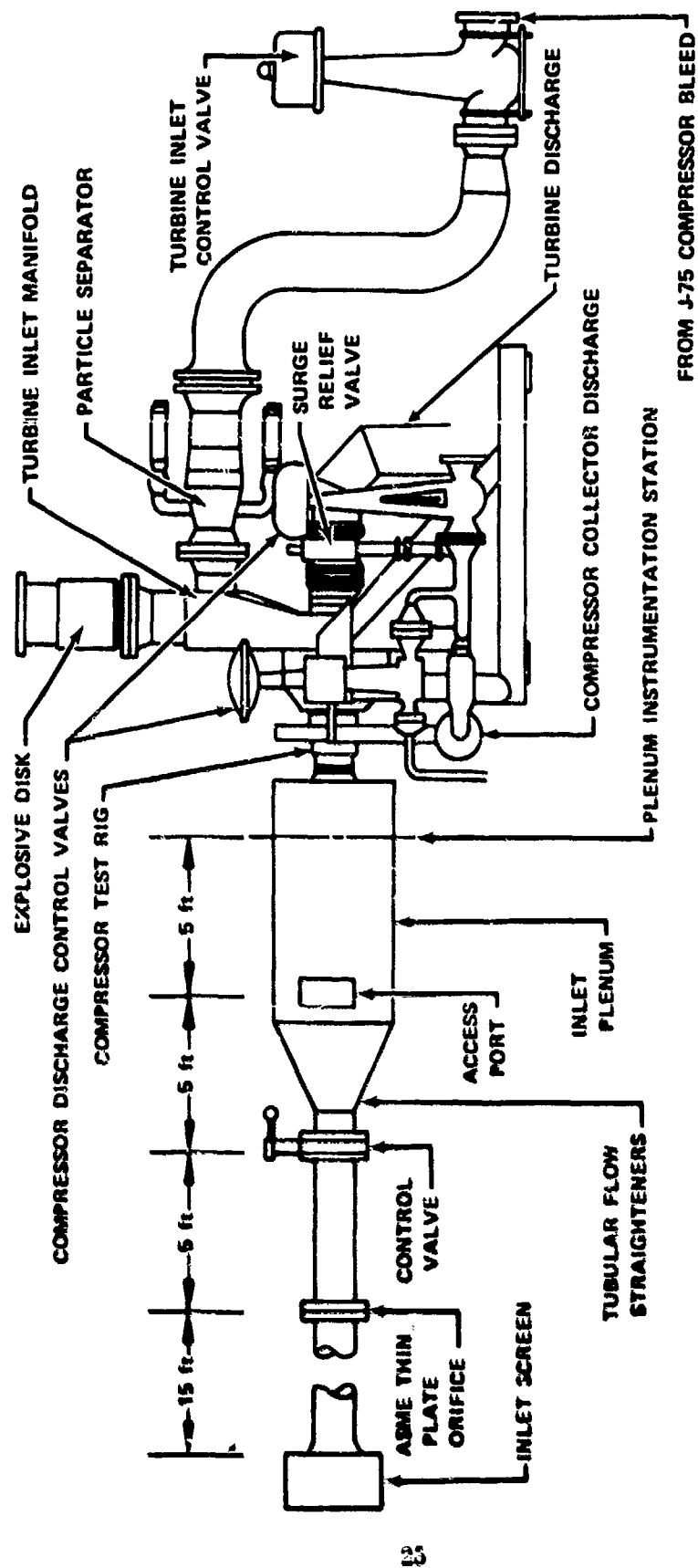


Figure 25. P&WA™ FRDC High-Speed Compressor Test Stand.

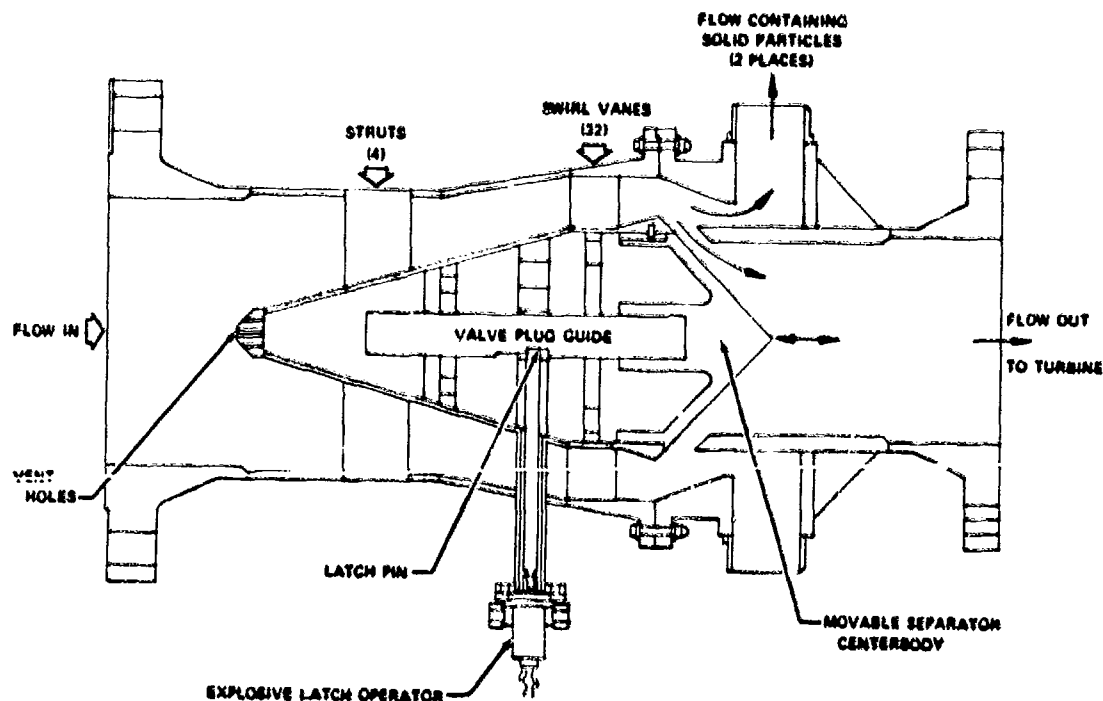


Figure 26. Particle Separator With Integral Fast-Acting Shutoff Valve.

TABLE III. TEST FACILITY SAFETY SYSTEMS	
<b>Rapid Shutdown System</b>	
Initiating Action	<ol style="list-style-type: none"> <li>1. Low thrust balance pressure</li> <li>2. Loss of control room A/C power</li> </ol>
Results	<ol style="list-style-type: none"> <li>1. Turbine inlet control valves closed</li> <li>2. Compressor discharge valve opened</li> <li>3. Slave engine throttled to idle</li> </ol>
<b>Rig Abort System</b>	
Initiating Action	<ol style="list-style-type: none"> <li>1. Low lubricating oil supply pressure</li> <li>2. Rotor overspeed</li> <li>3. Manual abort by test engineer</li> </ol>
Results	<ol style="list-style-type: none"> <li>1. Explosive-actuated turbine inlet valve closed</li> <li>2. If manual abort, turbine inlet manifold vented to ambient</li> <li>3. Turbine inlet control valves closed</li> <li>4. Compressor discharge valve opened</li> <li>5. Slave engine throttled to idle</li> </ol>

The installation of the compressor rig in the test facility is shown in Figure 27. The compressor inlet duct contains a sharp-edged flow measuring orifice, control valve, flow straightening tubes, and a plenum chamber. An inflatable rubber seal sealed the plenum to the compressor bellmouth. The control valve in the compressor inlet duct remained in a full-open position during all testing.

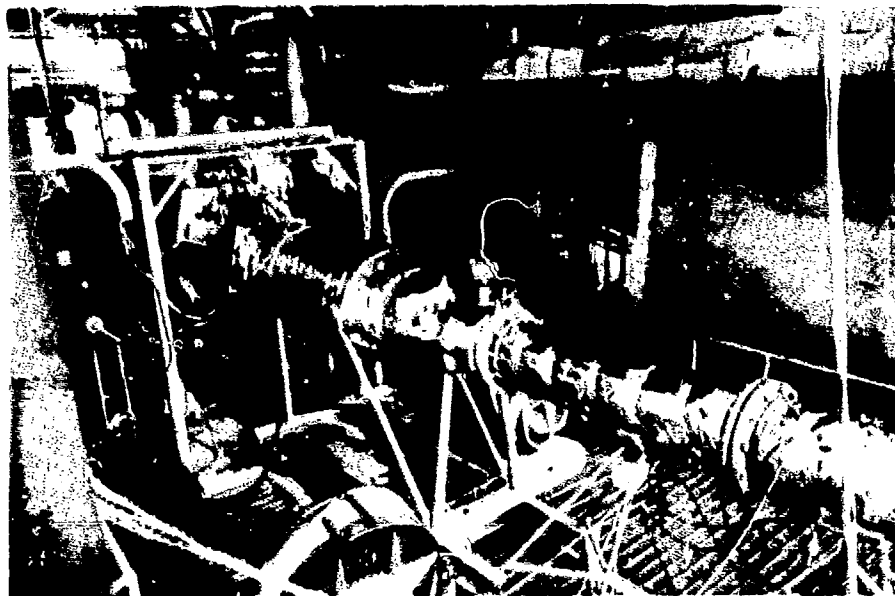


Figure 27. Compressor Rig Installed in B-2 Test Facility.

The compressor exhausted to atmosphere from the diffuser collector through two back-pressure control valves, one of which also acted as a burner control. By controlling the compressor discharge back pressure, it was possible to operate the compressor along a speedline with transients into and out of stall. A surge relief system was designed and used to detect the onset of surge. The system used a high-frequency response pressure sensing transducer in the diffuser collector. A control module allowed the selection of a rate of change of pressure that would actuate the system. If a higher rate of change of pressure was sensed, a fast-operating valve in the compressor discharge duct was opened. This reduced the compressor back pressure, thereby automatically allowing the compressor to move away from a surge condition.

A differential pressure control system was used between the impeller hub side backface and a buffer seal dam compartment (Figure 13). All performance data were taken with this delta pressure equal to zero to prevent flow out of or into the flow path at the impeller exit-diffuser entrance. This pressure differential could, however, be adjusted to either side of the zero delta pressure point, if desired.

The required thrust load on the ball bearing was maintained by supplying gaseous nitrogen to the impeller thrust balance cavity (Figure 13) through an automatic control valve. This valve was adjustable to any set point and was changed while the rig was in operation.

## INSTRUMENTATION

Instrumentation was provided to establish stage overall performance, stage component performance, and monitor rig operation. The instrumentation used to take these data and the instrumentation locations are described in this section. Major instrumentation stations for the test compressor are defined in Table IV, and the axial and radial locations of these stations are shown in Figure 28.

**TABLE IV. COMPRESSOR INSTRUMENTATION STATIONS**

00	-	Compressor Inlet-Plenum
0	-	Compressor Inlet-Bellmouth Throat
1.0	-	Inlet Guide Vane Exit
1.5	-	Inducer Exit
2.0	-	Impeller Exit
3.0	-	Diffuser Exit
3.5	-	Compressor Discharge Collector Manifold

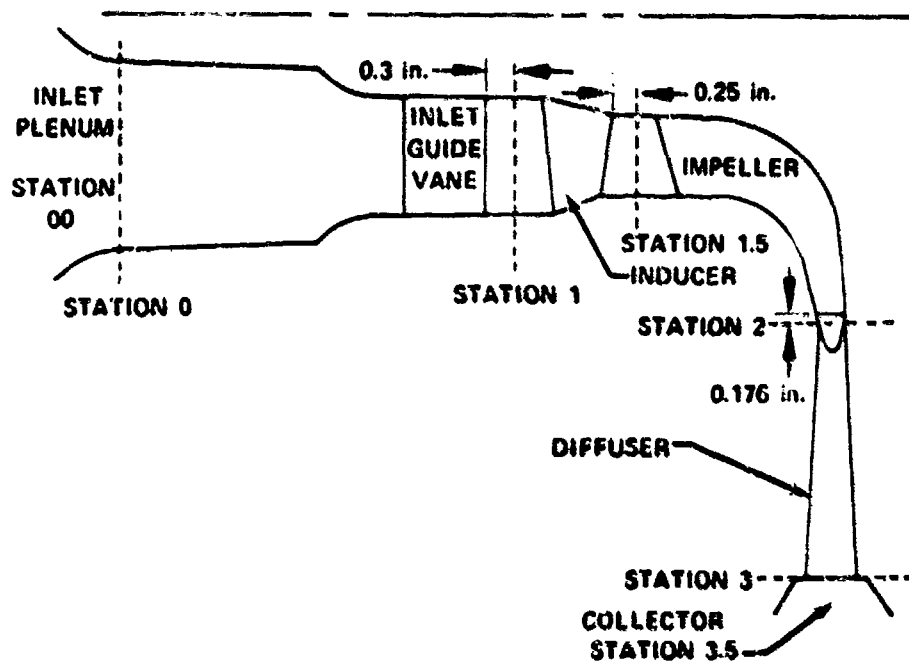


Figure 28. Compressor Instrumentation Station Locations.

### Overall Performance Instrumentation

Instrumentation was provided to obtain inlet flow rate, impeller speed, compressor inlet conditions (Station 00), and compressor discharge conditions (Stations 3.0 and 3.5). These data were combined to define overall performance in terms of total-pressure-to-total-pressure conditions (Stations 00 to 3.0) and total-pressure-to-static-pressure conditions (Stations 00 to 3.5).

Compressor inlet flow rate was calculated from data obtained from a 5.270-in.-diameter thin plate orifice installed upstream of the inlet plenum in a 12.5-in.-diameter inlet duct, as shown in Figure 29. The orifice was installed in accordance with ASME standards. Orifice upstream static pressure was measured by means of three static pressure taps, each sensed by a 0- to 15-psia transducer. Three orifice differential static pressures were each sensed by a 5-psid transducer. The temperature of the orifice flow was measured in the inlet plenum.

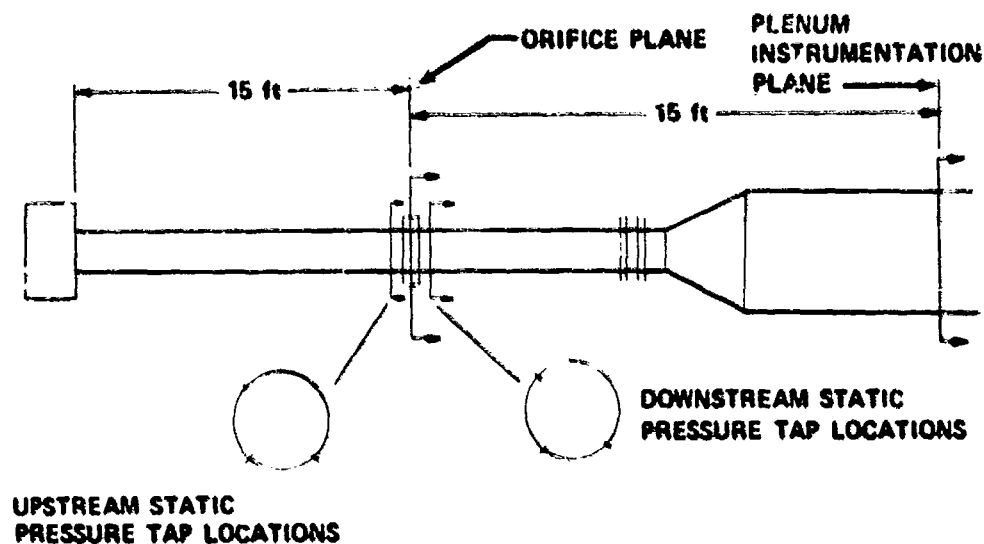
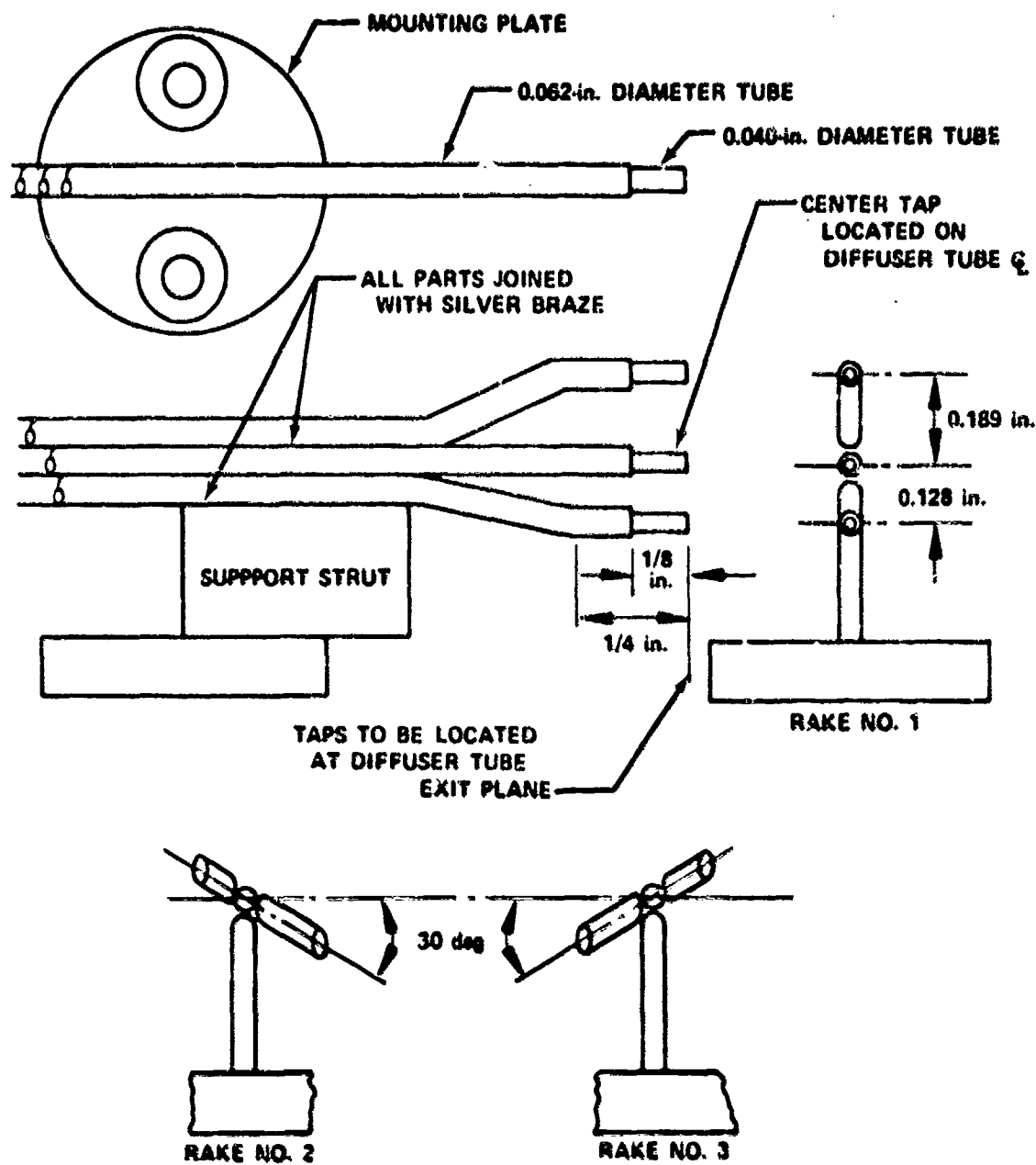


Figure 29. Inlet Orifice Installation.

Compressor inlet total pressure was measured with three Kiel-type total pressure probes, located in the inlet plenum. The probes were each sensed with a 0- to 15-psia transducer. Compressor inlet total temperature was measured with a Rosemount resistance thermometer in the inlet plenum. Redundant inlet temperature measurements were obtained with three half-shielded copper-constantan (C/C) thermocouples, also located in the inlet plenum. Beginning with Build No. 5 of the compressor, the C/C thermocouples were deleted and four additional Rosemount resistance thermometers were installed at various radial positions in the inlet plenum to accurately measure any radial variation in temperature.

Diffuser exit total pressure was measured by means of three total pressure rakes, each consisting of three elements, as shown in Figure 30. Each element was sensed by a pressure-scanning system using a 0- to 150-psia transducer. The rakes were installed at the exit of the diffuser tubes, shown in Figure 31. The locations of the nine total pressure probes superimposed onto one diffuser tube are shown in Figure 32. It was noted that the center probe of each rake was in the same relative position in each tube to provide redundant measurements at this point. Also shown in Figure 32 are the seven equal areas that were assigned to the total pressures measured by the rakes for mass-averaging purposes.



RAKES NO. 1, 2, AND 3 ARE THE SAME, EXCEPT FOR ANGLES SHOWN

Figure 30. Diffuser Exit Total Pressure Rakes.

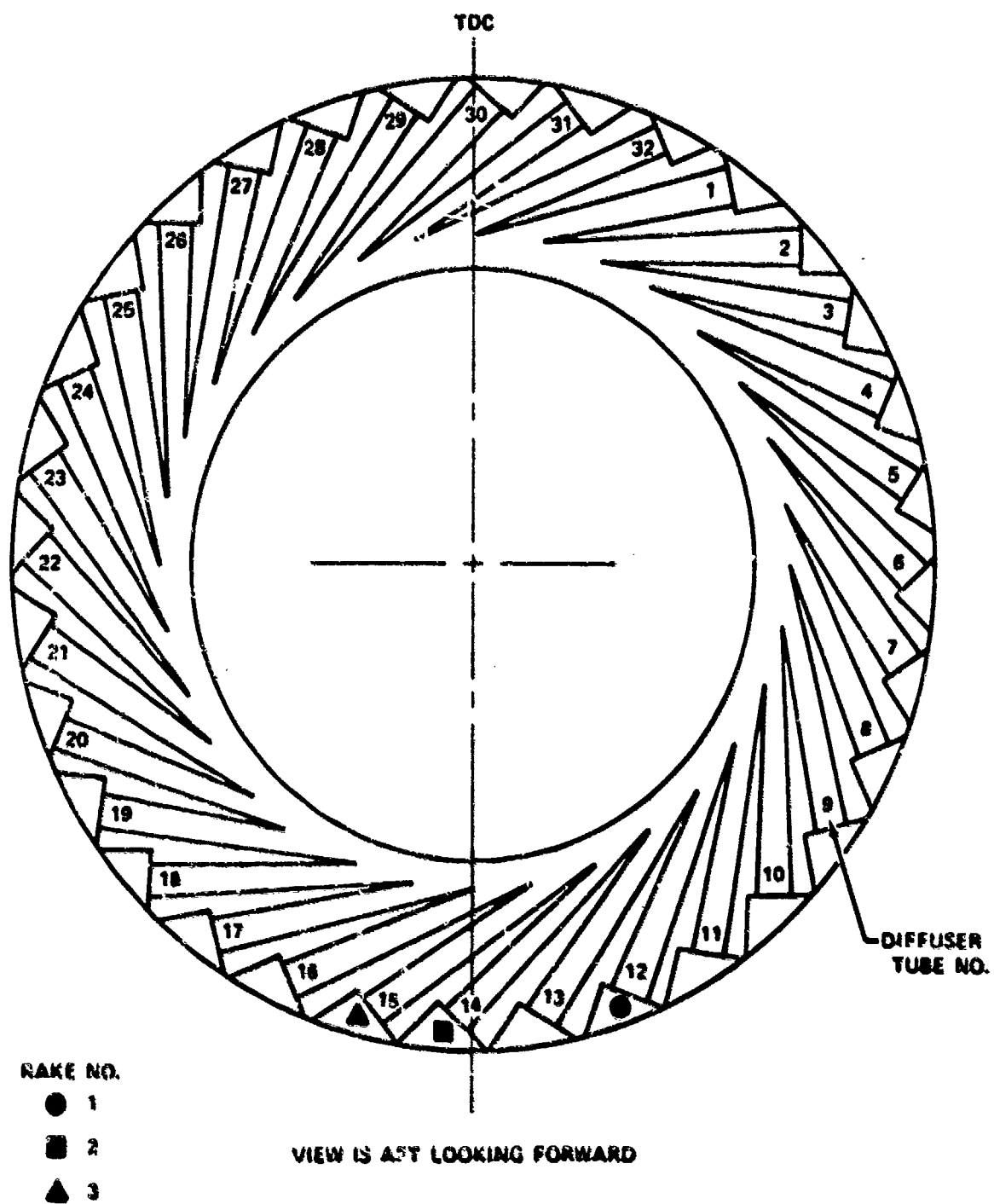


Figure 31. Location of Diffuser Exit Total Pressure Rakes.



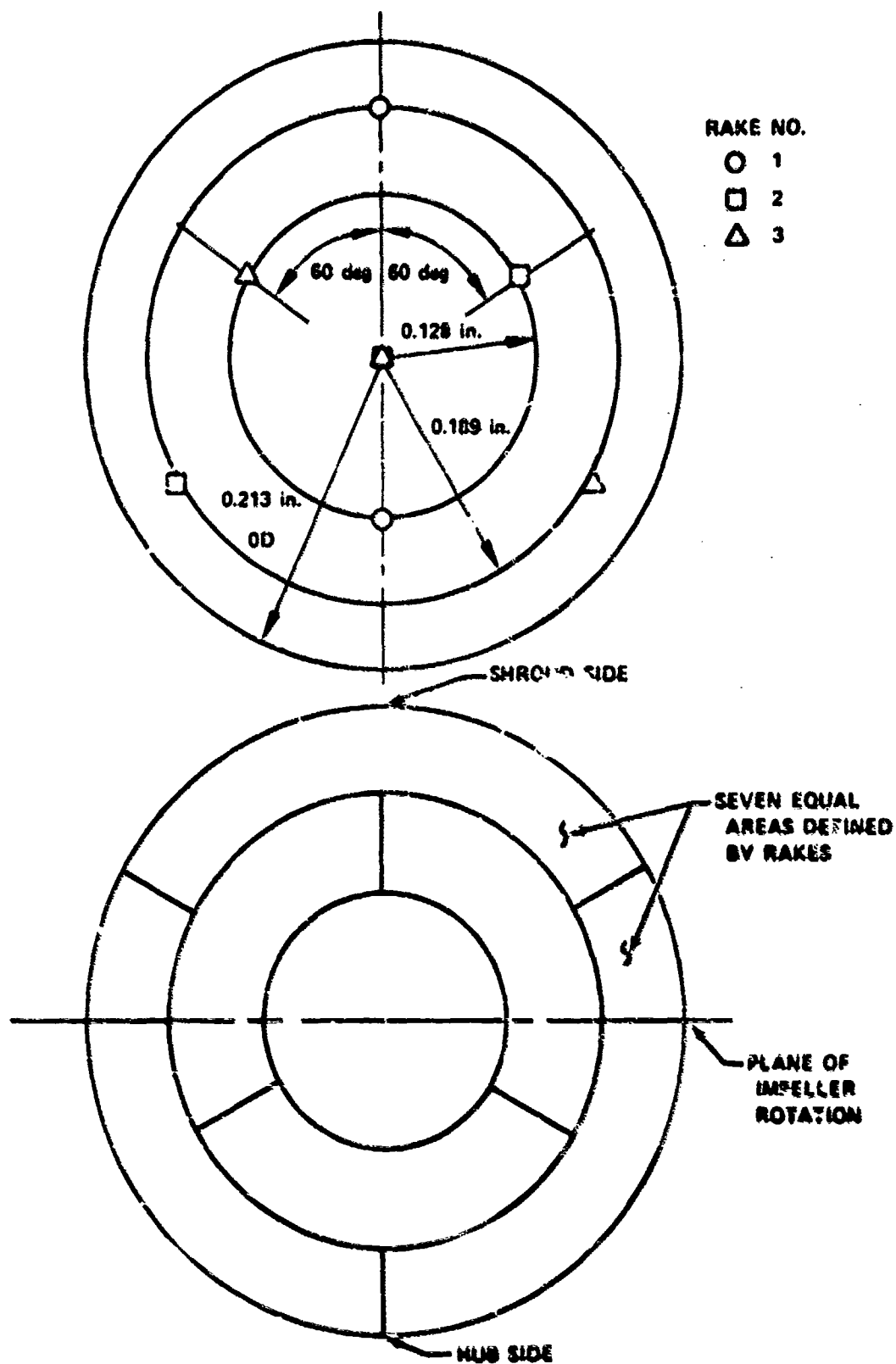


Figure 32. Placement of Total Pressure Probes in Diffuser Exit Plane Station.

Compressor exit static pressure was measured by means of eight static pressure taps in the collector, each connected to a pressure-scanning system using a 0- to 150-psia transducer. The taps were located on the shroud-side wall so that neither diffuser discharge velocity nor the collector struts interfered with the measurements. The design and location of these taps are shown in Figure 33. Compressor exit total temperature was measured with four chromel-alumel (C/A) shielded thermocouples in the exhaust collector. The thermocouple probes were axially located midway between the collector manifold walls and circumferentially located as shown in Figure 33. To increase the accuracy of the temperature measurement, the thermocouples were constructed from a single batch of calibrated special-limits-of-error wire. This wire was continuous from the thermocouple junction to the reference junction to eliminate errors caused by connectors and by the lower quality wire normally used between the connector and the reference junction. A thermocouple was attached to the shroud-side wall of the collector manifold to aid in estimation of potential radiation errors on the collector thermocouple measurements.

#### Component Performance Instrumentation

Instrumentation was provided to evaluate the component performance; namely, the inlet guide vane, inducer, impeller, and diffuser. The component performance instrumentation is described below and is also summarized in Table V.

Instrumentation was provided downstream of the inlet guide vane to measure wall static pressures and radial distributions of total pressure and air angle (and in Build No. 6, total temperature). Similar instrumentation downstream of the inducer was used to describe its performance, with the exception that total temperature was also measured at the exit of the inducer. The axial and circumferential locations of the inlet guide vane and inducer instrumentation are shown in Figure 34.

Static pressure at the leading and trailing edges of the inlet guide vanes was measured by one shroud wall static pressure tap at the leading-edge and single hub and shroud wall static taps at the trailing-edge plane to define the static pressure along the flow path. All three static pressure taps had to be deleted in the revised inlet case, Builds No. 4 through No. 6. Inlet guide vane exit (Station 1.0) wall static pressure data were obtained by four wall taps equally spaced about the circumference on both the hub and shroud walls. Builds No. 4 through No. 6 did not contain the hub wall taps as the revised inlet case prevented their installation. The hub wall taps were located approximately on design midchannel streamlines. It should be noted that the shroud wall taps were located on a circumferential traverse ring.

Static pressure at the leading and trailing-edge planes of the inducer was obtained by single hub and shroud wall taps at the leading-edge plane and a shroud wall tap at the trailing-edge plane. Additionally, four static pressure taps equally spaced about the circumference on the shroud wall were installed at the inducer exit traverse station (Station 1.5).

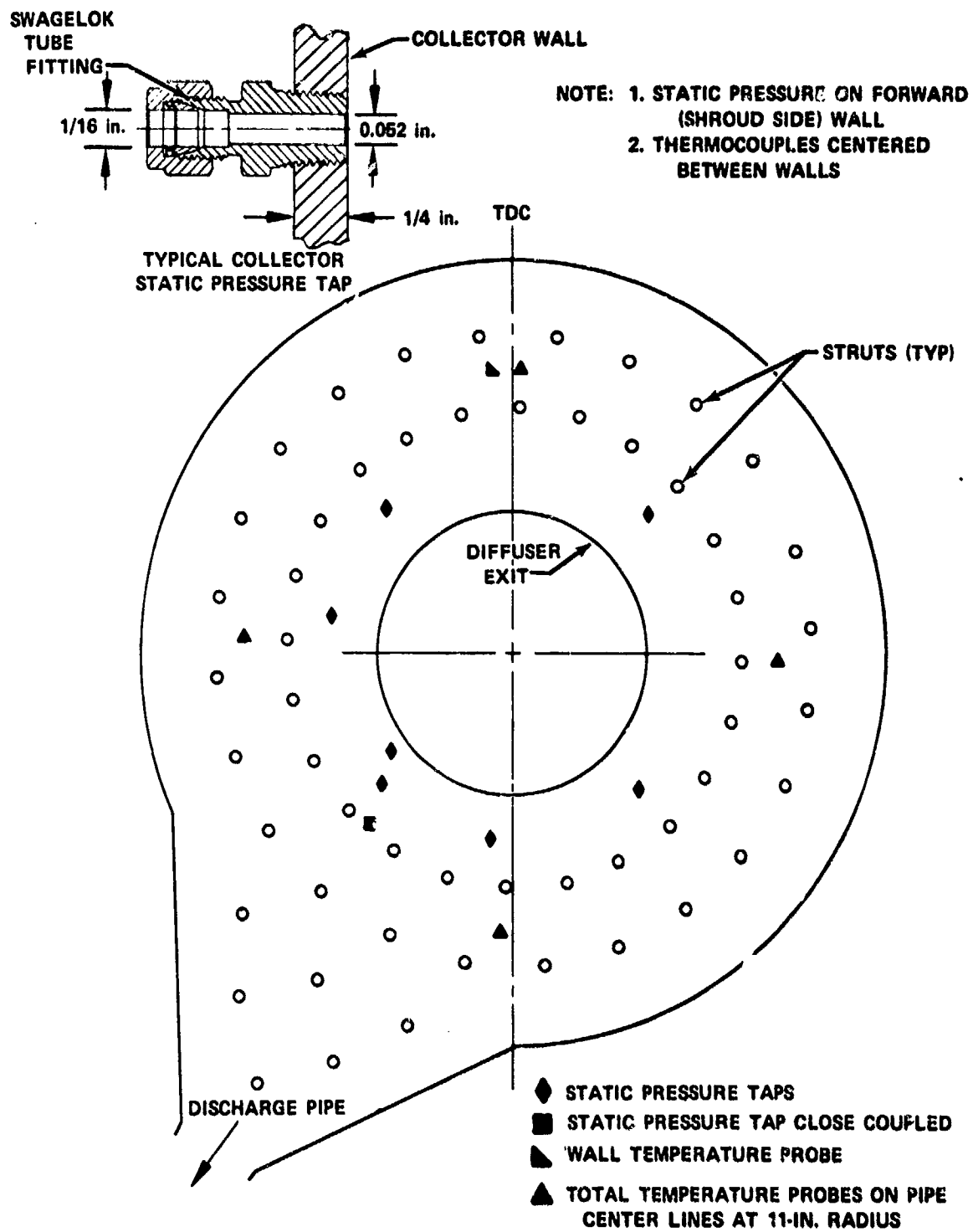


Figure 33. Collector Instrumentation Locations.

**TABLE V. COMPRESSOR COMPONENT PERFORMANCE  
INSTRUMENTATION SUMMARY**

Location	Flow Variable	Instrument Type	Quantity
Station 0	P	Wall Tap	4
Inlet Guide Vane	P	Shroud Wall Tap	2(1)
	P	Hub Wall Tap	1(1)
		Chord Angle Indicator	1
Station 1	P	Shroud Wall Tap	4
	P	Hub Wall Tap	4(1)
	P <sub>t</sub> , T	Circumferential and Radial Traversing Cobra Probe	1(2)
Inducer	P	Hub Wall Tap	1(1)
	P	Shroud Wall Tap	2
Station 1.5	P	Shroud Wall Tap	4
	P <sub>t</sub> , T	Radial Traversing Cobra Probe with Thermocouple	1
Impeller Shroud	P	Wall Tap	14
Impeller Tip Shroud Side	P	Communicating Groove	4
Impeller Tip Backface	P	Tube	2
Station 2	P	Shroud Wall Tap	4
	P	Hub Wall Tap	4
	P <sub>t</sub>	Axial Traversing Cobra Probe	1
	T	Axial Traversing Thermocouple	1
Diffuser	P	Shroud Wall Tap	32
	P	Hub Wall Tap	8

(1) Deleted from Build No. 6 due to relocation of front bearing compartment.

(2) No T<sub>t</sub> for Build No. 3.

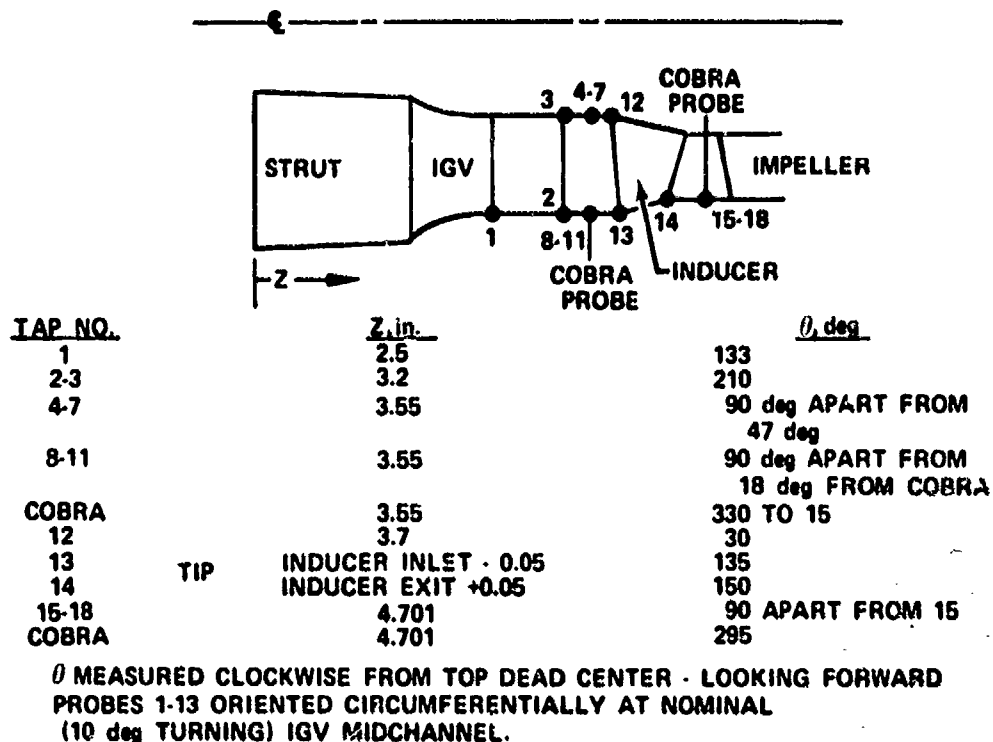


Figure 34. Axial Locations of Inlet and Inducer Instrumentation.

Radial distributions of total pressure and air angle (and total temperature in Build No. 6) at Station 1.0 were measured by means of a cobra probe that was traversed in both the radial and circumferential directions. The cobra probe was traversed circumferentially at five radial locations corresponding to 10, 30, 50, 70, and 90% spans. At each spanwise location, the probe was traversed through a 45-deg arc, which permitted measurement of total pressure and air angle data behind two inlet guide vanes and one inlet strut in the Build No. 1 through No. 3 configuration. In the redesigned inlet configuration, the probe was rotated through an arc of 52 deg. The cobra probe used was constructed of 0.020-in.-OD tubing and is shown in Figure 35. The Build No. 3, Station 1.0 cobra probe was not constructed with a thermocouple. Radial distributions of total pressure, total temperature, and air angle at the inducer exit (Station 1.5) were obtained by means of a radially traversing cobra probe.

Impeller instrumentation was provided to measure wall static pressures along the impeller shroud, impeller tip static pressure on both the shroud side and the hub side, total pressure and air angle distributions across the flow path at the impeller exit, and total temperature distribution across the flow path at the impeller exit. The locations of the 0.040-in.-diameter wall static pressure taps along the impeller shroud are shown in Figure 36. The positions of these taps were selected so that the data obtained from them would define the static pressure distribution at the impeller entrance, the splitter regions, areas of possible flow separation, and areas of possible flow distortion due to influence of the diffuser passages. The circumferential relationship of taps were superimposed onto one diffuser tube inlet.

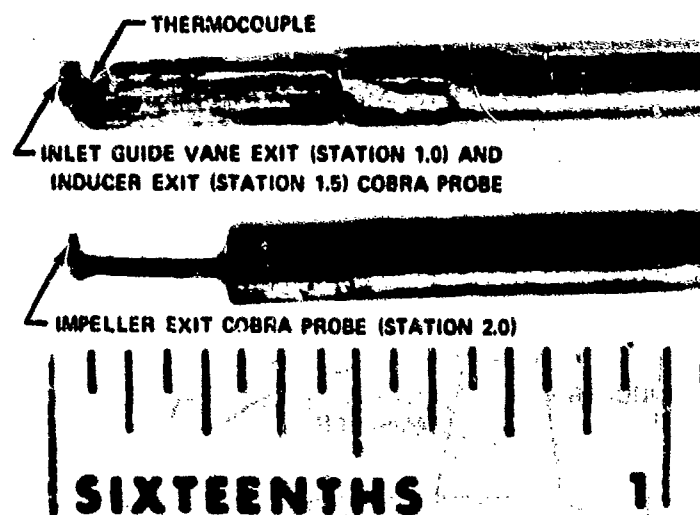


Figure 35. Construction of Traverse Cobra Probes.

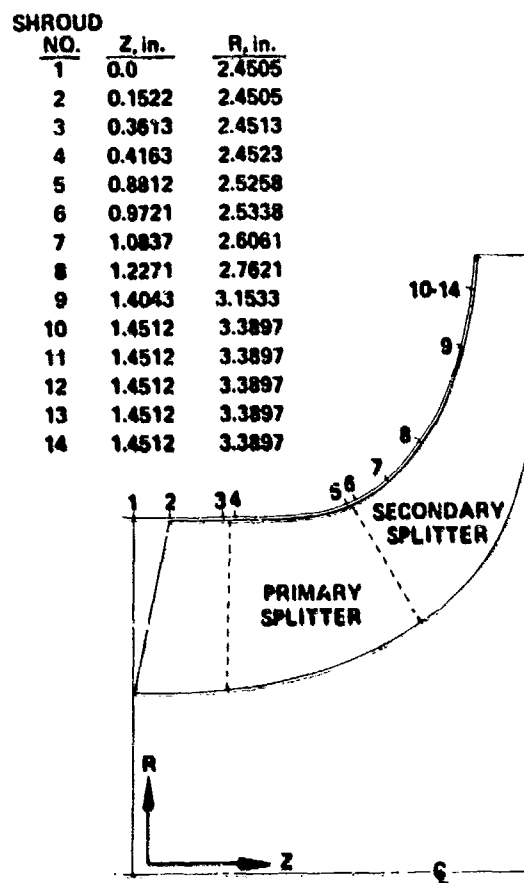


Figure 36. Location of Impeller Shroud Static Pressure Taps.

Impeller tip static pressure on the shroud side was obtained from measurements of the pressure in a circumferential passage that is connected with the flow path by a 0.015-in.-wide circumferential groove between the impeller shroud and the diffuser. Pressure was measured through four ports that were equally spaced around the circumference. This circumferential groove scheme is shown in Figure 37. Impeller tip backface pressure was measured by means of two 0.062-in.-diameter tubes installed 180 deg apart in the impeller tip backface cavity. Beginning with Build No. 5, one chromel-alumel thermocouple was located in the backface cavity to measure temperature.

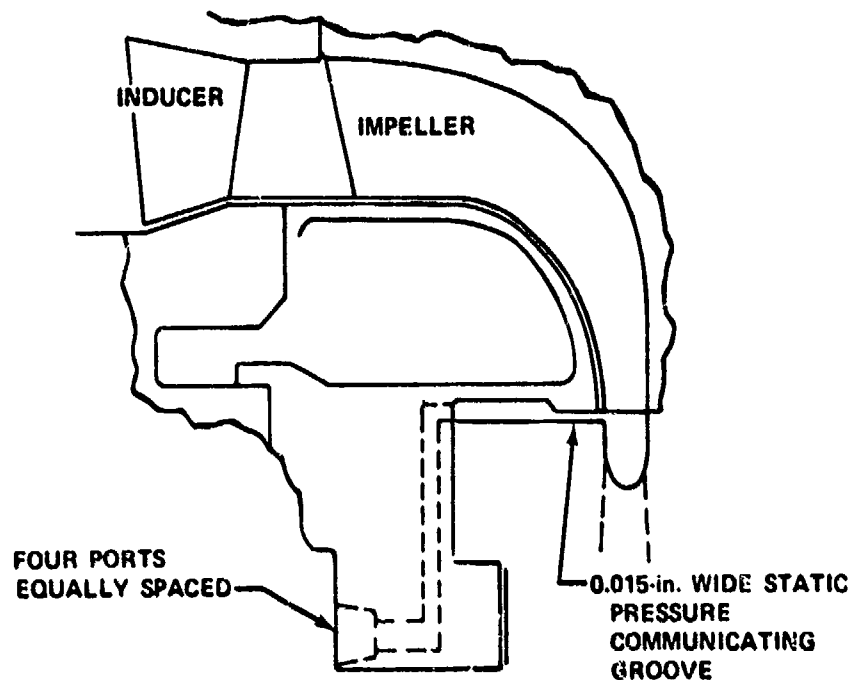


Figure 37. Impeller Tip Static Pressure Passage.

Impeller exit air angle and total pressure were measured at an impeller exit radius ratio of 1.05 by means of a cobra probe that was traversed across the impeller exit flow path in the plane of the rig centerline. The probe was installed as shown in Figure 38; the cobra probe is shown in Figure 35.

Total temperature across the flow path at the impeller exit was measured with the temperature probe shown in Figure 39. This probe was designed with an aspirated head to maximize the temperature recovery, and sheathed wire was used to minimize the conduction error. The temperature probe was installed in the same location as the cobra probe.

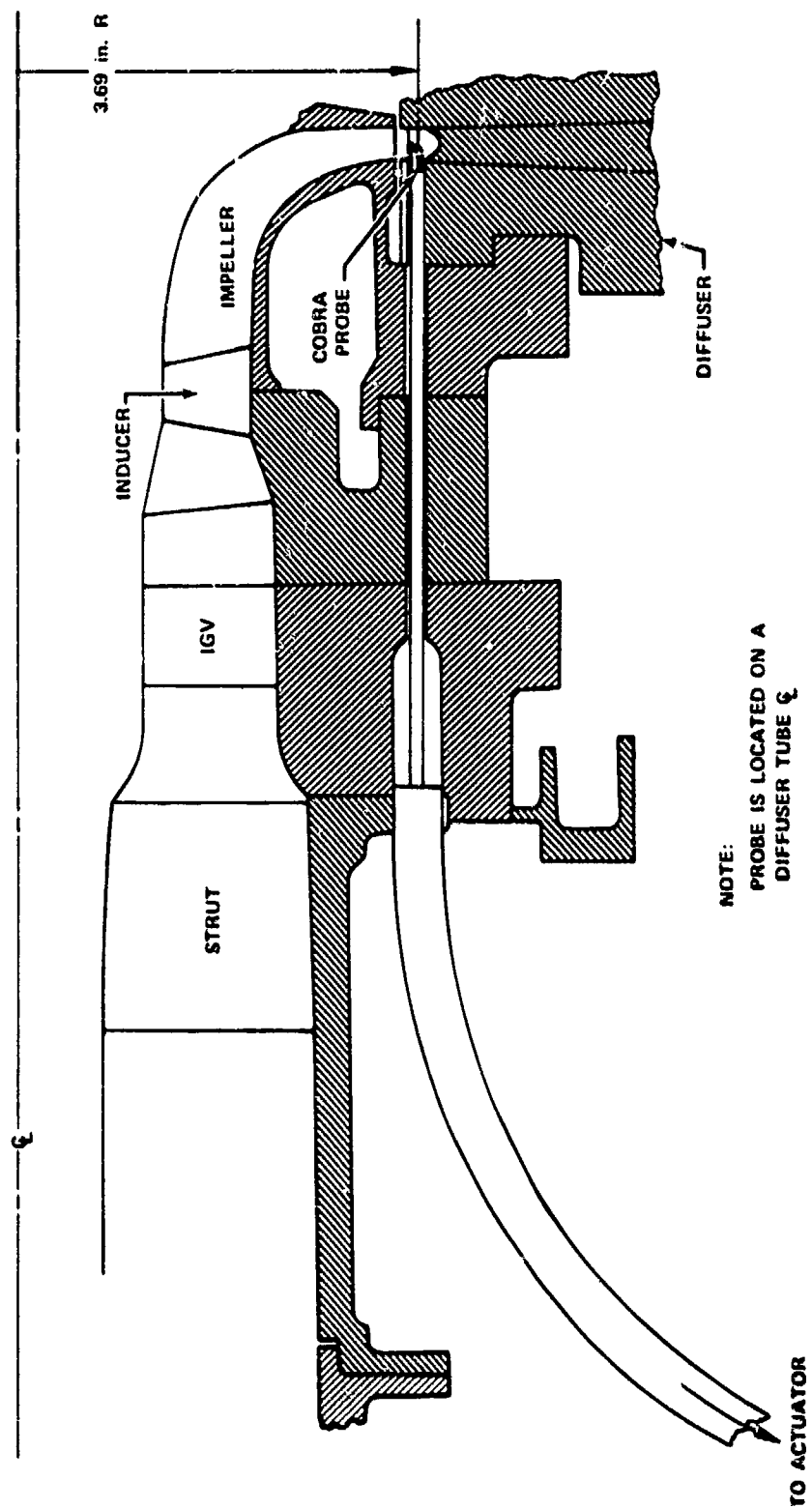
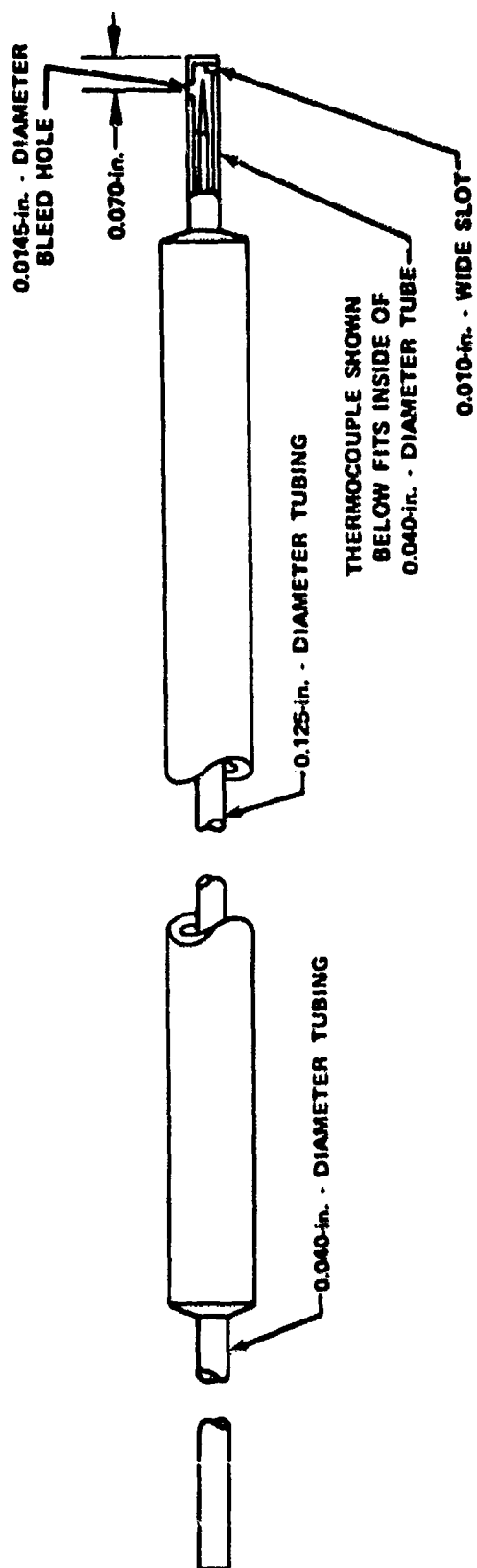
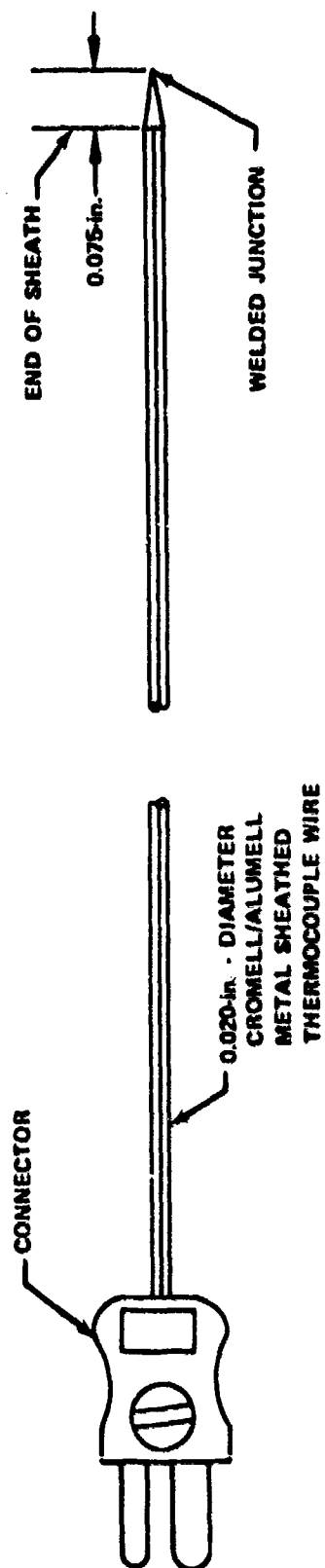


Figure 38. Impeller Exit Cobra Probe Installation.





#### A. THERMOCOUPLE HOUSING



#### B. THERMOCOUPLE

Figure 39. Impeller Exit Total Temperature Probe Construction.

The diffuser instrumentation consisted of 48 wall static pressure taps. The locations of the diffuser wall static pressure taps are shown in Figure 40. This figure also shows the location of the impeller exit cobra probe. Figure 40 shows that composite static pressure data were obtained in the vaneless space, diffuser throat, and along the diffuser length. The construction of the static pressure taps is also shown in this figure; the 0.020-in. -diameter taps were made by the electrical discharge machining process to eliminate drilling burrs and to ensure sharp edges at the intersection of the pressure port and the diffuser passage.

#### Special Instrumentation

Total pressure in the plenum, static pressure in the inlet bellmouth, total pressure in the diffuser exit, and static pressure in the collector manifold were measured with close-coupled transducers to achieve the fast response required to define overall performance during compressor stall. The transducers used had a frequency response of up to 100 Hz, and the data recording system could record each transducer at a maximum of 65 scans/sec. These response characteristics permitted good definition of stall characteristics.

High-frequency instrumentation, capable of response between 200 and 100,000 Hz, was installed in the compressor rig in the following locations:

1. Total pressure probe at Station 2 traversing location
2. Two static pressure probes on the Station 2 shroud walls
3. One static pressure probe at the diffuser exit.

Exact radial and circumferential locations in the diffuser are shown in Table VI.

TABLE VI. HIGH-FREQUENCY RESPONSE PROBE LOCATIONS		
Probe	Circumferential Location (CCW From TDC)	Radial Location, in.
Total Pressure	66 deg 5 min	3.69
Vaneless Space Static	29 deg 30 min	3.69
Vaneless Space Static	315 deg	3.69
Diffuser Exit Static	18 deg	

The total pressure probe that was inserted in the Station 2 traversing mechanism was a flush diaphragm Kulite XCELW-200A; the three static probes were Kulite CEL-125-200A probes. These sensors were mounted in probe housings, as shown in Figure 41. The probes were temperature compensated to 450°F and had a maximum operating temperature of 525°F (which corresponds to an exit temperature reached at less than 80% of design speed).

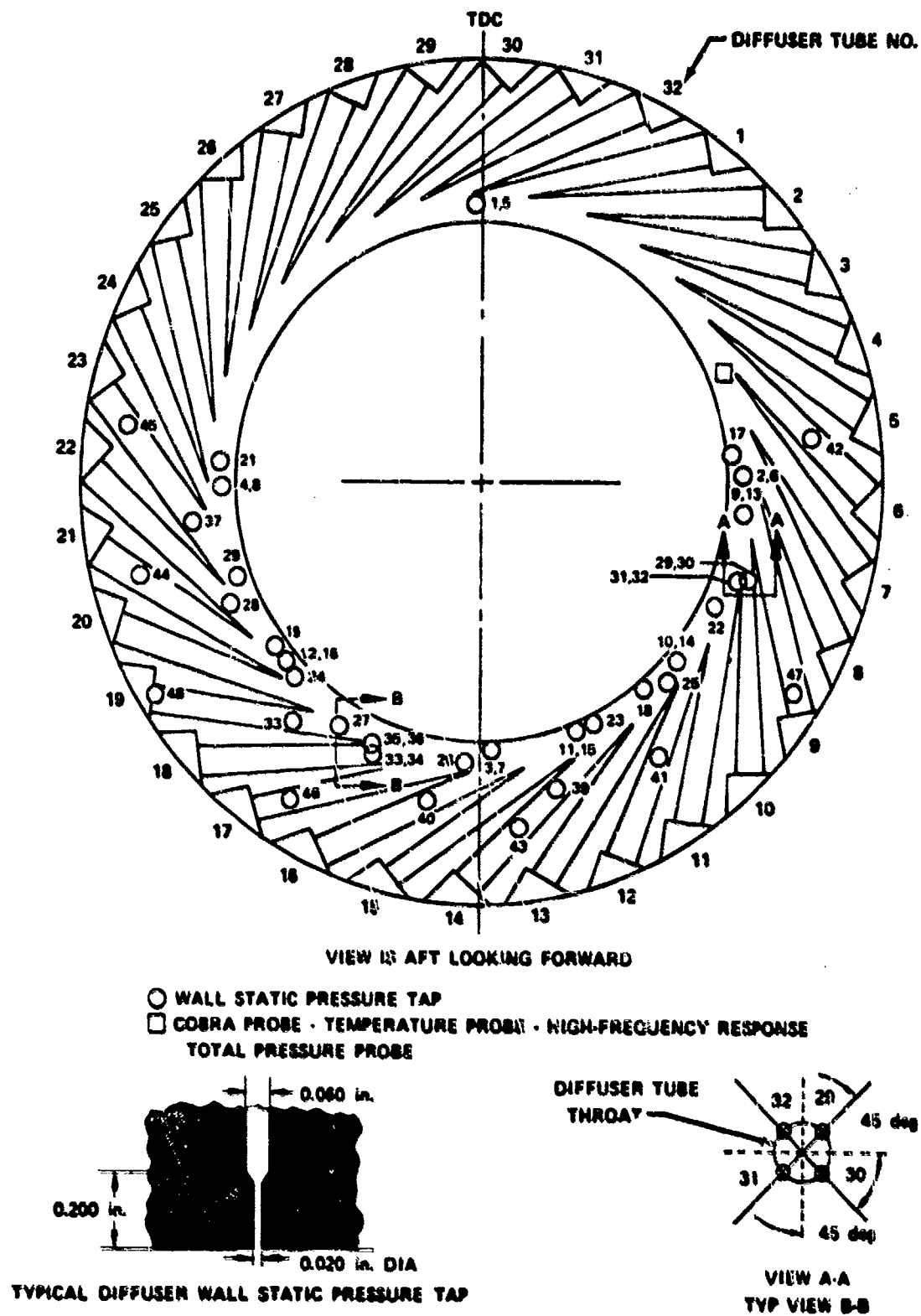


Figure 40. Location of Diffuser Static Pressure Instrumentation.

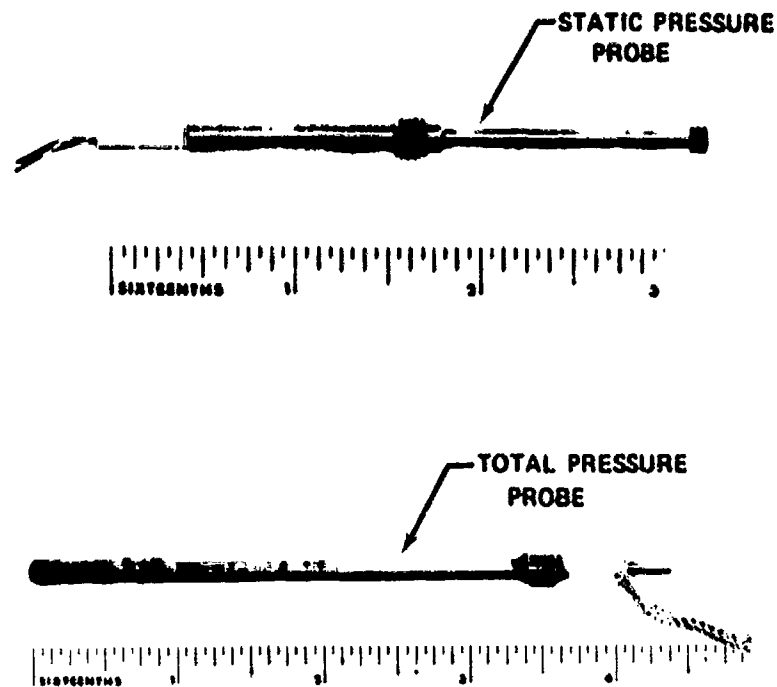


Figure 41. High-Frequency Response Kulites.

#### Data Readout and Recording Systems

The primary data recording system was an automatic digital magnetic tape recorder. This system recorded all compressor rig data except that from the high-frequency response transducers. The high-frequency data were recorded on analog magnetic tape.

Information needed for safe operation of the rig and for setting data points was displayed in the control room. Control room data readouts included rotor speed, rig vibration levels, bearing temperatures, oil pressures, inlet orifice differential pressure, thrust balance pressure, rig inlet pressure, and rig discharge pressure. Impeller rotational speed was obtained from two electromagnetic pickups mounted adjacent to a 6-tooth gear on the rear of the drive turbine rotor shaft.

When cobra probe data were obtained, the total pressure measured by the cobra probe was displayed on X-Y plotters, located adjacent to the traverse actuator controls. This allowed changing the speed, or, if necessary, stopping the cobra probe actuator to allow the probe to respond to changes in the air flow angle.

## PROCEDURES

### TEST PROCEDURES

#### Shakedown Test

Prior to the initiation of any performance testing, each build of the compressor test rig was subjected to a prerun (nonrotating) checkout of all rig systems and then a shakedown test. The objectives of this checkout and shakedown test were to (1) verify the mechanical integrity of the test rig and (2) check the instrumentation and the data acquisition system. Any difficulties encountered during the shakedown test, such as test equipment or instrumentation malfunction, were subsequently corrected prior to the initiation of the performance tests.

During the shakedown test, rig vibrations and bearing temperatures were monitored over the entire range of rig operation. Areas of high vibration and high temperatures were noted, and prolonged running in these areas during the performance tests was then avoided. A maximum allowable limit of 160 g's was set for extended life of the bearings; however, 220 g's were recorded during the Build No. 3 shakedown test. The extensive redesign of the rig bearing system reduced these vibrations to well within the acceptable level. Build No. 6 vibration levels are plotted as a function of speed in Figure 42. Vibration data were recorded continuously during the main portion of the test program on analog magnetic tape, too.

The thrust balance system for the test rig was checked out during each shakedown test, and the thrust load on the bearings was calculated at several speed conditions. Adjustments were made to the automatic surge relief system, as necessary, so that it responded to stall associated pressure fluctuations and not to the gradual pressure changes caused by closing the throttle valves or random pressure fluctuations.

The inducer radial, impeller radial, and impeller axial shroud clearances were measured with mechanical rub probes. These clearance probes were withdrawn and measured after a very low-speed rotation to obtain a cold clearance and then were similarly examined after the impeller rotational speed had reached 70, 85, 95, and 100% of design speed. Figures 43 through 45 show the clearance changes measured during the Builds No. 2, 3, and 6 shakedown tests, respectively.

All instrumentation was checked for continuity from the test rig back to the data recording system. Just prior to the start of each run, all transducer and thermocouple output voltages were calibrated over their operating ranges, and a set of ambient readings was recorded for all the instrumentation for comparison to true ambient conditions. During the shakedown test, overall performance, component performance, and transient data were obtained and processed through the data reduction system to determine if all the instrumentation was recording properly and to check the data acquisition and the data reduction systems.

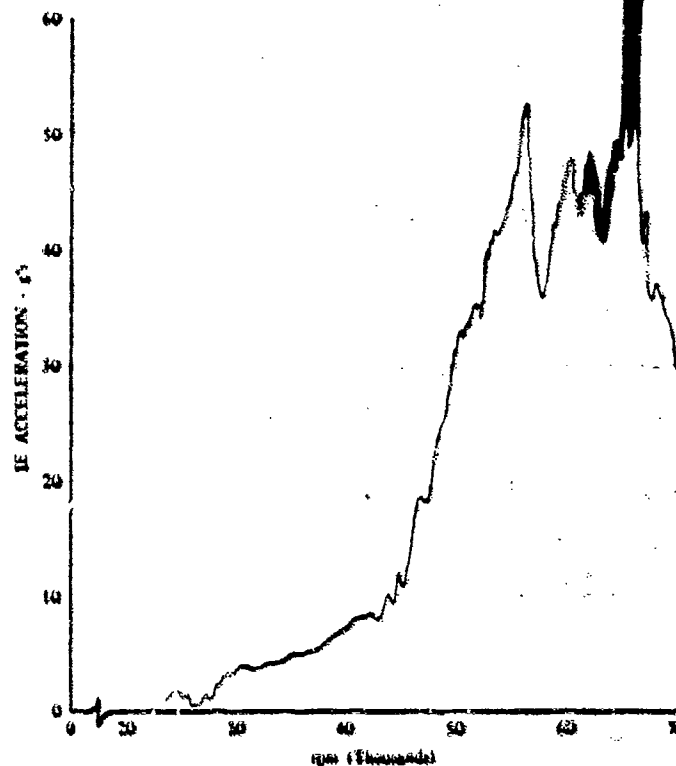


Figure 42. Maximum Front Bearing IE Acceleration, Build No. 6.

#### Overall Performance Data Acquisition

Each speedline was defined by a stall transient and by steady-state points at near-stall, wide-open discharge, and at several intermediate points. Since stall transients were first performed by recording data at a rate of 1 scan/sec, while closing the compressor discharge valve from its wide-open position, thus increasing back pressure, until the rig surged. During the transient, adjustments to the turbine inlet control valves were made to hold the rotor rpm constant. A near-stall point was then set, based on the collector static pressure, and the compressor again operated into stall while recording data at a higher scan rate. This recording rate was 10 scans/sec during Build No. 3 testing, and the maximum recording rate of approximately 65 scans/sec was used during Build No. 6 testing.

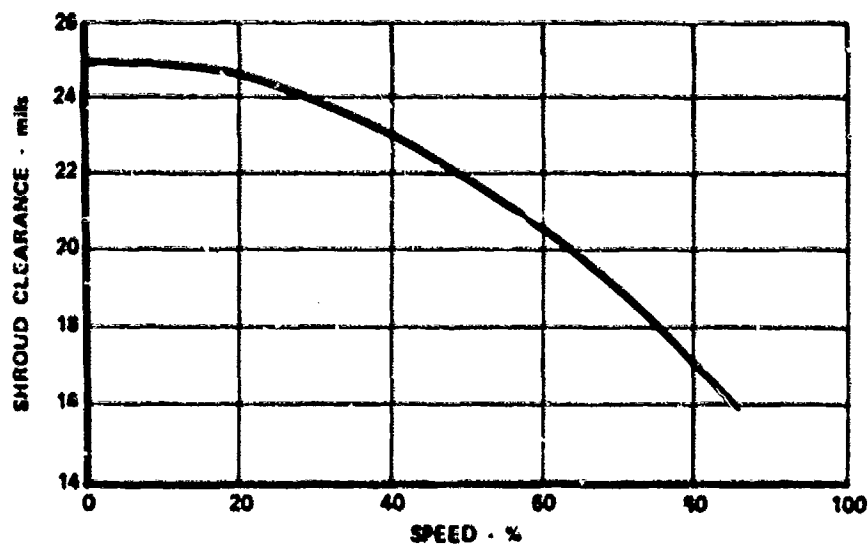


Figure 43. Impeller Tip Axial Shroud Clearance, Build No. 2.

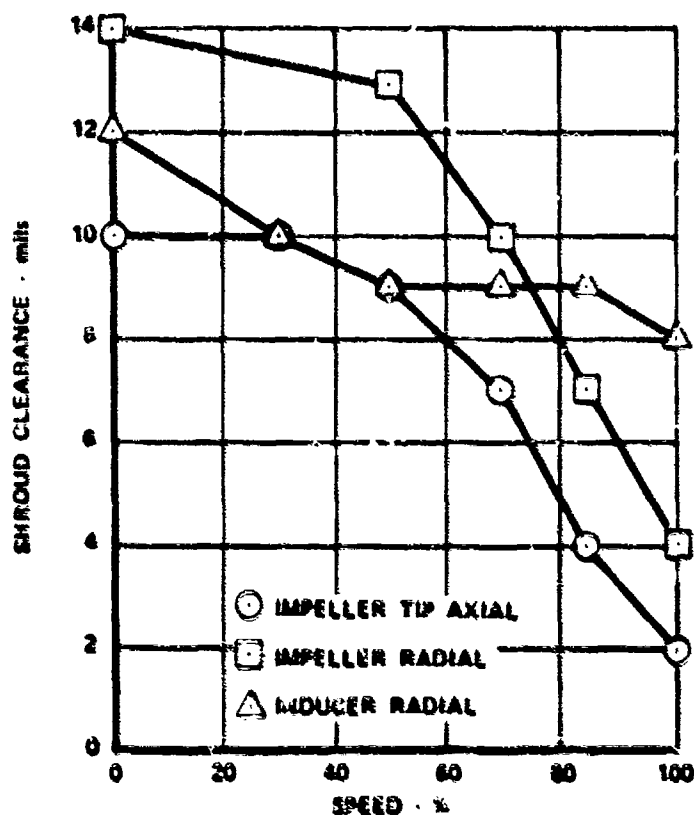


Figure 44. Clearance Probe Measurements, Build No. 3.

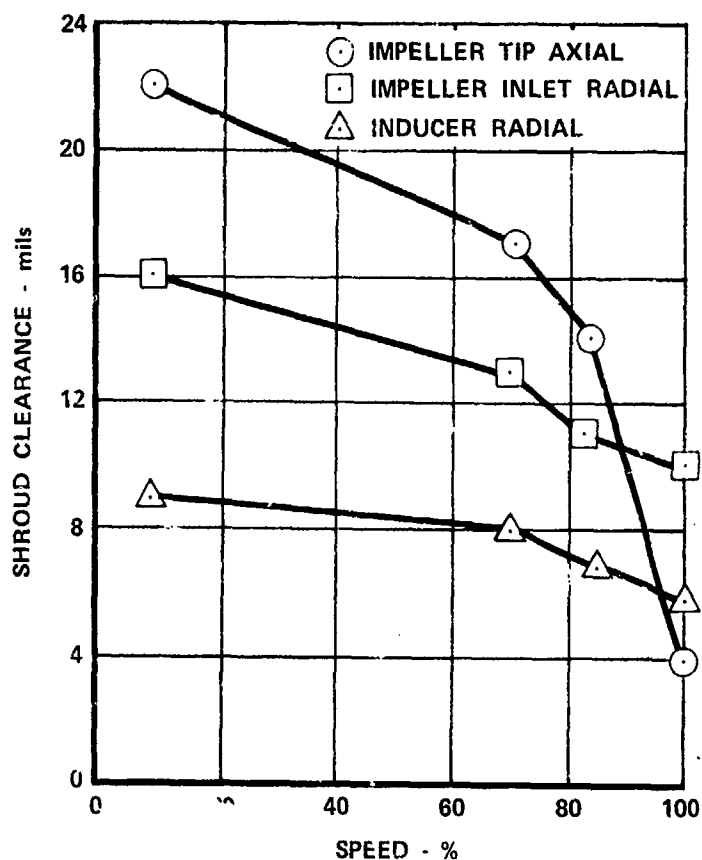


Figure 45. Shroud Clearance Measurements, Build No. 6.

Steady-state data points were distributed along a speedline, based on the collector static pressure range recorded during the first slow-stall transient. A steady-state point consisted of cycling the pressure scanning units twice at a rate of 2 ports/sec, followed by the recording of the rest of the rig instrumentation for 10 sec at a rate of 10 scans/sec. A detailed outline of all data points taken is shown in Table VII.

#### Component Performance Data Acquisition

Component performance data were obtained by radially traversing air angle, total pressure, and total temperature probes behind the inducer and the impeller and by both radially and circumferentially traversing behind the inlet guide vanes. The data recording rate for all traverses was 1 scan/sec. Total pressure vs radial or circumferential travel data could be monitored in the control room on an X-Y plotter and the traverse rate governed, as required, to obtain good profile definition in wakes and near the walls.



TABLE VII. DATA SUMMARY

TABLE VII. DATA SUMMARY

		Overall Performance						Component Performance						Remarks		
		IGV, deg	Steady-State Build No.	3	6	Stall Transient Build No.	6	IGV Exit Radial Traverse Build No.	6	Circumferential Traverse Build No.	3	6	Impeller Exit Traverse Build No.	3	6	
30%		0	6	1	1	1								3	3	
		10	6	1	1	1								3	3	
		20	6	1	1	1								3	3	
50%		0	6	1	1	1										
		10	6	1	1	1										
		20	6	1	1	1										
70%		0	6	1	1	1								3	3	
		10	6	1	1	1								3	3	
		20	6	1	1	1								3	3	
		30	6	4	1	2								1	1	
		40	6	4	1	1								1	1	
80%		0	6	1	1	1										
		10	6	1	1	1										
		20	6	1	1	1										
85%		0	4	1	1	1										
		20	4	1	1	1										
		30	4	1	1	1										
90%		0	6	1	1	1								1	1	
		10	6	1	1	1										
		20	6	1	1	1										
8/1		10	6	1	1	1										
		15	6	1	1	1										
95%		0	6	1	1	1										
		10	6	1	1	1										
		15	6	1	1	1										
		20	6	1	1	1										
100%		5	6	1	1	1										
		10	6	1	1	1										
		15	6	1	1	1										
101%		-4	6	1	1	1										
		-4	6	1	1	1										
		-3	6	1	1	1										
		0	6	1	1	1										
		5	6	1	1	1										

One transient. 95% + 500 rpm and one at 95% - 500 rpm.

With flange coolant.

(1) Additional stall transient performed with impeller exit cobra probe at approximately 15% from the shroud wall.

(2) Eight additional steady-states at near stall with various backface  $\Delta P$ 's.

(1) Additional stall transient performed with impeller exit cobra probe at approximately 15% from the shroud wall.

(2) 5.1g% additional steady-states at near stall with various backface  $\Delta P$ 's.

One transient, 95% + 500 rpm and one at 95% - 500 rpm.

With flange coolant.

Inlet guide vane traverse data were obtained at near-stall points for all speedlines at 70% speed or greater. Near-stall points were set as outlined for steady-state points. The inlet guide vane exit probe was first traversed radially inwards between inlet guide vane wakes from the shroud to the probe's maximum travel at 2.0% span (from hub). The probe was then retracted to the 10% span position and circumferentially traversed to include one IGV gap with a strut wake and one IGV gap without a strut wake. Circumferential traverses were then similarly performed at 30, 50, 70, and 90% spans to complete the inlet guide vane survey for that point.

Inducer exit radial traverses were performed by running the probe in to its limit and then recording data while slowly retracting the probe back out of the flow path.

Impeller exit traverse data were obtained on each speedline at the maximum possible back pressure with the traverse probe in the flow path. This point was set by decreasing the back pressure in small increments until the probe could be traversed across the span without causing the rig to surge. Data were then recorded while slowly traversing the probe from the hub wall back into the shroud. A steady-state point was recorded to coincide with each impeller exit traverse point. At the completion of impeller exit traversing with the air angle and total pressure cobra probe, this probe was replaced with a total temperature probe, and data were obtained at the same rig operating points.

One special test sequence involved performing stall transients with the impeller exit cobra probe, located at approximately 15% span. Data were recorded on six speedlines from wide-open discharge valve into stall at 1 scan/sec and from near stall into stall at 65 scans/sec.

#### Special Instrumentation Data Acquisition

High-frequency response data were obtained at 70 and 78% of design-corrected speed. Data were recorded on analog magnetic tape during a stall transient and near-stall steady-state point for each speedline. Transients and steady-state points were set as outlined in the overall performance data acquisition section.

#### DATA REDUCTION PROCEDURES

The reduction of data was accomplished in three steps: (1) reduction of overall performance data, (2) calculation of component performance and velocity triangles, and (3) reduction of high-frequency response and rig vibration data. The arithmetic mean value of data from redundant instrumentation was used for all calculations except where otherwise noted, and all performance data except orifice and plenum data were corrected to standard day inlet conditions as follows:

$$\text{corrected pressure} = \frac{\text{recorded pressure}}{\delta}$$

$$\text{corrected temperature} = \frac{\text{recorded temperature}}{\theta}$$

Under this system, inlet temperatures and pressures are always standard day conditions ( $T_0 = 518.688^\circ\text{R}$ ,  $P_{t0} = 14.694 \text{ psia}$ ).

## Overall Performance

The reduction of overall performance data was accomplished through the use of an IBM 360-75 computer program. A DRIL (Data Reduction Input Language) program converts raw test data into engineering units, ratios, pressures, and temperatures to standard day inlet conditions, averages data from redundant instrumentation and from successive data recording cycles, and performs overall performance calculations. Actual weight flow was calculated from the orifice equation

$$w_{act} = 14.675 \left[ 1 - 0.302 \left( \frac{\Delta P}{P} \right) \right] \left[ \frac{P \cdot \Delta P}{T_o} \right]^{1/2}$$

where

$P$  = upstream orifice static pressure  
 $\Delta P$  = orifice differential static pressure  
 $T_o$  = plenum total temperature

Both weight flow and speed were corrected to standard day inlet conditions as follows:

$$w_{cor} = w_{act} \frac{\sqrt{\theta}}{\delta}$$

and

$$N_{cor} = \frac{N}{\sqrt{\theta}}$$

Overall temperature ratio, total-to-static pressure ratio, and adiabatic efficiency are given, respectively, by

$$T_r = T_3 / 518.388$$

$$P_r = P_3 / 14.694$$

and

$$\eta = \frac{\text{ideal (isentropic) enthalpy change}}{\text{actual enthalpy change}} = \frac{\Delta hf(P_r)}{\Delta hf(T_r)}$$

where  $\Delta hf(P_r)$  and  $\Delta hf(T_r)$  were determined by fourth degree curve fits of change in enthalpy vs pressure ratio and temperature ratio data from Table I (Dry Air Tables) in Keenan and Kaye Gas Tables. Two separate pressure ratios and corresponding efficiencies were defined, depending on the type of data point. For steady-state points, the average of six collector static pressure taps was used for the values of  $P_3$  in the pressure ratio equation. During stall transients, the pressure ratio was based on the value of a single collector static pressure tap read through a close-coupled pressure transducer. The value of this tap generally agreed to within less than 0.3% of the collector average during steady-state points.

### Inlet Guide Vane Performance

Inlet guide vane performance was calculated by an inlet guide vane update routine to the main DRIL program, which includes the effects of the inlet struts, located upstream of the guide vanes. The static pressure distribution behind the inlet guide vanes was assumed to be a constant equal to the measured shroud static pressure at each point, and the temperature was assumed constant across the vanes.

Guide vane discharge total pressure and air angle traverse data were mass-averaged over both one gap including a strut wake and one gap without any strut effects at 10, 30, 50, 70, and 90% spans. These values were then weighted, based on the relative number of struts to number of inlet guide vanes, and combined to give a single mass-averaged value at each percent span as follows:

$$\bar{P}_t = \frac{3\bar{P}_{ts} + 7\bar{P}_{tv}}{10}$$

and

$$\bar{\alpha} = \frac{3\bar{\alpha}_s + 7\bar{\alpha}_v}{10}$$

where: the subscripts s and v pertain to gaps including a strut wake and gaps not including a strut wake, respectively. A spanwise mass-average total pressure ( $\bar{P}_{t1}$ ) and mass-average air angle ( $\bar{\alpha}_1$ ) were then calculated from these weighted values. The mass-average of any quantity (X) is given by

$$\bar{X} = \frac{\sum_{i=1}^n \Delta w X}{\sum_{i=1}^n \Delta w}$$

where

$$\Delta w = \frac{K(\Delta A)P_t}{\sqrt{T}} \sin \alpha$$

Losses were calculated based on the values of  $\bar{P}_{ts}$ ,  $\bar{P}_{tv}$ , and  $\bar{P}_t$  at each percent span and an overall loss was calculated, based on the spanwise mass-average total pressure. These losses were all of the form

$$\text{loss} = \frac{14.694 - P_t}{14.694}$$

Weight flow was calculated by two separate methods for comparison with the orifice flow calculation. The first method involved integrating the incremental flows,  $\Delta W_s$  and  $\Delta W_v$ , which were obtained during the inlet guide vane total pressure and air angle circumferential mass-average calculations across the blade passage. The results of these integrations were then weighted to reflect the relative number of struts and vanes and summed to yield an integrated flow. The second flow calculation was based on the IGV exit spanwise mass average total pressure:

$$w_{cal} = \frac{KA (\bar{P}_{t1}) \sin \bar{\alpha}_1}{\sqrt{T_1}}$$

where

$A$  = cross-sectional flow path area at the IGV exit  
 $T_1 = 518.688$ , same as inlet

Based on this calculated weight flow, an inlet flow coefficient was determined as follows:

$$C_d = \frac{w_{cal}}{w_{cor}}$$

Inlet guide vane exit velocity triangles were calculated by an IBM 1130 digital computer program, Centrifugal Compressor Data Reduction Program (CCDRP). Again, static pressure was assumed constant across the span. The ratio of specific heats ( $\gamma$ ) was determined from a curve fit of  $\gamma$  vs static temperature ( $T_s$ ) data and involved an iteration on the value of  $T_s$  to satisfy the following:

$$\frac{\bar{P}_{t1}}{P_1} = \left( \frac{T_1}{T_{s1}} \right)^{\gamma/\gamma-1}$$

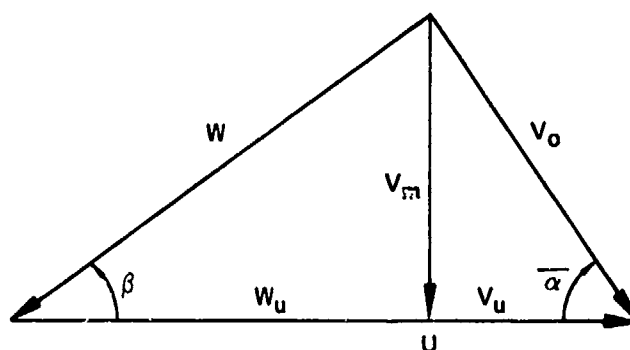
The absolute Mach number ( $Mo$ ) was calculated at each percent span by iterating on the value of  $Mo$  until

$$\frac{\bar{P}_t}{P_1} = \left( 1 + \frac{\gamma-1}{2} Mo^2 \right)^{\gamma/\gamma-1}$$

The local speed of sound was calculated by

$$a = (\gamma GRT_s)^{1/2}$$

From  $Mo$ ,  $a$ , and  $\bar{a}$  the components of the velocity triangles as defined below at each percent span were then calculated.



Inducer incidence ( $i$ ) was determined at each percent span by

$$i = \beta^+ - \beta$$

where  $\beta^+$  is the inducer leading edge metal angle at the corresponding percent span.

#### Inducer Performance

Total pressure, total temperature, and air angle data from each inducer traverse were first plotted vs percent span on a CALCOMP plotter. Up to 25 points from each plot were then selected and input into the 1130 CDRP program. A constant spanwise static pressure distribution equal to the measured shroud static was assumed. Values of  $\gamma$ ,  $T_s$ , and  $Mo$  were calculated for each point by the same iteration methods used in the inlet guide vane section. Total temperatures were corrected for Mach number effects by dividing the recorded temperatures by a recovery factor. The recovery factor used in the calculations was a linear approximation of the actual probe recovery factor vs Mach number calibration data. The maximum error created by this assumption is approximately 0.1% of the temperature reading.

Total pressure and total temperature were then mass-averaged across the span. The sum of the incremental weight flows from the mass-averaging routine was checked against the corresponding orifice flow, and an iteration was performed on the air angle values until the two flow calculations agreed. This air angle check was necessary since errors of 1 or 2 deg in the alignment of the air angle traverse probes on the test stand are not uncommon. Final mass-average total pressure ( $\bar{P}_{t1.5}$ ) and total temperature ( $\bar{T}_{1.5}$ ) values were then calculated, based on the adjusted air angle profile. Inducer pressure ratio and temperature ratio were calculated as follows:

$$P_{r(1-1.5)} = \frac{\bar{P}_{t1.5}}{\bar{P}_{t1}}$$

$$T_{r(1-1.5)} = \frac{\bar{T}_{1.5}}{518.7}$$

Inducer efficiency was calculated by the same methods as the overall efficiency. Inducer exit velocity triangles at 10, 30, 50, 70, and 90% span were determined by the same methods as in the inlet guide vane section.

Near-stall traverse data at 100% speed, 10-deg IGV setting and 101% speed, -4-deg IGV setting were also input into a streamline analysis computer program to calculate the actual spanwise static pressure distribution. This program satisfies the equations of motion and radial equilibrium using input values of total pressure and air angle, a description of the flow path, and a design blockage distribution. The blockages were adjusted until the measured shroud static pressures were matched. Linear approximations of the resulting static pressure distributions were then input into the IBM 1130 CDRP program, and new velocity triangles and inducer performance parameters were calculated for these two points.

### Impeller Performance

Impeller exit traverse data were reduced by nearly the same methods as the inducer exit data. Static pressure was assumed to vary linearly between the measured values at the hub and shroud. Total temperature was input in the form of traverse data and also as a single value equal to the collector total temperature, which was assumed constant across the span.

Flow at the impeller exit was supersonic across much of the span at the higher speed points, which would cause a shock to form in front of the traverse probe. For data taken where the local value of  $P_t/P$  was less than 1.893, the flow was assumed subsonic and impeller performance parameters and velocity triangles were calculated as in the inducer section. For values of  $P_t/P$  greater than 1.893, the flow was assumed supersonic, and a shock correction procedure was incorporated assuming a normal shock to determine the upstream flow conditions.

The mass-average radial velocity ( $\bar{V}_m$ ) and mass-average tangential velocity ( $\bar{V}_u$ ) were calculated, and from these a mass-average air angle was determined:

$$\bar{\alpha}_2 = \tan^{-1} \left( \frac{\bar{V}_m}{\bar{V}_u} \right)$$

The slip factor at the instrumentation station was calculated by

$$\text{slip factor} = \frac{\bar{V}_u}{U}$$

The slip factor at the actual impeller tip was determined from the instrumentation station slip factor by assuming constant angular momentum. Combined inducer-impeller performance was also defined by an internal flow analysis involving a solution of the equations of continuity and momentum. Input for the analysis consisted of overall total pressure ratio and total temperature ratio, rotor speed, mass flow, impeller exit static pressure, configuration geometry, flow factors at the leading edge of the inlet guide vanes and impeller exit, and a calculated temperature rise due to shroud friction, based on rotor speed, density, surface area, and friction coefficient for bladed disks.

### Diffuser Performance

Diffuser discharge coefficient was calculated as

$$C_d^* = \frac{w_{cor}}{w}$$

$$\text{where } W = \frac{KA^*P_{t2}}{\sqrt{T_3}}$$

$A^*$  = throat area

$P_{t2}$  = maximum  $P_t$  at impeller exit from traverse data

Throat blockage was then determined by:

$$B^* = 1 - C_d^*$$

Diffuser static pressure recovery coefficients were defined from the impeller exit to the collector and from the throat to the collector, respectively, as follows:

$$C_p = \frac{P_3 - P_2}{\bar{P}_{t2} - P_2}$$

$$C_p^* = \frac{P_3 - P^*}{\bar{P}_{t2} - P^*}$$

Diffuser effectiveness was defined as

$$\epsilon = \frac{C_p}{C_{pl}^*}$$

where  $C_{pl}^*$  is the ideal pressure recovery coefficient that would be obtained with a one-dimensional, isentropic flow through the same diffuser. For the  $C_{pl}^*$  calculation, a throat Mach number of 1.0 and a  $\gamma$  of 1.4 were assumed.

Diffuser losses were documented by the following:

$$\text{Diffuser loss (total-to-static)} = \frac{\bar{P}_{t2} - P_3}{\bar{P}_{t2}}$$

$$\text{Diffuser loss (total-to-total)} = \frac{\bar{P}_{t2} - \bar{P}_{t3}}{\bar{P}_{t2}}$$



$$\text{Diffuser loss coefficient} = \frac{\bar{P}_{t2} - P_3}{\bar{P}_{t2} - P_2}$$

$$\text{Dump loss} = \frac{\bar{P}_{t3} - P_3}{\bar{P}_{t3}}$$

where  $\bar{P}_{t3}$  is the mass-average total pressure at the diffuser exit.

Diffuser performance was also obtained by separating from overall performance the impeller exit conditions calculated by the internal flow analysis, described in the impeller section. Performance derived from this analysis was compared to that obtained from traverse data.

The Mach number profile at the diffuser exit was calculated, based on diffuser exit total pressure data and collector static pressure and assuming a  $\gamma$  of 1.4. Total pressure data from different pipes was first adjusted to match a single average value at the center of each pipe to eliminate scatter in the absolute profiles of individual pipes for this presentation.

#### High-Frequency Response and Rig Vibration Data

High-frequency response (Kulite) data recorded on analog magnetic tape was processed using a digital Fourier analyzer system to determine the magnitude of pressure fluctuations, blade wake definition, and rotating stall characteristics. Resultant data plots included spectral plots (amplitude vs frequency), tracking plots (amplitude vs time), and various correlation plots.

Rig vibration data recorded prior to the installation of the digital Fourier analyzer system was processed in a similar manner, except that a wave analyzer system was used in which the data were not first digitized. Resultant data plots were similar to those mentioned in preceding paragraphs.

#### VALIDATION OF TEST DATA

Estimates of the uncertainty of the data acquired from the compressor test rig are presented in Table VIII. These estimates include both the uncertainty of the sensor and of the recording device. All uncertainty calculations, with the exception of those for weight flow and efficiency, are applicable to any reading. Weight flow and efficiency uncertainty were calculated at the design point. Uncertainty of air angle assumes no alignment error. Both bias and precision errors (precision errors are two standard deviations from the mean) were used in the uncertainty analysis; these errors are also presented in Table VIII. When multiple probes were available for redundant measurement, the precision error was calculated by statistically averaging individual measurements by the root-sum-square method as illustrated below.

$$u = \frac{e}{\sqrt{n}}$$

TABLE VIII. ESTIMATE OF INSTRUMENTATION ACCURACY

Variable	Location (Station)	Type Instrument	Range	Number of Probes Averaged	Bias $\pm$	Precision $\pm$	Uncertainty $\pm$	Units
P	00	Transducer	0 to 15	3	0.04	0.01	0.05	psia
T	00	Resistance Thermometer	Ambient	5	0.27	0.07	0.34	$^{\circ}$ R
P	1 and 1.5	Pressure Scanner	0 to 15	4	0.05	0.02	0.07	psia
Air Angle	1, 1.5, and 2.0	Potentiometer	0 to 160	1	0.4	1.2	1.6	degree
P <sub>t</sub>	1.5	Transducer	0 to 25	1	0.40	0.30	0.43	psia
T	1.5	CA/TC	0 to 600	1	3.0	1.2	4.2	$^{\circ}$ F
P	1.5 to 2.0	Pressure Scanner	0 to 55	1	0.28	0.09	0.37	psia
P <sub>t</sub>	2.0	Transducer	0 to 170	1	0.46	0.29	0.74	psia
T	2.0	CA/TC	0 to 1150	1	3.5	1.5	5.0	$^{\circ}$ R
P	2.0 to 3.0 and 3.5	Pressure Scanner	0 to 150	1	0.43	0.34	0.77	psia
T	3.5	CA/TC	0 to 1150	4	1.08	0.49	1.57	$^{\circ}$ R
Flowrate	Inlet	Orifice	3.1	34P, 3P, 5 temperature	0.024	0.037	0.059	lb/sec
Efficiency	00 to 3.5	-	75%	-	-	-	0.553	percent

where  $u$  = overall uncertainty of flow variable

$e$  = uncertainty of individual sensor

$n$  = number of sensors recording the same flow variable

Table VIII also includes the effect of the data uncertainty on the uncertainty of the overall efficiency performance calculation. This performance uncertainty estimate was calculated by differentiating the efficiency equation and inputting the uncertainty values of Table VIII in the resulting relationship. The uncertainty of the efficiency value was 0.55 point in efficiency, which was considered to be satisfactory. The uncertainty of the weight flow was calculated by combining the total bias and precision involved in measuring weight flow with the inlet and instrumentation used for this program. The total uncertainty of  $\pm 0.059$  lb/sec is based on the design flow of 3.1 lb/sec.

At each steady-state point, approximately 20 scans of data recorded over a 2-sec interval were averaged. A typical printout from a near-stall, steady-state point at 101% design speed and -4-deg inlet guide vane setting is shown in Table IX. A 2-sec average value, the maximum and the minimum value recorded, and 3 sigma (three standard deviations from the mean) are also listed for each instrumentation. These provide a measure of the actual scatter in the data due both to the uncertainty in measurement and to slight speed and flow variations that may have occurred while recording the steady-state.

Integrated flows calculated from traverse data at each instrumentation station were checked for correspondence with the inlet orifice flow as is shown in Figures 46 through 48 for Build No. 6. Calculated weight flows, based on mass-averaged values of the total pressure and air angle, are also included on the inlet guide vane flow correspondence plot in Figure 46. The approximate 0.40 lbm/sec shift in the inducer exit integrated flow shown in Figure 47 can be attributed to two factors. The first of these is the constant spanwise static pressure distribution that was assumed for the reduction of most of the traverse data at this instrumentation station. As can be seen in Figure 47, the flow correspondence improved for the two near-stall points at 100 and 101% speed, which were reduced assuming a linear static pressure profile, which more closely approximated the calculated static pressure distribution at that station. The impeller exit integrated flow shown in Figure 48 correlates well with the orifice flow over most of the flow range, but falls off slightly at the higher flow rates. This can be attributed to larger differences between the actual static pressure profile and the assumed linear static pressure profile for these points.

Prior to the calculation of component performance parameters and velocity triangles, the inducer exit and the impeller exit integrated flows were adjusted to match the inlet orifice flow, and thus satisfy continuity requirements. This was accomplished by adding a constant value to the measured air angles so that the impeller exit airflow matched that measured. It was felt that the absolute value of the air angle measurement was the least accurate of the data used in the weight flow calculation, although the profile was considered accurate. However, as pointed out earlier, the assumed static pressure profiles at the inducer exit and the impeller exit and the assumed total temperature profile at the impeller exit also contributed significantly to the initial integrated flow variations, especially at the higher speed, higher pressure ratio points.

TABLE IX. TYPICAL PRINTOUT FOR A NEAR-STALL, STEADY-STATE POINT  
AT 101% DESIGN SPEED AND -4-DEG INLET GUIDE VANE SETTING

W	TIME 2205	PLAN 20, 1973	RIG NO. 2588	BUILD 06	RUN NO. 004-02	P-02
OVERALL FLOW TIME INTERNAL BEGINNING AT 2005-224						
MEASUREMENTS	UNIT	CHANNEL	OVERS	SCGMA	MAXIMUM	MINIMUM
SCANS USED	SCANS ELIMINATED					
0510	0	0-000	0-000	0-242	-0-704	0
0511	1	0-000	0-000	0-000	0-000	0
0512	2	0-000	0-000	0-000	0-000	0
0513	3	0-000	0-000	0-000	0-000	0
0514	4	0-000	0-000	0-000	0-000	0
0515	5	0-000	0-000	0-000	0-000	0
0516	6	0-000	0-000	0-000	0-000	0
0517	7	0-000	0-000	0-000	0-000	0
0518	8	0-000	0-000	0-000	0-000	0
0519	9	0-000	0-000	0-000	0-000	0
0520	10	0-000	0-000	0-000	0-000	0
0521	11	0-000	0-000	0-000	0-000	0
0522	12	0-000	0-000	0-000	0-000	0
0523	13	0-000	0-000	0-000	0-000	0
0524	14	0-000	0-000	0-000	0-000	0
0525	15	0-000	0-000	0-000	0-000	0
0526	16	0-000	0-000	0-000	0-000	0
0527	17	0-000	0-000	0-000	0-000	0
0528	18	0-000	0-000	0-000	0-000	0
0529	19	0-000	0-000	0-000	0-000	0
0530	20	0-000	0-000	0-000	0-000	0
0531	21	0-000	0-000	0-000	0-000	0
0532	22	0-000	0-000	0-000	0-000	0
0533	23	0-000	0-000	0-000	0-000	0
0534	24	0-000	0-000	0-000	0-000	0
0535	25	0-000	0-000	0-000	0-000	0
0536	26	0-000	0-000	0-000	0-000	0
0537	27	0-000	0-000	0-000	0-000	0
0538	28	0-000	0-000	0-000	0-000	0
0539	29	0-000	0-000	0-000	0-000	0
0540	30	0-000	0-000	0-000	0-000	0
0541	31	0-000	0-000	0-000	0-000	0
0542	32	0-000	0-000	0-000	0-000	0
0543	33	0-000	0-000	0-000	0-000	0
0544	34	0-000	0-000	0-000	0-000	0
0545	35	0-000	0-000	0-000	0-000	0
0546	36	0-000	0-000	0-000	0-000	0
0547	37	0-000	0-000	0-000	0-000	0
0548	38	0-000	0-000	0-000	0-000	0
0549	39	0-000	0-000	0-000	0-000	0
0550	40	0-000	0-000	0-000	0-000	0
0551	41	0-000	0-000	0-000	0-000	0
0552	42	0-000	0-000	0-000	0-000	0
0553	43	0-000	0-000	0-000	0-000	0
0554	44	0-000	0-000	0-000	0-000	0
0555	45	0-000	0-000	0-000	0-000	0
0556	46	0-000	0-000	0-000	0-000	0
0557	47	0-000	0-000	0-000	0-000	0
0558	48	0-000	0-000	0-000	0-000	0
0559	49	0-000	0-000	0-000	0-000	0

**TABLE IX. CONTINUED**

[illegible]

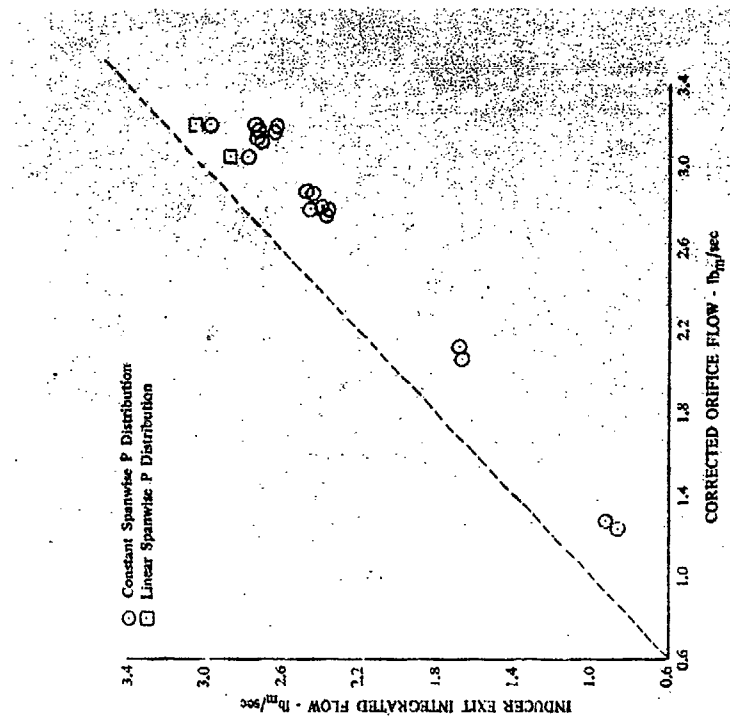


Figure 46. Inlet Guide Vane Exit Flow  
Correspondence, Build No. 6.

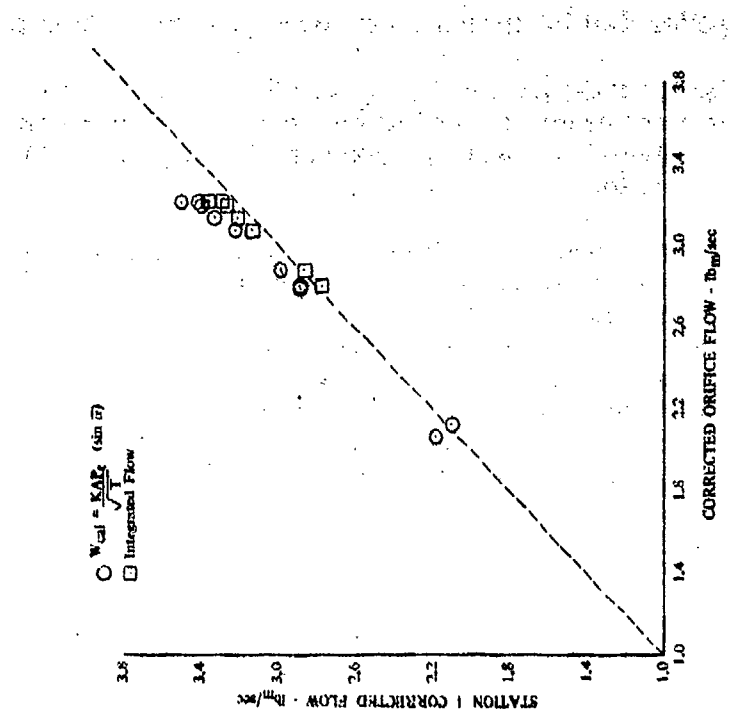


Figure 47. Inducer Exit Integrated Flow  
Correspondence, Build No. 6.

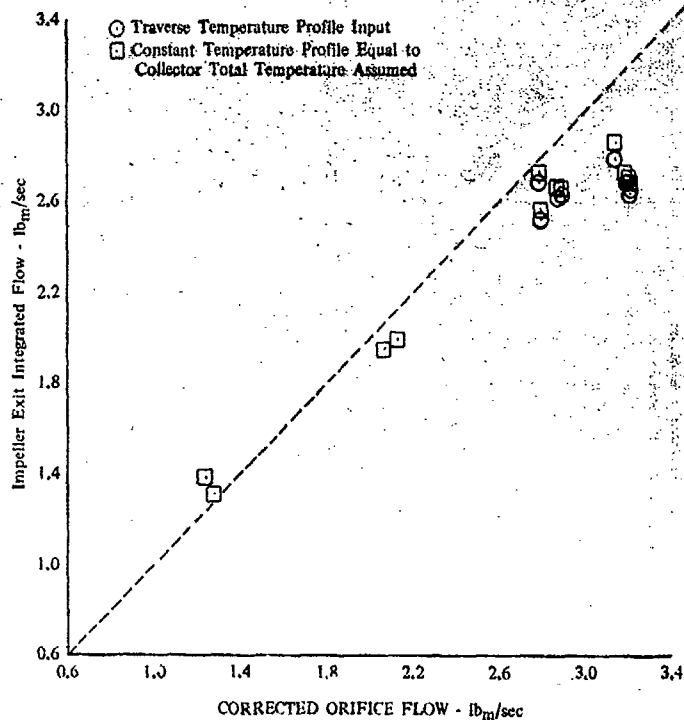


Figure 48. Impeller Exit Integrated Flow Correspondence, Build No. 6.

Measured collector static pressure readings from all taps were within the estimated precision of  $\pm 0.34$  psia and generally read within  $\pm 0.1$  psia. The measured collector temperatures exhibited an observed maximum deviation of  $\pm 0.75\%$  about the average at the same condition.

Combined inlet guide vane, inducer, and impeller performance obtained from traverse data showed the same trends as the performance generated by an internal flow analysis as previously defined in the Data Reduction Section, although the absolute performance levels from the traverse data were higher. Table X compares the performance obtained from traverse data and that obtained from the internal flow analysis for near-stall points at 95% speed and 10-deg inlet guide vane setting and 101% speed and 0-deg inlet guide vane. Also shown in the table are the diffuser losses obtained by subtracting the above inlet guide vane, inducer, and impeller performance from the overall performance at those points.

TABLE X. TRAVERSE DATA - INTERNAL FLOW ANALYSIS PERFORMANCE COMPARISON

	101% Speed, 0-Deg IGV rpm = 65,953 Flow = 3.185		95% Speed, 10-Deg IGV rpm = 62,426 Flow = 2.783	
	Traverse Data	Internal Flow Analysis	Traverse Data	Internal Flow Analysis
IGV, Inducer, Impeller Pressure Ratio, $P_o/P_{t2}$	11.812	11.210	9.655	9.260
IGV, Inducer, Impeller Adiabatic Efficiency, %	81.5	79.4	85.8	82.7
Diffuser Loss, $P_{t2} - P_3$ $P_{t2}$	0.182	0.139	0.167	0.115



## RESULTS AND DISCUSSION

### Initial Performance

Overall performance data obtained during the Build No. 2 shakedown test indicated the existence of a performance deficiency, which data analyses revealed to be caused by an impeller-diffuser mismatch. These analyses resulted in a decision to bore out the diffuser throat to provide a better match for the impeller discharge conditions.

The overall performance data indicated that, if the compressor had operated at design speed, the compressor would have been down appreciably in efficiency (Figure 49) and flow (Figure 50). The test data were used in conjunction with analytical computer programs to separate the impeller and diffuser performance characteristics to isolate the cause of this degradation in performance. This analysis resulted in two conclusions. First, the diffuser was setting the maximum flow rate for the compressor, as indicated by the diffuser loss characteristics shown in Figure 51. Vertical diffuser loss characteristics, such as those in Figure 51, are commonly associated with a flow-limited diffuser. The second conclusion was that, as a result of the reduced inlet flow rate caused by the choked diffuser, the impeller incidence values were higher than design, resulting in a loss in impeller efficiency.

Further analysis of the diffuser revealed that the diffuser was flow limited due to greater than anticipated throat blockages at 70, 80, and 85% of design speed, as can be seen in Figure 52. Extrapolating the throat blockage data to 100% speed indicates the blockage will be 14% compared to the design value of 8%. By assuming a 14% blockage at 100% design rotor speed and that the impeller will meet its design goals at design flow rate, i.e., incidence, it was determined that a diffuser throat area 7% greater than the current design was required. Therefore, it was decided to bore out the diffuser throat by 7% but to retain the diffuser design throat length-to-diameter ratio of 0.5 by also re boring the 3-deg cone. Changes in diffuser leading edge radius ratio, leading edge Mach number, and diffuser exit conditions resulting from the increased throat area were considered negligible.

### OVERALL PERFORMANCE

Overall performance data for Builds No. 3 and 6 of the compressor are presented in this section. Build No. 6 of the compressor was tested with a damaged diffuser, and its performance was somewhat impaired. An analytical representation of the performance that this stage would have produced without this damage was prepared using diffuser performance from Build No. 3; it is also presented in this section.

Data for Build No. 3 at the design inlet guide vane setting of 10 deg are presented in Figure 53 and for inlet guide vane angles of 0 and 20 deg in Figures 54 and 55. At the 10-deg design IGV setting, the flow rate was 3.03 lb/sec, compared to the goal of 3.1 lb/sec, an indication that the inducer-impeller was producing less pressure than anticipated. The maximum pressure ratio at design speed was 9.34 at an efficiency of 77.6%. A rotor speed of 95% of design produced a pressure ratio exceeding the required 8:1 pressure ratio at an efficiency slightly less than the 80% goal, 79.6%.

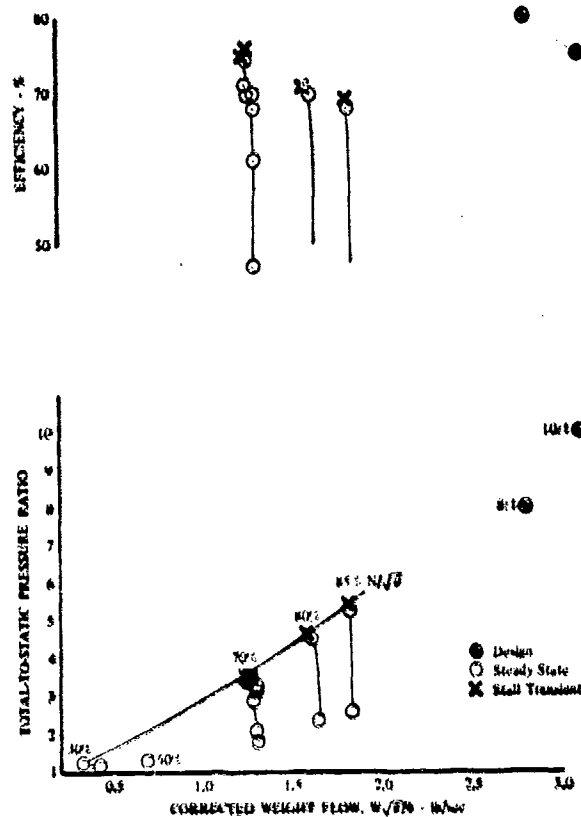


Figure 49. Overall Performance, Build No. 2 Shakedown Test.

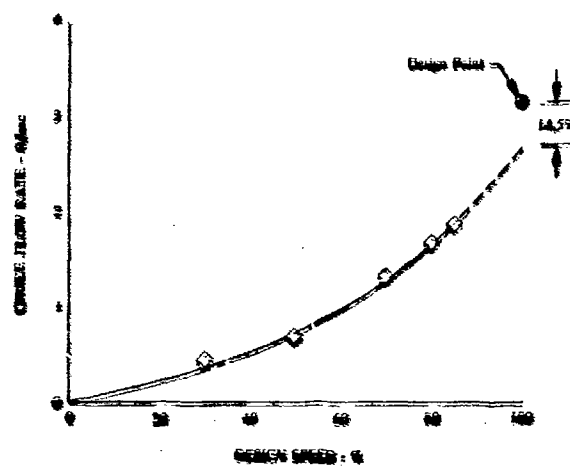


Figure 50. High-Speed Centrifugal Compressor Flow Characteristics.

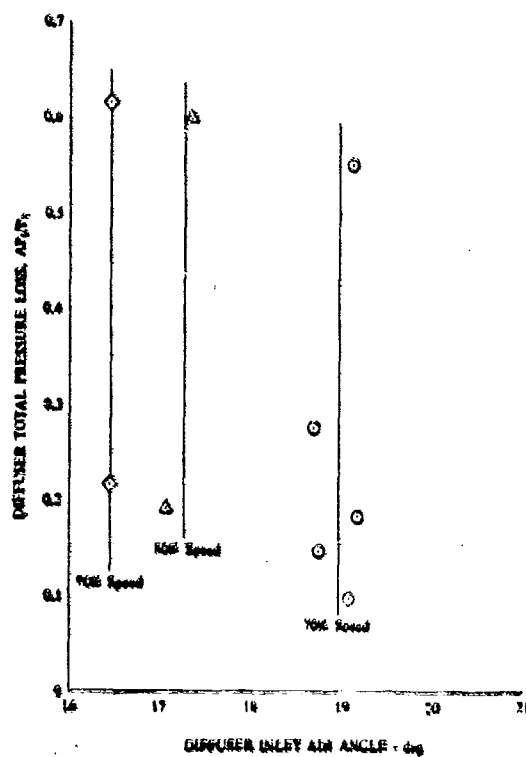


Figure 51. Diffuser Loss Characteristic, Build No. 2 Shakedown Test.

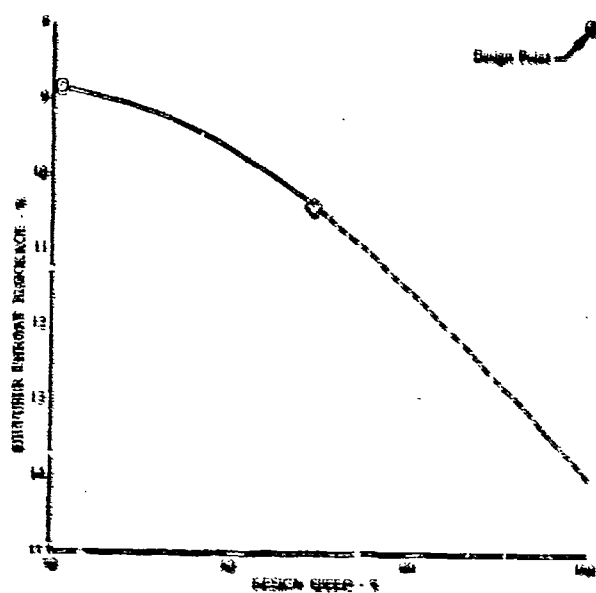


Figure 52. Diffuser Throat Blockage Characteristic, Build No. 2 Shakedown Test.

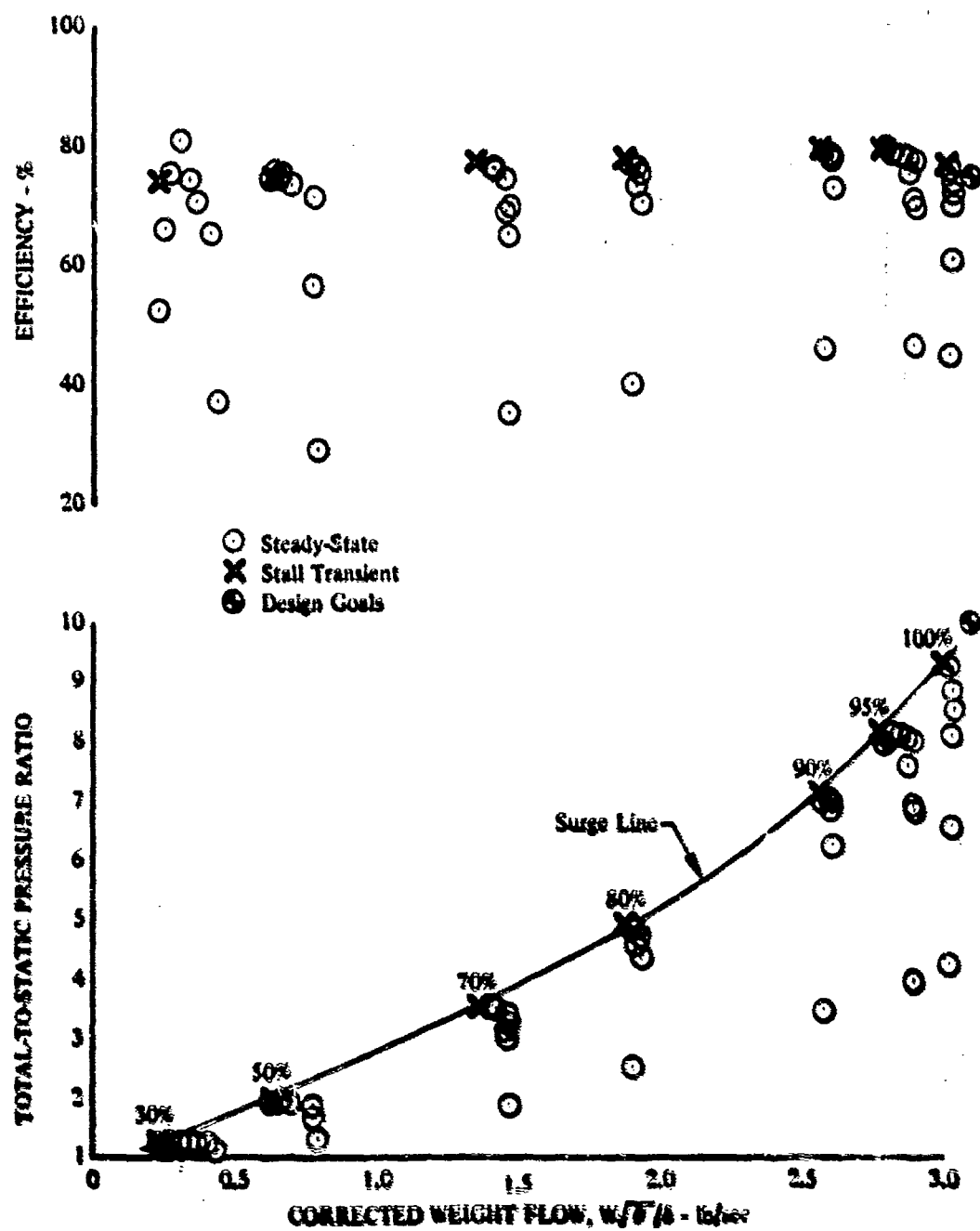


Figure 53. Overall Performance, Build No. 3, 10-deg IGV.

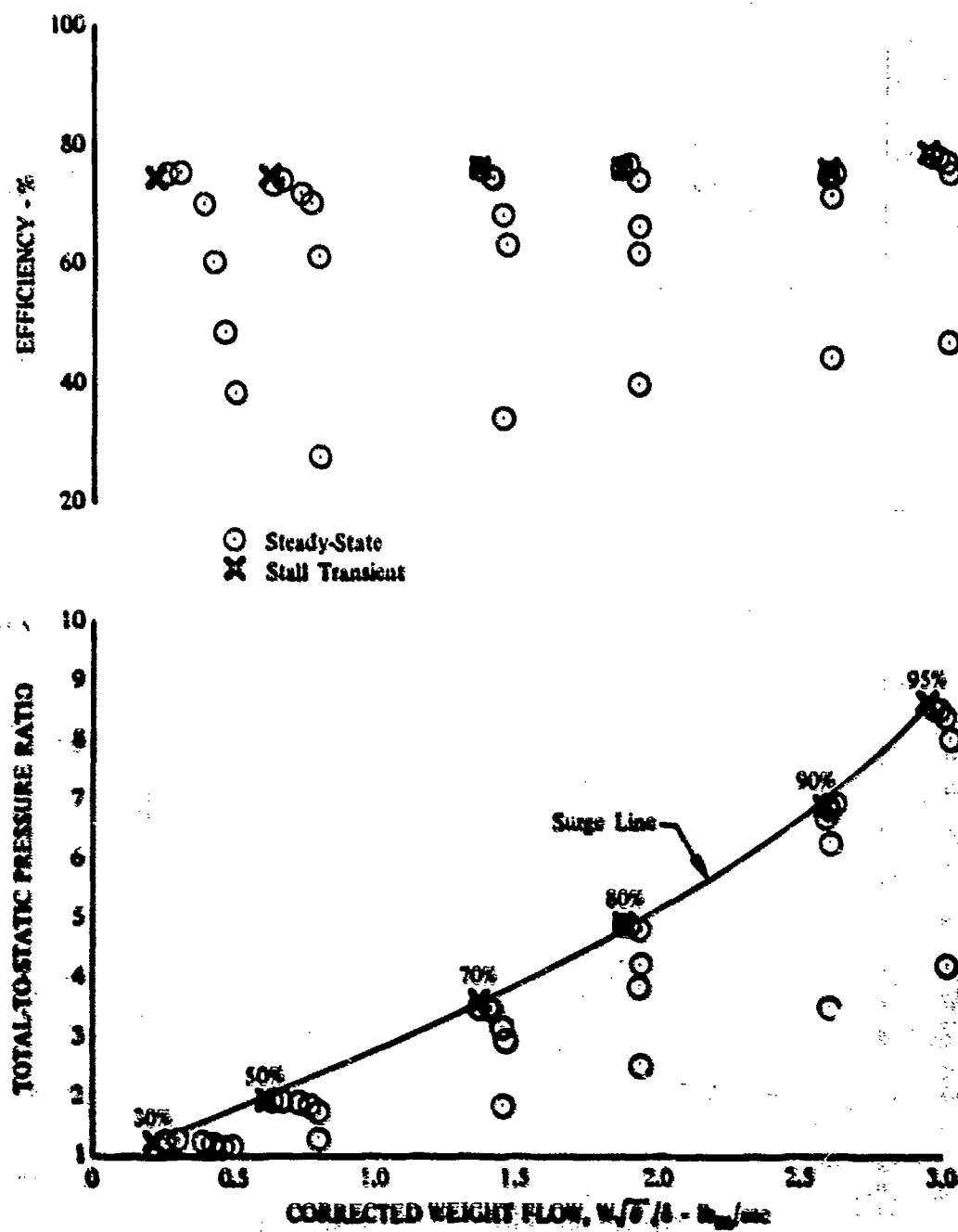


Figure 34. Overall Performance, Build No. 3, 0-deg IGV.

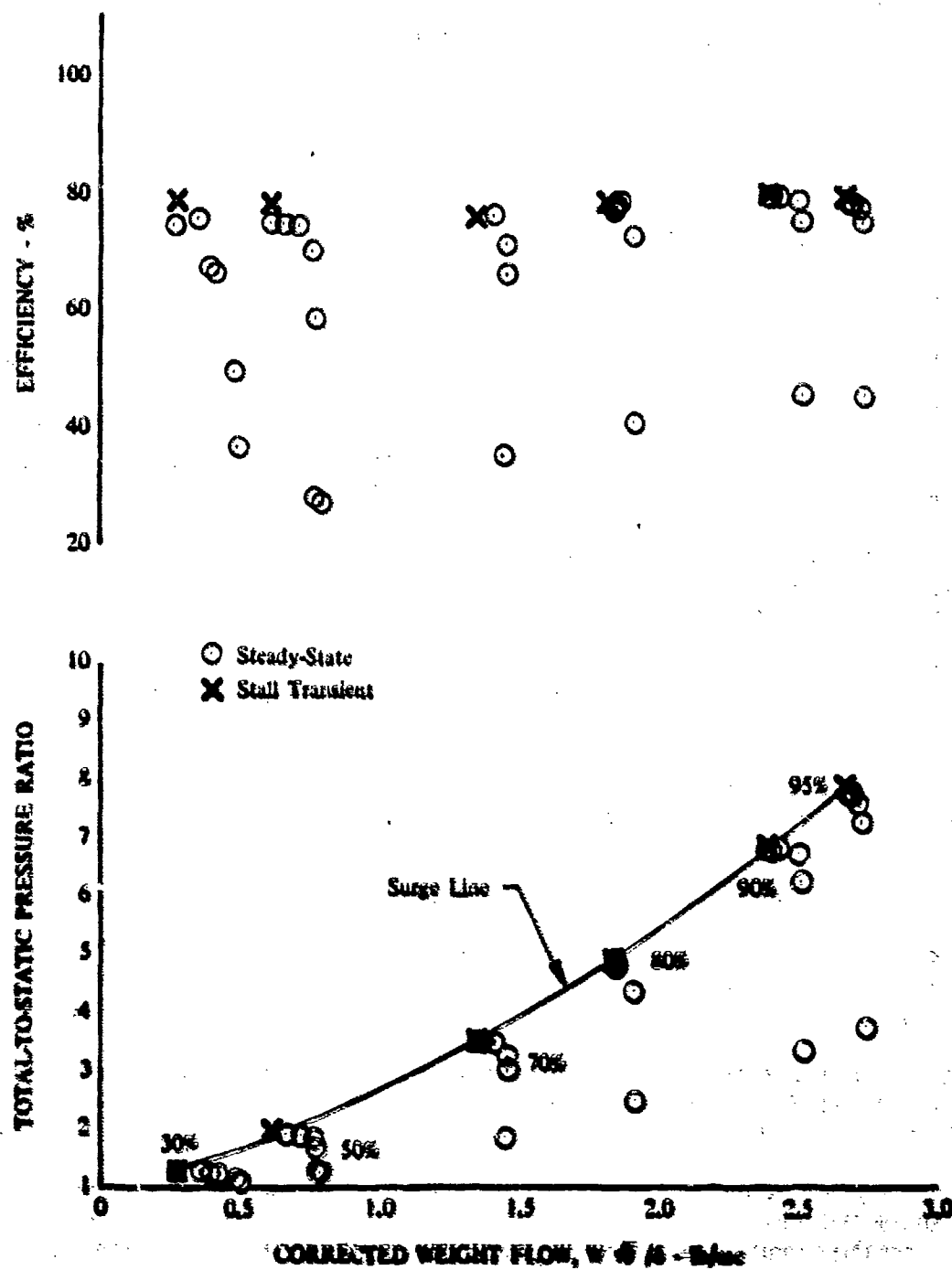


Figure 55. Build No. 3 Overall Performance, 20-deg IGV.

The trends exhibited by these data lead to an interesting speculation that the design conditions may have been attained by overspeeding the rotor approximately 2% at the design inlet guide vane setting. High rig vibrations prevented further high-speed testing.

The compressor maps obtained with inlet guide vane settings  $\pm 10$  deg from the nominal were limited to a maximum speed of 95% of design due to rotor vibrations. The higher rotor work capability of the 0-deg IGV setting raised the maximum pressure ratio from 8.2 for the design IGV setting at 95% of design speed to over 8.6 without measurable loss in efficiency. This change in IGV angle also increased airflow by 4.5%. The improved performance at the 0-deg IGV setting indicated that this setting may have offered the best compromise for attaining the performance goals at high-rotor speeds. Testing of Build No. 3 was, however, terminated due to a bearing failure associated with the vibration problems.

Performance testing of Build No. 6 after the redesign of the rig bearing and rotor system completed the high speed tests initiated with Build No. 3. Data are presented in Figure 56 for the various combinations of IGV settings and rotor speeds that were tested. The data show that the maximum pressure ratio reached at a -4-deg IGV setting was slightly above the design goal (10:03) at a rotor speed of 1% in excess of design, and the corresponding maximum efficiency was 1.2 percentage points low. At the 8:1 pressure ratio point, the efficiency decrement was 2 points below the goal.

Comparing this efficiency loss with the previous data led to the conclusion that the damage sustained by the diffuser was more serious than expected. Damage occurred when portions of the silver plating on the impeller shroud broke off and impinged on the leading edges of the diffuser during an earlier impeller-to-shroud rub. A complete discussion of the problem is presented in the diffuser component section. The Build No. 6 testing also included a special test in which nitrogen was used to cool a thermal dam machined between the impeller shroud flange and the inducer shroud flange to eliminate heat transfer and to create a thermal environment similar to that of Build No. 3 or a gas generator with thin cases.

This test generated a pressure ratio of 10.04:1 and an efficiency of 74.3% at 101% of design speed and -4-deg IGV setting. This was an improvement of 0.5% due to the thermal dam.

Using data from Builds No. 3 and 6 compressor tests, a composite performance map was formulated for this compressor. This map, Figure 57, uses the Build No. 3 data at rotor speeds of 95% of design and below. At design speed, data from a Build No. 6 stall transient (no steady-state data points were recorded) were used, but were adjusted to compensate for the reduced performance of the damaged diffuser using Build No. 3 diffuser performance data. This composite data map shows that the compressor achieved its major pressure ratio and efficiency goals. The efficiency throughout the speed range was optimized by varying the inlet guide vanes as noted on the figure.

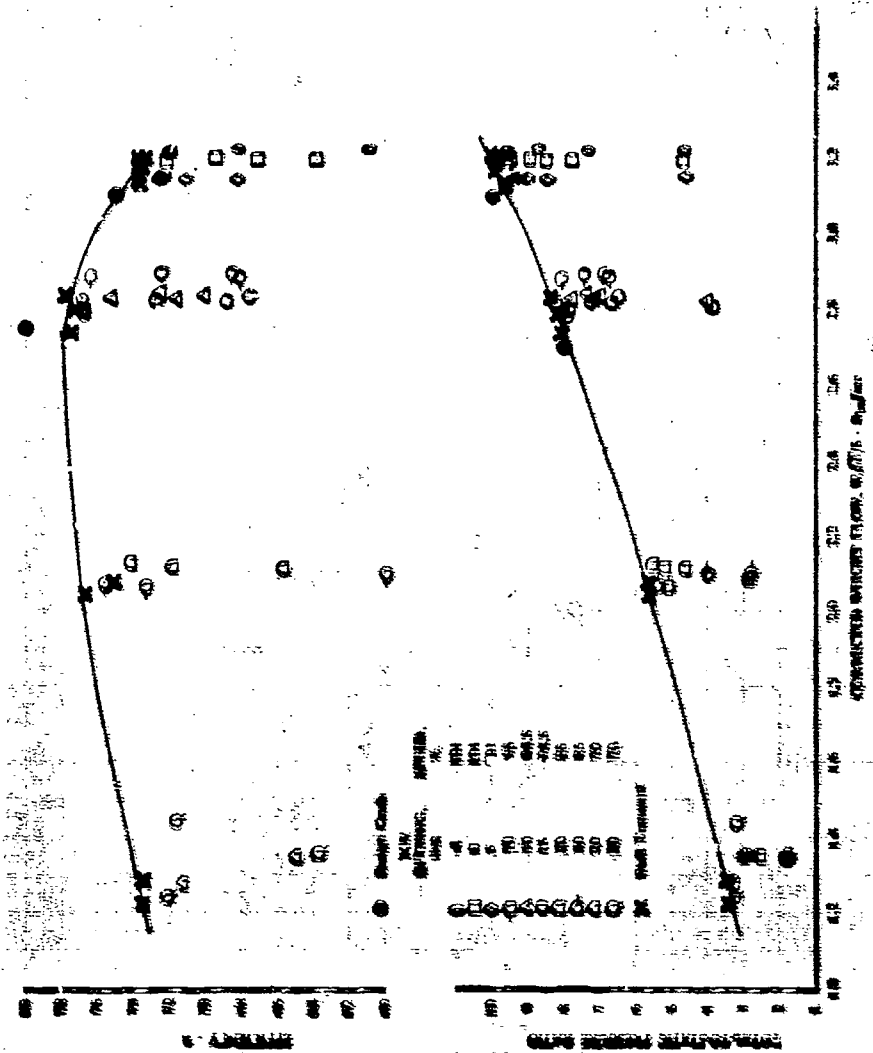


Figure 6C. Build No. 6 Overall Performance.



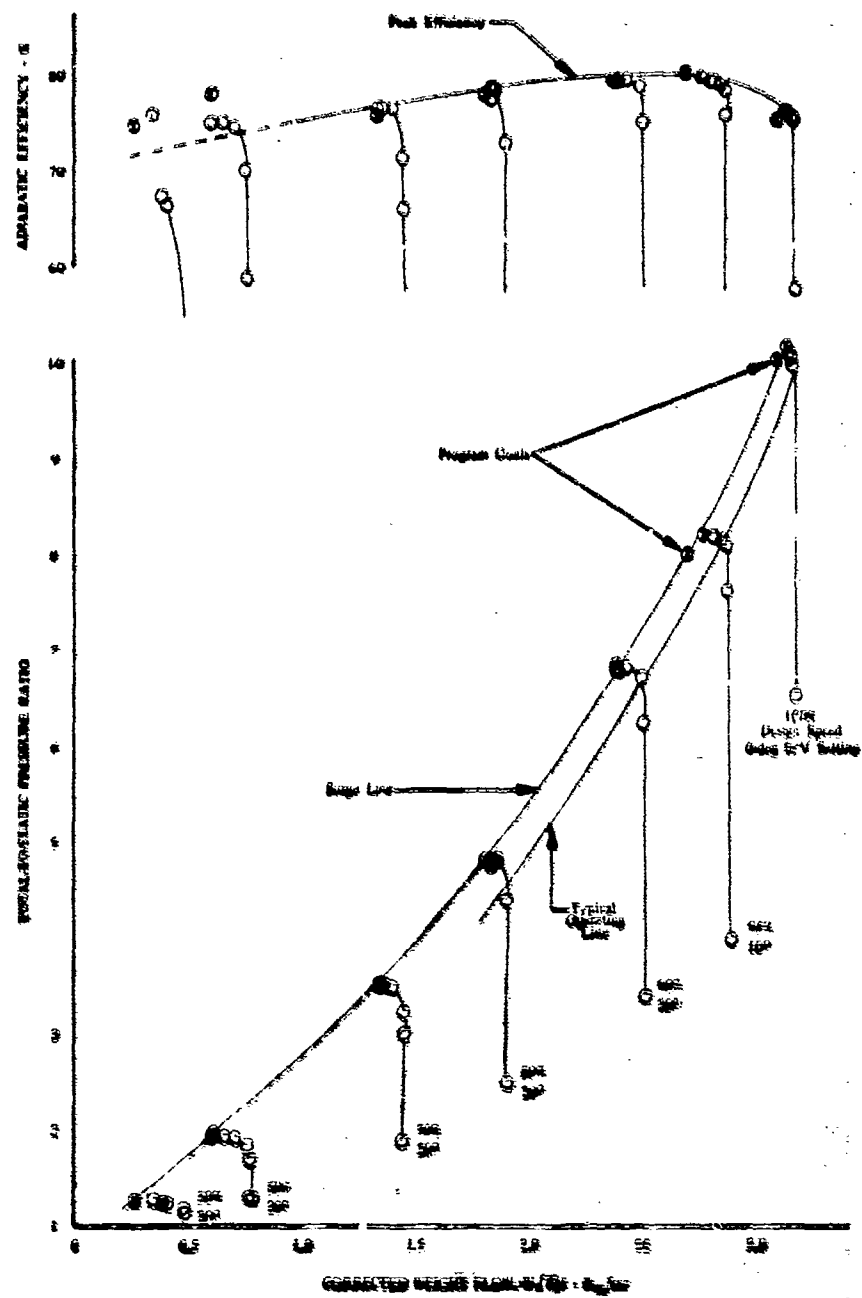


Figure 37. Composite Overall Performance Map.

## COMPONENT PERFORMANCE

A discussion of the performance of each compressor stage component is presented in this section. A representation of the cumulative performance at various stage component interfaces is presented in Figure 58 to provide a perspective on the contributions of the various components to the overall stage performance. Data from both Builds No. 3 and 6 are used in this representation. It may be noted that the inlet section, including the IGV losses, has a small effect on overall performance and that the impeller performance is not sensitive to operating conditions throughout the speed-flow regime. On the other hand, the inducer performance peaks at about 2.9 lb/sec flow and then drops sharply at higher flow, suggesting that a significant improvement in efficiency may be possible through an evaluation of the cause of this loss and the accomplishment of corrective modifications.

### Inlet and Inlet Guide Vanes

The inlet and inlet guide vanes were analyzed for the Builds No. 3 and 6 configurations. Tabulations of all inlet guide vane data are presented in Appendix I and can be used to further define the characteristics of individual vanes and struts. Inlet guide vane turning for the Build No. 6 configuration is shown in Figure 59 as mass average turning angle vs inlet guide vane setting. These data show that the mass average angles agree well with predicted turning angles. Although the average turning matches the design prediction, the flow was underturned at the tip, compensating for general overturning over the rest of the span, as demonstrated in Figure 60. This figure presents mass average exit air angle at five spanwise positions for the 10-deg IGV setting at three rotor speeds for Build No. 6 and one for Build No. 3. The different distribution is evidently related to the Build No. 6 converging configuration, since the Build No. 3 data using the same guide vanes and setting produced a more nearly constant distribution with slight overturning at the tip.

The redesigned inlet also produced a greater loss than the original design. Mass-averaged total pressure data from Builds No. 6 and 3, as shown in Figure 61, demonstrate this increase in inlet losses. A sample plot of the circumferential total pressure traverses used to generate this loss data is shown in Figure 62. A sample radial traverse is shown in Figure 63. The probe has been shimmed away from the hub wall by approximately 0.020 in. These data show the trend to increasing losses toward the tip of the guide vanes. This may also be seen in Figure 64 in which the losses from the hub through midspan are low, while 70 and 90% span losses are quite high for data taken at 100 and 101% of design speed. There is a considerable increase in losses generated when the guide vanes were set to produce negative turning. The increase in loss at 90% span with increasing prewhirl may be a function of the clearance between the vane end and the outer wall, which increased in any position except axial. At other spanwise locations the losses minimize at 10 deg, which was the design setting.

The inducer inlet conditions generated by the guide vanes are described completely for every traverse point in tabulations in Appendix I. A typical tabulation (e.g., 100% speed and 10 deg of prewhirl) is presented in Table XI. Inlet relative Mach number and incidence are presented as a function of spanwise position in Figure 65.

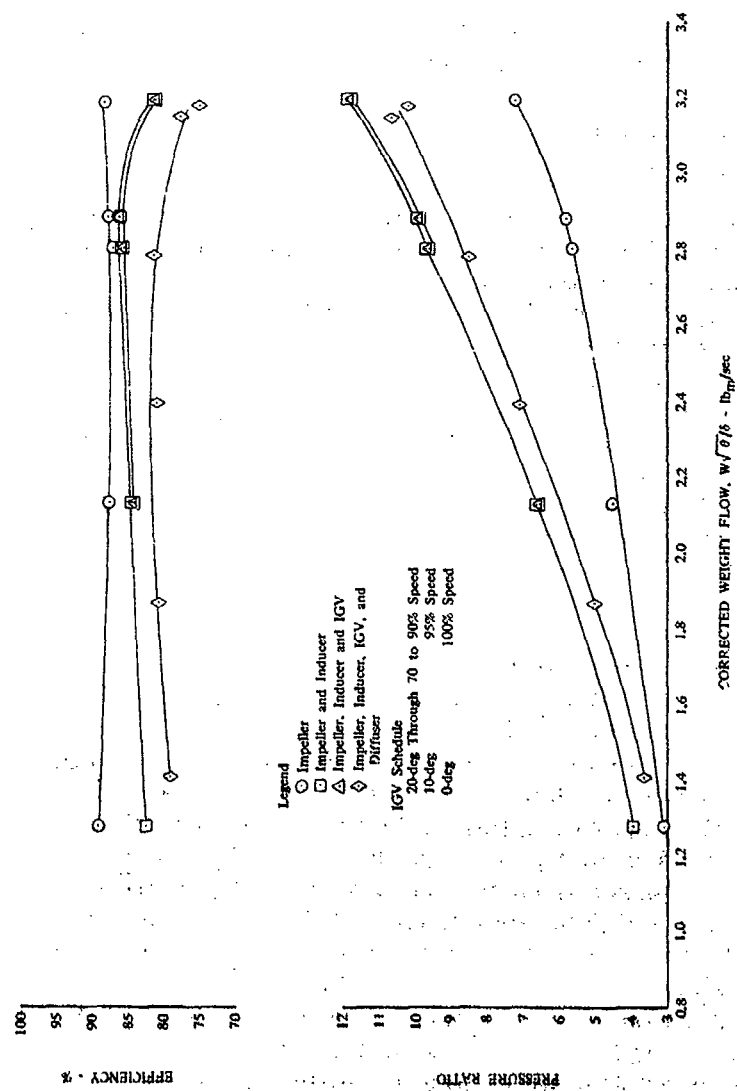


Figure 58. Component Efficiency Representation.

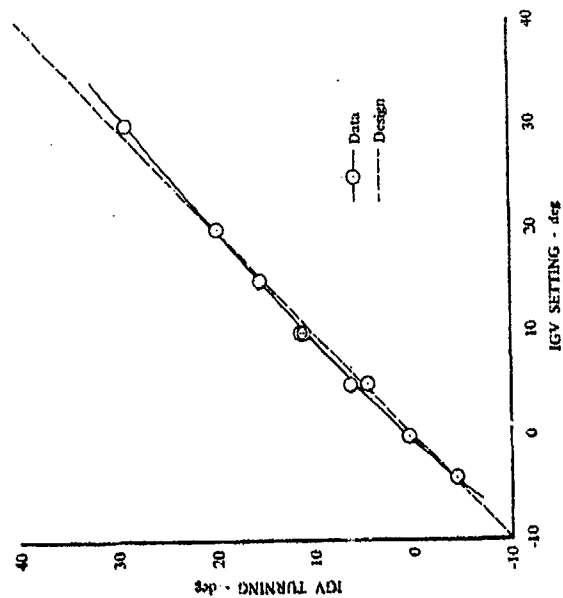


Figure 59. IGV Turning vs Setting, Build No. 6.

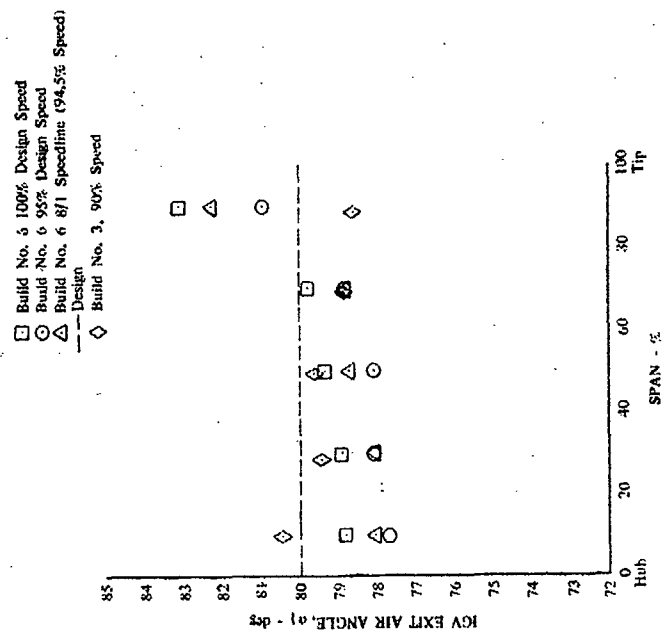


Figure 60. IGV Exit Prewirl Distribution, 10-deg IGV.

IGV Setting, deg	Build No.
10	6
5	6
15	6
4	6
20	6
10	3

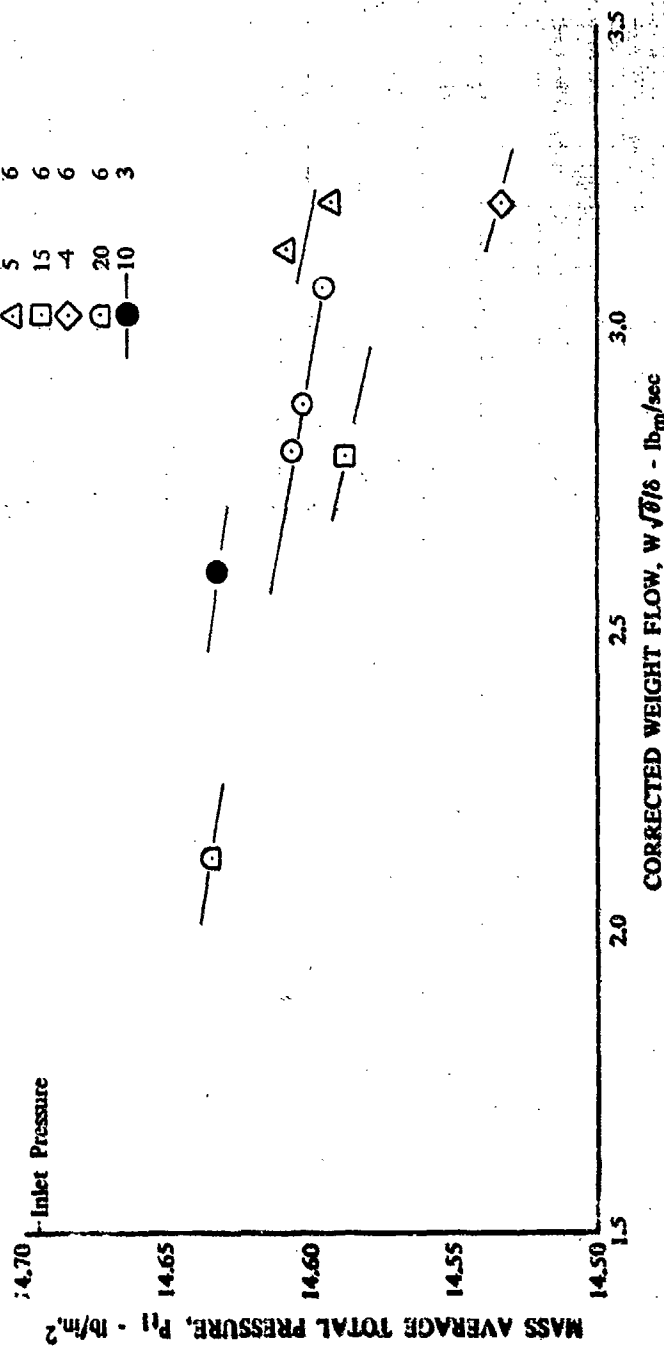


Figure 61. Inlet Section Total Pressure Loss Characteristics.

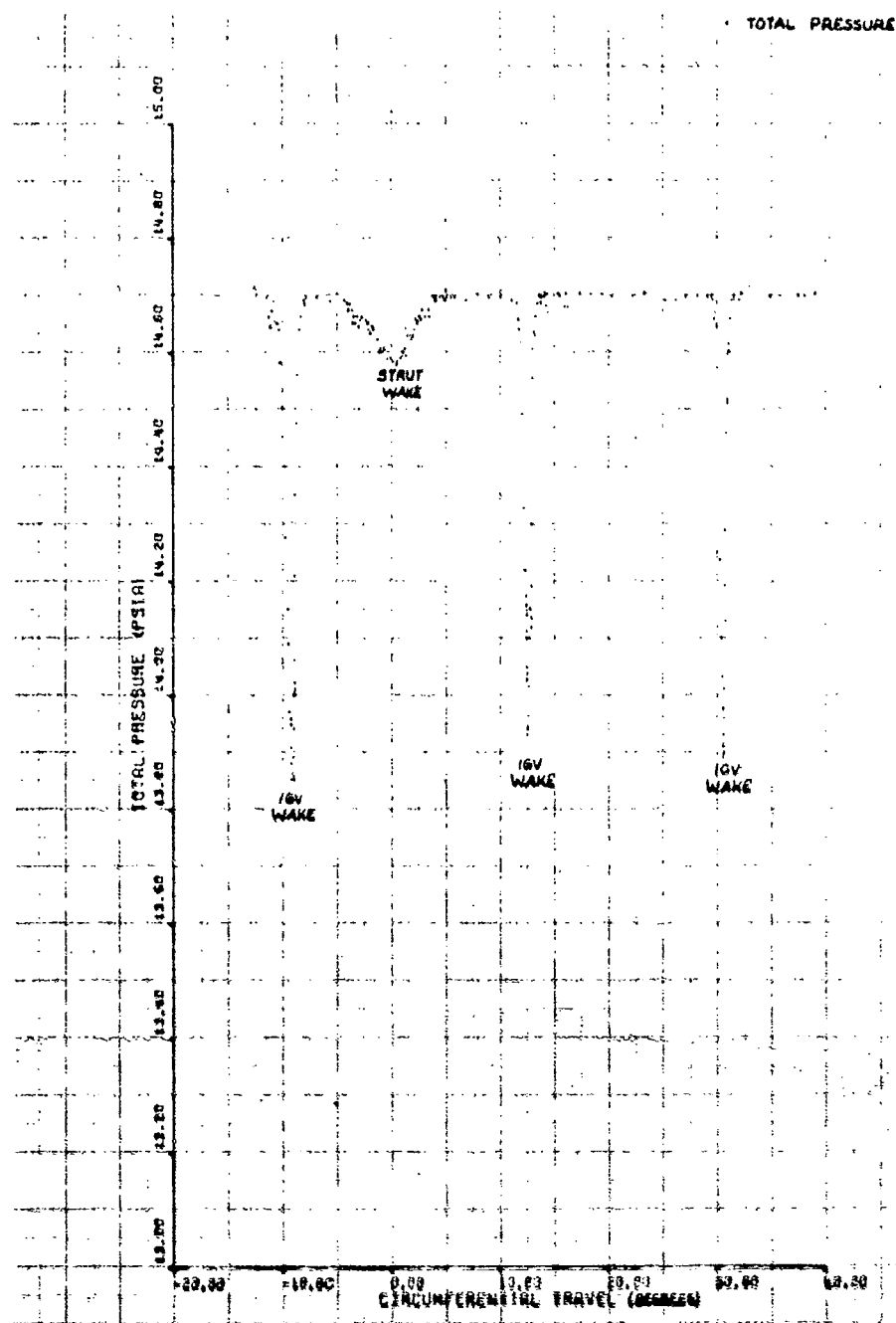


Figure 62. IGV Circumferential Traverse, Build No. 6, 100% Speed, 10-deg IGV, 50% Span.

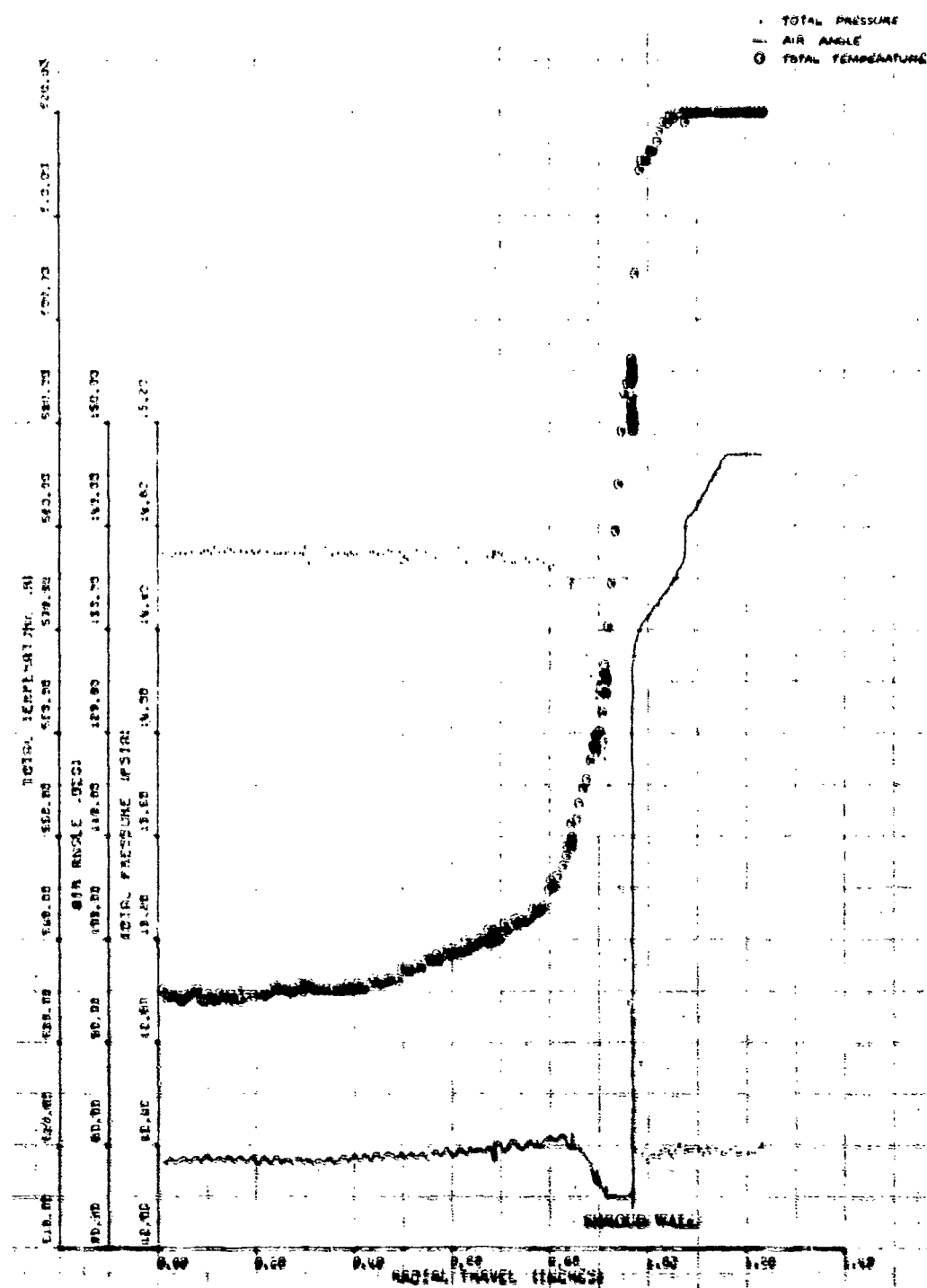


Figure 63. IGV Exit Radial Traverse, Build No. 6, 100% Speed, 10-deg IGV, Near Stall.

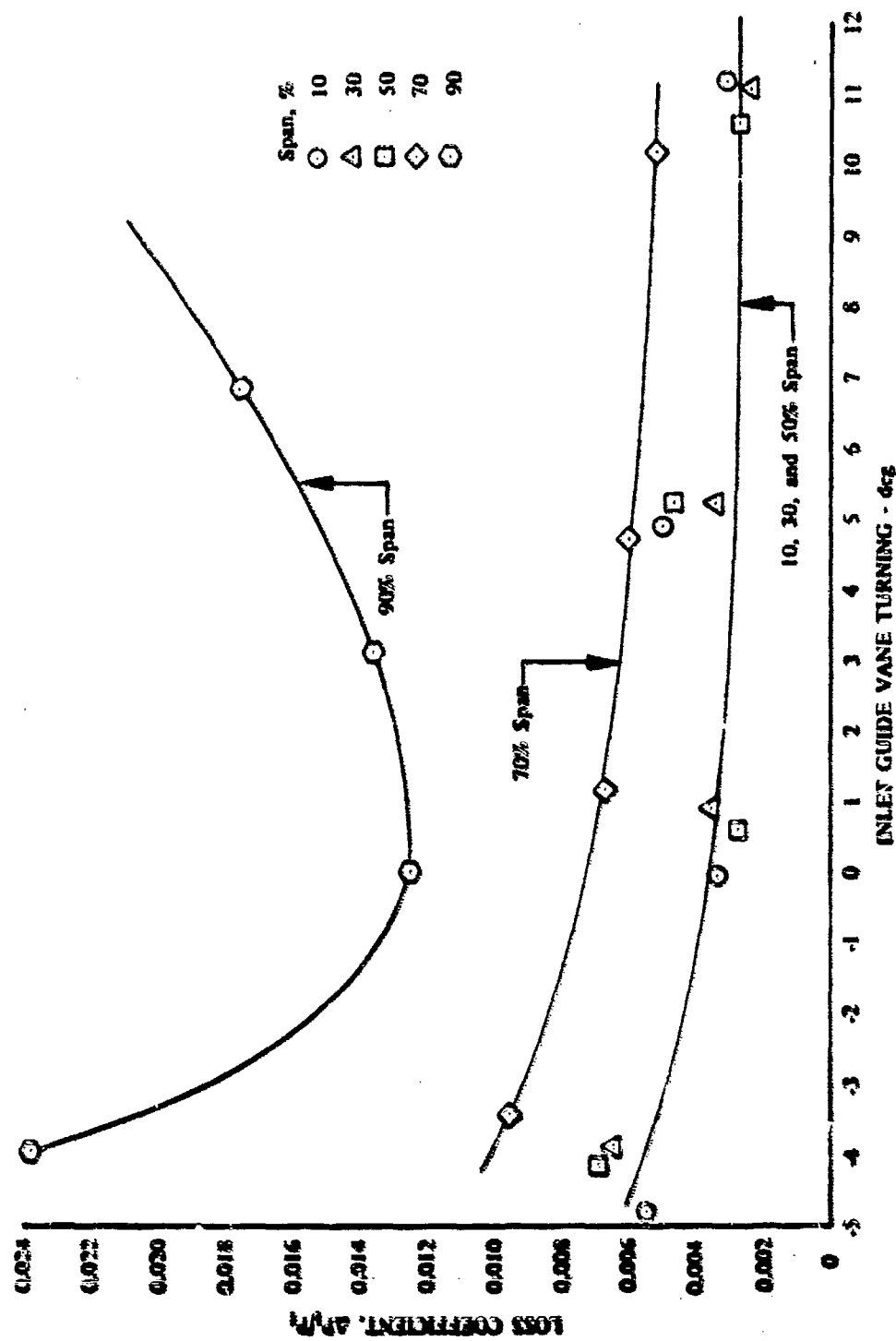


Figure 64. Build No. 6, Inlet Guide Vane Losses at Approximately 0.46 Mach Number.



TABLE XI. INLET GUIDE VANE CIRCUMFERENTIAL TRAVERSE DATA - 100% SPEED, 10-DEG IGV SETTING

Circumferentially Integrated Quantities					
Percent Span	10.1389	30.2170	50.2768	70.4209	90.2630
Strut Average Radial Travel	0.1014	0.3022	0.5028	0.7042	0.9026
Vane Average Radial Travel	0.1003	0.3018	0.5020	0.7046	0.9022
Average Hub Static Pressure	12.4440	12.4440	12.4440	12.4440	12.4440
Average Shroud Static Pressure	12.4440	12.4440	12.4440	12.4440	12.4440
Spanwise Static Pressure	12.4440	12.4440	12.4440	12.4440	12.4440
Incremental Flow (S)	0.0246	0.0294	0.0319	0.0354	0.0362
Incremental Flow (V)	0.0239	0.0293	0.0314	0.0355	0.0360
Mass Average Pressure (S)	14.5850	14.6153	14.6169	14.5801	14.4525
Mass Average Pressure (V)	14.6720	14.6751	14.6684	14.6332	14.4308
Mass Average Angle (S)	78.7595	78.9085	79.0077	79.6817	82.6728
Mass Average Angle (V)	78.8080	78.9434	79.5941	79.8631	83.2852
Weighted Pressure	14.6459	14.6572	14.6529	14.6172	14.4373
Weighted Angle	78.7934	78.9329	79.4182	79.8086	83.1014
Weighted Flow	0.0241	0.0293	0.0315	0.0355	0.0360
Loss Coefficient (S)	0.007419	0.005357	0.005250	0.007751	0.016435
Loss Coefficient (V)	0.001500	0.001283	0.001743	0.004141	0.017910
Weighted Loss Coefficient	0.003276	0.002505	0.002795	0.005224	0.017458
Total Integrated Quantities					
Total Incremental Flow	0.15652				
Spanwise Mass Average Total Pressure	14.59489				
Spanwise Mass Average Air Angle	79.94775				
Total Pressure Loss	0.00674				
Integrated Flow	3.13035				
Flow Coefficient of Inlet	0.95331				
Mach Number In	0.43984				
Guide Vane Angle	96.67302				

NOTE:

(S) denotes parameter pertaining to gaps containing both IGV and strut wakes.  
(V) pertains to gaps containing IGV wakes only.

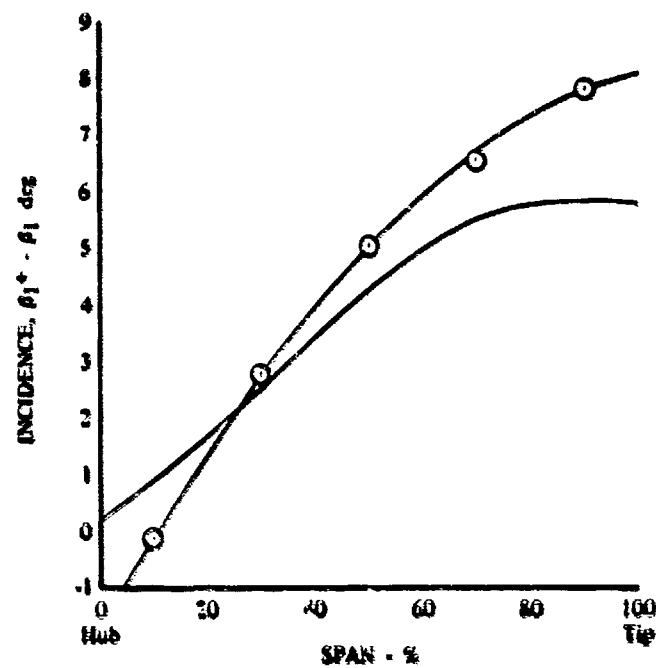
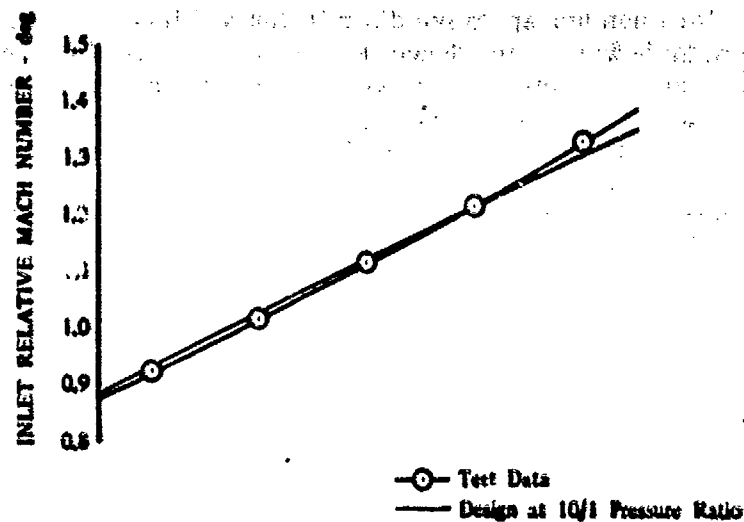


Figure 65. Inducer Inlet Conditions, 100% Speed, 10-deg IGV.

The inlet relative Mach number spanwise distribution and level are both in close agreement with design; however, incidence is more positive (stalled) in the outer half of the passage than anticipated. Increasing the speed and reducing the prewhirl (for instance, to 101% speed and -4-deg of prewhirl) raises the relative Mach number and increases the amount of stall incidence, as shown in Figure 66.

Static pressure profiles generated by wall taps through the inlet are presented in Appendix I for both Builds No. 3 and 6 at comparative conditions.

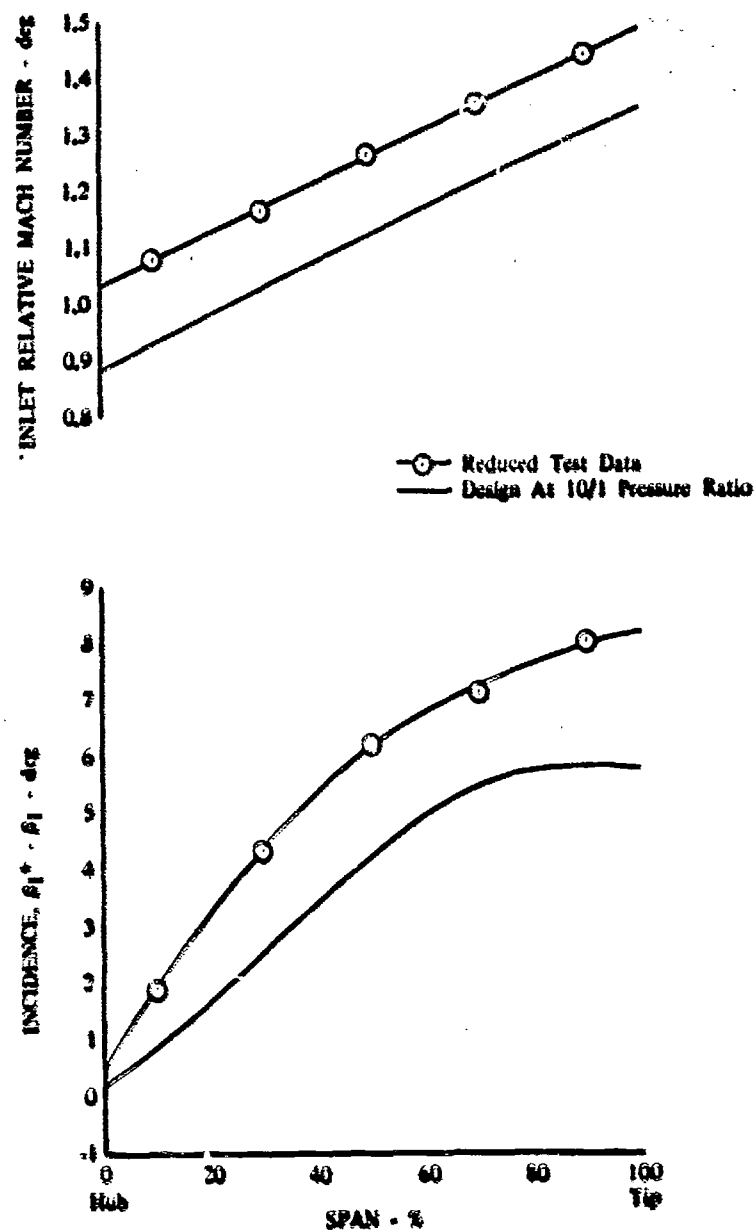


Figure 66. Inducer Inlet Conditions, 101% Speed, -4-deg IGV.

## Inducer

Analysis of inducer performance was divided into Builds No. 3 and 6, with a majority of the traverse data used obtained in Build No. 6. Build No. 3 inducer data at 95% speed and 10 deg of prewhirl were reduced using inlet conditions from the only available inlet guide vane traverse point during that build. These data are shown in Figure 67. Inlet relative Mach number distribution was in good agreement with design values, but lower overall due to the decreased speed (95%). The average inducer incidence angle was about 2 deg above the design value because flow rate and, consequently, axial velocity were slightly below design. The inducer pressure ratio and efficiency for this point were 1.67 and 85.6%, respectively.

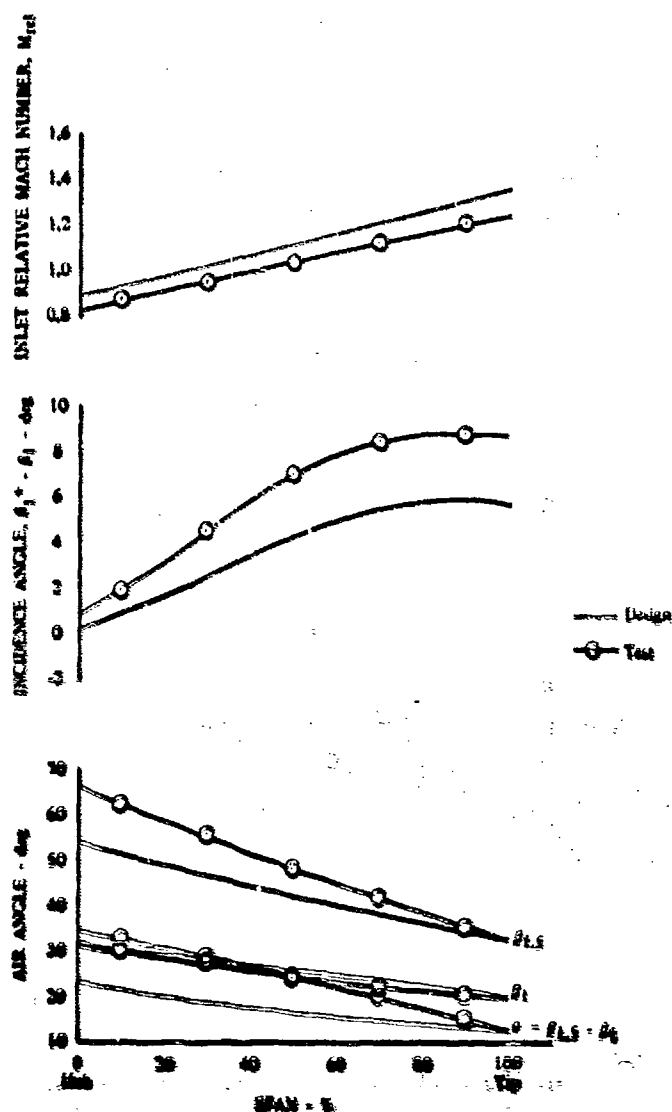


Figure 67. Inducer Inlet Conditions, Build No. 3, 95% Speed, 10-deg IGV, Near Stall.

The inducer discharge conditions calculated for this point indicated that the impeller was operating below design incidence over most of the span. The low incidence in the hub region was caused by overturning in the hub region of the inducer.

Sufficient data were obtained in Build No. 6 to completely define the blade element and overall performance of the inducer. Inducer pressure ratio and efficiency are presented as functions of weight flow in Figure 68. The inducer exceeded its design pressure ratio, but at a lower than goal efficiency. The efficiency of the inducer decreased markedly with speed above 95% of design speed; pressure ratio also decreased for constant inlet guide vane settings. The low prewhirls at 101% speed increased the pressure ratio and flow of the inducer, but efficiency monotonically decreased with increasing flow. Inducer exit traverse data also help explain the loss in performance at high speed. A traverse plot at 101% speed and -4-deg inlet guide vane setting in Figure 69 shows that a severe inducer exit air angle and total pressure profiles were generated when the inducer was operated at an inlet relative Mach number considerably higher than design. The radial travel increases from the hub to shroud, with the shroud wall being at approximately 0.62 in. Tabulated data for this point are presented in Table XII.

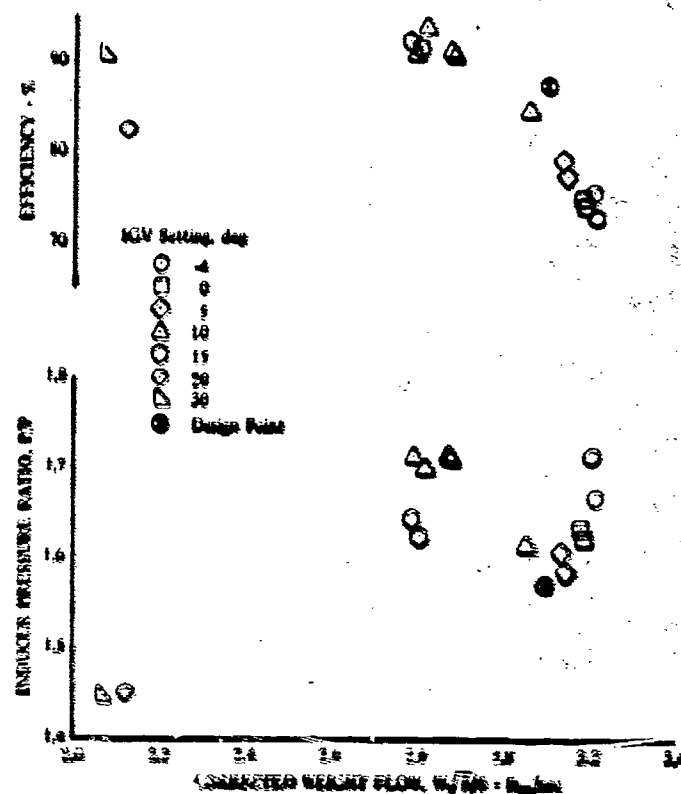


Figure 68. Inducer Performance, Build No. 6.

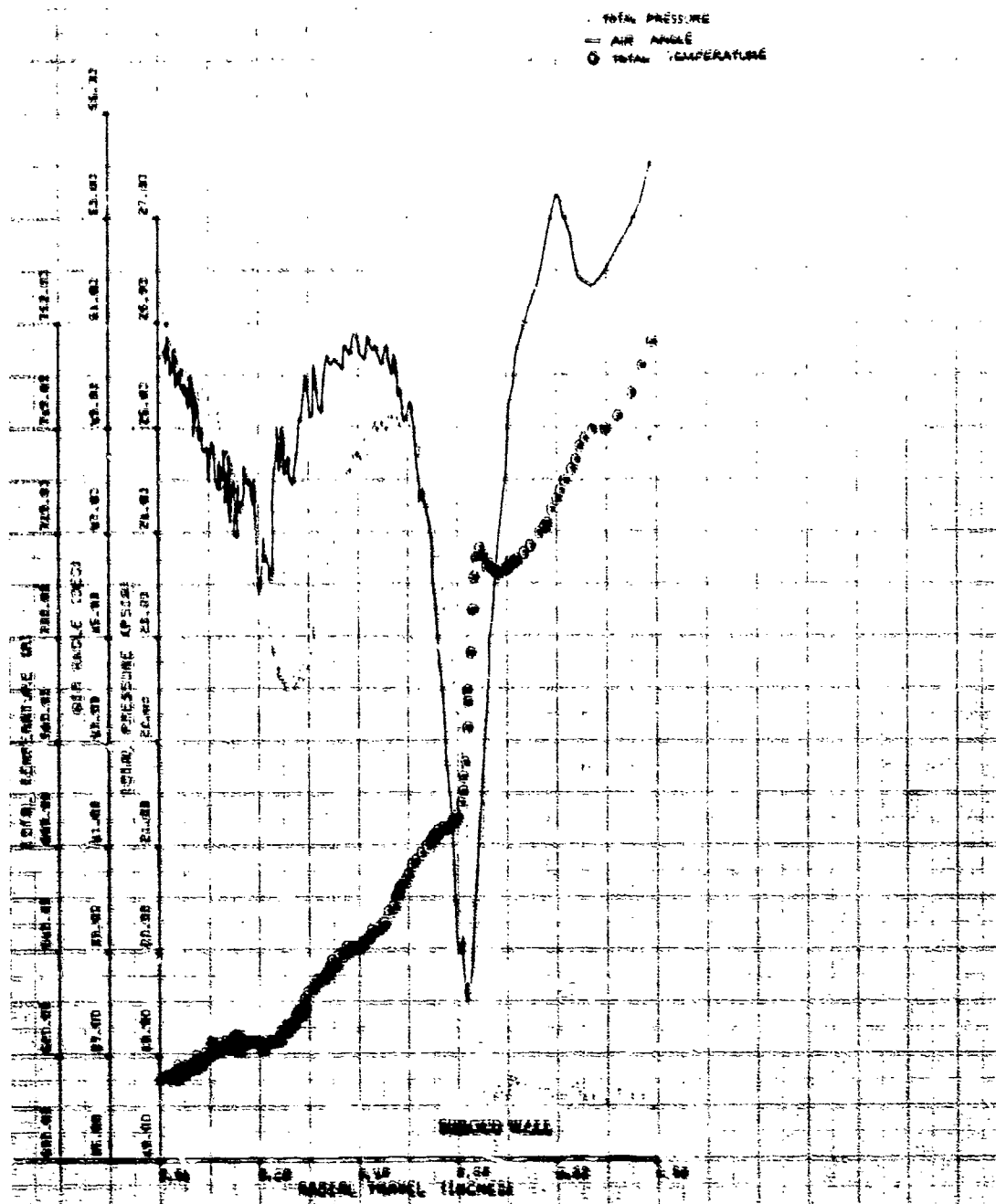


Figure 69. Inducer Exit Traverse, Build No. 6, 101% Speed, -4-deg IGV, Wide Open Discharge.

Reducing speed to 100% of design and increasing prewhirl to 10 deg, which allows the inducer to operate at design inlet Mach number, improved the midspan problem with the inducer. The majority of the inducer inefficiency at the design point appears near the tip as total pressure loss, overturning, and excessive temperature rise, as shown in Figure 70 and Table XIII. A further decrease in speed to 95% of design speed, as shown in Figure 71, continued to improve the performance of the inducer, allowing it to reach efficiencies of over 90% at pressure ratios of over 1.7:1.

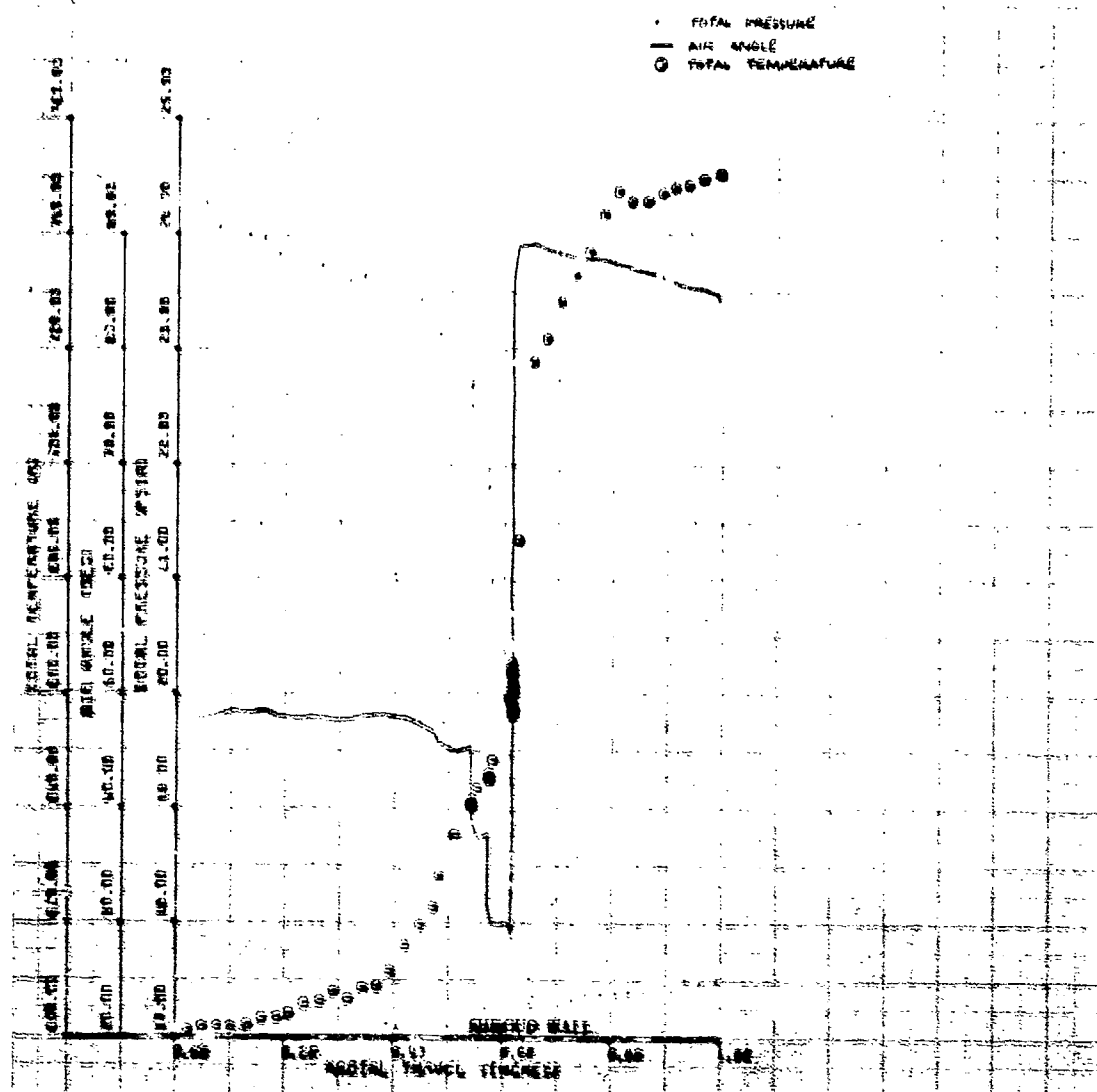


Figure 70. Inducer Exit Traverse, Build No. 6, 100% Speed, 10-deg IGV.

TABLE XII. INDUCER EXIT TRAVERSE DATA, 101% SPEED, -4-DEG IGV SETTING

* * * Inducer Exit * * *										
Mass Average Total Pressure										
24.923										
Mass Average Total Temperature										
631.963										
Inducer Pressure Ratio										
1.696										
Inducer Temperature Ratio										
1.218										
Inducer Efficiency										
0.745										
Inducer Exit Velocity Triangles										
MO	VO	ALPHA	VM	VU	U	WU	B	WO	MREL	I VO/VOMAX
10	0.697	808.673	35.740	472.362	656.374	1044.047	50.623	611.078	0.526	3.076
30	0.716	834.029	58.747	713.002	432.702	1126.575	45.779	994.903	0.854	3.626
50	0.582	691.862	53.639	557.156	410.182	1209.103	34.891	974.011	0.819	10.138
70	0.649	770.935	62.441	683.462	356.677	1291.630	36.167	1158.127	0.975	4.032
90	0.560	680.815	54.008	550.852	400.089	1374.158	29.488	1119.039	0.921	6.161
										0.816

TABLE XIII. INDUCER EXIT TRAVERSE DATA, 100% SPEED, 10-DEG IGV SETTING

* * * Inducer Exit * * *										
Mass Average Total Pressure										
23.577										
Mass Average Total Temperature										
607.093										
Inducer Pressure Ratio										
1.604										
Inducer Temperature Ratio										
1.170										
Inducer Efficiency										
0.850										
Inducer Exit Velocity Triangles										
MO	VO	ALPHA	VM	VU	U	WU	B	WO	MREL	I VO/VOMAX
10	0.708	812.781	55.115	666.729	464.848	1032.187	49.604	875.444	0.762	4.095
30	0.697	798.528	54.707	651.771	461.347	1113.778	44.971	922.210	0.805	4.428
50	0.683	785.786	54.003	635.744	461.831	1195.368	40.914	970.694	0.844	4.115
70	0.678	785.521	54.259	637.668	458.718	1276.959	37.929	1037.370	0.895	2.270
90	0.607	717.287	46.915	523.867	489.963	1358.549	31.095	1014.337	0.858	4.554
										0.882



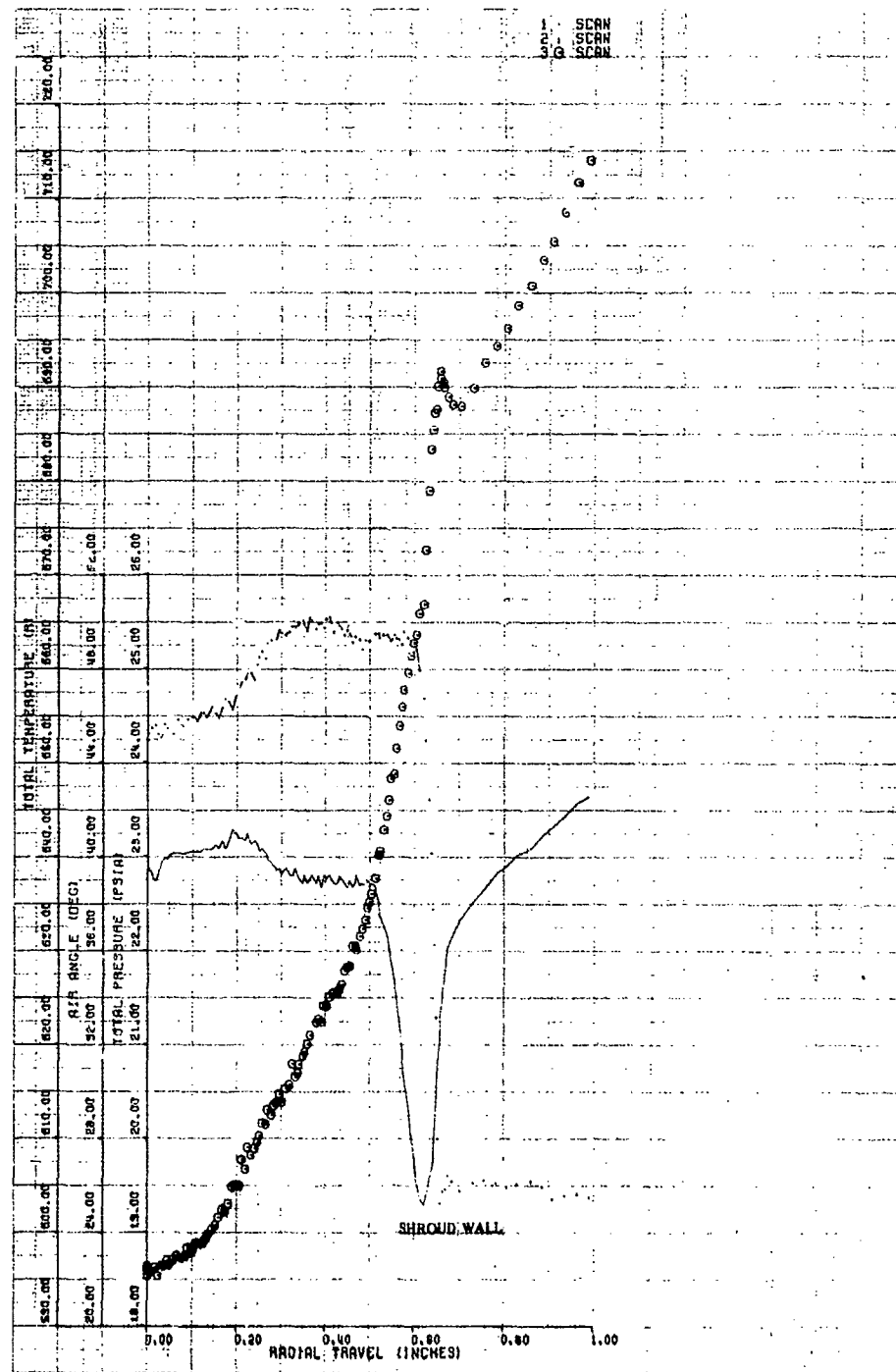


Figure 71. Inducer Exit Traverse, Build No. 6, 95% Speed, 10-deg IGV, Near Stall.

Inducer loss coefficient is presented in Figure 72 to demonstrate the level of improvement from overspeed (101%) to design (100%) conditions in conventional terms. The effect of the higher inlet Mach number and incidence on the inducer losses is easily seen in this figure. These data, coupled with the fact that the falloff in inducer efficiency at high flow shows a dependence on inlet guide vane setting, lead to the conclusion that these losses are largely dependent upon the high inlet relative Mach number.

Inducer exit traverse data are compared with impeller design inlet conditions in Figures 73 and 74 for 100% speed and 10 deg of prewhirl. Impeller inlet relative Mach number distribution and level agree well with the predicted design values; however, the incidence distribution shows the impeller incidence to be more negative than the design value, as did the data available from Build No. 3. The hub side overturning that causes this negative incidence is most apparent in Figure 74. Similar information is presented for the 101% design speed, -4-deg prewhirl condition in Figures 75 and 76.

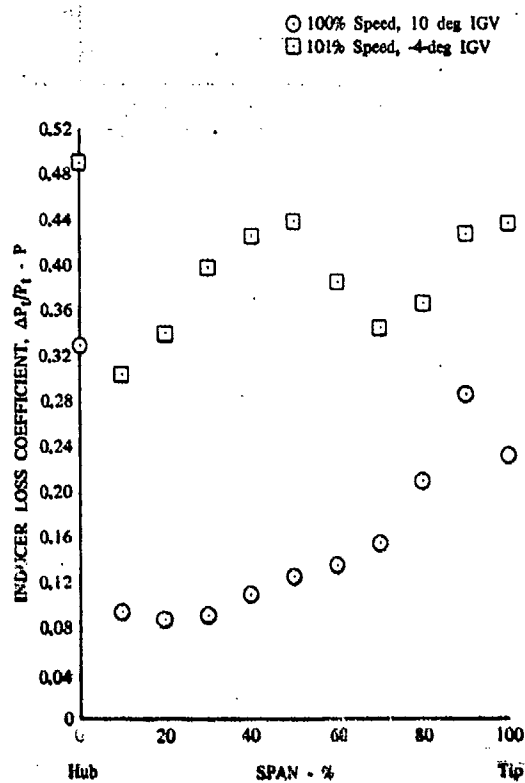


Figure 72. Inducer Losses.

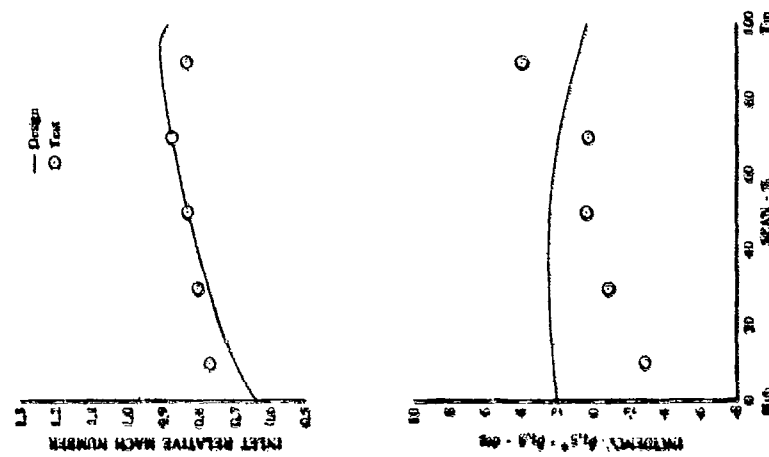


Figure 73. Impeller Inlet Conditions,  
100% Design Speed, 10-deg  
IGV.

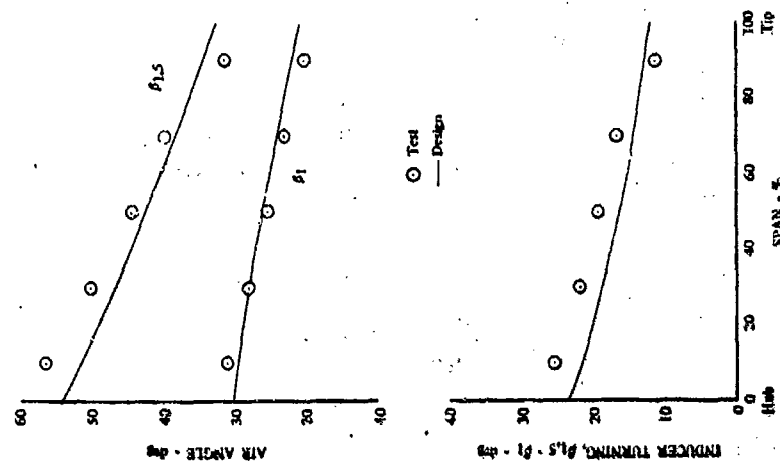


Figure 74. Inducer Exit Air Angle Profile,  
100% Design Speed, 10-deg  
IGV.

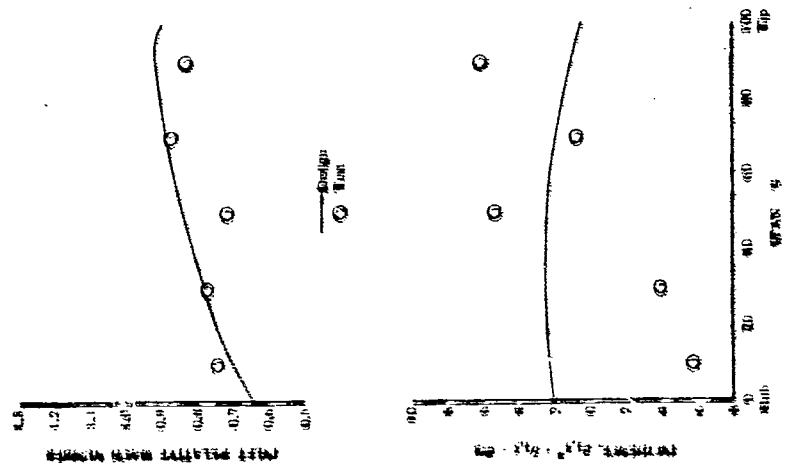


Figure 75. Impeller Inlet Conditions.  
101% Speed, -4-deg IGV.

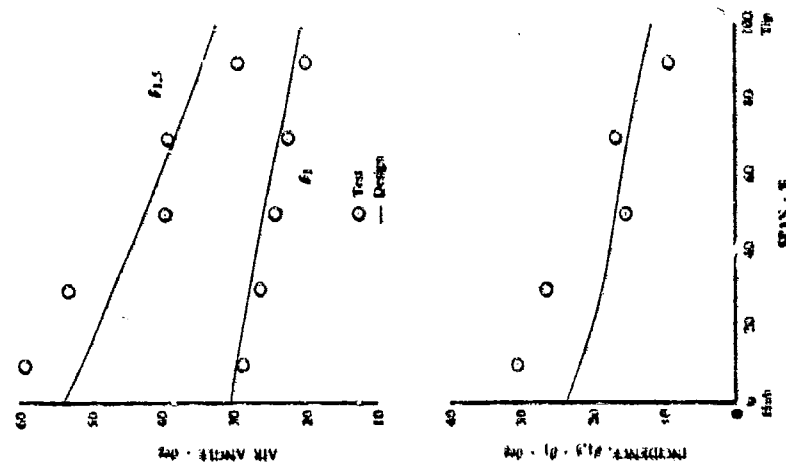


Figure 76. Inducer Exit Air Angle Profile.  
101% Speed, -4-deg IGV.

The bulk of the traverse data were reduced by assuming that the static pressure across the span behind the inlet guide vanes was a constant pressure equal to that of the shroud wall behind the inducer. This assumption was necessary due to the lack of static pressure taps on the hub wall or static pressure traverse data. Performance in these planes was also reduced for some points using static pressure distributions generated by inputting geometric and aerodynamic information into a streamline analysis computer program. The static pressure profile comparison for the IGV exit (inducer inlet) is shown in Figure 77, and the inducer exit static pressure distribution comparison is shown in Figure 78.

Since the data reduction program would only accept linear distribution of static pressure, the profile generated by the streamline analysis was approximated as shown by a straight line from hub to shroud. Use of these static pressures in the data reduction program resulted in the profiles previously presented in Figures 72 through 76. The use of the initial constant pressure assumption yielded the results shown in Figures 79 and 80. There was only a small effect on impeller inlet relative Mach number; however, the change in calculated hub incidence was quite large. Incidence at 10% span from the hub was increased. Relative inducer exit air angle was, of course, similarly affected. This difference in inducer exit conditions should be considered during use of any of the standard reduction printouts presented in Appendix I.

The effect of the inducer on overall performance, other than its pressure ratio and efficiency characteristics, was evaluated in terms of any limitations it may have imposed on the impeller or overall performance. The effect of the poor high-speed inducer performance on the impeller was minimal, and is discussed in the following impeller component performance section. With respect to overall performance, the inducer was initially thought to be the flow-limiting component in the compressor. The correlation of maximum or choke flow presented in Figure 81 is composed of Build No. 3 data and was used to develop this logic. The slope of the speed-flow curve decreases sharply above 95% speed at 0-deg prewhirl, above 90 to 95% at 10-deg prewhirl, and above 90% speed at 20-deg prewhirl. This change in slope is generally a precursor to choking of the annulus and was considered to be evidence of inducer choking. The vertically common maximum flow at lower speeds, regardless of prewhirl, is due to diffuser choking.

The same relationship for the Build No. 6 data (Figure 82) did not exhibit similar characteristics. Choke flow at 70% speed was somewhat lower than Build No. 3, possibly from increased blockage in the diffuser due to the leading-edge damage. The slope of the curve did not fall off rapidly at high speed and continued to increase with lower prewhirl at maximum speed. The high-speed choke flow in Build No. 6 exceeded that projected for Build No. 3.

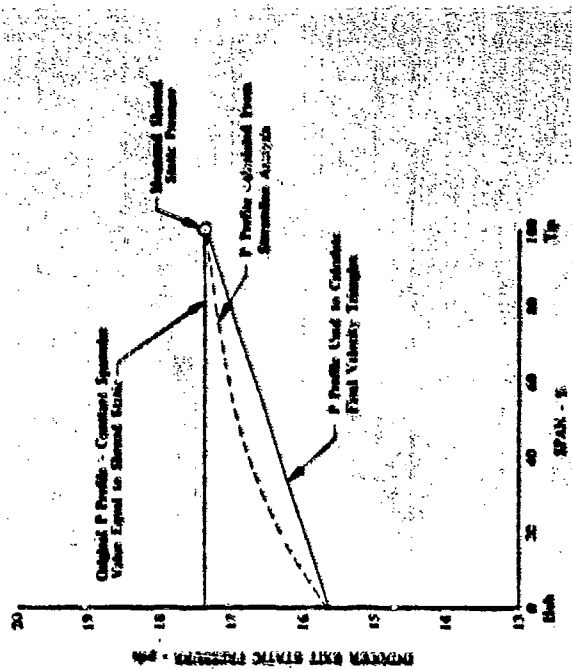


Figure 78. Inducer Exit Static Pressure Profile, 100% Speed, 10-deg IGV.

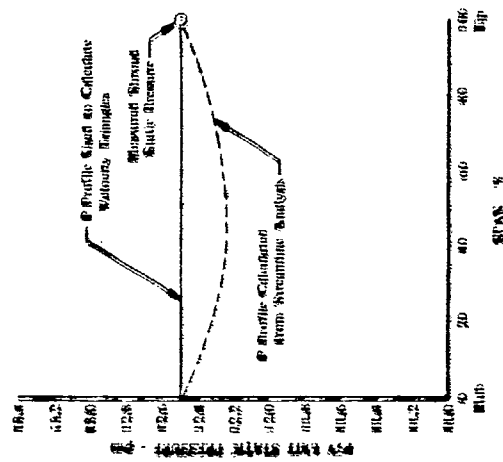


Figure 77. IGV Exit Static Pressure Profile, 100% Speed, 10-deg IGV.

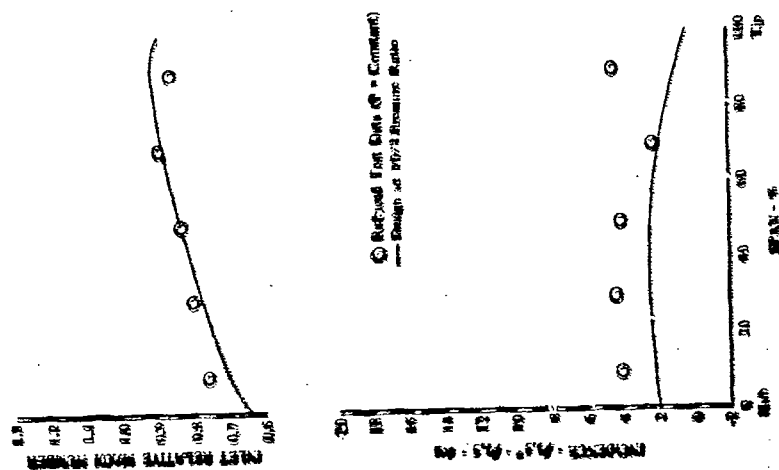


Figure 79. Impeller Inlet Conditions, 100% Speed, 10-deg IGV.

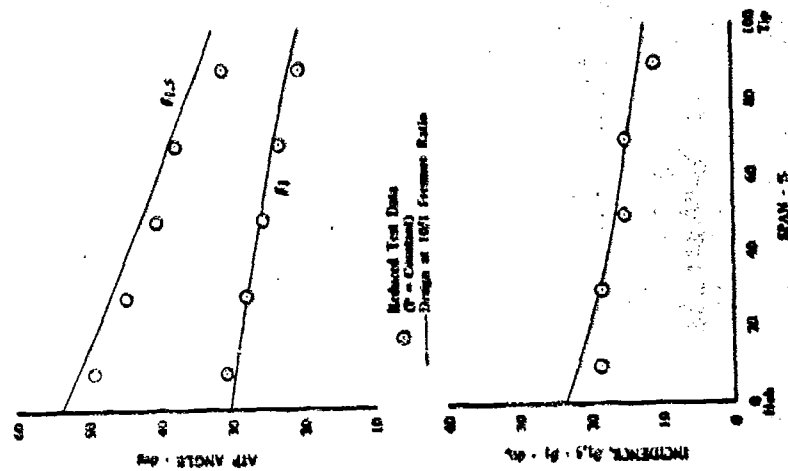


Figure 80. Inducer Exit Air Angle Profile, 100% Speed, 10-deg IGV.

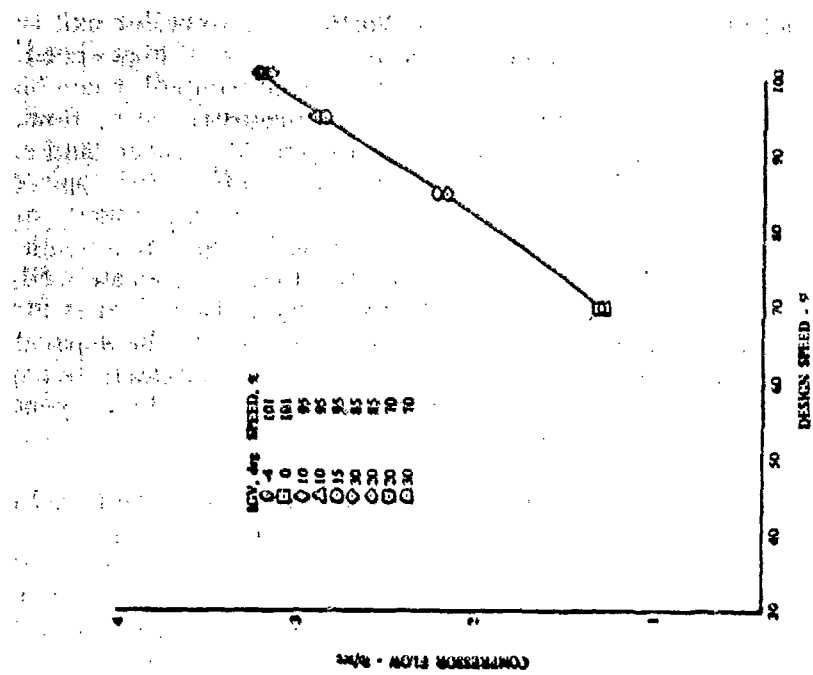


Figure 82. Build No. 6 Choke Point Flow as a Function of Rotor Speed.

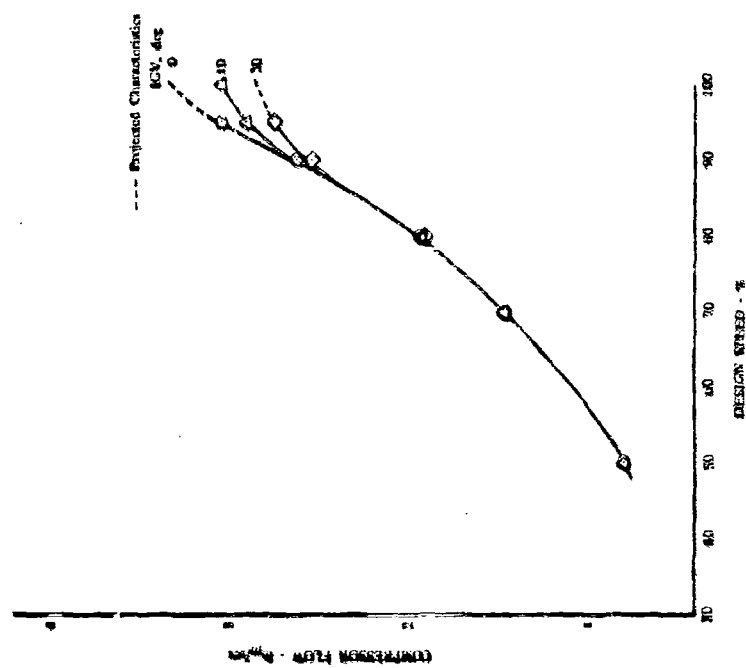


Figure 81. Choke Point Flow as a Function of Rotor Speed, Build No. 3.



## Impeller

Impeller performance was well defined from a combination of Builds No. 3 and 6 data. Low-speed definition was available from Build No. 3 impeller exit traverses, and Build No. 6 impeller exit traverses defined its operation at high speed. An internal flow analysis was also used to analyze the inducer-impeller combination and was available for every data point. The impeller pressure ratio, flow, and efficiency data from Build No. 6 are presented in Figure 83. These data showed that the impeller produced its design pressure ratio at an efficiency approximately 5 percentage points higher than its design goal and at a flow rate slightly higher than design. The consistent high efficiency of the impeller and the smooth pressure rise characteristic showed that the impeller continued to operate well, even when its inlet conditions were being affected by the large inducer losses at high speed. This good high-speed performance was due, in part, to the separate inducer-impeller concept as the impeller performance demonstrated its capability to work efficiently at conditions that would have severely affected a conventionally designed impeller with an integral inducer.

The tabulated data for the impeller performance can be found on the impeller traverse printouts in Appendix I. Since insufficient data were obtained to properly separate the impeller and inducer performance generated in Build No. 3, the combined performance is shown in Figure 84 with comparative Build No. 6 results. The Build No. 6 inducer-impeller pressure ratio was slightly higher than that of Build No. 3, possibly due in part to the Build No. 6 impeller having a 0.020-in. larger diameter.

Build No. 3 inducer and impeller performances from an internal flow analysis program are shown in Figure 85. Similar Build No. 6 inducer and impeller performance are shown in Figure 86.

Inducer and impeller efficiency as a function of incidence was also generated by the internal performance analysis and is presented in Figure 87 for Build No. 3 data and in Figure 88 for Build No. 6 data. A limited amount of data that were obtained in Build No. 2 with an undersized diffuser is also presented in Figure 87 for comparative purposes. The lower efficiency was due to the inducer operating in a stalled condition. Low-speed characteristics are essentially identical for Builds No. 3 and 6. The inducer-impeller was operating on the stalled side of its performance characteristic and efficiency decreased with increasing incidence. It appeared from the Build No. 3 characteristics, that the inducer-impeller and diffuser were matched at 95% speed, and at 100% speed and 10-deg prewhirl, the match may be on the negative or choke side of the incidence characteristics. Build No. 6 data could be interpreted similarly if only 10-deg IGV setting data were obtained at 100% speed; however, other 101% speed data at different prewhirls behaved in a manner no different than that observed at lower speeds. Build No. 6 data at 95% speed also failed to exhibit the peaking effect demonstrated in Build No. 3, hence it is probable that Build No. 6 operated at slightly positive (stall) incidence at 95 to 101% speeds.

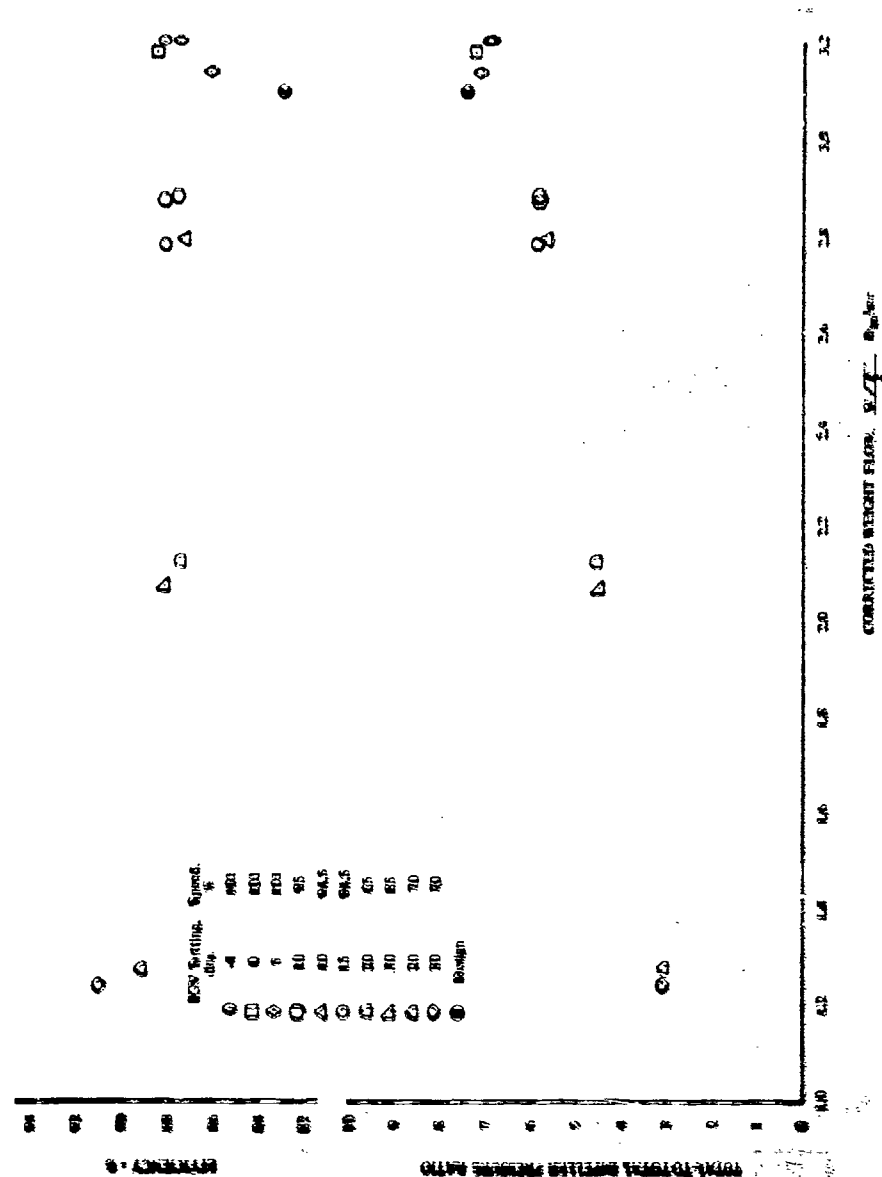


Figure 83. Build No. 6 Impeller Performance Derived From Traverse Data.

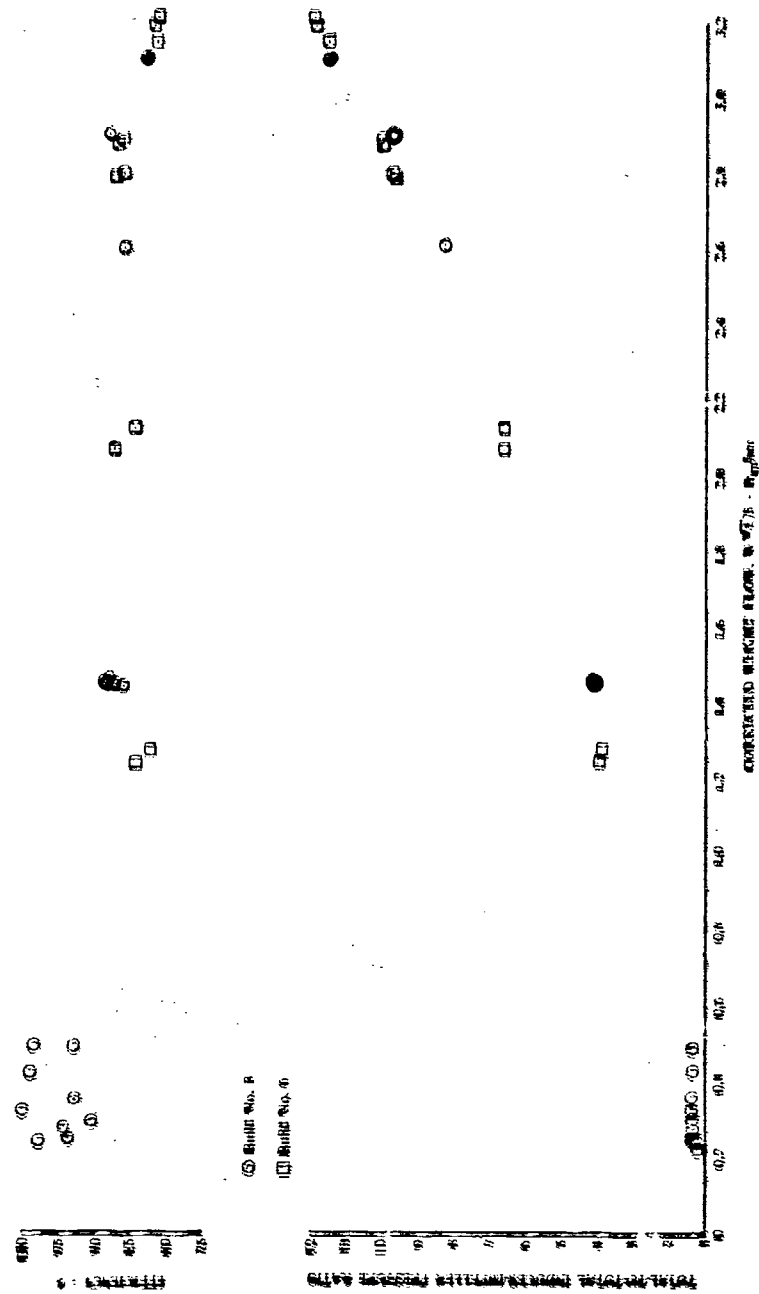


Figure 84. Inducer-Impeller Performance Derived From Traverse Data.

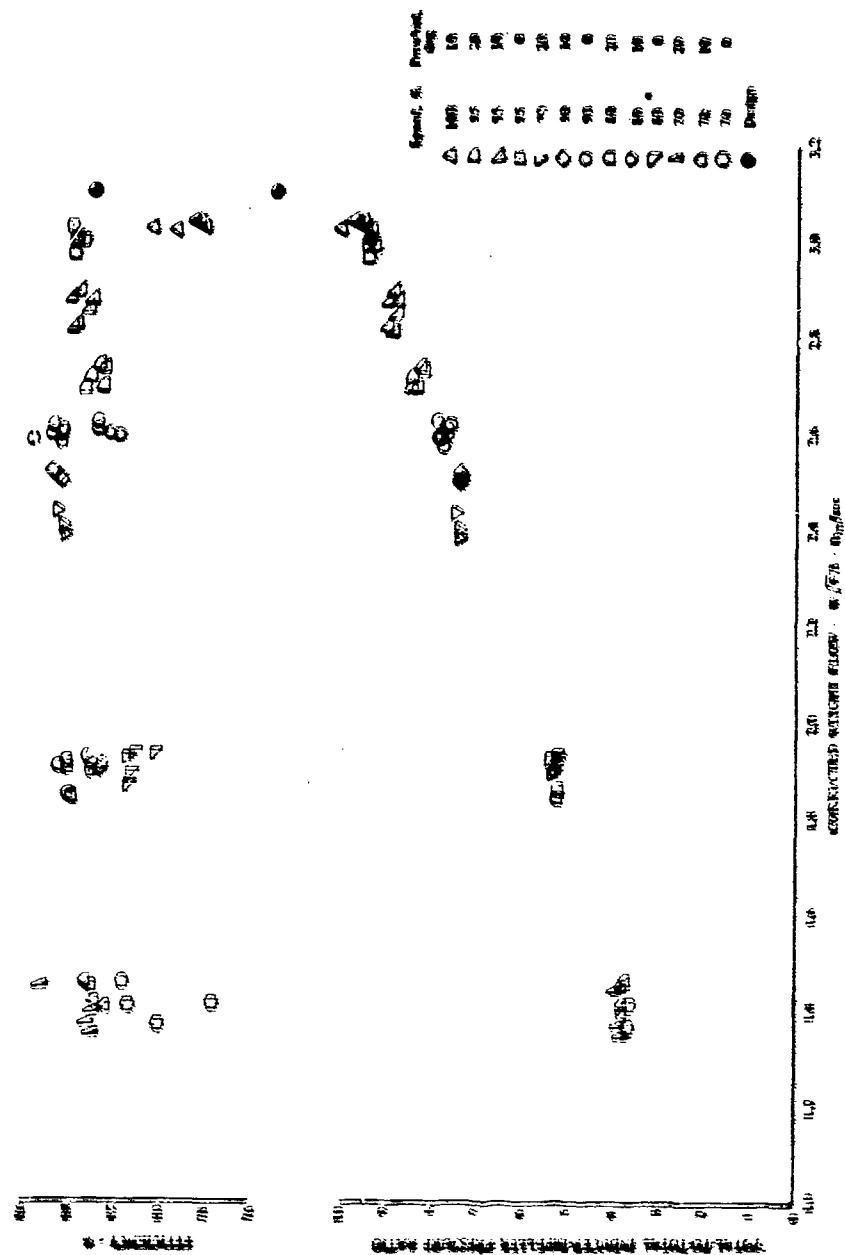


Figure 65. Build No. 3 Impeller Performance Map Derived From Internal Flow Analysis.

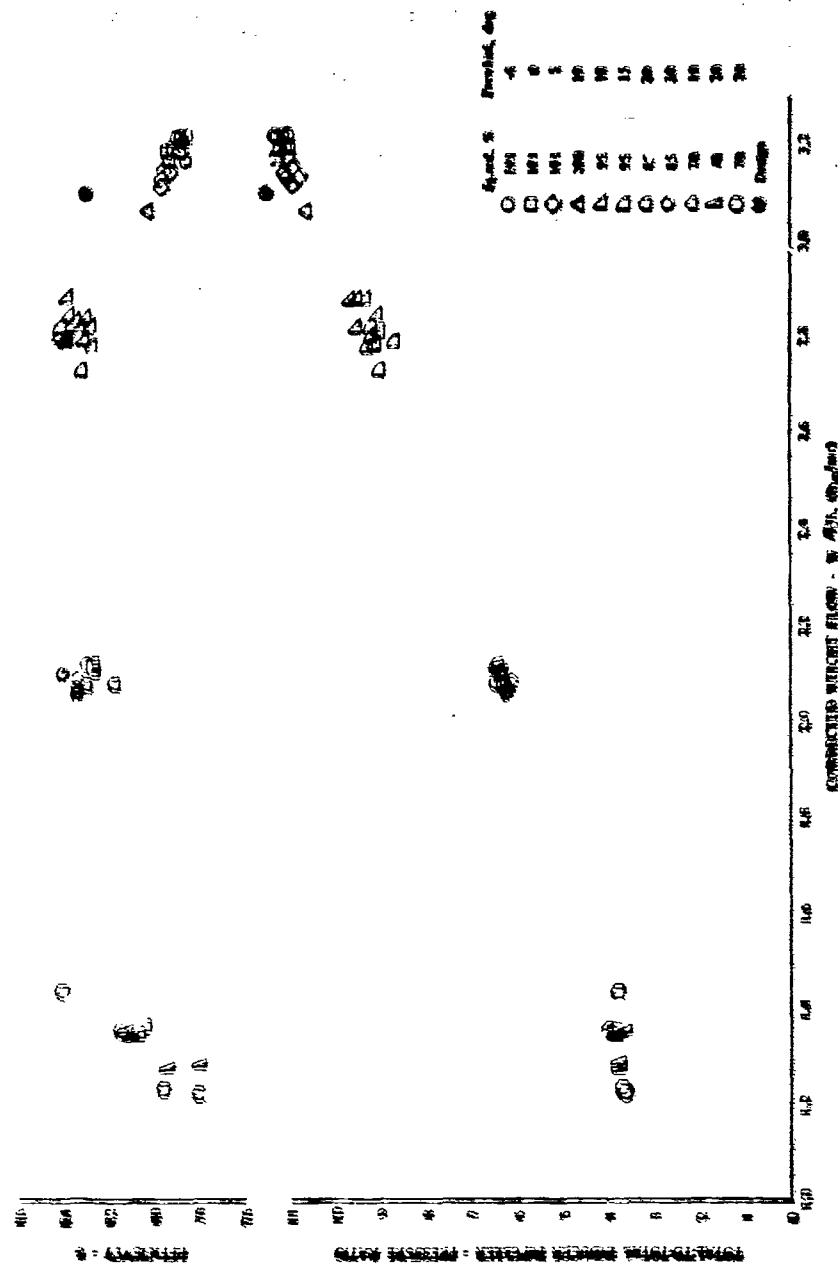


Figure 66. Build No. 6 Inducer-Impeller Performance Map Derived From Internal Analysis.

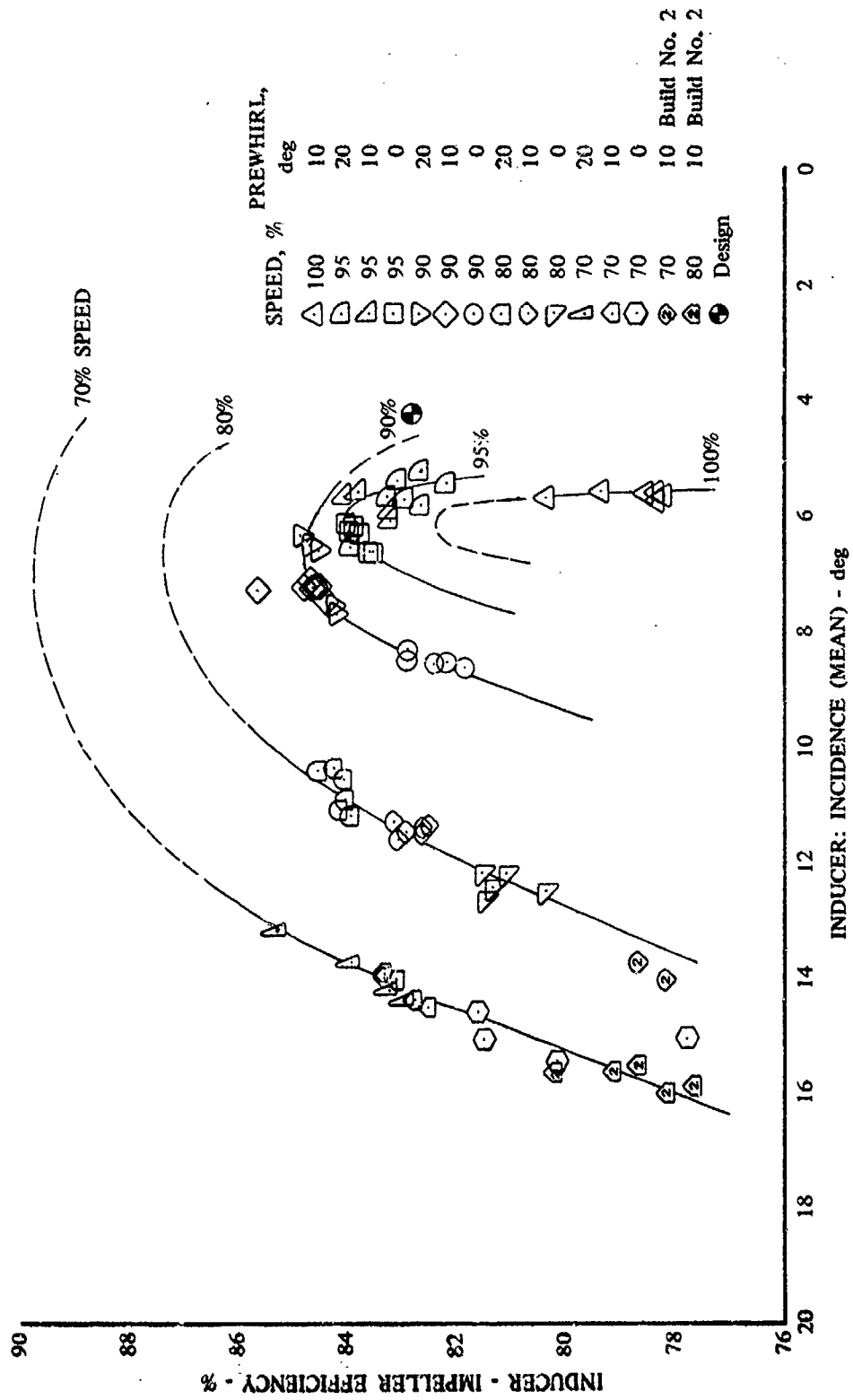


Figure 87. Build No. 3 Impeller Efficiency-Incidence Characteristic.

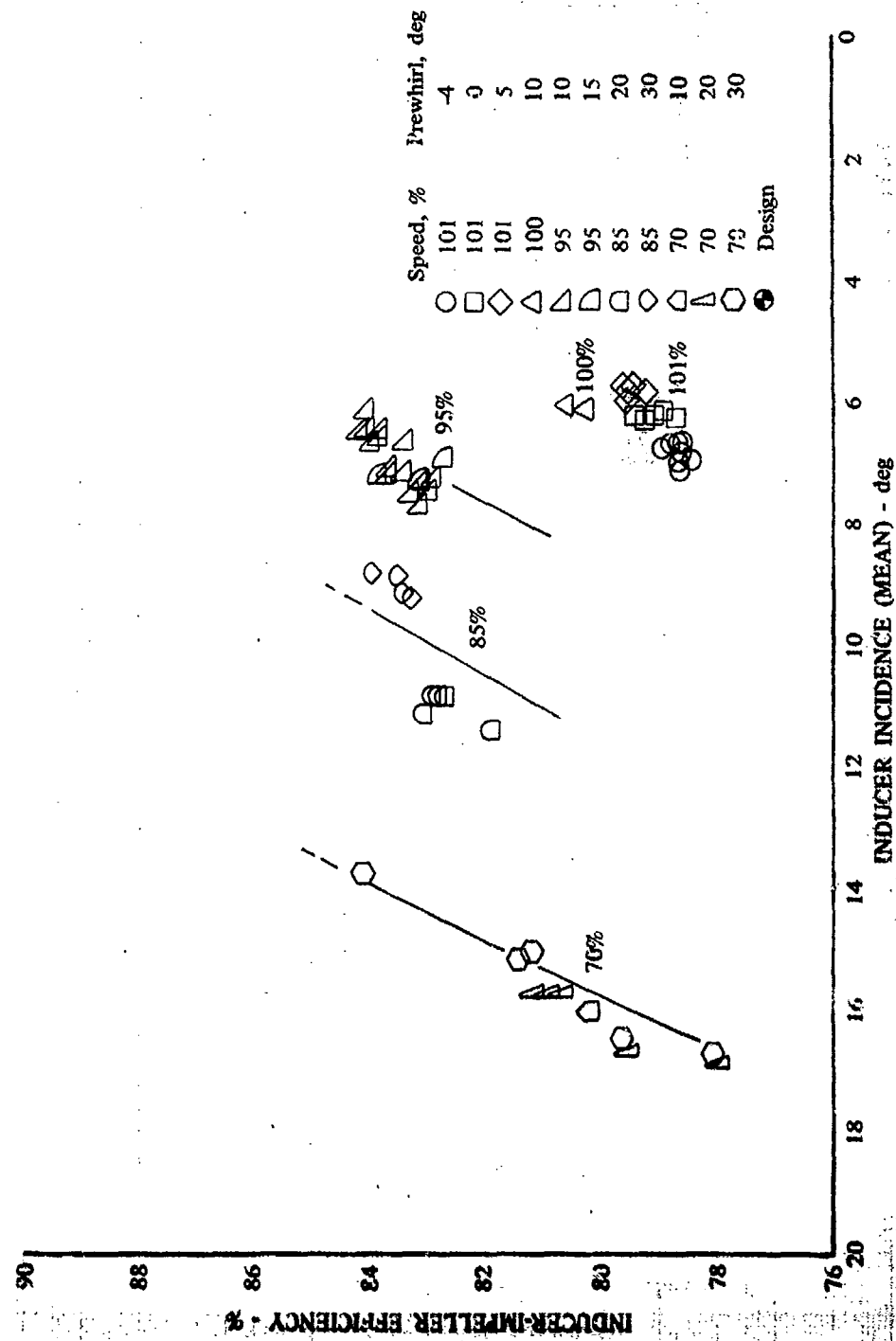


Figure 88. Build No. 6 Inducer-Impeller Efficiency-Incidence Characteristic.

The internal performance analysis was also used to demonstrate the effect of prewhirl on inducer-impeller performance, as shown in Figure 89 at 101% speed. The increase in efficiency with prewhirl was due to reduced shock losses as the inlet relative Mach number was lowered, and also due to reduced profile losses as the incidence was improved. The 100% speed Build No. 3 data showed nearly the same incidence and efficiency.

Comparison of the two builds at 95% speed is shown in Figure 90. The Build No. 6 inducer-impeller was operating at a more positive incidence most probably because of the reduced airflow at this speed caused by the smaller effective diffuser throat area in the damaged Build No. 6 diffuser.

Slip factor calculated at the impeller tip (discharge) from traverse data of Builds No. 3 and 6 is presented as a function of corrected flow rate in Figure 91. The general trend of both data sets was similar and the level at near design was also similar. Low-speed data exhibit an indication of higher slip factors for the Build No. 6 testing. Impeller exit discharge coefficients calculated by using impeller exit mass average data to generate weight flow which is compared to orifice flow are presented for the same data in Figure 92. These discharge coefficients were used to generate input for the internal flow analysis for both builds. While levels varied from build to build, both exhibited the trend of high blockage at low speed, which decreased with an increase in speed and flowed to a low blockage value at flow rates corresponding to 90 to 95%. Higher speed and flow conditions again showed a considerable increase in blockage.

Impeller exit traverse data summaries for every traverse point from Builds No. 3 and 6 are presented in Appendix I. An example of these data are presented in Figure 93 for 101% speed and -4 deg of prewhirl. Examples of impeller exit traverse data for 95% speed 10-deg prewhirl from Builds No. 3 and 6 are shown in Figures 94 and 95, respectively. Impeller exit total pressure data indicated a larger boundary layer development on the shroud side than on the hub. The air angles shifted toward tangential on both hub and shroud sides, corresponding roughly to areas of falloff in total pressure. Normalized distributions of radial velocity for Build No. 6 101% speed, -4-deg prewhirl and Builds No. 3 and 6 at 95% speed are shown in Figures 96 through 98, respectively. Builds No. 3 and 6 show essentially the same characteristic as the higher speed Build No. 6 data. Generally, velocity was less than design on the shroud side, with a peak greater than design near the hub.

Temperature traverses were also obtained behind the impeller. All of the temperature traverse data are presented in Appendix I. These data were input into the traverse reduction deck and a mass average temperature was calculated. This temperature was considerably different from the average temperature measured in the exhaust collector; for example, at 101% speed and 0-deg prewhirl, the average impeller exit temperature was 40-deg hotter than the collector. Since the impeller exit temperature was measured with a one-of-a-kind experimental thermocouple and since the resultant data differed not only in level from the average collector temperature but also in profile characteristics from the check-out of this probe during a previous test, the data were considered faulty.



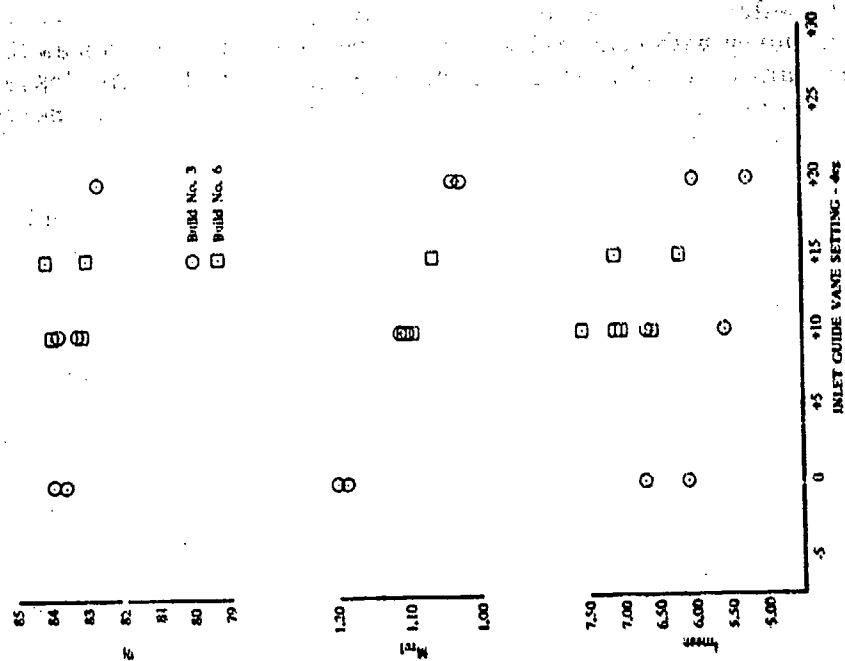


Figure 69. Effect of Prewirl on Inducer-Impeller Performance Near 10:1 Pressure Ratio.

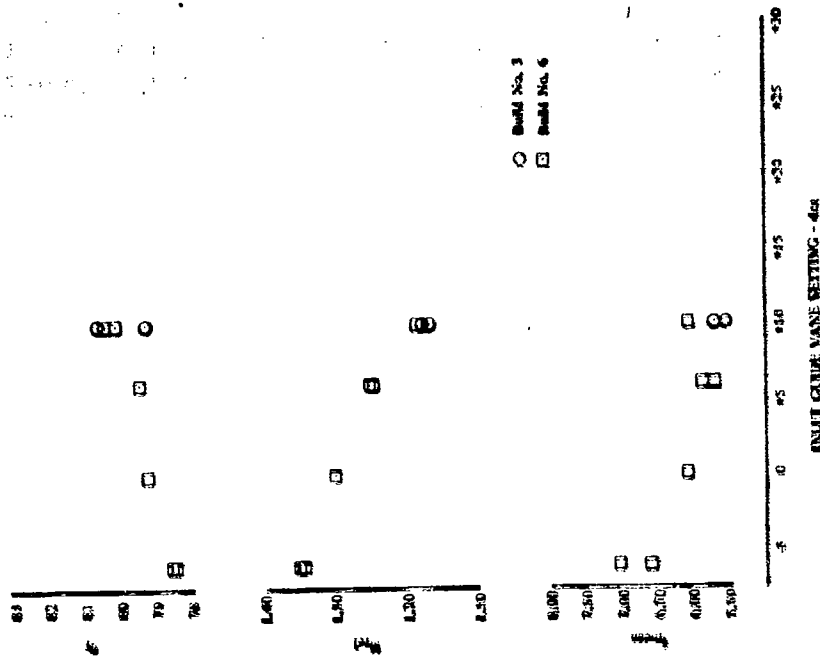


Figure 90. Effect of Prewirl on Inducer-Impeller Performance Near 8:1 Pressure Ratio.

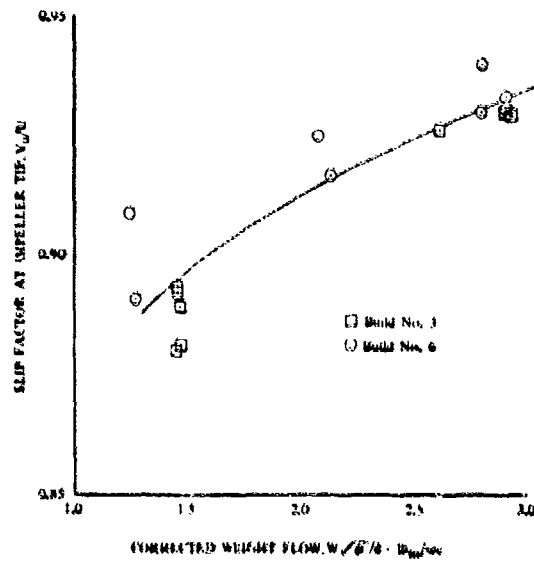


Figure 91. Impeller Exit Slip Factor.

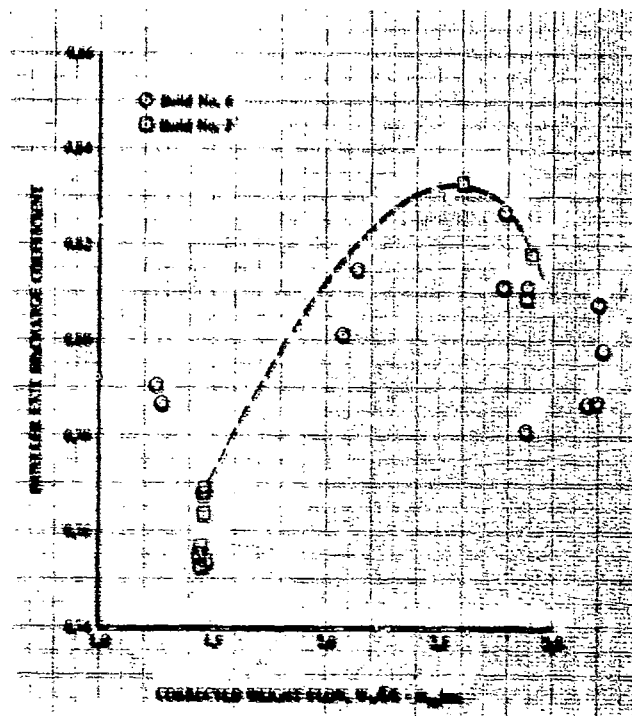


Figure 92. Impeller Exit Discharge Coefficient.

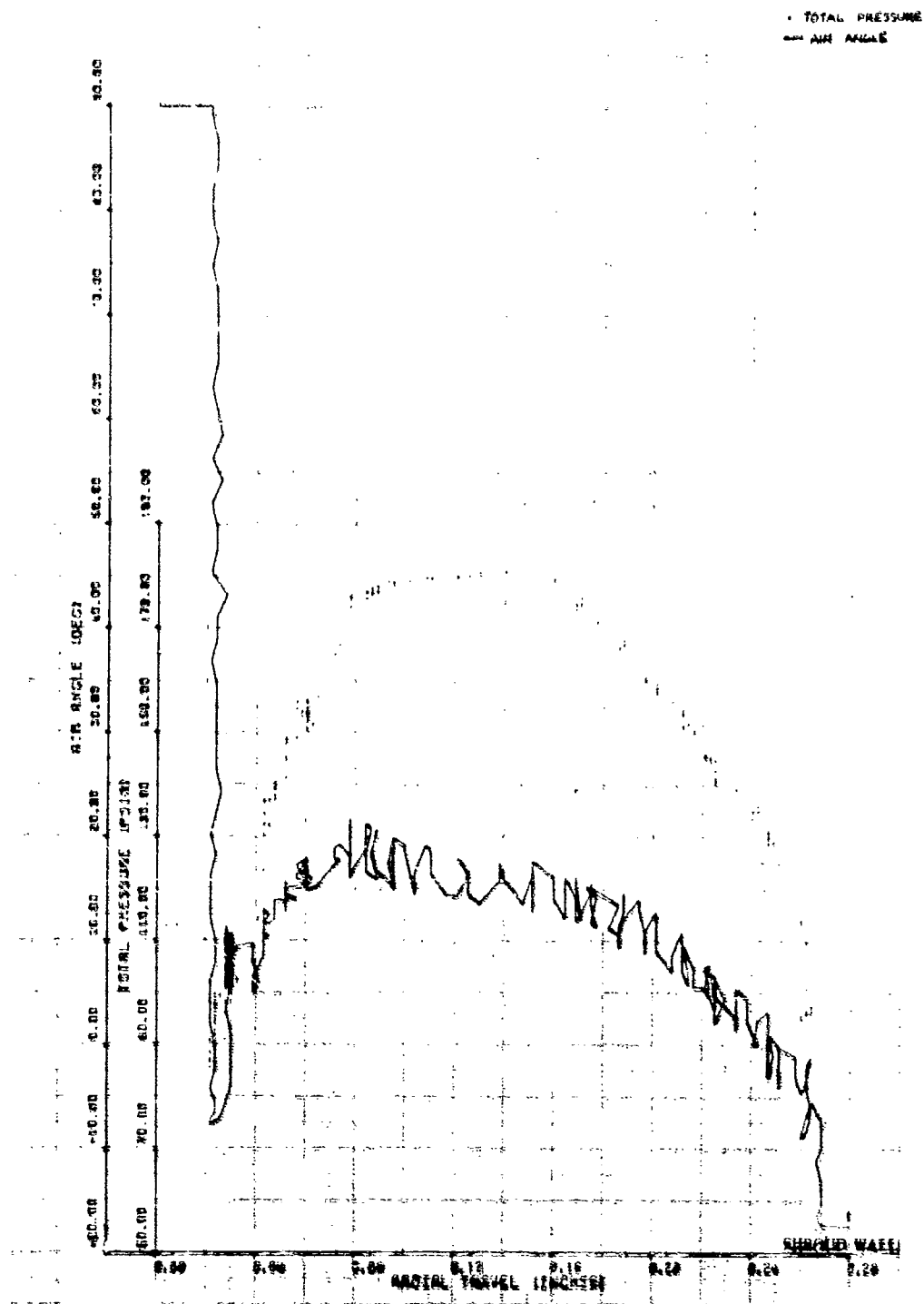


Figure 93. Impeller Exit Traverse, Build No. 6, 101% Speed, -4-deg IGV, Near Stall.

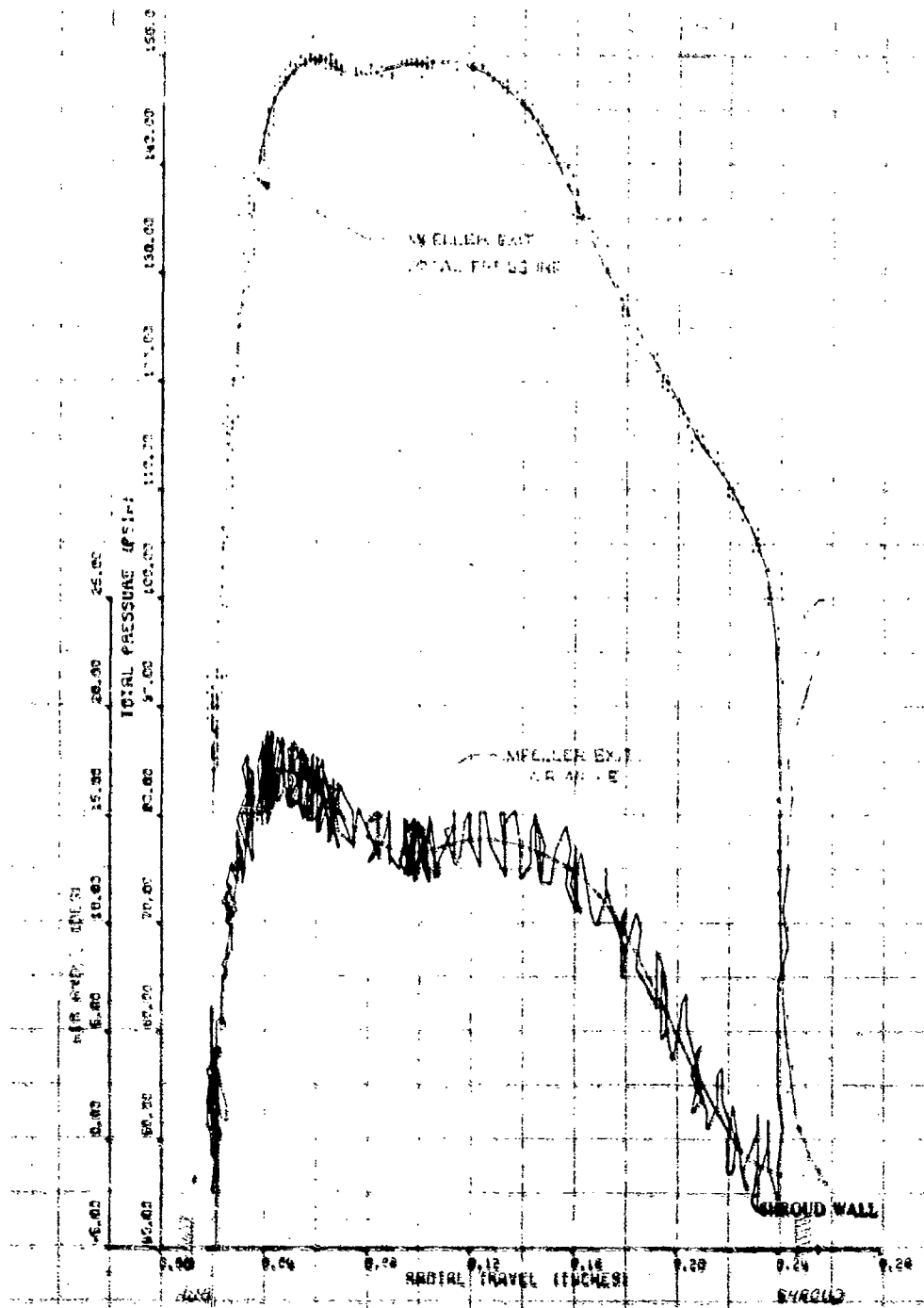


Figure 94. Impeller Exit Traverse, Build No. 3, 95% Speed, 10-deg IGV, Near Stall.

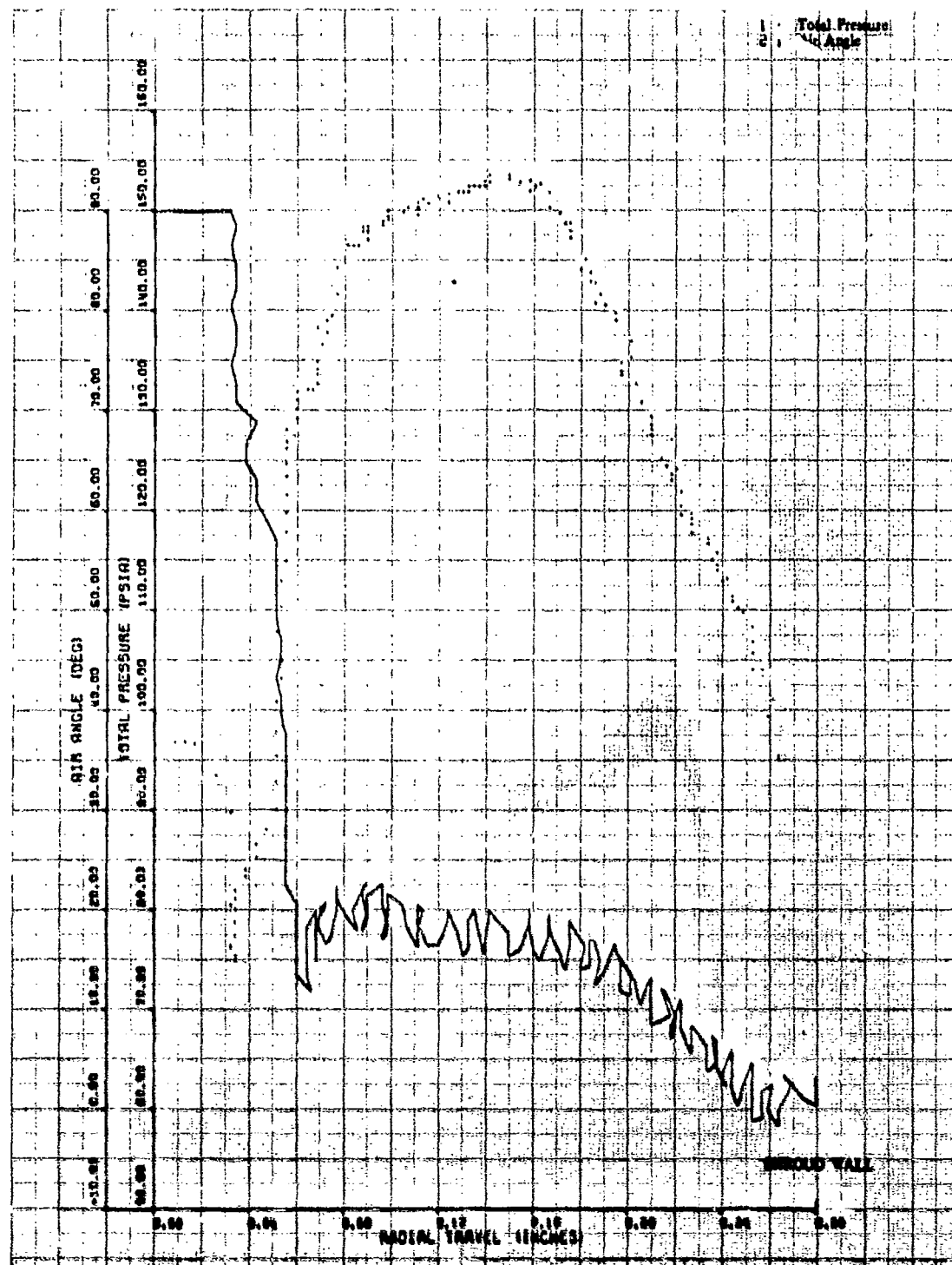


Figure 95. Impeller Exit Traverse, Build No. 6, 95% Speed, 10-deg IGV, Near Stall.

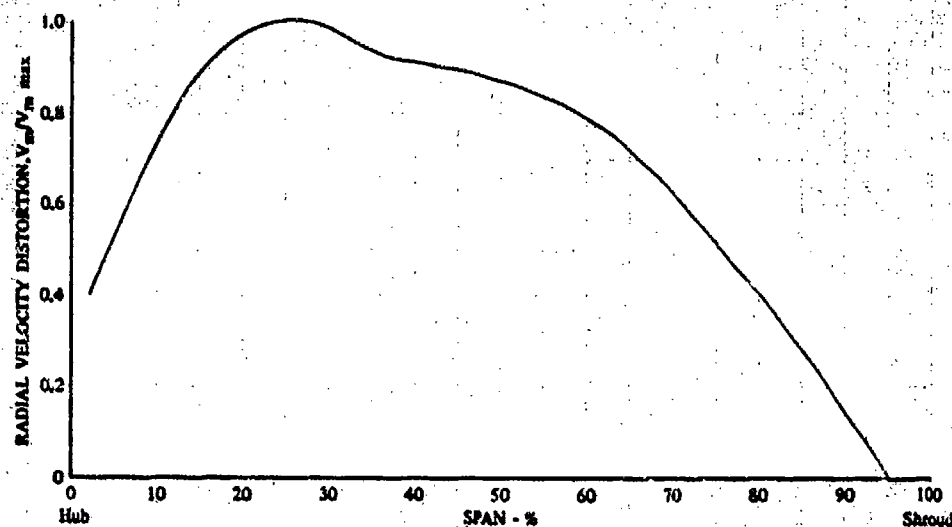


Figure 96. Normalized Radial Velocity Distribution, Build No. 6, 101% Speed, -4-deg IGV.

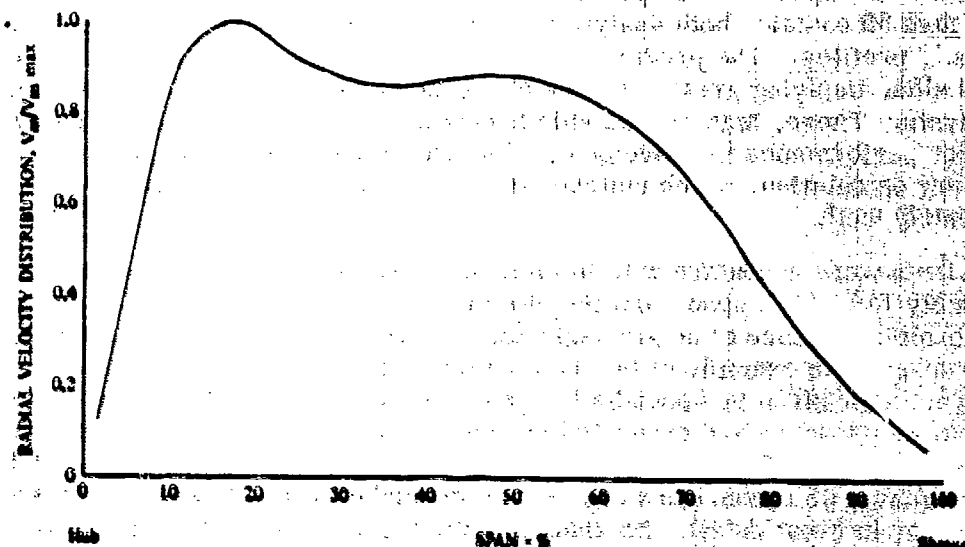


Figure 97. Normalized Radial Velocity Distribution, Build No. 3, 95% Speed, 10-deg IGV.

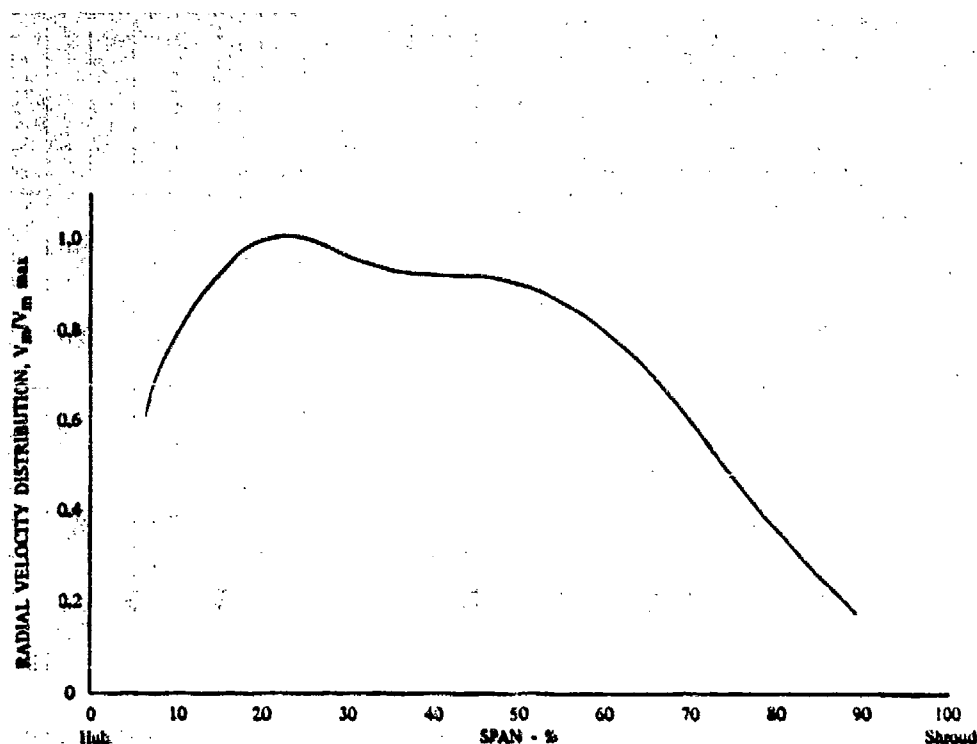


Figure 98. Normalized Radial Velocity Distribution, Build No. 6, 95%  $N/\sqrt{\theta}$  Design, 10-deg IGV.

A boundary layer analysis program was used to predict the impeller exit velocity profile for the 95% speed 10-deg prewhirl near stall points for both Builds No. 3 and 6. Figure 99 contains both analytical predictions and experimentally obtained velocity ratio profiles. The predicted boundary layer thickness was too small on the shroud side, implying greater losses along the shroud wall than were assumed in the analysis. There, high shroud side losses also pointed to an area for potential impeller performance improvement. The predictions allowed an accurate potential flow calculation, which matched the experimental profile from 20 to 60% span extremely well.

Stall transients were conducted with the impeller exit traverse probe positioned at approximately 15% of the span from the shroud wall. These transients were expected to exhibit evidence of an air angle shift toward tangential flow immediately preceding surge. An example of the data obtained is presented in Figure 100, with the remainder given in Appendix I. Impeller exit total pressure, angle, and collector static pressure are presented vs time. A tabulation of speed and flow vs time is also given. Data from two different transients at scanning rates of 1 and approximately 65 scans/sec were used to describe overall trends and to show surge behavior in great detail. No change in air angle could be determined from the typical searching pattern observed in these data. In nearly every case, there was a drop in impeller exit total pressure accompanied by an increase in speed

and a slight decrease in weight flow before surge. Collector static pressure continued to rise even though the impeller exit total pressure decreased, which indicated either a shift in the impeller exit profile causing a pressure decrease at 15% span or that the diffusion efficiency increased faster than the rate of impeller exit pressure decrease.

Static pressure information was recorded along the shroud wall for every steady-state data point. Figure 101 shows Builds No. 3, 6, and design data for the 95% speed, 10-deg IGV setting condition. The trend of static pressure showed no significant change from build to build. True evaluation of the significance of these profiles was difficult since it was not possible to separate the contribution due to impeller work and diffusion; however, no obvious discontinuity showing areas of separation was visible. Most of the static pressure rise occurred after the transition from axial to radial flow, with some decrease in the magnitude of pressure rise near the exit of the impeller.

The five static pressure taps near the exit were located in such a way as to allow determination of the effect of diffuser pipes on the static pressure distribution in the impeller. No effect was seen, most likely due to the large vaneless space. Other examples of this static pressure distribution are presented in Appendix 1. All show the same trends as the examples. The distribution and level do not change from near stall to wide open discharge; however, at a constant speed the level of static pressure is highest for the inlet guide vane setting that allows the impeller to do the most work.

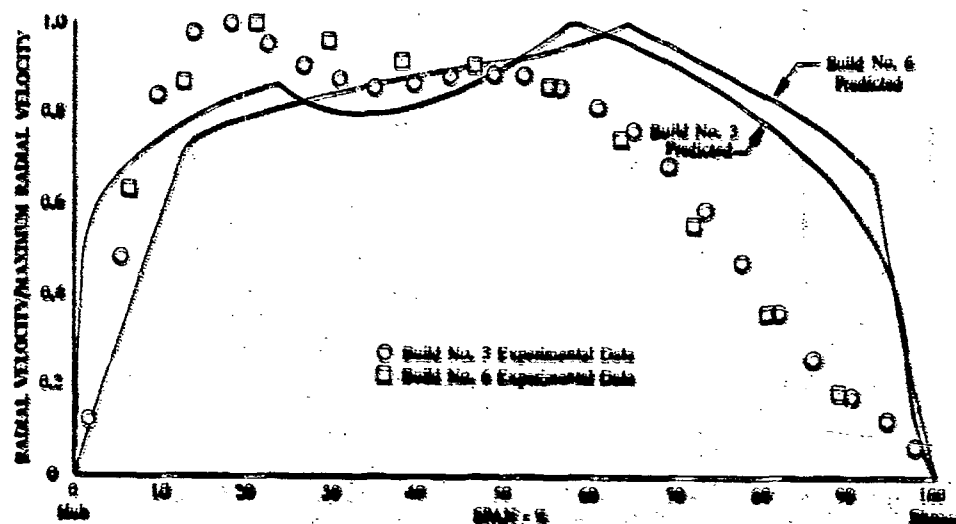


Figure 99. Discharge Velocity Ratio Comparisons.



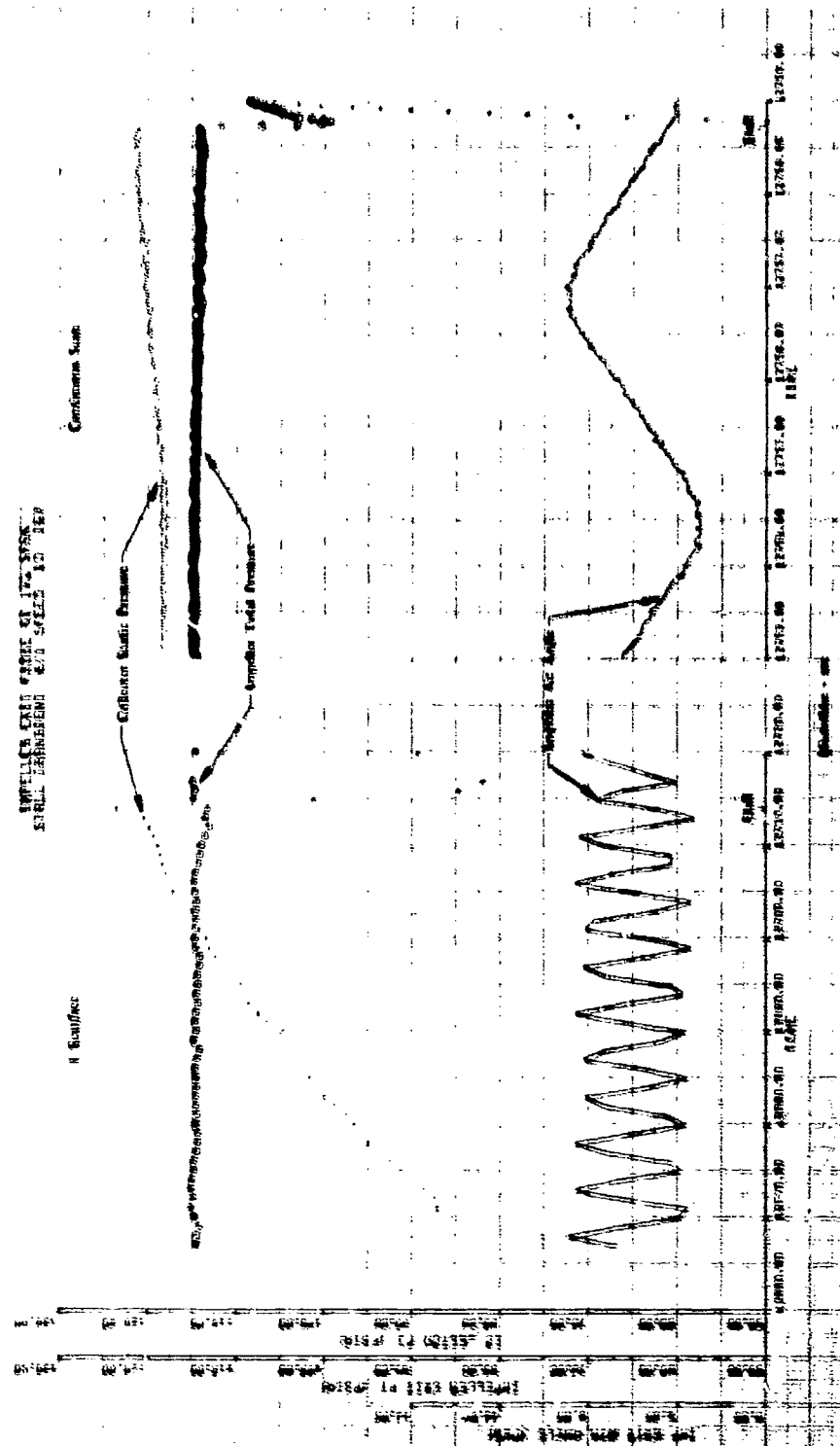


Figure 100. Stall Transient Data at 1 Scan/sec and Continuous Scan.

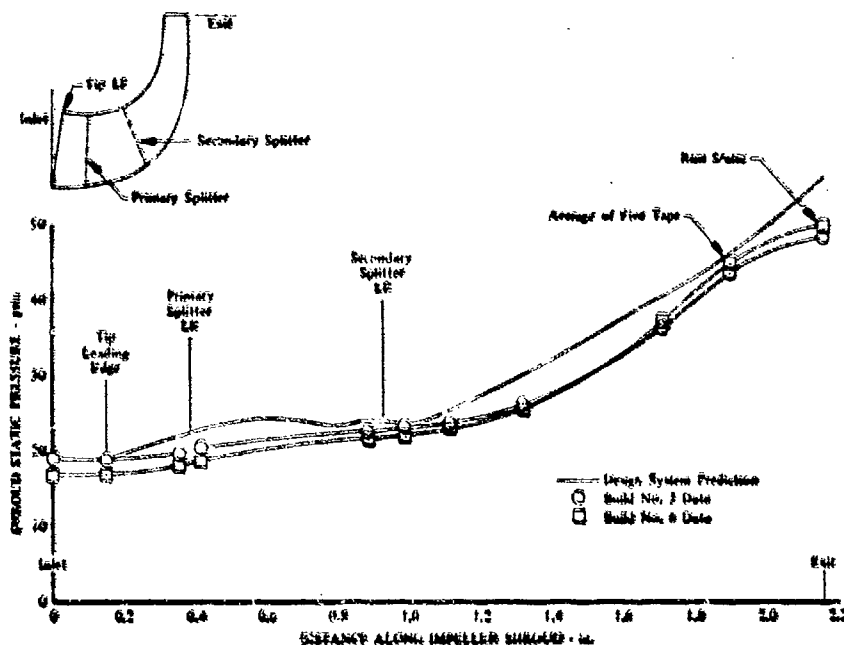


Figure 101. Static Pressure Variation Along Impeller Shroud, 95% Speed, Near Stall, 10-deg IGV.

#### Diffuser Performance

Diffuser performance evaluation, including an evaluation of the diffusion process and an assessment of the total pressure losses incurred during the diffusion process, will be presented in the form of static pressure distributions throughout the diffuser, total pressure profiles at the diffuser exit, and various loss correlations. Since the diffuser was damaged prior to the Build No. 6 performance testing, the discussion will include the Build No. 3 diffuser performance, the nature of the damage to the diffuser, and the resulting performance losses seen in Build No. 6. All diffuser performance data are available from tabulations of performance in Appendix 1.

Build No. 3 static pressure distributions along the length of the diffuser pipes on the shroud side are shown at near stall and at minimum back pressure for 95% speed and 10-deg IGV and at near stall for 100% speed and 10-deg IGV in Figures 102 and 103. The strong normal shock, located approximately 1 in. from the diffuser exit at minimum back pressure, moves upstream of the throat to slightly strengthen the inlet shock in that region at near stall as is shown in Figure 102. The near stall static pressure distribution plots at 95 and 100% speed in Figures 102 and 103 show that the effective throat (i.e., where the diffusion process begins) is located approximately 0.230-in. upstream of the geometric throat. The region between the tangency point and the effective throat is essentially a region for flow adjustment and alignment and is marked by shock wave-boundary-layer interactions and areas of flow acceleration so that there is little if any diffusion. Figure 104 presents the static pressure distributions on the hub and shroud walls across one diffuser gap at the tangency radius for several points and

illustrates the complex nature of the flow in this region. This is also evident in the diffuser shroud side isobar map in Figure 105. The representations shown in Figures 104 and 105 are composites generated from static pressure information from several locations and may, therefore, contain scatter as a result of pipe-to-pipe variation. Downstream of the effective throat, where essentially all the diffusion takes place, no evidence of separation is noted. The circumferential static pressure distribution at the geometric throat, as shown in Figure 106 for 95% speed and 10-deg IGV, is fairly uniform especially near stall.

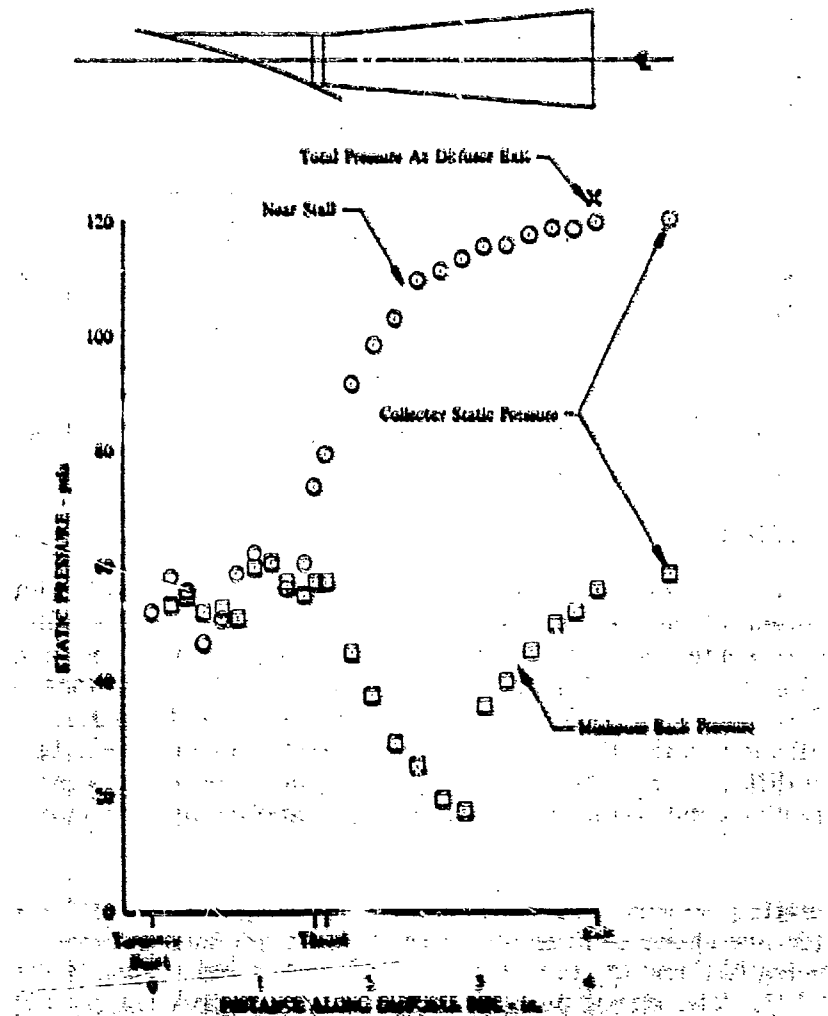


Figure 102. Diffuser Static Pressure Profile: Build No. 3, 95% Speed, 10-deg IGV.

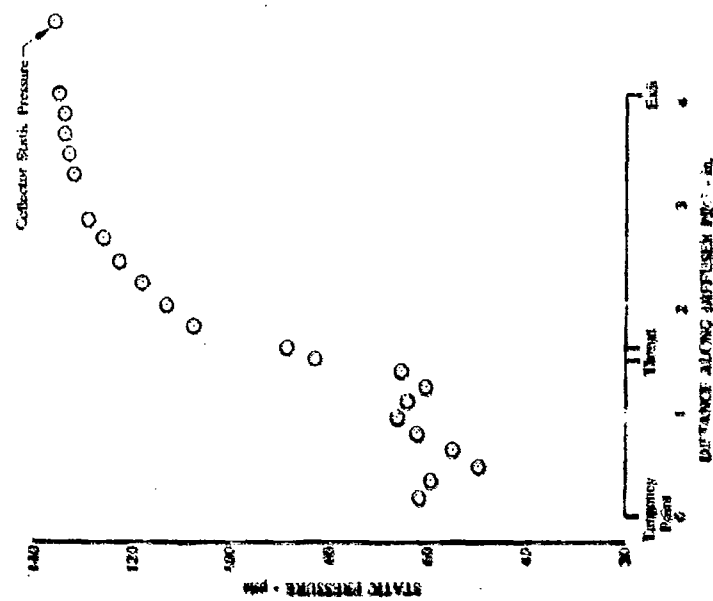


Figure 103. Diffuser Static Pressure Profile:  
Build No. 3, 100% Speed, 10-deg IGV,  
Near Stall.

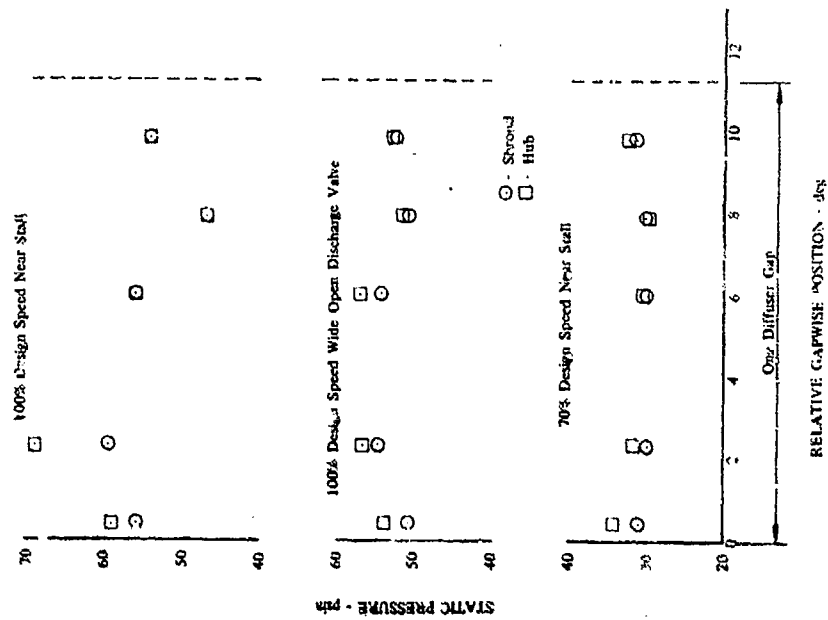


Figure 104. Diffuser Capwise Static Pressure  
Distributions Along the Tangency  
Radius: Build No. 3, 10-deg IGV Setting.

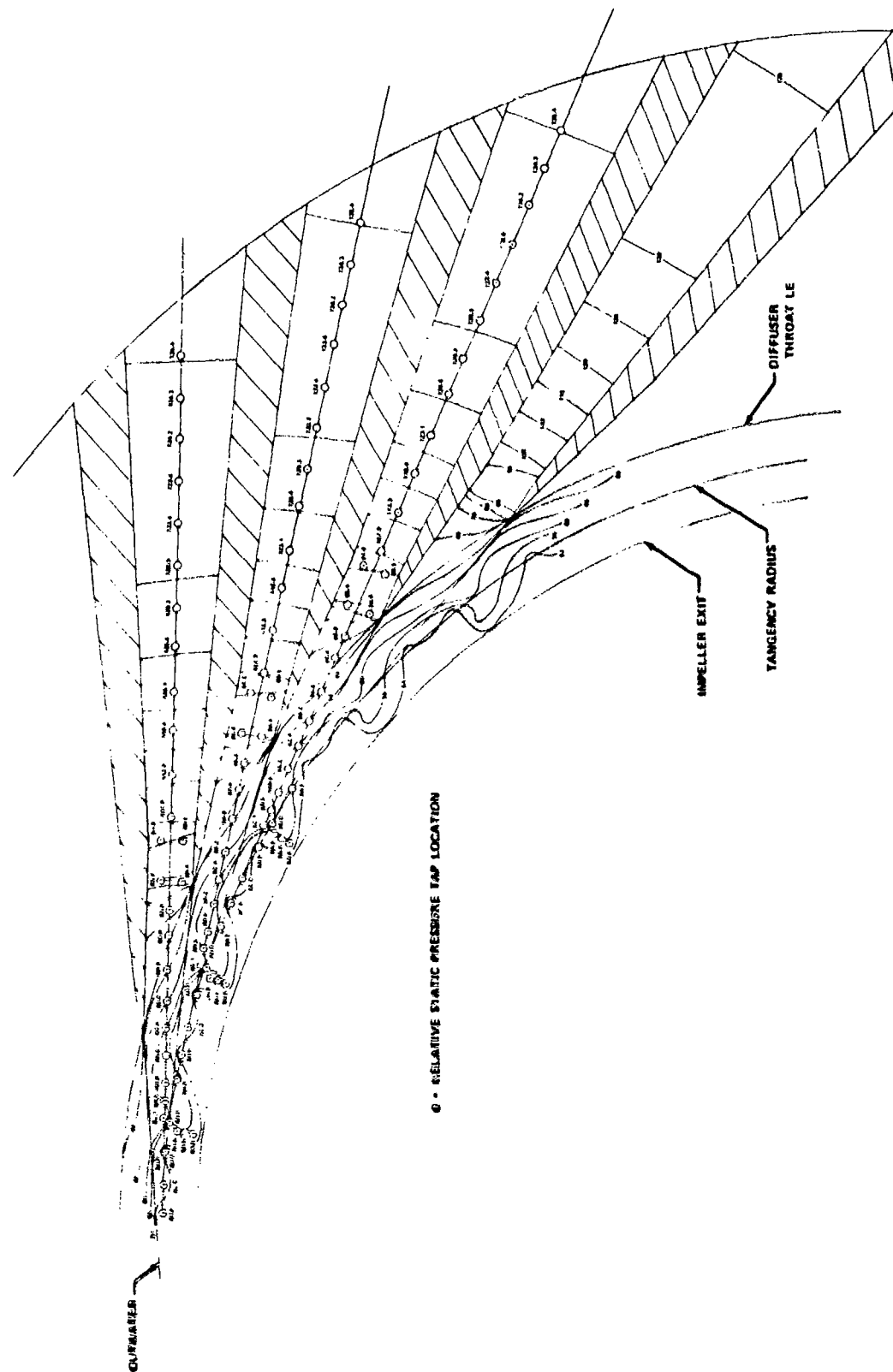


Figure 165. Diffuser Shroud Static Pressure Contours: Build No. 3, 100% Speed, 10-deg IGV.

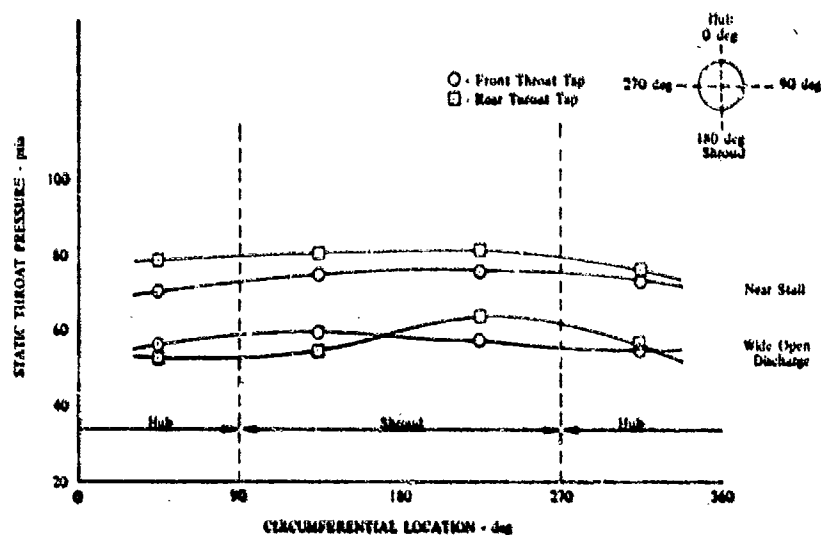


Figure 106. Diffuser Throat Static Pressure Distribution: Build No. 3, 95% Speed, 10-deg IGV.

During Build No. 4 testing (mechanical checkout of redesigned rig bearing and rotor system), a rub occurred between the impeller and the stationary shroud, spewing pieces of the shroud silver plating through the diffuser and causing damage to the diffuser pipe throat leading edges. Photographs of this damage from several typical pipes are shown in Figure 107. For comparison, a photograph of an undamaged diffuser pipe is shown in Figure 108. Prior to the Build No. 6 performance tests, all the diffuser pipes were polished to remove any burrs extending into the flow path along the damaged throat leading edges. One diffuser pipe found to be slightly oversized was nickel plated to the same size as the rest of the pipes. At the completion of the Build No. 6 testing during the rig teardown, it was discovered that a considerable amount of rust had formed in the diffuser pipes, as is shown in Figure 109. This rust probably also contributed to the loss in performance noted in Build No. 6, although it is impossible to predict the degree to which the diffuser pipes were rusted at any given point in the test program. The diffuser material, 410 Stainless Steel, was chosen because its thermal expansion closely matched that of the titanium impeller; however, it appears that for aerodynamic reasons a corrosion-resistant material would be better.

The effects of the damaged diffuser can be seen in the Build No. 6 static pressure distribution plots for 95 and 100% speeds and 10-deg IGV in Figures 110 and 111. The effective throat region has moved downstream from its Build No. 3 location and nearly coincides with the geometric throat. Also, regions of flow separation are now evident in some of the pipes toward the diffuser exit. The individual points shown on the plots are not necessarily from the same diffuser pipe, so the inconsistent nature of the static pressure data near the diffuser exit indicates

varying amounts of separation from pipe to pipe for those pipes in which separation does occur. Figure 112 shows Build No. 6 static pressure distributions for 101% speed and -4-deg IGV at both near stall and minimum back pressure.

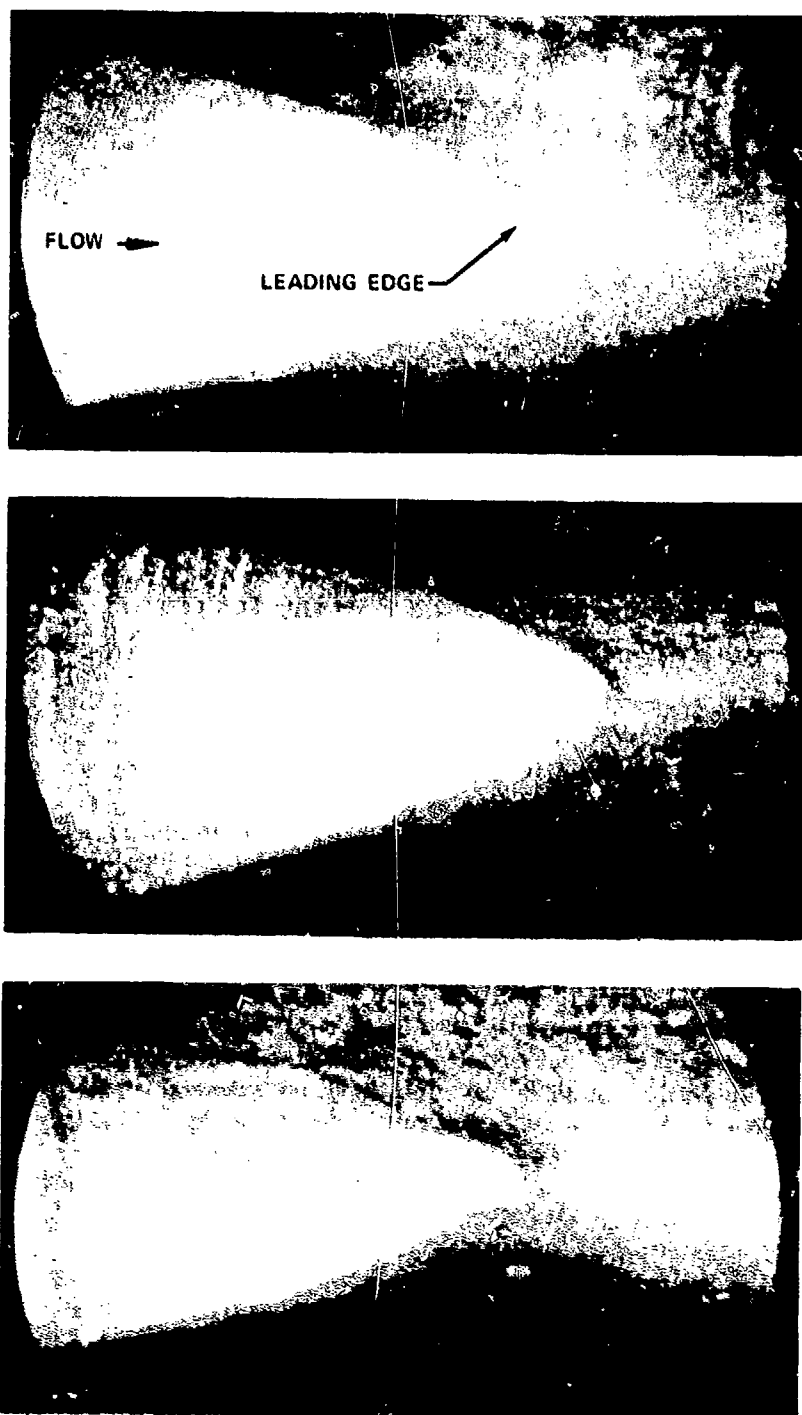


Figure 107. Damaged Diffuser Pipe Leading Edges.



Figure 108. Typical Undamaged Diffuser Pipe Loading Edge.



Figure 109. Post-Test Condition of Diffuser.



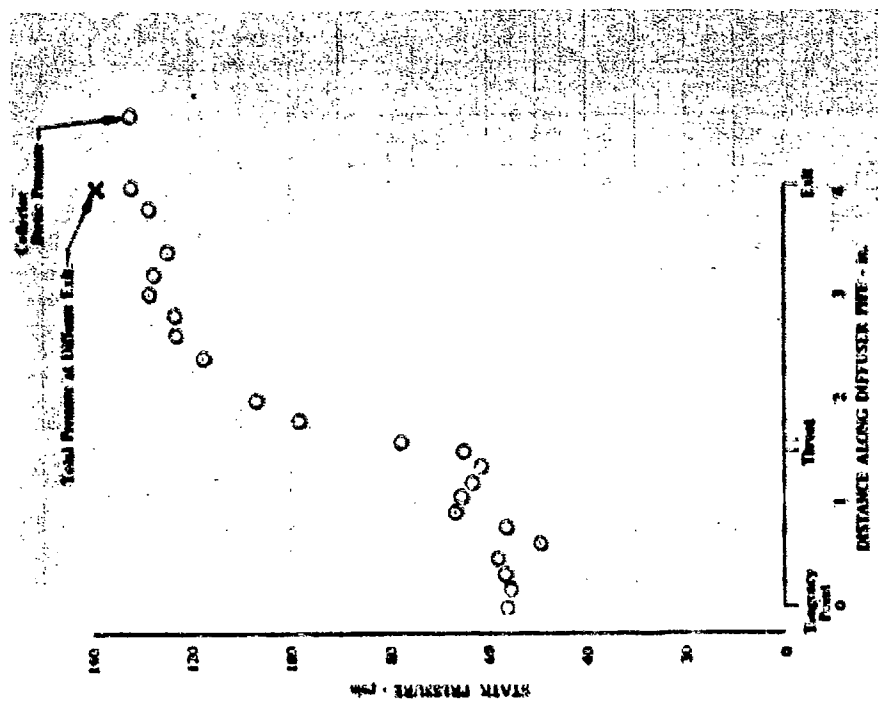


Figure 111. Diffuser Static Pressure Profile:  
Build No. 6, 100% Speed, 10-deg  
IGV, Near Stall.

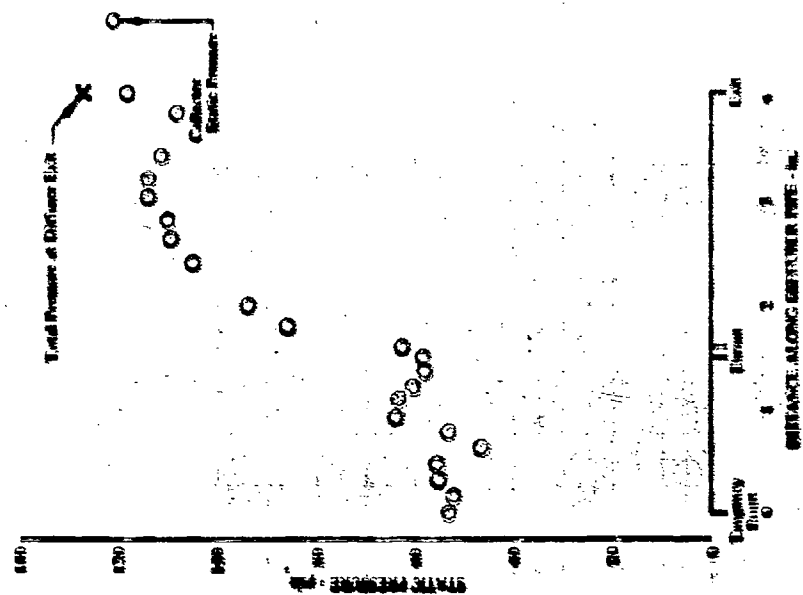


Figure 110. Diffuser Static Pressure Profile:  
Build No. 6, 95% Speed, 10-deg  
IGV, Near Stall.

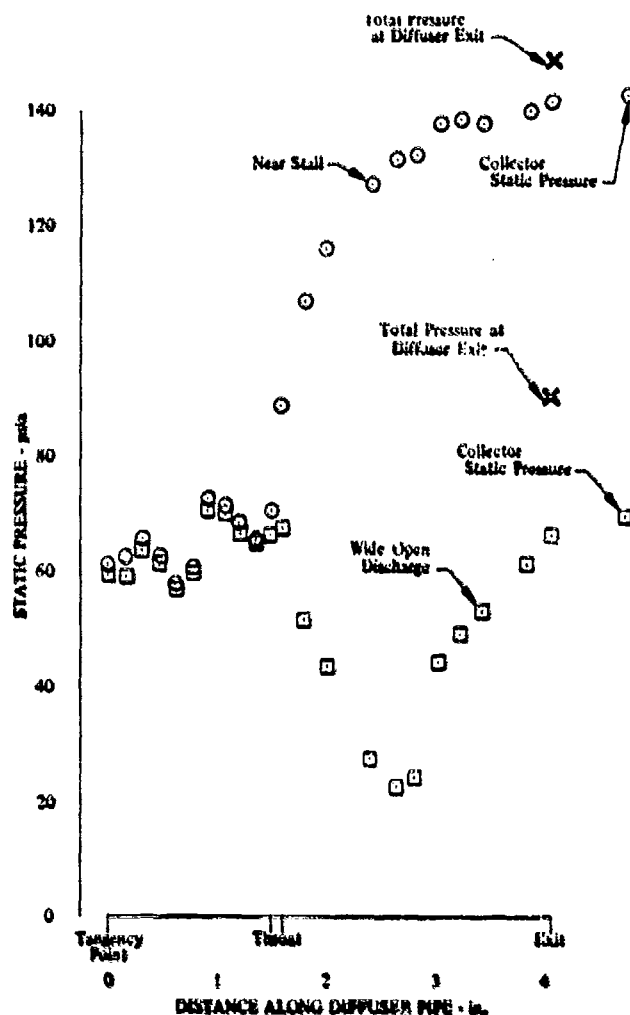
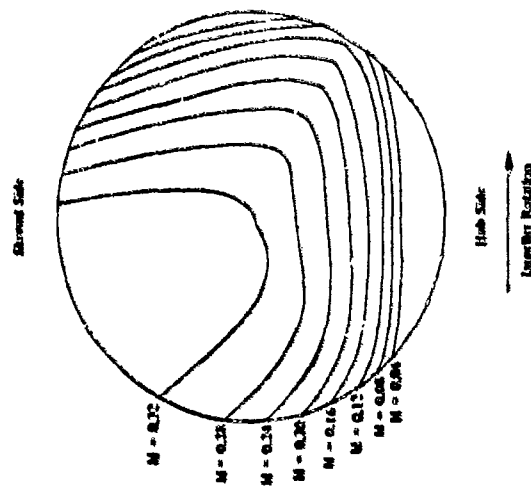


Figure 112. Diffuser Static Pressure Profile: Build No. 6, 101% Speed, -4-deg IGV.

Diffuser exit Mach number profiles were generated, based on diffuser exit total pressure rake data and collector static pressure. A resultant profile for Build No. 3 at 95% speed, near stall, and 10-deg IGV is shown in Figure 113. The profile is marked by a large low-diffusion region on the shroud side and by a low-flow region on the hub side, which probably represents a large boundary layer and flow separation. The Build No. 6 profile for the same point is presented in Figure 114 and has the same high-loss region on the hub side, but has a commensurately larger low-diffusion zone than Build No. 3. Profiles at 100 and 101% speed from Build No. 6, shown in Figures 115 and 116, have the same general characteristics as the 95% speed profile. Figure 117 shows the diffuser exit Mach number profile at minimum back pressure at 101% speed, which is characterized by very low diffusion with large high-loss regions.





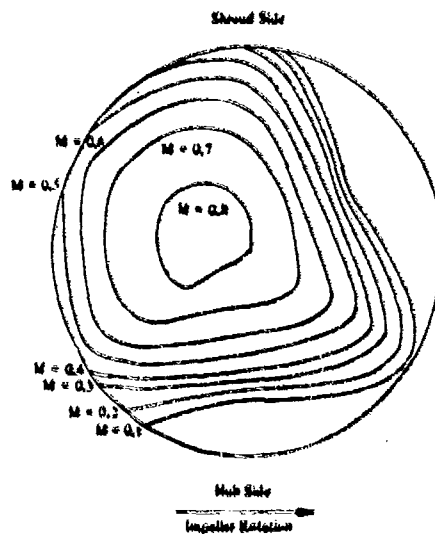


Figure 117. Diffuser Exit Mach Number Profile: Build No. 6, 101% Speed, -4-deg IGV, Wide Open Discharge.

Diffuser total pressure and diffuser dump losses are plotted as a function of corrected weight flow and impeller exit Mach number for both Builds No. 3 and 6 in Figures 118 and 119. The total pressure diffuser losses were essentially identical for both builds, although the Build No. 6 dump losses were higher. This can be directly attributed to the lower diffusion levels and resultant higher diffuser exit Mach numbers for Build No. 6, as is shown in Figure 120. The Build No. 6 static pressure rise coefficient values were considerably lower than the Build No. 3 levels, as shown in Figure 121.

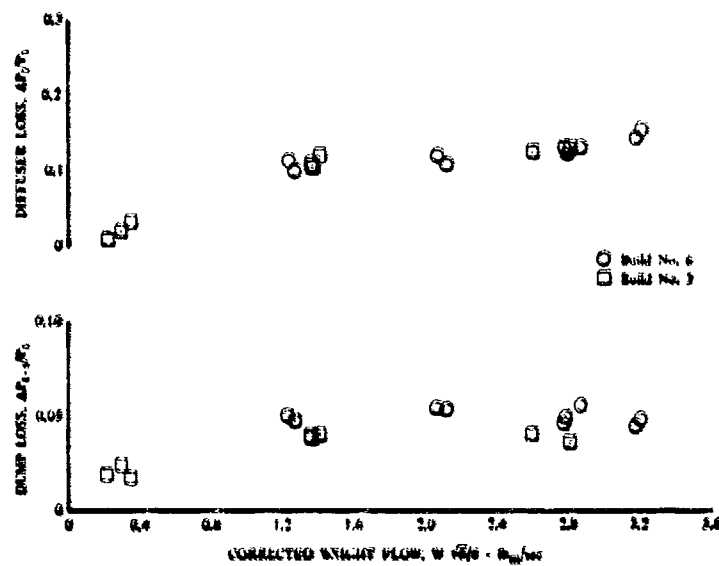


Figure 118. Diffuser Losses vs Corrected Weight Flow, Near Stall.

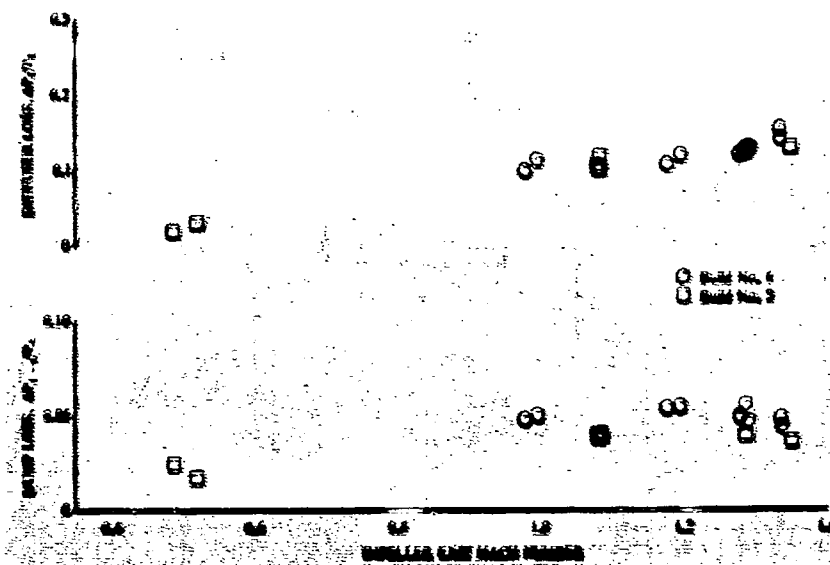


Figure 119. Diffuser Losses vs Impeller Exit Mach Number, Near Stall.

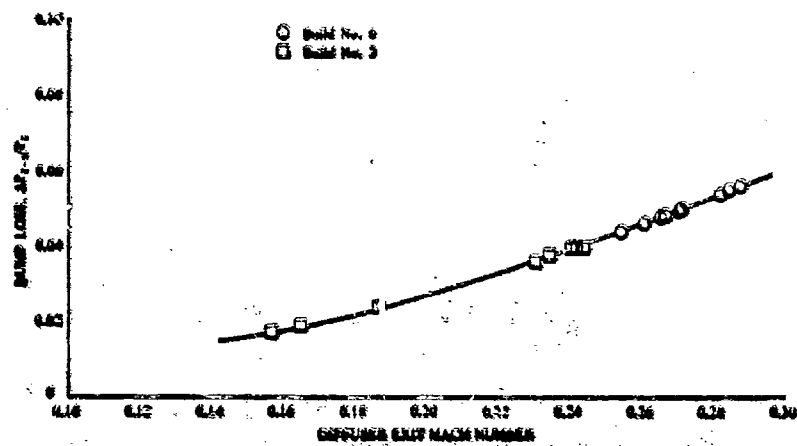


Figure 120. Diffuser Dump Losses Near Stall.

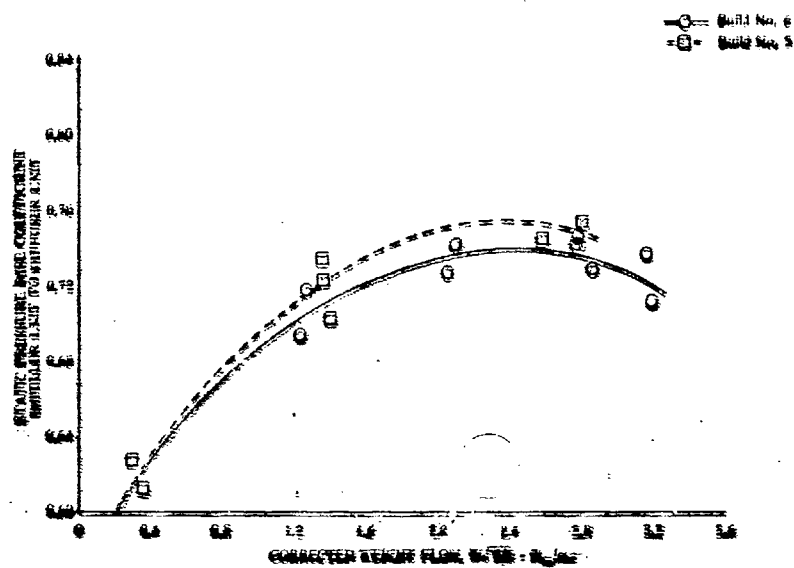


Figure 121. Diffuser Static Pressure Rise Coefficient vs Corrected Weight Flow.

## HIGH-FREQUENCY RESPONSE DATA

High-frequency response data were recorded at two speeds, 70 and 78% of design speed, during Build No. 6 testing. These speeds were selected because they were the highest speeds for which performance data were available and which did not exceed the temperature limitations of the high-response KULITE™ pressure transducers. Data were recorded at steady-state conditions, near stall and during transient operation into stall for the following four pressures:

1. Total pressure at the impeller exit
2. Two static pressures in the vaneless space
3. Static pressure at the diffuser discharge.

These pressures were recorded using KULITE pressure transducers capable of frequencies from dc to 100,000 Hz; however, due to the high magnetic tape speed required to attain resolution at the high frequencies, data below 200 Hz are not reliable.

Typical data are presented in Figures 122 and 123 for 70 and 78% of design speed, respectively, and show the response of the four measured pressures during a 10-ms period including the surge event. Typically, these data define surge both in the form of an amplitude change and a frequency change. The amplitude difference between the two vaneless space static measurements is believed to be due to a faulty gain setting on one channel (PSDVK1); however, the wave form is unaffected.

Additional data from each of the high-response probes during the steady-state point and at 2.5-ms increments into the stall transient are presented in Appendix I in the form of pressure amplitude vs time and pressure amplitude vs frequency. These data indicate the presence of strong discrete fluctuations at frequencies corresponding to 12 E, 24 E, and 48 E (E - rotor speed). These frequencies correspond to excitations from the impeller blading, which has 12 full blades, 12 primary splitters, and 24 secondary splitters. Prior to surge, the dominant frequency observed was generally 24 E which seems to indicate a differential work input between the secondary splitters and the full blades and primary splitters. Correlations which were performed on these data, however, failed to identify the 24 E signal with the various types of blades and splitters.

Following surge, the dominant frequency became 48 E, which appears to be the pressure field associated with the stalled blading. This pattern of frequency change was observed for both the 70 and 78% speed. No evidence of rotating stall prior to surge was noted; however, the local distortion of the impeller discharge flow field due to the insertion of the relatively large high-frequency pressure probe caused surge to occur significantly below the undistorted surge line. This asymmetry may have prevented the formation of rotating stall cells.



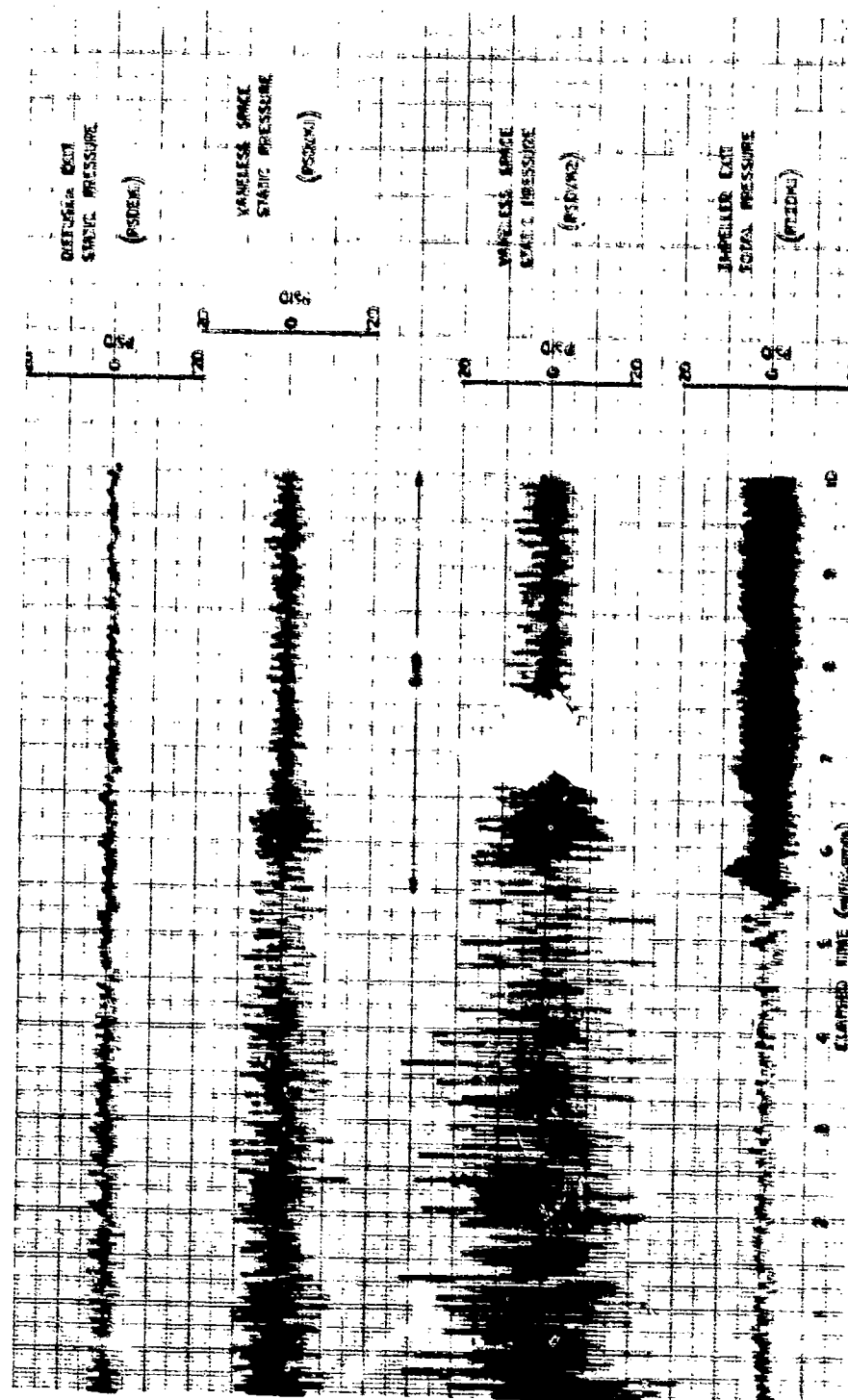


Figure 122. High-Frequency Response Data at 70% Speed.

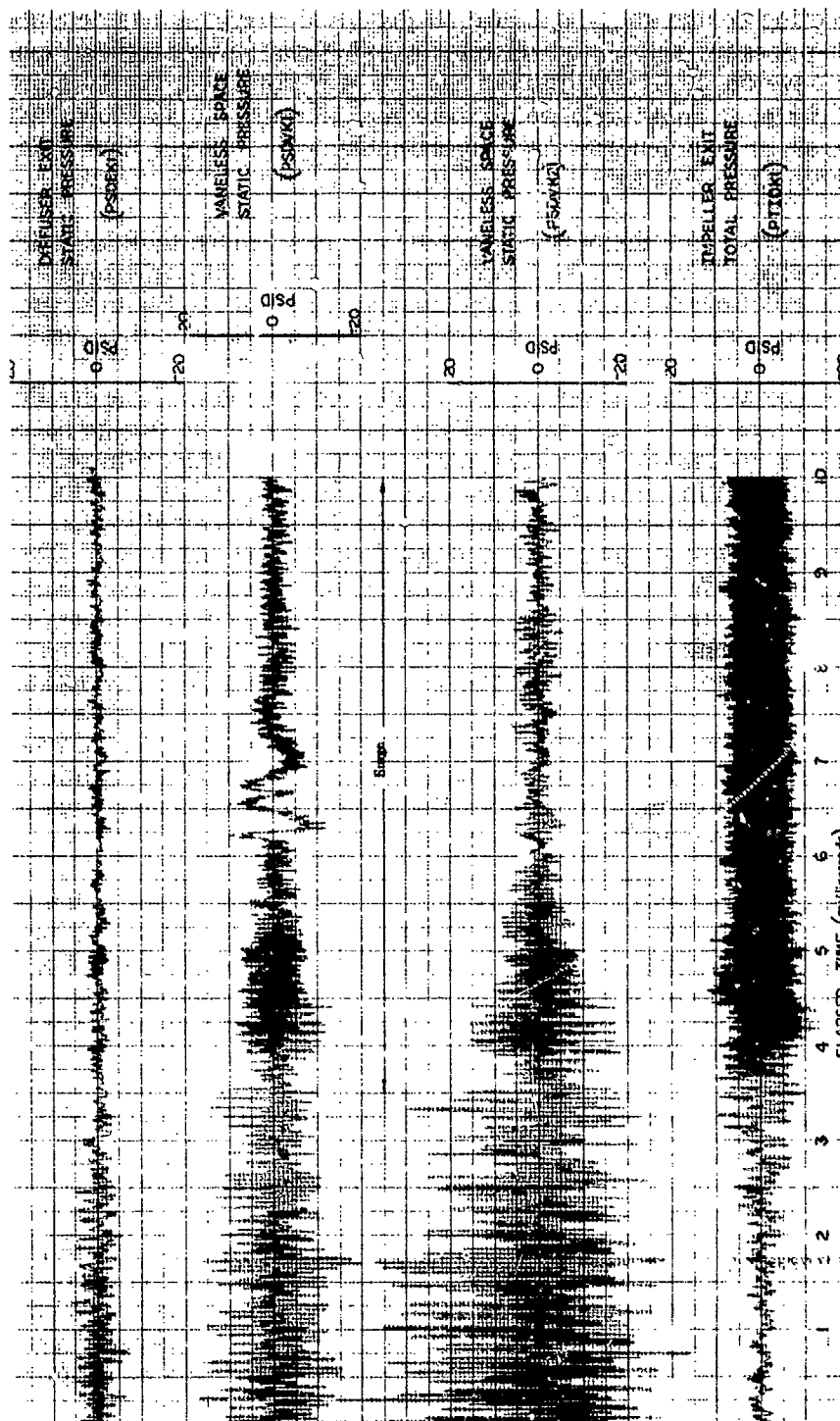


Figure 123. High-Frequency Response Data at 78% Speed.

## CONCLUSIONS

The overall total-to-static pressure ratio and efficiency of this compressor came very close to meeting design goals and, for all practical purposes has demonstrated that high-pressure ratio, high-efficiency, single-stage centrifugal compressors can be developed. If the diffuser had not been damaged, the 10:1 pressure ratio 75% efficiency goal likely would have been surpassed, as shown by the composite compressor map generated assuming undamaged diffuser losses on the overall compressor performance.

The basic approach taken for the aerodynamic design has proven to be sound. The use of variable inlet guide vanes has allowed obtaining optimum performance data throughout the range of operating speeds and generation of an inlet guide vane schedule for potential use of this compressor in a gas generator configuration.

The inducer operated well until it was run at conditions beyond its intended design. When it was discovered that the overall pressure ratio was low at design speed and prewhirl, it was necessary to produce more work in the inducer-impeller. This involved a decrease in prewhirl, an increase in speed, or both. Either condition increased the inlet relative Mach number into the inducer and forced a more stalled incidence, generating high losses and resulting in low efficiency. The remote inducer, which was included in the design to accept shock losses should they be higher than expected and to allow separation on the inducer without destroying impeller performance, also functioned properly in this situation as the impeller operation was not influenced by the poor inducer exit characteristics.

The inlet guide vanes were set to produce less prewhirl, and rotor speed was increased to produce the required rotor pressure ratio. The impeller efficiency was above predicted, indicating that additional tip diameter would also have obtained the design performance.

The diffuser, including the entry region, is the most critical element in the performance of this compressor. The mismatch caused by the undersized diffuser in Build No. 2 and the resulting improved performance obtained in Build No. 3 by only increasing the throat diameters from 0.228 to 0.235 in. demonstrates the small latitude in dimensioning the diffuser throat and predicting impeller exit conditions and diffuser throat blockage.

The losses and static pressure rise generated by the resized diffuser were quite good and would have allowed the overall performance goal of 10:1 pressure ratio at 75% efficiency to have been surpassed in Build No. 3 at a lower prewhirl than 10 deg if the rig had functioned properly mechanically. Damage to the leading edge region of the diffuser, resulting from silver impingement when the impeller rubbed the shroud in a mechanical checkout of the redesigned bearing support and rotor system, resulted in enough change in the diffuser characteristics to cause the performance to be short of the goal. The change in throat blockage causes the flow rate to change and the static pressure rise to decrease. This behavior also points to the critical nature of the diffuser in a compressor such as this.

## RECOMMENDATIONS

Analysis of the data obtained during this program to design and test a 10:1 pressure ratio single-stage centrifugal compressor leads to the following recommendations to improve its aerodynamic performance:

1. The inducer should be redesigned to operate efficiently at the conditions required to produce 10:1 pressure ratio. The inducer redesign would be based on the optimum inlet guide vane exit conditions and the desired impeller inlet conditions and could improve the design speed efficiency up to three points.
2. The modified inducer should be tested with a new diffuser to eliminate the detrimental effects of the damage leading edges of the current diffuser.
3. The potential performance increase that could be attained through reducing impeller blade-to-shroud friction heating should be evaluated. This friction heating could be minimized through the use of a shrouded impeller. The shrouded impeller also would eliminate the problem of impeller-to-shroud rubs encountered in this and other programs as a result of the small clearances required for conventional open-faced impellers to achieve good performance. A shrouded impeller would also permit extension of hub and shroud walls to form a mechanically practical rotating vaneless space to reduce diffuser entrance losses.
4. Means for improving the range characteristics of this compressor should be evaluated. The useful performance of the compressor in an engine or gas generator application would be substantially improved if peak efficiency could be achieved off the surge line. Several approaches have shown potential for improving the near-vertical speedline characteristics of high-pressure-rise, single-stage centrifugal compressors. Particular attention should be given to the impeller exit/diffuser entrance region, which, to a large degree, controls range from choke to surge. Specific recommendations at the 10:1 pressure ratio design point include reducing the number of diffuser passages to increase range, as well as using sweptback impeller blading.

APPENDIX I  
OVERALL PERFORMANCE TABULATIONS

The tabulations of overall performance data used to construct the performance plots in the text are shown in Tables XIV through XVII. Table XIV contains data through the range of operation for Build No. 3 zero degrees of prewhirl. All steady-state data points and the incipient stall point located by stall transients are included. Similar Build No. 3 data for 10- and 20-deg inlet guide vane settings are shown on Tables XV and XVI, respectively. Table XVII contains similar data for all prewhirl conditions during Build No. 6. Data points are listed in sequential order down the speedline from the incipient stall point.

TABLE XIV. OVERALL PERFORMANCE TABULATION -  
BUILD NO. 3, 0-DEG PREWHIRL

Speed, %	IGV Setting, deg	Weight Flow, lb/sec	Pressure Ratio	Efficiency, %
30	0	0.213	1.257	0.747
		0.253	1.272	0.753
		0.302	1.281	0.758
		0.389	1.259	0.704
		0.425	1.218	0.606
		0.466	1.168	0.487
		0.494	1.142	0.383
50	0	0.620	1.953	0.751
		0.638	1.942	0.736
		0.667	1.959	0.742
		0.737	1.907	0.721
		0.769	1.877	0.704
		0.794	1.749	0.617
		0.801	1.301	0.276
70	0	1.370	3.603	0.764
		1.369	3.539	0.756
		1.412	3.515	0.748
		1.414	3.505	0.747
		1.452	3.196	0.686
		1.464	2.999	0.638
		1.454	1.878	0.346
80	0	1.879	4.904	0.767
		1.873	4.872	0.769
		1.897	4.878	0.771
		1.932	4.812	0.745
		1.936	4.202	0.669
		1.934	3.861	0.623
		1.938	2.531	0.402
90	0	2.597	6.935	0.761
		2.600	6.921	0.761
		2.624	6.926	0.760
		2.603	6.865	0.761
		2.597	6.714	0.751
		2.604	6.296	0.719
		2.605	3.496	0.446
95	0	2.954	8.661	0.791
		2.965	8.563	0.788
		2.969	8.555	0.786
		2.989	8.520	0.784
		3.019	8.376	0.778
		3.031	8.019	0.755
		3.026	4.198	0.472

**TABLE XV. OVERALL PERFORMANCE TABULATION -  
BUILD NO. 3, 10-DEG PREWHIRL**

Speed, %	IGV Setting, deg	Weight Flow, lb/sec	Pressure Ratio	Efficiency, %
30	10	0.223	1.200	0.526
		0.246	1.223	0.662
		0.224	1.251	0.741
		0.269	1.261	0.756
		0.301	1.271	0.811
		0.337	1.251	0.746
		0.360	1.241	0.709
		0.407	1.226	0.653
		0.432	1.120	0.372
50	10	0.637	1.950	0.746
		0.625	1.941	0.747
		0.655	1.941	0.748
		0.663	1.955	0.753
		0.649	1.928	0.743
		0.646	1.947	0.759
		0.698	1.919	0.737
		0.777	1.871	0.717
		0.776	1.664	0.567
70	10	0.790	1.305	0.291
		1.355	3.555	0.772
		1.406	3.503	0.763
		1.417	3.480	0.762
		1.453	3.408	0.742
		1.462	3.202	0.697
		1.460	3.006	0.653
		1.457	3.152	0.688
		1.463	1.884	0.352
80	10	1.874	4.943	0.779
		1.898	4.851	0.769
		1.910	4.836	0.766
		1.930	4.720	0.752
		1.914	4.549	0.734
		1.933	4.384	0.708
		1.903	2.500	0.401
90	10	2.562	7.137	0.797
		2.575	7.046	0.790
		2.595	7.046	0.789
		2.605	6.973	0.786
		2.607	6.882	0.781
		2.611	6.258	0.734
		2.586	3.496	0.461

TABLE XV - Continued				
Speed, %	IGV Setting, deg	Weight Flow, lb/sec	Pressure Ratio	Efficiency, %
95	10	2.778	8.192	0.796
		2.818	8.261	0.791
		2.816	8.176	0.791
		2.819	8.174	0.791
		2.854	8.145	0.788
		2.873	8.083	0.782
		2.902	8.006	0.777
		2.878	7.610	0.757
		2.895	6.927	0.710
		2.902	6.825	0.700
		2.898	3.990	0.467
		2.895	3.978	0.467
100	10	3.005	9.338	0.770
		3.025	9.288	0.762
		3.037	8.885	0.742
		3.039	8.575	0.723
		3.034	8.135	0.703
		3.033	6.594	0.611
		3.025	4.287	0.451

TABLE XVI. OVERALL PERFORMANCE TABULATION - BUILD NO. 3, 20-DEG PREWHIRL				
Speed, %	IGV Setting, deg	Weight Flow, lb/sec	Pressure Ratio	Efficiency, %
30	20	0.275	1.253	0.785
		0.269	1.259	0.747
		0.358	1.272	0.759
		0.394	1.235	0.674
		0.419	1.229	0.664
		0.484	1.168	0.497
		0.494	1.119	0.367
50	20	0.614	1.976	0.780
		0.611	1.942	0.750
		0.664	1.923	0.750
		0.718	1.918	0.746
		0.762	1.842	0.701
		0.774	1.686	0.588
		0.790	1.289	0.274
		0.777	1.297	0.278



TABLE XVI - Continued				
Speed, %	IGV Setting, deg	Weight Flow, lb/sec	Pressure Ratio	Efficiency, %
70	20	1.345	3.508	0.758
		1.372	3.506	0.764
		1.350	3.498	0.764
		1.409	3.488	0.764
		1.458	3.230	0.713
		1.459	3.004	0.660
		1.448	1.886	0.354
80	20	1.818	4.818	0.780
		1.841	4.817	0.783
		1.848	4.809	0.784
		1.865	4.817	0.784
		1.841	4.752	0.774
		1.910	4.393	0.727
		1.919	2.483	0.409
90	20	2.389	6.849	0.793
		2.388	6.805	0.792
		2.402	6.772	0.792
		2.436	6.821	0.794
		2.501	6.712	0.788
		2.510	6.232	0.751
		2.520	3.385	0.456
95	20	2.664	7.882	0.792
		2.697	7.749	0.783
		2.696	7.732	0.783
		2.691	7.726	0.783
		2.721	7.593	0.775
		2.733	7.236	0.752
		2.740	3.740	0.454

**TABLE XVII. OVERALL PERFORMANCE TABULATION -  
BUILD NO. 6**

Speed, %	IGV Setting, deg	Weight Flow, lb./sec	Pressure Ratio	Efficiency, %
70	30	1.227	3.405	0.735
		1.242	3.320	0.722
		1.441	3.255	0.717
		1.357	2.952	0.638
		1.346	1.874	0.349
70	20	1.288	3.500	0.734
		1.279	3.346	0.713
		1.353	3.044	0.650
		1.353	2.598	0.544
		1.359	1.829	0.334
85	30	2.044	5.624	0.767
		2.071	5.425	0.756
		2.065	5.168	0.733
		2.097	4.040	0.600
		2.101	2.866	0.426
85	20	2.078	5.690	0.751
		2.125	5.553	0.742
		2.117	5.234	0.719
		2.113	4.692	0.657
		2.088	2.925	0.422
94.5	15	2.734	8.079	0.775
		2.787	7.957	0.768
		2.797	7.913	0.768
		2.823	7.298	0.728
		2.819	6.703	0.689
		2.833	6.539	0.676
		2.807	3.945	0.461
94.5	10	2.792	8.169	0.773
		2.796	8.037	0.768
		2.827	7.808	0.753
		2.841	7.414	0.726
		2.828	7.273	0.717
		2.837	7.015	0.701
		2.823	4.059	0.471
95	10	2.833	8.388	0.778
		2.819	8.238	0.769
		2.883	8.122	0.764
		2.894	7.487	0.725
		2.894	6.897	0.686
		2.881	6.792	0.681

TABLE XVII - Continued				
Speed, %	IGV Setting, deg	Weight Flow, lb/sec	Pressure Ratio	Efficiency, %
101	5	3.129	9.661	0.735
		3.136	9.693	0.737
		3.142	9.444	0.726
		3.147	9.360	0.724
		3.144	9.119	0.712
		3.142	8.520	0.683
		3.150	4.679	0.448
101	0	3.183	9.882	0.737
		3.185	9.649	0.727
		3.192	9.552	0.722
		3.197	8.993	0.695
		3.194	8.516	0.672
		3.195	7.830	0.639
		3.192	4.743	0.450
101	-4	3.196	10.034	0.738
		3.198	9.965	0.733
		3.209	9.698	0.721
		3.217	9.672	0.721
		3.221	8.786	0.682
		3.222	7.398	0.610
		3.221	4.728	0.442

## TRAVERSE PLOTS

This section contains plots of traverse data obtained during Builds No. 3 and 6 testing. Total pressure and total temperature are ratioed to standard day conditions, but are otherwise uncorrected. The keys on the plots identify the correct scale to the symbol from right to left in increasing number. The temperature sensor on the Station 1 and 1.5 traverse probe is offset 0.045 in. from the pressure sensing ports. Both the Station 1 and 1.5 probes were stopped prior to the hub wall and traversed into recesses in the shroud wall.

Figures 124 through 152 contain Station 1 (inlet guide vane exit) radial plots of total pressure, air angle, total temperature, and circumferential plots of total pressure. The radial traverses are from hub to shroud, while the circumferential traverses were made at five discrete spanwise locations. Figures 153 through 174 contain Station 1.5 (inducer exit) radial traverses of total pressure, air angle, and temperature vs travel. Figures 175 through 210 contain Station 2 (impeller exit) traverse plots of total pressure and air angle from hub to shroud. The probe was traversed from a recess in the shroud wall to a recess in the hub wall, and data were recorded on the return traverse. Figures 211 through 219 are impeller exit temperature traverse plots taken in the same manner as total pressure and air angle.

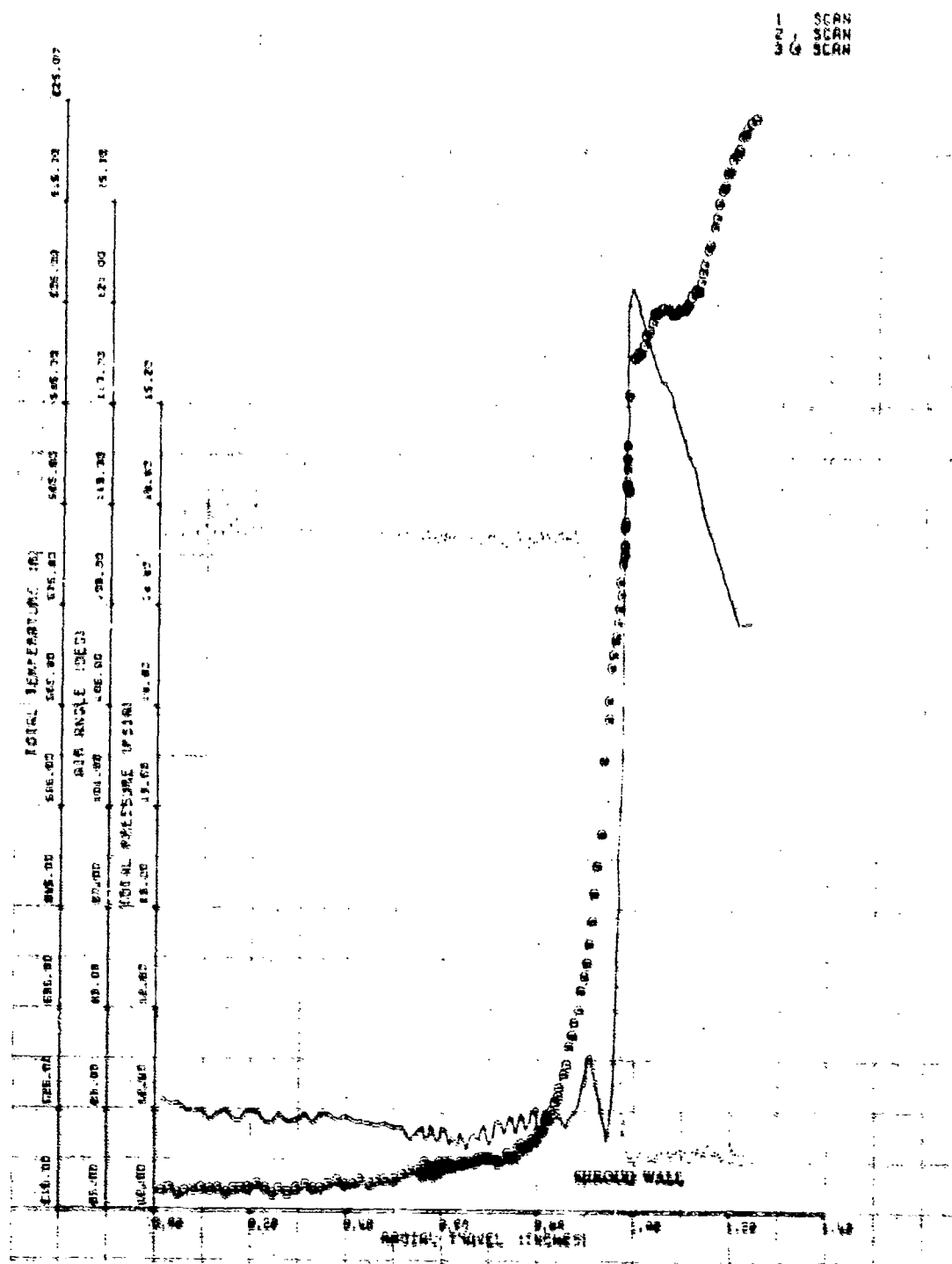


Figure 124. IGV Exit Radial Traverse, Build No. 6, 101% Speed, 0-deg IGV, Near Stall.

1 SCAN

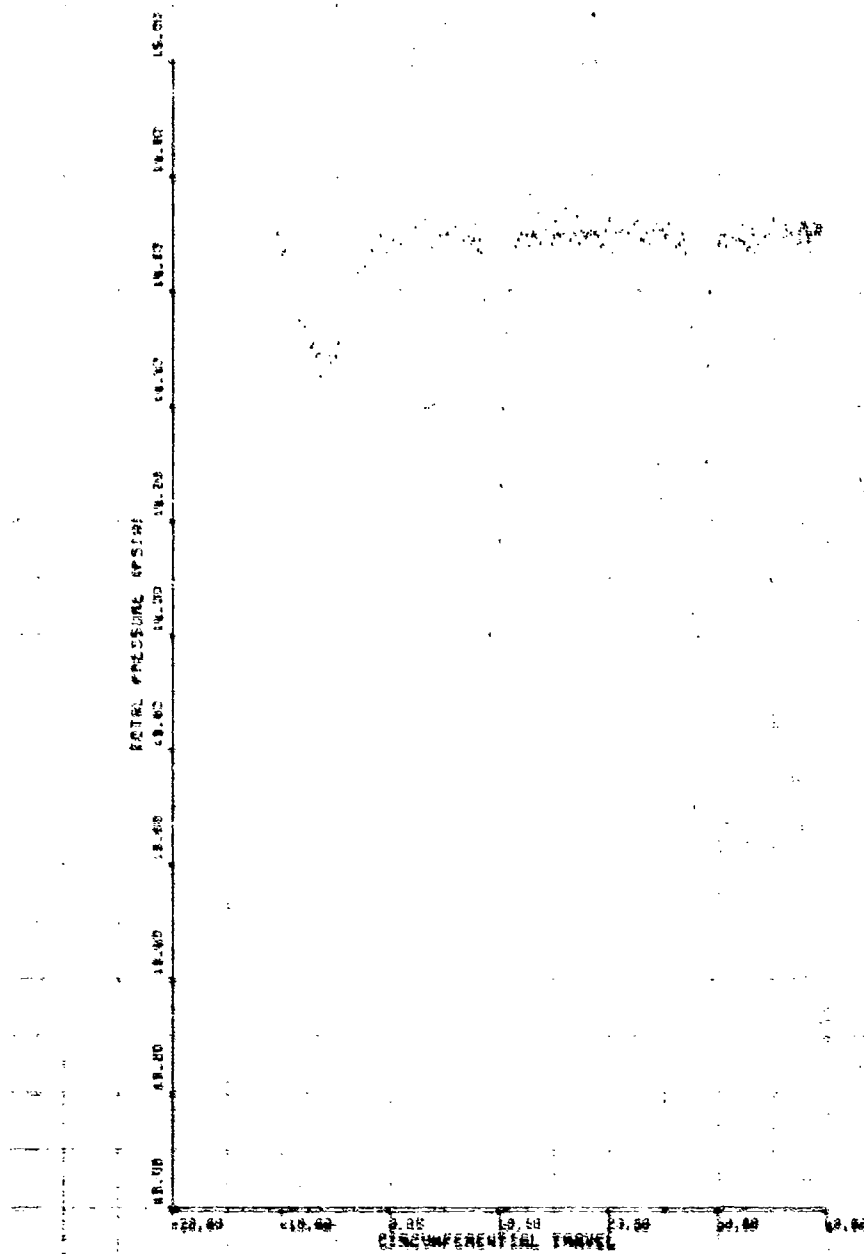


Figure 125. IGV Circumferential Traverse, Build No. 6,  
1017 Speed, 0-deg IGV, 10% Span.



Figure 126. IGV Circumferential Traverse, Build No. 6,  
1017 Speed, 0-deg IGV, 30% Span.

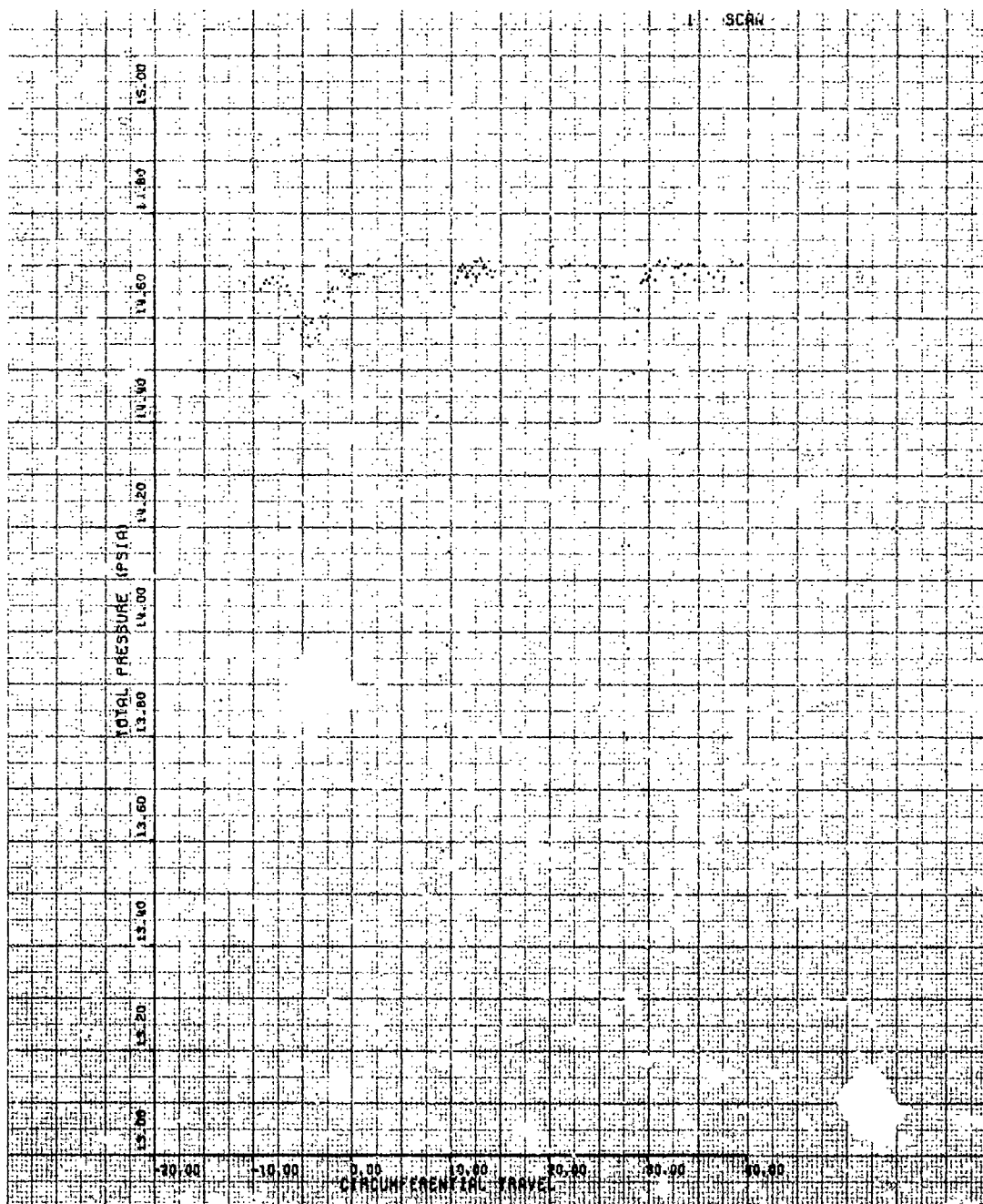


Figure 127. IGV Circumferential Traverse, Build No. 6,  
101% Speed, 0-deg IGV, 50% Span.



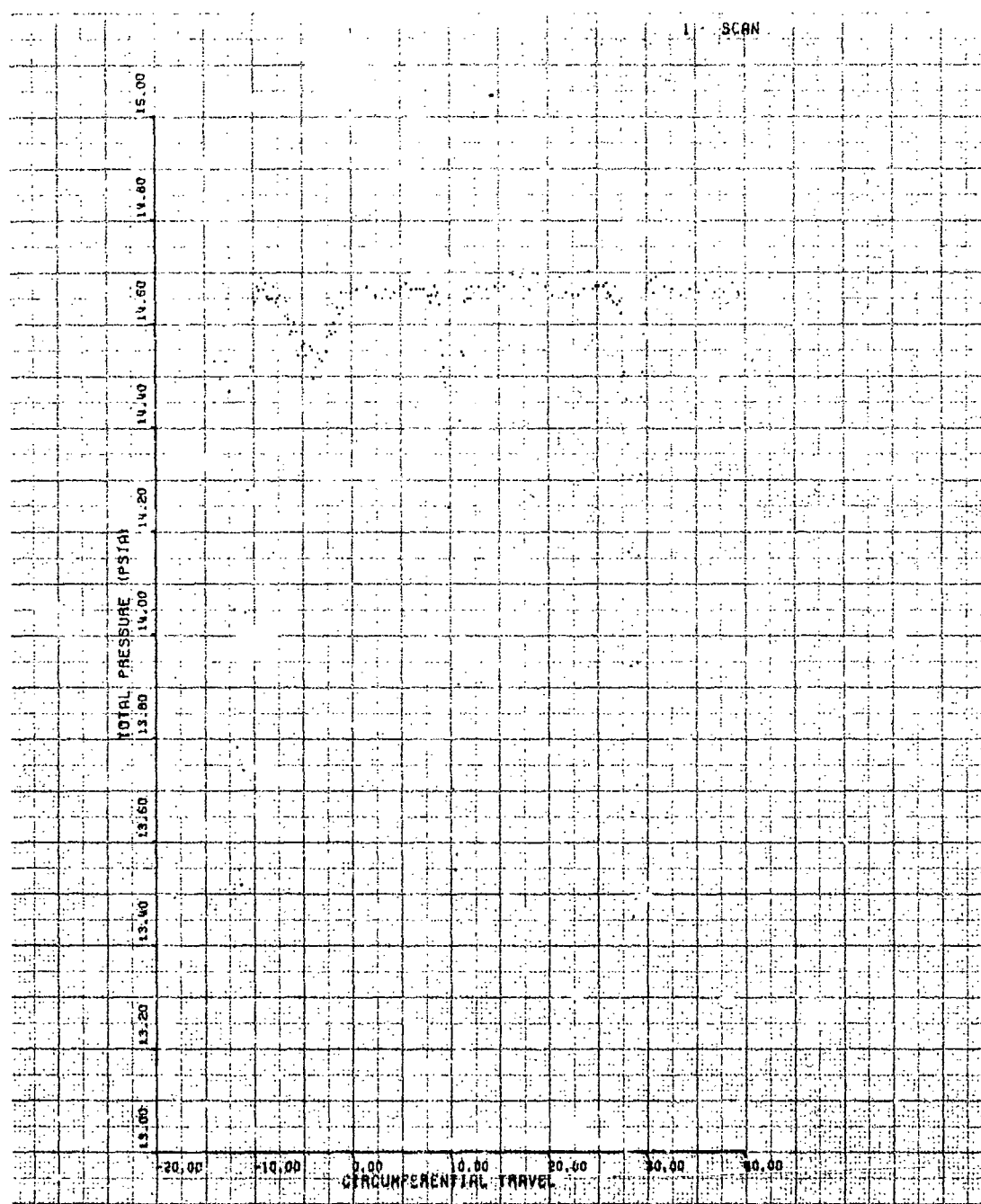


Figure 128. IGV Circumferential Traverse, Build No. 6,  
101% Speed, 0-deg IGV, 70% Span.

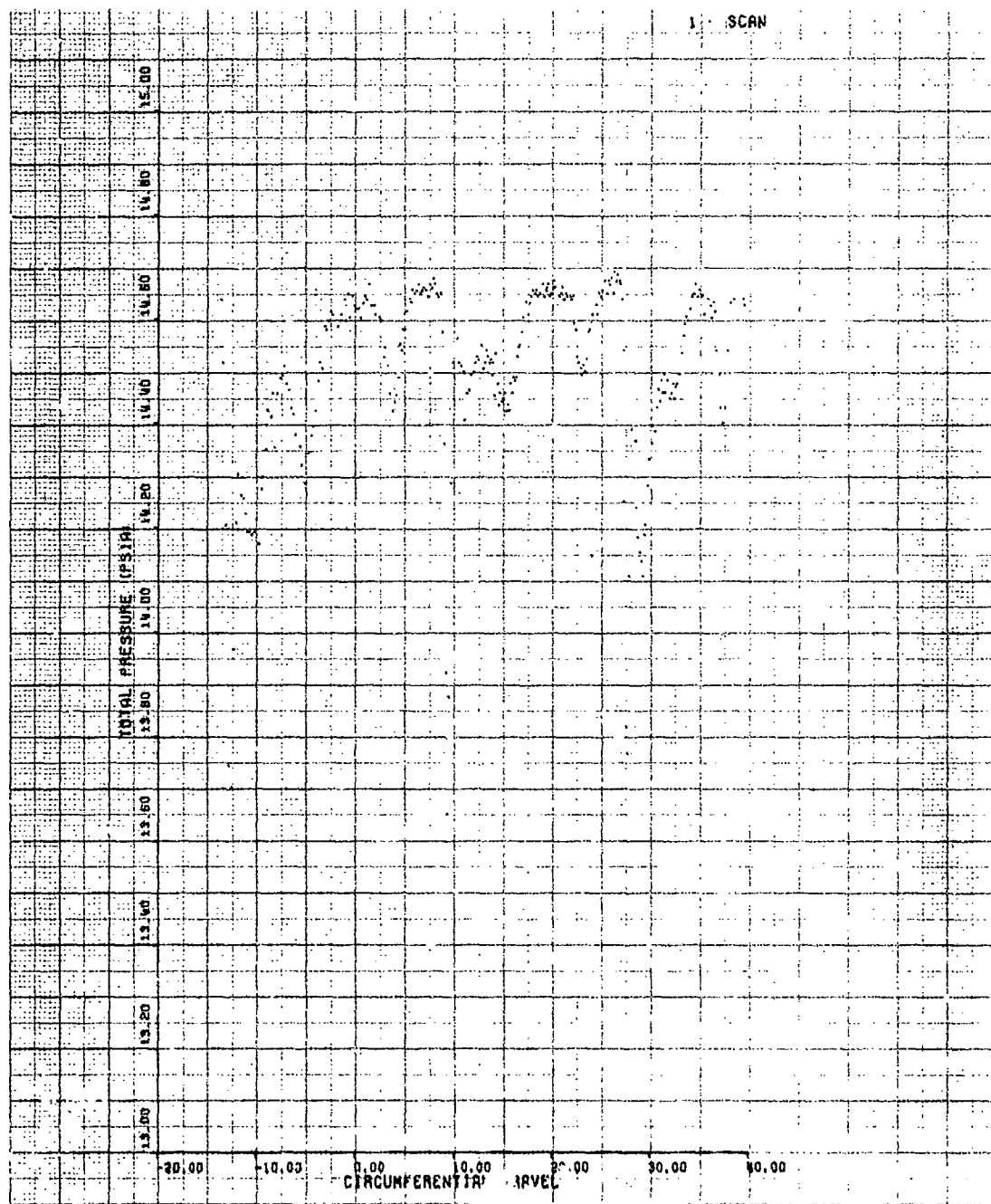


Figure 129. IGV Circumferential Traverse, Build No. 6,  
101% Speed, 0-deg IGV, 90% Span.

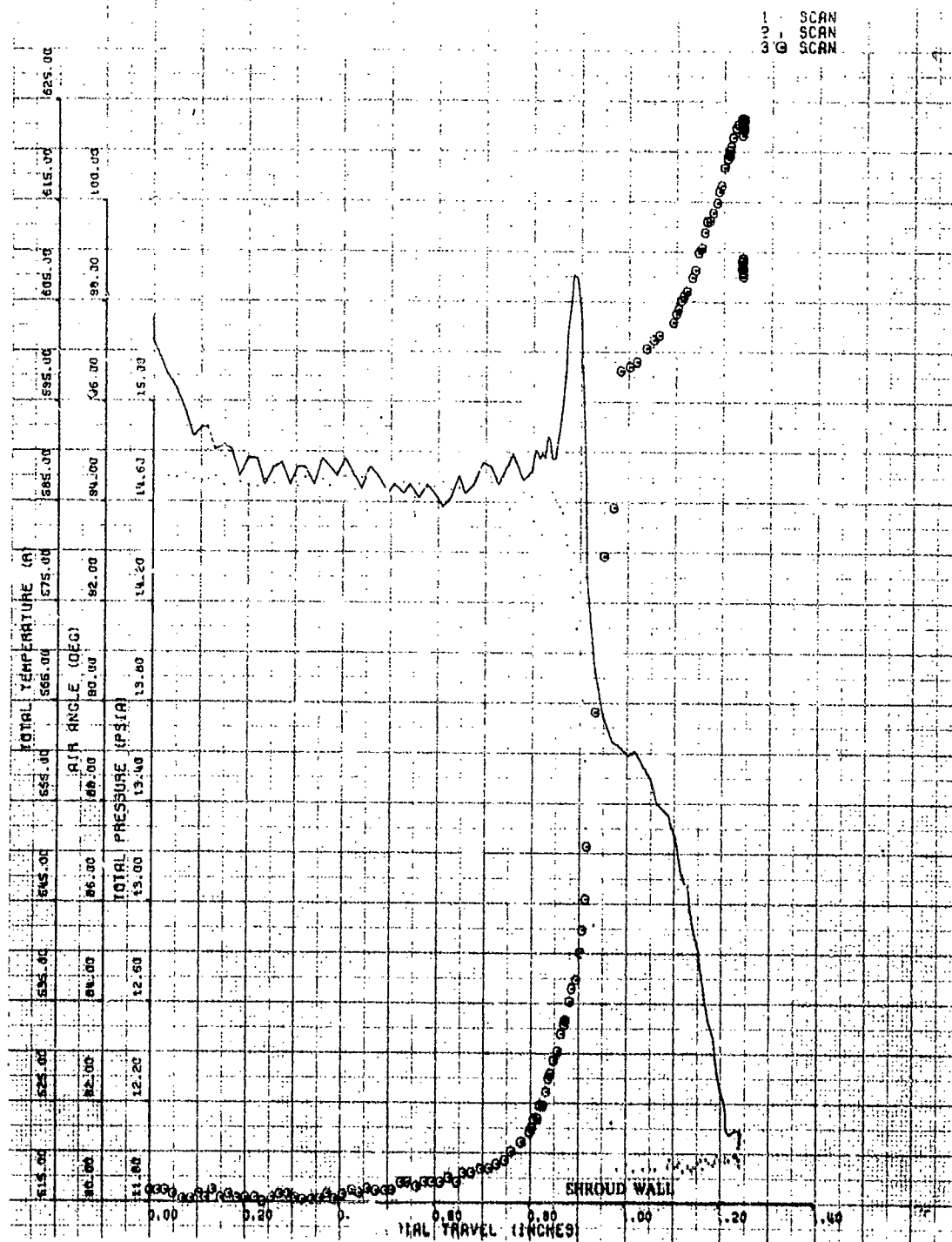


Figure 130. IGV Exit Radial Traverse, Build No. 6, 101% Speed, -4-deg IGV.

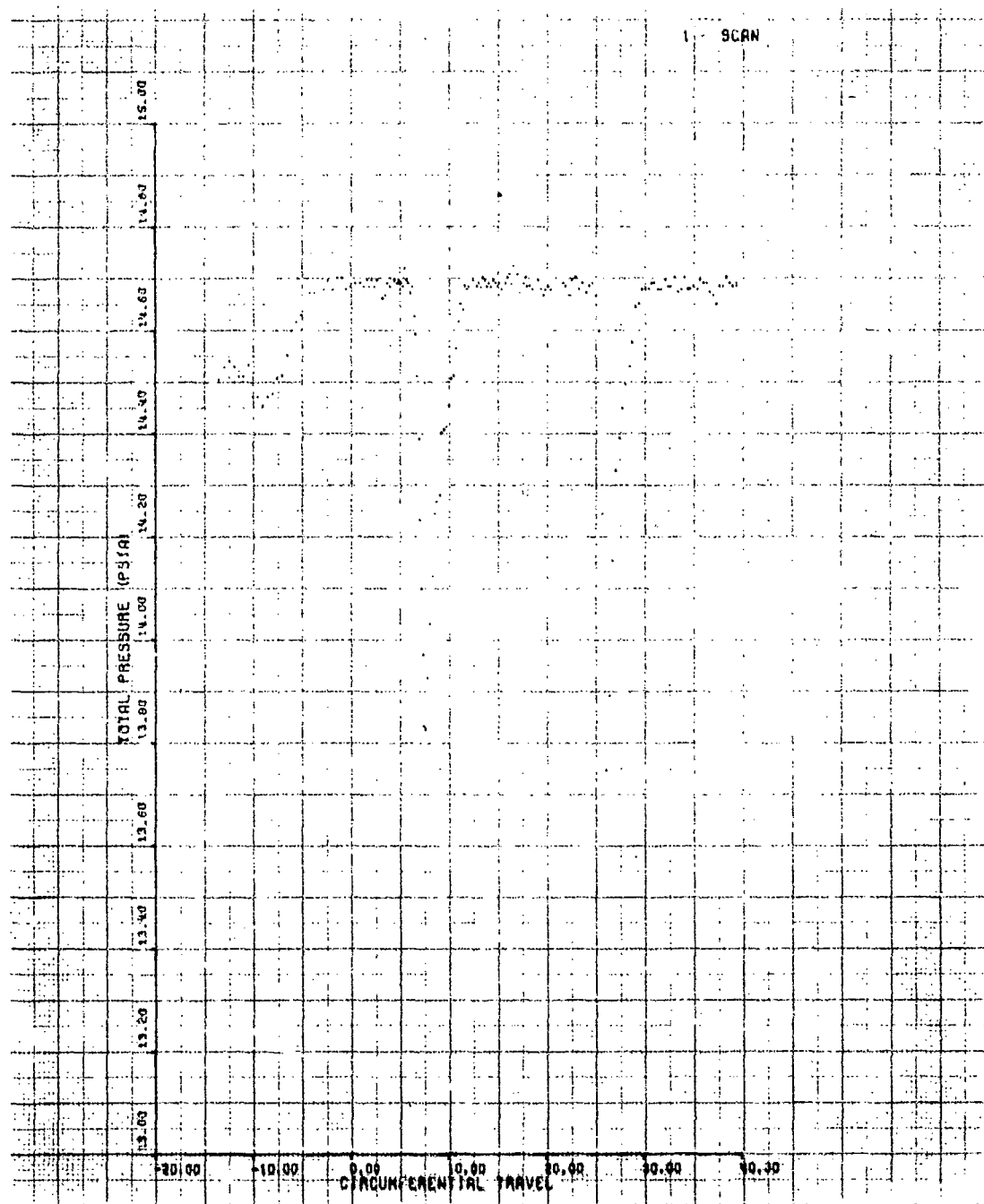


Figure 131. IGV Circumferential Traverse, Build No. 6,  
101% Speed, -4-deg IGV, 10% Span.

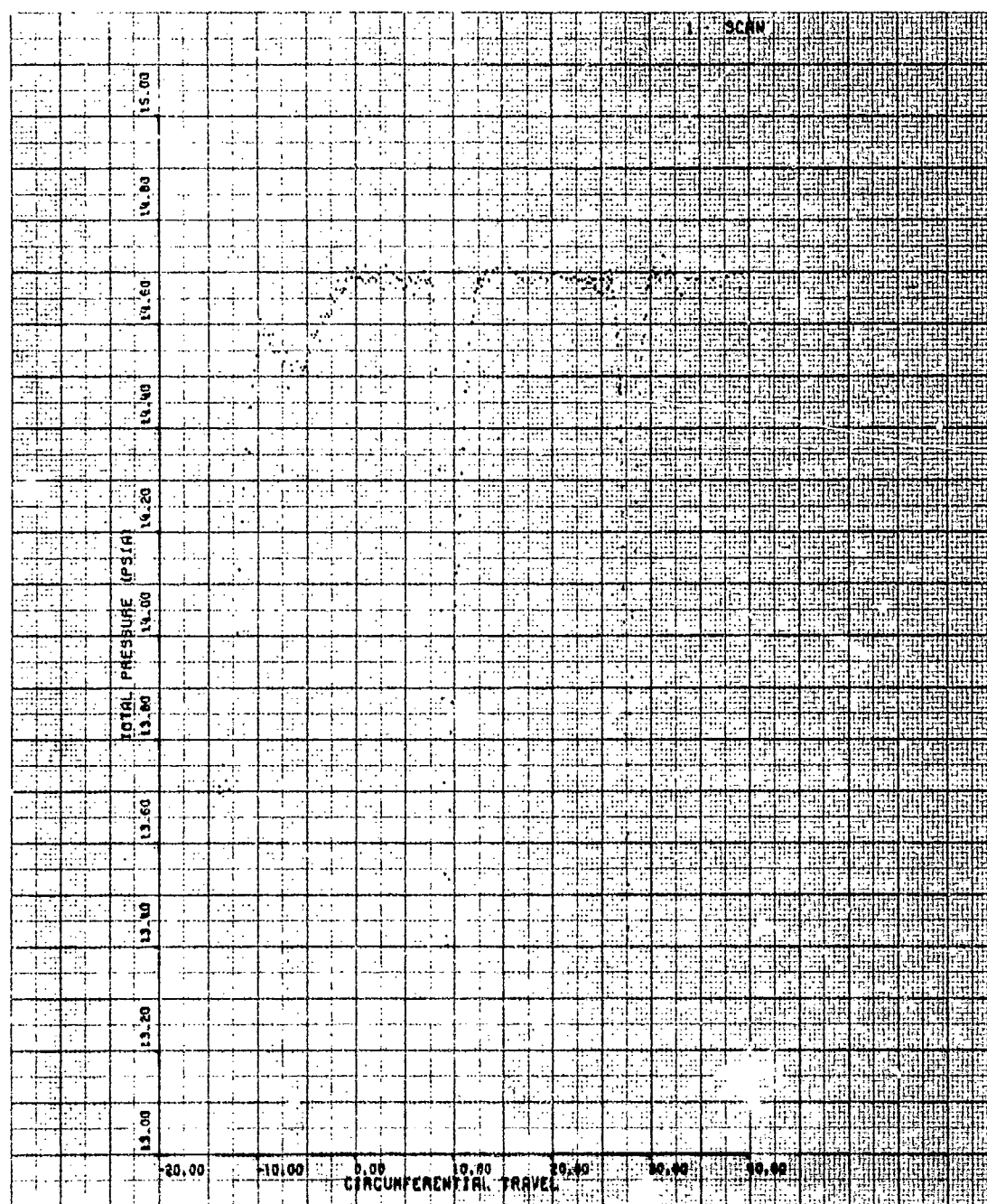


Figure 132. IGV Circumferential Traverse, Build No. 6,  
101% Speed, -4-deg IGV, 30% Span.

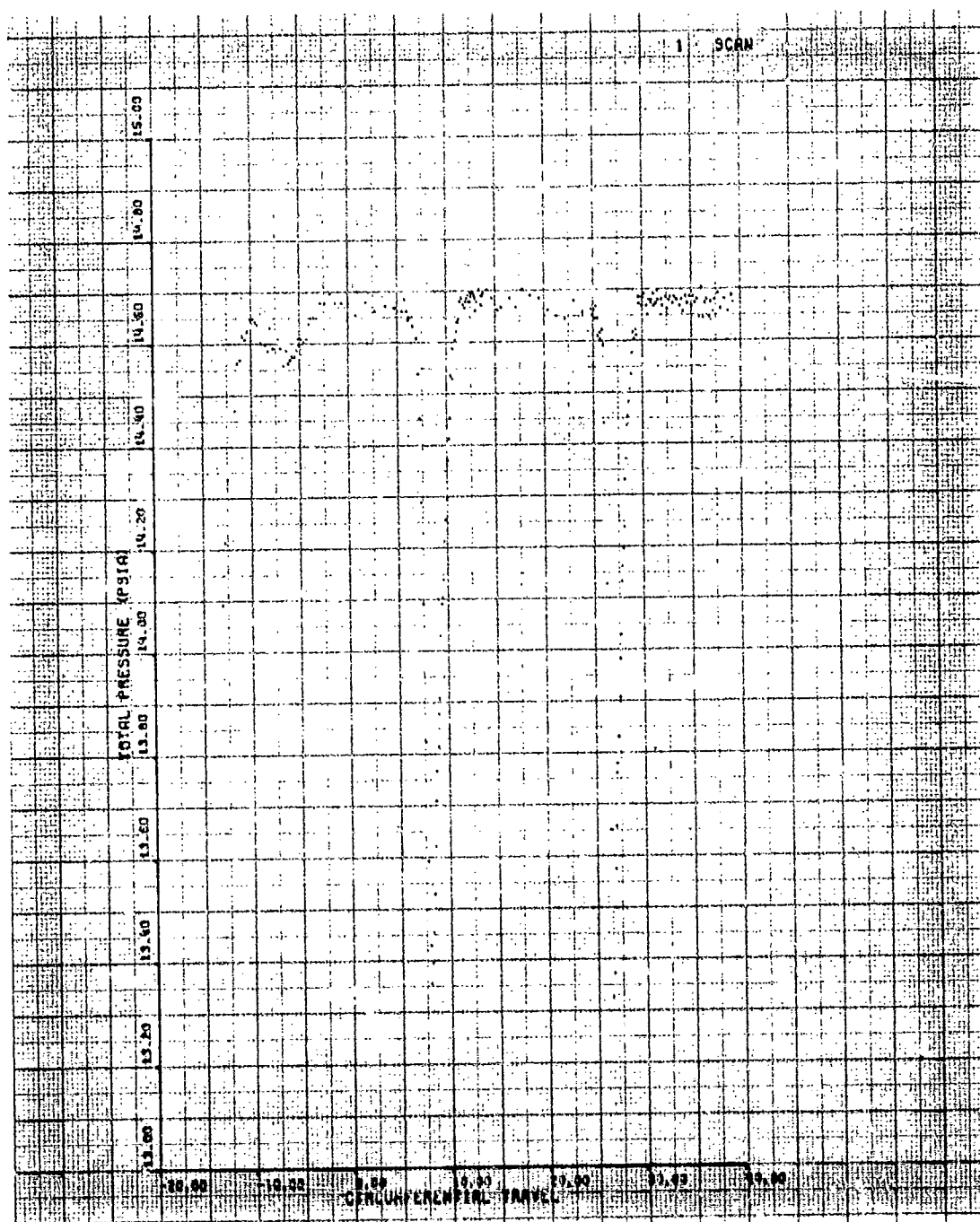


Figure 133. IGV Circumferential Traverse, Build No. 6,  
101% Speed, -4-deg IGV, 50% Span.

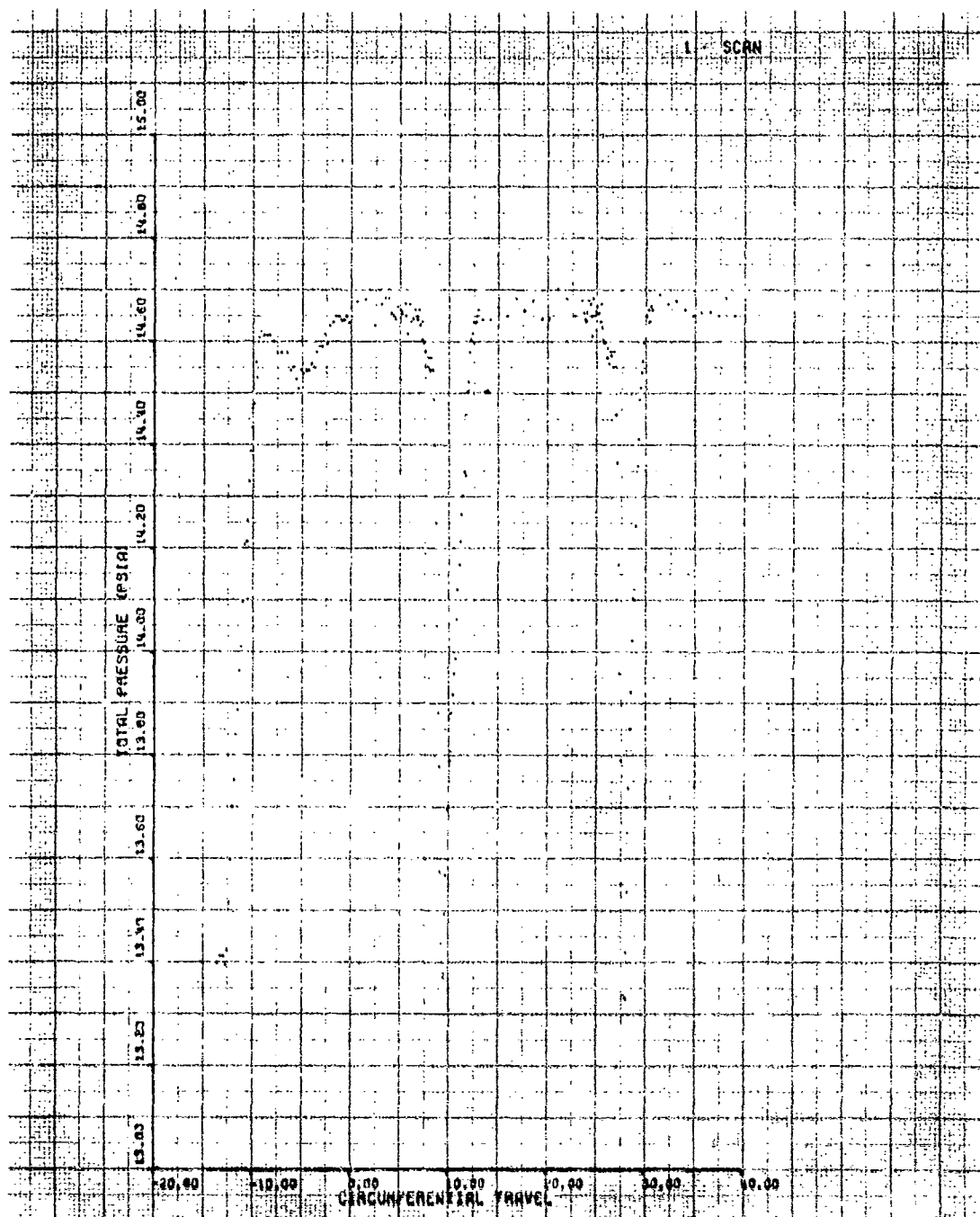


Figure 134. IGV Circumferential Traverse, Build No. 6,  
101% Speed, -4-deg IGV, 70% Span.

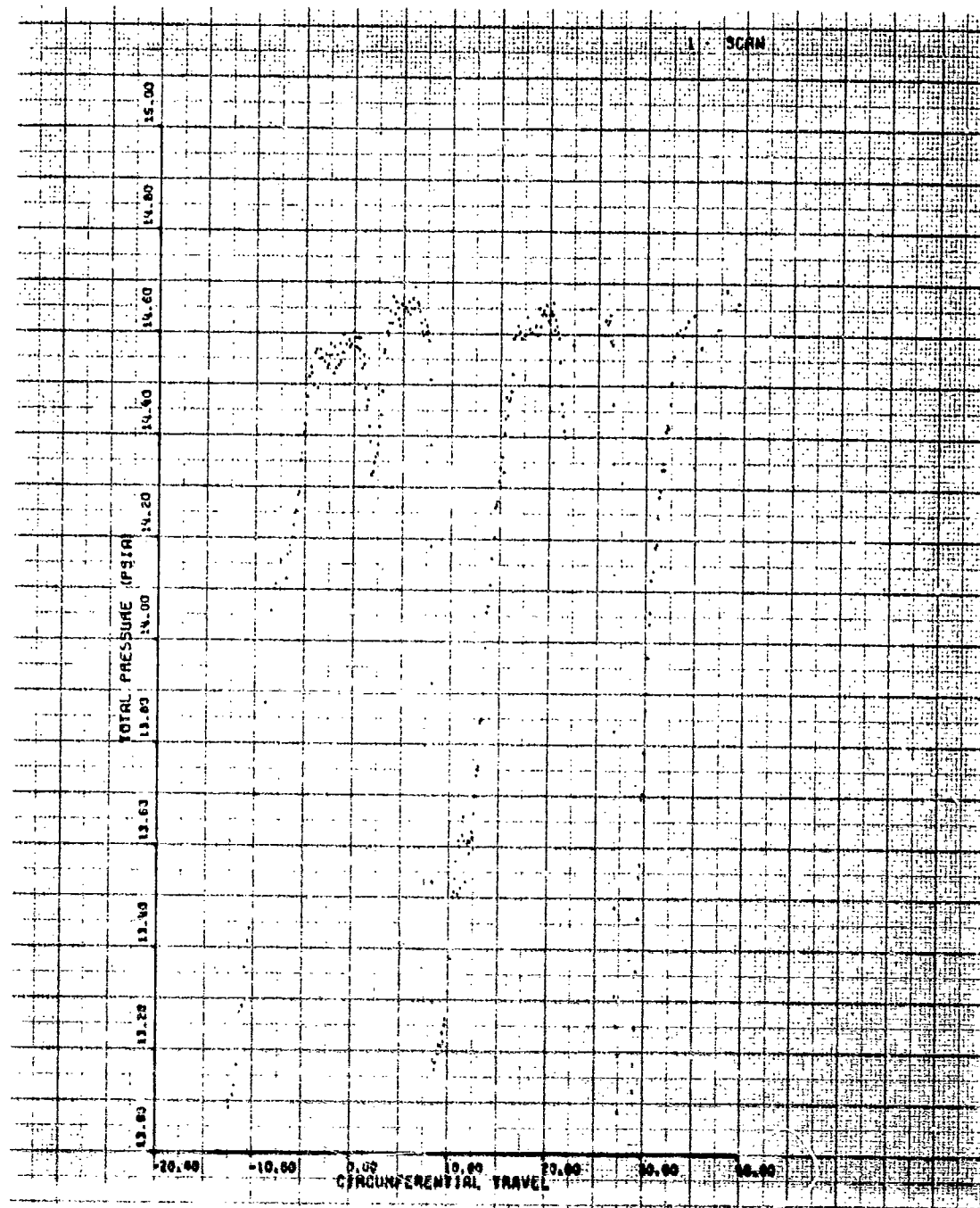


Figure 135. IGV Circumferential Traverse, Build No. 6,  
101% Speed, -4-deg IGV, 90% Span.



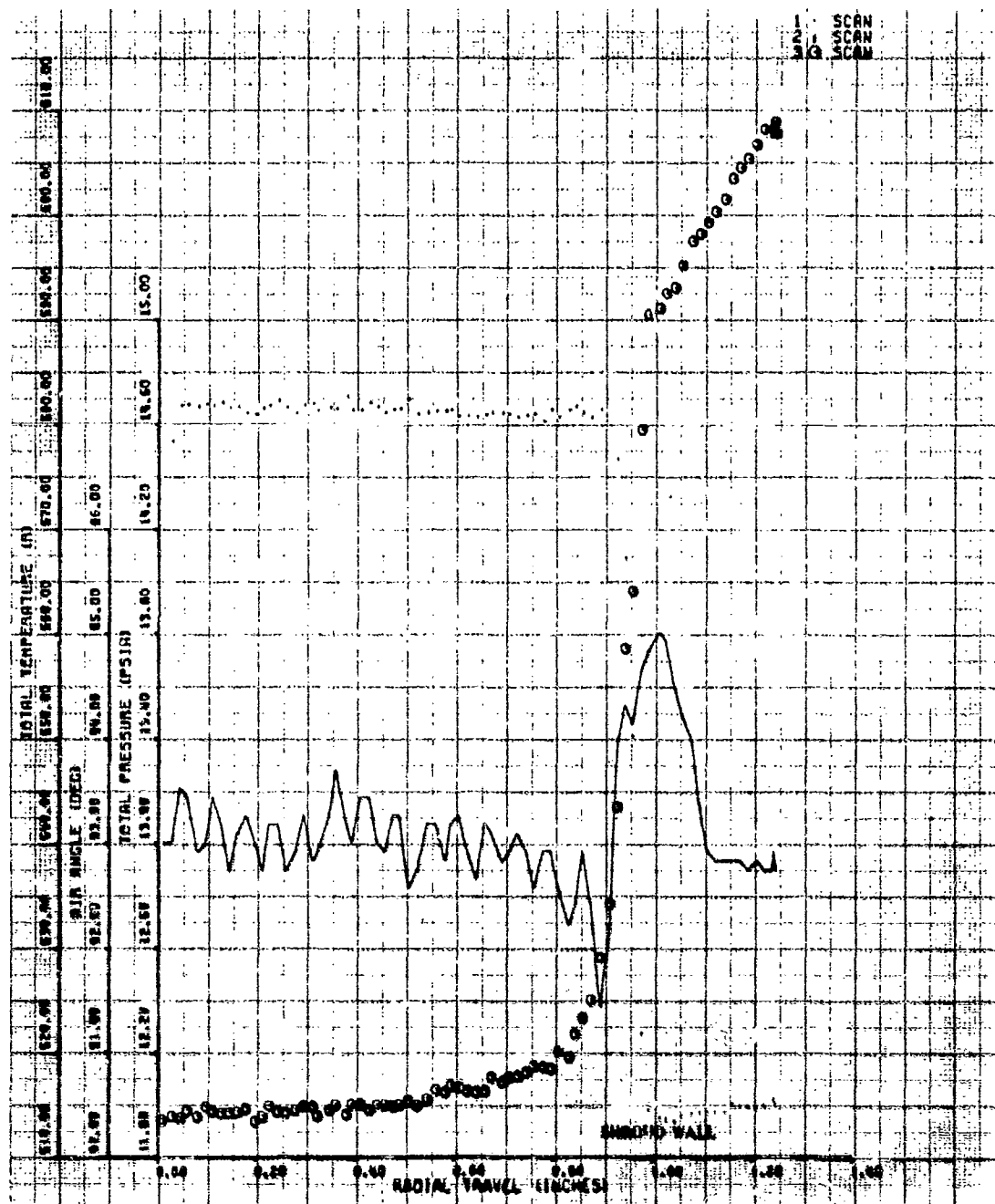


Figure 136. IGV Exit Radial Traverse, Build No. 6,  
1017 Speed, -5-deg IGV.

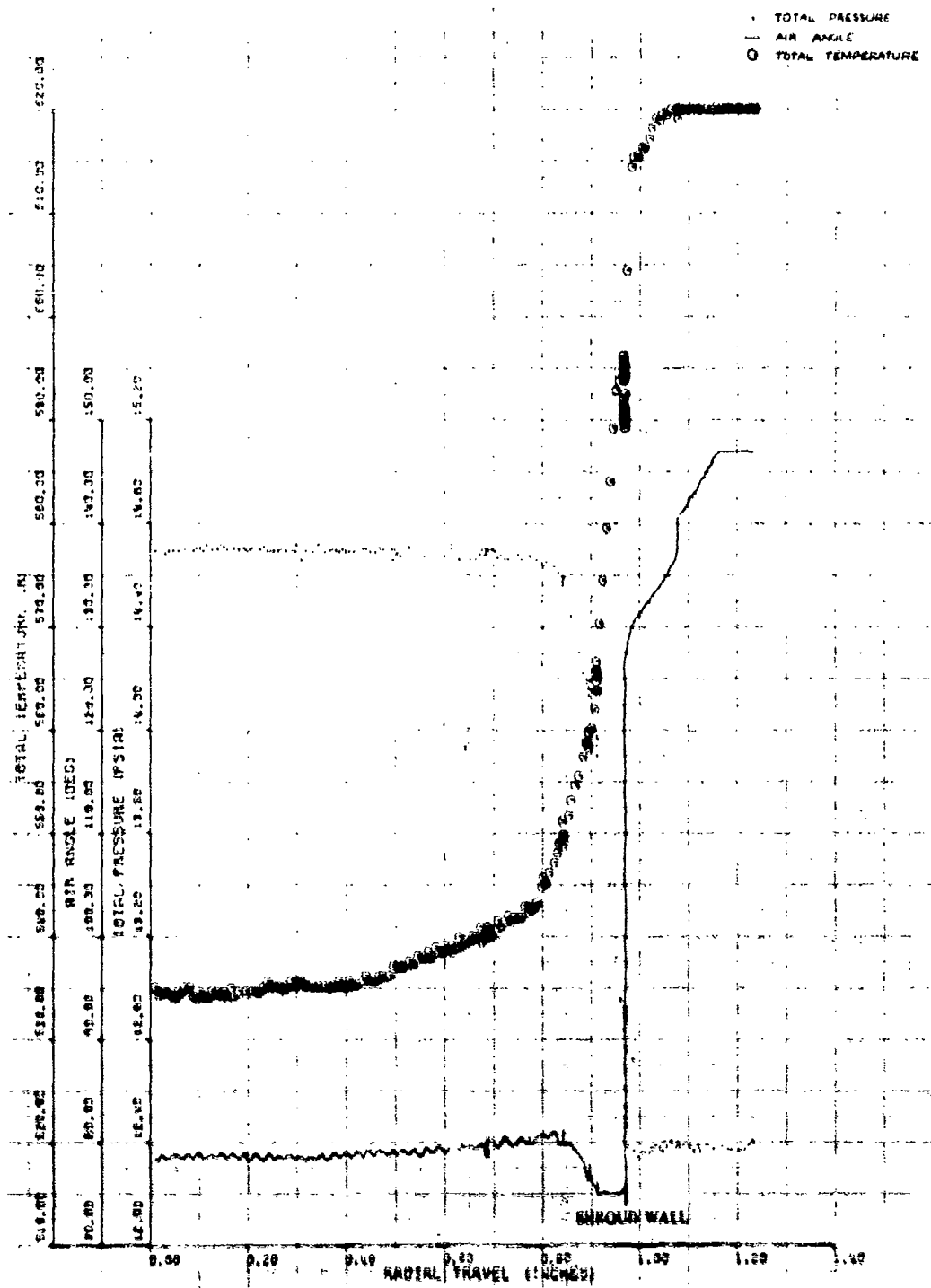


Figure 137. 10V Exit Radial Traverse, Build No. 6, 100% Speed, 10-deg 10V, Near Stall.

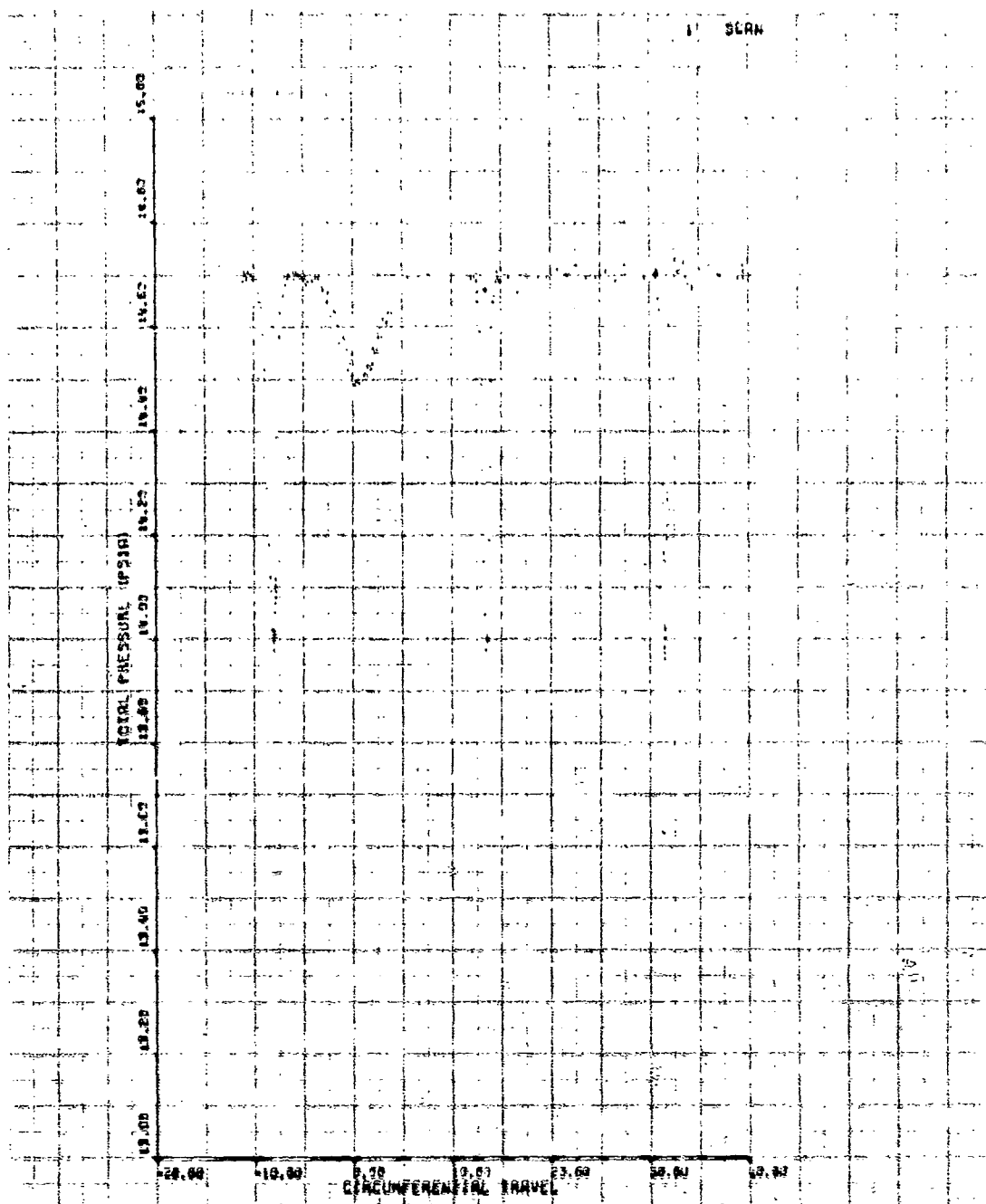


Figure 138. IGV Circumferential Traverse, Build No. 6,  
100% Speed, 10-deg IGV, 10% Span.

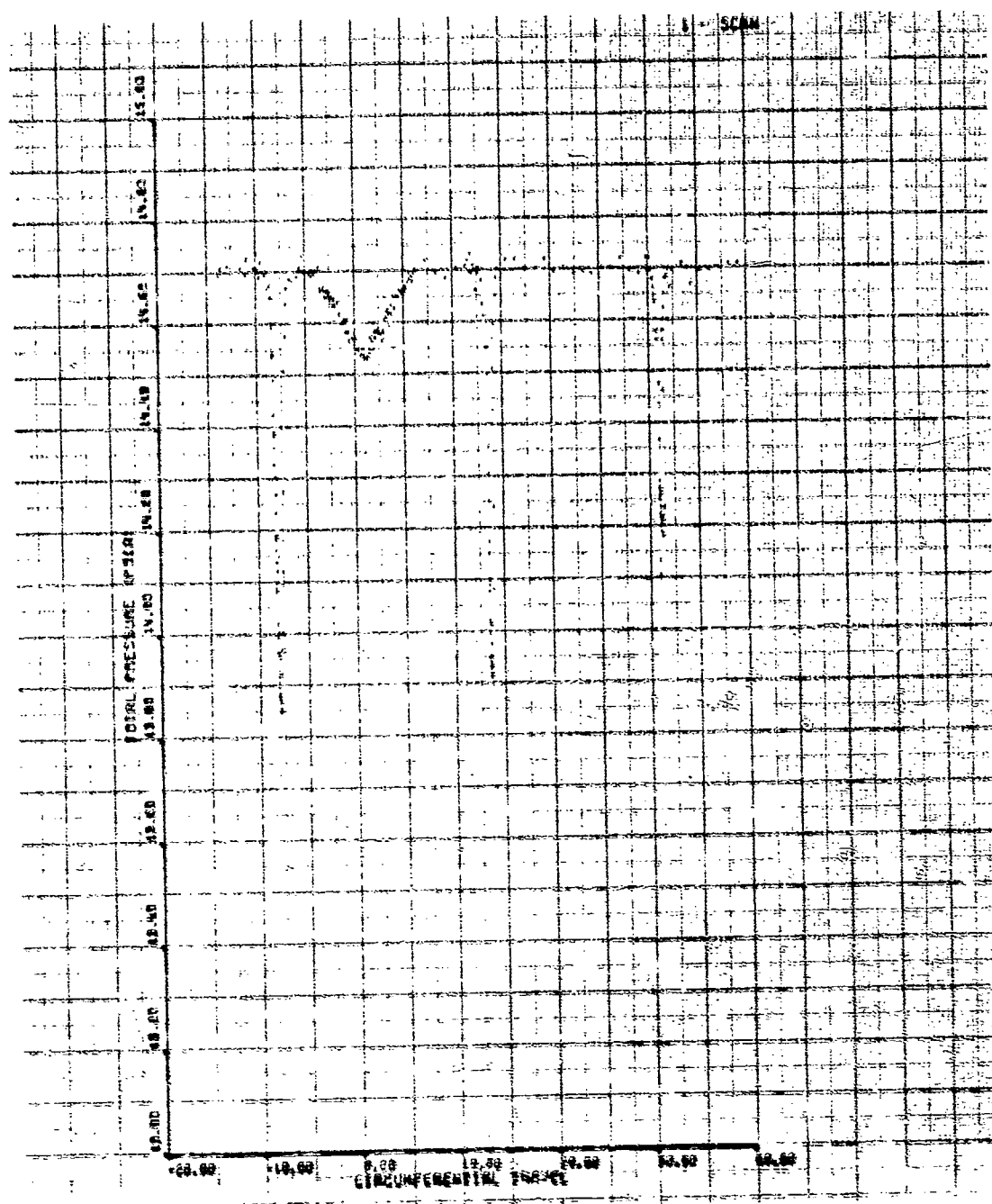


Figure 139. IGV Circumferential Traverse, Build No. 6,  
100% Speed, 10-deg IGV, 30° Span.

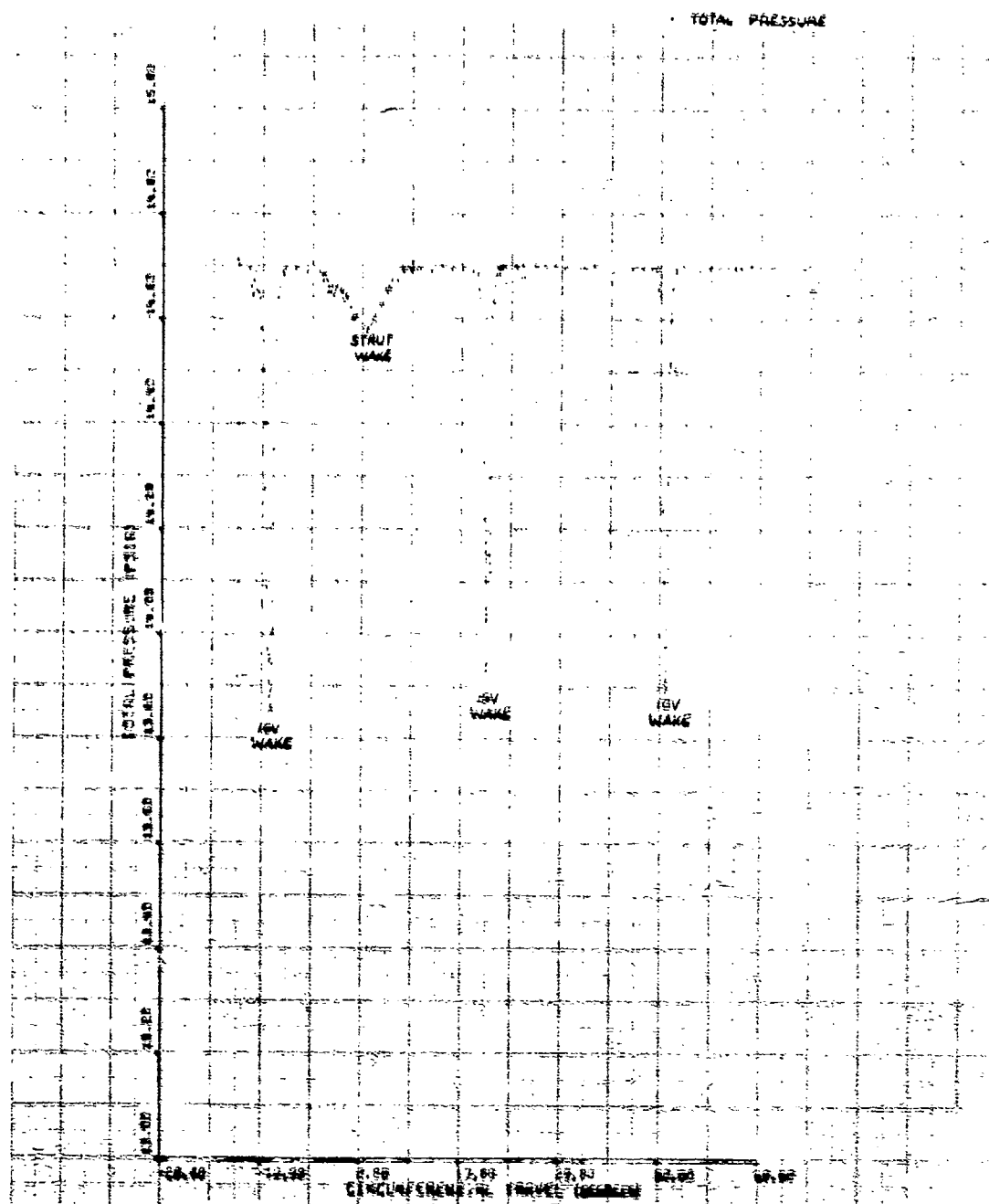


Figure 140. IGV Circumferential Traverse, Build No. 6,  
100% Speed, 10-deg IGV, 50% Span.

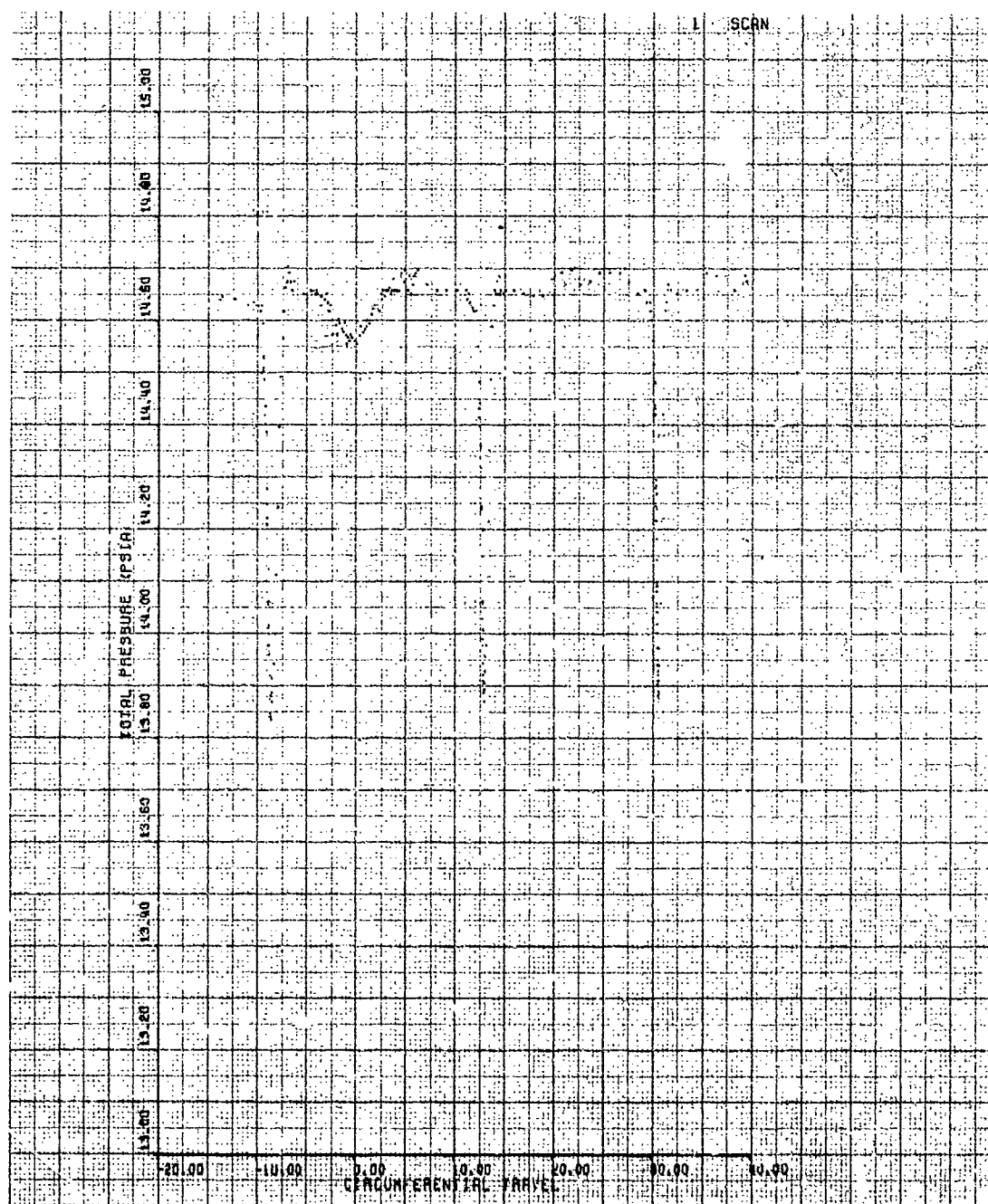


Figure 141. IGV Circumferential Traverse, Build No. 6,  
100% Speed, 10-deg IGV, 70% Span.

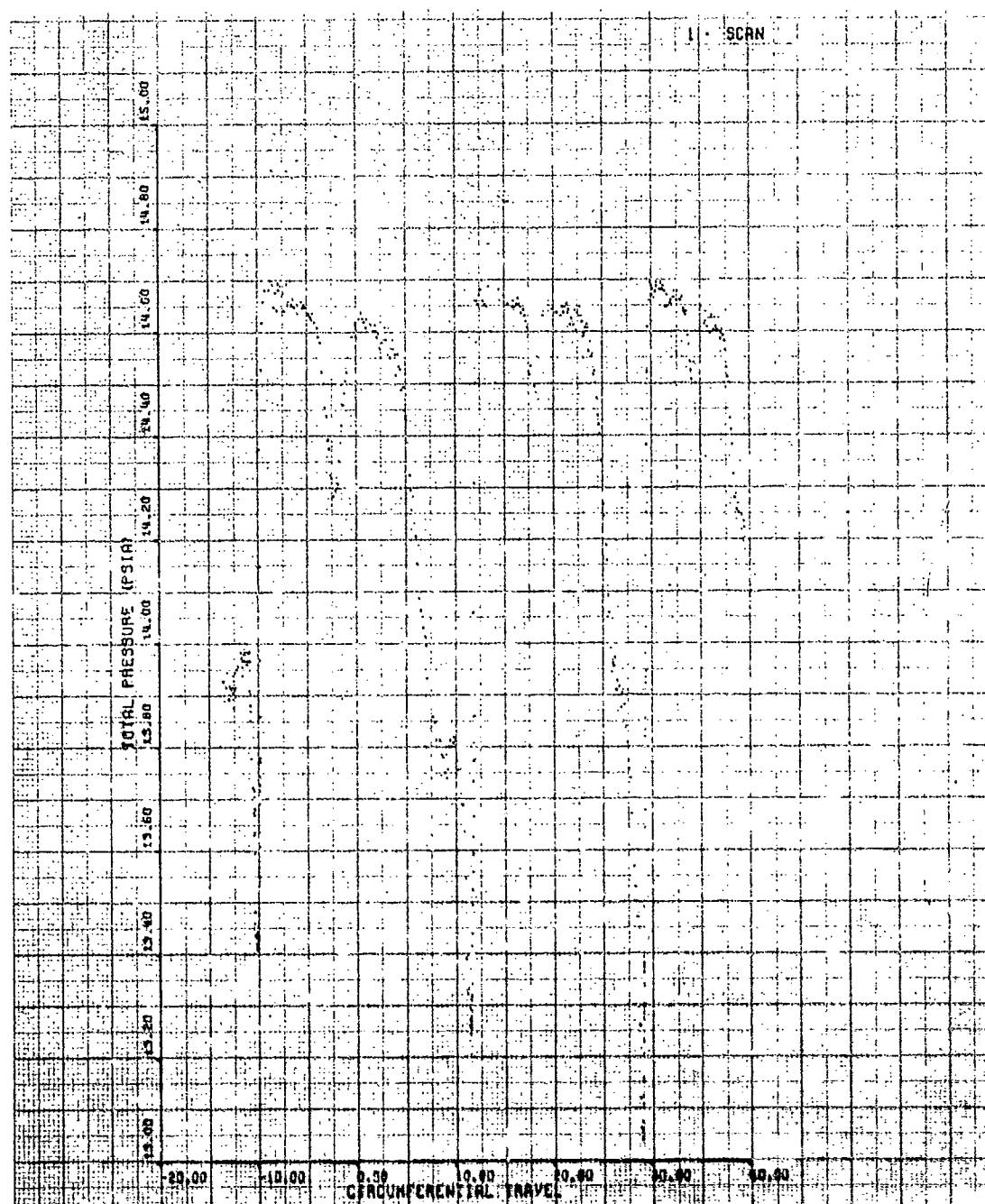


Figure 142. IGV Circumferential Traverse, Build No. 6,  
100% Speed, 10-deg IGV, 90% Span.

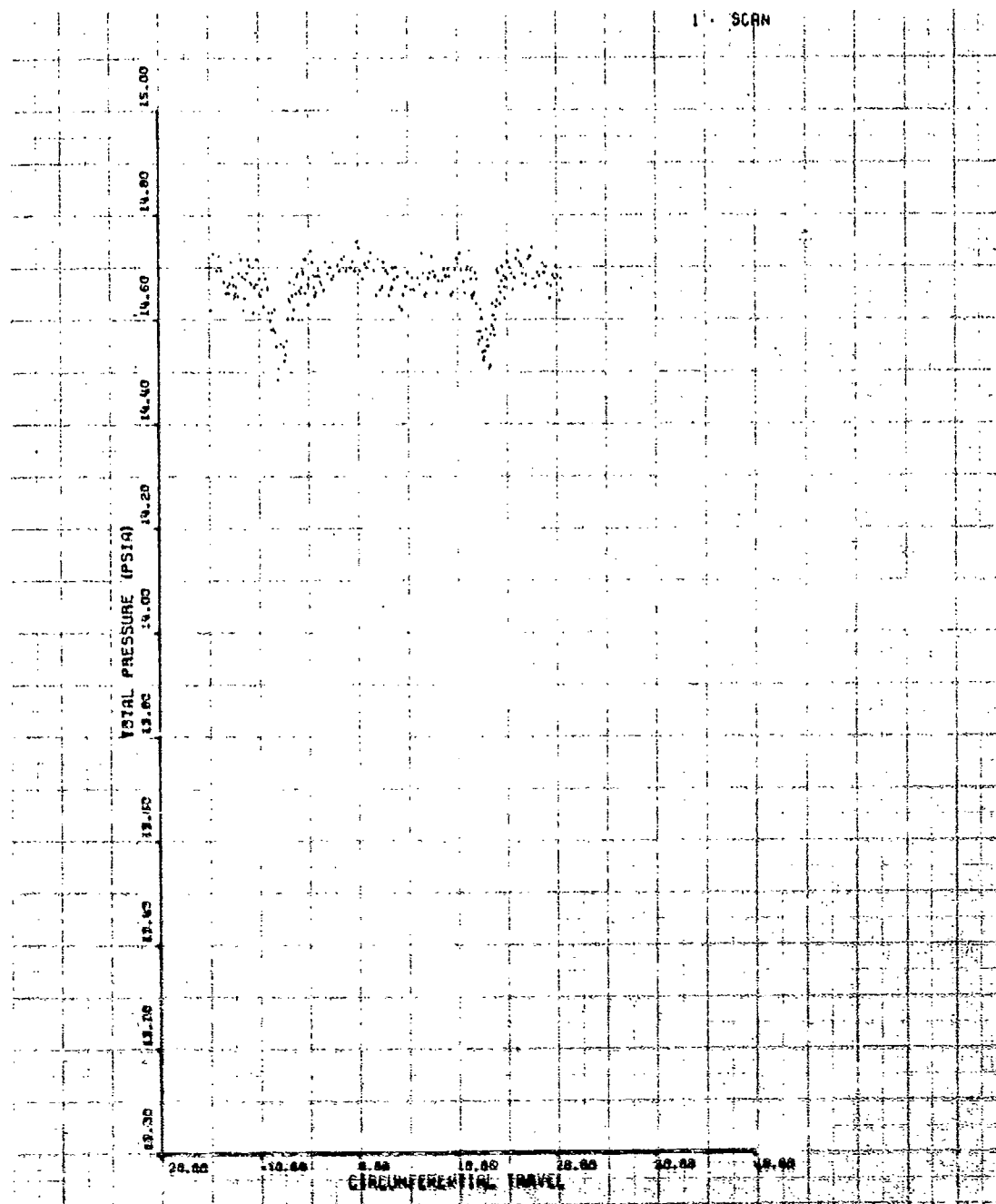


Figure 143. IGV Circumferential Traverse, Build No. 3,  
70% Speed, 10-deg IGV, 10% Span.



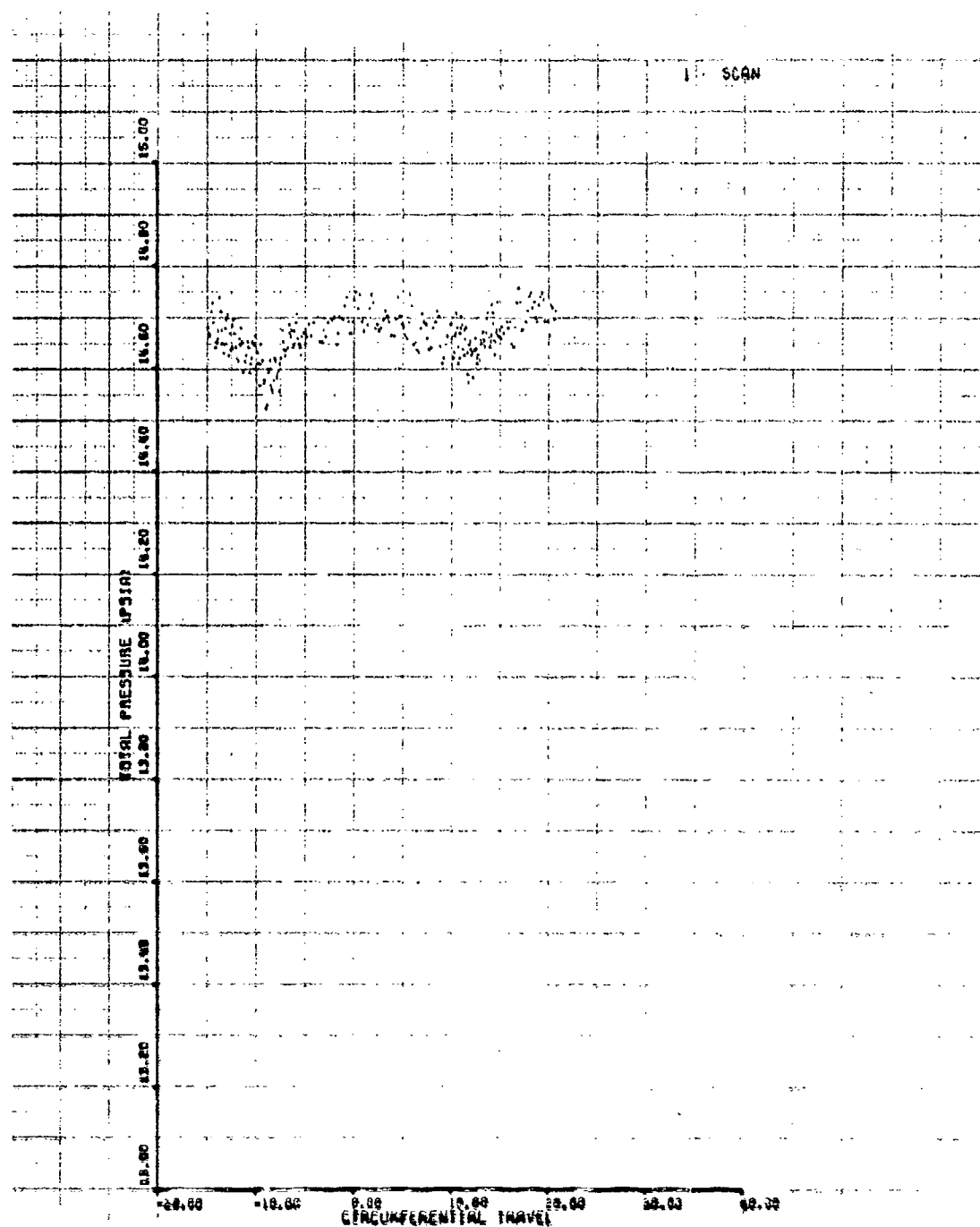


Figure 144. IGV Circumferential Traverse, Build No. 3,  
70% Speed, 10-deg IGV, 30" Span.

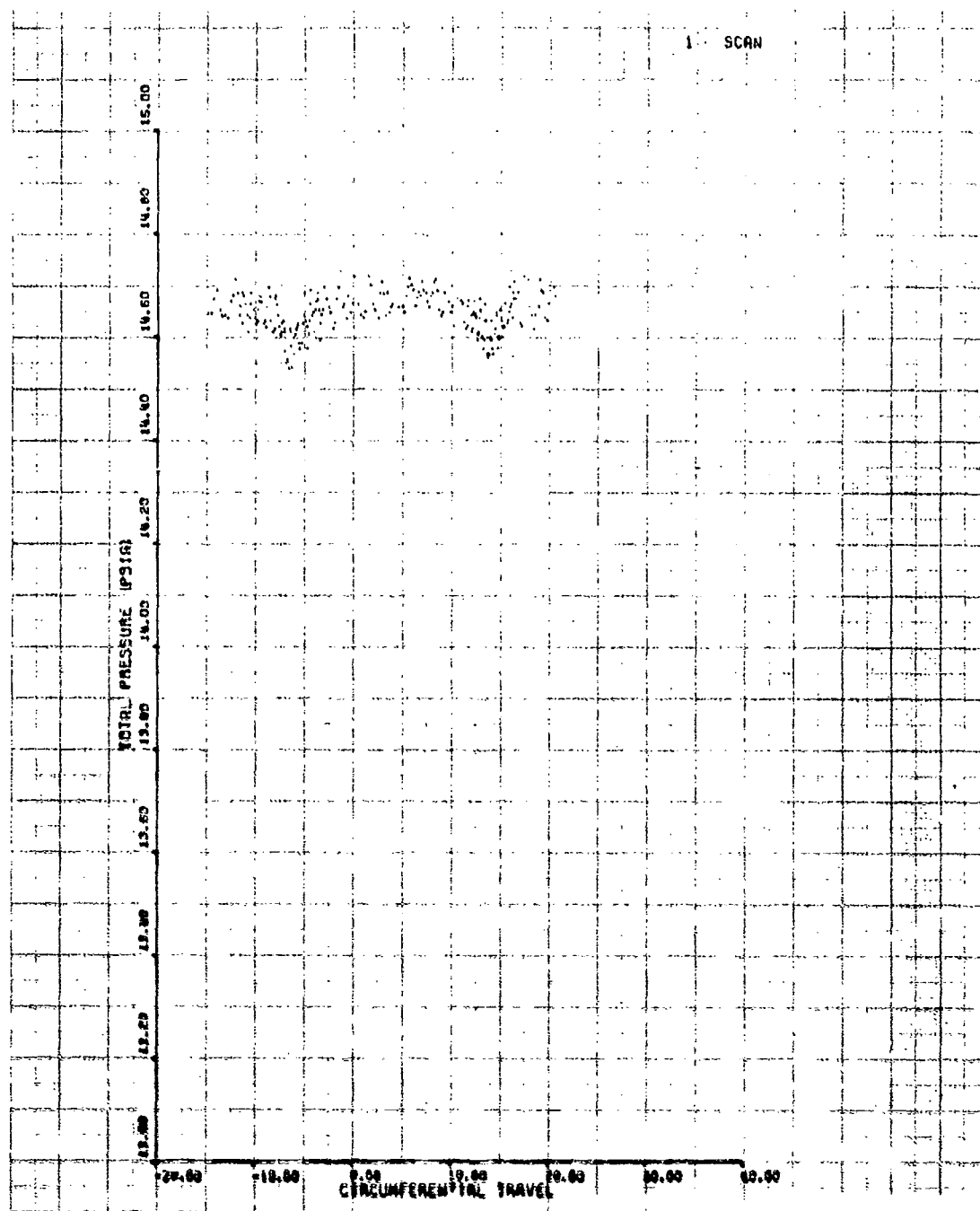


Figure 145. IGV Circumferential Traverse, Build No. 3,  
70% Speed, 10-deg IGV, 50% Span.

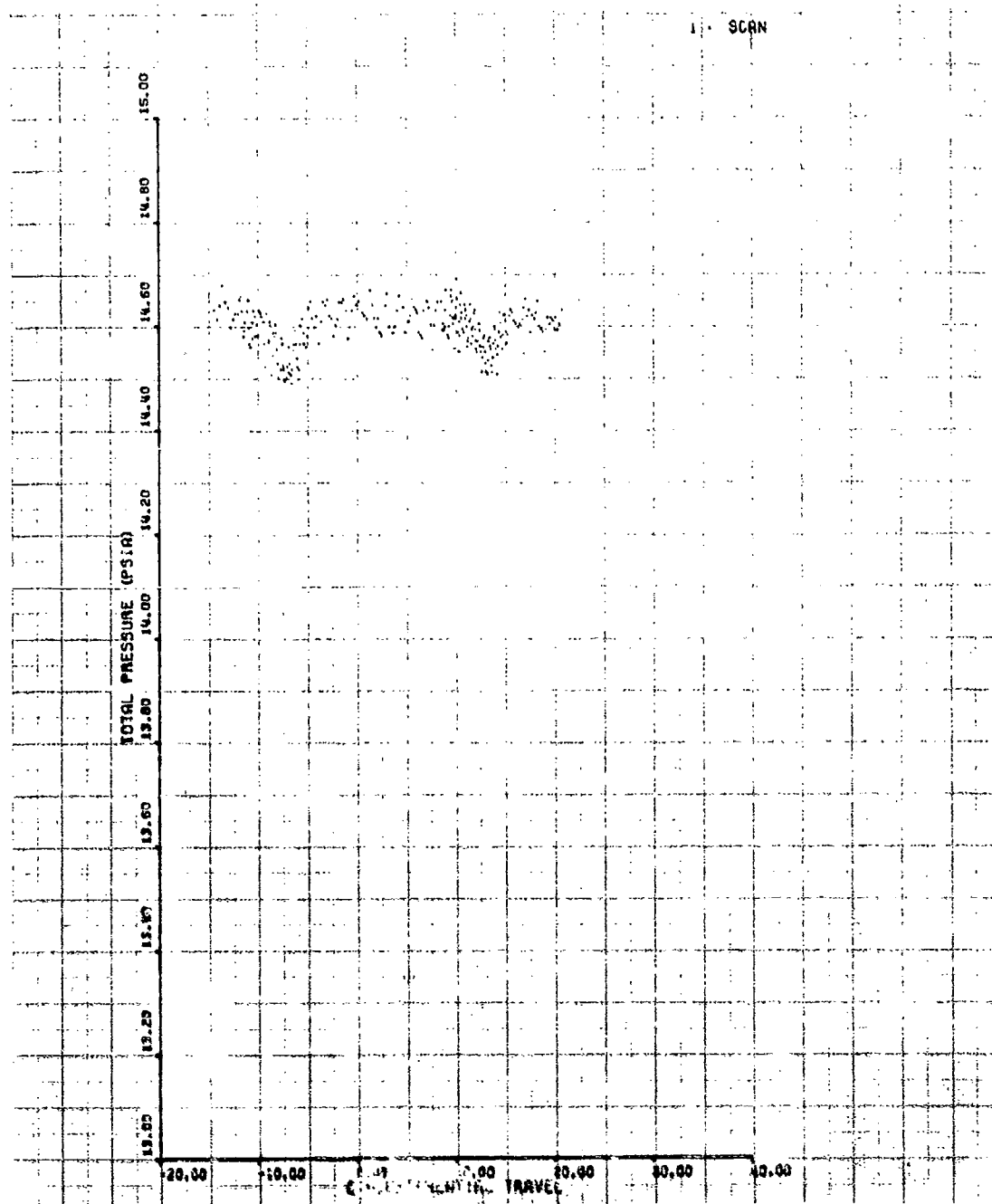


Figure 146. IGV Circumferential Traverse, Build No. 3,  
70% Speed, 10-deg IGV, 70% Span.

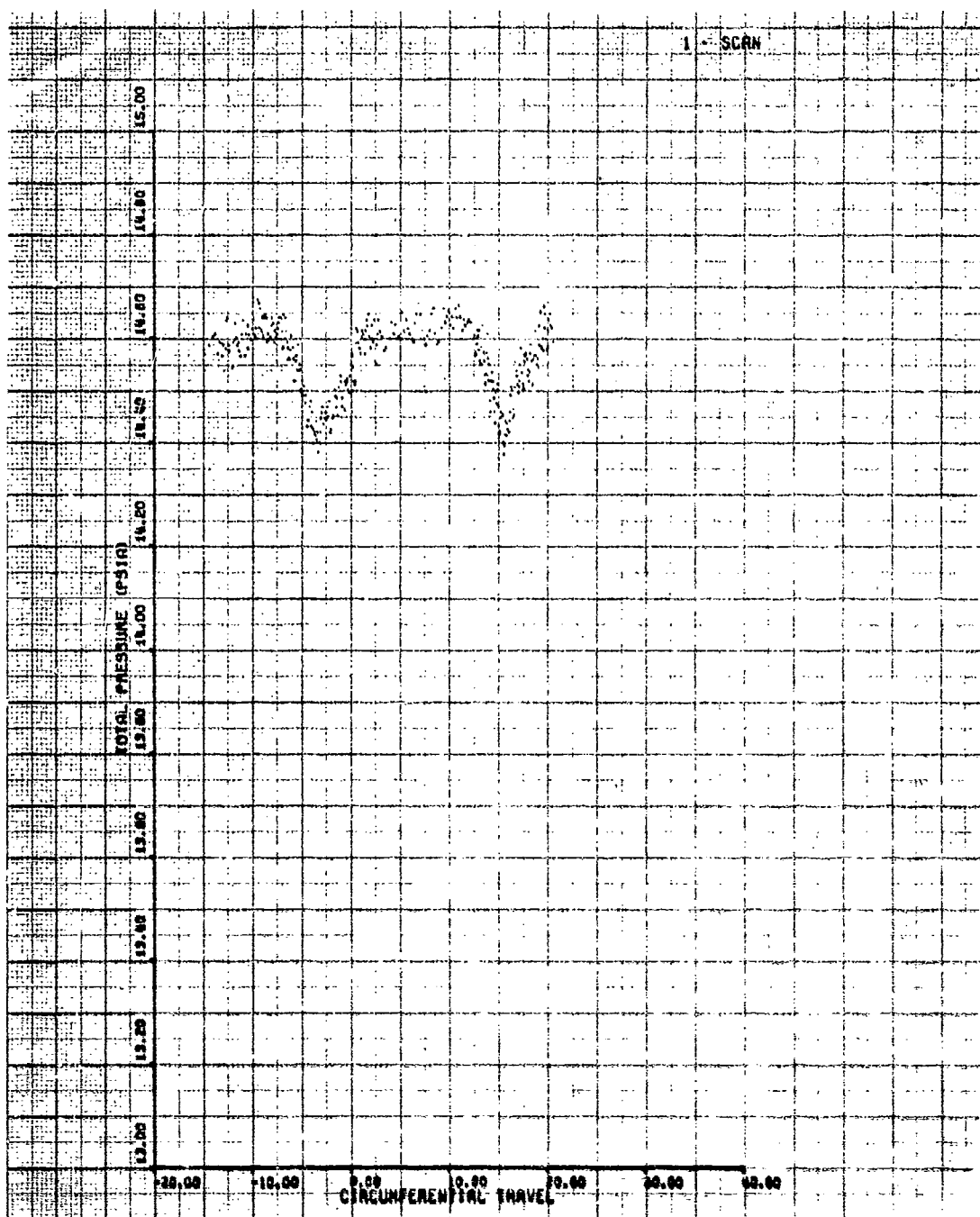


Figure 147. IGV Circumferential Traverse, Build No. 3,  
70% Speed, 10-deg IGV, 90% Span.

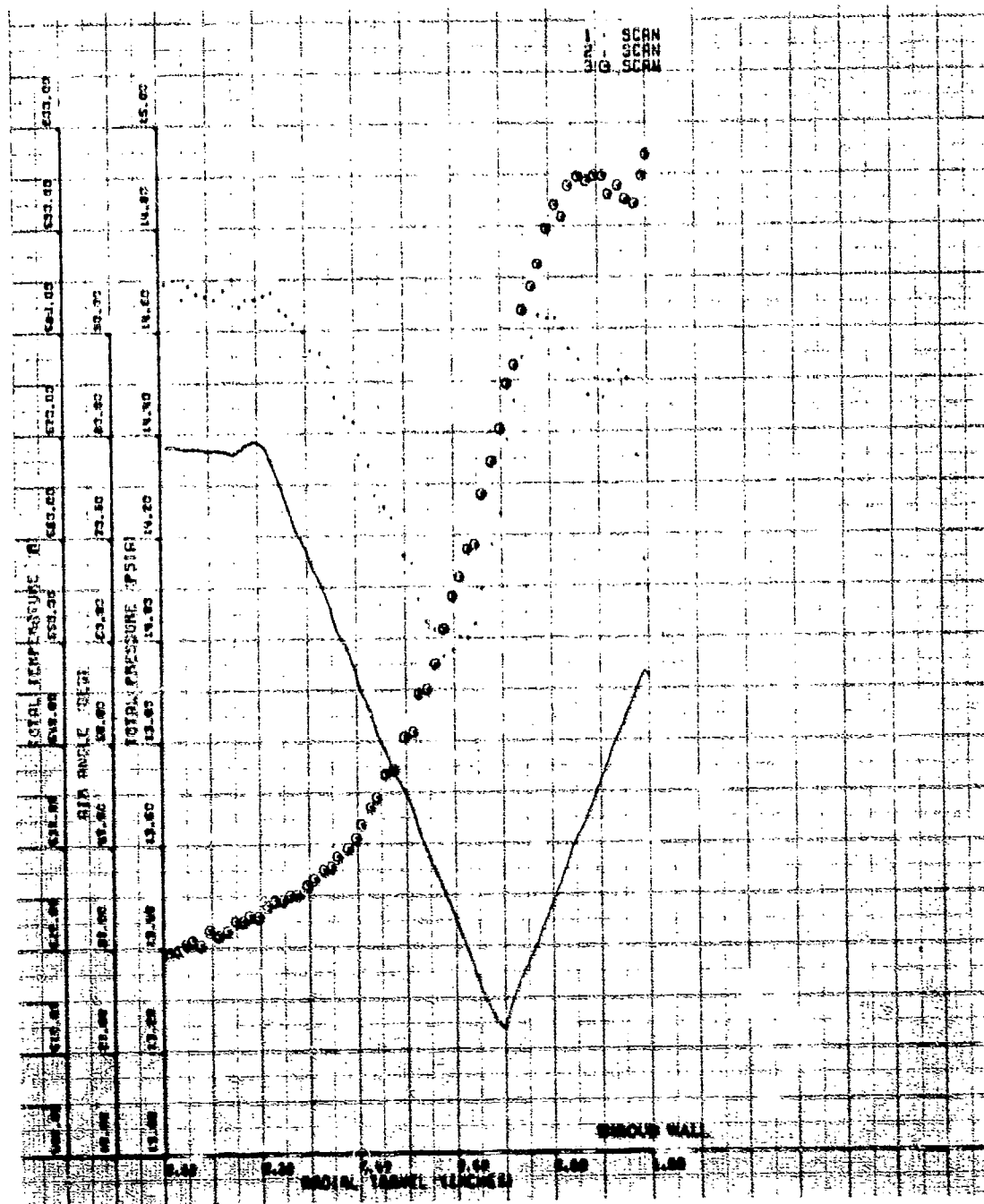


Figure 148. IGV Exit Radial Traverse, Build No. 6,  
70% Speed, 10-deg IGV, Near Stall.

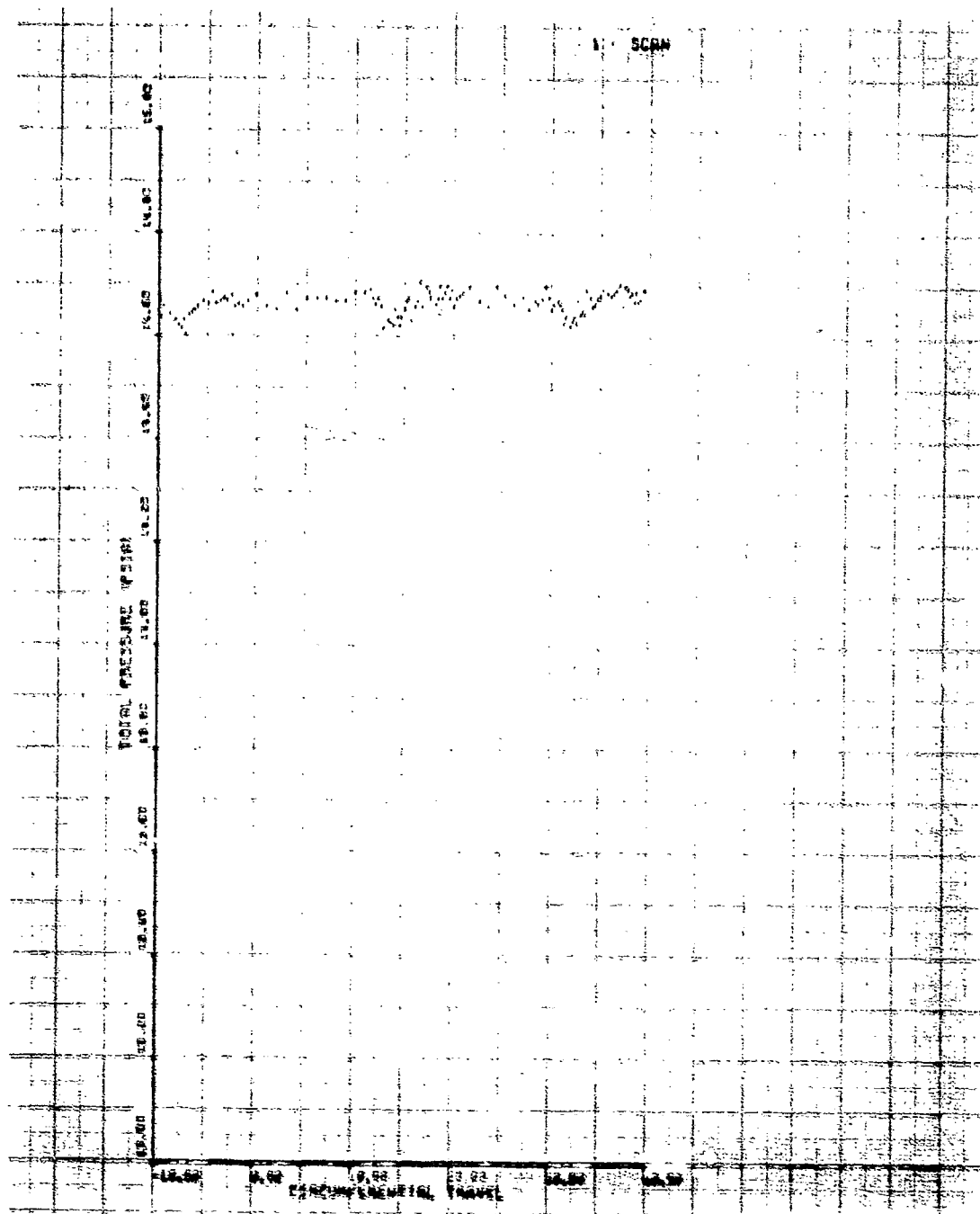


Figure 149. IGV Circumferential Travel, Build No. 6,  
70% Speed, 10-deg IGV, 10% Span.

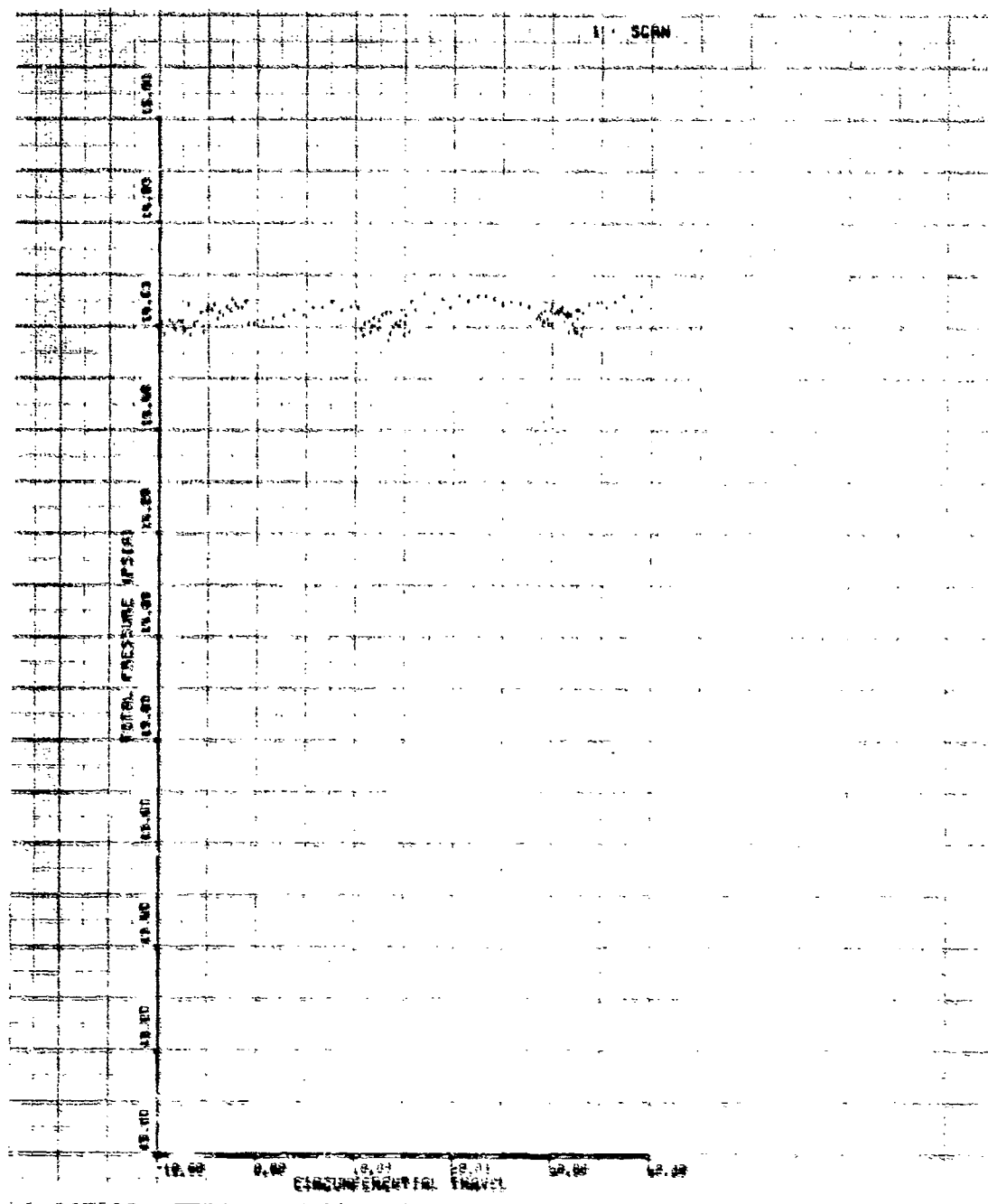


Figure 150. IGV Circumferential Traverse, Build No. 6,  
70% Speed, 10-deg IGV, 30% Span.

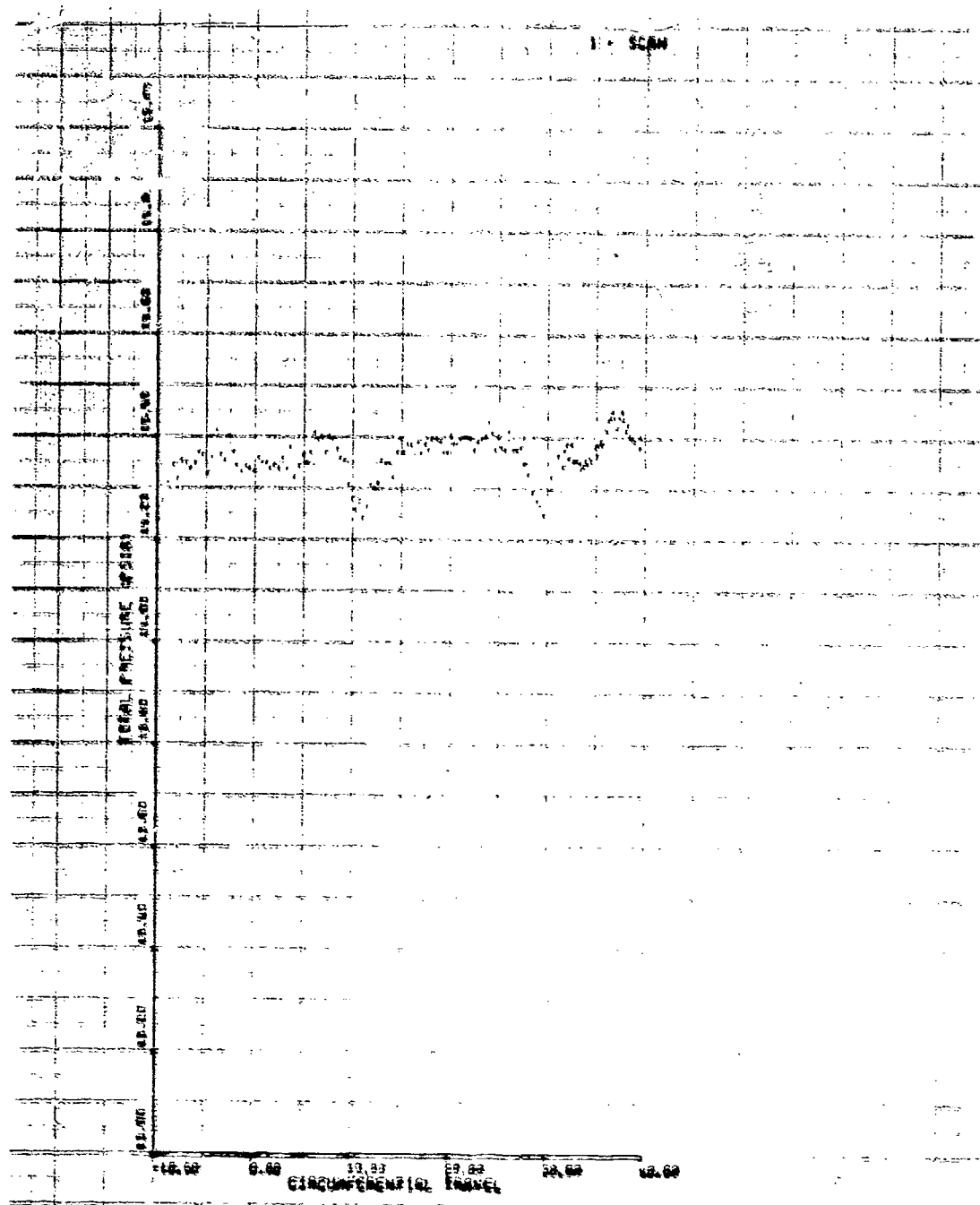


Figure 131. IGV Circumferential Traverse, Build No. 6,  
70% Speed, 10-deg IGV, 30% Span.



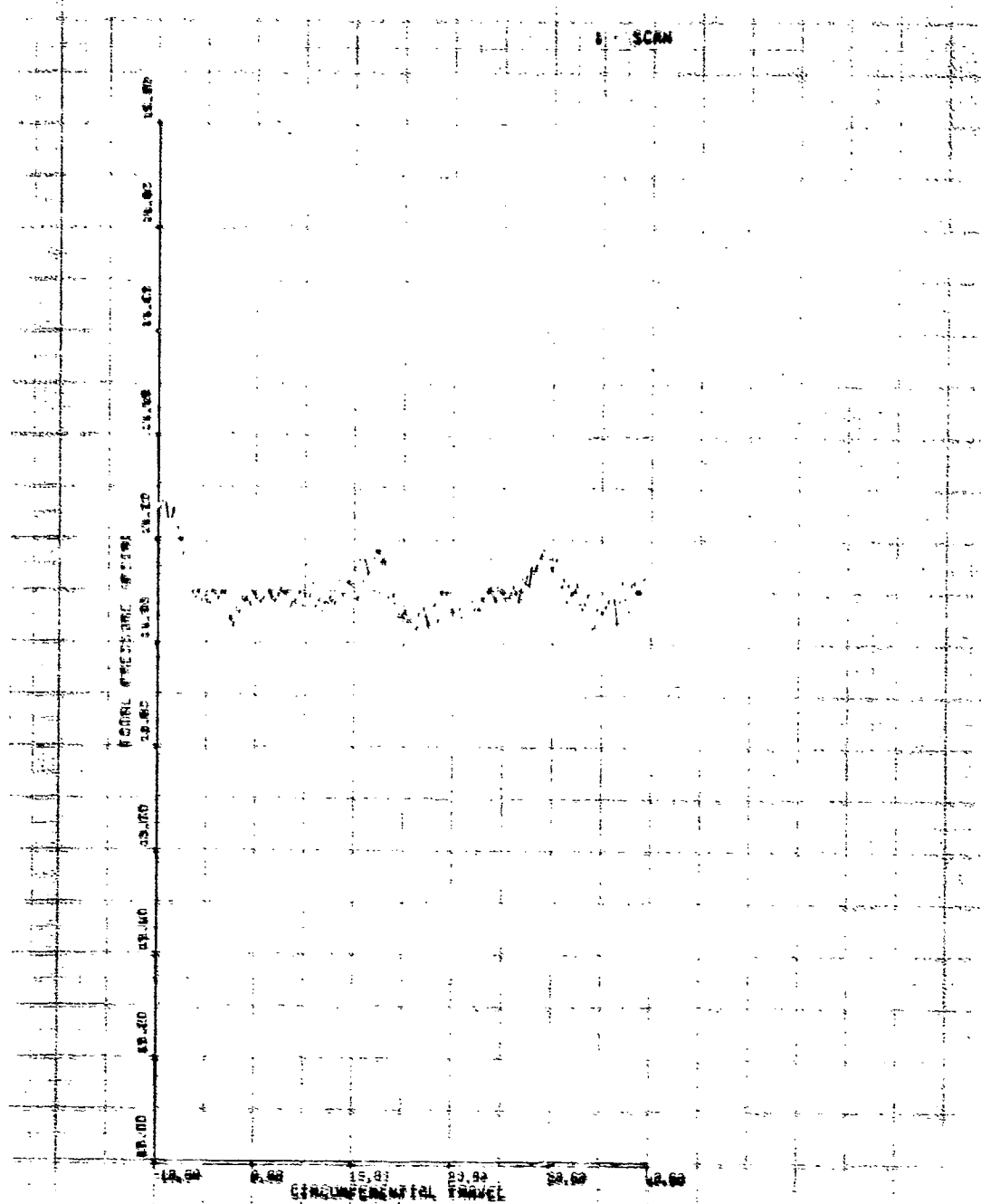


Figure 152. IGV Circumferential Traverse, Build No. 6,  
70% Speed, 10-deg IGV, 70% Span.

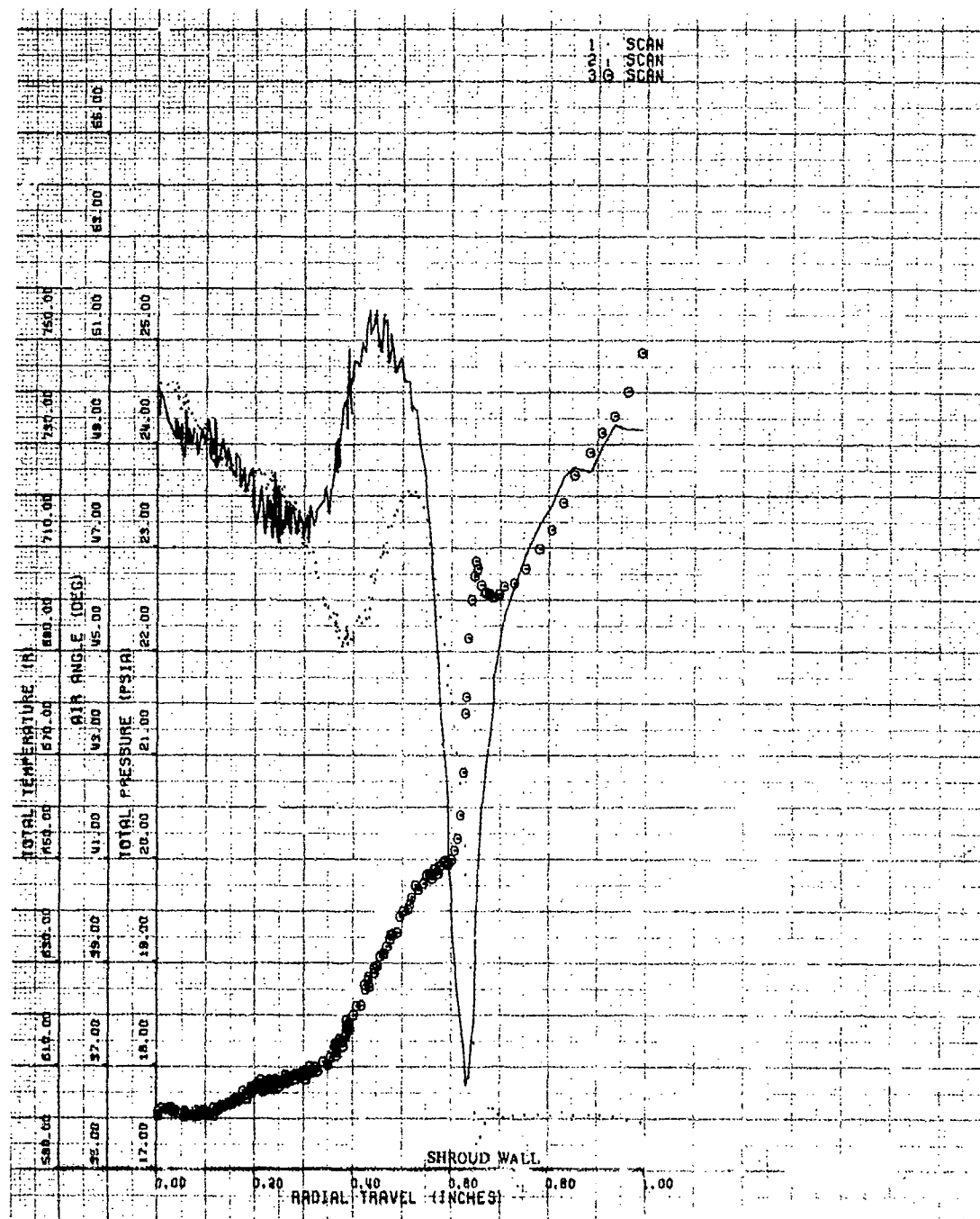


Figure 153. Inducer Exit Traverse, Build No. 6, 101% Speed, 5-deg IGV, Wide Open Discharge.

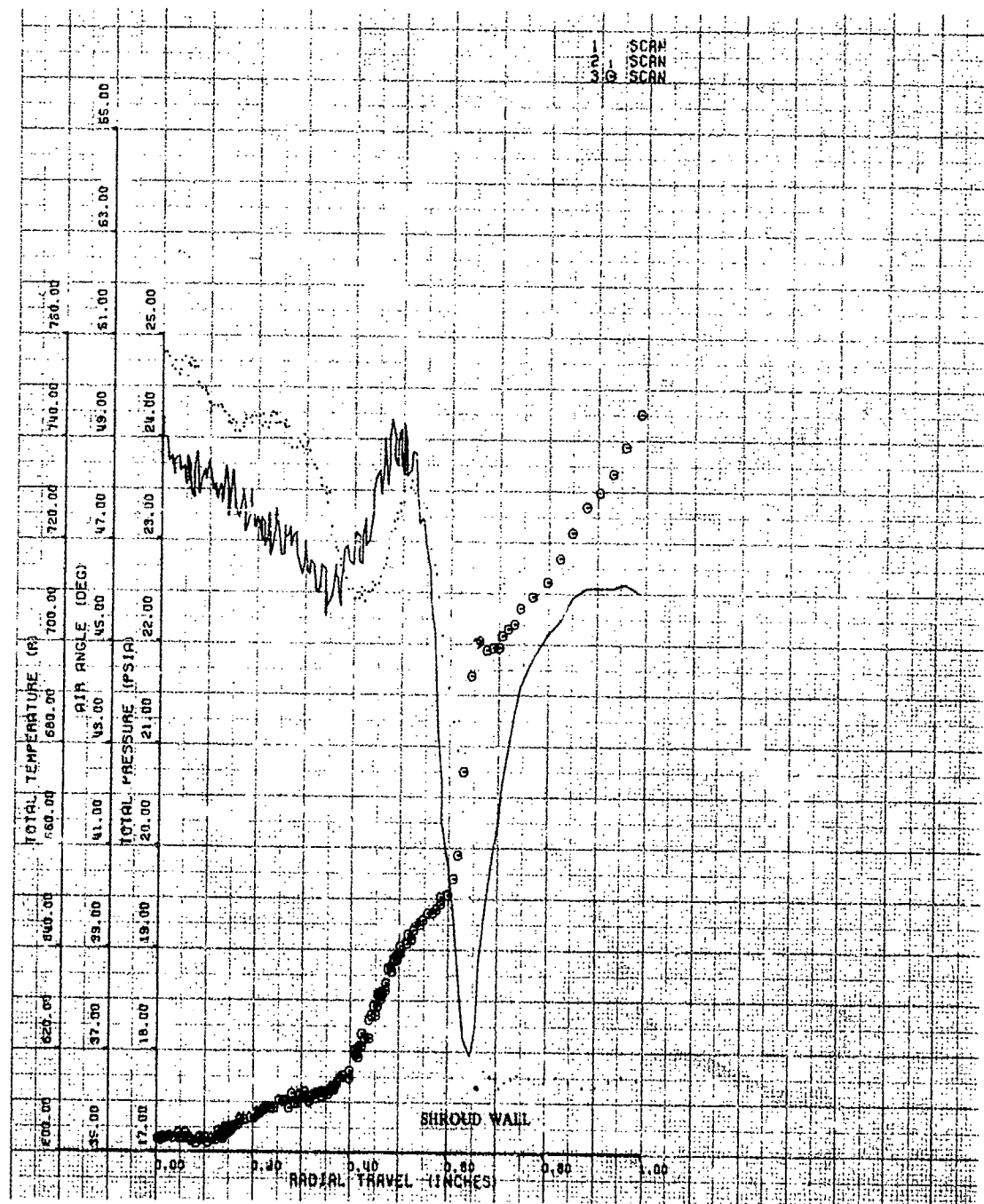


Figure 154. Inducer Exit Traverse, Build No. 6, 101% Speed, 5-deg IGV, Near Stall.

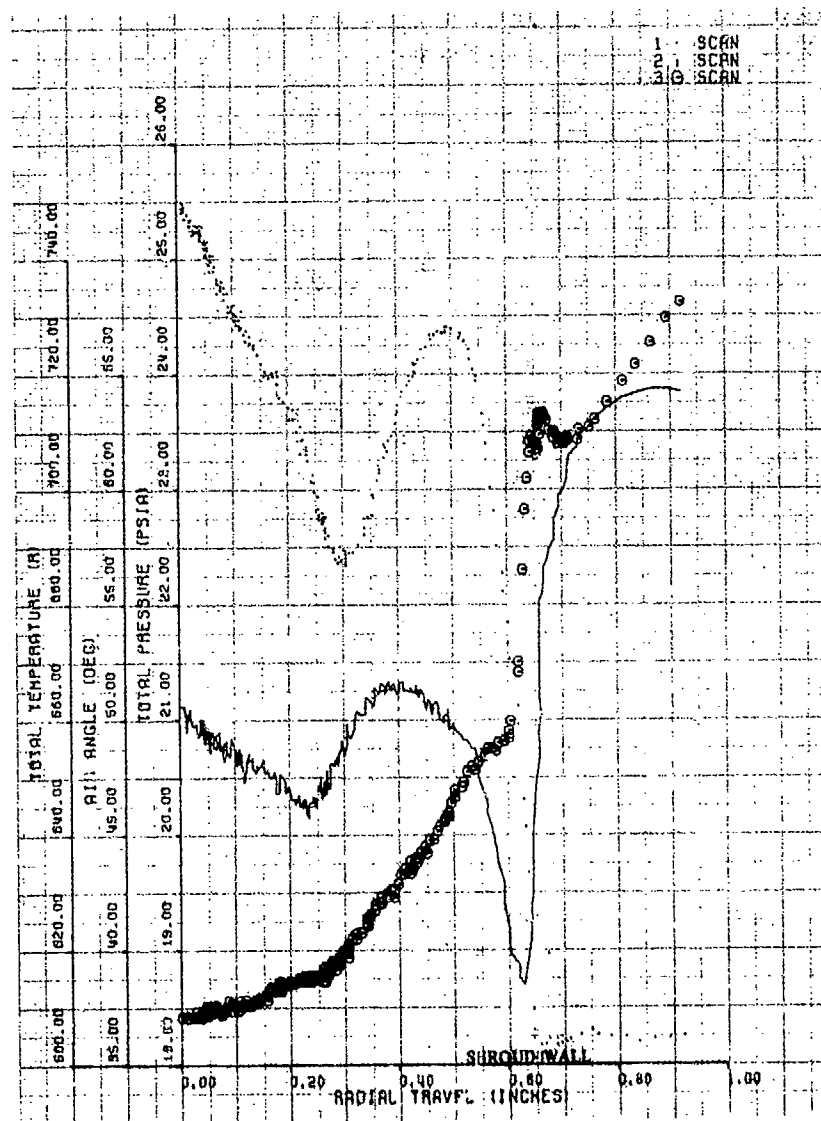


Figure 155. Inducer Exit Traverse, Build No. 6, 101% Speed, 0-deg IGV, Wide Open Discharge.

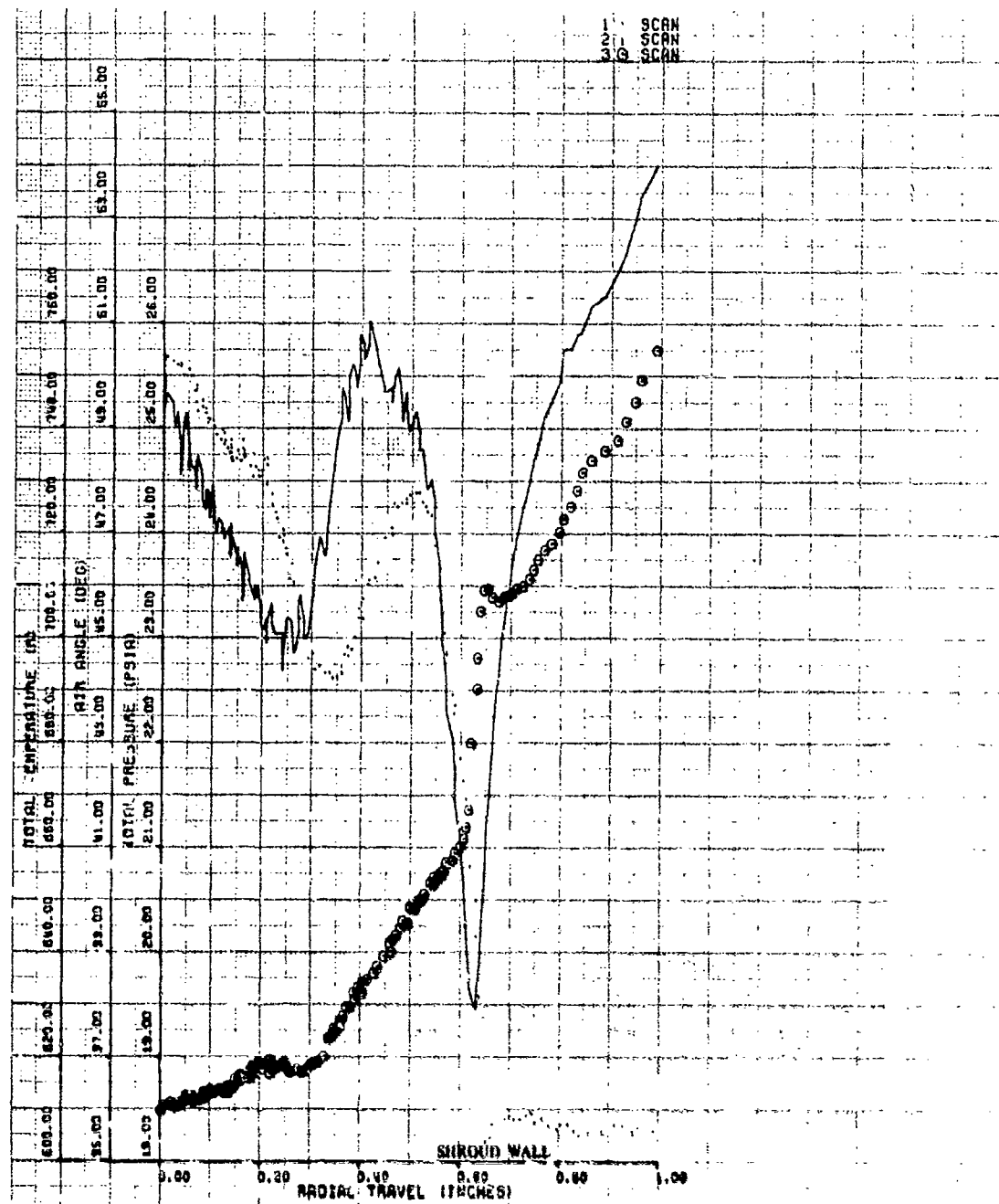


Figure 156. Inducer Exit Traverse, Build No. 6, 101% Speed, 0-deg IGV, Near Stall.

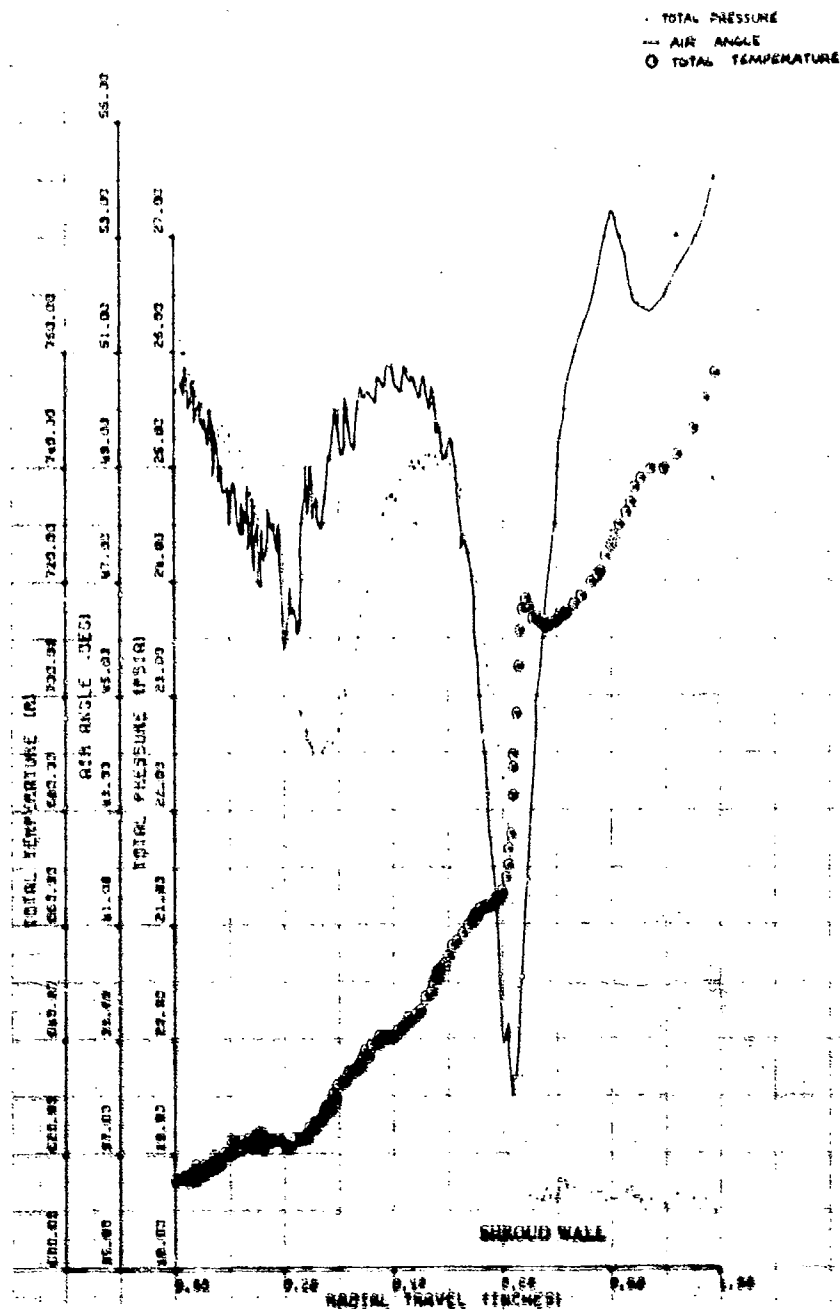


Figure 137. Inducer Exit Traverse, Build No. 6, 101% Speed, -4-deg IGV, Wide Open Discharge.

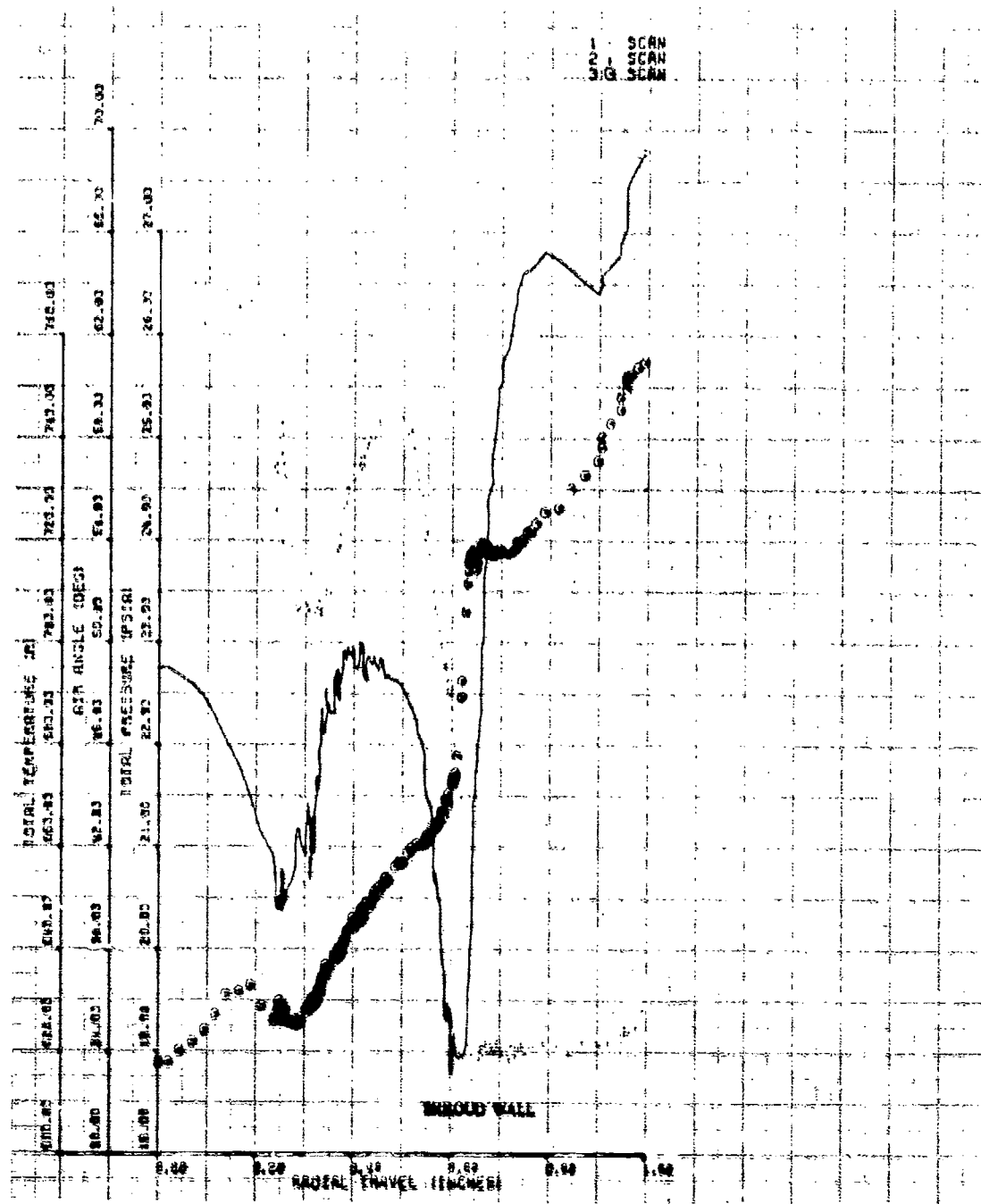


Figure 158. Inducer Exit Traverse, Build No. 6, 101% Speed, -4-deg IGV, Near Stall.

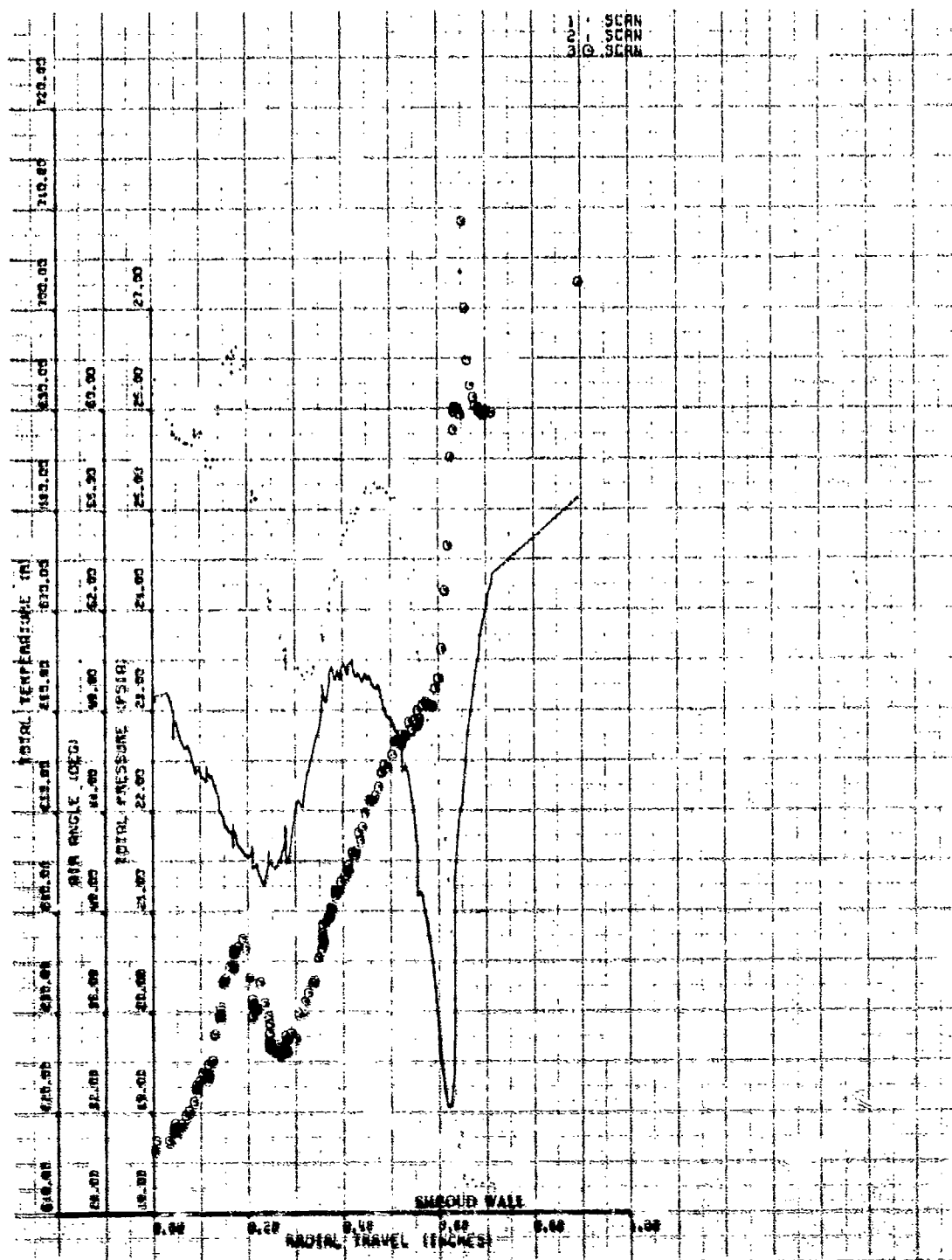


Figure 139. Inducer Exit With Coolant, Build No. 6, 101% Speed, -4-deg IGV, Near Stall.



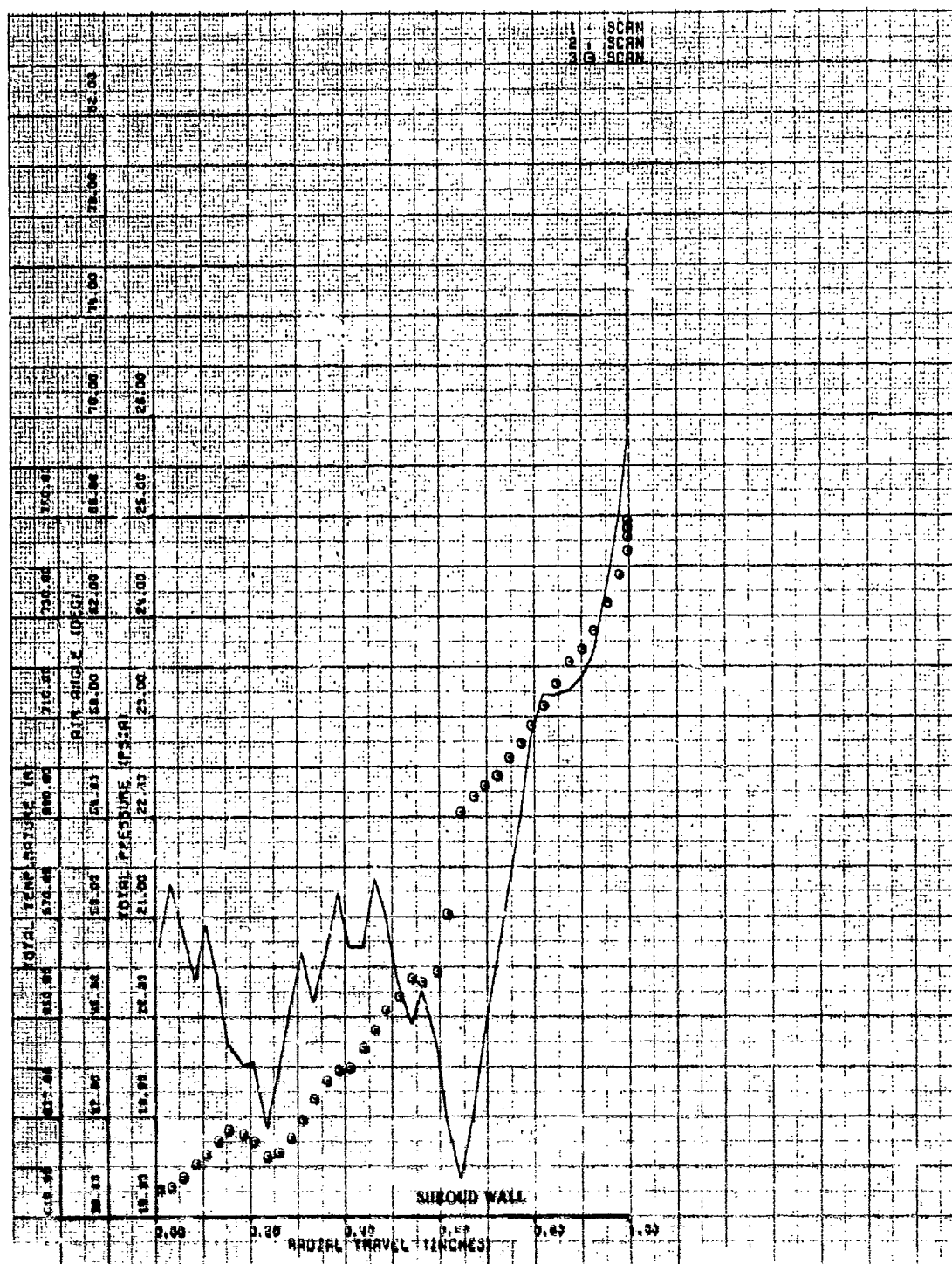


Figure 160. Inducer Exit Traverse, Build No. 6, 101% Speed, -5-deg IGV.

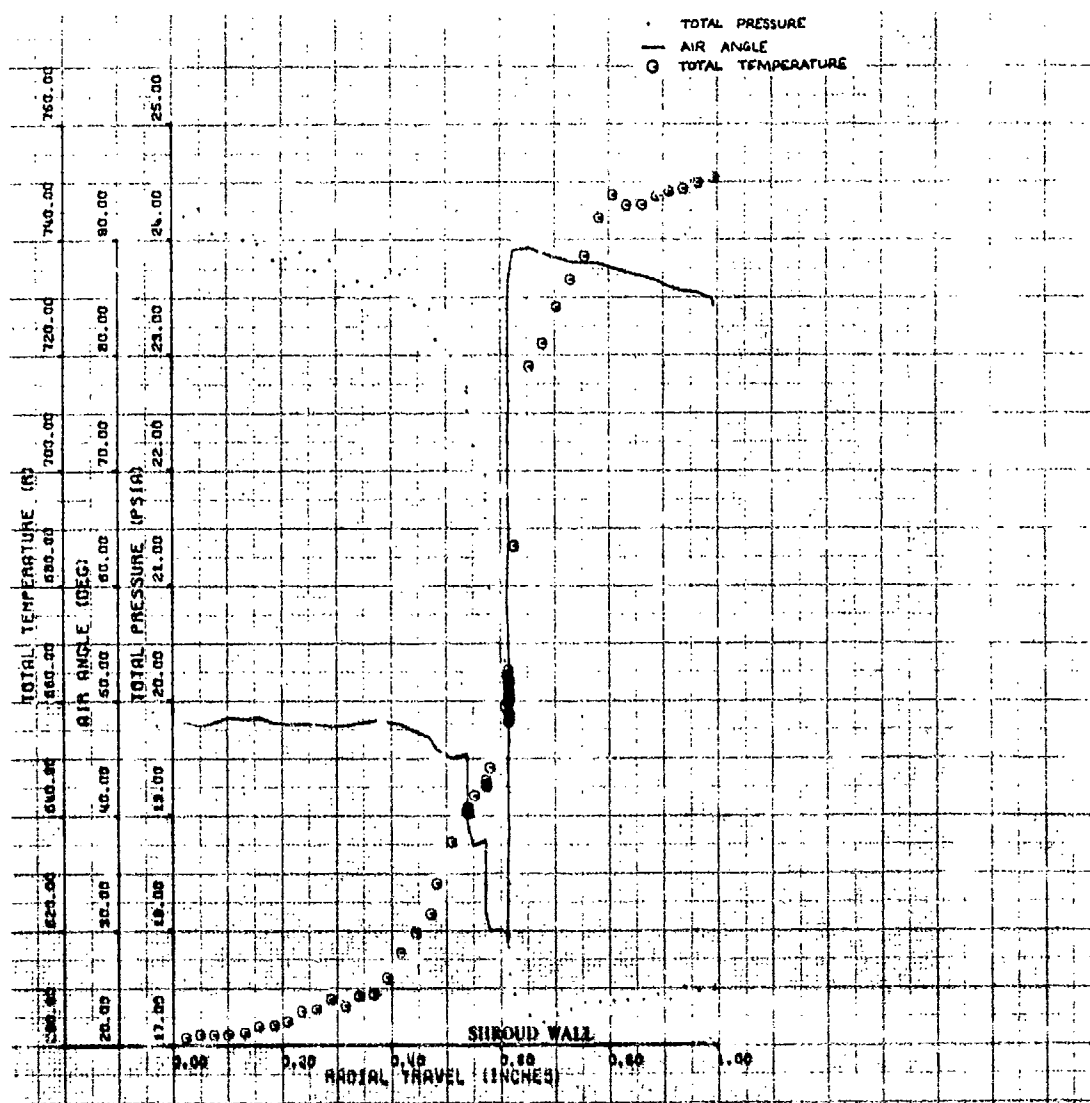


Figure 161. Inducer Exit Traverse, Build No. 6, 100% Speed, 10-deg IGV.

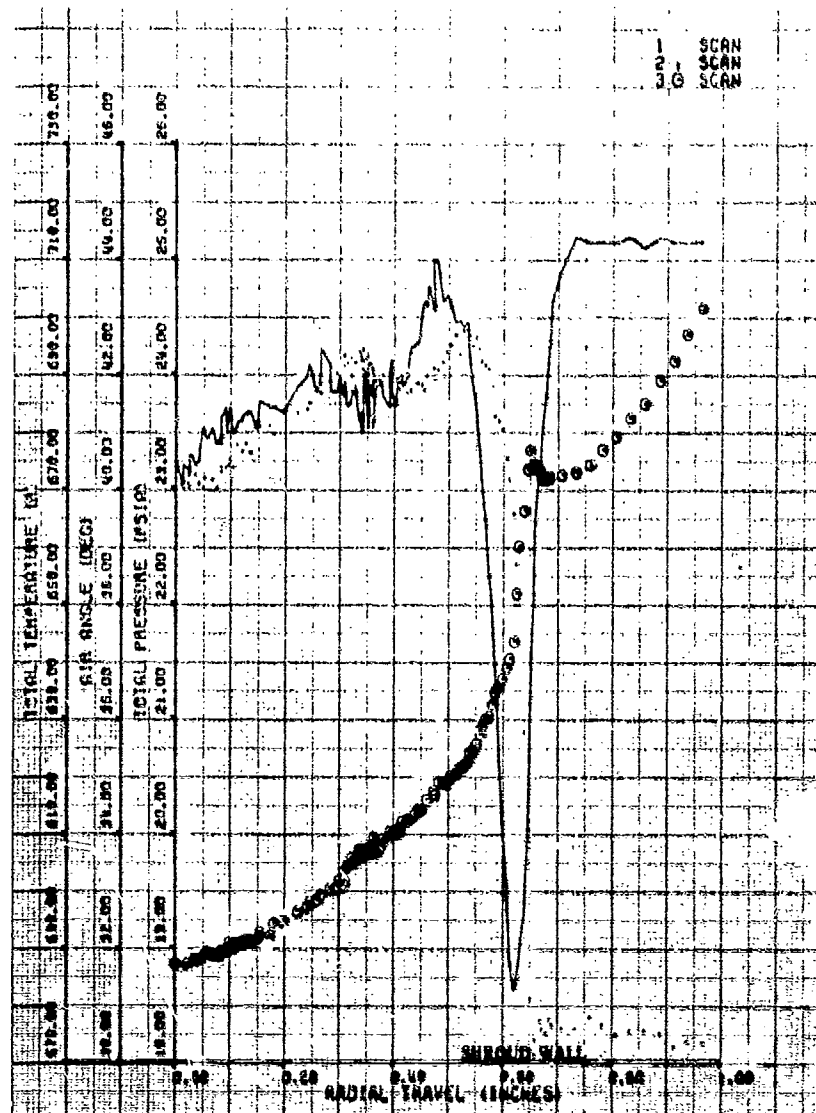


Figure 162. Inducer Exit Traverse, Build No. 6, 95% Speed, 15-deg IGV, Wide Open Discharge.

21.50  
21.50  
21.50

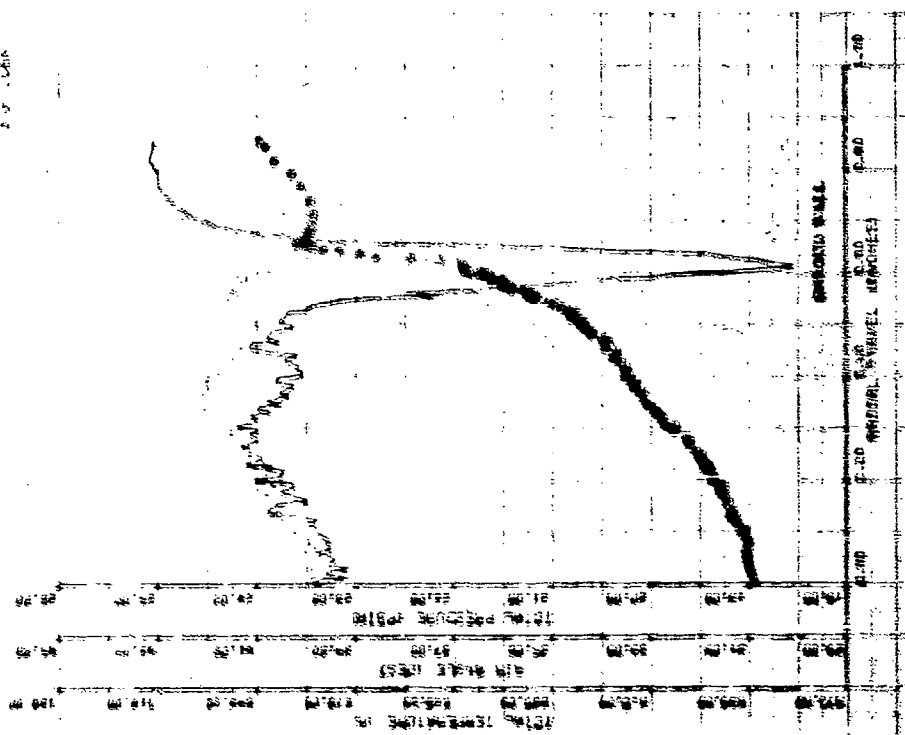


Figure 163. Inducer Exit Traverse, Build No. 6.  
95% Speed, 15-deg IGV, Near Stall.

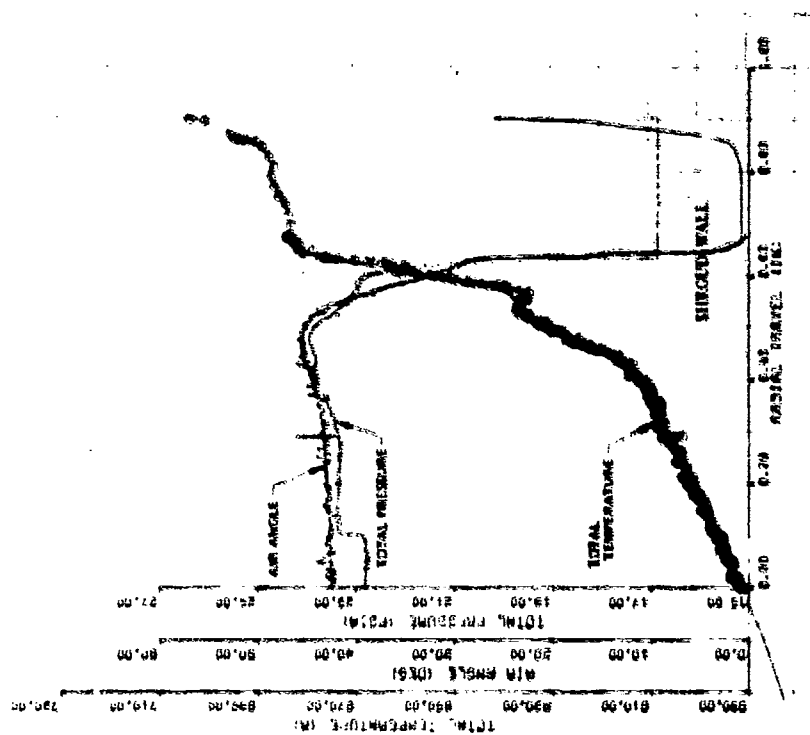


Figure 164. Inducer Exit Traverse, Build No. 3.  
95% Speed, 10-deg IGV, Wide Open  
Discharge.

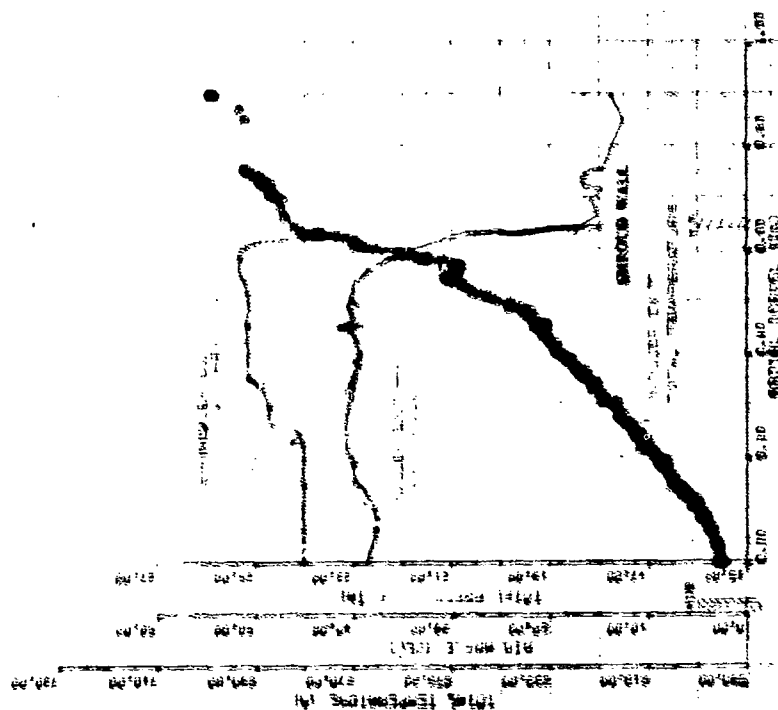


Figure 165. Inducer Exit Traverse, Build No. 3.  
95% Speed, 10-deg IGV, Near Stall.

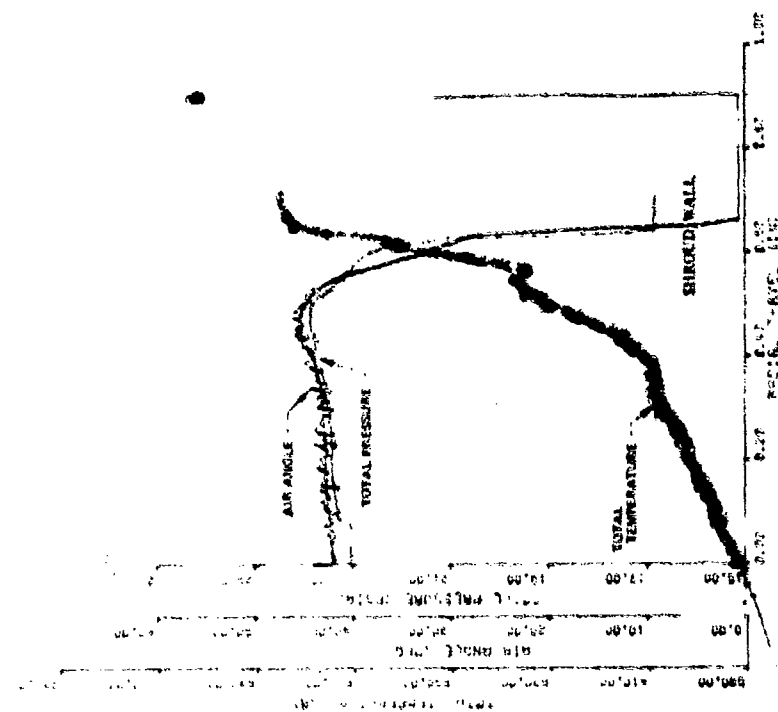


Figure 166. Inducer Exit Traverse, Build No. 3.  
95% Speed, 10-deg IGV, Below Near  
Stall.

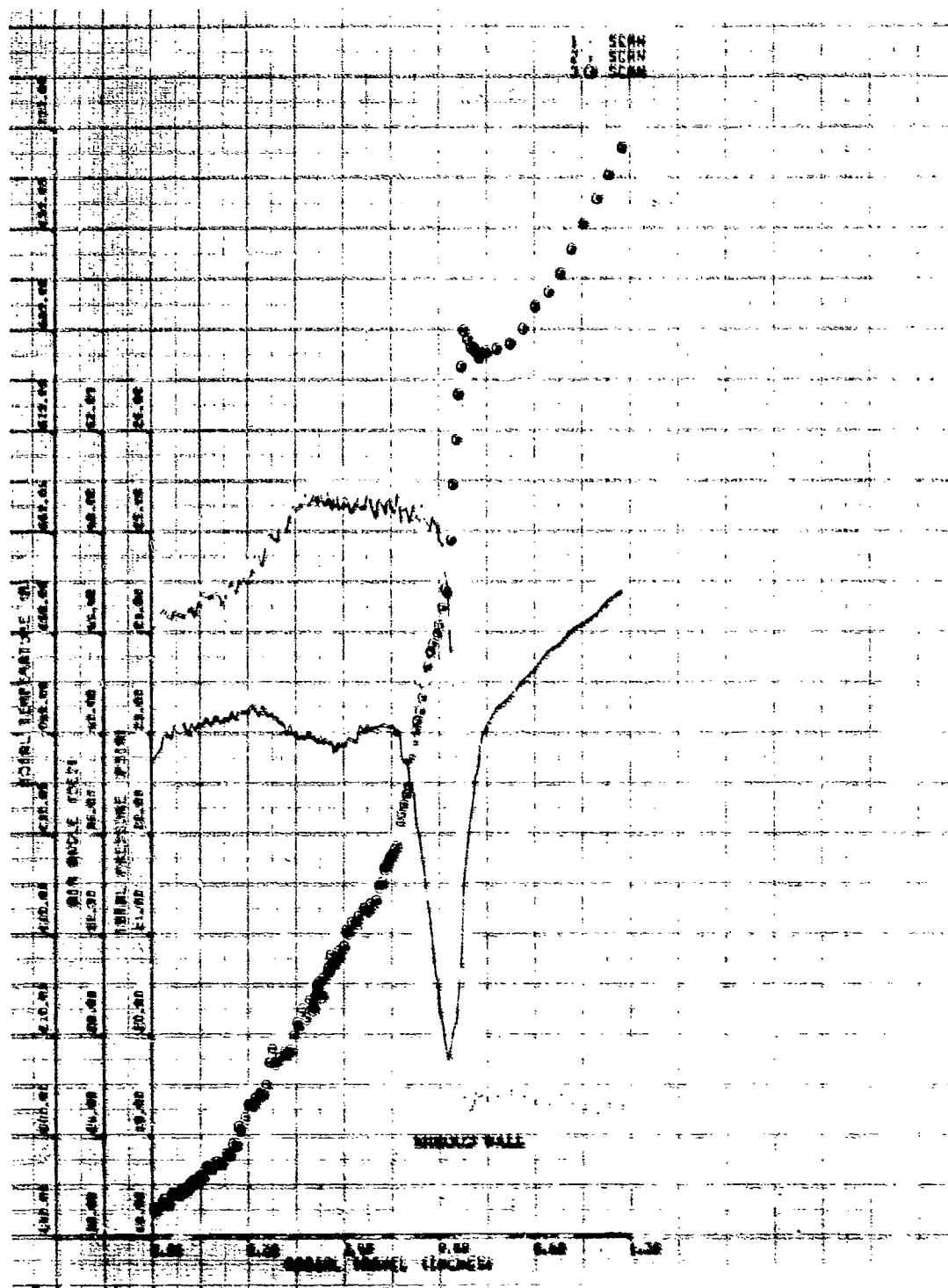


Figure 167. Inducer Exit Traverse, Build No. 6, 95% Speed,  
10-deg ICV, Wide Open Discharge.

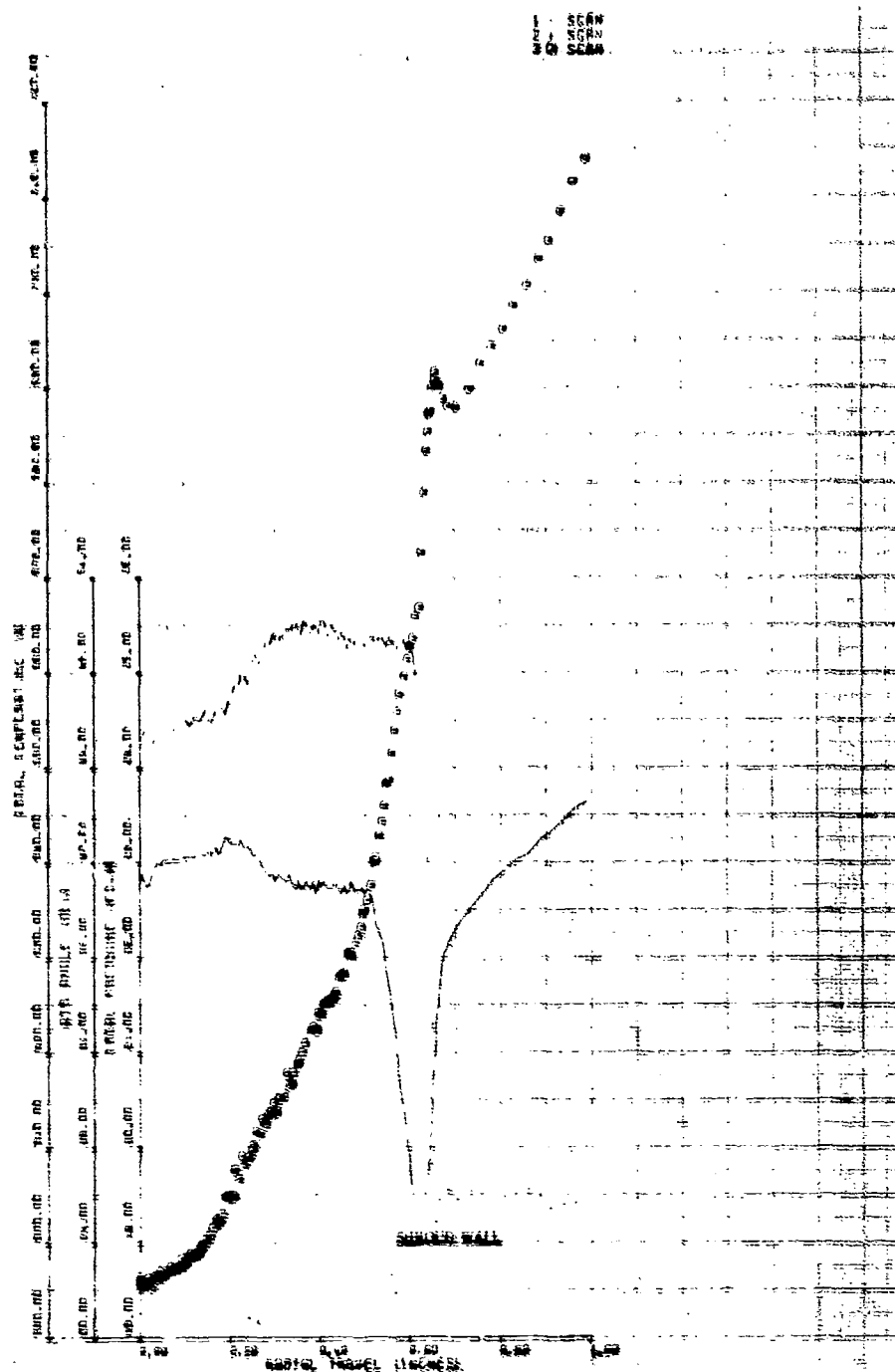


Figure 168. Inducer Exit Tracerse, Build No. 6, 95% Speed, 19-deg ICV, Near Stall.

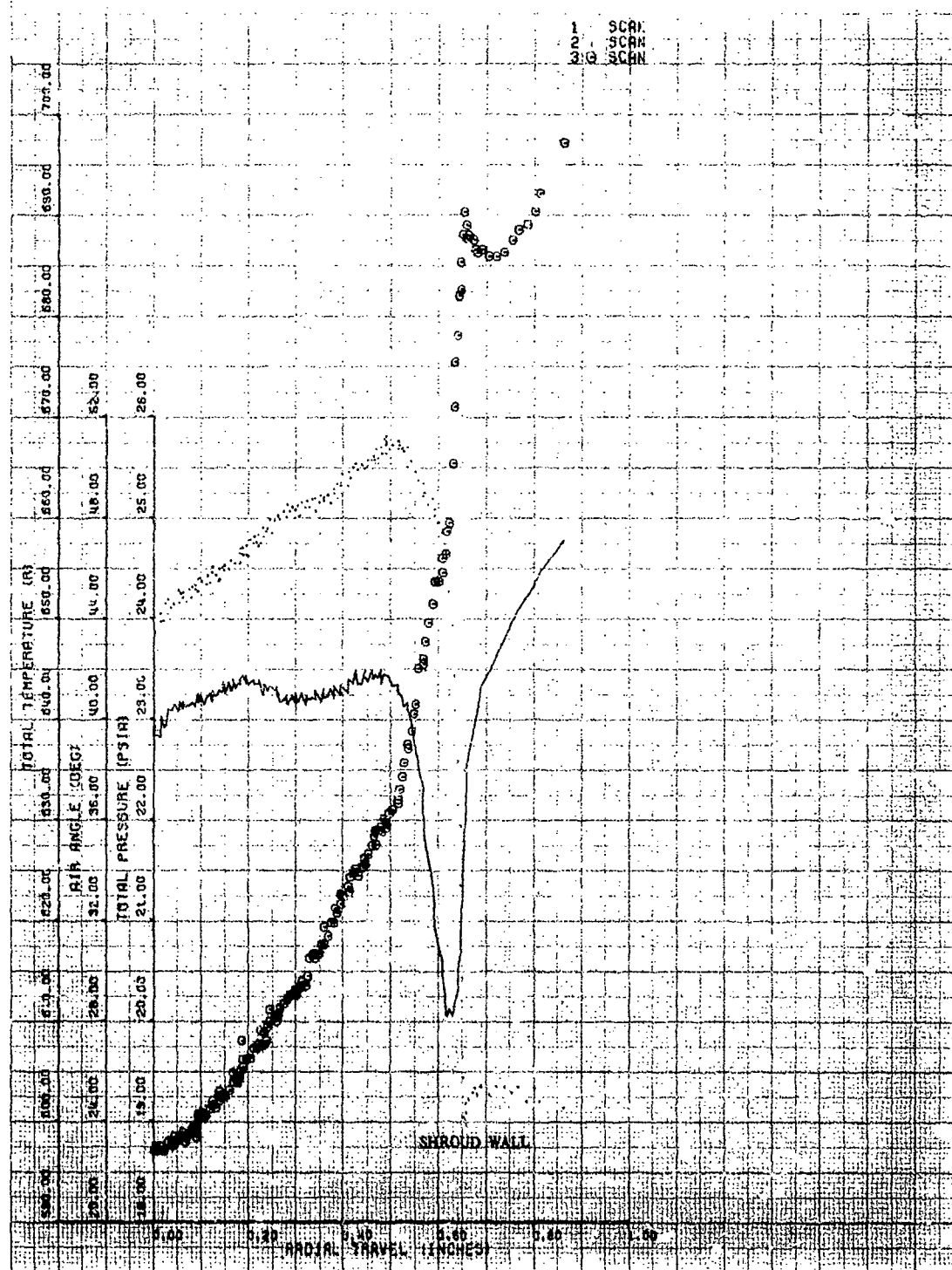


Figure 169. Inducer Exit Traverse, Build No. 6, 95% Speed, 10-deg IGV, Wide Open Discharge.



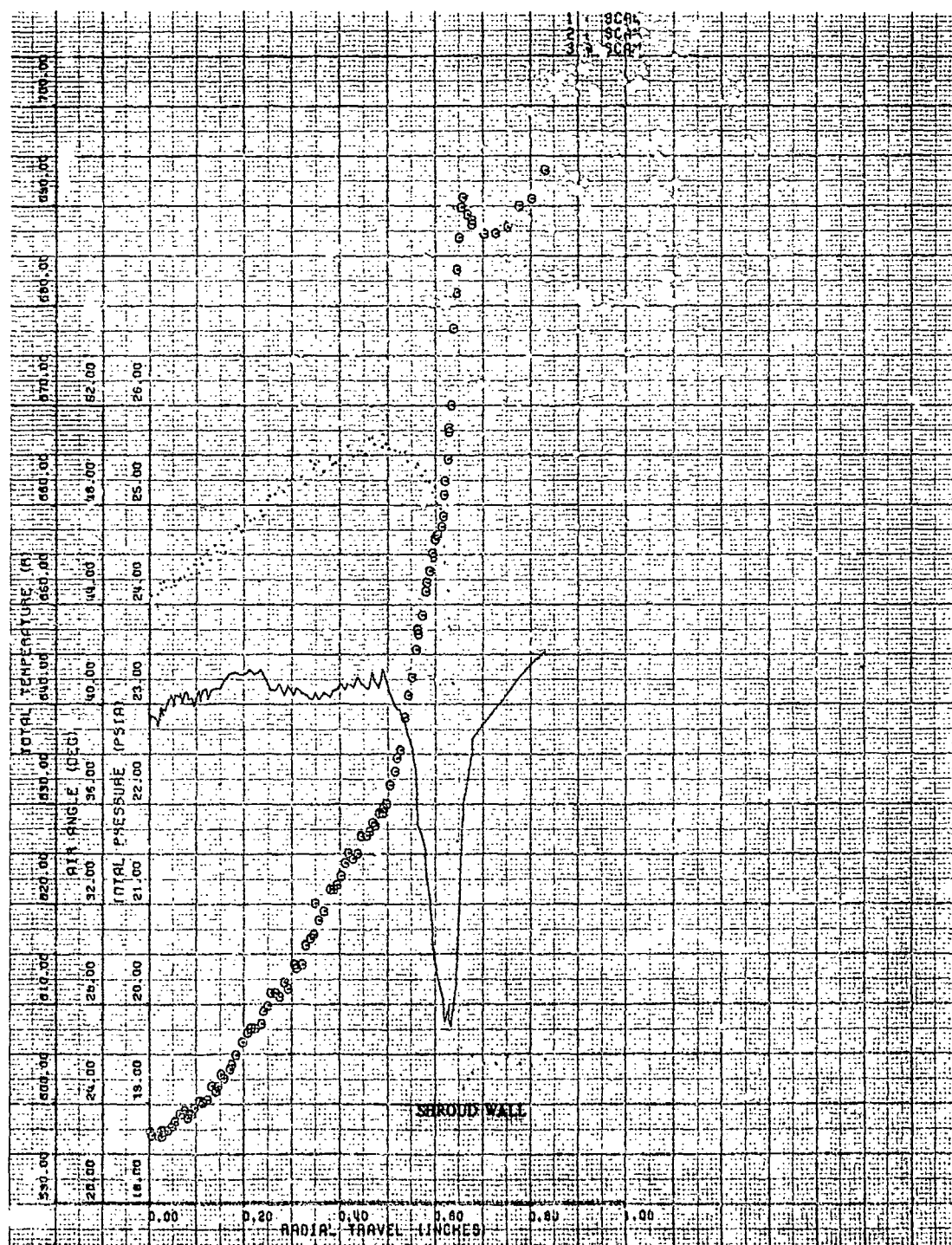


Figure 170. Inducer Exit Traverse, Build No. 6, 95% Speed, 10-deg IGV, Near Stall.

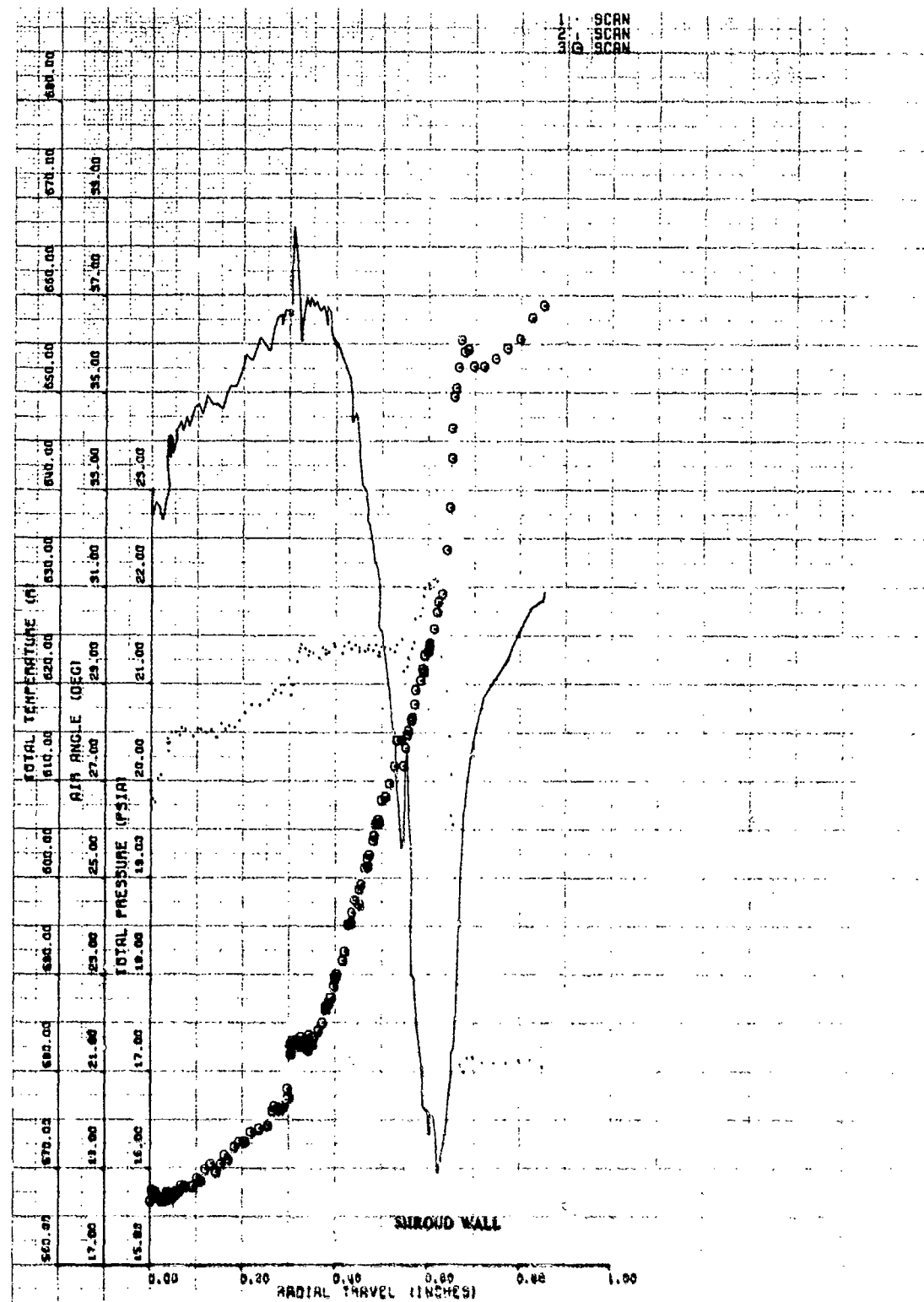


Figure 171. Inducer Exit Traverse, Build No. 6, 85% Speed, 30-deg IGV, Near Stall.

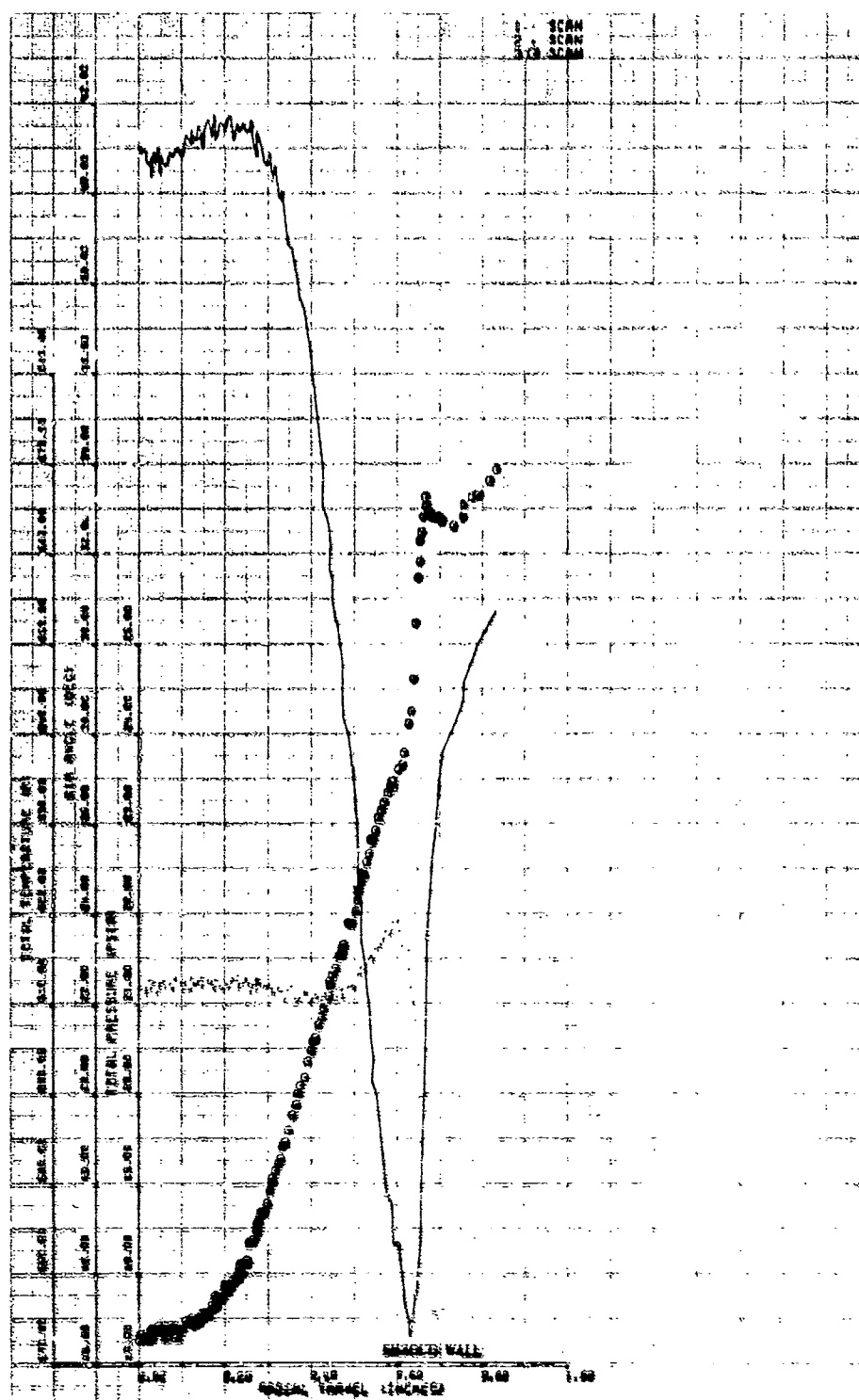


Figure 172. Inducer Exit Traverse, Build No. 6, 85% Speed, 20-deg IGV, Near Stall.

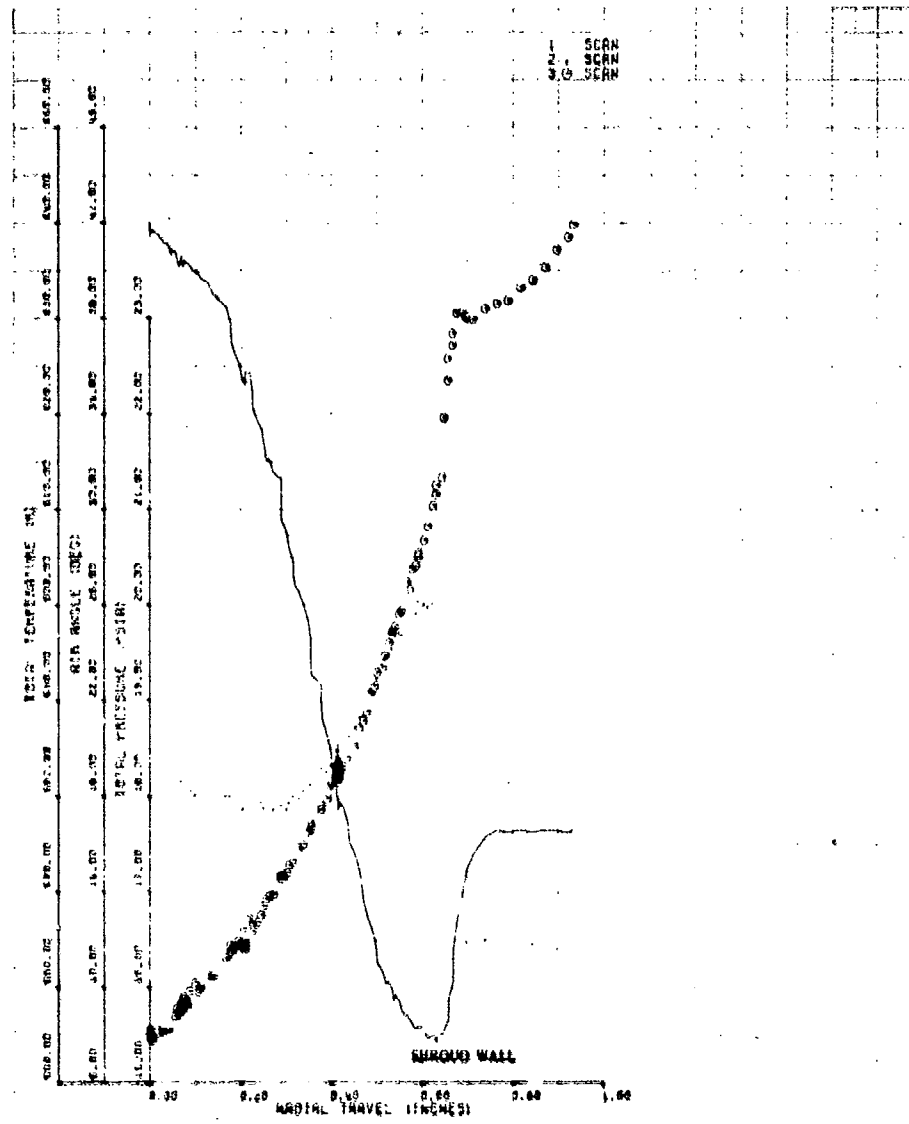


Figure 173. Inducer Exit Traverse, Build No. 6, 70% Speed, 30-deg IGV, Near Stall.

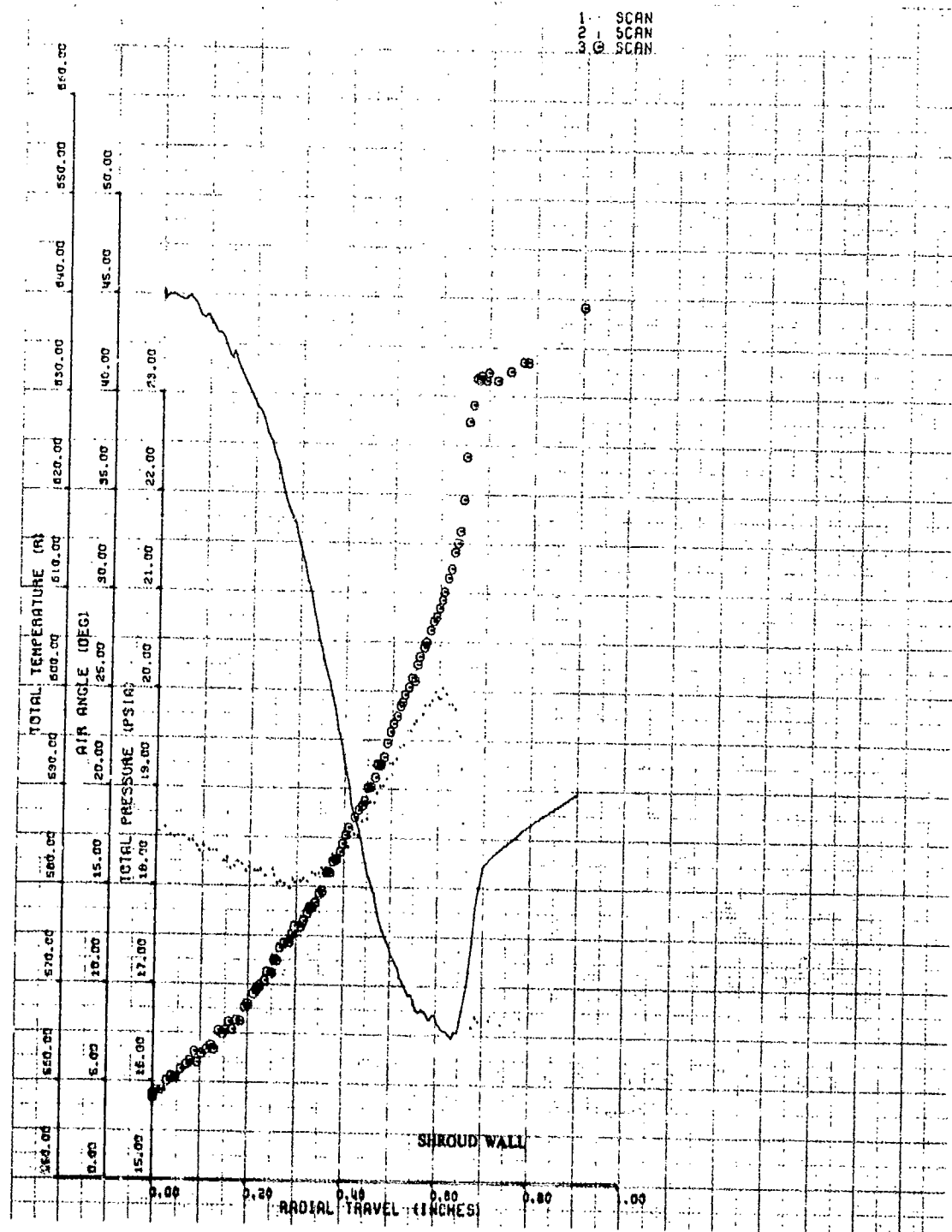


Figure 174. Inducer Exit Traverse, Build No. 6, 70% Speed, 20-deg IGV, Near Stall.

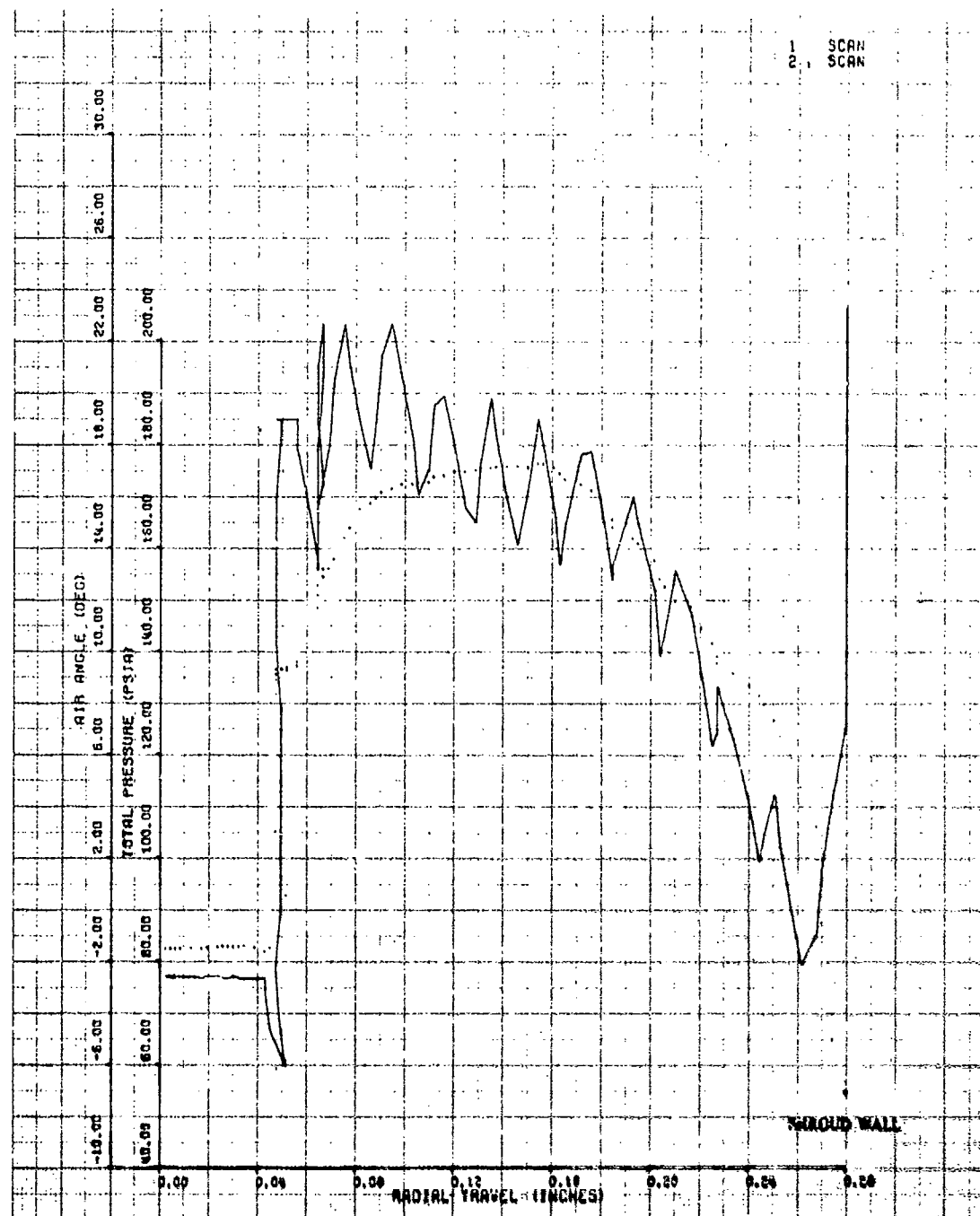
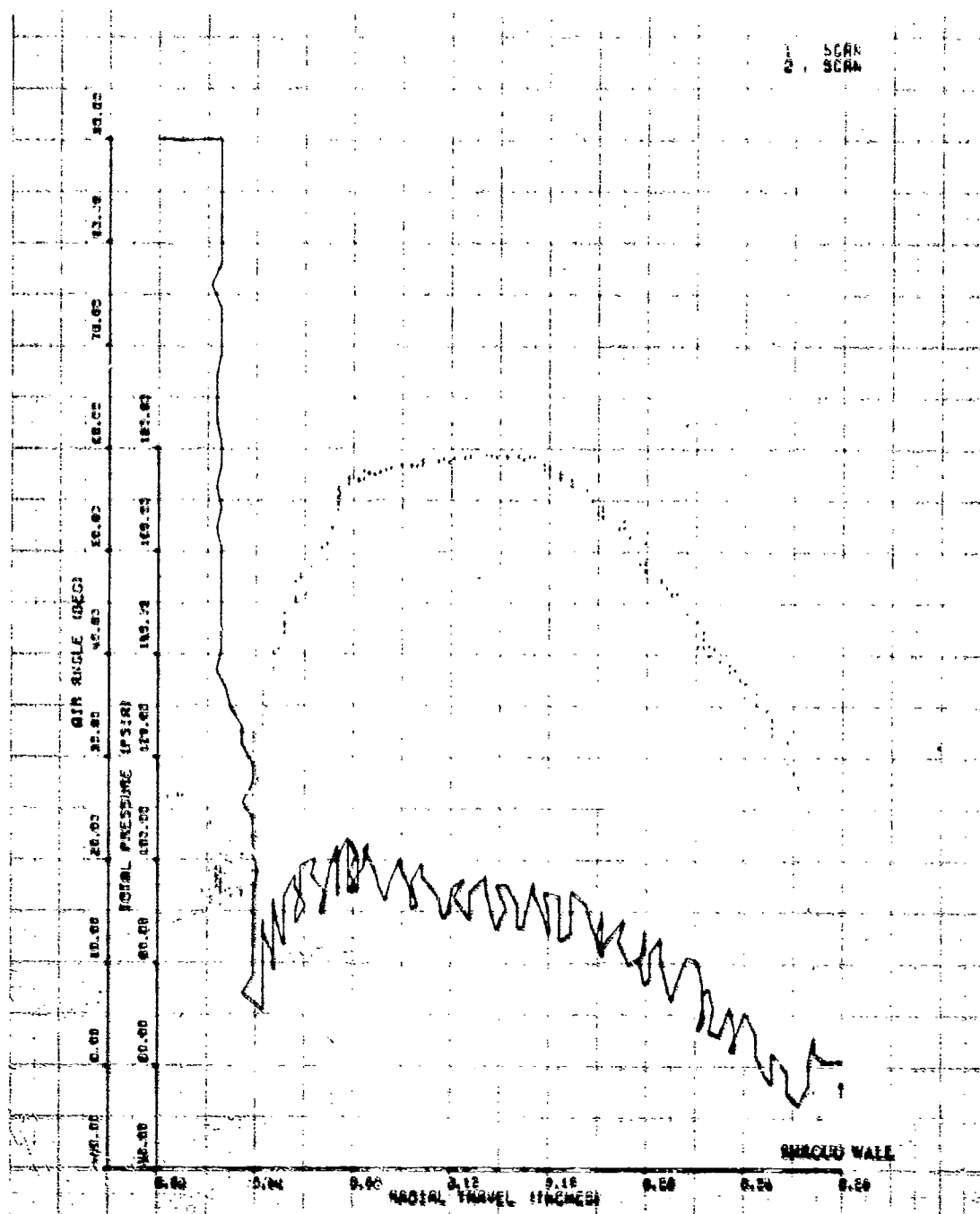


Figure 175. Impeller Exit Traverse, Build No. 6, 101% Speed, 5-deg IGV, Near Stall.



**Figure 176. Impeller Exit Traverse, Build No. 6, 1017 Speed, 0-deg ICV, Near Stall.**

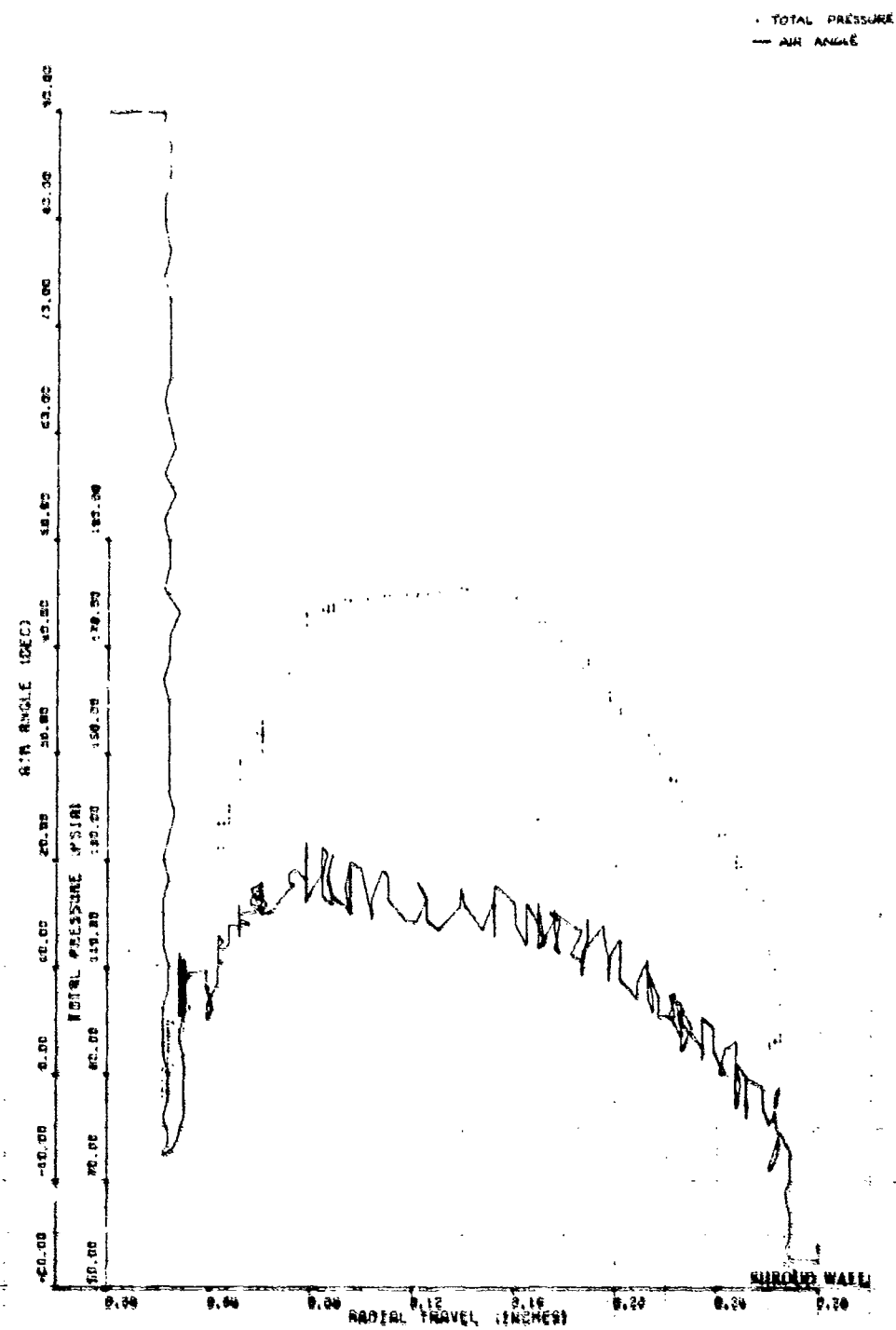


Figure 177. Impeller Exit Traverse, Build No. 6, 101% Speed, -4-deg IGV, Near Stall.



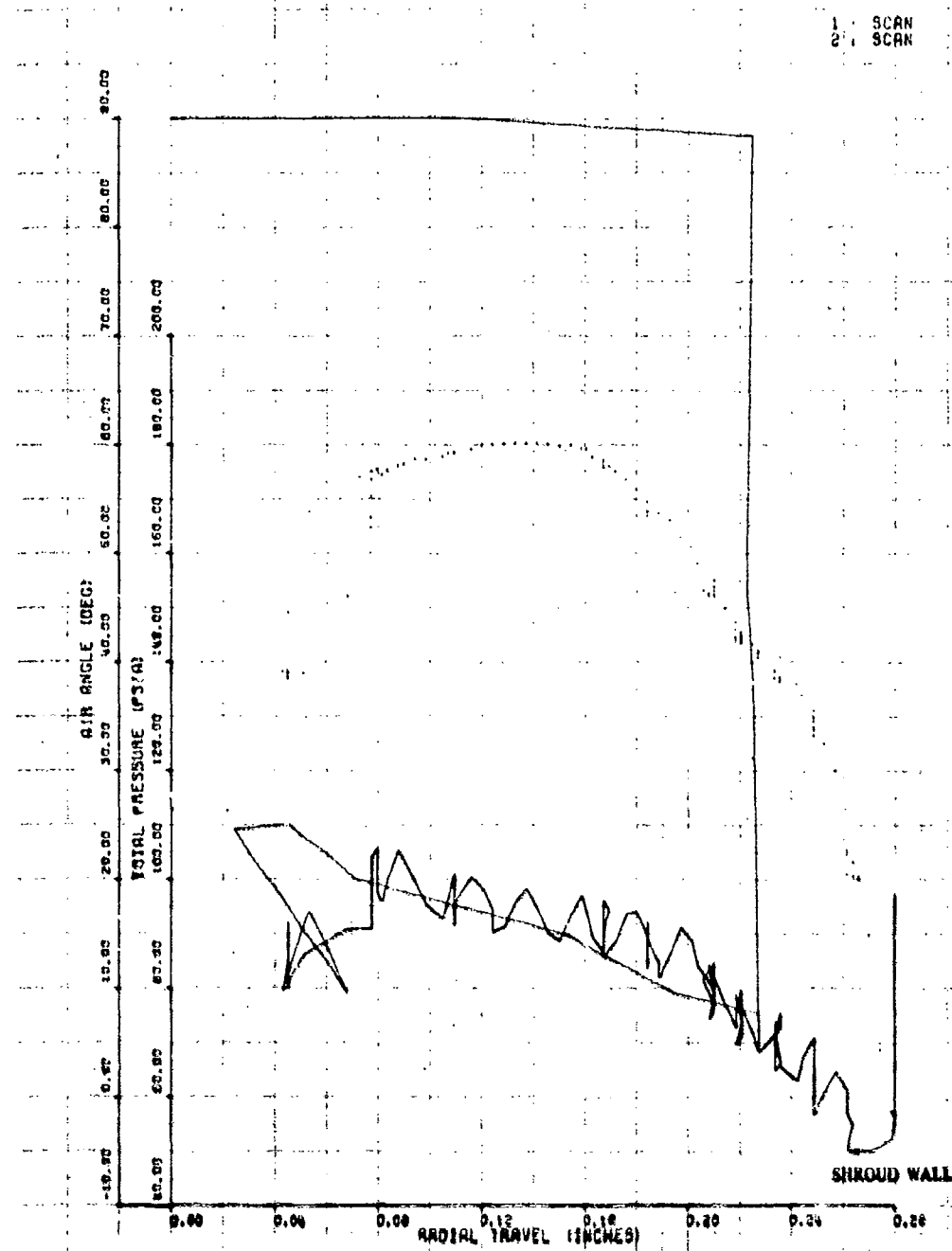


Figure 178. Impeller Exit Traverse With Flange Coolant, Build No. 6, 101% Speed, -4-deg IGV.

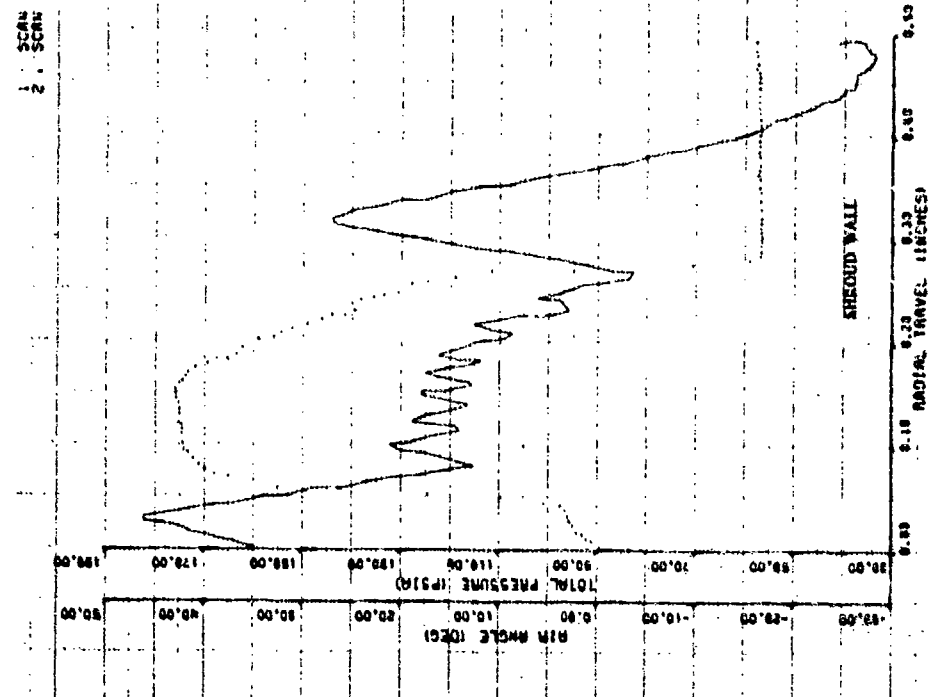


Figure 180. Impeller Exit Traverse, Build No. 6,  
101% Speed, -5-deg IGV.

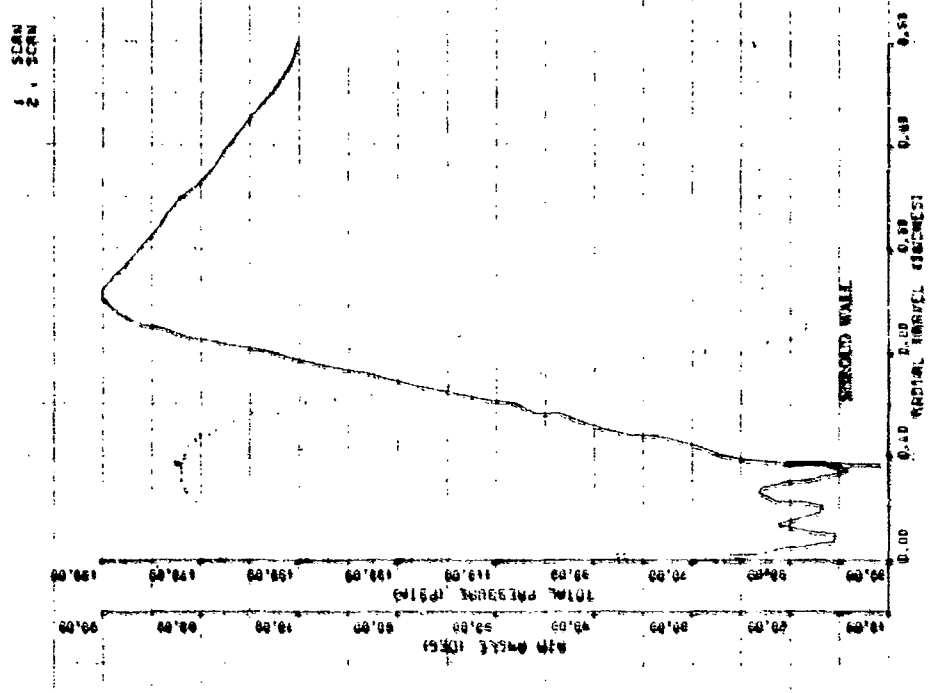


Figure 179. Impeller Exit Traverse, Build  
No. 6, 101% Speed, -5-deg IGV.

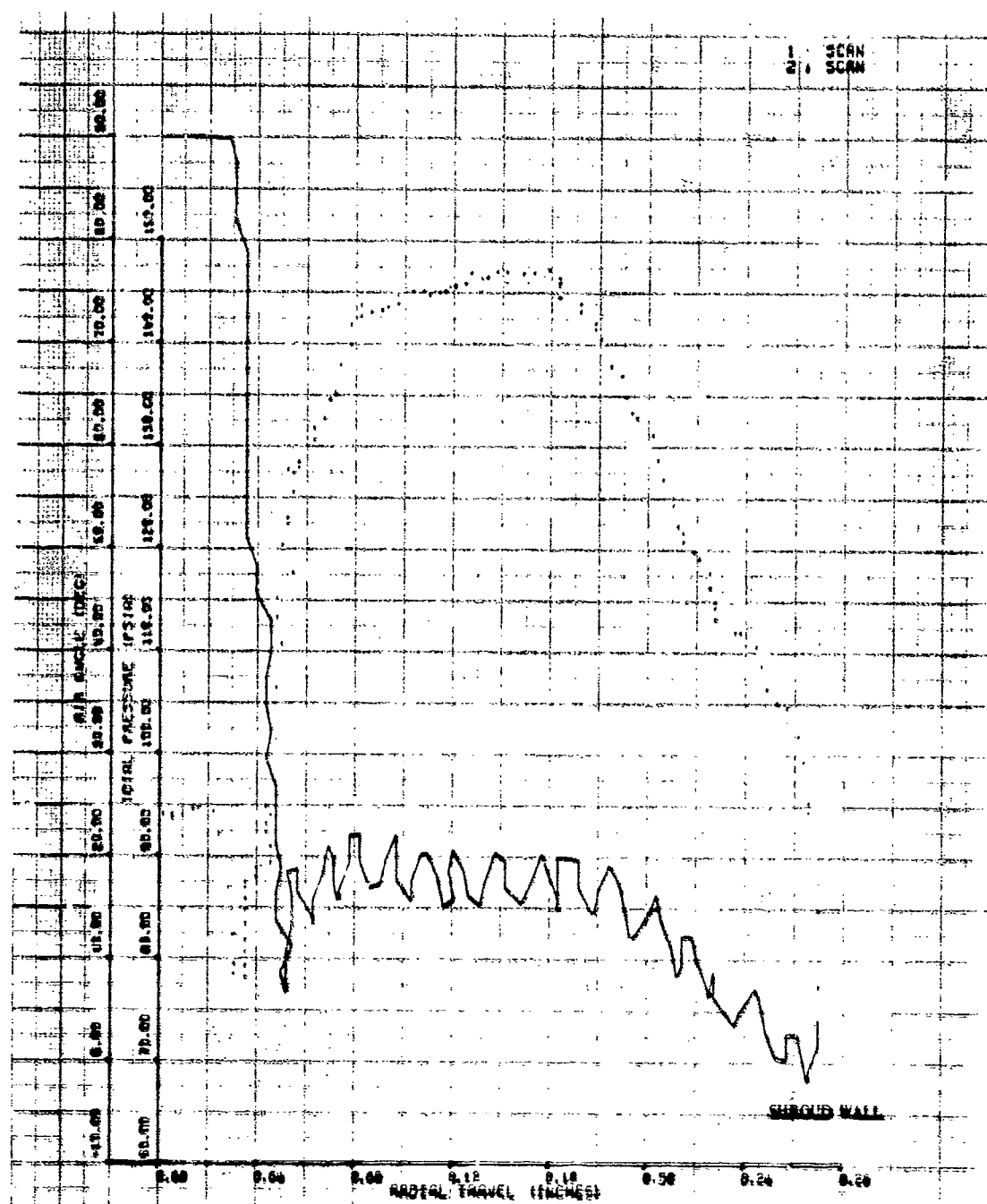


Figure 181. Impeller Exit Traverse, Build No. 6, 95% Speed, 13-deg IGV.

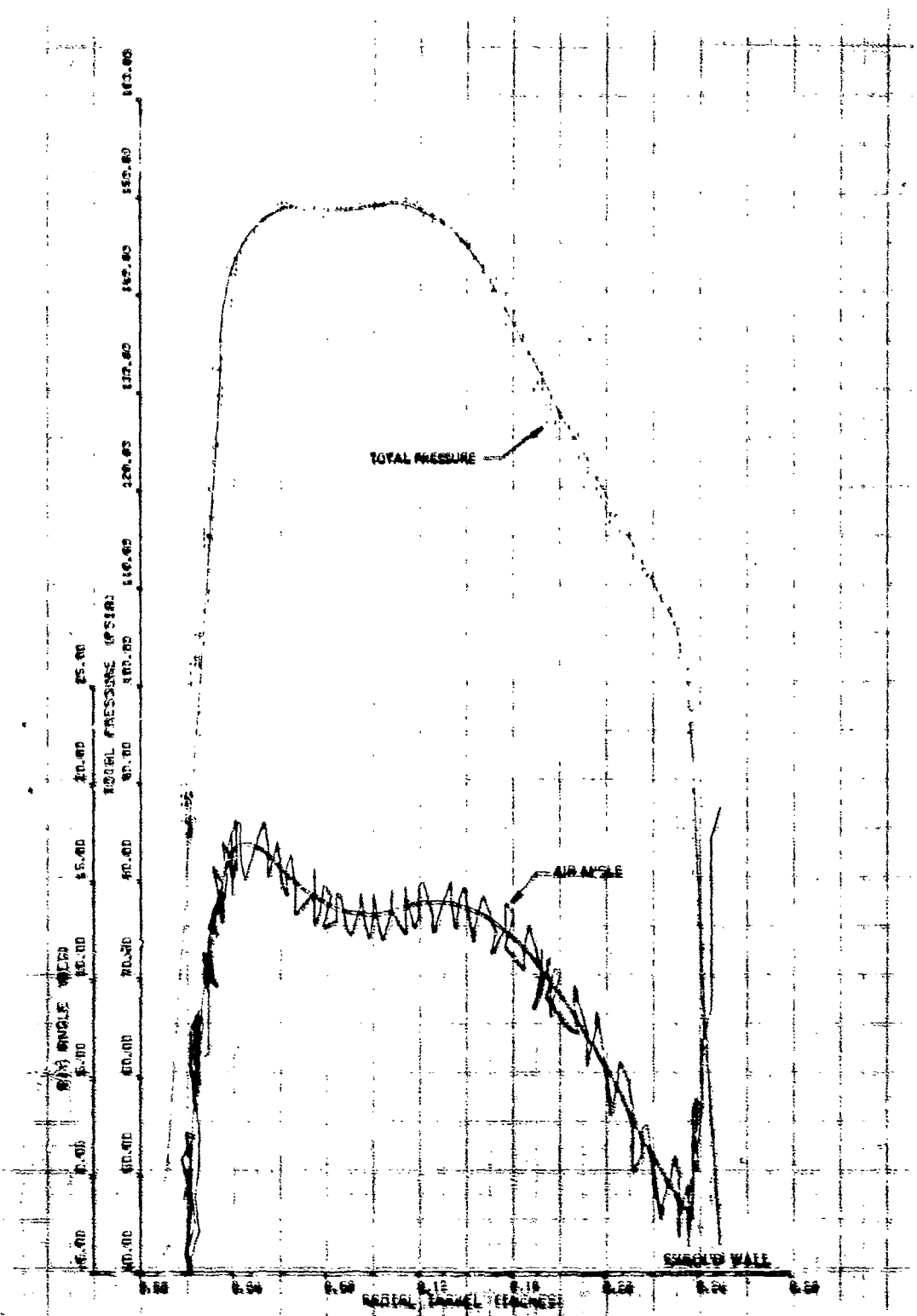


Figure 132. Impeller Exit Traverse, Build No. 3, 95% Speed, 10-deg 10V, Wide Open Discharge.

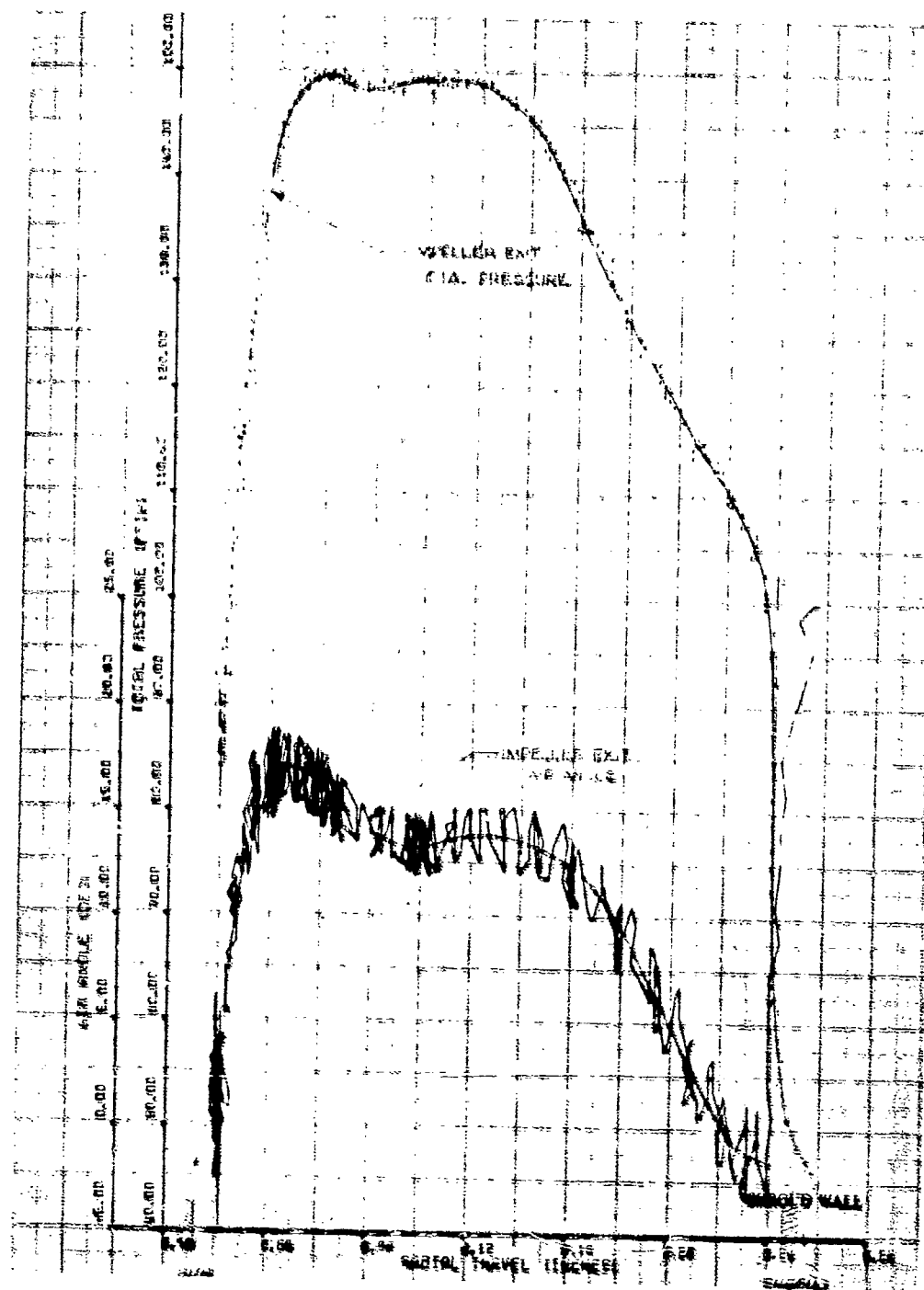


Figure 183. Impeller Exit Traverse, Build No. 3, 95% Speed, 10-deg IGV, Near Stall.

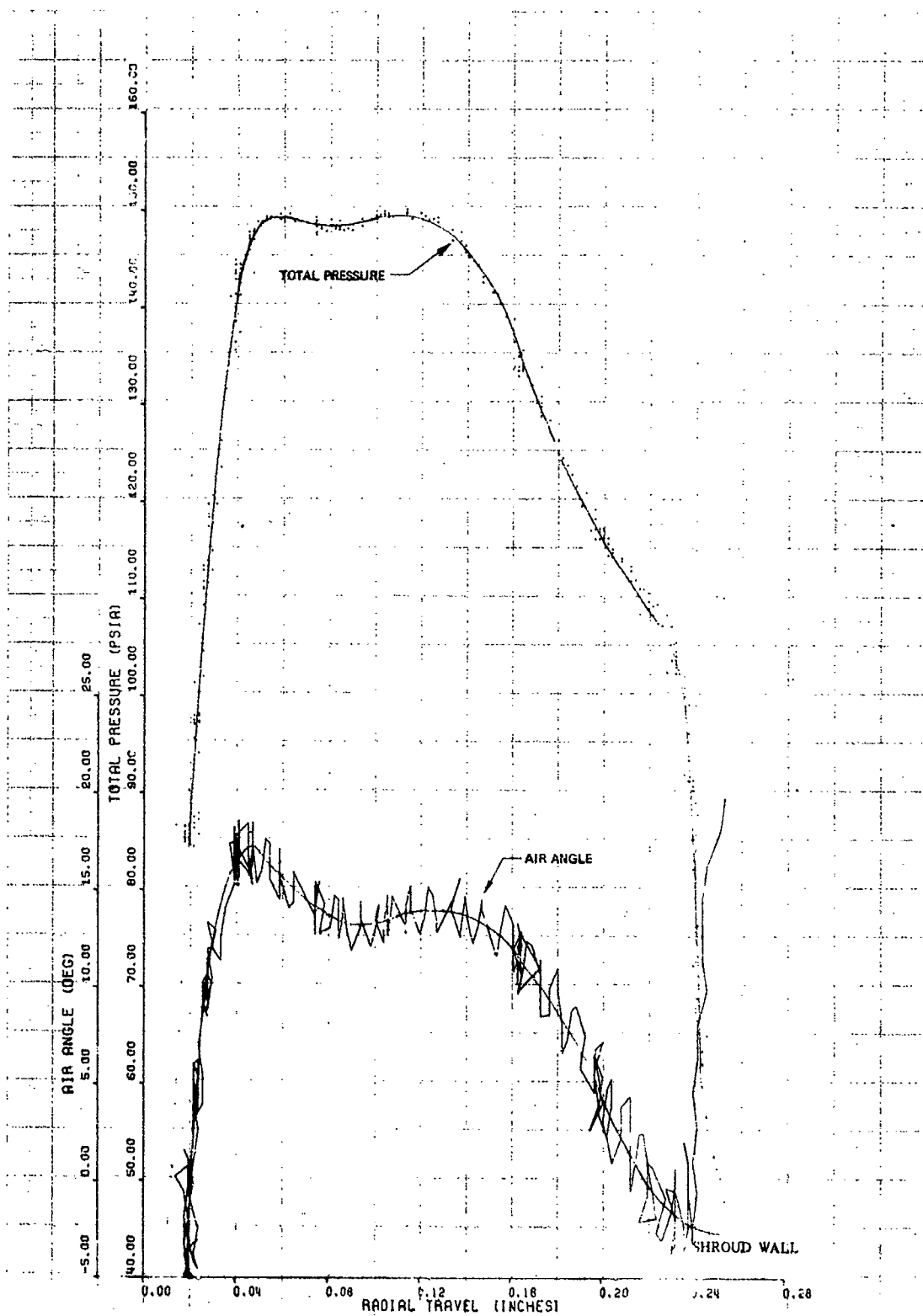


Figure 184. Impeller Exit Traverse, Build No. 3, 95% Speed, 10-deg IGV, Below Near stall.

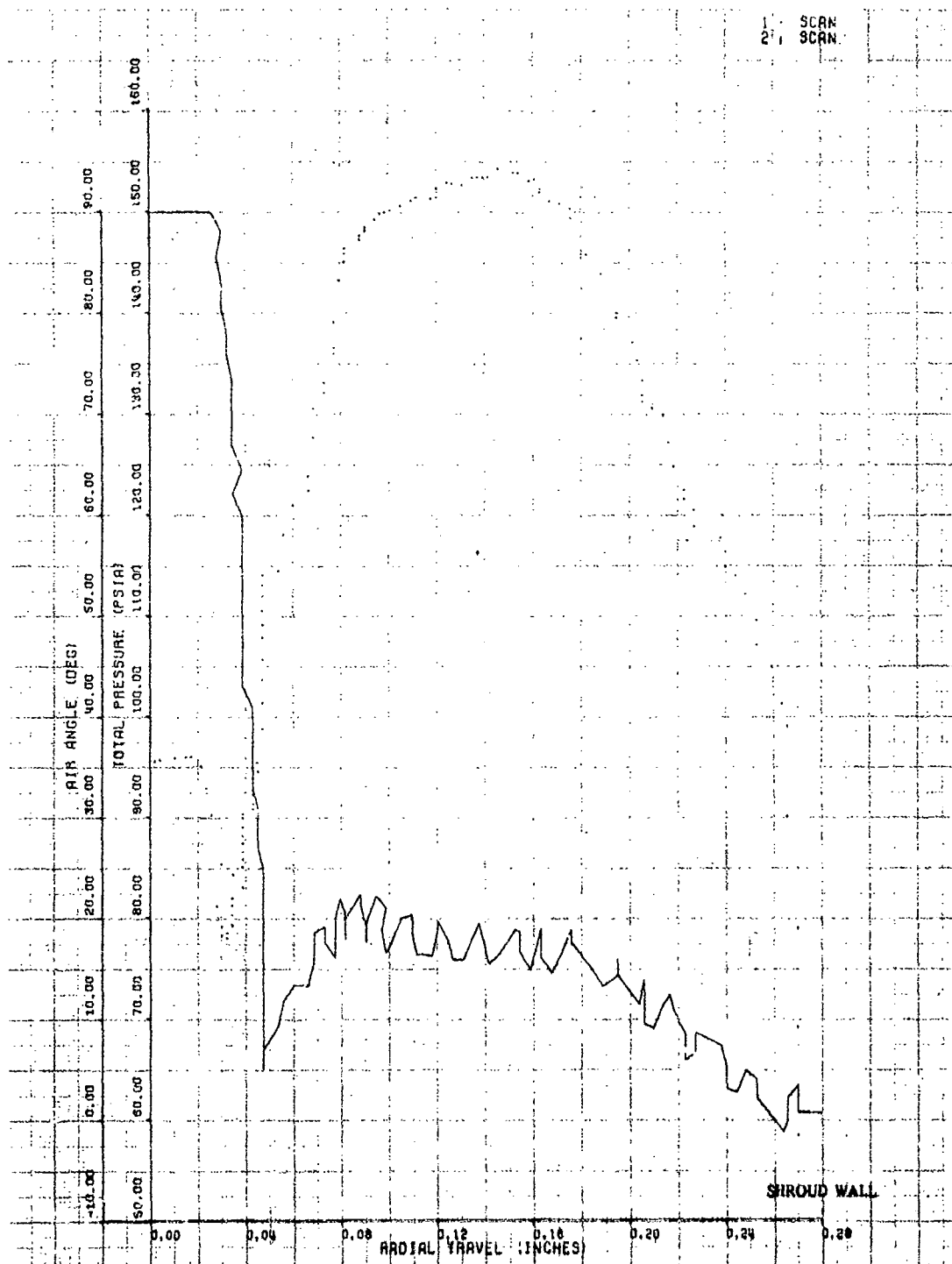


Figure 185. Impeller Exit Traverse, Build No. 6, 95% Speed, 10-deg IGV, Wide Open Discharge.

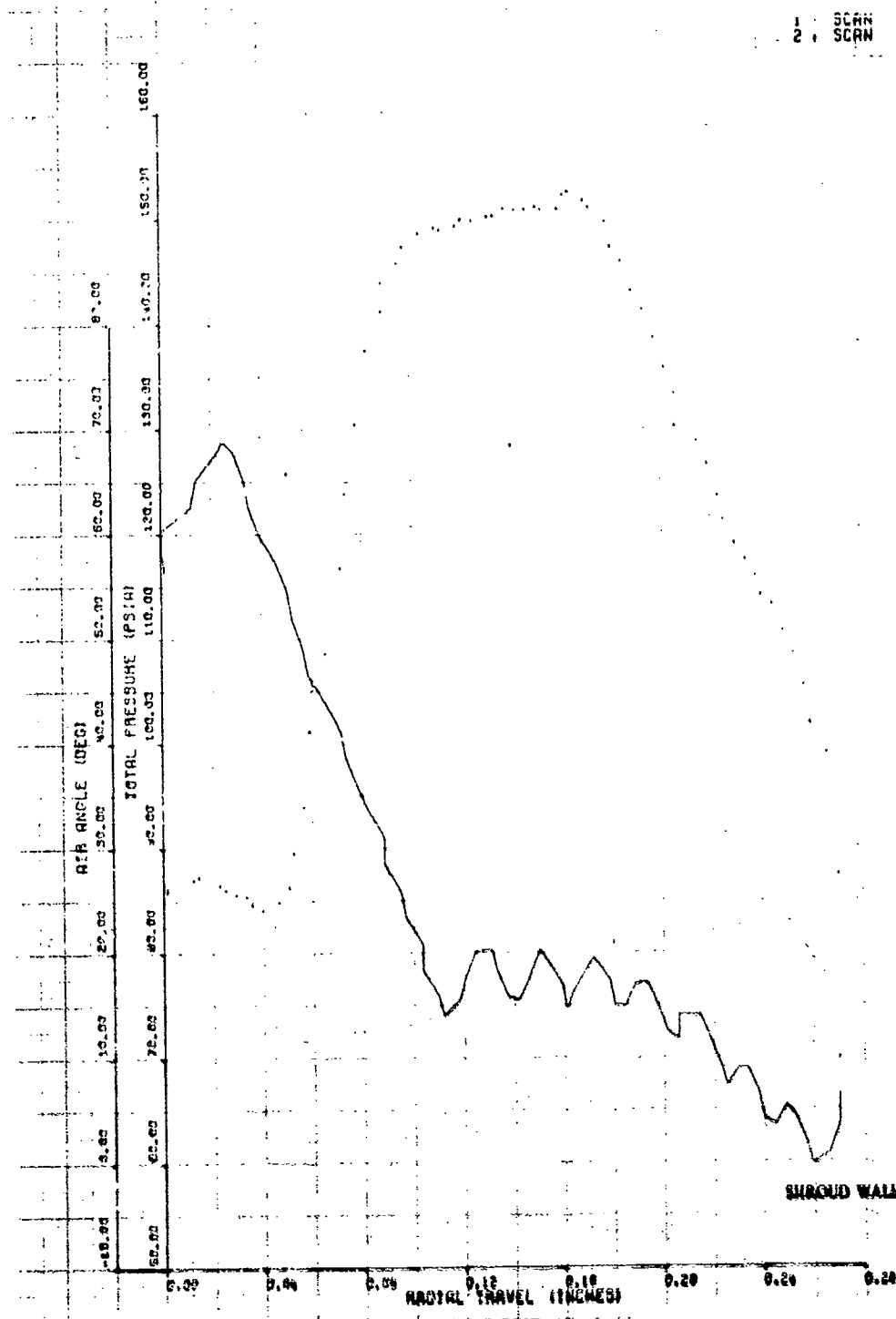


Figure 186. Impeller Exit Traverse, Build No. 6, 95% Speed, 10-deg IGV.



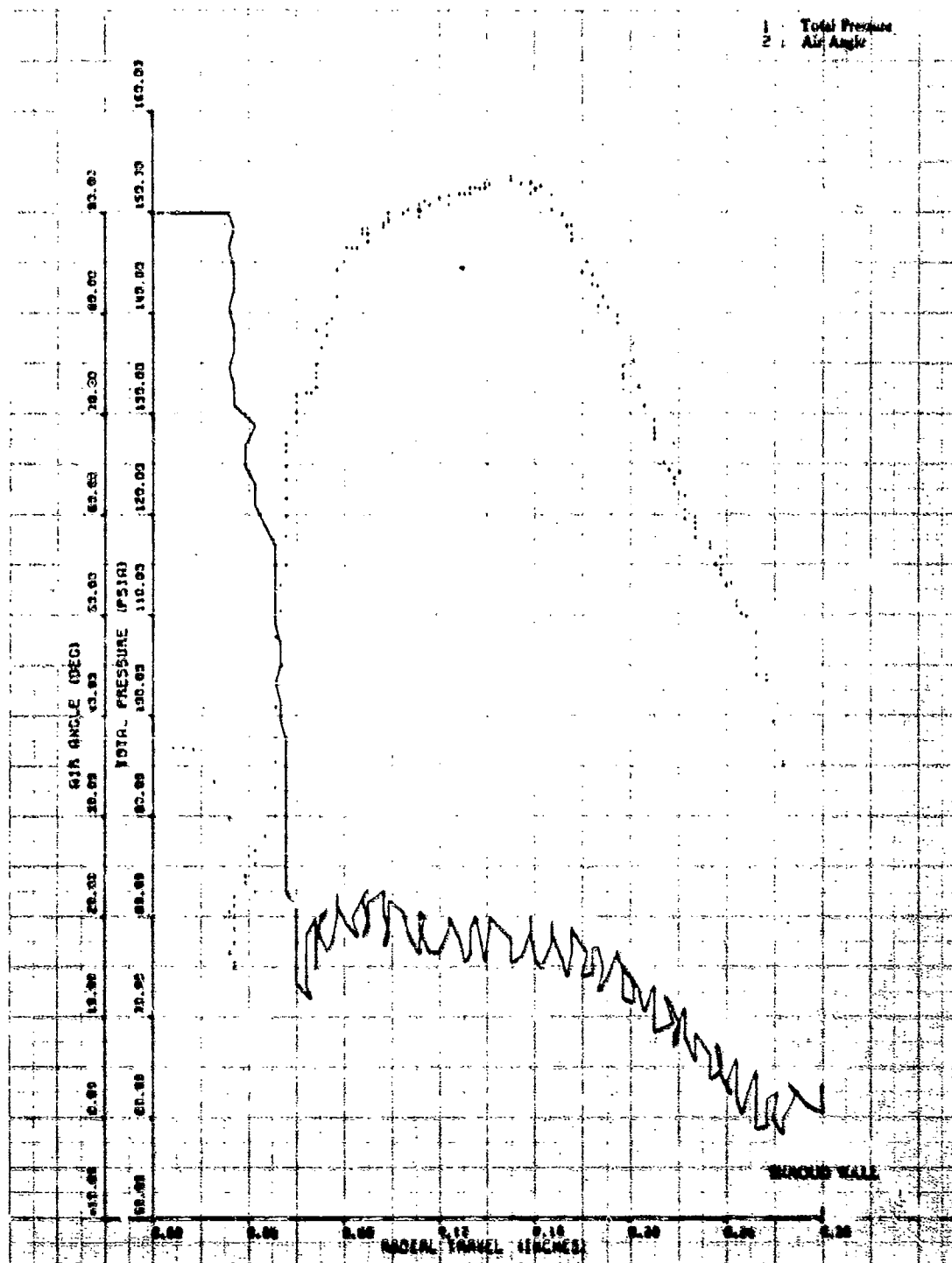


Figure 187. Impeller Exit Traverse, Build No. 6, 95% Speed, 10-deg IGV, Near Stall.

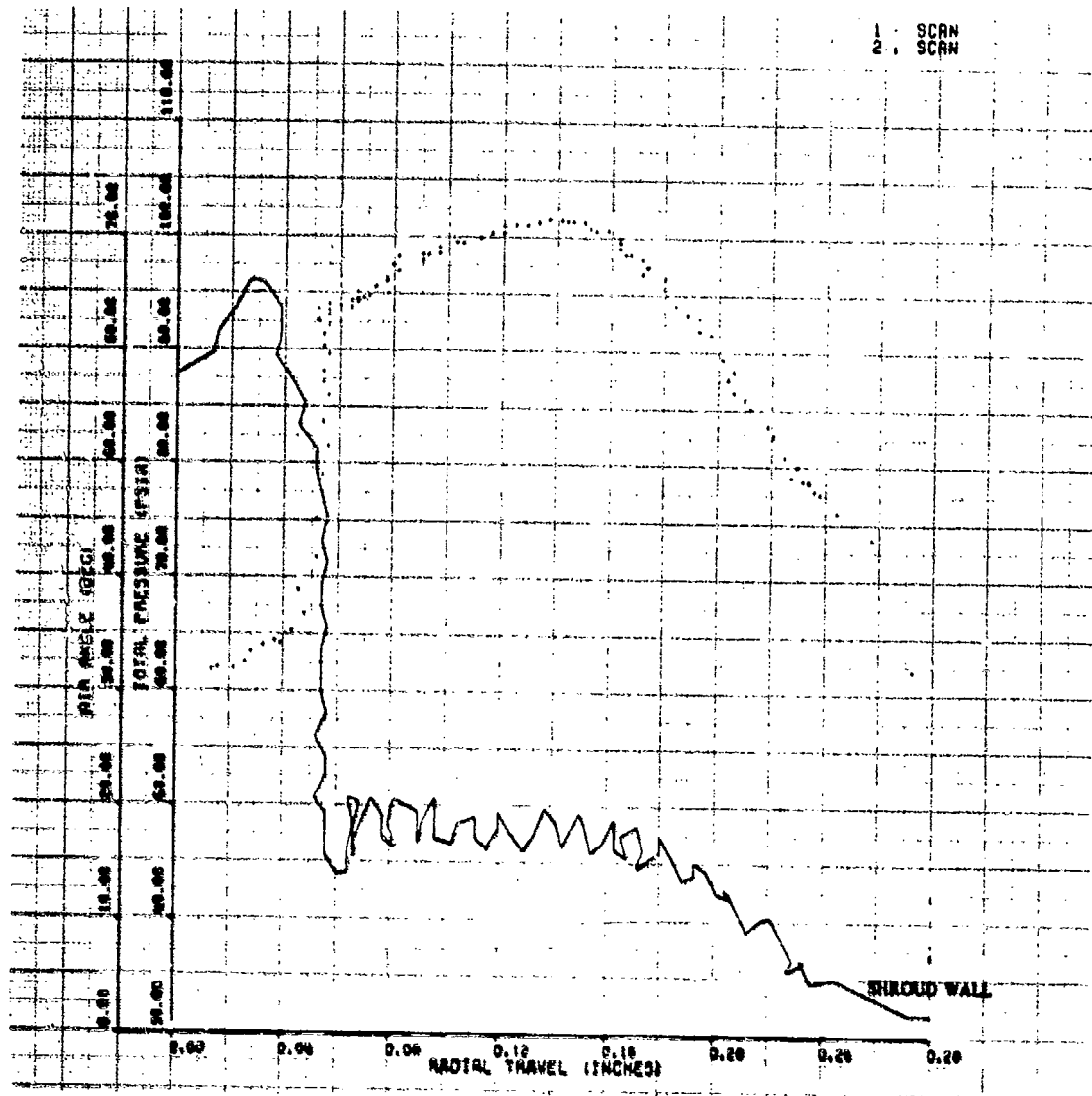


Figure 188. Impeller Exit Traverse, Build No. 6, 85% Speed, 30-deg IGV.

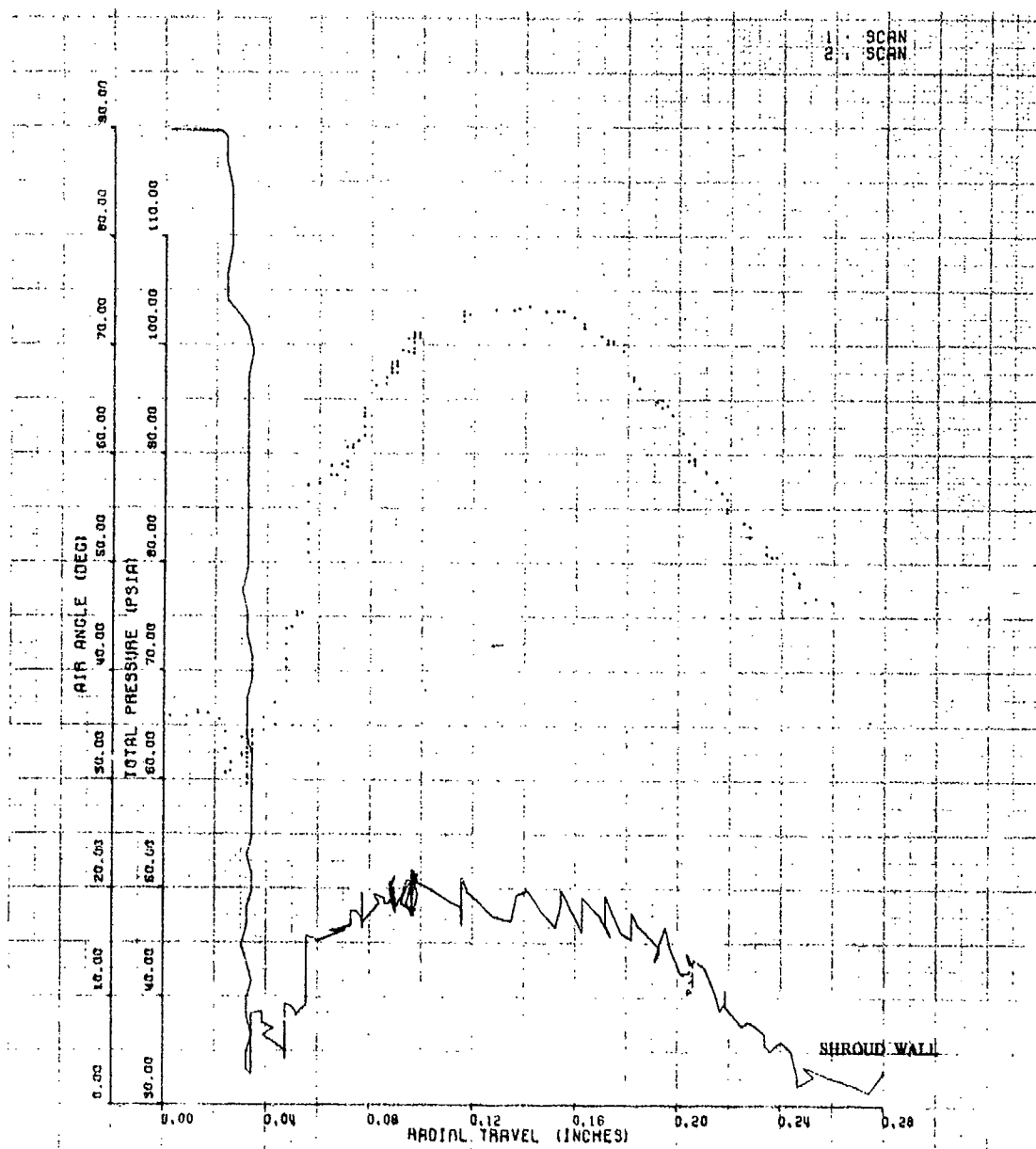


Figure 189. Impeller Exit Traverse, Build No. 6, 85% Speed, 20-deg IGV, Near Stall.

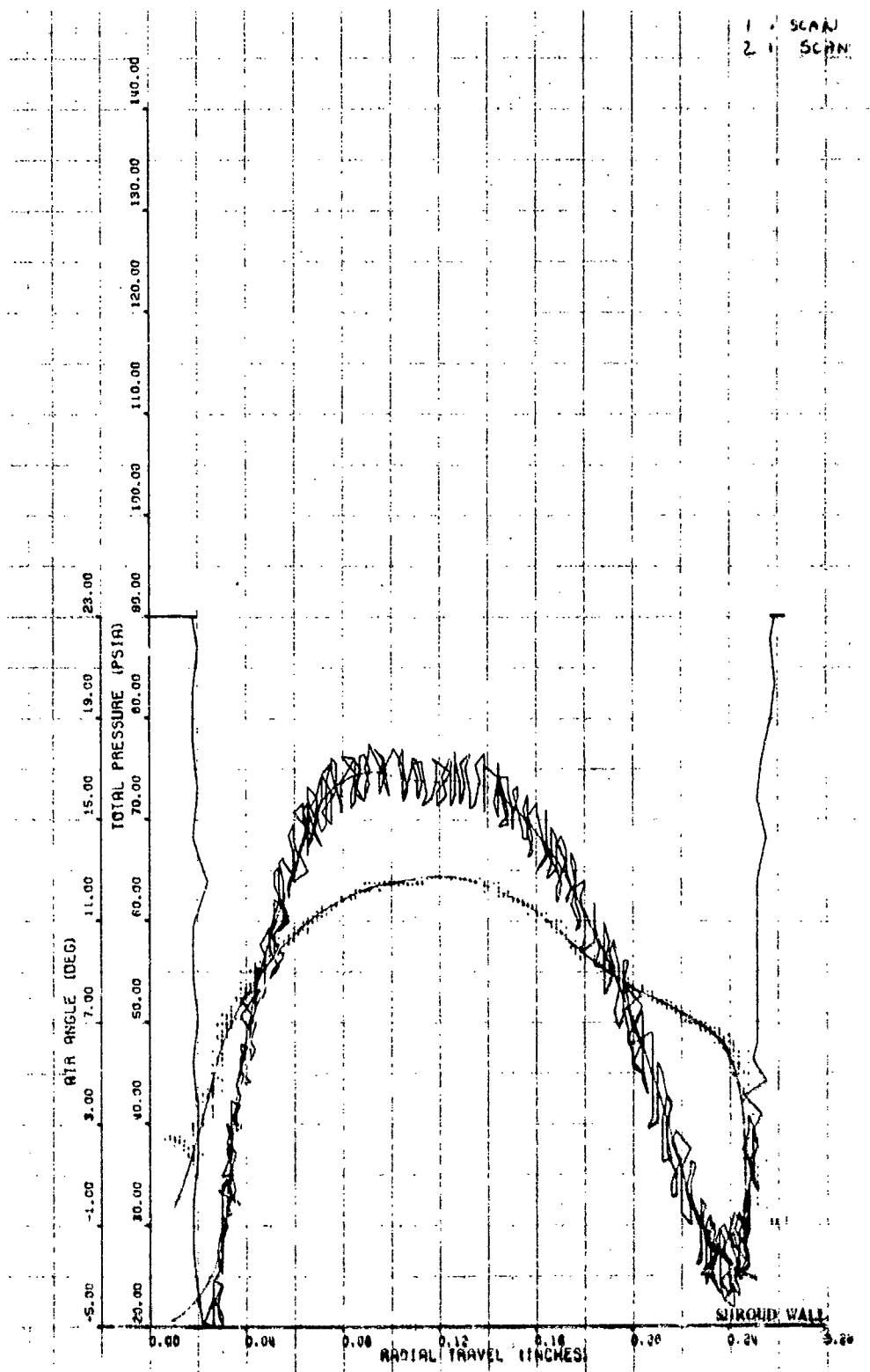


Figure 190. Impeller Exit Traverse, Build No. 3, 70% Speed, 20-deg IGV, Wide Open Discharge.

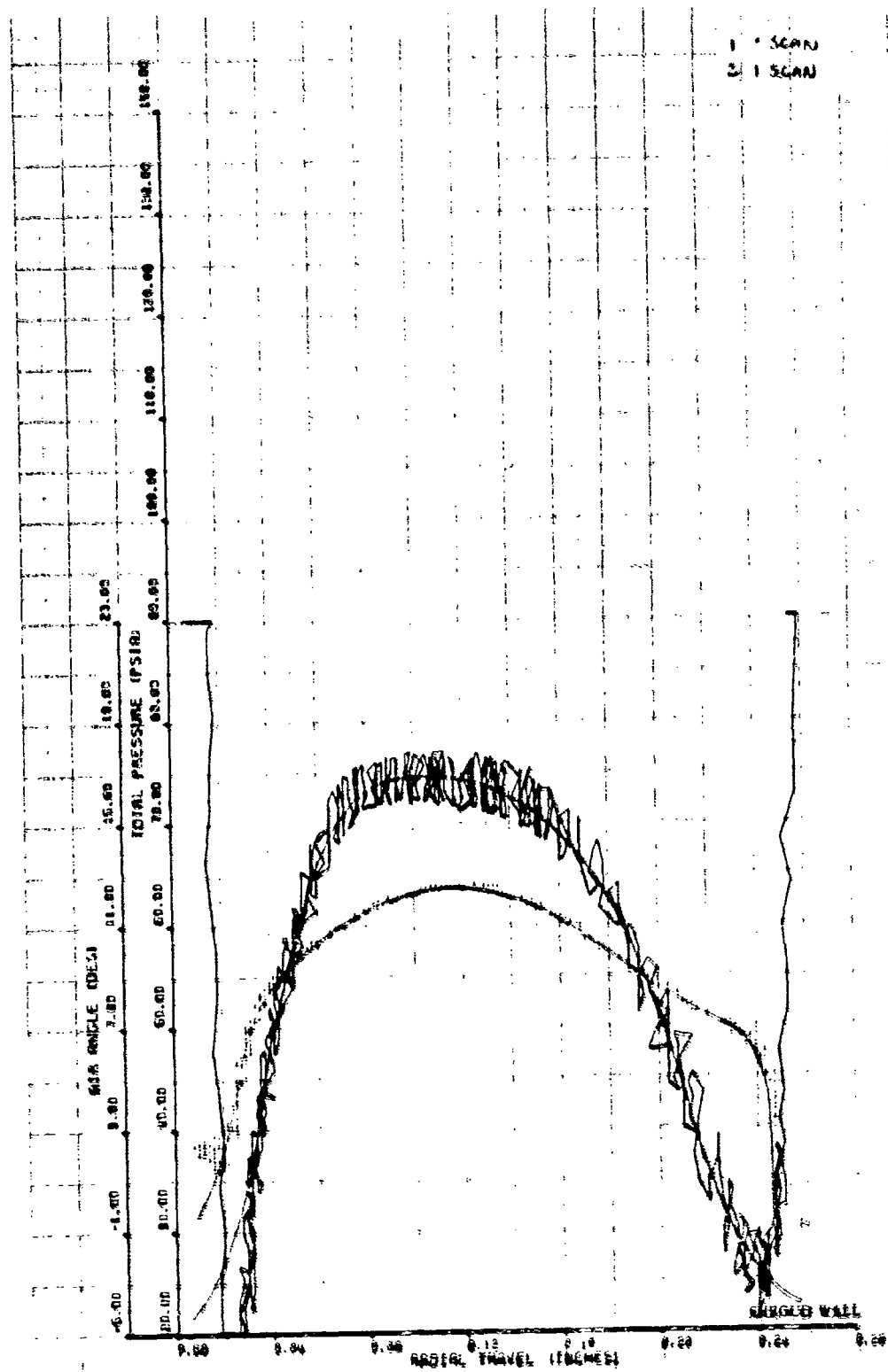


Figure 191. Impeller Exit Traverse, Build No. 3, 70% Speed, 20-deg IGV, Near Stall.

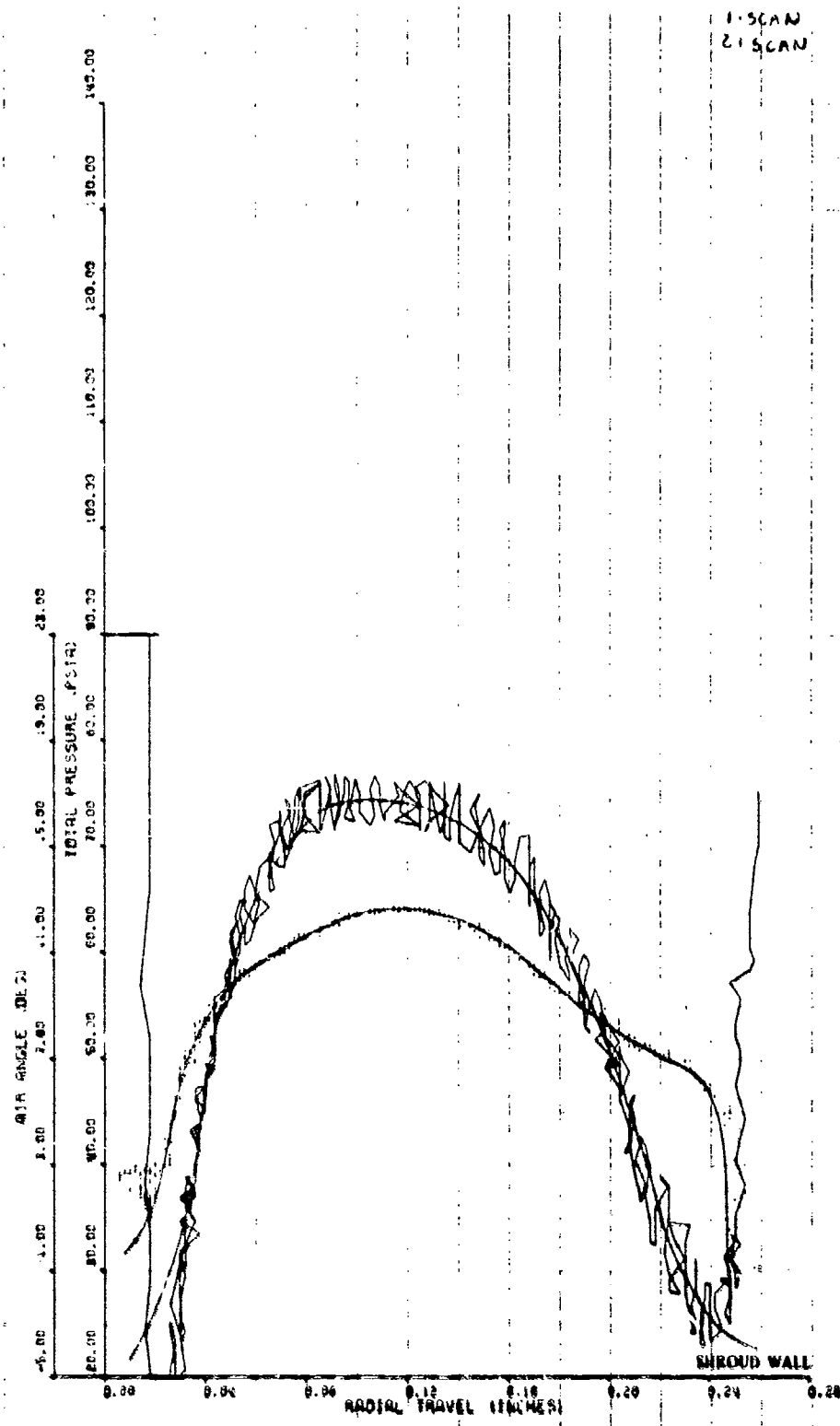


Figure 192. Impeller Exit Traverse, Build No. 3, 70% Speed, 20-deg IGV, Below Near Stall.

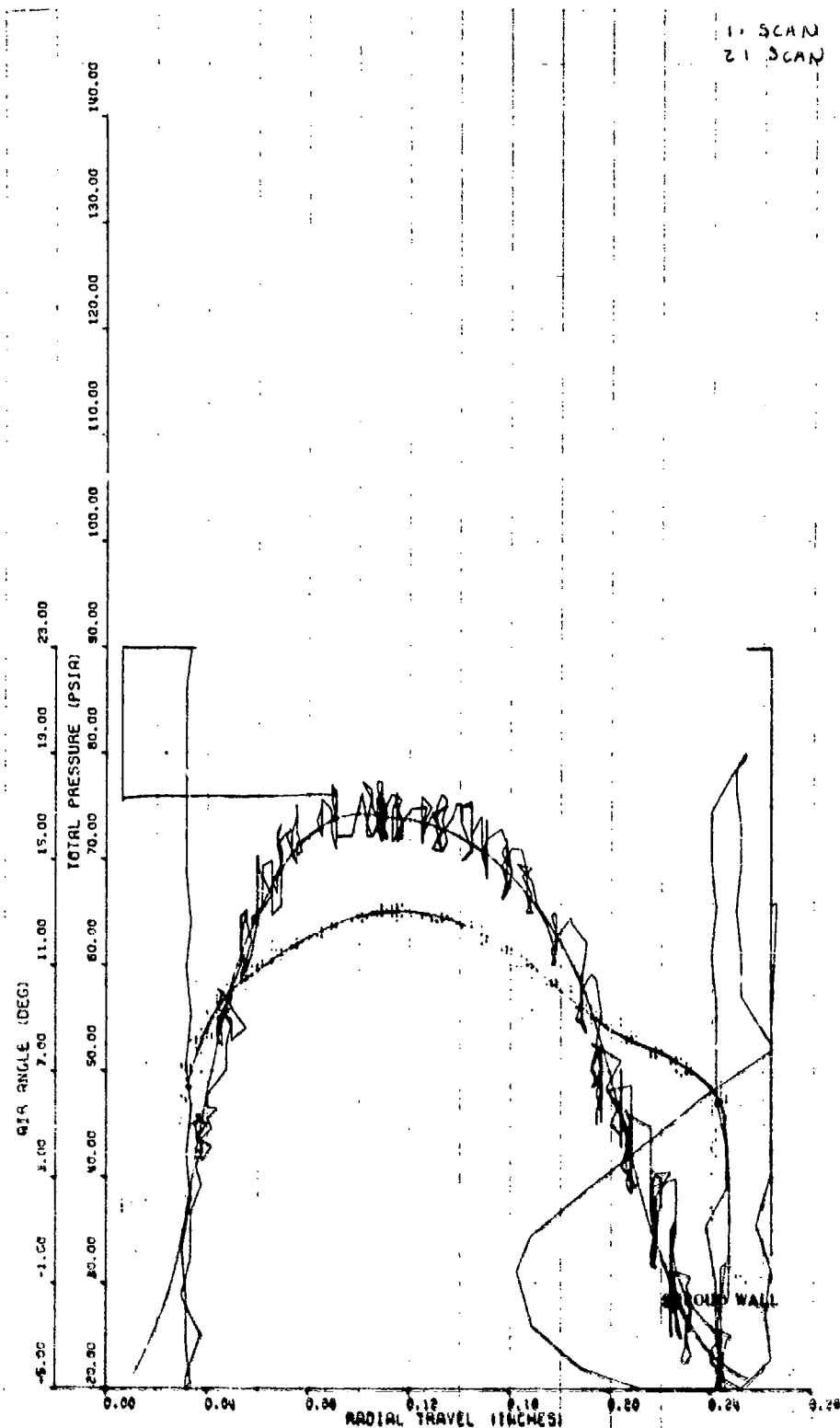


Figure 193. Impeller Exit Traverse, Build No. 3, 70% Speed, 10-deg IGV, Wide Open Discharge.

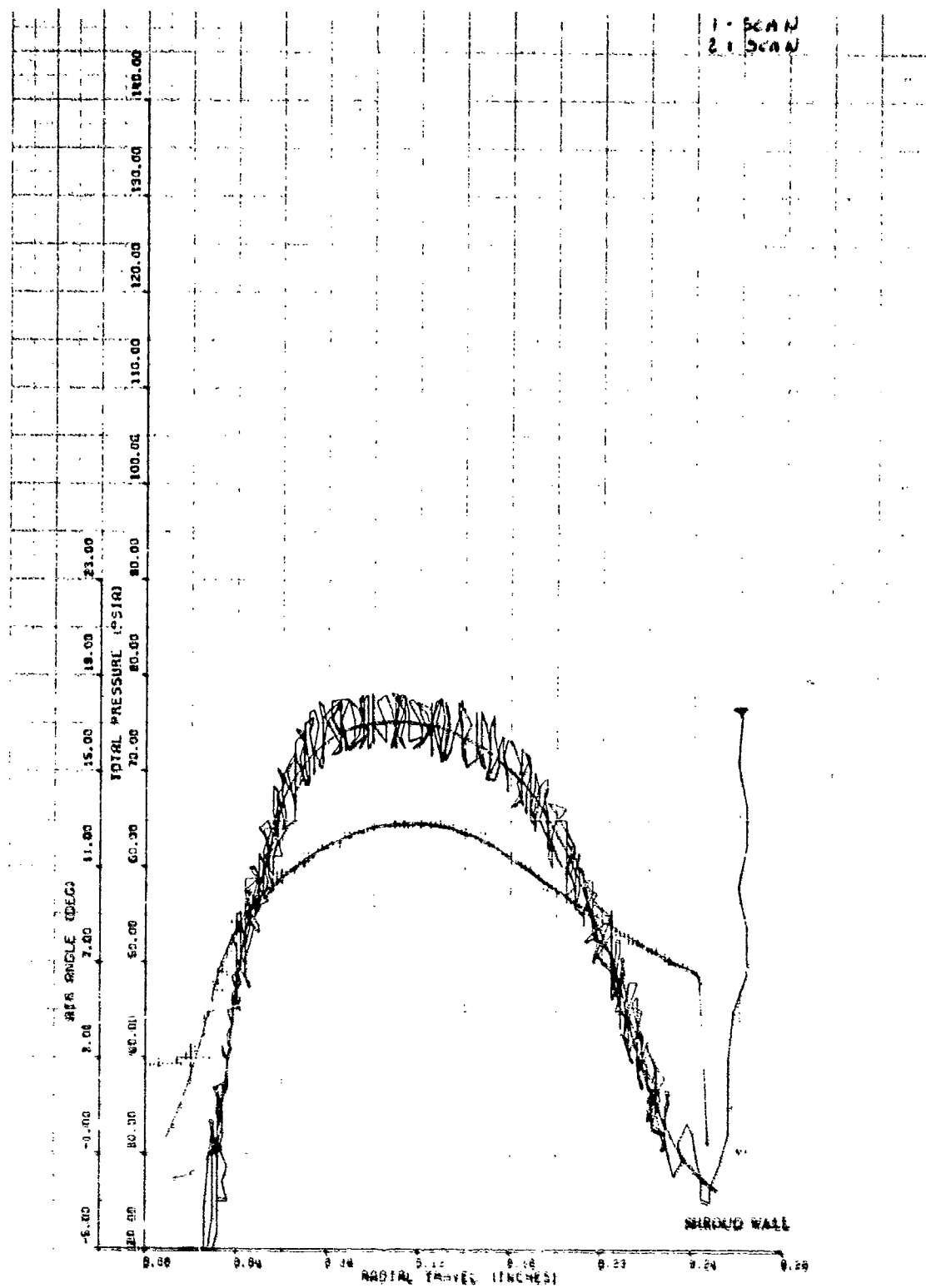


Figure 194. Impeller Exit Traverse, Build No. 3, 70% Speed, 10-deg IGV, Near Stall.



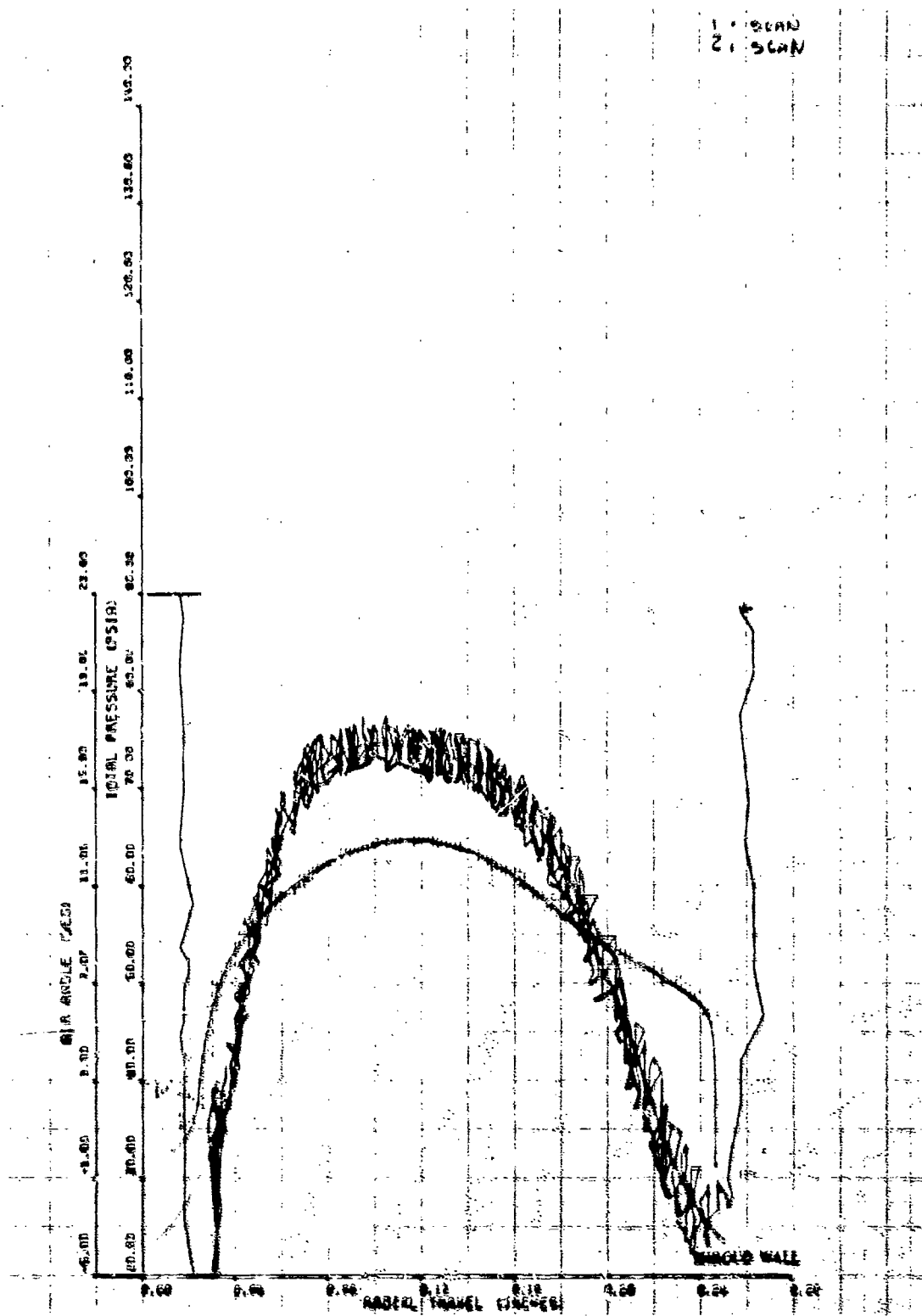


Figure 195. Impeller Exit Traverse, Build No. 3, 70% Speed, 10-deg IGV, Below Near Stall.

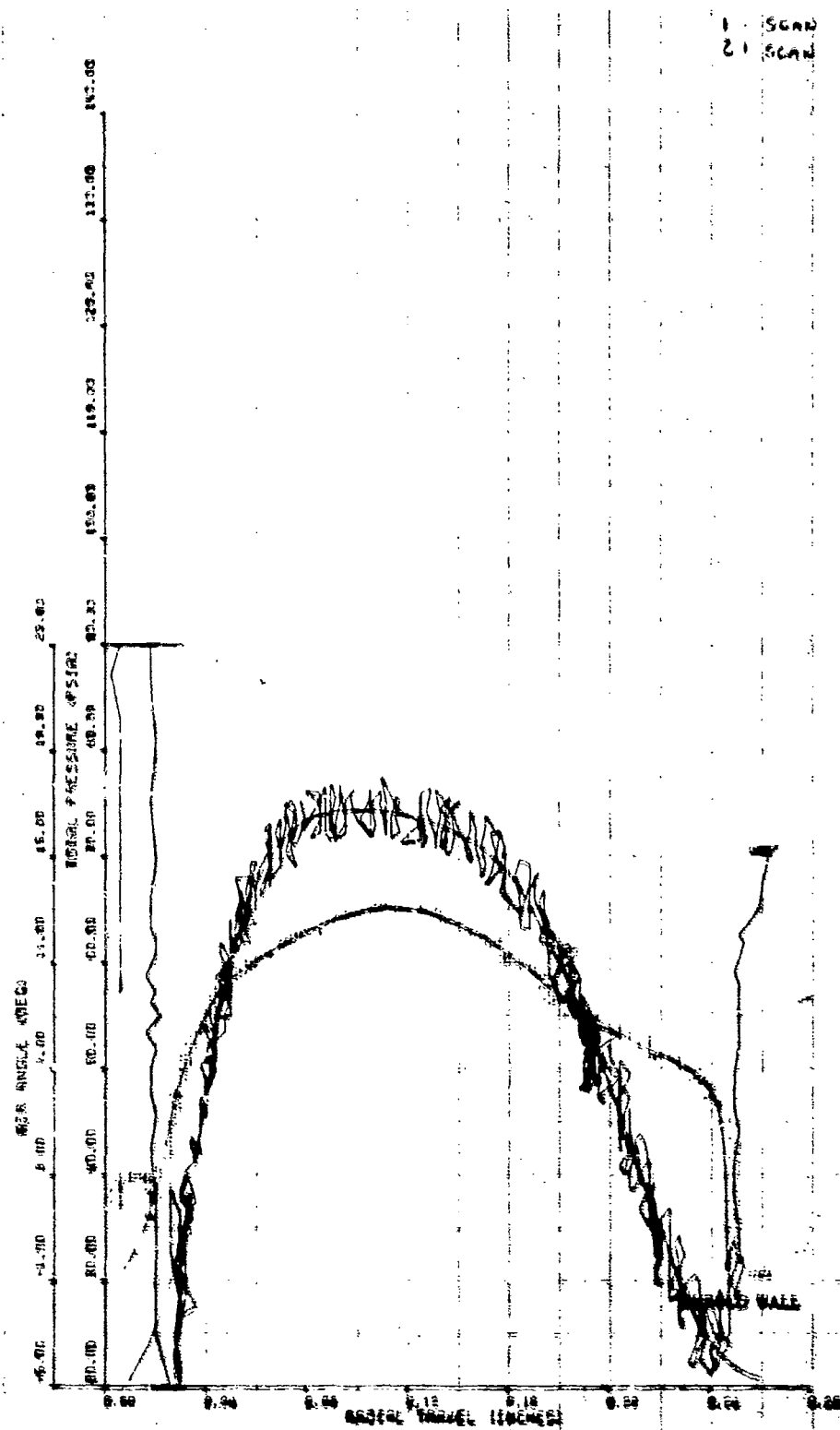


Figure 186. Impeller Exit Traverse, Build No. 3, 70% Speed,  
0-deg IGV, Wide Open Discharge.

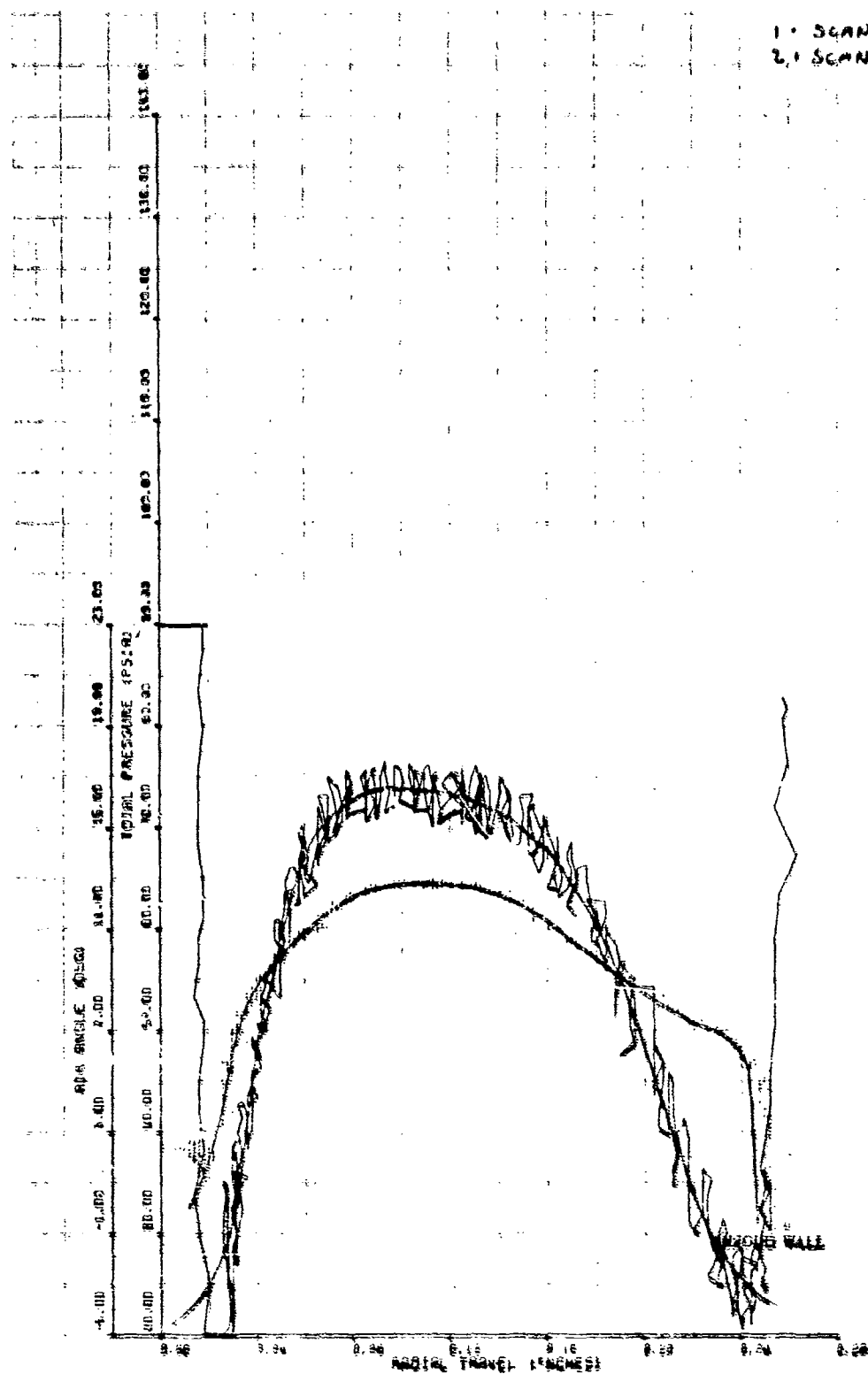


Figure 197. Impeller Exit Traverse, Build No. 3, 70% Speed, 0-deg IGV, Near Stall.

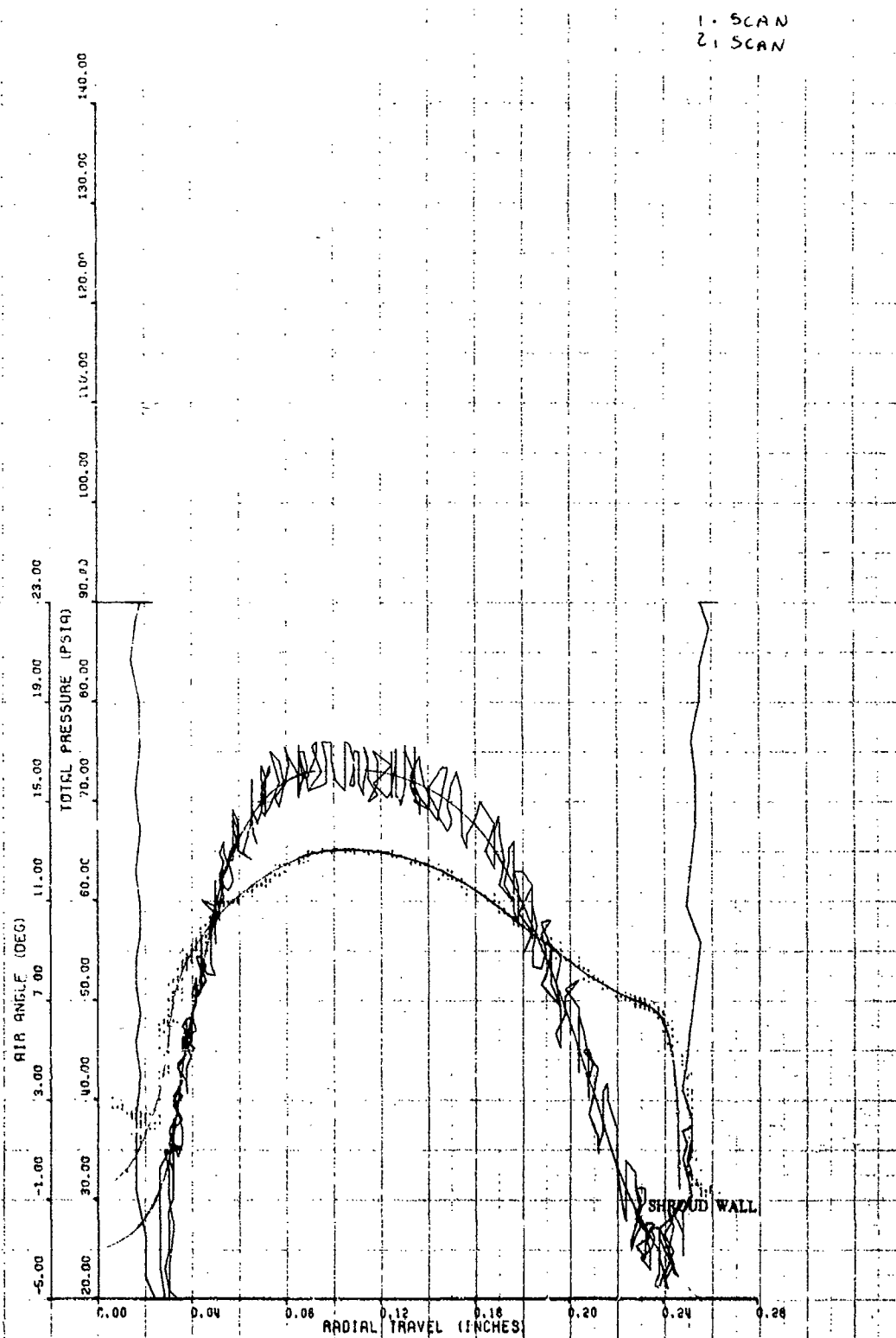


Figure 198. Impeller Exit Traverse, Build No. 3, 70% Speed, 0-deg IGV, Below Near Stall.

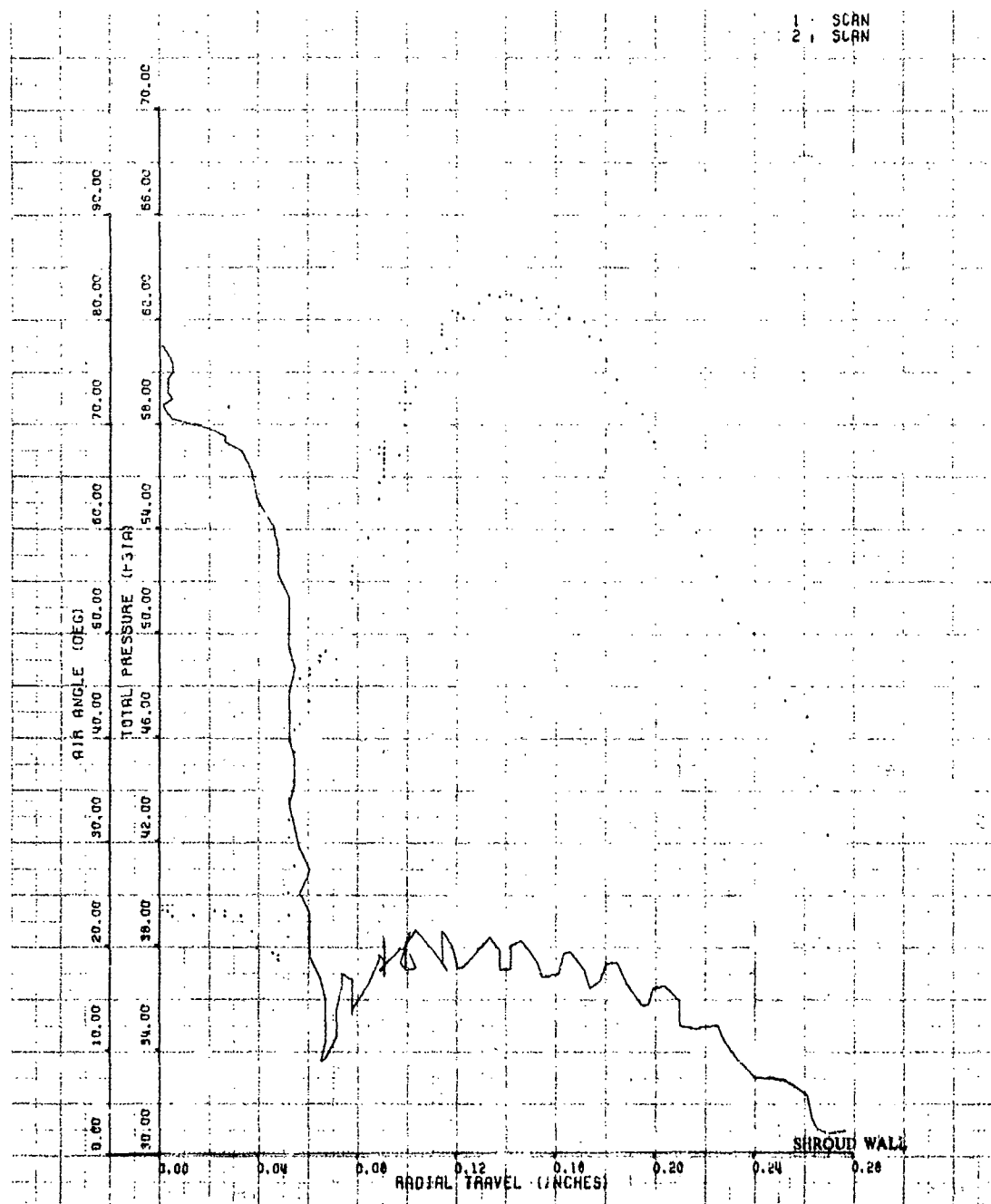


Figure 1f9. Impeller Exit Traverse, Build No. 6, 70% Speed, 30-deg IGV.

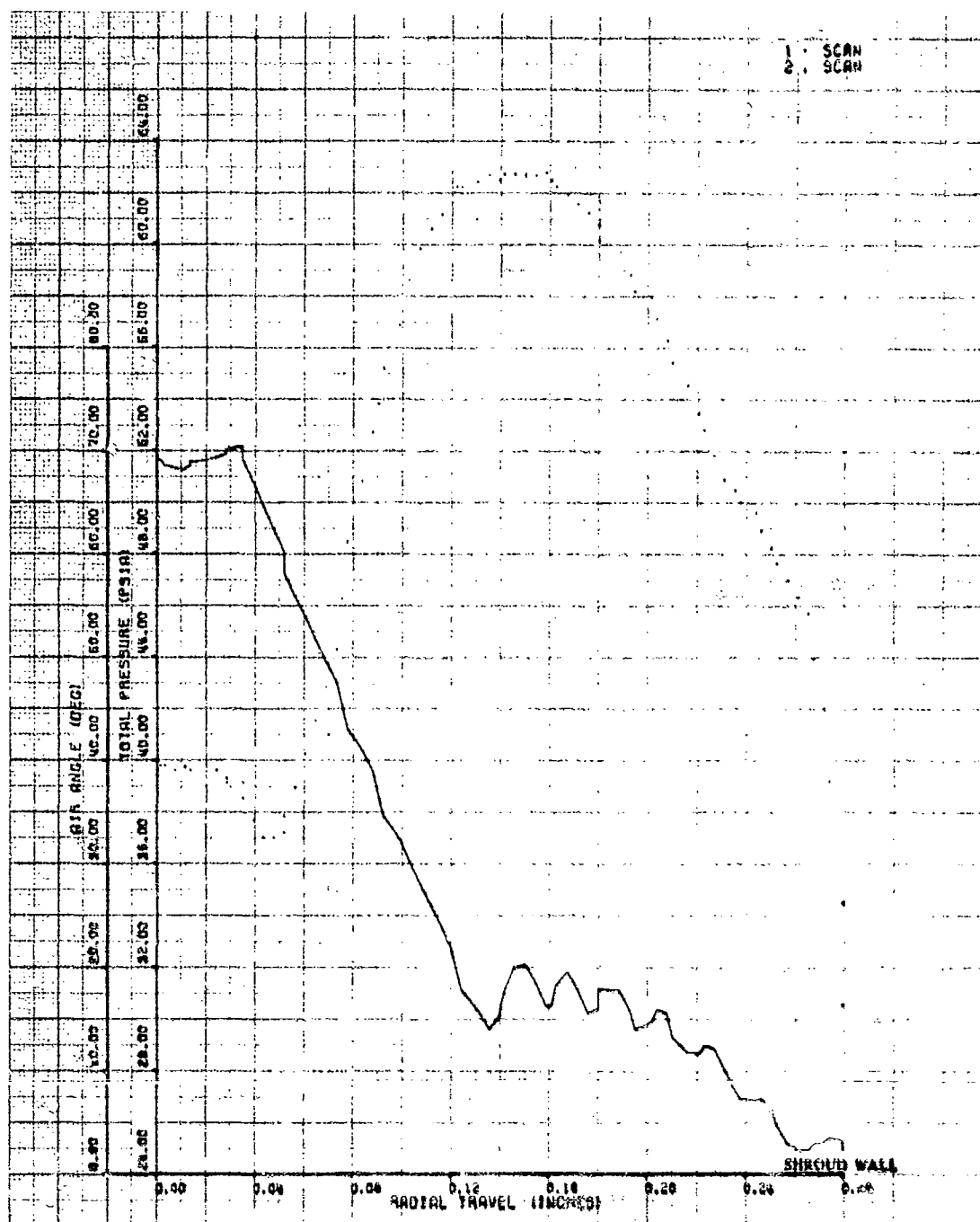


Figure 200. Impeller Exit Traverse, Build No. 6, 70% Speed, 20-deg IGV.

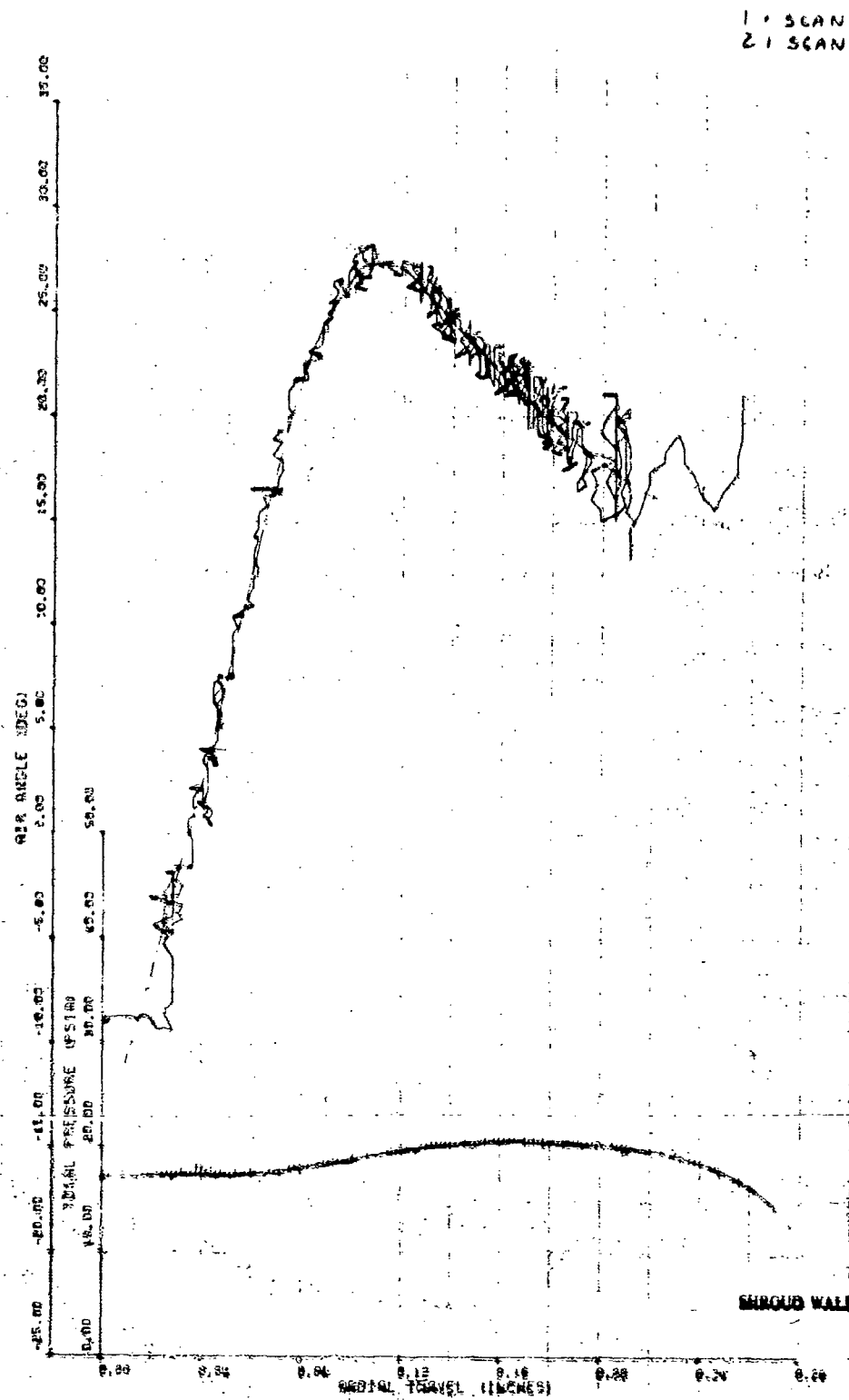


Figure 261. Impeller Exit Traverse, Build No. 3, 30% Speed, 20-deg IGV, Wide Open Discharge.

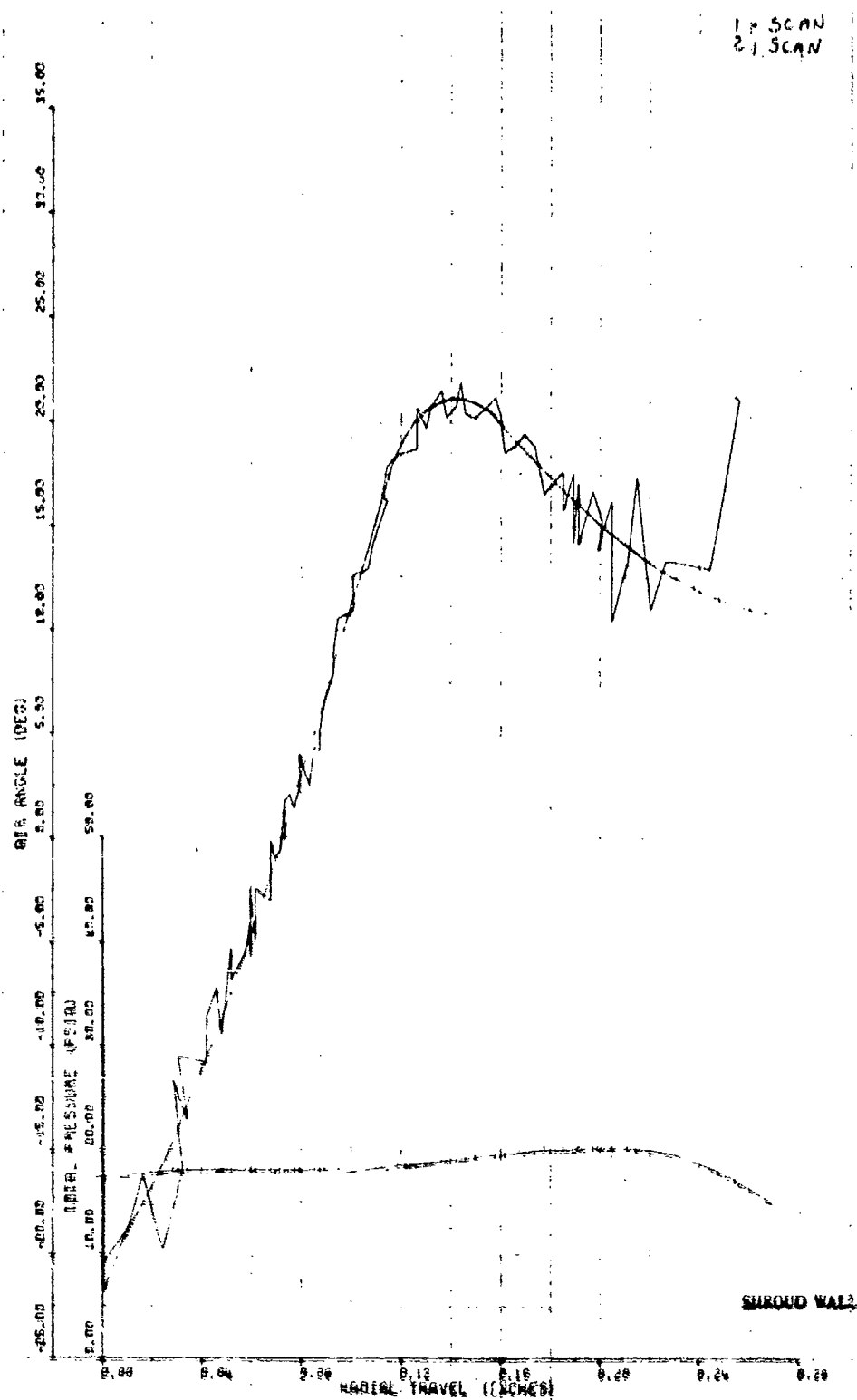


Figure 202. Impeller Exit Traverse, Build No. 3, 30% Speed, 20-deg IGV, Near Stall.



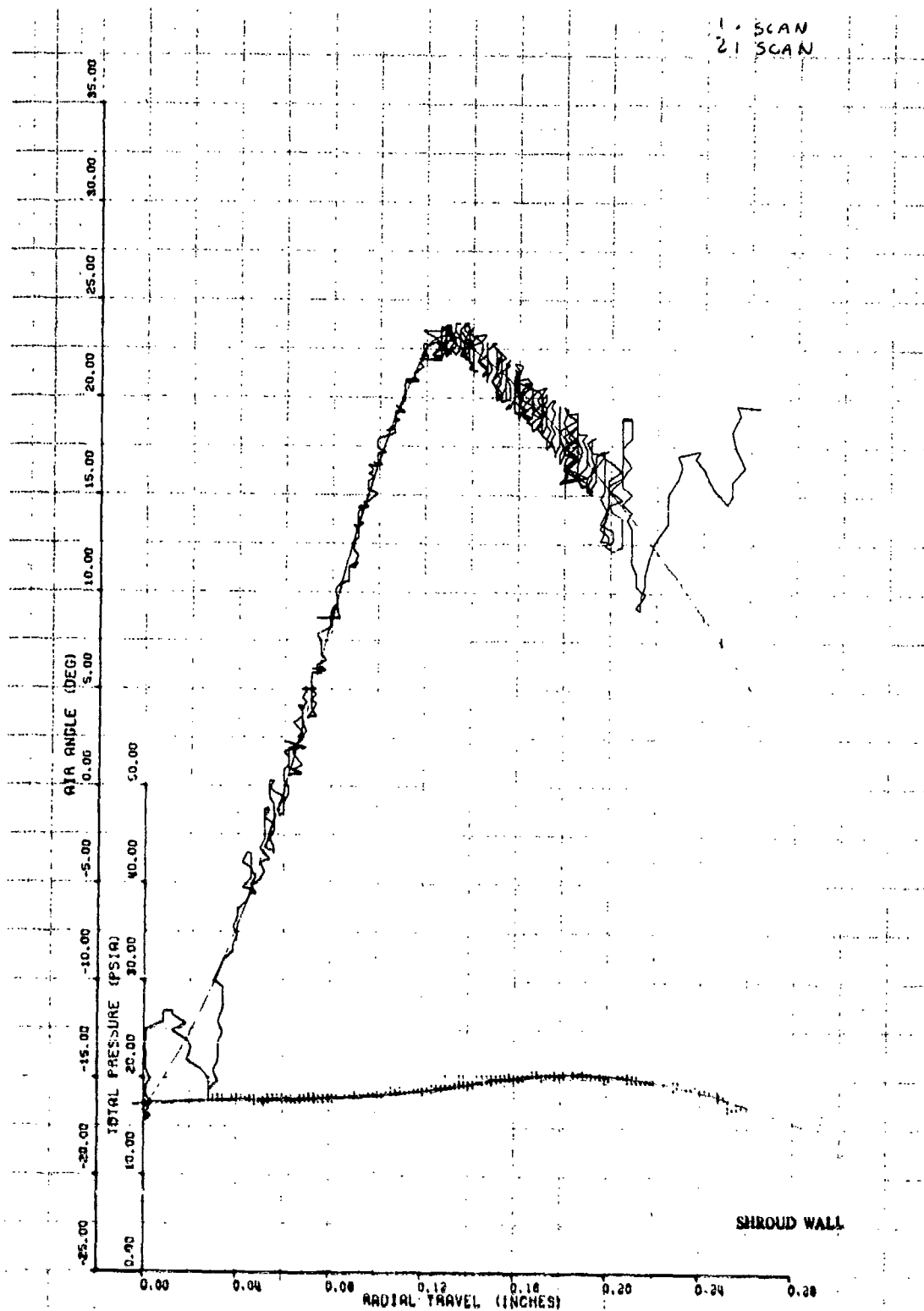


Figure 203. Impeller Exit Traverse, Build No. 3, 30% Speed, 20-deg IGV, Below Near Stall.

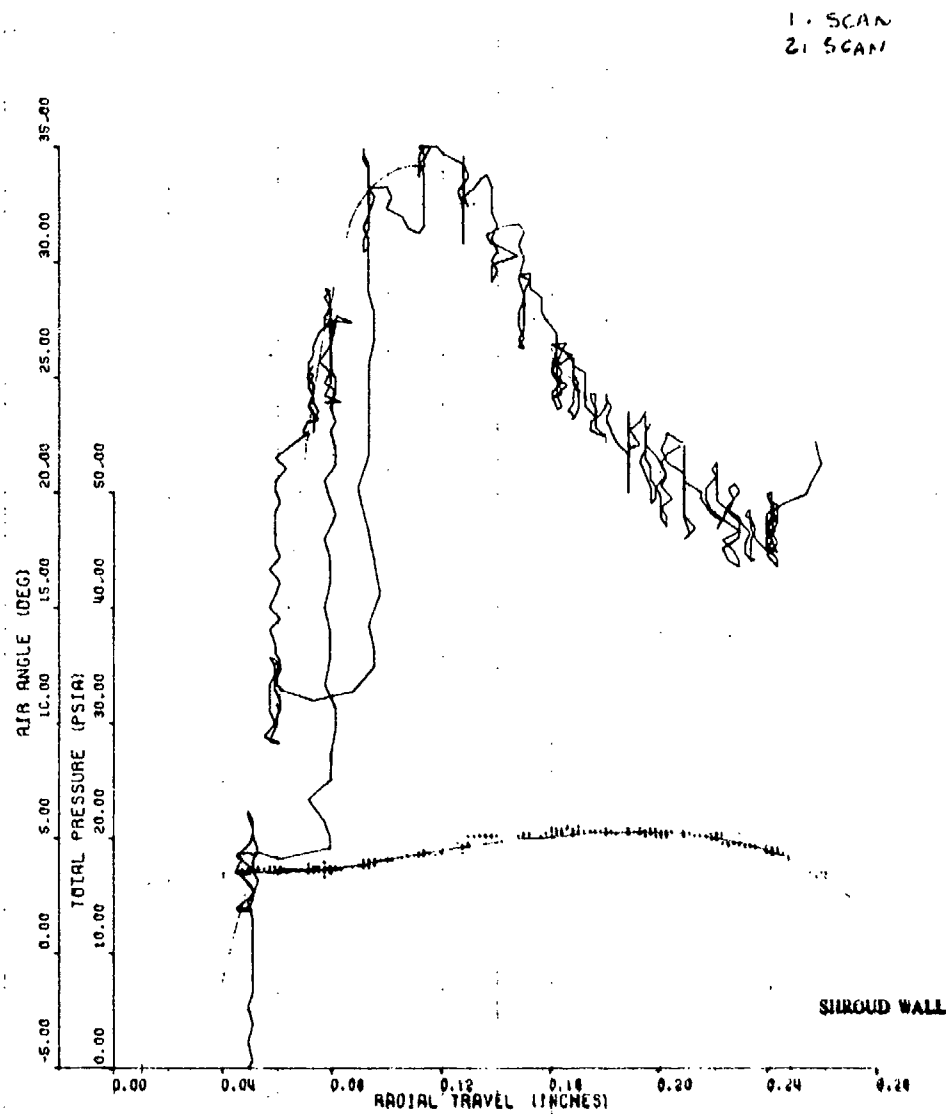


Figure 204. Impeller Exit Traverse, Build No. 3, 30% Speed, 10-deg IGV, Wide Open Discharge.

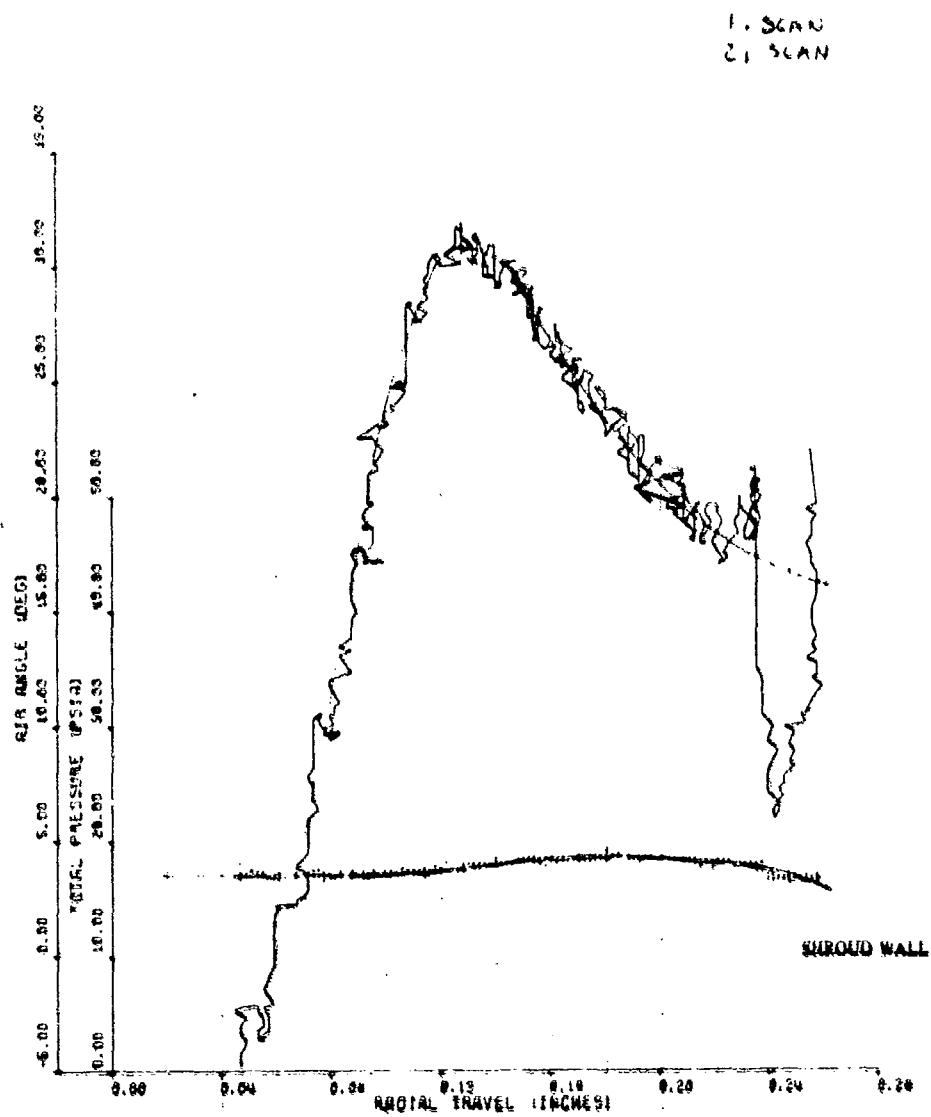


Figure 20E. Impeller Exit Traverse, Build No. 3, 30% Speed, 10-deg iGV, Near Stall.

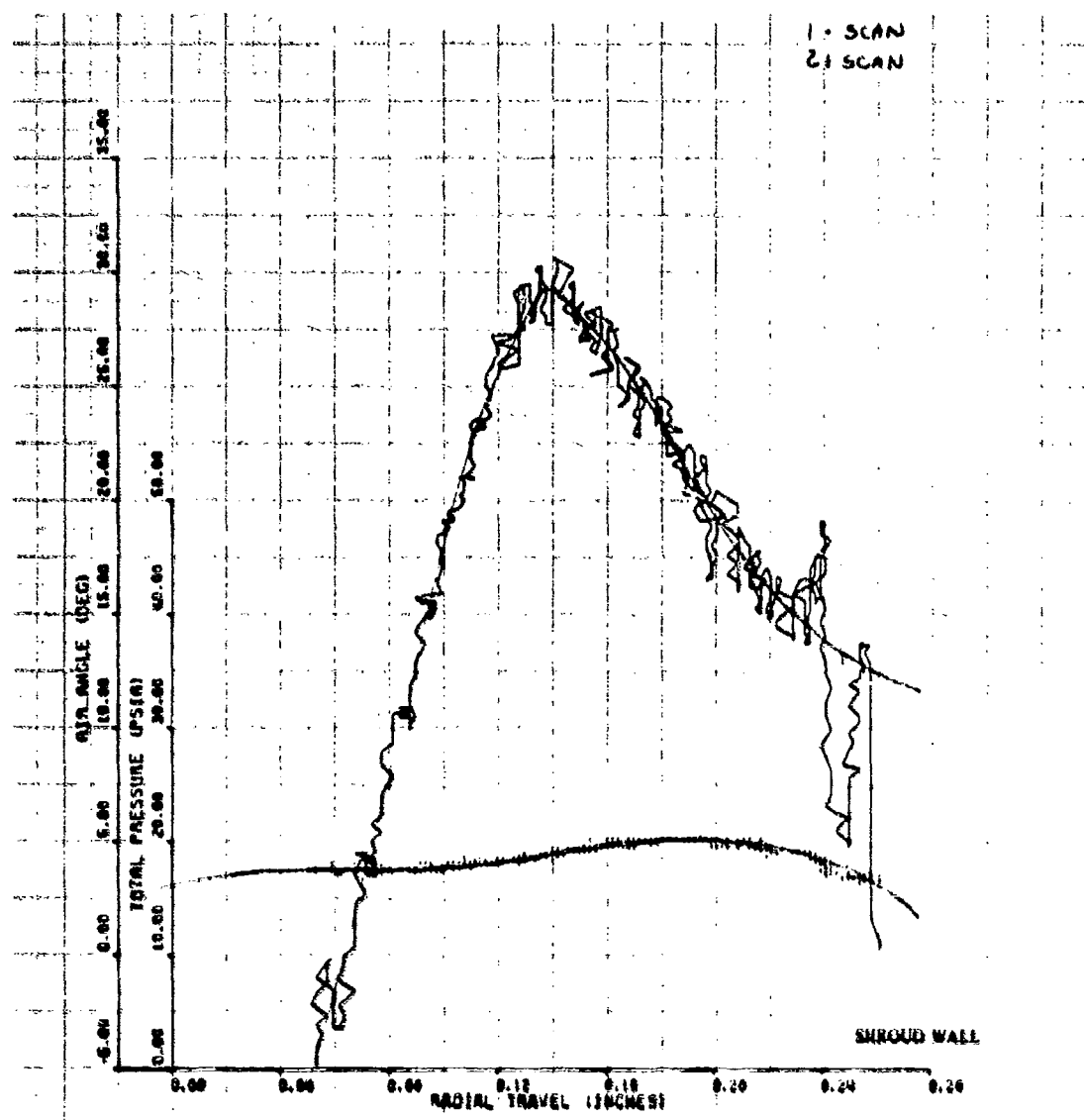


Figure 206. Impeller Exit Traverse, Build No. 3, 30% Speed, 10-deg IGV, Below Near Stall.

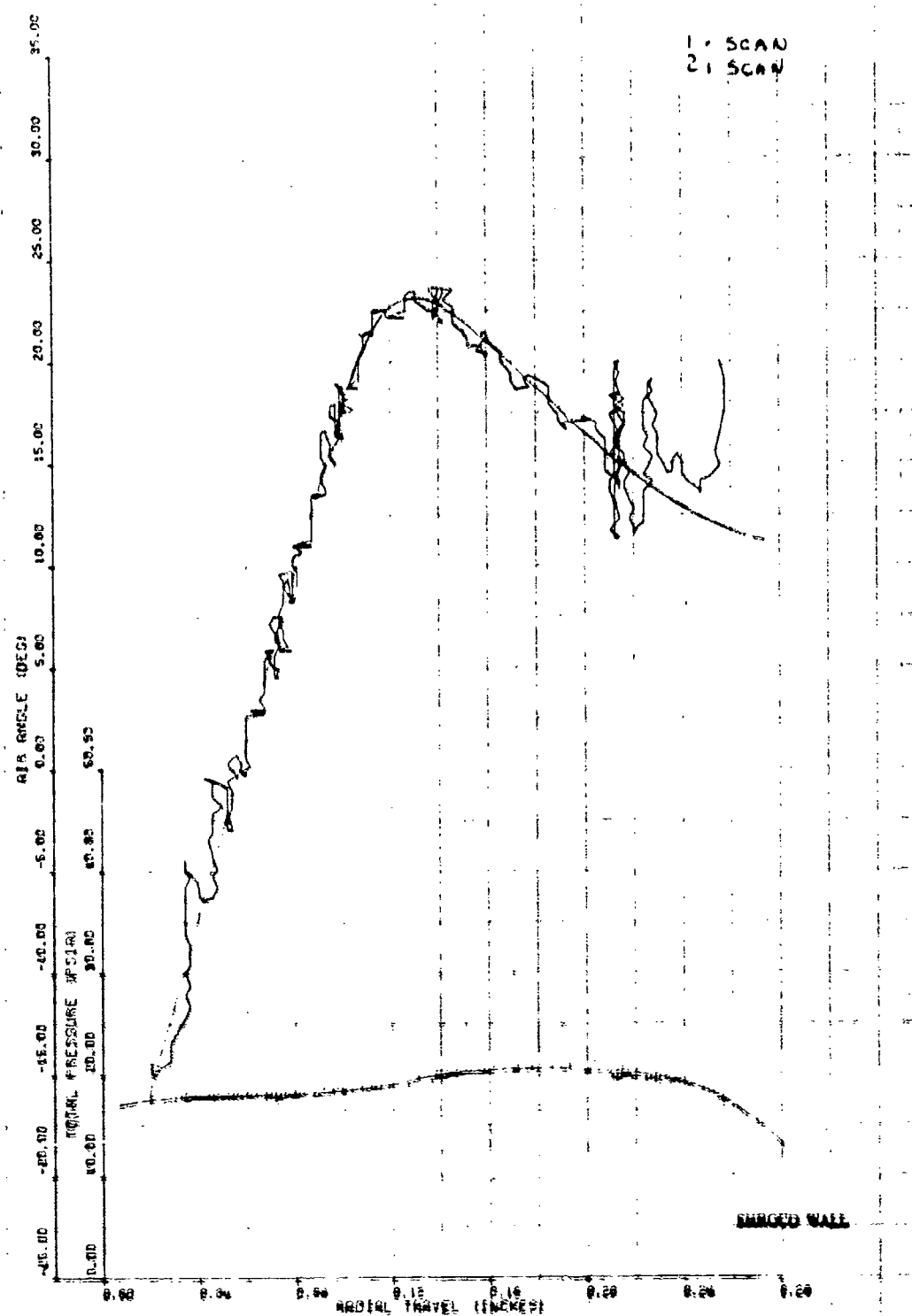


Figure 307. Impeller Exit Traverse, Build No. 3, 30% Speed, 10-deg ICV, Below Near Stall.

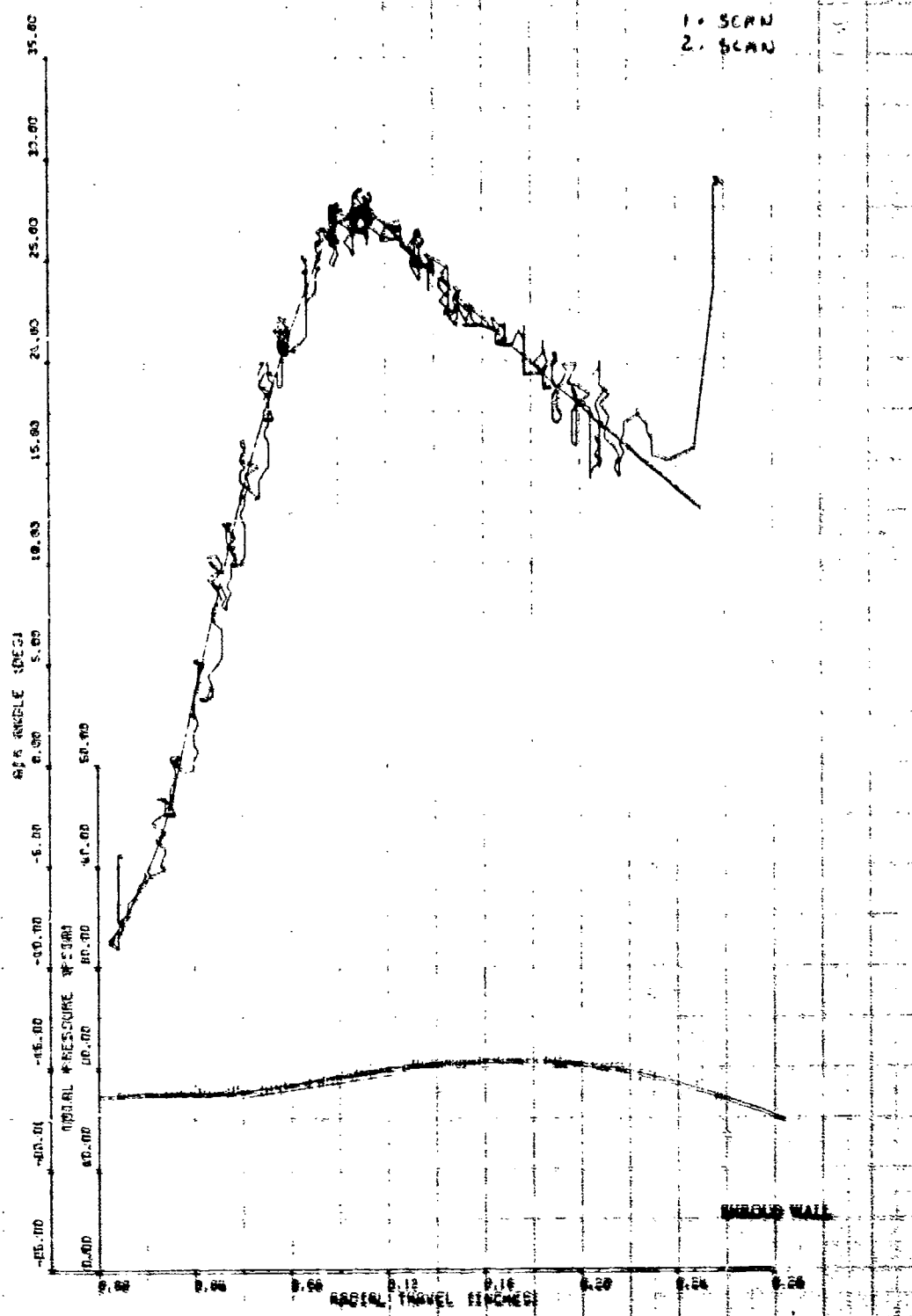


Figure 20s. Impeller Exit Traverse, Build No. 3, 30% Speed,  
0-deg ICV, Wide Open Discharge.

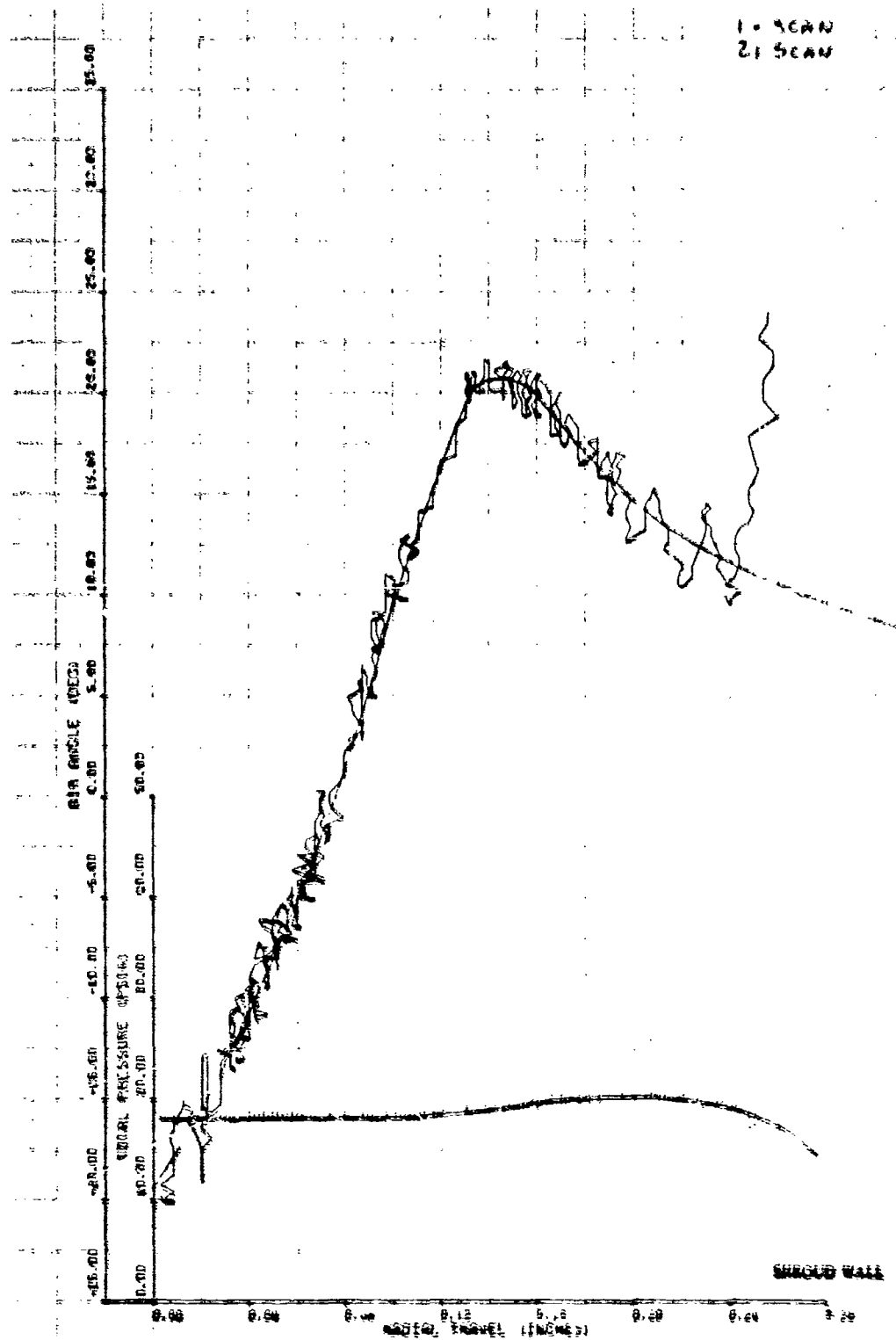


Figure 209. Impeller Exit Traverse, Build No. 3, 30% Speed, 0-deg IGV, Near Stall.

323



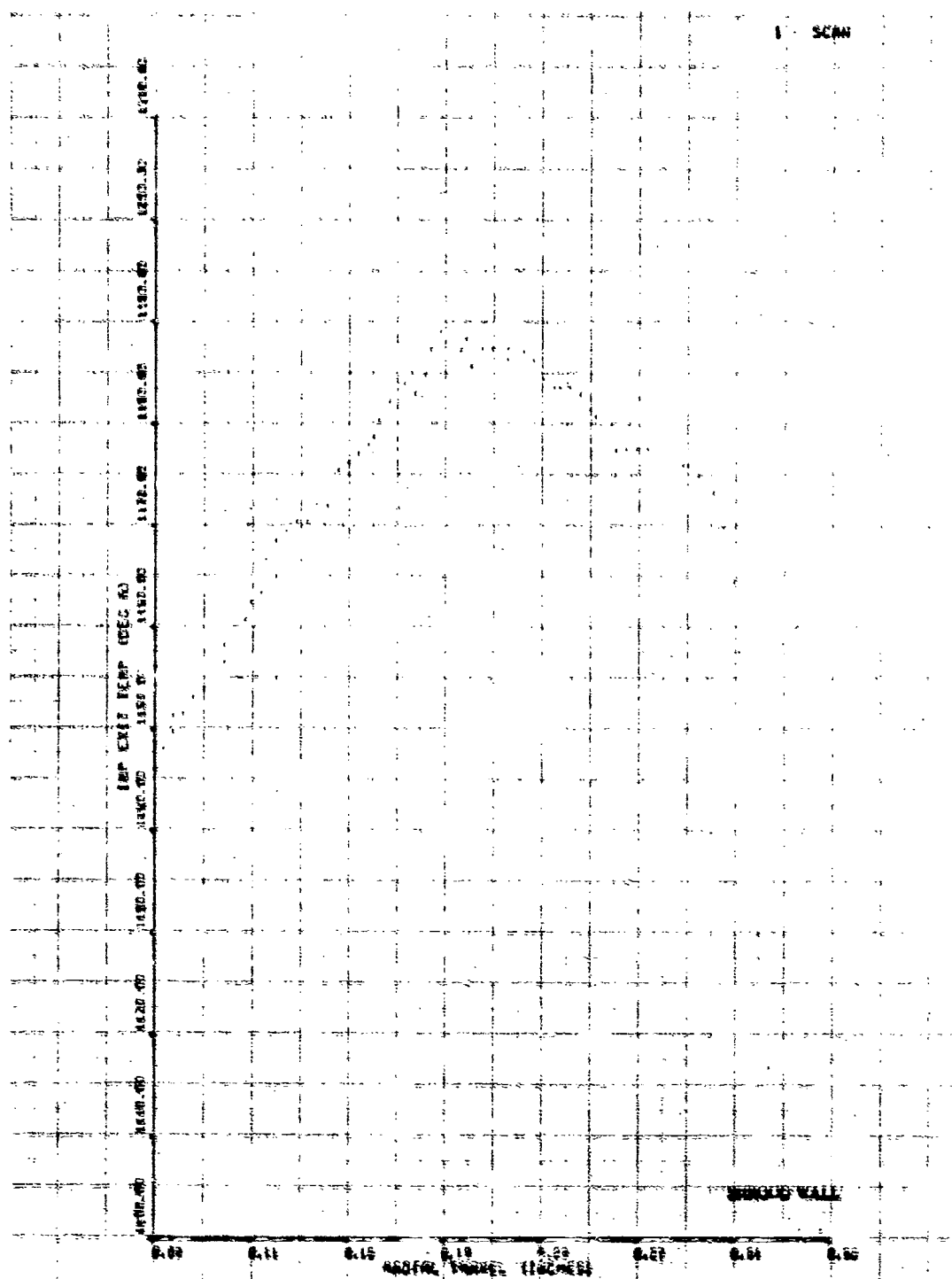


Figure 211. Impeller Exit Temperature Traverse, Build No. 6,  
1017 Speed, 5-deg IGV.

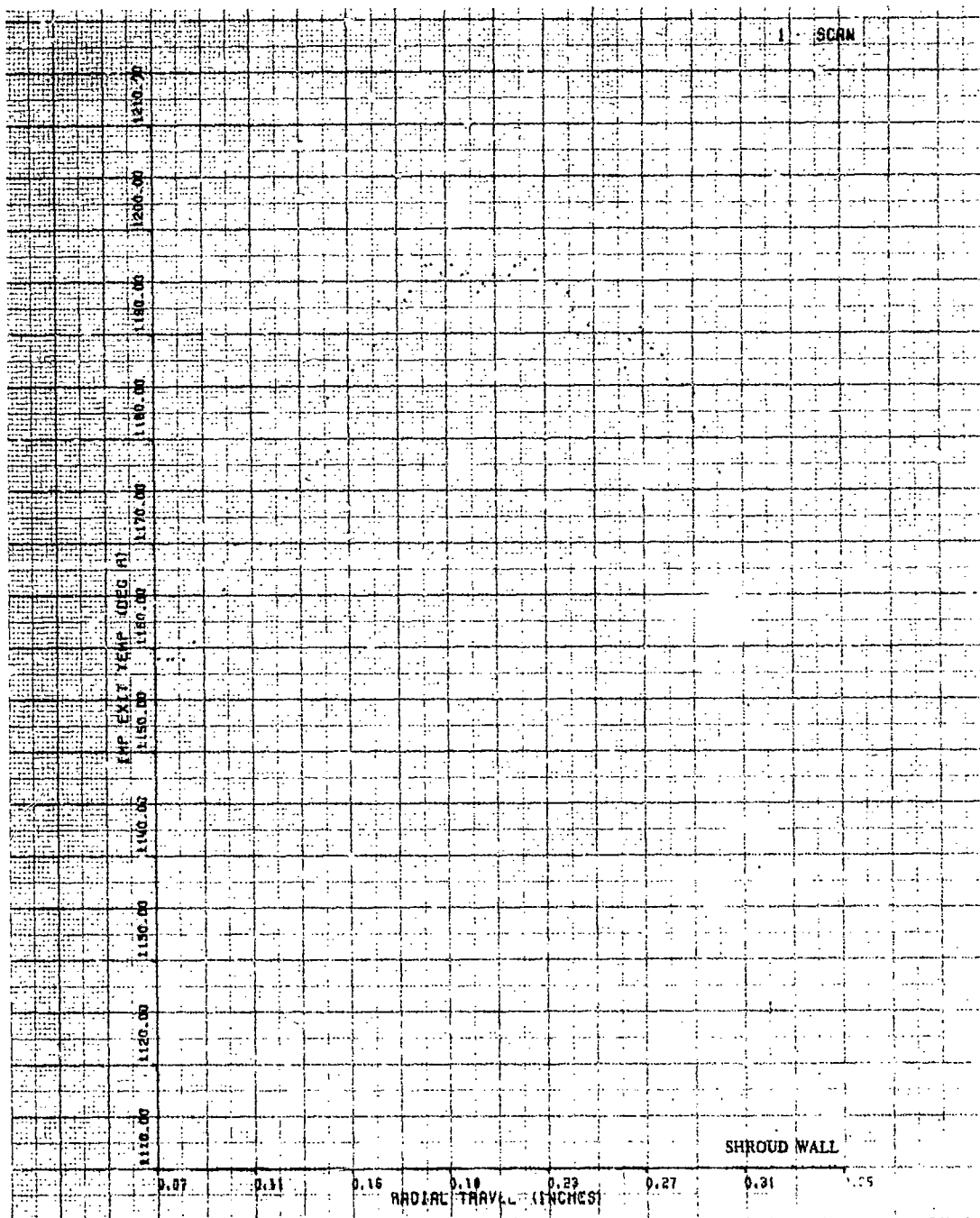


Figure 212. Impeller Exit Temperature Traverse, Build No. 6,  
101% Speed, 0-deg IGV.

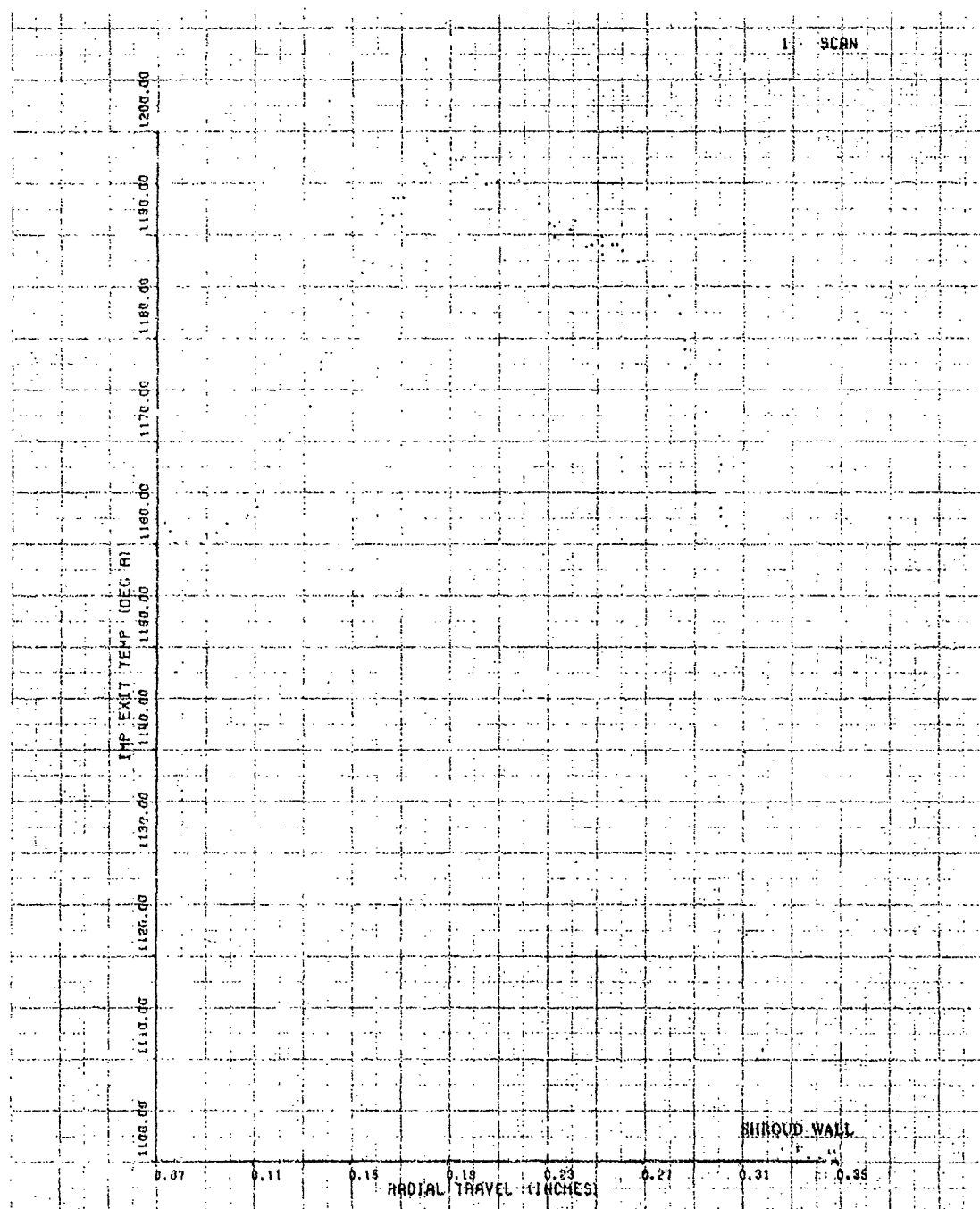


Figure 213. Impeller Exit Traverse With Coolant, Build No. 6,  
101% Speed, -4-deg IGV.

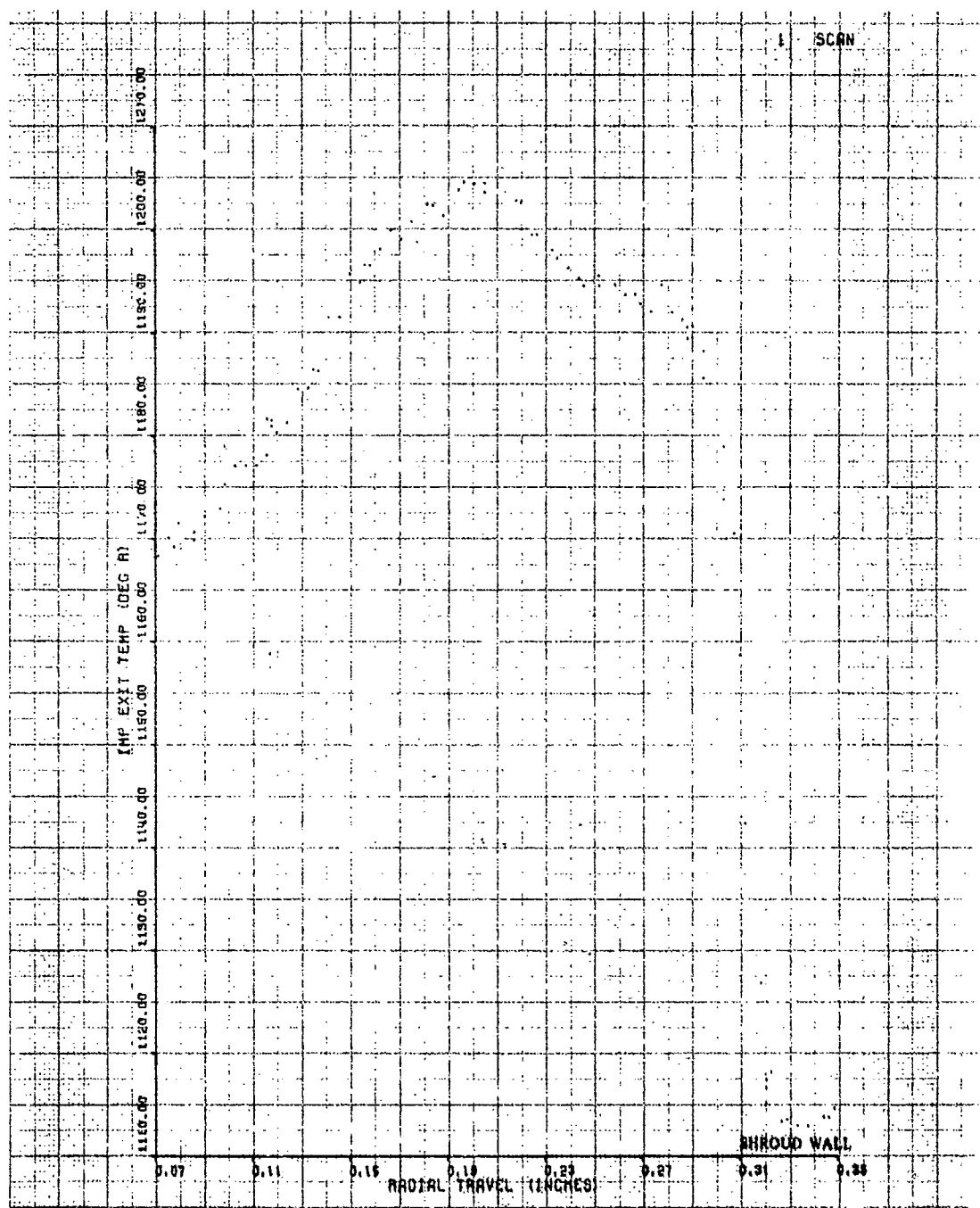


Figure 214. Impeller Exit Traverse With Coolant, Build No. 6,  
101% Speed, -4-deg IGV.

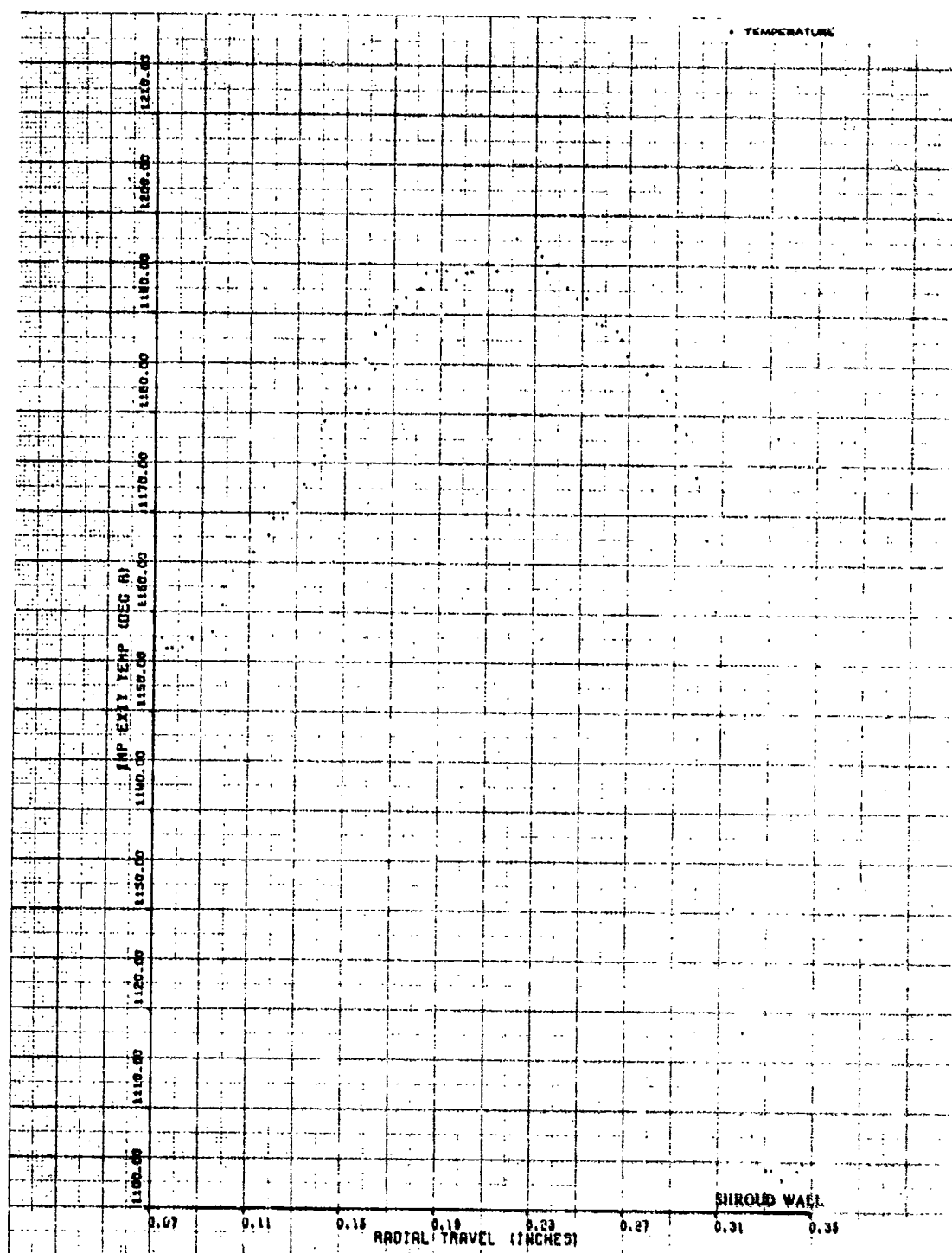


Figure 215. Impeller Exit Temperature Traverse, Build No. 6, 101% Speed, -4-deg IGV.

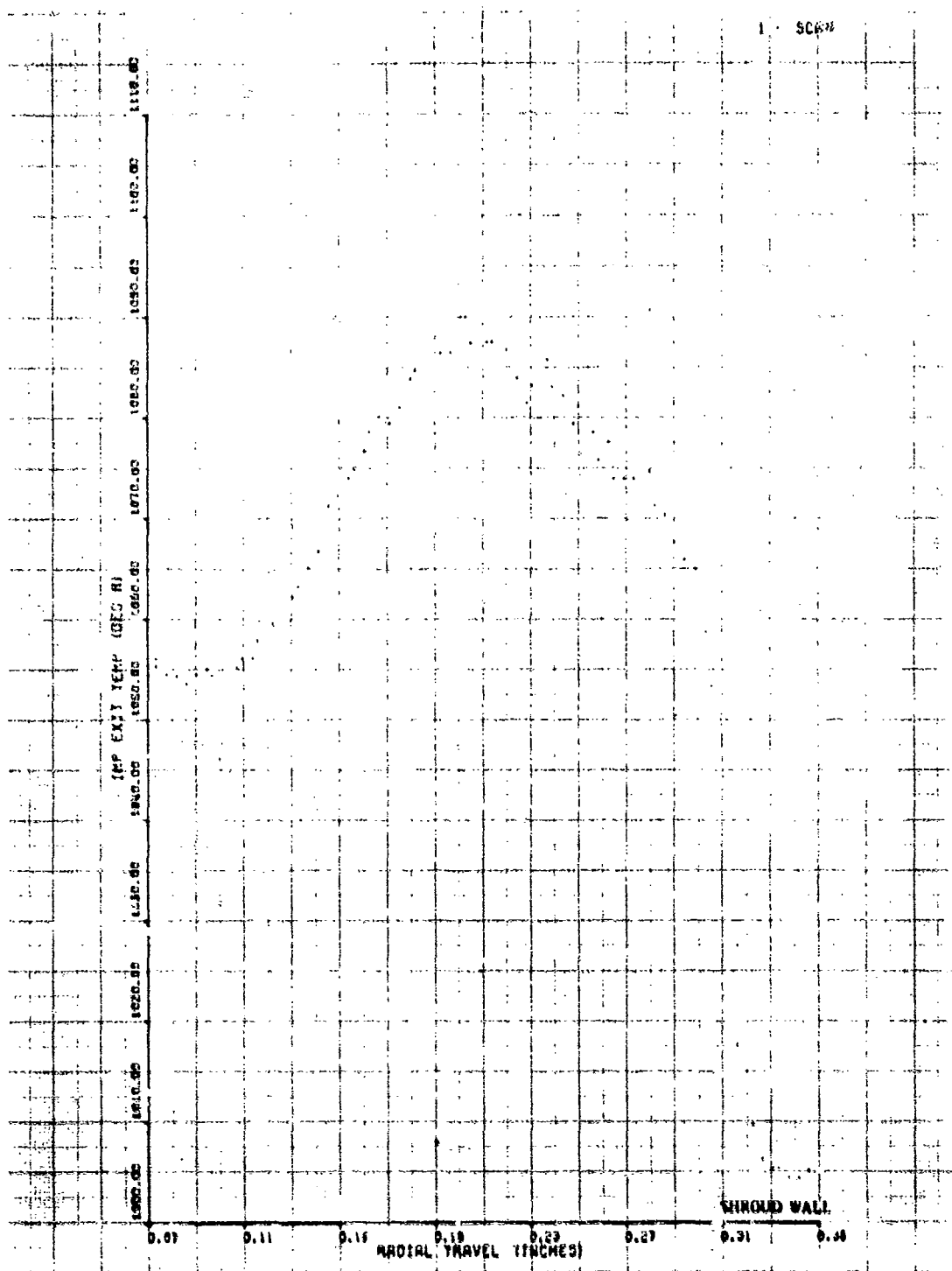


Figure 216. Impeller Exit Temperature Traverse, Build No. 6,  
94.5% Speed, 15-deg IGV.

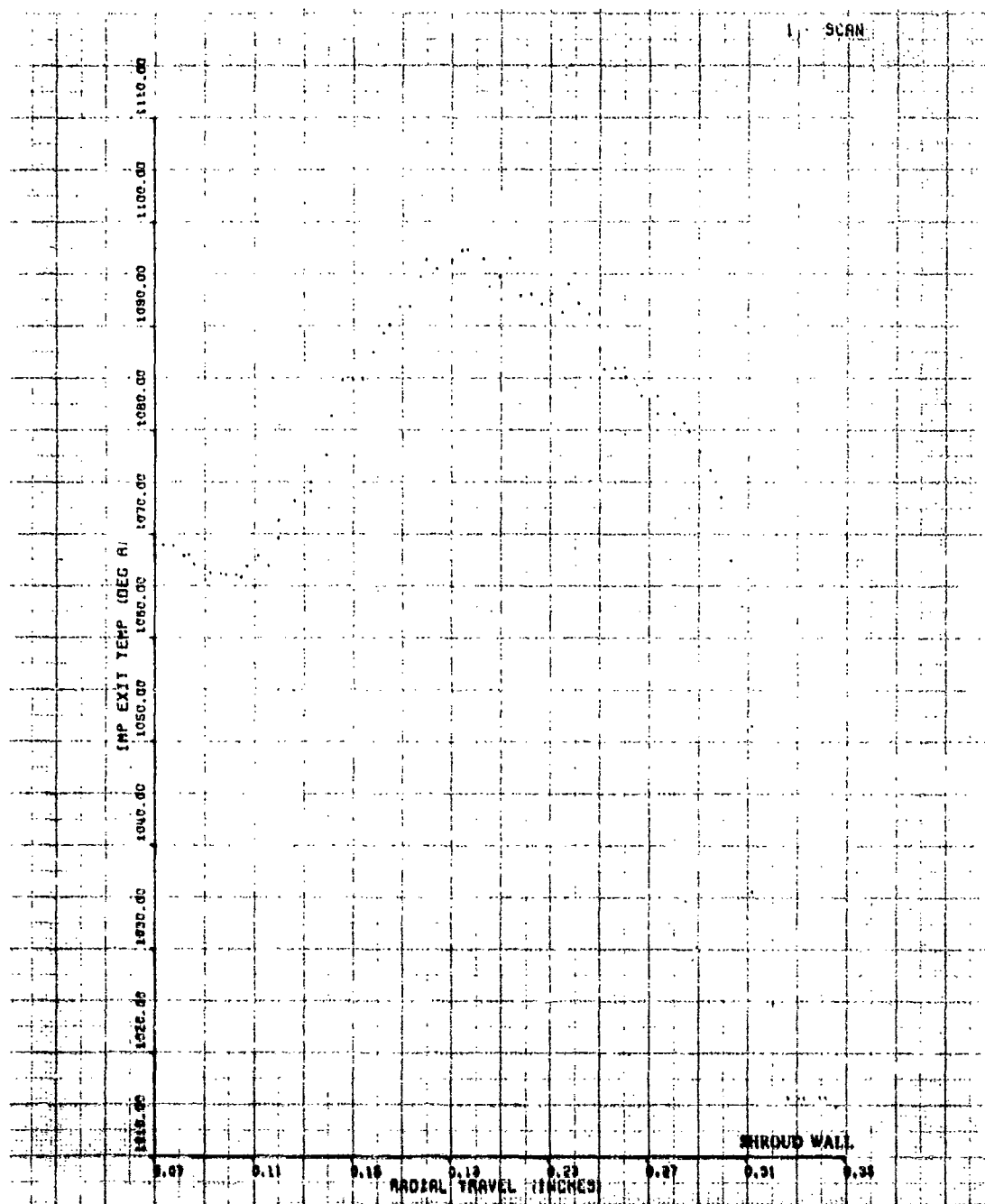


Figure 217. Impeller Exit Temperature Traverse, Build No. 6,  
94.5% Speed, 10-deg IGV.

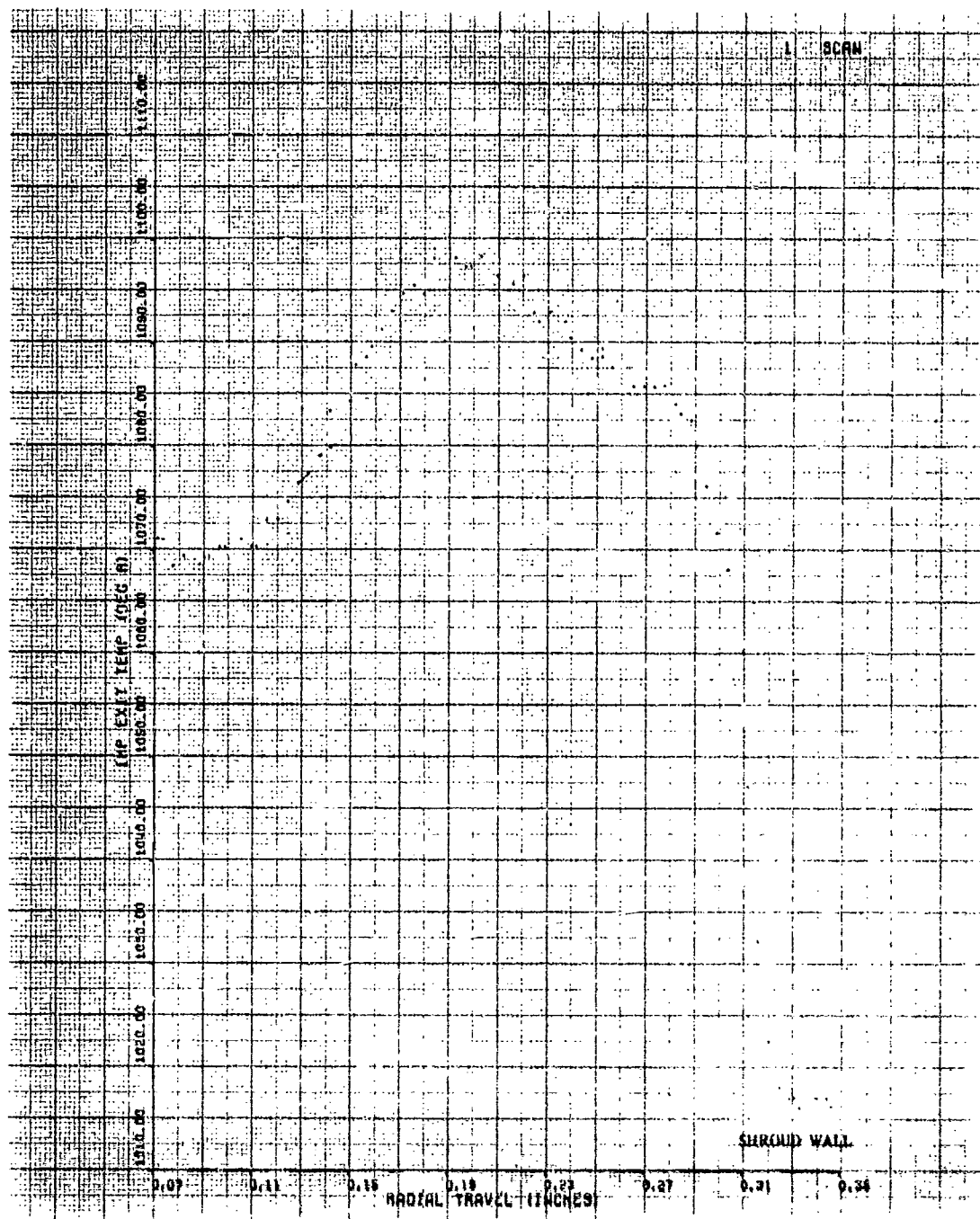


Figure 218. Impeller Exit Temperature Traverse, Build No. 6,  
95% Speed, 10-deg IGV, Wide Open Discharge.



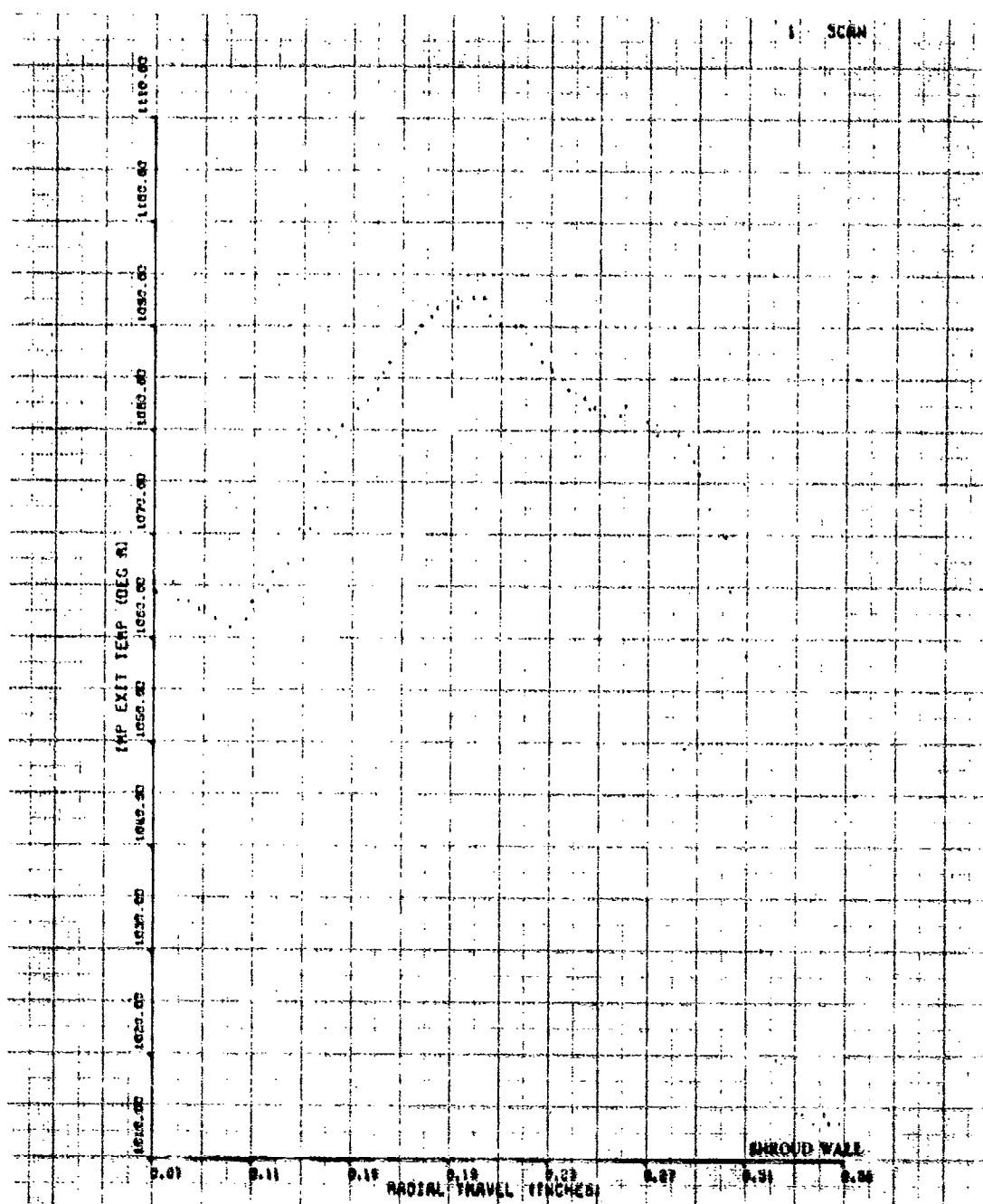


Figure 219. Impeller Exit Temperature Traverse, Build No. 6,  
95% Speed, 10-deg IGV.

### INLET GUIDE VANE PERFORMANCE PRINTOUTS

Summary printouts from the inlet guide vane circumferential traverse data reduction program are shown in Tables XVIII through XXIX for Builds No. 3 and 6. Parameters pertaining to inlet guide vane gaps, including both a strut wake and an inlet guide vane wake, are denoted by an (S), and those parameters pertaining to gaps that include only an inlet guide vane wake are denoted by a (V). Values of these parameters were then weighted, based on the relative number of struts to number of inlet guide vanes, and combined to yield the "weighted" values at each percent span. All other parameters listed in the printout are self-explanatory. A complete discussion of the data reduction procedures can be found in the main body of this report.

TABLE XVIII. INLET GUIDE VANE PERFORMANCE PRINTOUT, 70% SPEED,  
10-DEG IG, NEAR STALL, BUILD NO. 3

CIRCUMFERENTIALLY INTEGRATED QUANTITIES

PERCENT SPAN	6.0674	27.7380	47.4821	67.2579	86.9221
STANT AVG RADIAL TRAVEL	C.06C7	C.2774	C.4748	0.6726	0.8652
VANE AVG RADIAL TRAVEL	C.06C6	C.2775	C.4752	0.6724	0.8691
AVG SUB STATIC PRESS	14.1174	14.1174	14.1174	14.1174	14.1174
AVG SPREAD STATIC PRESS	14.4541	14.4541	14.4541	14.4541	14.4541
SPANWISE STATIC PRESS	14.1418	14.2073	14.2736	14.3405	14.4060
INCREMENTAL FLOW (S)	C.01C8	0.0167	C.0115	0.0145	0.0112
INCREMENTAL FLOW (V)	C.0111	C.0170	0.0118	0.0148	0.0122
MASS AVG PRESS (S)	14.6707	14.6646	14.6488	14.6057	14.5791
MASS AVG PRESS (V)	14.6704	14.6776	14.6587	14.6062	14.5963
MASS AVG ANGLE (S)	75.9365	78.9362	75.2388	78.4661	78.7722
MASS AVG ANGLE (V)	EC.5531	79.6017	75.7161	78.9684	78.2834
WEIGHTED PRESS	14.6702	14.6750	14.6567	14.6061	14.5928
WEIGHTED ANGLE	EC.4297	79.4686	79.6206	78.8680	78.3811
WEIGHTED FLOW	C.011C	C.0169	0.0118	0.0147	0.0120
LOSS COEFFICIENT (S)	G.001567	C.002001	0.003074	0.006008	0.007818
LOSS COEFFICIENT (V)	C.001605	C.001113	0.002405	0.005976	0.006652
WEIGHTED LOSS COEFFICIENT	C.001602	C.001291	C.002539	C.005983	0.006886

TOTAL INTEGRATED QUANTITIES

TOTAL INCREMENTAL FLOW	0.06640
SPANWISE MASS AVG TOTAL PRESS	14.64088
SPANWISE MASS AVG AIR ANGLE	79.02205
TOTAL PRESSURE LOSS	0.00361
INTEGRATED FLOW	1.32801
FLOW COEFFICIENT OF INLET	1.06268
MACH NUMBER IN	0.14435
GUIDE VANE ANGLE	50.7413

TABLE XIX. INLET GUIDE VANE PERFORMANCE PRINTOUT, 90% SPEED,  
10-DEG IGV, NEAR STALL, BUILD NO. 3

CIRCUMFERENTIALLY INTEGRATED QUANTITIES

PERCENT SPAN	18.7715	36.9858	45.2982	63.0581	80.8799
STRUT AVG RADIAL TRAVEL	0.1877	0.1659	0.4530	0.6306	0.6088
VANE AVG RADIAL TRAVEL	0.1882	0.1659	0.4535	0.6305	0.6088
AVG HUB STATIC PRESS	13.2041	13.2041	13.2041	13.2041	13.2041
AVG SHROUD STATIC PRESS	13.3549	13.3549	13.3549	13.3549	13.3549
SPANWISE STATIC PRESS	13.2307	13.2578	13.2714	13.2979	13.3243
INCREMENTAL FLOW (S)	0.0404	0.0007	0.0217	0.0266	0.0398
INCREMENTAL FLOW (V)	0.0422	0.0005	0.0221	0.0250	0.0419
MASS AVG PRESS (S)	14.6328	14.4383	14.6575	14.6156	14.5291
MASS AVG PRESS (V)	14.6767	14.4747	14.6792	14.6370	14.5824
MASS AVG ANGLE (S)	78.0359	82.1828	83.5815	74.8915	82.3076
MASS AVG ANGLE (V)	81.9529	82.4576	83.6800	75.7240	83.7035
WEIGHTED PRESS	14.6679	14.4659	14.6748	14.6327	14.5717
WEIGHTED ANGLE	81.1694	82.8026	83.6402	75.5574	83.4243
WEIGHTED FLOW	0.0418	0.0005	0.0220	0.0254	0.0414
LOSS COEFFICIENT (S)	0.004164	0.004334	0.002486	0.005334	0.011226
LOSS COEFFICIENT (V)	0.001177	0.001311	0.001010	0.003977	0.007598
WEIGHTED LOSS COEFFICIENT	0.001774	0.001916	0.001305	0.004168	0.008324

TOTAL INTEGRATED QUANTITIES

TOTAL INCREMENTAL FLOW	0.13118
SPANWISE MASS AVG TOTAL PRESS	14.63187
SPANWISE MASS AVG AIR ANGLE	79.72418
TOTAL PRESSURE LOSS	0.00423
INTEGRATED FLOW	2.62368
FLOW COEFFICIENT OF INLET	0.97841
MACH NUMBER IN	0.35615
GUIDE VANE ANGLE	96.32941

TABLE XX. INLET GUIDE VANE PERFORMANCE PRINTOUT, 85% SPEED,  
20-DEG IGV, NEAR STALL, BUILD NO. 6

CIRCUMFERENTIALLY INTEGRATED QUANTITIES

PERCENT SPAN	10.0683	30.1750	50.2230	70.3277	90.1872
STAY AVG RADIAL TRAVEL	0.1009	0.3018	0.5022	0.7033	0.9019
VANE AVG RADIAL TRAVEL	C.1008	C.3015	0.5013	0.7026	0.9019
AVG HUB STATIC PRESS	13.6100	13.6100	13.6100	13.6100	13.6100
AVG SHROUD STATIC PRESS	13.6100	13.6100	13.6100	13.6100	13.6100
SPANWISE STATIC PRESS	13.6100	13.6100	13.6100	13.6100	13.6100
INCREMENTAL FLOW (SI)	C.0171	C.0202	0.0210	C.0245	0.0212
INCREMENTAL FLOW (V)	C.0174	C.0205	0.0220	C.0248	0.0224
MASS AVG PRESS (SI)	14.6352	14.6460	14.6545	14.6350	14.4871
MASS AVG PRESS (V)	14.6572	14.6492	14.6826	14.6718	14.5358
MASS AVG ANGLE (SI)	67.6903	68.0322	69.1018	70.2325	75.7120
MASS AVG ANGLE (V)	68.3452	68.6402	69.5150	70.5767	74.2330
WEIGHTED PRESS	14.6506	14.6488	14.6743	14.6607	14.5212
WEIGHTED ANGLE	67.1467	68.4620	69.3910	70.4734	74.6767
WEIGHTED FLOW	C.0173	C.0204	C.0217	C.0247	C.0220
LOSS COEFFICIENT (SI)	0.004001	0.001749	C.002688	0.004018	0.014082
LOSS COEFFICIENT (V)	C.002503	0.001689	C.000761	0.001514	0.010764
WEIGHTED LOSS COEFFICIENT	0.002953	0.001713	0.001339	0.002265	0.011760

TOTAL INTEGRATED QUANTITIES

TOTAL INCREMENTAL FLOW	C.10607
SPANWISE MASS AVG TOTAL PRESS	14.63443
SPANWISE MASS AVG AIR ANGLE	70.30234
TOTAL PRESSURE LOSS	C.00409
INTEGRATED FLOW	2.12135
FLOW COEFFICIENT OF INLET	1.01750
MACH NUMBER IN	0.25409
GUIDE VANE ANGLE	106.94604

TABLE XXI. INLET GUIDE VANE PERFORMANCE PRINTOUT, 85% SPEED,  
30-DEG IGV, NEAR STALL, BUILD NO. 6

CIRCUMFERENTIALLY INTEGRATED QUANTITIES

PERCENT SPAN	10.1117	30.0473	50.1771	70.3378	90.2058
STRTN AVG RADIAL TRAVEL	0.1011	0.3005	0.5018	0.7034	0.9021
VANE AVG RADIAL TRAVEL	0.1003	0.3023	0.5018	0.7034	0.9021
AVG HUB STATIC PRESS	13.1000	13.1000	13.1000	13.1000	13.1000
AVG SHROUD STATIC PRESS	13.1000	13.1000	13.1000	13.1000	13.1000
SPANWISE STATIC PRESS	13.1000	13.1000	13.1000	13.1000	13.1000
INCREMENTAL FLOW (S)	0.0161	0.0197	0.0223	0.0238	0.0211
INCREMENTAL FLOW (V)	0.0163	0.0220	0.0226	0.0274	0.0244
MASS AVG PRESS (S)	14.6005	14.5950	14.5141	14.4904	14.2913
MASS AVG PRESS (V)	14.5927	14.6351	14.5512	14.5608	14.4411
MASS AVG ANGLE (S)	56.6160	56.9463	59.5749	60.6313	71.3820
MASS AVG ANGLE (V)	56.3248	57.9089	60.6805	62.4249	69.0164
WEIGHTED PRESS	14.5931	14.6230	14.5443	14.5397	14.3961
WEIGHTED ANGLE	56.1121	57.6187	60.3348	61.8868	69.7261
WEIGHTED FLOW	0.0163	0.0213	0.0225	0.0263	0.0234
LOSS COEFFICIENT (S)	0.006364	0.006740	0.012240	0.013856	0.027405
LOSS COEFFICIENT (V)	0.006892	0.004010	0.009307	0.009064	0.017214
WEIGHTED LOSS COEFFICIENT	0.006734	0.004829	0.010187	0.010503	0.020271

TOTAL INTEGRATED QUANTITIES

TOTAL INCREMENTAL FLOW	0.11182
SPANWISE MASS AVG TOTAL PRESS	14.53548
SPANWISE MASS AVG AIR ANGLE	61.14932
TOTAL PRESSURE LOSS	0.01079
INTEGRATED FLOW	2.23641
FLOW COEFFICIENT OF INLET	.95170
MACH NUMBER IN	0.27533
GUIDE VANE ANGLE	117.612.0

TABLE XXII. INLET GUIDE VANE PERFORMANCE PRINTOUT, 8/1 SPEED,  
10-DEG IGV, NEAR STALL, BUILD NO. 6

CIRCUMFERENTIALLY INTEGRATED QUANTITIES

PERCENT SPAN	10.0552	30.2590	50.1402	70.3766	90.2529
STRTUT AVG RADIAL TRAVEL	0.1006	0.3026	0.5014	0.7038	0.9025
VANE AVG RADIAL TRAVEL	0.0998	0.3027	0.5022	0.7036	0.9021
AVG HUB STATIC PRESS	12.9410	12.9410	12.9410	12.9410	12.9410
AVG SHROUD STATIC PRESS	12.9410	12.9410	12.9410	12.9410	12.9410
SPANWISE STATIC PRESS	12.9410	12.9410	12.9410	12.9410	12.9410
INCREMENTAL FLOW (S)	0.0221	0.0268	0.0261	0.0318	0.0315
INCREMENTAL FLOW (V)	0.0229	0.0263	0.0276	0.0325	0.0298
MASS AVG PRESS (S)	14.6063	14.6262	14.6315	14.6058	14.4885
MASS AVG PRESS (V)	14.6670	14.6746	14.6679	14.6471	14.4332
MASS AVG ANGLE (S)	77.8664	77.8808	78.3391	78.5037	81.5074
MASS AVG ANGLE (V)	78.1397	78.1188	78.8347	78.9413	82.5757
WEIGHTED PRESS	14.6488	14.6599	14.6570	14.6347	14.4498
WEIGHTED ANGLE	78.0577	78.0474	78.7280	78.8100	82.2551
WEIGHTED FLOW	0.0226	0.0265	0.0271	0.0323	0.0303
LOSS COEFFICIENT (S)	0.005968	0.004611	0.004257	0.006004	0.013985
LOSS COEFFICIENT (V)	0.001834	0.001335	0.001776	0.003139	0.017745
WEIGHTED LOSS COEFFICIENT	0.003074	0.002318	0.002521	0.004034	0.016617

TOTAL INTEGRATED QUANTITIES

TOTAL INCREMENTAL FLOW	0.13892
SPANWISE MASS AVG TOTAL PRESS	14.605185
SPANWISE MASS AVG AIR ANGLE	78.90396
TOTAL PRESSURE LOSS	0.00600
INTEGRATED FLOW	2.77640
FLOW COEFFICIENT OF INLET	0.97114
MACH NUMBER IN	0.39162
GUIDE VANE ANGLE	98.49242

TABLE XXIII. INLET GUIDE VANE PERFORMANCE PRINTOUT, 8/1 SPEED,  
15-DEG ICV, NEAR STALL, BUILD NO. 6

CIRCUMFERENTIALLY INTEGRATED QUANTITIES

PERCENT SPAN	10.0496	30.3265	50.2566	70.4075	90.2598
STRUT AVG RADIAL TRAVEL	0.1001	0.3033	0.5026	0.7041	0.9026
VANE AVG RADIAL TRAVEL	0.1003	0.3035	0.5031	0.7041	0.9027
AVG HUB STATIC PRESS	12.8556	12.8556	12.8556	12.8556	12.8556
AVG SHROUD STATIC PRESS	12.8556	12.8556	12.8556	12.8556	12.8556
SPANWISE STATIC PRESS	12.8556	12.8556	12.8556	12.8556	12.8556
INCREMENTAL FLOW (S)	0.0219	0.0266	0.0267	0.0322	0.0287
INCREMENTAL FLOW (V)	0.0226	0.0261	0.0277	0.0308	0.0297
MASS AVG PRESS (S)	14.5899	14.6359	14.6251	14.6040	14.3389
MASS AVG PRESS (V)	14.6366	14.6714	14.6548	14.6587	14.4054
MASS AVG ANGLE (S)	72.7570	72.9513	73.4628	74.0750	78.5647
MASS AVG ANGLE (V)	73.3160	73.2807	74.2171	74.5319	78.3494
WEIGHTED PRESS	14.6226	14.6607	14.6459	14.6423	14.2855
WEIGHTED ANGLE	73.1483	73.1819	73.9508	74.3948	78.4140
WEIGHTED FLOW	0.0224	0.0262	0.0274	0.0312	0.0294
LOSS COEFFICIENT (S)	0.007086	0.003956	0.004690	0.006124	0.024163
LOSS COEFFICIENT (V)	0.003906	0.001538	0.002665	0.002402	0.019640
WEIGHTED LOSS COEFFICIENT	0.004860	0.002264	0.003273	0.003519	0.020997

TOTAL INTEGRATED QUANTITIES

TOTAL INCREMENTAL FLOW	0.13662
SPANWISE MASS AVG TOTAL PRESS	14.58814
SPANWISE MASS AVG AIR ANGLE	74.48524
TOTAL PRESSURE LOSS	0.00720
INTEGRATED FLOW	2.73239
FLOW COEFFICIENT OF INLET	0.96963
MACH NUMBER IN	0.38997
GUIDE VANE ANGLE	103.82545



TABLE XXIV. INLET GUIDE VANE PERFORMANCE PRINTOUT, 101% SPEED,  
5-DEG IGV, BELOW NEAR STALL, BUILD NO. 6

CIRCUMFERENTIALLY INTEGRATED QUANTITIES

PERCENT SPAN	10.1119	30.2659	50.3228	70.4516	90.2988
STKUT AVG RADIAL TRAVEL	0.1011	0.3027	0.5032	0.7045	0.9030
VANE AVG RADIAL TRAVEL	0.1015	0.3027	0.5032	0.7033	0.9032
AVG HUB STATIC PRESS	12.1371	12.1371	12.1371	12.1371	12.1371
AVG SHROUD STATIC PRESS	12.1371	12.1371	12.1371	12.1371	12.1371
SPANWISE STATIC PRESS	12.1371	12.1371	12.1371	12.1371	12.1371
INCREMENTAL FLOW (S)	0.0268	0.0302	0.0327	0.0359	0.0368
INCREMENTAL FLOW (V)	0.0266	0.0300	0.0379	0.0371	0.0385
MASS AVG PRESS (S)	14.5646	14.5786	14.6200	14.5716	14.5138
MASS AVG PRESS (V)	14.6423	14.6674	14.6250	14.6172	14.4867
MASS AVG ANGLE (S)	85.4214	84.5930	85.0027	85.4967	86.2876
MASS AVG ANGLE (V)	84.9313	84.8281	84.6319	85.1310	87.0897
WEIGHTED PRESS	14.6190	14.6408	14.6235	14.6025	14.4948
WEIGHTED ANGLE	85.0783	84.7576	84.7431	85.2407	86.8490
WEIGHTED FLOW	0.0267	0.0301	0.0364	0.0368	0.0380
LOSS COEFFICIENT (S)	0.00809	0.007851	0.005037	0.008330	0.012265
LOSS COEFFICIENT (V)	0.003518	0.001809	0.004695	0.005226	0.014109
WEIGHTED LOSS COEFFICIENT	0.005105	0.003622	0.004798	0.006157	0.013556

TOTAL INTEGRATED QUANTITIES

TOTAL INCREMENTAL FLOW	0.16786
SPANWISE MASS AVG TOTAL PRESS	14.59239
SPANWISE MASS AVG AIR ANGLE	85.39484
TOTAL PRESSURE LOSS	0.00692
INTEGRATED FLOW	3.35720
FLOW COEFFICIENT OF INLET	0.91697
MACH NUMBER IN	0.45503
GUIDE VANE ANGLE	91.96770

TABLE XXV. INLET GUIDE VANE PERFORMANCE PRINTOUT, 95% SPEED,  
10-DEG IGV, NEAR STALL, BUILD NO. 6

CIRCUMFERENTIALLY INTEGRATED QUANTITIES

PERCENT SPAN	10.1383	30.2356	50.2806	70.3858	90.2598
STRUT AVG RADIAL TRAVEL	0.1014	0.3024	0.5028	0.7039	0.9026
VANE AVG RADIAL TRAVEL	0.1020	0.3023	0.5016	0.7037	0.9024
AVG HUB STATIC PRESS	12.8193	12.8193	12.8193	12.8193	12.8193
AVG SHROUD STATIC PRESS	12.8193	12.8193	12.8193	12.8193	12.8193
SPANWISE STATIC PRESS	12.8193	12.8193	12.8193	12.8193	12.8193
INCREMENTAL FLOW (S)	0.0242	0.0262	0.0282	0.0317	0.0313
INCREMENTAL FLOW (V)	0.0239	0.0268	0.0291	0.0334	0.0307
MASS AVG PRESS (S)	14.6256	14.6206	14.6461	14.6077	14.4051
MASS AVG PRESS (V)	14.6731	14.6716	14.6740	14.6551	14.4139
MASS AVERAGE ANGLE (S)	77.5509	77.8978	77.8740	78.4593	81.4951
MASS AVG ANGLE (V)	77.7449	78.1520	78.1554	78.9947	80.6293
WEIGHTED PRESS	14.6588	14.6563	14.6656	14.6409	14.4112
WEIGHTED ANGLE	77.6866	78.0757	78.0710	78.8340	80.8891
WEIGHTED FLOW	0.0260	0.0266	0.0289	0.0329	0.0309
LOSS COEFFICIENT (S)	0.004657	0.004993	0.003262	0.005872	0.019662
LOSS COEFFICIENT (V)	0.001423	0.001524	0.001360	0.002645	0.019063
WEIGHTED LOSS COEFFICIENT	0.002393	0.002565	0.001931	0.003613	0.019243

TOTAL INTEGRATED QUANTITIES

TOTAL INCREMENTAL FLOW	0.14317
SPANWISE MASS AVG TOTAL PRESS	14.60225
SPANWISE MASS AVG AIR ANGLE	78.73923
TOTAL PRESSURE LOSS	0.00624
INTEGRATED FLOW	2.86339
FLOW COEFFICIENT OF INLET	0.96458
MACH NUMBER IN	0.40224
GUIDE VANE ANGLE	97.09309

TABLE XXVI. INLET GUIDE VANE PERFORMANCE PRINTOUT, 100% SPEED,  
10-DEG IGV, NEAR STALL, BUILD NO. 6

CIRCUMFERENTIALLY INTEGRATED QUANTITIES

PERCENT SPAN	10.1389	30.2170	50.2768	70.4209	90.1630
STRUT AVG RADIAL TRAVEL	0.1014	0.3122	0.5028	0.7042	0.9026
VANE AVG RADIAL TRAVEL	0.1003	0.3018	0.5020	0.7046	0.9022
AVG SHROUD STATIC PRESS	12.4440	12.4440	12.4440	12.4440	12.4440
SPANWISE STATIC PRESS	12.4440	12.4440	12.4440	12.4440	12.4440
INCREMENTAL FLOW (S)	0.0246	0.0294	0.0319	0.0354	0.0362
INCREMENTAL FLOW (V)	0.0239	0.0293	0.0314	0.0355	0.0360
MASS AVG PRESS (S)	14.5350	14.6153	14.6169	14.5801	14.4525
MASS AVG PRESS (V)	14.6720	14.6751	14.6684	14.6332	14.4308
MASS AVG ANGLE (S)	78.7595	78.9085	79.0077	79.6817	82.6728
MASS AVG ANGLE (V)	78.8080	78.9434	79.5941	79.8631	83.2852
WEIGHTED PRESS	14.6459	14.6572	14.6529	14.6172	14.4373
WEIGHTED ANGLE	78.7934	78.9329	79.4182	79.8086	83.1014
WEIGHTED FLOW	0.0241	0.0293	0.0315	0.0355	0.0360
LOSS COEFFICIENT (S)	0.007419	0.005357	0.005250	0.007751	0.016435
LOSS COEFFICIENT (V)	0.001500	0.001283	0.001743	0.004141	0.017910
WEIGHTED LOSS COEFFICIENT	0.003276	0.002505	0.002795	0.005224	0.017468

TOTAL INTEGRATED QUANTITIES

TOTAL INCREMENTAL FLOW	0.15652
SPANWISE MASS AVG TOTAL PRESS	14.59489
SPANWISE MASS AVG AIR ANGLE	79.94775
TOTAL PRESSURE LOSS	0.00674
INTEGRATED FLOW	3.13035
FLOW COEFFICIENT OF INLET	0.95331
MACH NUMBER IN	0.43984
GUIDE VANE ANGLE	96.67302

TABLE XXVII. INLET GUIDE VANE PERFORMANCE PRINTOUT, 101% SPEED,  
-4-DEG IGV, NEAR STALL, BUILD NO. 6

CIRCUMFERENTIALLY INTEGRATED QUANTITIES

PERCENT SPAN	9.8964	30.2122	50.3212	70.3874	90.2370
STRUT AVG RADIAL TRAVEL	0.0990	0.3021	0.5032	0.7039	0.9024
VANE AVG RADIAL TRAVEL	0.0991	0.3007	0.5016	0.7039	0.9016
AVG HUB STATIC PRESS	12.1129	12.1129	12.1129	12.1129	12.1129
AVG SHROUD STATIC PRESS	12.1129	12.1129	12.1129	12.1129	12.1129
SPANWISE STATIC PRESS	12.1129	12.1129	12.1129	12.1129	12.1129
INCREMENTAL FLOW (S)	0.0271	0.0321	0.0326	0.0383	0.0355
INCREMENTAL FLOW (V)	0.0267	0.0318	0.0317	0.0376	0.0360
MASS AVG PRESS (S)	14.6131	14.5628	14.6225	14.5173	14.2661
MASS AVG PRESS (V)	14.6115	14.6120	14.5774	14.5673	14.3767
MASS AVG ANGLE (S)	94.6648	94.4430	94.0580	93.9955	95.0706
MASS AVG ANGLE (V)	94.8274	93.6026	94.1533	93.1720	93.4334
WEIGHTED PRESS	14.6120	14.5973	14.5909	14.5523	14.3435
WEIGHTED ANGLE	94.7786	93.8547	94.1247	93.4190	93.9245
WEIGHTED FLOW	0.0268	0.0319	0.0320	0.0378	0.0359
LOSS COEFFICIENT (S)	0.005506	0.008926	0.004863	0.012022	0.029119
LOSS COEFFICIENT (V)	0.005615	0.005579	0.007935	0.008620	0.021592
WEIGHTED LOSS COEFFICIENT	0.005582	0.006583	0.007014	0.009641	0.023850

TOTAL INTEGRATED QUANTITIES

TOTAL INCREMENTAL FLOW	0.16436
SPANWISE MASS AVG TOTAL PRESS	14.53274
SPANWISE MASS AVG AIR ANGLE	94.43839
TOTAL PRESSURE LOSS	0.01097
INTEGRATED FLOW	3.28720
FLOW COEFFICIENT OF INLET	0.94047
MACH NUMBER IN	0.46587
GUIDE VANE ANGLE	82.89236

TABLE XXVIII. INLET GUIDE VANE PERFORMANCE PRINTOUT, 101% SPEED,  
0-DEG IGV, NEAR STALL, BUILD NO. 6

CIRCUMFERENTIALLY INTEGRATED QUANTITIES

PERCENT SPAN	9.9113	30.1065	50.1109	70.3106	90.1169
STRUT AVG RADIAL TRAVEL	0.0991	0.3011	0.5011	0.7031	0.9012
VANE AVG RADIAL TRAVEL	0.0993	0.3007	0.5013	0.7026	0.9010
AVG HUB STATIC PRESS	12.2522	12.2522	12.2522	12.2522	12.2522
AVG SHROUD STATIC PRESS	12.2522	12.2522	12.2522	12.2522	12.2522
SPANWISE STATIC PRESS	12.2522	12.2522	12.2522	12.2522	12.2522
INCREMENTAL FLOW (S)	0.0250	0.0318	0.0303	0.0370	0.0368
INCREMENTAL FLOW (V)	0.0263	0.0307	0.0314	0.0368	0.0385
MASS AVG PRESS (S)	14.6243	14.5840	14.6544	14.5578	14.4463
MASS AVG PRESS (V)	14.6494	14.6625	14.6495	14.6093	14.5373
MASS AVG ANGLE (S)	90.2377	89.3547	89.1071	89.0439	90.1648
MASS AVG ANGLE (V)	89.8768	88.9055	89.4831	88.6835	89.8621
WEIGHTED PRESS	14.6419	14.6390	14.6509	14.5939	14.5100
WEIGHTED ANGLE	89.9850	89.0402	89.3703	88.7916	89.9529
WEIGHTED FLOW	0.0260	0.0310	0.0311	0.0369	0.0380
LOSS COEFFICIENT (S)	0.004742	0.007488	0.002695	0.009267	0.016858
LOSS COEFFICIENT (V)	0.003038	0.002140	0.003032	0.005761	0.010662
WEIGHTED LOSS COEFFICIENT	0.003549	0.003745	0.002931	0.006813	0.012521

TOTAL INTEGRATED QUANTITIES

TOTAL INCREMENTAL FLOW	0.16290
SPANWISE MASS AVG TOTAL PRESS	14.60144
SPANWISE MASS AVG AIR ANGLE	89.56659
TOTAL PRESSURE LOSS	0.00630
INTEGRATED FLOW	3.25810
FLOW COEFFICIENT OF INLET	0.93972
MACH NUMBER IN	0.46187
GUIDE VANE ANGLE	86.63223

TABLE XXIX. INLET GUIDE VANE PERFORMANCE PRINTOUT, 101% SPEED,  
5-DEG IGV, NEAR STALL, BUILD NO. 6

CIRCUMFERENTIALLY INTEGRATED QUANTITIES

PERCENT SPAN	10.0578	30.2659	50.2744	70.3934	90.2602
STRUT AVG RADIAL TRAVEL	0.1006	0.3027	0.5027	0.7039	0.9026
VANE AVG RADIAL TRAVEL	0.1010	0.3026	0.5029	0.7039	0.9025
AVG HUB STATIC PRESS	12.3762	12.3762	12.3762	12.3762	12.3762
AVG SHROUD STATIC PRESS	12.3762	12.3762	12.3762	12.3762	12.3762
SPANWISE STATIC PRESS	12.3762	12.3762	12.3762	12.3762	12.3762
INCREMENTAL FLOW (S)	0.0247	0.0303	0.0313	0.0365	0.0372
INCREMENTAL FLOW (V)	0.0264	0.0303	0.0317	0.0360	0.0366
MASS AVG PRESS (S)	14.5844	14.6044	14.6155	14.5832	14.5323
MASS AVG PRESS (V)	14.6633	14.6736	14.6579	14.6298	14.5038
MASS AVG ANGLE (S)	83.9771	82.7935	83.0604	83.1970	85.5105
MASS AVG ANGLE (V)	82.9403	82.7175	83.4629	83.1833	85.8735
WEIGHTED PRESS	14.6396	14.6529	14.6452	14.6158	14.5123
WEIGHTED ANGLE	82.9813	82.7403	83.3421	83.1873	85.7646
WEIGHTED FLOW	0.0259	0.0303	0.0315	0.0362	0.0368
LOSS COEFFICIENT (S)	0.007461	0.006097	0.005343	0.007538	0.011008
LOSS COEFFICIENT (V)	0.002089	0.001385	0.002458	0.004372	0.012943
WEIGHTED LOSS COEFFICIENT	0.003701	0.002799	0.003324	0.005322	0.012362

TOTAL INTEGRATED QUANTITIES

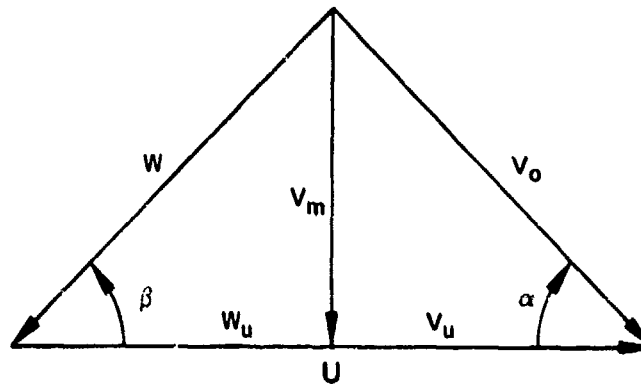
TOTAL INCREMENTAL FLOW	0.16071
SPANWISE MASS AVG TOTAL PRESS	14.60872
SPANWISE MASS AVG AIR ANGLE	83.60435
TOTAL PRESSURE LOSS	0.00580
INTEGRATED FLOW	3.21425
FLOW COEFFICIENT OF INLET	0.94337
MACH NUMBER IN	0.44827
GUIDE VANE ANGLE	92.37350

## TRAVERSE DATA REDUCTION PRINTOUTS

Component performance parameters and velocity triangles calculated from traverse data are presented in Tables XXX through LXXXII for all Builds No. 3 and 6 traverse points. Tables XXX through LIV include all Build No. 3 traverse data reduction printouts, and Tables LV through LXXII include all the Build No. 6 traverse printouts in which the data were reduced following the basic set of assumptions and procedures set forth in the data reduction procedures section of this report. For both builds, tables are arranged in order of increasing speed. Information in the title is self-explanatory, with WOD (wide open discharge), knee, and near stall, referring to the back pressure condition on the speedline.

In Tables LXXIV and LXXV, the inducer exit traverse data were reduced assuming a linear spanwise static pressure distribution instead of a constant static pressure distribution for near-stall points at 100% speed, 10-deg IGV and 101% speed, -4-deg IGV, respectively. All impeller exit traverse data in Tables XXX through LXXV were reduced assuming a constant spanwise total temperature profile equal to the collector total temperature. Tables LXXVI through LXXXII include impeller exit printouts in which the traverse data were reduced using the total temperature profiles obtained from impeller exit total temperature traverses.

Component performance parameters and velocity triangle components are given in the summaries for each traverse station. Velocity triangle components listed in the tables are defined per the following.



Other parameters calculated for each percent span include incidence ( $I$ ), absolute Mach number ( $MO$ ), and relative Mach number ( $MREL$ ).

TABLE XXX.

10/1 CENT COMP, I/P TRAV 30 PCT SP, MDCV, RUN 3.06  
 IGV = 0 DEG  
 FLOW RATE = 0.494 SPEED = 19700.0

*** I-PELLER EXIT ***										INITIAL INTEGRATED FLOW 0.461									
PCT SPAN	R	%O	VO/V MAX	ALP	VM	VM/VM MAX	VU	U	WU	B	WU	WU	WU	WU	WU	WU	WU	WU	WU
0.0169	0.0040	0.2078	0.4074	-5.102	-21.58	-0.0841	241.71	605.62	363.90	33.593	363.90	363.90	363.90	363.90	363.90	363.90	363.90	363.90	363.90
0.0764	0.0180	0.2078	0.4072	0.297	1.25	0.0049	242.55	605.62	363.90	33.744	363.90	363.90	363.90	363.90	363.90	363.90	363.90	363.90	363.90
0.1612	0.0380	0.2242	0.4390	9.697	4.004	0.1717	257.74	605.62	363.90	36.534	363.90	363.90	363.90	363.90	363.90	363.90	363.90	363.90	363.90
0.2461	0.0579	0.2734	0.5339	18.647	101.68	0.3964	301.30	605.62	363.90	44.715	363.90	363.90	363.90	363.90	363.90	363.90	363.90	363.90	363.90
0.3310	0.0779	0.3664	0.7115	25.397	181.75	0.7086	382.81	605.62	363.90	59.799	363.90	363.90	363.90	363.90	363.90	363.90	363.90	363.90	363.90
0.4159	0.0979	0.4457	0.8598	25.197	241.95	0.9433	451.29	605.62	363.90	71.120	363.90	363.90	363.90	363.90	363.90	363.90	363.90	363.90	363.90
0.5008	0.1179	0.4949	0.9503	25.947	256.49	1.0000	504.53	605.62	363.90	82.938	363.90	363.90	363.90	363.90	363.90	363.90	363.90	363.90	363.90
0.5857	0.1379	0.5195	0.9951	25.997	246.68	0.9617	538.86	605.62	363.90	94.314	363.90	363.90	363.90	363.90	363.90	363.90	363.90	363.90	363.90
0.6706	0.1579	0.5485	1.0000	22.347	226.44	0.8828	550.82	605.62	363.90	105.659	363.90	363.90	363.90	363.90	363.90	363.90	363.90	363.90	363.90
0.7555	0.1779	0.5885	0.9748	25.147	195.98	0.7796	545.06	605.62	363.90	117.031	363.90	363.90	363.90	363.90	363.90	363.90	363.90	363.90	363.90
0.8404	0.1979	0.6468	0.8945	18.097	165.48	0.6451	506.37	605.62	363.90	128.631	363.90	363.90	363.90	363.90	363.90	363.90	363.90	363.90	363.90
0.9252	0.2179	0.7173	0.7311	16.097	120.73	0.4707	418.35	605.62	363.90	140.281	363.90	363.90	363.90	363.90	363.90	363.90	363.90	363.90	363.90
0.9838	0.2317	0.7307	0.5857	14.647	85.21	0.3439	337.50	605.62	363.90	151.931	363.90	363.90	363.90	363.90	363.90	363.90	363.90	363.90	363.90

MASS AVERAGE TOTAL PRESSURE 19.836  
 MASS AVERAGE TOTAL TEMPERATURE 568.804  
 MASS AVG VN 103.033 VU 476.284 ANGLE 23.087  
 FLOW FACTOR 0.736 SLIP FACTOR INS. STA. 0.766 I-PELLER TIP 0.824  
 IMP. PRESS. RATIO 0.000 IMP. TEMP. RATIO 0.000 EFFICIENCY 0.300  
 IMP. IND. PRESS. RATIO 1.354 IMP. IND. TEMP. RATIO 1.096 EFFICIENCY 0.942  
 IMP. IND. IGV PRESS. RATIO 1.390 IMP. IND. IGV TEMP. RATIO 1.096 EFFICIENCY 0.930

\*\*\* DIFFUSER \*\*\*

CD DIFFUSER THROAT FRONT 0.808 REAR 0.765  
 STATIC PRESSURE RISE COEFFICIENT I-PELLER EXIT/DIFFUSER EXIT -0.112  
 DIFFUSER THROAT RISE/DIFFUSER EXIT 0.473 DIFFUSER THROAT REAR/DIFFUSER EXIT 0.676  
 DIFFUSER LOSSES TOTAL TO STATIC 0.153 TOTAL TO TOTAL 0.121  
 DIFFUSER LOSS COEFFICIENT 1.112



TABLE XXXI.

10/1 CENTRIFUGAL COMPRESSOR, 1 IMPELLER TRAVERSE 30 PCT SPEED, BELOW NEAR STALL,  
 RUN 3-06  
 ISV SETTING=0 DEG  
 FLOW RATE = 0.302 SPEED = 19420.0

\*\*\* I PELLER EXIT \*\*\* INITIAL INTEGRATED FLOW 0.296

PCT. SPAN	K	%C	VO	VO/VMAX	ALP	VM	VM/VMAX	VU	U	WU	B	WO
0.0109	0.3040	0.2600	280.42	0.2009	-13.774	-50.75	-0.3555	272.35	597.01	324.66	39.993	-103.88
0.0176	0.3180	0.2624	305.59	0.2539	-9.874	-52.40	-0.2790	301.07	597.01	295.74	43.492	-73.48
0.01812	0.3380	0.2734	318.05	0.2682	-3.574	-19.82	-0.1955	317.43	597.01	279.57	48.628	-20.42
0.02461	0.3579	0.2734	317.53	0.2680	3.775	20.93	0.1115	317.25	597.01	279.75	48.594	27.91
0.03310	0.3779	0.3007	349.20	0.6238	12.025	72.75	0.3874	341.53	597.01	255.47	53.202	90.80
0.04159	0.3979	0.3390	392.62	0.7014	19.125	128.64	0.6850	370.95	597.01	228.06	58.641	150.64
0.05308	0.4174	0.3937	454.12	0.8113	22.225	171.77	0.9147	420.38	597.01	176.63	67.239	180.32
0.06706	0.4379	0.4457	511.79	0.9153	21.525	187.75	1.0000	476.09	597.01	120.92	75.748	193.74
0.07555	0.4579	0.4785	547.81	0.9786	14.225	140.34	0.9606	517.24	597.01	79.75	81.234	162.52
0.08404	0.4779	0.4894	559.73	1.0000	16.775	161.55	0.8603	535.91	597.01	61.10	83.695	162.60
0.09252	0.4974	0.4974	535.67	0.9570	14.825	137.07	0.7299	517.83	597.01	79.17	81.306	138.66
0.09830	0.5217	0.4074	498.90	0.8377	13.525	109.67	0.5840	455.90	597.01	141.11	72.801	114.80
	0.5217	0.3261	378.76	0.6786	12.925	84.94	0.4523	370.13	597.01	220.87	58.493	99.63

MASS AVERAGE TOTAL PRESSURE 19.706

MASS AVERAGE TOTAL TEMPERATURE 568.805

MASS AVG VM 165.456 VU 475.229 ANGLE 19.303

FLOW FACTOR 0.555 SLIP FACTOR INS. STA. 0.796

IMP. PRESS. RATIO 0.000 IMP. TEMP. RATIO 0.000

IMP.IND. PRESS. RATIO 1.345 IMP.IND. TEMP. RATIO 1.096

IMP.IND. IC/ PRESS. RATIO 1.341 IMP.IND. ICV TEMP. RATIO 1.096

EFFICIENCY 0.920

EFFICIENCY 0.909

\*\*\* DIFFUSER \*\*\*

CD DIFFUSER THROAT FRONT 0.625 REAR 0.625

STATIC PRESSURE RISE COEFFICIENT IMPELLER EXIT/DIFFUSER EXIT 0.627

DIFFUSER THROAT FRONT/DIFFUSER EXIT 0.668

DIFFUSER LOSSES TOTAL TO STATIC 0.044

DIFFUSER LOSS COEFFICIENT 0.372

TOTAL TO TOTAL 0.021

REAR/DIFFUSER EXIT 0.668

EFFICIENCY 0.920

EFFICIENCY 0.909

EFFICIENCY 0.920

EFFICIENCY 0.909

EFFICIENCY 0.920

EFFICIENCY 0.909

EFFICIENCY 0.920

EFFICIENCY 0.909

EFFICIENCY 0.920

EFFICIENCY 0.909

TABLE XXXII.

10/1 CENTRIFUGAL COMPRESSOR. IMPELLER TRAVERSE 30 PCT SPEED. NEAR STALL. RUN 3-06  
 FLOW SETTING DEG  
 FLOW RATE = 0.233 SPEED = 19537.0

*** IMPELLER EXIT ***									
INITIAL INTEGRATED FLOW 0.223									
PCENT	SPAN	X	NO	VO	VO/VMAX	ALP	VM	VM/VMAX	NO
0.0169	0.0040	0.2898	336.41	0.6020	-15.091	-87.41	-0.4660	325.07	49.714
0.0174	0.0180	0.2898	336.61	0.6020	-11.801	-68.84	-0.3828	329.50	50.523
0.0182	0.0260	0.2863	330.26	0.5906	-6.703	-35.54	-0.2143	328.01	50.270
0.02461	0.0379	0.2789	323.91	0.5793	-0.651	-3.68	-0.0204	327.89	49.491
0.0310	0.0379	0.2843	330.15	0.5904	6.448	38.22	0.2125	327.89	50.236
0.04159	0.0379	0.3117	341.27	0.6481	14.048	87.89	0.4874	350.46	54.483
0.0508	0.1179	0.3609	416.86	0.7435	19.698	140.51	0.7812	392.47	62.061
0.0587	0.1379	0.4183	481.07	0.8603	21.698	176.29	0.9802	447.60	71.127
0.0706	0.1379	0.4568	532.25	0.9519	19.748	179.84	1.0000	500.95	78.748
0.0755	0.1779	0.4894	559.13	1.0000	14.498	154.78	0.8429	536.11	83.140
0.0804	0.1979	0.4939	553.08	0.9891	14.348	137.06	0.7621	535.83	83.107
0.0822	0.2179	0.4320	495.82	0.8867	13.698	115.73	0.6435	482.13	76.193
0.0838	0.2317	0.3836	419.58	0.7554	12.496	92.23	0.5128	409.32	64.921

MASS AVERAGE TOTAL PRESSURE 19.756

MASS AVERAGE TOTAL TEMPERATURE 567.685

FLOW FACTOR 174.800 VU 485.693 ANGLE 19.793

IMP. PRESS. RATIO 0.444 SLIP FACTOR INS. STA. 0.008

IMP. PRESS. RATIO 0.000 IMP. TEMP. RATIO 0.000

IMP. IND. PRESS. RATIO 1.349 IMP. IND. TEMP. RATIO 1.094

IMP. IND. IGV PRESS. RATIO 1.344 IMP. IND. IGV TEMP. RATIO 1.094

EFFICIENCY 0.949

EFFICIENCY 0.938

\*\*\* DIFFUSER \*\*\*

CD DIFFUSER THROAT FRONT 0.546 REAR 0.565

STATIC PRESSURE RISE COEFFICIENT IMPELLER EXIT/DIFFUSER EXIT 0.583

DIFFUSER THROAT FRONT/DIFFUSER EXIT 0.548 DIFFUSER THROAT REAR/DIFFUSER EXIT 0.500

DIFFUSER LOSSES TOTAL TO STATIC 0.054 TOTAL TO TOTAL 0.031

DIFFUSER LOSS COEFFICIENT 0.416

TABLE XXXIII.

10/1 CENTRIFUGAL COMPRESSOR, IMPELLER TRAVERSE 30 PCT SPEED, WDCV, RUN 3.05  
 IGV SETTING=10 DEG  
 FLOW RATE = 0.432 SPEED = 19798.0

INITIAL INTEGRATED FLOW 0.511									
PCTN SPAN	R	NO	VO	VO/VNA	ALP	VN	VN/VMAX	VU	U
0.016	0.0060	0.1093	127.55	0.2120	-12.806	-28.27	-0.1172	124.37	608.63
0.0746	0.0180	0.1312	152.95	0.2562	-8.306	-23.09	-0.0916	151.35	608.63
0.1612	0.0380	0.1367	159.27	0.2667	0.863	2.34	0.0087	159.35	608.63
0.2461	0.0579	0.1804	209.91	0.3489	15.663	56.60	0.2346	202.14	608.63
0.3310	0.0779	0.2734	316.68	0.5263	27.363	145.46	0.4030	281.30	608.63
0.4159	0.0979	0.3691	424.84	0.7061	29.543	212.06	0.5791	368.13	608.63
0.5008	0.1179	0.4637	539.70	0.8671	28.243	241.20	0.7500	449.02	608.63
0.5857	0.1379	0.5503	599.48	0.9465	24.463	235.65	0.9269	518.44	608.63
0.6706	0.1579	0.6249	599.87	0.9804	20.443	212.02	0.9790	556.87	608.63
0.7555	0.1779	0.6804	601.44	1.0000	16.143	187.35	0.7767	571.73	608.63
0.8404	0.1979	0.6285	577.88	0.9804	16.243	161.64	0.6701	554.21	608.63
0.9252	0.2179	0.6367	497.19	0.9263	14.993	128.63	0.5332	480.26	608.63
0.9856	0.2317	0.5617	393.51	0.8360	14.663	98.15	0.4069	381.07	608.63

MASS AVERAGE TOTAL PRESSURE 19.593

MASS AVERAGE TOTAL TEMPERATURE 563.692

FLOW AVG VM 169.579 VU 472.482

SLIP FACTOR INS. STA. 0.776

IMP. PRESS. RATIO 0.000 IMP. TEMP. RATIO 0.000

IMP. IND. PRESS. RATIO 1.338 IMP. IND. TEMP. RATIO 1.086

IMP. IND. IGV PRESS. RATIO 1.333 IMP. IND. IGV TEMP. RATIO 1.086

EFFICIENCY 1.009 EFFICIENCY 0.992

CD DIFFUSER FRONT 0.698 REAR 0.672

STATIC PRESSURE RISE COEFFICIENT IMPELLER EXIT/DIFFUSER EXIT -0.218

DIFFUSER THROAT FRONT/DIFFUSER EXIT 0.476 DIFFUSER THROAT REAR/DIFFUSER EXIT 0.668

DIFFUSER LOSSES TOTAL TO STATIC 0.160 TOTAL TO TOTAL 0.121

DIFFUSER LOSS COEFFICIENT 1.218

LOW CENTRIFUGAL COMPRESSOR, 1" PELLER TRAVERSE 30 DEG SPEED, KNEE, RUN 3.00  
1.00 DETINUED DEG  
FLW. RATE = 0.337 SPEED = 19877.0

[illegible]

TABLE XXXV.

10/1 CENTRIFUGAL COMPRESSOR. IMPELLER TRAVERSE 30 PCT SPEED. BELOW MR 57.  
 10V SETTING=10 DEG  
 FLOW RATE = 3.246  
 SPEED = 19647.0

* * * IMPELLER EXIT * * *									
PC/LN	SPAN	E	MO	WU	WU/MIN	ALP	MR	VM/MIN	U
0.0109	0.0040	0.1812	159.09	0.2139	-0.2816	-21.887	-58.36	162.17	603.99
0.0114	0.0180	0.1816	222.67	0.2583	-0.2339	-17.737	-67.83	212.09	603.99
0.0112	0.0380	0.2301	273.85	0.4763	-0.1736	-10.837	-51.36	268.18	603.99
0.0141	0.0939	0.2806	319.31	0.4832	-0.0331	-2.187	-10.05	279.10	603.99
0.0210	0.0779	0.2826	304.33	0.2237	7.382	7.382	40.05	301.48	603.99
0.0130	0.0870	0.2882	334.07	0.4121	14.312	14.312	99.05	339.81	603.99
0.0200	0.1170	0.2930	437.28	0.7396	21.982	21.982	163.36	405.36	603.99
0.0257	0.1379	0.3066	522.82	0.9089	22.612	22.612	200.71	481.89	603.99
0.0706	0.1579	0.3876	566.78	0.9248	19.812	19.812	190.26	333.89	603.99
0.0753	0.1779	0.3638	575.60	1.0000	19.812	19.812	190.08	333.82	603.99
0.0806	0.1979	0.3812	548.78	0.9236	12.182	12.182	115.82	338.46	603.99
0.0832	0.2179	0.3992	658.16	0.7959	8.482	8.482	75.32	451.93	603.99
0.0886	0.2317	0.2915	291.45	0.5083	8.112	8.112	61.13	288.93	603.99
MASS AVERAGE TOTAL PRESSURE 19.689 MASS AVERAGE TOTAL TEMPERATURE 569.003 MASS AVG MR 186.918 FLOW FACTOR 0.021 IMP. PRESS. RATIO 0.009 IMP.IND. PRESS. RATIO 1.366 IMP.IND. FLOW PRESS. RATIO 1.329									
WU 311.979 SLIP FACTOR 0.008 IMP. TEMP. RATIO 0.000 IMP.IND. TEMP. RATIO 1.089 IMP.IND. FLOW TEMP. RATIO 1.089									
ANGLE 19.783 STA. 0.844 IMPELLER YIP 0.007 EFFICIENCY 0.000 EFFICIENCY 0.993 EFFICIENCY 0.993									

\* \* \* DIFFUSER \* \* \*

CD DIFFUSER THROAT FRONT	0.501	GEAR	0.501
STATIC PRESSURE RISE COEFFICIENT IMPELLER EXIT/DIFFUSER EXIT	0.359		
DIFFUSER THROAT FRONT/DIFFUSER EXIT	0.428	DIFFUSER THROAT REAR/DIFFUSER EXIT	0.433
DIFFUSER LOSSES TOTAL TO STATIC	0.087	TOTAL TO TOTAL	0.080
DIFFUSER LOSS COEFFICIENT	0.044		

TABLE XXXVI.

10/1 CENTRIFUGAL COMPRESSOR, IMPELLER TRAVERSE 30 PCT SPEED, N/S, RUN 3.05  
 IGV SETTING=10 DEG  
 FLOW RATE = 0.223 SPEED = 19422.0

** IMPELLER EXIT **		INITIAL INTEGRATED FLOW 0.262									
PCT SPAN	R	MO	VO	VO/VMAX	ALP	VM	VM/VMAX	VU	U	WU	WO
0.0169	0.0040	0.0874	102.47	0.2490	-16.834	-29.67	-0.1760	98.08	597.07	498.99	-153.87
0.0764	0.0180	0.0874	102.47	0.2490	-13.334	-23.63	-0.1401	99.71	597.07	497.36	-120.23
0.1612	0.0380	0.0874	102.47	0.2490	-8.834	-12.19	-0.0723	101.74	597.07	495.33	-60.60
0.2461	0.0579	0.0874	102.49	0.2491	2.665	4.76	0.0282	102.38	597.07	494.69	23.51
0.3310	0.0779	0.0984	115.24	0.2801	14.465	28.78	0.1707	111.59	597.07	485.48	128.50
0.4159	0.0979	0.1749	204.43	0.4969	23.865	62.70	0.4905	186.95	597.07	410.12	199.40
0.5008	0.1179	0.2734	318.05	0.7730	27.165	145.21	0.8613	282.97	597.07	314.10	216.95
0.5857	0.1379	0.3390	392.82	0.9548	23.415	168.59	1.0000	354.81	597.07	242.26	204.14
0.6706	0.1579	0.3554	411.40	1.0000	21.865	153.21	0.9088	381.81	597.07	215.26	175.89
0.7555	0.1778	0.3554	411.40	1.0000	18.715	132.00	0.7829	389.65	597.07	207.42	169.54
0.8404	0.1979	0.3363	389.66	0.9471	16.265	109.13	0.8473	374.06	597.07	223.01	127.06
0.9252	0.2179	0.2296	267.71	0.6507	14.515	67.10	0.3980	259.17	597.07	337.90	110.25
0.9838	0.2317	0.0437	51.24	0.1245	13.665	12.10	0.0718	49.79	597.07	547.28	133.61

MASS AVERAGE TOTAL PRESSURE 18.172  
 MASS AVERAGE TOTAL TEMPERATURE 571.141  
 MASS AVG VM 136.331 VU 334.721 ANGLE 72.160  
 FLOW FACTOR 0.518 SLIP FACTOR INS. STA. 0.360 IMPELLER TIP 0.587  
 IMP. PRESS. RATIO 0.000 IMP. TEMP. RATIO 0.000 EFFICIENCY 0.000  
 IMP.,IND.,PRESS. RATIO 1.241 IMP.,IND.,TEMP. RATIO 1.101 EFFICIENCY 0.630  
 IMP.,IND.,IGV PRESS. RATIO 1.236 IMP.,IND.,IGV TEMP. RATIO 1.101 EFFICIENCY 0.619

\*\* DIFFUSER \*\*

CD DIFFUSER THROAT FRONT 0.643 REAR 0.625  
 STATIC PRESSURE RISE COEFFICIENT IMPELLER EXIT/DIFFUSER EXIT 0.507  
 DIFFUSER THROAT/DIFFUSER EXIT 0.626 DIFFUSER THROAT REAR/DIFFUSER EXIT 0.656  
 DIFFUSER LOSSES TOTAL TO STATIC 0.029 TOTAL TO TOTAL 0.010  
 DIFFUSER LOSS COEFFICIENT 0.492

TABLE XXXVII.

10/1 CENT COMP, IMP TRAV 30 PCT SP, WDCV, RUN 3.06  
 IGV=20 DEG  
 FLOW RATE = 0.494 SPEED = 19874.0

*** IMPELLER EXIT ***												
PCT SPAN	R	HO	VO	VO/VMAX	ALP	VM	VM/VMAX	VU	U	WU	B	WO
0.0169	0.0040	0.2132	248.21	0.4040	-7.667	-33.11	-0.1307	245.99	610.97	364.97	33.979	-59.25
0.0764	0.0180	0.2351	273.29	0.4449	-1.467	-7.00	-0.0276	273.20	610.97	337.76	38.967	-11.13
0.1612	0.0380	0.2460	285.80	0.4652	8.232	40.92	0.1615	282.86	610.97	328.10	40.764	62.67
0.2461	0.0579	0.2898	335.80	0.5466	18.082	104.22	0.4113	319.22	610.97	291.75	47.574	141.20
0.3310	0.0779	0.3718	428.59	0.6977	25.082	181.68	0.7170	388.17	610.97	222.79	60.146	209.48
0.4159	0.0979	0.4402	504.52	0.8213	27.532	233.21	0.9204	447.38	610.97	163.28	69.915	248.31
0.5008	0.1179	0.5003	570.20	0.9282	26.382	253.37	1.0060	510.81	610.97	100.15	78.900	288.19
0.5857	0.1379	0.5986	611.35	0.9953	24.482	231.42	0.9999	556.42	610.97	54.54	84.400	254.58
0.6706	0.1579	0.5414	614.27	1.0090	22.132	200.45	0.7911	568.01	610.97	41.95	85.782	232.05
0.7555	0.1779	0.5304	602.52	0.9808	19.432	170.79	0.6741	537.37	610.97	42.77	85.694	201.02
0.8404	0.1979	0.4949	563.86	0.9179	17.632	134.04	0.5290	457.42	610.97	73.59	82.201	172.39
0.9252	0.2179	0.4156	476.66	0.7759	16.332	98.69	0.3895	352.72	610.97	153.54	71.444	141.39
0.9838	0.2377	0.3171	366.27	0.5962	15.632					258.24	53.790	122.32

MASS AVERAGE TOTAL PRESSURE 19.771

MASS AVG VM 205.486

SLIP FACTOR 0.733

IMP. PRESS. RATIO 0.000

IMP. IND. PRESS. RATIO 1.350

IMP. IND. IGV PRESS. RATIO 1.345

IMP. IND. IGV TEMP. RATIO 1.090

EFFICIENCY 0.999

EFFICIENCY 0.987

\*\*\* DIFFUSER \*\*\*

CD DIFFUSER THROAT FRONT 0.811

REAR 0.755

STATIC PRESSURE RISE COEFFICIENT IMPELLER EXIT/DIFFUSER EXIT -0.234

DIFFUSER THROAT FRONT/DIFFUSER EXIT 0.402

DIFFUSER THROAT REAR/DIFFUSER EXIT 0.643

DIFFUSER LOSSES TOTAL TO STATIC 0.168

TOTAL TO TOTAL 0.126

DIFFUSER LOSS COEFFICIENT 1.234

TABLE XXXVIII.

10/1 CENT COMP. IMP TRAV 30 PCT SP. BELOW NR ST. RUN 3.06  
 FLOW RATE = 0.358 SPEED = 19912.0

*** I-PELLER EXIT ***			I-INITIAL INTEGRATED FLOW 0.306							
PCT SPAN	R	MO	VO	VO/VMAX	ALP	VM	VM/VMAX	VU	U	WU
0.0169	0.0040	0.2187	254.49	0.4304	-11.332	-50.00	-0.2320	249.52	612.14	362.61
0.0764	0.0180	0.2406	279.65	0.4730	-7.732	-37.62	-0.1746	277.10	612.14	335.03
0.1612	0.0380	0.2734	317.23	0.5366	-1.382	-7.65	-0.0355	317.14	612.14	294.99
0.2461	0.0579	0.2843	329.69	0.5577	6.517	37.42	0.1736	327.56	612.14	284.57
0.3310	0.0779	0.3007	348.35	0.5832	14.867	89.38	0.4148	336.69	612.14	275.44
0.4159	0.0979	0.3499	404.09	0.6835	21.867	150.50	0.6984	375.01	612.14	257.12
0.5008	0.1179	0.4101	471.38	0.7973	24.767	197.47	0.9164	428.80	612.14	184.11
0.5857	0.1379	0.4703	537.84	0.9098	23.617	215.47	1.0000	492.80	612.14	119.34
0.6706	0.1579	0.5113	582.45	0.9852	21.267	211.26	0.9804	542.79	612.14	69.35
0.7555	0.1779	0.5195	591.16	1.0000	18.717	189.70	0.8803	559.89	612.14	52.24
0.8404	0.1979	0.4867	555.61	0.9398	15.817	151.44	0.7728	534.58	612.14	77.56
0.9252	0.2179	0.4101	471.22	0.7971	13.117	106.94	0.4963	458.92	612.14	153.21
0.9838	0.2317	0.3390	391.46	0.6621	11.717	79.49	0.3689	383.30	612.14	228.83

MASS AVERAGE TOTAL PRESSURE 19.678  
 MASS AVERAGE TOTAL TEMPERATURE 567.340  
 MASS AVG VM 180.601 VU 483.062 ANGLE 20.499  
 FLOW FACTOR 0.610 SLIP FACTOR INS. STA. 0.789 IMPPELLER TIP 0.827  
 IMP. PRESS. RATIO 0.000 IMP. TEMP. RATIO 0.000 EFFICIENCY 0.000  
 IMP. IND. PRESS. RATIO 1.343 IMP. IND. TEMP. RATIO 1.093 EFFICIENCY 0.943  
 IMP. IND. IGV PRESS. RATIO 1.339 IMP. IND. IGV TEMP. RATIO 1.093 EFFICIENCY 0.931

\*\*\* DIFFUSER \*\*\*

CD DIFFUSER THROAT FRONT 0.702 REAR 0.689  
 STATIC PRESSURE RISE COEFFICIENT IMPELLER EXIT/DIFFUSER EXIT 0.612  
 DIFFUSER THROAT FRONT/DIFFUSER EXIT 0.656 DIFFUSER THROAT REAR/DIFFUSER EXIT 0.677  
 DIFFUSER LOSSES TOTAL TO STATIC 0.050 TOTAL TO TOTAL 0.033  
 DIFFUSER LOSS COEFFICIENT 0.287



TABLE XXXIX.

10/1 CENT COMP. IAP TRAV 30 PCT SP. NEAR STALL, RUN 3.06  
 IGV=20 DEG  
 FLOW RATE = 0.269 SPEED = 19458.0

I. INITIAL INTEGRATED FLOW 0.239												
PCT SP.	A	NO	VO	VO/V*AX	ALP	VM	VM/VM*AX	VU	U	WU	B	WO
0.0169	0.0040	0.2570	297.99	0.5371	-16.243	-83.35	-0.4623	246.10	598.18	312.08	42.512	-123.35
0.0764	0.0180	0.2789	322.90	0.5821	-12.593	-70.40	-0.3904	313.13	598.18	289.04	48.071	-94.63
0.1612	0.0380	0.2898	335.33	0.6045	-6.593	-38.50	-0.2135	333.12	598.18	265.06	51.490	-49.20
0.2461	0.0579	0.2953	341.54	0.6157	0.456	2.72	0.0150	341.53	598.18	256.64	53.076	3.40
0.3310	0.0779	0.2953	341.54	0.6157	8.306	49.34	0.2736	337.95	598.18	240.22	52.405	62.27
0.4159	0.0979	0.3199	369.19	0.6660	16.306	103.74	0.5753	354.63	598.18	243.55	55.519	123.85
0.5008	0.1179	0.3718	427.99	0.7715	21.306	155.51	0.8625	398.74	598.18	199.44	63.426	173.88
0.5857	0.1379	0.4238	485.81	0.8757	21.706	179.57	0.9965	451.36	598.18	146.82	71.981	188.94
0.6706	0.1579	0.4648	530.83	0.9569	19.856	180.30	1.0000	499.27	598.18	98.90	78.794	183.80
0.7555	0.1779	0.4867	554.62	0.9998	17.506	166.83	0.9233	523.93	598.18	69.24	82.541	168.26
0.8404	0.1979	0.4867	554.72	1.0000	15.456	147.83	0.8199	534.66	598.18	63.52	83.224	148.87
0.9252	0.2179	0.4183	479.62	0.8646	13.806	114.45	0.6348	465.76	598.18	132.41	74.129	118.99
0.9838	0.2317	0.2953	341.30	0.6152	12.956	76.52	0.4244	332.61	598.18	255.56	51.396	97.92

MASS AVERAGE TOTAL PRESSURE 19.557  
 MASS AVERAGE TOTAL TEMPERATURE 565.596  
 MASS AVG V 178.116 VU 479.570 ANGLE 20.375  
 FLOW FACTOR 0.472 SLIP FACTOR I.I.S. STA. 0.801 IMPPELLER TIP 0.840  
 I.P. PRESS. RATIO 0.000 I.P. TEMPERATURE 0.000 EFFICIENCY 0.000  
 I.P.I.D. PRESS. RATIO 1.335 I.P.I.D. TEMP. RATIO 1.090 EFFICIENCY 0.957  
 I.P.I.D.IGV PRESS. RATIO 1.330 I.P.I.D.IGV TEMP. RATIO 1.090 EFFICIENCY 0.945

\*\*\* DIFFUSEX \*\*\*  
 CO DIFFUSEX THROAT FRONT 0.590 REAR 0.614  
 STATIC PRESSURE RISE COEFFICIENT I.P. EXIT/DIFFUSER EXIT 0.556  
 DIFFUSEX THROAT FRONT/DIFFUSER EXIT 0.537 DIFFUSER THROAT REAR/DIFFUSER EXIT 0.479  
 DIFFUSEX LOSSES TOTAL TO STATIC 0.054 TOTAL TO TOTAL 0.034  
 DIFFUSEX LOSS COEFFICIENT 0.443

TABLE XL.

10/1 CENTRIFUGAL COMPRESSOR, IMPELLER TRAVERSE  
70 PCT SPEED, WIDE OPEN DISCHARGE, RUN 3.07  
IGV TURNING= 0 DEG

FLOW RATE = 1.454 SPEED = 45557.0

INITIAL INTEGRATED FLOW 1.049

\*\*\* IMPELLER EXIT \*\*\*

PCT SPAN	R	MO	VO	VO/VMAX	ALP	VM	VM/VMAX	VU	U	WU	B	MO
0.0169	0.0040	0.3281	449.50	0.3407	0.645	5.06	0.0107	449.47	1400.52	951.05	25.295	11.84
0.0251	0.0130	0.6439	857.79	0.6503	3.045	45.56	0.0967	856.58	1400.52	543.94	57.584	53.97
0.0976	0.0230	0.8312	1080.96	0.8192	7.445	140.06	0.2972	1071.85	1400.52	328.67	72.952	146.50
0.1400	0.0329	0.9132	1173.35	0.8895	12.792	259.85	0.5515	1144.21	1400.52	256.31	77.373	266.29
0.1825	0.0429	0.9556	1220.24	0.9250	16.795	352.58	0.7483	1168.19	1400.52	232.33	78.751	359.49
0.2249	0.0529	0.9930	1249.83	0.9475	19.045	407.83	0.8656	1181.41	1400.52	219.11	79.493	414.78
0.2674	0.0629	1.0042	1272.52	0.9647	20.245	460.33	0.9346	1193.90	1400.52	206.62	80.181	466.88
0.3098	0.0729	1.0218	1291.44	0.9790	20.745	457.44	0.9709	1207.71	1400.52	192.81	80.929	463.23
0.3522	0.0829	1.0347	1305.09	0.9894	20.945	466.53	0.9902	1218.85	1400.52	181.67	81.522	471.68
0.3967	0.0929	1.0441	1315.00	0.9969	20.995	471.14	1.0000	1227.70	1400.52	172.82	81.987	475.79
0.4371	0.1030	1.0476	1319.04	1.0000	20.845	469.37	0.9962	1232.71	1400.52	167.81	82.247	473.70
0.4796	0.1129	1.0441	1315.76	0.9975	20.595	462.83	0.9823	1231.67	1400.52	168.85	82.194	467.16
0.5220	0.1229	1.0359	1307.32	0.9911	20.245	452.38	0.9601	1226.56	1400.52	173.96	81.927	456.90
0.5645	0.1329	1.0242	1295.52	0.9821	19.745	437.67	0.9289	1219.35	1400.52	181.17	81.548	442.47
0.6059	0.1429	1.0066	1277.32	0.9683	18.995	415.75	0.8824	1207.76	1400.52	192.76	80.932	421.01
0.6494	0.1529	0.9843	1253.88	0.9505	17.795	383.20	0.8133	1193.89	1400.52	206.63	80.180	388.90
0.6918	0.1629	0.9583	1226.15	0.9295	16.145	340.95	0.7236	1177.79	1400.52	222.73	79.291	347.00
0.7342	0.1729	0.9296	1194.76	0.9057	14.145	291.97	0.6197	1158.53	1400.52	241.99	78.201	298.27
0.7767	0.1829	0.9050	1167.98	0.8854	11.795	238.74	0.5067	1143.32	1400.52	257.20	77.321	244.71
0.8191	0.1929	0.8832	1143.83	0.8671	9.195	182.78	0.3879	1129.13	1400.52	271.39	76.485	187.98
0.8616	0.2029	0.8640	1122.72	0.8511	6.545	127.97	0.2716	1115.40	1400.52	285.12	75.660	132.08
0.9040	0.2129	0.8421	1097.86	0.8323	4.045	77.44	0.1643	1095.12	1400.52	305.40	74.417	80.39
0.9465	0.2229	0.8121	1063.21	0.8060	1.845	34.23	0.0726	1062.66	1400.52	337.86	72.362	35.92
0.9825	0.2314	0.5769	777.80	0.5896	0.545	7.39	0.0157	777.76	1400.52	622.76	51.315	9.47

MASS AVERAGE TOTAL PRESSURE 60.960

MASS AVERAGE TOTAL TEMPERATURE 812.199

MASS AVG VM 388.346 VU 1191.270 ANGLE 18.055

FLOW FACTOR 0.755 SLIP FACTOR INS. STA. 0.850 IMPELLER TIP 0.891

IMP. PRESS. RATIO 0.000 IMP. TEMP. RATIO 0.000 EFFICIENCY 0.000

IMP. IND. PRESS. RATIO 4.163 IMP. IND. TEMP. RATIO 1.565 EFFICIENCY 0.879

IMP. IND. IGV PRESS. RATIO 4.148 IMP. IND. IGV TEMP. RATIO 1.565 EFFICIENCY 0.877

\*\*\* DIFFUSER \*\*\*

TO DIFFUSER THROAT FRONT 0.857 REAR 0.871

STATIC PRESSURE RISE COEFFICIENT IMPELLER EXIT/DIFFUSER EXIT -0.045

DIFFUSER THROAT FRONT/DIFFUSER EXIT -0.224 DIFFUSER THROAT REAR/DIFFUSER EXIT -0.039

DIFFUSER LOSSES TOTAL TO STATIC 0.547 TOTAL TO TOTAL 0.454

DIFFUSER LOSS COEFFICIENT 1.045

TABLE XLI.

10/1 CENTRIFUGAL COMPRESSOR. IMPELLER TRAVERSE  
70 PCT SPEED. BELOW NEAR STALL, RUN 3.07  
IGV TURNING= 0 DEG

FLOW RATE = 1.464 SPEED = 45712.0

INITIAL INTEGRATED FLOW 1.029

IMPELLER EXIT \*\*\*

PCT SPAN	R	MO	VO	VO/VMAX	ALP	VM	VM/VMAX	VU	U	WU	B	WO
0.0169	0.0040	0.2624	361.69	0.2736	2.494	15.74	0.0334	361.34	1405.29	1043.94	19.092	48.12
0.0551	0.0130	0.5796	775.32	0.5896	4.094	55.64	0.1183	777.33	1405.29	627.95	51.067	71.52
0.0976	0.0230	0.8093	1057.93	0.8004	8.144	149.87	0.3186	1047.26	1405.29	358.02	71.126	158.38
0.1400	0.0329	0.9146	1177.39	0.8907	13.294	270.74	0.5756	1145.84	1405.29	259.44	77.241	277.59
0.1825	0.0429	0.9597	1227.21	0.8484	16.844	355.61	0.7561	1174.56	1405.29	230.73	78.886	362.40
0.2249	0.0529	0.9698	1259.59	0.9429	18.844	406.84	0.8650	1192.08	1405.29	213.20	79.859	413.30
0.2674	0.0629	1.0125	1284.02	0.9714	19.994	439.03	0.9335	1206.63	1405.29	198.66	80.650	444.95
0.3098	0.0729	1.0317	1304.04	0.9866	20.594	458.69	0.9753	1220.71	1405.29	184.58	81.401	463.90
0.3522	0.0829	1.0417	1315.10	0.9949	20.794	466.87	0.9927	1229.43	1405.29	175.85	81.859	471.62
0.3927	0.0929	1.0464	1320.25	0.9988	20.844	469.78	0.9988	1233.84	1405.29	171.44	82.089	474.29
0.4371	0.1050	1.0476	1321.73	1.0000	20.844	470.30	1.0000	1235.22	1405.29	170.06	82.160	474.74
0.4766	0.1129	1.0441	1316.44	0.9975	20.844	464.83	0.9883	1233.78	1405.29	171.51	82.085	469.30
0.5220	0.1229	1.0371	1311.45	0.9922	20.844	455.92	0.9694	1229.64	1405.29	175.64	81.870	460.56
0.5645	0.1329	1.0265	1300.73	0.9841	19.844	441.95	0.9388	1223.49	1405.29	181.79	81.548	446.60
0.6089	0.1429	1.0101	1283.61	0.9711	19.044	418.84	0.8905	1213.36	1405.29	191.93	81.011	426.04
0.6494	0.1529	0.9896	1262.10	0.9548	17.994	389.89	0.8290	1200.37	1405.29	204.92	80.312	395.53
0.6916	0.1629	0.9652	1235.94	0.9350	16.444	349.87	0.7439	1185.38	1405.29	219.90	79.490	355.84
0.7342	0.1729	0.9378	1206.31	0.9126	14.994	299.87	0.6376	1168.44	1405.29	236.85	78.541	305.97
0.7767	0.1829	0.9105	1176.66	0.8902	11.944	243.52	0.5177	1151.18	1405.29	254.10	77.552	269.38
0.8191	0.1929	0.8832	1146.34	0.8673	9.244	184.15	0.3915	1131.45	1405.29	273.84	76.394	189.44
0.8616	0.2029	0.8565	1118.64	0.8463	6.394	124.28	0.2644	1111.68	1405.29	293.60	75.205	128.85
0.9040	0.2129	0.8267	1093.57	0.8274	3.844	73.32	0.1559	1091.21	1405.29	316.07	73.942	76.30
0.9465	0.2229	0.8066	1059.44	0.8015	1.994	36.88	0.0783	1058.80	1405.29	346.49	71.879	34.79
0.9884	0.2314	0.7714	772.55	0.5845	0.844	11.38	0.0242	772.47	1405.29	632.82	50.675	14.71

MASS AVERAGE TOTAL PRESSURE 61.060

MASS AVERAGE TOTAL TEMPERATURE 815.582

MASS AVG VM 389.721 VU 1194.779 ANGLE 18.065

FLOW FACTOR 0.760 SLIP FACTOR 145. STA. 0.850 IMPELLER I/P 0.891

IMP. PRESS. RATIO 0.000 IMP. TEMP. RATIO 0.000 EFFICIENCY 0.000

IMP. IND. PRESS. RATIO 4.160 IMP. IND. TEMP. RATIO 1.572 EFFICIENCY 0.870

IMP. IND. TOTAL PRESS. RATIO 0.155 IMP. IND. TOTAL TEMP. RATIO 1.572 EFFICIENCY 0.868

\*\*\* DIFFUSER \*\*\*

CO DIFFUSER THROAT FLOW 0.866 REAR 0.000

STATIC PRESSURE RISE COEFFICIENT IMPELLER EXIT/DIFFUSER EXIT 0.469

DIFFUSER THROAT FLOW/DIFFUSER EXIT 0.378 DIFFUSER THROAT REAR/DIFFUSER EXIT 0.471

DIFFUSER LOSSES TOTAL TO STATIC 0.378 TOTAL TO TOTAL 0.224

DIFFUSER LOSS COEFFICIENT 0.52

100% CENTRIFUGAL COMPRESSORS, IMPELLER INVERSE  
70 PCT SPEED, NEAR STALL, RUN 3-07  
1GV TURNING= 9 DEG  
FLOW RATE = 1.452 SPEED = 65242.0

[illegible]

中華民國二十九年五月十四日

[illegible]

TABLE XLIII.

10/1 CENTRIFUGAL COMPRESSOR, IMPELLEN TRAVERSE  
TO 200 SPEED, WIDE OPEN DISCHARGE, RUN 3.07  
16V TURNING 10 DEG

FLOW RATE = 1.463 SPEED = 45606.0

INITIAL INTEGRATED FLOW 1.037

PERCENT IMPELLER	W	MD	MD	MD/VMAX	ALP	W	W/VMAX	WU	WU	WU	WU	WU
0.0189	0.0040	0.2953	404.75	0.3060	1.066	7.57	0.0161	594.67	1508.18	1003.50	21.962	20.52
0.0331	0.0130	0.5766	776.36	0.5870	3.586	48.56	0.1022	774.84	1408.18	633.33	50.738	42.72
0.0576	0.0320	0.7888	1062.89	0.7885	7.259	142.09	0.2012	1033.03	1408.18	375.15	70.041	52.24
0.1400	0.0829	0.9105	1168.53	0.8823	12.819	256.63	0.4202	1169.00	1408.18	268.17	76.762	243.63
0.1925	0.0929	0.9342	1216.03	0.9107	16.118	338.08	0.7116	1168.51	1408.18	239.67	72.608	363.32
0.2249	0.0929	0.9342	1245.95	0.9420	18.236	382.91	0.8207	1168.37	1408.18	220.80	72.263	398.88
0.1674	0.0929	1.0018	1274.22	0.9394	19.036	429.25	0.9235	1169.74	1408.18	208.43	80.164	435.68
0.3083	0.0729	1.0353	1292.89	0.9713	20.876	452.63	0.9291	1202.93	1408.18	198.25	80.684	441.74
0.3522	0.0729	1.0353	1307.57	0.9816	21.916	470.43	0.9902	1228.81	1408.18	188.16	81.232	470.00
0.4373	0.0929	1.0468	1317.54	0.9961	21.916	475.04	1.0000	1228.81	1408.18	173.77	81.986	478.43
0.4766	0.1129	1.0523	1322.86	0.9954	22.836	470.19	0.9897	1235.40	1408.18	172.77	82.038	474.74
0.5210	0.1229	1.0616	1317.42	0.9924	22.446	460.97	0.9703	1233.82	1408.18	174.36	81.956	463.54
0.5675	0.1229	1.0362	1307.62	0.9887	19.986	446.14	0.9408	1228.86	1408.18	179.31	81.898	451.68
0.6055	0.1029	1.0230	1292.18	0.9770	19.286	426.79	0.8984	1219.66	1408.18	188.52	81.213	431.86
0.6386	0.1029	1.0007	1284.79	0.9593	18.286	398.11	0.8320	1204.72	1408.18	203.46	80.413	403.74
0.6718	0.1229	0.9748	1241.52	0.9387	16.986	352.70	0.7634	1197.23	1408.18	220.82	79.464	388.92
0.7052	0.1429	0.9460	1216.75	0.9154	15.286	319.21	0.6719	1167.91	1408.18	249.26	78.375	323.89
0.7387	0.1629	0.9149	1161.03	0.8929	12.786	261.38	0.5502	1151.74	1408.18	258.43	77.447	267.78
0.7721	0.1829	0.8553	1155.31	0.8735	9.386	188.42	0.4366	1139.84	1408.18	268.23	76.752	193.57
0.8056	0.2029	0.8777	1135.42	0.8568	5.986	138.46	0.3293	1129.62	1408.18	278.55	76.147	122.01
0.8400	0.2229	0.8585	1104.40	0.8426	3.286	63.89	0.2144	1112.56	1408.18	292.61	75.119	64.10
0.8743	0.2429	0.8344	1075.66	0.8192	1.636	26.96	0.0567	1075.22	1408.18	332.95	74.794	28.44
0.9085	0.2629	0.8006	993.43	0.7599	0.536	7.43	0.0156	793.30	1408.18	614.78	52.628	8.44

MASS AVERAGE TOTAL PRESSURE 60.914

MASS AVERAGE TOTAL TEMPERATURE 604.661

MASS AVG W 308.061 WU 1255.834 ANGLE 18.202

FLOW FACTOR 0.753 S. 12 FACTOR INS. STA. 15.648 IMPELLEN JIP 0.8829

IMP. PRESS. RATIO 0.806 IMP. TEMP. RATIO 0.800 EFFICIENCY 0.8829

IMP. IND. PRESS. RATIO 0.140 IMP. IND. TEMP. RATIO 0.559 EFFICIENCY 0.8829

IMP. IND. LOSS COEFFICIENT 0.147

CO. COEFFICIENT 0.147

CO. COEFFICIENT 0.147

CO. COEFFICIENT 0.147

CO. COEFFICIENT 0.147

CO. COEFFICIENT 0.147

CO. COEFFICIENT 0.147

CO. COEFFICIENT 0.147

CO. COEFFICIENT 0.147

CO. COEFFICIENT 0.147

CO. COEFFICIENT 0.147

CO. COEFFICIENT 0.147

CO. COEFFICIENT 0.147

CO. COEFFICIENT 0.147

CO. COEFFICIENT 0.147

CO. COEFFICIENT 0.147

CO. COEFFICIENT 0.147

CO. COEFFICIENT 0.147

CO. COEFFICIENT 0.147

10/1 CENTRIFUGAL COMPRESSOR, IMPELLER TRAVELSE  
TO PCV SPEED, BELOW NEAR STALL, JUN 2007  
ICV TURNING 10 DEG

FLOW RATE = 1.463 SPEED = 5883.0

INITIAL INTEGRATED FLOW 1.056

[illegible]

WEEKS AVERAGE TOTAL PRESSURE 60.400

[illegible][illegible]

CO DIFFUSER WINDWAY FRONT	Q. 0.008
STATIC PRESSURE WIDE COEFFICIENT	
DIFFUSER WINDWAY FRONT DIFFUSION FACT	0.008
DIFFUSION LOSSES	0.008
DIFFUSION LOSS COEFFICIENT	0.008

PC-4 CENTRIFUGAL COMPRESSOR IMPELLER TWENTY  
TO FC1 SPEED. NEAR STALL RUN 307  
1GW TURNING TO DEG

246

Q000 CENTRIFUGAL COMPRESSION, IMP-INT. INVENTS  
Q001 FCT SPEED, WIDE OPEN DISCHARGE, RND BODY  
Q002 TURNING= PE DIE

[illegible]



POOR SCIENTIFIC COMPLIANCE. IMPROVE TAYLOR  
AND PIERCE'S BEHAVIOR NEAR ST. LOUIS BOAT  
BOY TRAINING. PI. DES.

264

TABLE XLVIII.

10/1 CENTRIFUGAL COMPRESSOR, IMPELLER TRAVERSE  
70 PCT SPEED, NEAR STALL, RUN 3.07  
IGV TURNING= 20 DEG

FLOW RATE = 1.458 SPEED = 45913.0

## INITIAL INTEGRATED FLOW 1.057

## \*\*\* IMPELLER EXIT \*\*\*

PCT SPAN	R	MO	VO	VO/VMAX	ALP	VM	VM/VMMAX	VU	U	WU	B	MO
0.0169	0.0040	0.3554	484.59	0.3698	1.344	11.37	0.0242	484.46	1411.47	927.01	27.591	24.55
0.0551	0.0130	0.6453	856.73	0.6539	3.544	52.97	0.1131	855.09	1411.47	556.37	56.949	63.20
0.0976	0.0230	0.8271	1072.70	0.8188	7.744	144.56	0.3086	1062.92	1411.47	348.55	71.844	152.13
0.1400	0.0329	0.9037	1159.11	0.8847	12.344	247.81	0.5291	1132.31	1411.47	279.16	76.150	255.23
0.1825	0.0429	0.9433	1202.83	0.9181	15.894	329.42	0.7034	1156.84	1411.47	254.62	77.586	337.31
0.2249	0.0529	0.9734	1235.54	0.9431	18.494	391.94	0.8368	1171.73	1411.47	239.74	78.436	400.06
0.2674	0.0629	0.9980	1262.06	0.9633	19.944	430.51	0.9192	1186.36	1411.47	225.11	79.255	438.19
0.3098	0.0729	1.0160	1281.07	0.9778	20.994	452.72	0.9666	1198.41	1411.47	213.06	79.918	459.82
0.3522	0.0829	1.0371	1303.48	0.9949	21.944	468.08	0.9994	1208.73	1411.47	202.73	80.478	470.34
0.3947	0.0929	1.0571	1324.48	0.9982	20.994	468.08	0.9994	1208.73	1411.47	194.93	80.896	474.05
0.4371	0.1030	1.0406	1307.14	0.9977	20.994	468.08	0.9994	1208.73	1411.47	191.11	81.099	474.03
0.4796	0.1129	1.0429	1310.08	1.0000	20.994	465.11	0.9931	1224.74	1411.47	186.73	81.331	470.48
0.5220	0.1229	1.0371	1304.24	0.9955	20.944	455.58	0.9727	1222.09	1411.47	189.38	81.191	461.02
0.5645	0.1329	1.0277	1294.71	0.9882	19.944	441.65	0.9430	1217.06	1411.47	194.41	80.924	447.25
0.6069	0.1429	1.0148	1281.44	0.9781	19.194	421.31	0.8996	1210.20	1411.47	201.25	80.557	427.10
0.6494	0.1529	0.9966	1262.51	0.9536	18.194	394.22	0.8417	1199.38	1411.47	212.09	79.971	400.33
0.6918	0.1629	0.9734	1238.01	0.9247	15.944	360.82	0.7704	1184.25	1411.47	227.20	79.139	367.40
0.7342	0.1729	0.9483	1211.52	0.8949	15.244	318.56	0.6802	1168.88	1411.47	242.58	78.275	325.35
0.7767	0.1829	0.9242	1185.08	0.9045	12.994	266.48	0.5690	1154.73	1411.47	256.73	77.465	272.39
0.8191	0.1929	0.8968	1154.83	0.8914	10.244	205.39	0.4385	1136.42	1411.47	275.04	76.394	211.32
0.8616	0.2029	0.8633	1131.03	0.8633	7.094	139.59	0.2982	1122.37	1411.47	299.09	75.556	144.25
0.9040	0.2129	0.8331	1106.39	0.8445	4.244	81.89	0.1748	1103.36	1411.47	308.11	74.397	85.03
0.9465	0.2229	0.8121	1059.51	0.8087	2.244	41.50	0.0886	1058.69	1411.47	352.77	71.571	43.74
0.9825	0.2314	0.5769	774.86	0.5214	1.144	15.48	0.0330	774.71	1411.47	636.76	50.582	24.04

MASS AVERAGE TOTAL PRESSURE 59.796

MASS AVERAGE TOTAL TEMPERATURE 806.000

MASS AVG VM 386.852 VU 1185.619 ANGLE 18.070

FLOW FACTOR 0.768 SLIP FACTOR INS. STA. 0.839 IMPELLER TIP 0.880

IMP. PRESS. RATIO 0.000 IMP. TEMP. RATIO 0.000 EFFICIENCY 0.000

IMP.,IND. PRESS. RATIO 4.083 IMP.,IND. TEMP. RATIO 1.553 EFFICIENCY 0.883

IMP.,IND.,IGV PRESS. RATIO 4.069 IMP.,IND.,IGV TEMP. RATIO 1.553 EFFICIENCY 0.881

\*\*\* DIFFUSER \*\*\*

CD DIFFUSER THROAT FRONT 0.878 REAR 0.888

STATIC PRESSURE RISE COEFFICIENT IMPELLER EXIT/DIFFUSER EXIT 0.603

DIFFUSER THROAT FRONT/DIFFUSER EXIT 0.530 DIFFUSER THROAT REAR/DIFFUSER EXIT 0.601

DIFFUSER LOSSES TOTAL TO STATIC 0.226 TOTAL TO TOTAL 0.155

DIFFUSER LOSS COEFFICIENT 0.396

TABLE XLIX.

10/1 CENTRIFUGAL COMPRESSOR, IMPELLER EXIT TRAVERSE  
90 PSI SPEED, NEAR STALL, RUN 3.08  
IGV TURNING = 0 DEG

FLOW RATE = 2.604      SPEED = 58529.6

\* \* \* INLET GUIDE VANE EXIT \* \* \*

MO	VO	ALPHA	VM	VU	U	WU	B	WO	MREL	I	VO/VO MAX
10	0.380	418.452	90.000	418.452	0.000	868.998	868.997	25.712	964.499	0.876	5.187
30	0.371	409.658	90.000	409.657	0.000	971.233	971.232	22.869	1054.093	0.956	8.030
50	0.366	403.789	90.000	403.789	0.000	1073.468	1073.467	20.614	1136.899	1.040	9.946
70	0.360	397.915	90.000	397.915	0.000	1175.703	1175.702	18.698	1241.215	1.125	10.971
90	0.355	392.036	90.000	392.036	0.000	1277.930	1277.937	17.054	1336.719	1.212	11.095

\* \* \* INDUCER EXIT \* \* \*      INITIAL INTEGRATED FLOW 2.268

MASS AVERAGE TOTAL PRESSURE 24.129  
MASS AVERAGE TOTAL TEMPERATURE 627.447  
INDUCER PRESSURE RATIO 1.642  
INDUCER TEMPERATURE RATIO 1.209  
INDUCER EFFICIENCY 0.725

INDUCER EXIT VELOCITY TRIANGLES

MO	VO	ALPHA	VM	VU	U	WU	B	WO	MREL	I	VO/VO MAX
10	0.576	670.063	50.474	320.846	426.446	926.096	499.649	32.706	592.795	0.511	20.993
30	0.576	673.292	51.821	528.466	416.167	999.399	583.232	42.179	787.042	0.674	7.220
50	0.604	711.078	50.908	551.898	448.372	1072.701	624.325	41.476	833.291	0.708	3.553
70	0.601	720.104	47.902	529.243	428.325	1148.004	657.678	38.824	844.180	0.705	1.375
90	0.609	743.462	34.470	445.780	614.873	1219.306	604.733	36.395	751.280	0.614	-0.745

TABLE XLIX. (Continued)

\*\*\* IMPELLER EXIT \*\*\* INITIAL INTEGRATED FLOW 1.799

PCENT SPAN	R	MO	VO	VO/VMAX	ALP	VM	VM/VMAX	VU	U	WU	B	WO
0.0148	0.0035	0.3773	575.41	0.3302	6.810	68.23	0.1203	571.35	1799.33	1227.98	24.951	161.74
0.0468	0.0114	0.7628	1119.44	0.6424	11.010	213.79	0.3770	1098.83	1799.33	700.50	57.482	253.54
0.0912	0.0214	1.0664	1495.13	0.8580	14.760	380.92	0.6718	1445.79	1799.33	353.54	76.259	392.14
0.1358	0.0319	1.2164	1661.52	0.9535	17.410	497.14	0.8768	1585.40	1799.33	213.92	82.315	501.65
0.1782	0.0419	1.2585	1705.24	0.9786	18.960	534.05	0.9772	1612.72	1799.33	186.61	83.399	557.74
0.2419	0.0569	1.2714	1718.84	0.9864	19.260	550.97	1.0000	1622.64	1799.33	176.69	83.785	570.22
0.3036	0.0719	1.2773	1725.04	0.9900	18.960	550.48	0.9885	1631.45	1799.33	167.88	84.124	563.44
0.3480	0.0820	1.2832	1731.22	0.9935	18.810	558.20	0.9845	1638.76	1799.33	150.57	84.403	560.87
0.3904	0.0919	1.2902	1738.52	0.9977	18.810	560.55	0.9886	1645.67	1799.33	153.66	84.665	562.99
0.4329	0.1019	1.2937	1742.38	1.0000	18.810	561.80	0.9908	1649.32	1799.33	150.01	84.802	564.12
0.4753	0.1120	1.2914	1740.10	0.9986	18.810	561.06	0.9895	1647.16	1799.33	152.17	84.721	563.45
0.5178	0.1219	1.2832	1731.65	0.9938	18.810	558.34	0.9847	1639.17	1799.33	160.16	84.419	561.00
0.5602	0.1319	1.2703	1718.12	0.9860	18.810	553.98	0.9770	1626.35	1799.33	172.97	83.928	557.10
0.6027	0.1419	1.2562	1704.17	0.9780	18.810	549.48	0.9691	1613.16	1799.33	186.17	83.416	553.13
0.6451	0.1519	1.2363	1683.78	0.9663	18.110	523.39	0.9231	1600.37	1799.33	198.96	82.913	527.42
0.6876	0.1620	1.2117	1657.54	0.9513	15.910	424.38	0.8814	1524.05	1799.33	205.28	82.661	458.13
0.7300	0.1719	1.1835	1627.71	0.9341	13.110	369.20	0.6511	1385.28	1799.33	214.05	82.310	272.55
0.7724	0.1819	1.1519	1553.31	0.9144	10.810	298.83	0.5270	1565.03	1799.33	234.30	81.485	302.16
0.8149	0.1920	1.1214	1559.61	0.8951	8.360	226.76	0.3999	1543.03	1799.33	246.29	80.569	223.86
0.8573	0.2019	1.0992	1534.73	0.8808	6.760	180.66	0.3186	1524.06	1799.33	275.27	79.761	183.58
0.8998	0.2119	1.0804	1513.45	0.8686	5.810	153.21	0.2702	1505.87	1799.33	292.65	78.963	154.09
0.9422	0.2220	1.0464	1474.28	0.8461	4.910	126.19	0.2222	1468.87	1799.33	330.46	77.320	129.34
0.9741	0.2294	0.9570	1367.76	0.7849	4.810	114.69	0.2022	1362.94	1799.33	436.38	72.245	120.43
0.9910	0.2334	0.6535	973.18	0.5585	4.810	81.60	0.1439	969.76	1799.33	829.57	49.454	107.39

MASS AVERAGE TOTAL PRESSURE 121.325

MASS AVERAGE TOTAL TEMPERATURE 1010.599

MASS AVG VM 490.723

FLOW FACTOR 0.834

SLIP FACTOR INS. STA. 17.142

IMP. PRESS. RATIO 5.028

IMP. TEMP. RATIO 0.884

IMP. IND. PRESS. RATIO 8.256

IMP. IND. IG/ PRESS. RATIO 8.256

IMP. IND. IG/ TEMP. RATIO 1.948

EFFICIENCY 0.859

EFFICIENCY 0.859

EFFICIENCY 0.859

EFFICIENCY 0.859

EFFICIENCY 0.859

EFFICIENCY 0.859

EFFICIENCY 0.859

EFFICIENCY 0.859

EFFICIENCY 0.859

EFFICIENCY 0.859

EFFICIENCY 0.859

EFFICIENCY 0.859

EFFICIENCY 0.859

EFFICIENCY 0.859

EFFICIENCY 0.859

EFFICIENCY 0.859

EFFICIENCY 0.859

EFFICIENCY 0.859

EFFICIENCY 0.859

EFFICIENCY 0.859

EFFICIENCY 0.859

\*\*\* DIFFUSER \*\*\*

CD DIFFUSER THROAT FRONT 0.957

REAR 0.892

STATIC PRESSURE RISE COEFFICIENT 0.578

IMPELLER EXIT/DIFFUSER EXIT 0.623

DIFFUSER THROAT FRONT/DIFFUSER EXIT 0.578

DIFFUSER THROAT REAR/DIFFUSER EXIT 0.572

DIFFUSER LOSSES TOTAL TO STATIC 0.238

TOTAL TO TOTAL 0.237

DIFFUSER LOSS COEFFICIENT 0.376

TABLE L.

10/1 CENTRIFUGAL COMPRESSOR, IND AND IMP TRAV 8/1 LINE, WIDE OPEN DISCHARGE,  
 RJN 3.09 IGV TURNING=10 DEG SPEED = 61877.0  
 FLOW RATE = 2.898

## \*\*\* INLET GUIDE VANE EXIT \*\*\*

MO	VO	ALPHA	VM	VU	U	WU	B	WO	MREL	I	VO/VOMAX
10	0.451	493.938	60.450	487.092	81.949	918.697	30.204	968.198	0.884	0.695	1.000
30	0.448	491.040	79.450	482.739	89.907	1026.780	27.260	1053.930	0.962	3.639	0.994
50	0.442	485.241	79.600	477.269	87.596	1134.862	24.500	1150.892	1.050	6.059	0.982
70	0.434	476.533	78.850	467.538	92.152	1242.944	22.110	1242.141	1.133	7.559	0.964
90	0.432	473.721	78.620	464.407	93.473	1351.026	20.268	1340.565	1.222	7.881	0.959

## \*\*\* INDUCER EXIT \*\*\*

INITIAL INTEGRATED FLOW 2.879

MASS AVERAGE TOTAL PRESSURE 23.133  
 MASS AVERAGE TOTAL TEMPERATURE 605.739  
 INDUCER PRESSURE RATIO 1.574  
 INDUCER TEMPERATURE RATIO 1.167  
 INDUCER EFFICIENCY 0.826

## INDUCER EXIT VELOCITY TRIANGLES

MO	VO	ALPHA	VM	VU	U	WU	B	WO	MREL	I	VO/VOMAX
10	0.797	893.467	42.474	603.320	659.005	979.061	62.054	682.958	0.609	-8.254	1.000
30	0.782	883.420	42.972	602.182	646.380	1056.556	55.739	728.607	0.644	-6.339	0.988
50	0.741	846.064	43.729	584.841	611.379	1134.031	48.212	784.363	0.686	-3.182	0.946
70	0.735	847.143	43.567	604.926	593.056	1211.546	44.364	865.138	0.751	-4.164	0.948
90	0.661	780.083	39.170	492.722	604.776	1289.041	35.756	843.204	0.715	-0.106	0.873

TABLE L. (Continued)

TABLE L. (Continued)													
*** IMPELLER EXIT ***				INITIAL INTEGRATED FLOW 2.034									
PCLNT	SPAN	R	MO	VO	VO/VMAX	ALP	VM	VM/VMAX	VU	U	WU	B	WU
0.0169	0.0040	0.0040	0.6343	962.17	0.5242	2.192	36.81	0.0558	961.46	1902.24	940.77	45.623	51.50
0.0551	0.0130	0.0130	1.0195	1466.70	0.7992	10.192	259.54	0.3938	1443.55	1902.24	458.68	72.372	272.33
0.0976	0.0230	0.0230	1.2351	1711.63	0.9326	18.692	548.56	0.8324	1621.34	1902.24	230.89	80.171	556.73
0.1400	0.0329	0.0329	1.3265	1806.67	0.9844	21.392	658.99	1.0000	1682.20	1902.24	220.04	82.547	664.61
0.1825	0.0429	0.0429	1.3459	1823.62	0.9936	20.892	650.33	0.9868	1703.71	1902.24	198.52	83.353	654.73
0.2249	0.0529	0.0529	1.3476	1828.17	0.9961	19.792	619.05	0.9393	1720.17	1902.24	182.07	83.958	622.50
0.2674	0.0629	0.0629	1.3488	1829.76	0.9970	18.792	589.44	0.8944	1732.22	1902.24	170.02	84.394	592.28
0.3098	0.0729	0.0729	1.3499	1831.35	0.9978	18.192	571.77	0.8676	1739.81	1902.24	162.43	84.666	574.25
0.3522	0.0829	0.0829	1.3511	1832.03	0.9982	17.992	565.90	0.8587	1742.44	1902.24	159.80	84.760	568.28
0.3947	0.0929	0.0929	1.3535	1836.75	0.9997	18.092	569.79	0.8646	1744.04	1902.24	158.20	84.816	572.13
0.4371	0.1030	0.1030	1.3535	1835.21	1.0000	18.392	579.05	0.8786	1741.46	1902.24	160.77	84.725	581.52
0.4796	0.1129	0.1129	1.3476	1829.08	0.9966	18.592	583.17	0.8849	1733.61	1902.24	168.62	84.444	585.93
0.5220	0.1229	0.1229	1.3371	1818.80	0.9910	18.392	573.88	0.8708	1725.89	1902.24	176.35	84.165	576.86
0.5645	0.1329	0.1329	1.3207	1802.66	0.9822	17.892	553.84	0.8404	1715.48	1902.24	186.76	83.786	557.11
0.6069	0.1429	0.1429	1.2972	1778.44	0.9590	17.192	525.68	0.7977	1698.98	1902.24	203.26	83.177	529.43
0.6494	0.1529	0.1529	1.2726	1753.55	0.9555	16.092	486.07	0.7375	1684.84	1902.24	217.40	82.647	490.09
0.6918	0.1629	0.1629	1.2445	1723.80	0.9392	14.592	434.30	0.6590	1668.20	1902.24	234.04	82.013	438.55
0.7342	0.1729	0.1729	1.2164	1693.59	0.9228	12.892	377.88	0.5734	1650.90	1902.24	251.34	81.343	382.23
0.7767	0.1829	0.1829	1.1882	1662.93	0.9061	10.992	317.09	0.4811	1632.42	1902.24	269.82	80.614	321.39
0.8191	0.1929	0.1929	1.1578	1629.26	0.8877	8.792	249.04	0.3779	1610.11	1902.24	292.13	79.716	253.11
0.8616	0.2029	0.2029	1.1273	1595.06	0.8691	6.592	183.12	0.2778	1584.51	1902.24	317.73	78.661	186.77
0.9040	0.2129	0.2129	1.1308	1599.31	0.8714	4.592	128.05	0.1943	1594.17	1902.24	308.06	79.062	130.42
0.9465	0.2229	0.2229	0.9884	1431.88	0.7802	2.692	67.26	0.1020	1430.30	1902.24	471.93	71.739	70.83
0.9825	0.2314	0.2314	0.5742	878.12	0.4784	1.392	21.34	0.0323	877.86	1902.24	1024.37	40.595	32.79
MASS AVERAGE TOTAL PRESSURE 143.471													
MASS AVERAGE TOTAL TEMPERATURE 1049.316													
MASS AVG VM 527.176													
FLOW FACTOR 0.809													
SLIP FACTOR INS. STA. 17.318													
IMP. PRESS. RATIO 6.201													
IMP. TEMP. RATIO 1.732													
IMP. IND. PRESS. RATIO 9.797													
IMP. IND. TEMP. RATIO 2.022													
IMP. IND. IGV PRESS. RATIO 9.763													
IMP. IND. IGV TEMP. RATIO 2.022													
EFFICIENCY 0.883													
EFFICIENCY 0.881													
*** DIFFUSER ***													
CD DIFFUSER THROAT FRONT 0.889													
REAR 0.889													
STATIC PRESSURE RISE COEFFICIENT IMPELLER EXIT/DIFFUSER EXIT 0.120													
DIFFUSER THROAT FRONT/DIFFUSER EXIT 0.012													
DIFFUSER THROAT REAR/DIFFUSER EXIT 0.013													
DIFFUSER LOSSES TOTAL TO STATIC 0.591													
TOTAL TO TOTAL 0.503													
DIFFUSER LOSS COEFFICIENT 0.879													

TABLE LI.

10/1 CENTRIFUGAL COMPRESSOR, INDUCER TRAVERSE 8/1 LINE, BELOW NEAR STALL, RUN 3.09  
 IGV TURNING=10 DEG  
 FLOW RATE = 2.902 SPEED = 61921.0

## \*\*\* INLET GUIDE VANE EXIT \*\*\*

MO	VO	ALPHA	VM	VU	U	WU	B	WO	MREL	I	VO/VOMAX
10	0.448	490.944	80.450	484.140	81.452	919.351	837.898	30.019	967.712	0.883	0.999
30	0.448	491.040	79.450	482.739	89.907	1027.510	937.602	27.242	1054.579	0.963	1.000
50	0.442	485.241	79.600	477.269	87.596	1135.668	1048.072	24.483	1151.626	1.051	0.988
70	0.437	479.530	78.850	470.479	92.731	1243.827	1151.096	22.230	1243.532	1.134	0.976
90	0.432	473.721	78.620	464.407	93.473	1351.987	1258.513	20.254	1341.466	1.223	0.964

## \*\*\* INDUCER EXIT \*\*\*

INITIAL INTEGRATED FLOW 2.894

MASS AVERAGE TOTAL PRESSURE 23.268  
 MASS AVERAGE TOTAL TEMPERATURE 604.322  
 INDUCER PRESSURE RATIO 1.583  
 INDUCER TEMPERATURE RATIO 1.165  
 INDUCER EFFICIENCY 0.851

## INDUCER EXIT VELOCITY TRIANGLES

MO	VO	ALPHA	VM	VU	U	WU	B	WO	MREL	I	VO/VOMAX
10	0.803	899.789	41.807	599.828	670.691	979.757	309.066	62.739	674.771	0.602	1.000
30	0.782	880.994	42.579	596.091	648.711	1057.307	408.596	55.570	722.686	0.641	0.975
50	0.768	850.630	42.888	578.920	623.235	1134.857	511.622	48.531	772.597	0.678	0.945
70	0.731	843.554	44.548	591.707	601.079	1212.407	611.327	41.80	850.787	0.737	0.937
90	0.657	775.248	38.240	479.854	608.892	1289.957	681.065	35.167	833.132	0.706	0.861

TABLE LI.

10/1 CENTRIFUGAL COMPRESSOR, IMPELLER TRAVERSE  
8/1 LINE, BELOW NEAR STALL, RUN 3.09  
IGV TURNING=10 DEG

FLOW RATE = 2.902 SPEED = 61904.0

## INITIAL INTEGRATED FLOW 2.002

## \*\*\* IMPELLER EXIT \*\*\*

PCT SPAN	R	MO	VO	VO/VMAX	ALP	VM	VM/VMAX	VU	U	WU	B	WO
0.0169	0.0040	0.6480	981.95	0.5349	4.299	73.61	0.1111	979.19	1903.07	923.87	46.655	101.20
0.0551	0.0130	1.0453	1498.21	0.8161	11.899	308.92	0.4666	1466.02	1903.07	437.05	73.399	322.35
0.0976	0.0230	1.2421	1719.74	0.9368	19.199	565.54	0.8542	1624.09	1903.07	278.97	80.293	573.83
0.1400	0.0329	1.3253	1806.41	0.9840	21.499	662.03	1.0000	1680.72	1903.07	222.35	82.463	667.80
0.1825	0.0429	1.3476	1828.62	0.9961	21.099	658.28	0.9943	1706.03	1903.07	197.04	83.411	662.65
0.2249	0.0529	1.3488	1850.21	0.9970	19.899	622.94	0.99409	1720.93	1903.07	182.13	83.958	626.42
0.2674	0.0629	1.3476	1829.53	0.9966	18.999	595.61	0.8996	1729.86	1903.07	173.21	84.282	580.59
0.3098	0.0729	1.3476	1829.53	0.9966	18.399	577.47	0.8722	1736.00	1903.07	167.06	84.503	578.79
0.3522	0.0829	1.3499	1831.80	0.9978	18.199	572.11	0.8641	1740.17	1903.07	162.90	84.652	574.61
0.3947	0.0929	1.3535	1835.66	1.0000	18.299	576.36	0.8706	1742.83	1903.07	160.23	84.747	578.79
0.4371	0.1030	1.3535	1835.66	1.0000	18.599	585.48	0.8843	1739.79	1903.07	163.27	84.638	588.05
0.4796	0.1129	1.3499	1832.26	0.9981	18.799	590.45	0.8918	1734.51	1903.07	168.55	84.449	593.23
0.5220	0.1229	1.3406	1823.13	0.9931	18.699	584.50	0.8828	1726.90	1903.07	176.17	84.175	587.53
0.5645	0.1329	1.3253	1807.73	0.9847	18.199	564.60	0.8528	1717.30	1903.07	185.76	83.826	567.89
0.6069	0.1429	1.3019	1784.01	0.9718	17.299	530.50	0.8013	1703.31	1903.07	199.76	83.310	534.13
0.6494	0.1529	1.2679	1749.18	0.9528	15.999	482.12	0.7282	1681.43	1903.07	221.64	82.490	486.29
0.6918	0.1629	1.2281	1706.71	0.9297	14.399	424.42	0.6410	1653.09	1903.07	249.97	81.401	429.24
0.7342	0.1729	1.1953	1671.61	0.9106	12.599	364.63	0.5507	1631.35	1903.07	271.71	80.543	369.65
0.7767	0.1829	1.1636	1636.38	0.8914	10.299	292.57	0.4419	1610.01	1903.07	293.05	79.683	297.37
0.8191	0.1929	1.1355	1605.21	0.8744	7.799	217.83	0.3290	1590.36	1903.07	312.70	78.876	242.00
0.8616	0.2029	1.1097	1575.85	0.8584	5.299	145.54	0.2198	1569.11	1903.07	333.95	77.984	148.80
0.9040	0.2129	1.0804	1541.79	0.8399	3.399	91.42	0.1380	1539.07	1903.07	363.99	76.693	93.94
0.9465	0.2229	0.9570	1393.74	0.7592	2.399	58.34	0.0881	1392.51	1903.07	510.55	69.865	62.14
0.9825	0.2314	0.6343	964.40	0.5253	1.899	31.96	0.0482	963.86	1903.07	939.20	45.742	44.62

MASS AVERAGE TOTAL PRESSURE 143.401

MASS AVERAGE TOTAL TEMPERATURE 1050.140

MASS AVG VM 593.751 VU 1686.440 ANGLE 17.562

FLOW FACTOR 0.800 SLIP FACTOR INS. STA. 0.886 IMPELLER TIP 0.928

IMP. PRESS. RATIO 0.000 IMP. TEMP. RATIO 0.000 EFFICIENCY 0.000

IMP. IND. PRESS. RATIO 9.793 IMP. IND. TEMP. RATIO 2.024 EFFICIENCY 0.881

IMP. IND. IGV PRESS. RATIO 9.759 IMP. IND. IGV TEMP. RATIO 2.024 EFFICIENCY 0.880

## \*\*\* DIFFUSER \*\*\*

CD DIFFUSER THROAT FRONT 0.891 REAR 0.890

STATIC PRESS. REAR COEFFICIENT IMPELLER EXIT/DIFFUSER EXIT 0.553

DIFFUSER THROAT FRONT/DIFFUSER EXIT 0.498 DIFFUSER THROAT REAR/DIFFUSER EXIT 0.497

DIFFUSER LOSSES TOTAL TO STATIC 0.300 TOTAL TO TOTAL 0.253

DIFFUSER LOSS COEFFICIENT 0.446



TABLE III.

RUN 3.05 10/1 CENTRIFUGAL COMPRESSOR, INDUCER T 8/1 LINE, NEAR STALL,  
IGV TURNING=10 DEG  
FLOW RATE = 2.818 SPEED = 62035.0

\*\*\* INLET GUIDE VANE EXIT \*\*\*

MO	VO	ALPHA	VM	VU	U	WU	B	WO	MREL	I	VO/VUMAX
10	0.432	473.721	80.450	467.155	78.594	921.043	842.448	29.009	963.304	0.878	1.890
30	0.432	473.721	79.450	465.712	86.736	1029.401	942.665	26.291	1051.431	0.958	1.000
50	0.423	464.997	79.600	457.357	83.941	1137.760	1053.518	23.460	1148.786	1.047	0.981
70	0.415	456.351	78.850	447.737	88.249	1246.117	1157.868	21.141	1241.422	1.130	0.963
90	0.410	450.521	78.620	441.664	88.895	1354.476	1265.580	19.238	1340.433	1.220	0.951

\*\*\* INDUCER EXIT \*\*\*

INITIAL INTEGRATED FLOW 2.823

MASS AVERAGE TOTAL PRESSURE 24.553  
MASS AVERAGE TOTAL TEMPERATURE 614.449  
INDUCER PRESSURE RATIO 1.670  
INDUCER TEMPERATURE RATIO 1.184  
INDUCER EFFICIENCY 0.856

INDUCER EXIT VELOCITY TRIANGLES

MO	VO	ALPHA	VM	VU	U	WU	B	WO	MREL	I	VO/VUMAX
10	0.765	865.835	38.641	540.666	676.276	981.561	305.284	60.549	620.902	0.549	1.000
30	0.724	827.332	38.992	520.465	643.112	1059.254	416.141	51.355	666.376	0.583	0.955
50	0.716	825.388	40.639	537.568	626.327	1136.947	510.619	46.472	741.426	0.643	0.953
70	0.705	823.548	39.296	521.578	637.329	1214.639	577.310	42.096	778.030	0.666	0.951
90	0.675	803.224	37.251	486.200	639.358	1292.332	652.974	36.671	814.104	0.684	0.927

TABLE LIV.													
10/1 CENTRIFUGAL COMPRESSOR, IMPELLER TRAV 8/1 LINE, NEAR STALL.													
MUN 3.09													
IGV TURNING=10 DEG													
FLOW RATE = 2.895													
SPEED = 62126.0													
INITIAL INTEGRATED FLOW 2.040													
PCENT	SPAN	B	MO	VO	VO/VMAX	ALP	VN	VN/VMAX	VU	U	MU	B	MO
0.0169	0.0040	0.6535	979.43	0.5311	4.841	82.66	0.1262	975.94	1909.89	933.95	46.259	114.41	
0.0551	0.0130	1.0558	1495.26	0.8108	12.091	313.22	0.4782	1462.09	1909.89	447.80	72.971	327.58	
0.0976	0.0230	1.2656	1727.04	0.9366	18.641	552.05	0.8428	1636.46	1909.89	273.43	80.514	559.70	
0.1400	0.0329	1.3335	1796.94	0.9744	20.891	640.79	0.9783	1678.81	1909.89	231.08	82.162	646.83	
0.1825	0.0429	1.3598	1820.04	0.9870	23.091	656.95	1.0000	1698.11	1909.89	211.78	82.890	660.03	
0.2249	0.0529	1.3593	1823.83	0.9890	19.991	623.53	0.9520	1713.93	1909.89	195.96	83.477	627.59	
0.2674	0.0629	1.3593	1824.76	0.9895	18.991	593.83	0.9066	1725.43	1909.89	184.46	83.897	597.21	
0.3008	0.0729	1.3640	1830.12	0.9924	18.741	572.67	0.8746	1738.15	1909.89	171.74	84.357	575.66	
0.3522	0.0829	1.3699	1836.58	0.9959	17.841	562.70	0.8591	1748.26	1909.89	161.43	84.717	565.10	
0.3967	0.0929	1.3746	1841.93	0.9988	17.941	567.40	0.8663	1752.36	1909.89	157.53	84.863	569.49	
0.4371	0.1030	1.3757	1843.97	1.0000	18.241	577.20	0.8812	1751.30	1909.89	158.59	84.825	579.57	
0.4796	0.1129	1.3734	1842.23	0.9990	18.391	581.24	0.8874	1748.14	1909.89	161.75	84.713	583.72	
0.5220	0.1229	1.3675	1837.63	0.9965	18.241	575.22	0.8782	1745.28	1909.89	164.61	84.611	577.77	
0.5645	0.1329	1.3535	1824.25	0.9893	17.841	558.92	0.8533	1736.51	1909.89	173.38	84.298	561.70	
0.6069	0.1429	1.3289	1800.50	0.9764	17.241	533.67	0.8148	1719.54	1909.89	190.30	83.684	536.92	
0.6496	0.1529	1.3007	1772.87	0.9614	16.341	498.82	0.7616	1701.24	1909.89	208.65	83.007	502.55	
0.6918	0.1629	1.2726	1744.71	0.9461	15.941	449.84	0.6868	1685.72	1909.89	224.17	82.424	453.80	
0.7342	0.1729	1.2437	1716.82	0.9310	15.941	384.49	0.5870	1673.22	1909.89	236.67	81.948	388.32	
0.7767	0.1829	1.2210	1691.34	0.9172	15.941	310.88	0.4746	1662.52	1909.89	247.37	81.537	314.30	
0.8191	0.1929	1.1953	1666.23	0.9025	8.241	238.56	0.3642	1647.04	1909.89	262.85	80.932	241.58	
0.8616	0.2029	1.1718	1639.59	0.8891	5.991	171.14	0.2513	1630.83	1909.89	279.26	80.281	173.63	
0.9040	0.2129	1.1437	1608.73	0.8724	4.241	118.98	0.1816	1604.33	1539.89	305.56	79.216	121.12	
0.9465	0.2229	0.9748	1410.87	0.7651	3.291	81.00	0.1236	1408.54	1909.89	501.35	77.407	85.98	
0.9825	0.2316	0.5984	910.88	0.4939	2.841	45.15	0.0689	909.76	1909.89	1000.13	72.290	67.10	
MASS AVERAGE TOTAL PRESSURE 143.537													
MASS AVERAGE TOTAL TEMPERATURE 1049.316													
MASS AVG VM 528.091													
FLOW FACTOR 0.817													
IMP. PRESS. RATIO 0.000													
IMP.IND. PRESS. RATIO 9.832													
IMP.IND.IGV PRESS. RATIO 9.768													
IMP.IND.IGV TEMP. RATIO 2.022													
IMPELLER TIP EFFICIENCY 0.883													
IMPELLER TIP EFFICIENCY 0.000													
IMPELLER TIP EFFICIENCY 0.882													
CD DIFFUSER THROAT FRONT 0.889													
CD DIFFUSER THROAT REAR 0.888													
STATIC PRESSURE RISE COEFFICIENT IMPELLER EXIT/DIFFUSER EXIT 0.567													
DIFFUSER THROAT FRONT/DIFFUSER EXIT 0.513													
DIFFUSER THROAT REAR/DIFFUSER EXIT 0.512													
DIFFUSER LOSSES TOTAL TO STATIC 0.290													
DIFFUSER LOSSES TOTAL TO TOTAL 0.245													
DIFFUSER LOSS COEFFICIENT 0.432													
CD DIFFUSER * * *													

TABLE LV.

10/1 CENTRIFUGAL COMPRESSOR, IND AND IMP TRAV  
70 PCT SPEED, NEAR STALL, 20 DEG IGV TURNING  
BUILD 6

FLOW RATE = 1.279 SPEED = 45948.9

\*\*\* INDUCER EXIT \*\*\*

INITIAL INTEGRATED FLOW 0.926

MASS AVERAGE TOTAL PRESSURE 18.603  
MASS AVERAGE TOTAL TEMPERATURE 973.003  
INDUCER PRESSURE RATIO 1.284  
INDUCER TEMPERATURE RATIO 1.104  
INDUCER EFFICIENCY 0.657

INDUCER EXIT VELOCITY TRIANGLES

MD	VO	ALPHA	VM	VU	U	KU	Q	WO	MREL	I	VO/VO MAX
10	0.392	416.490	55.283	328.950	248.701	720.667	471.965	37.254	592.956	0.519	16.445
20	0.380	413.942	51.558	324.239	257.351	777.633	520.281	31.929	613.034	0.534	17.470
30	0.344	388.671	41.448	263.769	290.872	834.599	535.926	26.205	597.320	0.516	18.824
40	0.415	483.032	25.821	210.242	434.877	891.365	456.687	24.719	502.758	0.432	15.480
50	0.510	605.971	18.610	193.443	574.265	948.531	374.264	27.332	421.302	0.361	8.317
											1.000

TABLE LV. (Continued)

*** IMPELLER EXIT ***										INITIAL INTEGRATED FLOW 1.039									
CLM	AREA	N	MD	YD	YD	YD	YD	YD	YD	YD	YD	YD	YD	YD	YD	YD	YD	YD	YD
1.0228	0.0055	1.0765	770.00	10.00	10.00	10.00	10.00	10.00	10.00	10.00	10.00	10.00	10.00	10.00	10.00	10.00	10.00	10.00	10.00
1.0048	0.0200	0.7574	10.00	10.00	10.00	10.00	10.00	10.00	10.00	10.00	10.00	10.00	10.00	10.00	10.00	10.00	10.00	10.00	10.00
1.0067	0.0000	0.0000	0.0000	0.0000	0.0000	0.0000	0.0000	0.0000	0.0000	0.0000	0.0000	0.0000	0.0000	0.0000	0.0000	0.0000	0.0000	0.0000	0.0000
1.0340	0.0000	0.0000	0.0000	0.0000	0.0000	0.0000	0.0000	0.0000	0.0000	0.0000	0.0000	0.0000	0.0000	0.0000	0.0000	0.0000	0.0000	0.0000	0.0000
1.0343	0.0000	0.0000	0.0000	0.0000	0.0000	0.0000	0.0000	0.0000	0.0000	0.0000	0.0000	0.0000	0.0000	0.0000	0.0000	0.0000	0.0000	0.0000	0.0000
1.0244	0.0000	0.0000	0.0000	0.0000	0.0000	0.0000	0.0000	0.0000	0.0000	0.0000	0.0000	0.0000	0.0000	0.0000	0.0000	0.0000	0.0000	0.0000	0.0000
1.0058	0.0000	0.0000	0.0000	0.0000	0.0000	0.0000	0.0000	0.0000	0.0000	0.0000	0.0000	0.0000	0.0000	0.0000	0.0000	0.0000	0.0000	0.0000	0.0000
1.0342	0.0000	0.0000	0.0000	0.0000	0.0000	0.0000	0.0000	0.0000	0.0000	0.0000	0.0000	0.0000	0.0000	0.0000	0.0000	0.0000	0.0000	0.0000	0.0000
1.0001	0.0000	0.0000	0.0000	0.0000	0.0000	0.0000	0.0000	0.0000	0.0000	0.0000	0.0000	0.0000	0.0000	0.0000	0.0000	0.0000	0.0000	0.0000	0.0000
1.0041	0.0000	0.0000	0.0000	0.0000	0.0000	0.0000	0.0000	0.0000	0.0000	0.0000	0.0000	0.0000	0.0000	0.0000	0.0000	0.0000	0.0000	0.0000	0.0000
1.0025	0.0000	0.0000	0.0000	0.0000	0.0000	0.0000	0.0000	0.0000	0.0000	0.0000	0.0000	0.0000	0.0000	0.0000	0.0000	0.0000	0.0000	0.0000	0.0000
1.0050	0.0000	0.0000	0.0000	0.0000	0.0000	0.0000	0.0000	0.0000	0.0000	0.0000	0.0000	0.0000	0.0000	0.0000	0.0000	0.0000	0.0000	0.0000	0.0000
MASS AVERAGE TOTAL PRESSURE 57.465																			
MASS AVERAGE TOTAL TEMPERATURE 810.000																			
MASS AVG VM 34.043																			
FLOW FACTOR 0.787																			
IMP. PRESS. RATIO 3.000																			
IMP. IND. PRESS. RATIO 3.010																			
IMP. IND. FLOW PRESS. RATIO 3.010																			
IMP. IND. FLOW PRESS. RATIO 3.010																			
IMP. IND. FLOW PRESS. RATIO 3.010																			
IMP. IND. FLOW PRESS. RATIO 3.010																			
IMP. IND. FLOW PRESS. RATIO 3.010																			
IMP. IND. FLOW PRESS. RATIO 3.010																			
IMP. IND. FLOW PRESS. RATIO 3.010																			
IMP. IND. FLOW PRESS. RATIO 3.010																			
IMP. IND. FLOW PRESS. RATIO 3.010																			
IMP. IND. FLOW PRESS. RATIO 3.010																			
IMP. IND. FLOW PRESS. RATIO 3.010																			
IMP. IND. FLOW PRESS. RATIO 3.010																			
IMP. IND. FLOW PRESS. RATIO 3.010																			
IMP. IND. FLOW PRESS. RATIO 3.010																			
IMP. IND. FLOW PRESS. RATIO 3.010																			
IMP. IND. FLOW PRESS. RATIO 3.010																			
IMP. IND. FLOW PRESS. RATIO 3.010																			
IMP. IND. FLOW PRESS. RATIO 3.010																			
IMP. IND. FLOW PRESS. RATIO 3.010																			
IMP. IND. FLOW PRESS. RATIO 3.010																			
IMP. IND. FLOW PRESS. RATIO 3.010																			
IMP. IND. FLOW PRESS. RATIO 3.010																			
IMP. IND. FLOW PRESS. RATIO 3.010																			
IMP. IND. FLOW PRESS. RATIO 3.010																			
IMP. IND. FLOW PRESS. RATIO 3.010																			
IMP. IND. FLOW PRESS. RATIO 3.010																			
IMP. IND. FLOW PRESS. RATIO 3.010																			
IMP. IND. FLOW PRESS. RATIO 3.010																			
IMP. IND. FLOW PRESS. RATIO 3.010																			
IMP. IND. FLOW PRESS. RATIO 3.010																			
IMP. IND. FLOW PRESS. RATIO 3.010																			
IMP. IND. FLOW PRESS. RATIO 3.010																			
IMP. IND. FLOW PRESS. RATIO 3.010																			
IMP. IND. FLOW PRESS. RATIO 3.010																			
IMP. IND. FLOW PRESS. RATIO 3.010																			
IMP. IND. FLOW PRESS. RATIO 3.010																			
IMP. IND. FLOW PRESS. RATIO 3.010																			
IMP. IND. FLOW PRESS. RATIO 3.010																			
IMP. IND. FLOW PRESS. RATIO 3.010																			
IMP. IND. FLOW PRESS. RATIO 3.010																			
IMP. IND. FLOW PRESS. RATIO 3.010																			
IMP. IND. FLOW PRESS. RATIO 3.010																			
IMP. IND. FLOW PRESS. RATIO 3.010																			
IMP. IND. FLOW PRESS. RATIO 3.010																			
IMP. IND. FLOW PRESS. RATIO 3.010																			
IMP. IND. FLOW PRESS. RATIO 3.010																			
IMP. IND. FLOW PRESS. RATIO 3.010																			
IMP. IND. FLOW PRESS. RATIO 3.010																			
IMP. IND. FLOW PRESS. RATIO 3.010																			
IMP. IND. FLOW PRESS. RATIO 3.010																			
IMP. IND. FLOW PRESS. RATIO 3.010																			
IMP. IND. FLOW PRESS. RATIO 3.010																			
IMP. IND. FLOW PRESS. RATIO 3.010																			
IMP. IND. FLOW PRESS. RATIO 3.010																			
IMP. IND. FLOW PRESS. RATIO 3.010																			
IMP. IND. FLOW PRESS. RATIO 3.010																			
IMP. IND. FLOW PRESS. RATIO 3.010																			
IMP. IND. FLOW PRESS. RATIO 3.010																			
IMP. IND. FLOW PRESS. RATIO 3.010																			
IMP. IND. FLOW PRESS. RATIO 3.010																			
IMP. IND. FLOW PRESS. RATIO 3.010																			
IMP. IND. FLOW PRESS. RATIO 3.010																			
IMP. IND. FLOW PRESS. RATIO 3.010																			
IMP. IND. FLOW PRESS. RATIO 3.010																			
IMP. IND. FLOW PRESS. RATIO 3.010																			
IMP. IND. FLOW PRESS. RATIO 3.010																			
IMP. IND. FLOW PRESS. RATIO 3.010																			
IMP. IND. FLOW PRESS. RATIO 3.010																			
IMP. IND. FLOW PRESS. RATIO 3.010																			
IMP. IND. FLOW PRESS. RATIO 3.010																			
IMP. IND. FLOW PRESS. RATIO 3.010																			
IMP. IND. FLOW PRESS. RATIO 3.010																			
IMP. IND. FLOW PRESS. RATIO 3.010																			
IMP. IND. FLOW PRESS. RATIO 3.010																			
IMP. IND. FLOW PRESS. RATIO 3.010																			
IMP. IND. FLOW PRESS. RATIO 3.010																			
IMP. IND. FLOW PRESS. RATIO 3.010																			
IMP. IND. FLOW PRESS. RATIO 3.010																			
IMP. IND. FLOW PRESS. RATIO 3.010																			
IMP. IND. FLOW PRESS. RATIO 3.010																			
IMP. IND. FLOW PRESS. RATIO 3.010																			
IMP. IND. FLOW PRESS. RATIO 3.010																			
IMP. IND. FLOW PRESS. RATIO 3.010																			
IMP. IND. FLOW PRESS. RATIO 3.010																			
IMP. IND. FLOW PRESS. RATIO 3.010																			
IMP. IND. FLOW PRESS. RATIO 3.010																			
IMP. IND. FLOW PRESS. RATIO 3.010																			
IMP. IND. FLOW PRESS. RATIO 3.010																			
IMP. IND. FLOW PRESS. RATIO 3.010																			
IMP. IND. FLOW PRESS. RATIO 3.010																			
IMP. IND. FLOW PRESS. RATIO 3.010																			
IMP. IND. FLOW PRESS. RATIO 3.010																			
IMP. IND. FLOW PRESS. RATIO 3.010																			
IMP. IND. FLOW PRESS. RATIO 3.0																			

TABLE LVI.

10/1 CENTRIFUGAL COMPRESSOR, 1ND AND 1MP TRAV  
TO 0CT SPEED, NEAR STALL, 90 DEG IGV TURNING  
BUILD 6

FLOW RATE = 1.242      SPEED = 45928.7

\*\*\* INDUCER EXIT \*\*\*      INITIAL INTEGRATED FLOW 0.869

MASS AVERAGE TOTAL PRESSURE 19.442  
MASS AVERAGE TOTAL TEMPERATURE 570.390  
INDUCER PRESSURE RATIO 1.256  
INDUCER TEMPERATURE RATIO 1.099  
INDUCER EFFICIENCY 0.877

INDUCER EXIT VELOCITY TRIANGLES															
WD	VD	ALPHA	PM	WM	WU	U	WU	B	NO	MREL	I	VO/VOHAX			
10	0.880	422.481	51.768	319.721	267.137	720.348	432.710	36.885	566.001	0.497	16.814	0.684			
30	0.840	400.544	48.427	290.655	255.787	777.289	511.502	30.363	592.813	0.516	19.036	0.636			
50	0.800	419.658	38.592	259.105	224.908	834.229	509.320	26.981	571.530	0.496	18.048	0.638			
70	0.822	500.018	25.465	215.149	451.363	891.170	439.806	26.067	489.611	0.423	14.132	0.791			
90	0.844	631.519	18.717	202.656	598.119	948.971	349.971	30.071	404.429	0.348	5.576	1.000			

[illegible]

中華民國二十九年五月二十日

TABLE LVII.

10% CENTRIFUGAL COMPRESSOR, 1ND AND 1ND 1RAW  
85 ACFT SPEED, NEAR STALL, 20 DEG 1CV TURNING  
CLOUD 5

FLOW RATE = 2.125 SPEED = 55003.1

\*\*\* ENLIER GUIDE WANE EXIT \*\*\*

WD	VD	ALPHA	VM	VU	U	WU	B	WO	WREL	I	VO/VOMAX
10	0-303	339-094	48-148	311-761	125-020	626-866	701-668	23-950	767-979	0-483	0-969
20	0-306	379-094	48-148	312-199	126-400	624-918	800-117	21-501	839-982	0-777	0-999
30	0-308	316-161	49-391	317-110	119-251	102-979	908-728	19-339	938-806	0-886	0-999
40	0-306	338-096	70-473	319-367	61-741	1219-716	1008-439	17-605	1035-911	0-934	1-000
50	0-278	309-013	76-878	298-027	61-661	1210-261	1136-599	14-717	1173-089	1-058	0-911

\*\*\* INDUCER EXIT \*\*\*

INITIAL INTEGRATED FLOW 1.087

MASS AVERAGE TOTAL PRESSURE 21.209  
MASS AVERAGE TOTAL TEMPERATURE 989.548  
INDUCER PRESSURE RATIO 1.443  
INDUCER TEMPERATURE RATIO 1.136  
INDUCER EFFICIENCY 0.881

INDUCER EXIT VELOCITY TRIANGLES

WD	VD	ALPHA	VM	VU	U	WU	B	WO	WREL	I	VO/VOMAX
10	0-312	339-010	50-979	373-921	810-692	908-170	42-527	689-482	0-600	11-172	0-887
20	0-324	399-094	51-732	371-367	850-307	978-940	39-134	748-406	0-639	10-269	0-892
30	0-316	363-013	50-818	376-010	1019-923	943-912	33-439	792-311	0-687	9-392	0-886
40	0-316	390-011	51-124	384-989	492-214	1088-938	31-787	748-786	0-641	8-412	0-893
50	0-367	371-067	56-727	400-199	1159-153	938-954	28-400	635-432	0-536	7-249	1-000

TABLE LVII. (Continued)

TABLE LVII. (Continued)														
*** IMPELLER EXIT ***			INITIAL INTEGRATED FLOW 1.985											
PCENT	SPAN	R	MO	VO	VO/V <sub>max</sub>	ALP	VM	VM/V <sub>max</sub>	VU	U	WU	B	WD	
0.0233	0.0054	0.9378	1269.55	0.7757	8.507	187.82	0.3377	1255.57	1711.21	455.63	70.054	199.80		
0.0536	0.0149	1.0382	1422.02	0.8689	13.007	320.07	0.5754	1385.53	1711.21	325.68	76.772	328.79		
0.1273	0.0300	1.1343	1528.12	0.9337	17.007	446.97	0.8036	1461.29	1711.21	249.92	80.294	453.47		
0.2122	0.0500	1.1929	1590.38	0.9718	19.757	537.61	0.9666	1496.75	1711.21	214.46	81.846	543.11		
0.2971	0.0699	1.2269	1625.54	0.9932	20.007	556.17	1.0000	1527.43	1711.21	183.77	83.139	560.18		
0.3820	0.0899	1.2374	1636.52	1.0000	19.507	546.49	0.9825	1542.58	1711.21	168.63	83.761	549.74		
0.4568	0.1099	1.2351	1634.27	0.9986	19.007	532.27	0.9570	1545.16	1711.21	166.04	83.866	535.34		
0.5517	0.1299	1.2152	1613.79	0.9861	18.007	498.89	0.8970	1534.74	1711.21	176.47	83.440	502.18		
0.6366	0.1499	1.1730	1569.84	0.9592	15.757	426.32	0.7665	1510.84	1711.21	200.36	82.445	430.05		
0.7215	0.1699	1.1132	1505.73	0.9200	12.007	313.26	0.5632	1472.78	1711.21	238.42	80.804	317.33		
0.8064	0.1899	1.0523	1438.13	0.8787	8.007	200.34	0.3602	1424.10	1711.21	287.10	78.601	204.37		
0.8913	0.2099	1.0054	1385.07	0.8463	4.757	114.88	0.2065	1380.30	1711.21	330.91	76.518	118.15		
0.9550	0.2249	0.9624	1335.05	0.8157	2.757	64.23	0.1154	1333.51	1711.21	377.70	74.185	66.76		
MASS AVERAGE TOTAL PRESSURE 96.838														
MASS AVERAGE TOTAL TEMPERATURE 951.700														
MASS AVG VM 459.504 VU 1497.800 ANGLE 17.055														
FLOW FACTOR 0.815 SLIP FACTOR INS. STA. 0.875 IMPELLER TIP 0.917														
IMP. PRESS. RATIO 4.565 IMP. TEMP. RATIO 1.614 EFFICIENCY 0.875														
IMP.,IND.,PRESS. RATIO 6.617 IMP.,IND.,TEMP. RATIO 1.834 EFFICIENCY 0.846														
IMP.,IND.,IGV PRESS. RATIO 6.590 IMP.,IND.,IGV TEMP. RATIO 1.834 EFFICIENCY 0.844														
*** DIFFUSER ***														
CO DIFFUSER THROAT FRONT 0.862 REAR 0.862														
STATIC PRESSURE RISE COEFFICIENT IMPELLER EXIT/DIFFUSER EXIT 0.742														
DIFFUSER THROAT FRONT/DIFFUSER EXIT 0.684 DIFFUSER THROAT REAR/DIFFUSER EXIT 0.685														
DIFFUSER LOSSES TOTAL TO STATIC 0.157 TOTAL TO TOTAL 0.109														
DIFFUSER LOSS COEFFICIENT 0.257														



TABLE LVIII.

10/1 CENTRIFUGAL COMPRESSOR, IND AND IMP TRAV  
85 PCT SPEED, NEAR STALL, 30 DEG IGV TURNING  
BUILD 6

FLOW RATE = 2.071      SPEED = 55505.1

\*\*\* INLET GUIDE VANE EXIT \*\*\*

MO	VO	ALPHA	VM	VU	U	WU	B	WO	MREL	I	VO/VO MAX
10	0.352	389.096	56.112	323.000	216.948	607.686	27.991	688.195	0.623	2.908	0.992
30	0.355	392.036	57.618	331.075	209.956	711.319	24.959	784.593	0.711	5.940	1.000
50	0.344	380.266	60.334	330.425	188.206	830.650	21.692	893.958	0.809	8.867	0.969
70	0.344	380.266	61.886	335.401	179.187	937.400	19.667	995.597	0.902	9.982	0.969
90	0.322	356.600	69.726	334.507	123.565	1089.334	17.070	1139.537	1.031	11.079	0.909

\*\*\* INDUCER EXIT \*\*\*

INITIAL INTEGRATED FLOW 1.677

MASS AVERAGE TOTAL PRESSURE 21.018  
MASS AVERAGE TOTAL TEMPERATURE 582.301  
INDUCER PRESSURE RATIO 1.430  
INDUCER TEMPERATURE RATIO 1.122  
INDUCER EFFICIENCY 0.880

INDUCER EXIT VELOCITY TRIANGLES

MO	VO	ALPHA	VM	VU	U	WU	B	WO	MREL	I	VO/VO MAX
10	0.481	549.178	37.670	335.614	434.695	878.193	37.116	556.172	0.487	16.583	0.789
30	0.511	581.828	46.027	418.724	403.973	947.610	37.604	686.200	0.603	11.795	0.836
50	0.552	629.403	48.446	471.003	417.498	1017.028	38.153	762.417	0.669	6.876	0.904
70	0.557	642.781	42.089	430.849	477.008	1086.446	35.258	746.355	0.647	4.941	0.923
90	0.596	695.748	29.660	344.295	604.587	1155.864	31.986	649.958	0.556	3.663	1.000

TABLE LVIII. (Continued)

*** IMPELLER EXIT ***													
PCENT SPAN	R	MO	VO	VO/VMAX	ALP	VM	VM/VMAX	VU	U	WU	B	WO	
0.0366	0.0149	1.0722	1447.72	0.8668	17.420	433.43	0.8154	1381.32	1706.35	325.03	76.758	445.26	
0.1273	0.0300	1.1988	1582.88	0.9696	18.670	506.73	0.9533	1499.58	1706.35	206.77	82.149	511.52	
0.2122	0.0500	1.2234	1608.57	0.9853	19.295	531.54	1.0000	1518.21	1706.35	188.14	82.935	535.61	
0.2971	0.0699	1.2374	1622.74	0.9940	19.045	529.53	0.9962	1533.90	1706.35	172.44	83.585	535.87	
0.3820	0.0899	1.2468	1632.41	1.0000	18.920	529.32	0.9958	1544.21	1706.35	162.14	84.005	532.23	
0.4658	0.1099	1.2457	1631.31	0.9993	18.420	515.48	0.9697	1547.73	1706.35	158.62	84.148	518.18	
0.5517	0.1299	1.2234	1609.00	0.9856	17.170	475.01	0.8936	1537.28	1706.35	169.07	83.723	477.87	
0.6366	0.1499	1.1789	1563.11	0.9575	15.170	409.06	0.7695	1508.63	1706.35	197.72	82.523	412.56	
0.7215	0.1699	1.1203	1501.18	0.9196	11.920	310.08	0.5833	1468.81	1706.35	237.54	80.813	314.11	
0.8064	0.1899	1.0570	1432.50	0.8775	7.920	197.40	0.3713	1418.83	1706.35	287.52	78.544	201.41	
0.8913	0.2099	1.0031	1371.53	0.8401	4.920	117.64	0.2213	1366.48	1706.35	339.87	76.092	121.23	
0.9530	0.2249	0.9296	1285.88	0.7877	3.420	76.72	0.1443	1283.59	1706.35	422.76	71.770	80.78	
MASS AVERAGE TOTAL PRESSURE 96.112													
MASS AVERAGE TOTAL TEMPERATURE 937.399													
MASS AVG VM 460.575 VU 1506.133													
FLOW FACTOR 0.601 SLIP FACTOR INS. STA. ANGLE 17.003													
IMP. PRESS. RATIO 4.572 IMP. TEMP. RATIO 1.609 IMPELLER TIP 0.925													
IMP..IND..IGV PRESS. RATIO 6.612 IMP..IND..IGV TEMP. RATIO 1.807 EFFICIENCY 0.882													
IMP..IND..IGV PRESS. RATIO 6.540 IMP..IND..IGV TEMP. RATIO 1.807 EFFICIENCY 0.869													
*** DIFFUSER ***													
CD DIFFUSER THROAT FRONT 0.865 REAR 0.850													
STATIC PRESSURE RISE COEFFICIENT IMPELLER EXIT/DIFFUSER EXIT 0.727													
DIFFUSER THROAT FRONT/DIFFUSER EXIT 0.443 DIFFUSER THROAT REAR/DIFFUSER EXIT 0.662													
DIFFUSER LOSSES TOTAL TO STATIC 0.169 TOTAL TO TOTAL 0.121													
DIFFUSER LOSS COEFFICIENT 0.272													

TABLE LIX.

10/1 CENTRIFUGAL COMPRESSOR, INDUCER TRAVERSE  
8/1 SPEEDLINE, MOD. 10 DEG IGV TURNING  
BUILD 6

FLOW RATE = 2.823      SPEED = 61657.2

## \*\*\* INLET GUIDE VANE EXIT \*\*\*

WD	VO	ALPHA	VM	VU	U	WU	B	WO	MREL	I	VO/VOMAX
10	0.437	479.510	78.037	99.228	915.732	816.504	29.881	941.691	0.859	1.018	1.000
30	0.437	479.437	78.057	99.393	1024.528	925.234	26.882	1037.333	0.946	4.017	0.999
50	0.437	479.437	78.728	93.714	1131.586	1037.871	24.372	1159.410	1.039	6.187	0.999
70	0.437	479.530	78.810	93.059	1240.557	1147.497	22.291	1240.178	1.131	7.378	1.000
90	0.415	456.440	82.255	61.511	1347.590	1286.078	19.575	1363.287	1.241	8.774	0.951

## \*\*\* INDUCER EXIT \*\*\*

INITIAL INTEGRATED FLOW 2.413

MASS AVERAGE TOTAL PRESSURE 24.844  
MASS AVERAGE TOTAL TEMPERATURE 609.773  
INDUCER PRESSURE RATIO 1.690  
INDUCER TEMPERATURE RATIO 1.175  
INDUCER EFFICIENCY 0.923

## INDUCER EXIT VELOCITY TRIANGLES

WD	VO	ALPHA	VM	VU	U	WU	B	WO	MREL	I	VO/VOMAX
10	0.579	668.925	47.995	497.059	447.641	975.530	527.889	43.277	725.083	0.628	10.422
30	0.579	685.659	49.096	518.230	448.960	1052.542	603.682	40.644	795.610	0.688	8.755
50	0.627	727.050	48.597	545.346	480.831	1129.754	648.922	40.043	847.646	0.731	4.986
70	0.637	744.509	48.355	556.359	494.729	1206.866	712.136	37.998	903.700	0.773	2.201
90	0.631	747.979	39.527	476.044	576.935	1283.978	707.043	33.951	852.366	0.719	1.698
											1.000

TABLE LX.

10/1 CENTRIFUGAL COMPRESSOR, IND AND IMP TRAV  
8/1 SPEEDLINE, NEAR STALL, 10 DEG IGV TURNING  
BUILD 6

FLOW RATE = 2.796      SPEED = 61819.2

## \*\*\* INLET GUIDE VANE EXIT \*\*\*

MD	VC	ALPHA	VM	VU	U	WU	S	WO	MREL	I	VO/VOMAX
10	0.423	484.997	78.037	454.932	96.220	918.137	821.916	28.964	939.421	0.856	1.935
30	0.426	487.806	78.047	457.781	96.905	1027.219	930.214	28.199	1036.836	0.945	4.700
50	0.426	487.997	78.728	458.989	91.478	1134.559	1043.080	23.750	1139.592	1.038	6.809
70	0.421	482.087	78.810	453.302	89.674	1243.816	1154.142	21.442	1239.970	1.129	8.227
90	0.399	438.847	82.255	434.843	59.140	1351.130	1291.989	18.601	1363.204	1.240	9.548
											0.937

## \*\*\* INDUCER EXIT \*\*\*

INITIAL INTEGRATED FLOW 2.371

MASS AVERAGE TOTAL PRESSURE 25.029  
MASS AVERAGE TOTAL TEMPERATURE 613.736  
INDUCER PRESSURE RATIO 1.703  
INDUCER TEMPERATURE RATIO 1.183  
INDUCER EFFICIENCY 0.898

## INDUCER EXIT VELOCITY TRIANGLES

MD	VC	ALPHA	VM	VU	U	WU	S	WO	MREL	I	VO/VOMAX
10	0.582	674.075	47.813	499.467	452.669	978.093	525.423	43.549	724.940	0.626	10.150
30	0.592	684.401	48.986	516.417	449.130	1055.407	606.277	40.423	796.404	0.687	8.976
50	0.626	727.476	48.182	542.166	485.053	1132.722	647.668	39.932	844.641	0.727	5.097
70	0.628	738.170	47.596	545.078	497.779	1210.036	712.257	37.426	896.895	0.764	2.773
90	0.637	738.319	37.753	464.295	599.564	1287.351	687.786	34.021	829.831	0.697	1.628
											1.000

TABLE LX. (Continued)

TABLE LX. (Continued)												
*** IMPELLER EXIT ***												
INITIAL INTEGRATED FLOW 2.560												
PCT SPAN	R	MO	VO	VO/VMAX	ALP	VM	VM/VMAX	VU	U	WU	B	WO
0.0445	0.0104	0.9624	1407.03	0.7613	12.526	305.17	0.5150	1373.54	1900.46	526.92	69.011	326.86
0.1273	0.0300	1.1613	1642.40	0.8886	15.276	432.73	0.7303	1584.36	1900.46	316.10	78.716	441.26
0.2122	0.0500	1.2960	1787.98	0.9674	17.526	538.45	0.9087	1704.98	1900.46	195.48	83.459	541.97
0.2971	0.0699	1.3394	1832.27	0.9914	18.526	582.19	0.9825	1737.32	1900.46	163.14	84.635	584.75
0.3820	0.0899	1.3476	1840.80	0.9960	18.776	592.51	1.0000	1742.83	1900.46	157.62	84.832	594.93
0.4668	0.1079	1.3546	1848.15	1.0000	18.526	587.24	0.9910	1752.37	1900.46	148.09	85.169	589.33
0.5517	0.1299	1.3464	1840.10	0.9956	17.776	561.79	0.9481	1752.24	1900.46	148.22	85.164	563.80
0.6366	0.1499	1.3054	1797.90	0.9728	16.276	503.90	0.8504	1725.84	1900.46	174.62	84.222	506.48
0.7215	0.1699	1.2363	1725.35	0.9335	13.776	410.67	0.6934	1675.72	1900.46	224.74	82.361	414.55
0.8064	0.1892	1.1613	1643.14	0.8890	9.776	279.01	0.709	1619.28	1900.46	281.18	80.148	283.19
0.8913	0.2099	1.0746	1543.24	0.8350	4.526	121.79	0.255	1538.43	1900.46	362.03	76.757	125.12
0.9550	0.2249	0.9707	1417.83	0.7671	1.526	37.77	0.0637	1417.33	1900.46	483.13	71.176	39.90
MASS AVERAGE TOTAL PRESSURE 141.880												
MASS AVERAGE TOTAL TEMPERATURE 1059.800												
MASS AVG VM 498.571 VU 1687.611 ANGLE 16.458												
FLOW FACTOR 0.827 SLIP FACTOR INS. STA. 0.887 IMPELLER TIP 0.930												
IMP. PRESS. RATIO 5.668 IMP. TEMP. RATIO 1.726 EFFICIENCY 0.873												
IMP. IND. PRESS. RATIO 9.713 IMP. IND. TEMP. RATIO 2.043 EFFICIENCY 0.861												
IMP. IND. IGV PRESS. RATIO 9.655 IMP. IND. IGV TEMP. RATIO 2.043 EFFICIENCY 0.858												
*** DIFFUSER ***												
CD DIFFUSER THROAT FRONT 0.832 REAR 0.817												
STATIC PRESSURE RISE COEFFICIENT IMPELLER EXIT/DIFFUSER EXIT 0.747												
DIFFUSER THROAT FRONT/DIFFUSER EXIT 0.697 DIFFUSER THROAT REAR/DIFFUSER EXIT 0.669												
DIFFUSER LOSSES TOTAL TO STATIC 0.167 TOTAL TO TOTAL 0.123												
DIFFUSER LOSS COEFFICIENT 0.252												

TABLE LXI.

10/1 CENTRIFUGAL COMPRESSOR, INDUCER TRAVERSE  
8/1 SPEEDLINE, WOD, 15 DEG IGV TURNING  
BUILD 6

FLOW RATE = 2.807      SPEED = 61605.6

## \*\*\* INLET GUIDE VANE EXIT \*\*\*

MO	VO	ALPHA	VM	VU	U	WU	B	WO	MREL	I	VO/VOMAX
10	0.440	482.340	73.148	461.627	139.828	914.936	775.107	30.776	902.159	0.823	0.123
30	0.445	488.141	73.181	467.262	141.236	1024.033	882.796	27.892	998.831	0.911	3.007
50	0.442	485.241	73.990	466.422	133.826	1131.265	957.438	25.061	1101.105	1.005	1.000
70	0.442	485.335	74.394	467.445	130.559	1239.685	109.125	22.853	1203.604	1.098	0.994
90	0.412	453.437	78.414	444.197	91.068	1346.496	1255.429	19.484	1331.697	1.212	0.928

## \*\*\* INDUCER EXIT \*\*\*

INITIAL INTEGRATED FLOW 2.455

MASS AVERAGE TOTAL PRESSURE 29.717  
MASS AVERAGE TOTAL TEMPERATURE 602.838  
INDUCER PRESSURE RATIO 1.614  
INDUCER TEMPERATURE RATIO 1.162  
INDUCER EFFICIENCY 0.905

## INDUCER EXIT VELOCITY TRIANGLES

MO	VO	ALPHA	VM	VU	U	WU	B	WO	MREL	I	VO/VOMAX
10	0.593	680.376	47.731	503.477	457.626	974.713	517.086	44.236	721.711	0.629	9.463
30	0.609	700.055	48.824	526.928	460.894	1031.760	590.866	41.726	791.692	0.689	7.673
50	0.642	739.289	49.396	561.290	481.146	1128.808	647.662	40.913	857.037	0.744	4.116
70	0.639	742.718	50.191	570.548	475.505	1205.855	730.350	37.996	926.788	0.798	2.203
90	0.637	747.798	43.451	514.287	542.872	1282.903	740.030	34.797	901.186	0.767	0.852

TABLE LXII.

10/1 CENTRIFUGAL COMPRESSOR, IND AND IMP TRAV  
8/1 SPEEDLINE, NEAR STALL, 15 DEG IGV TURNING  
BUILD 6

FLOW RATE = 2.787      SPEED = 61700.7

\*\*\* INLET GUIDE VANE EXIT \*\*\*

MO	VO	ALPHA	VM	VU	U	WU	B	WO	MREL	I	VO/VO MAX
10	0.432	473.721	73.148	453.378	137.330	916.350	779.019	30.158	901.345	0.822	0.701
30	0.437	479.530	73.181	459.020	138.745	1025.614	886.869	27.364	998.617	0.921	3.535
50	0.434	476.523	73.990	458.052	131.424	1133.012	1001.517	24.575	1101.358	1.004	5.984
70	0.434	476.533	74.394	458.967	128.191	1241.600	1113.408	22.402	1204.296	1.098	7.267
90	0.404	444.772	78.414	439.710	89.328	1348.576	1259.250	19.086	1332.499	1.212	9.063
											0.927

\*\*\* INDUCER EXIT \*\*\*

INITIAL INTEGRATED FLOW 2.386

MASS AVERAGE TOTAL PRESSURE 23.903  
MASS AVERAGE TOTAL TEMPERATURE 605.103  
INDUCER PRESSURE RATIO 1.632  
INDUCER TEMPERATURE RATIO 1.166  
INDUCER EFFICIENCY 0.904

INDUCER EXIT VELOCITY TRIANGLES

MO	VO	ALPHA	VM	VU	U	WU	B	WO	MREL	I	VO/VO MAX
10	0.579	666.698	47.545	491.896	450.027	976.219	526.192	43.070	720.306	0.626	10.629
30	0.607	698.146	48.609	523.762	461.607	1053.385	591.777	41.510	790.271	0.687	7.869
50	0.637	734.801	49.662	563.097	475.629	1130.552	654.922	40.537	861.761	0.747	4.492
70	0.628	732.665	48.966	552.667	480.996	1207.718	726.722	37.252	912.998	0.783	2.947
90	0.631	744.500	42.493	502.915	548.960	1284.885	735.924	34.347	891.352	0.756	1.302
											0.895
											0.937
											0.986
											0.984
											1.000

TABLE LXII. (Continued)

*** IMPELLER EXIT ***													
PCENT SPAN	R	MO	VO	VO/VMAX	ALP	VM	VM/VMAX	VU	U	WU	S	WO	
U.0233	0.0054	1.0968	1562.07	0.8503	13.050	352.72	0.5878	1521.73	1896.82	375.09	76.153	363.27	
C.0036	0.0149	1.2391	1715.67	0.9339	15.800	467.14	0.7785	1650.85	1896.82	245.97	81.525	472.30	
J.1273	0.0300	1.2843	1768.00	0.9624	18.050	547.81	0.9129	1680.99	1896.82	215.83	82.683	552.31	
O.2122	0.0500	1.3300	1815.46	0.9882	19.300	600.03	1.0000	1713.43	1896.82	183.39	83.890	603.46	
O.2971	0.0699	1.382	1823.98	0.9928	19.050	595.33	0.9921	1724.08	1896.82	172.73	84.278	598.31	
O.3620	0.0899	1.4353	1831.51	0.9968	18.675	586.38	0.9772	1734.89	1896.82	161.93	84.667	588.33	
U.4668	0.1099	1.4911	1837.02	1.0000	18.425	580.61	0.9676	1742.85	1896.82	153.97	84.951	582.87	
O.5517	0.1299	1.5312	1817.06	0.9891	17.550	547.91	0.9131	1732.48	1896.82	164.33	84.581	550.37	
O.6366	0.1499	1.5867	1772.08	0.9646	15.050	460.14	0.7668	1711.29	1896.82	185.52	83.812	462.84	
O.7215	0.1699	1.6234	1704.98	0.9281	11.300	334.08	0.5567	1671.93	1896.82	224.89	82.339	337.09	
O.8064	0.1899	1.1578	1632.98	0.8689	7.300	207.49	0.3458	1619.74	1896.82	277.08	80.292	210.51	
O.8913	0.2099	1.0921	1558.51	0.8483	3.300	89.71	0.1495	1555.92	1896.82	340.89	77.641	91.84	
O.9550	0.2249	1.0007	1449.40	0.7889	0.800	20.23	0.0337	1449.26	1896.82	447.56	72.838	21.16	
MASS AVERAGE TOTAL PRESSURE 141.475													
MASS AVG VM 514.998													
MASS AVG VM 1701.057													
FLOW FACTOR 0.811													
IMP. PRESS. RATIO 5.896													
IMP.IND. PRESS. RATIO 9.698													
IMP.IND.IGV PRESS. RATIO 9.628													
IMP.IND.IGV TEMP. RATIO 2.030													
IMP.IND.IGV TEMP. RATIO 2.030													
IMPELLER TIP 0.940													
EFFICIENCY 0.882													
EFFICIENCY 0.872													
EFFICIENCY 0.868													
*** DIFFUSER ***													
CD DIFFUSER THROAT FRONT 0.846													
CD DIFFUSER THROAT REAR 0.832													
STATIC PRESSURE RISE COEFFICIENT IMPELLER EXIT/DIFFUSER EXIT 0.742													
DIFFUSER THROAT FRONT/DIFFUSER EXIT 0.682													
DIFFUSER THROAT REAR/DIFFUSER EXIT 0.632													
DIFFUSER LOSSES TOTAL TO STATIC 0.172													
DIFFUSER LOSSES TOTAL TO TOTAL 0.132													
DIFFUSER LOSS COEFFICIENT 0.257													



TABLE LXIII.

10/1 CENTRIFUGAL COMPRESSOR. IND AND IMP TRAV  
95 FCT SPEED. MOD. 1C DEG IGW TURNING  
BUILD 6

SPEED = 62114.1

FLC# RATE = 2.005

## \*\*\* INLET GUIDE VANE EXIT \*\*\*

MO	VO	ALPHA	VM	VU	U	WU	B	WO	MREL	I	VO/VOMAX
10	8.446	491.000	77.000	679.744	104.719	922.966	30.383	946.518	0.266	0.316	0.999
20	8.448	491.126	78.079	680.538	101.478	930.513	27.312	1047.209	0.956	3.387	1.000
30	8.448	491.000	78.071	680.436	101.498	930.234	24.811	1144.914	1.053	5.748	0.999
70	8.443	488.101	78.836	678.901	94.930	1269.799	22.513	1250.397	1.141	7.194	0.993
90	8.418	499.204	80.889	693.670	72.723	1397.612	19.439	1362.962	1.241	8.710	0.935

## \*\*\* INDUCER EXIT \*\*\*

INITIAL INTEGRATED FLOW 2.493

MASS AVERAGE TOTAL PRESSURE 24.976  
MASS AVERAGE TOTAL TEMPERATURE 613.630  
INDUCER PRESSURE RATIO 1.599  
INDUCER TEMPERATURE RATIO 1.183  
INDUCER EFFICIENCY 0.895

## INDUCER EXIT VELOCITY TRIANGLES

MO	VO	ALPHA	VM	VU	U	WU	B	WO	MREL	I	VO/VOMAX
10	0.992	474.601	49.390	904.121	448.362	982.799	43.330	734.655	0.624	10.369	0.884
20	0.901	497.196	49.361	928.897	454.257	1060.442	41.104	804.462	0.694	8.293	0.924
30	0.826	527.977	48.737	967.388	479.913	1128.123	39.747	858.082	0.736	9.282	0.934
70	0.932	562.822	49.411	979.118	496.169	1219.809	38.824	923.720	0.789	1.973	1.000
90	0.639	798.193	61.296	900.351	569.656	1293.492	34.654	879.930	0.742	0.935	0.994

TABLE LXIII. (Continued)

*** IMPELLER EXIT ***														INITIAL INTEGRATED FLOW 2.654													
PCENT	SPAN	R	MD	VO	VO/YMAR	ALP	VM	VM/VNMAX	VU	U	WU	S	WO														
0.0233	0.0034	1.0150	1478.07	0.7993	0.7993	8.224	211.43	0.3371	1482.87	1909.53	446.46	73.020	221.06														
0.0234	0.0149	1.1399	1410.94	0.8797	0.8797	12.224	342.79	0.5465	1502.24	1909.53	327.29	78.312	350.04														
0.0273	0.0308	1.2228	1727.86	0.9365	0.9365	17.224	511.57	0.8156	1650.14	1909.53	259.35	81.067	517.85														
0.0282	0.0300	1.3148	1816.28	0.9813	0.9813	20.224	627.18	1.0000	1702.43	1909.53	207.10	83.064	631.81														
0.0271	0.0409	1.3371	1837.86	0.9937	0.9937	19.724	619.99	0.9885	1729.27	1909.53	180.25	84.049	623.35														
0.0228	0.0839	1.3488	1848.88	1.0000	1.0000	18.974	601.08	0.9583	1748.24	1909.53	161.29	84.728	603.63														
0.0268	0.1099	1.3488	1848.88	0.9911	0.9911	18.474	585.80	0.9340	1753.42	1909.53	156.11	84.912	588.12														
0.0317	0.1299	1.3224	1832.38	0.9911	0.9911	17.724	557.84	0.8894	1745.40	1909.53	146.12	84.628	560.30														
0.0349	0.1499	1.2902	1788.80	0.9876	0.9876	15.724	484.77	0.7729	1721.86	1909.53	187.67	83.779	487.64														
0.0215	0.1899	1.2140	1707.24	0.9234	0.9234	12.224	361.48	0.5763	1608.53	1909.53	260.99	81.781	369.23														
0.0264	0.1899	1.1484	1634.41	0.8840	0.8840	8.224	233.79	0.3727	1617.60	1909.53	291.92	79.770	237.57														
0.0313	0.2099	1.0831	1561.43	0.8446	0.8446	4.474	121.80	0.1942	1596.69	1909.53	332.84	77.229	124.89														
0.0330	0.2249	0.9488	1395.73	0.7548	0.7548	2.224	54.16	0.0863	1394.70	1909.53	514.83	69.739	57.74														
MASS AVERAGE TOTAL PRESSURE 149.016																											
MASS AVERAGE TOTAL TEMPERATURE 1067.709																											
MASS AVG VM 918.074																											
FLOW FACTOR 0.811																											
IMP. PRESS. RATIO 9.846																											
IMP.-IND. PRESS. RATIO 9.997																											
IMP.-IND.-IGV PRESS. RATIO 9.937																											
IMP.-IND.-IGV TEMP. RATIO 2.038																											
IMPELLER TIP EFFICIENCY 0.939																											
EFFICIENCY 0.876																											
EFFICIENCY 0.863																											
EFFICIENCY 0.860																											
*** DIFFUSER ***																											
CD DIFFUSER THROAT FRONT 0.078																											
REAR 0.866																											
STATIC PRESSURE RISE COEFFICIENT 0.042																											
IMPELLER EXIT/DIFFUSER EXIT 0.132																											
DIFFUSER THROAT FRONT/DIFFUSER EXIT 0.042																											
DIFFUSER THROAT REAR/DIFFUSER EXIT 0.007																											
DIFFUSER LOSSES TOTAL TO STATIC 0.580																											
TOTAL TO TOTAL 0.887																											
DIFFUSER LOSS COEFFICIENT 0.887																											

TABLE LXIV.

10/1 CENTRIFUGAL COMPRESSOR, 1ND AND IMP TRAV  
95 PCT SPEED, NEAR STALL, 10 DEG IGV TURNING  
BUILD 6

FLOW RATE = 2.077 SPEED = 62133.6

\*\*\* INLET GUIDE VANE EXIT \*\*\*

MD	VD	ALPHA	VM	VU	U	WU	B	VO	MBEL	I	VO/VO MAX
10	0.442	489.335	77.686	474.170	103.502	923.236	819.833	30.044	947.082	0.864	0.859
20	0.442	489.335	78.075	474.862	100.280	1032.404	932.123	26.996	1046.111	0.954	1.000
30	0.442	489.335	78.071	474.834	100.319	1141.187	1040.868	24.522	1144.049	1.044	1.000
40	0.442	489.335	78.834	479.209	93.406	1250.298	1156.891	22.246	1249.925	1.140	0.993
50	0.412	499.437	80.889	447.716	71.800	1358.154	1286.353	19.190	1362.041	1.240	0.934

\*\*\* INDUCER EXIT \*\*\*

INITIAL INTEGRATED FLOW 2.453

MASS AVERAGE TOTAL PRESSURE 25.026  
MASS AVERAGE TOTAL TEMPERATURE 613.479  
INDUCER PRESSURE RATIO 1.103  
INDUCER TEMPERATURE RATIO 1.183  
INDUCER EFFICIENCY 0.898

INDUCER EXIT VELOCITY TRIANGLES

MD	VD	ALPHA	VM	VU	U	WU	B	VO	MBEL	I	VO/VO MAX
10	0.574	685.105	47.972	494.348	445.931	983.150	937.599	42.690	730.337	0.430	0.497
20	0.574	691.067	49.463	529.242	449.149	1060.385	911.715	40.830	806.273	0.695	0.922
30	0.621	735.829	49.285	556.219	478.670	1138.579	956.908	40.126	869.052	0.742	0.979
40	0.639	745.485	49.555	570.381	484.202	1214.293	730.091	37.998	926.482	0.790	1.000
50	0.628	748.835	40.336	493.408	589.280	1294.008	724.727	33.704	871.156	0.733	0.986

[illegible]

201

TABLE LXV.

10/1 CENTRIFUGAL COMPRESSOR. INDUCER TRAVERSE  
100 PCT SPEED. NEAR STALL, 10 DEG IGV TURNING  
BUILD 6

FLOW RATE = 3.050 SPEED = 60250 RPM

\*\*\* INLET GUIDE VANE EXIT \*\*\*

MD	VD	ALPHA	VM	VU	U	WU	W	VO	MREL	I	VO/VO MAX
10	0.450	930.950	79.773	920.953	103.193	969.393	880.197	31.019	1010.137	0.926	0.119
20	0.450	933.953	79.732	924.032	102.499	1083.791	981.281	28.103	1112.449	1.019	0.790
30	0.450	933.953	79.619	924.082	98.097	1180.085	1100.028	25.308	1218.837	1.117	0.091
40	0.450	928.254	79.088	919.970	93.459	1312.859	1239.399	23.090	1323.396	1.214	0.080
50	0.450	908.210	67.191	904.931	61.043	1623.913	1384.869	20.287	1433.130	1.330	0.031

\*\*\* INDUCER EXIT \*\*\*

INITIAL INTEGRATED FLOW 2.179

MASS AVERAGE TOTAL PRESSURE 29.977  
MASS AVERAGE TOTAL TEMPERATURE 600.276  
INDUCER PRESSURE RATIO 1.424  
INDUCER TEMPERATURE RATIO 1.176  
INDUCER EFFICIENCY 0.829

INDUCER EXIT VELOCITY TRIANGLES

MD	VD	ALPHA	VM	VU	U	WU	W	VO	MREL	I	VO/VO MAX
10	0.100	612.781	93.438	649.903	460.843	1032.107	971.342	49.923	880.131	0.764	0.176
20	0.107	798.320	96.863	653.576	459.334	1113.778	696.226	44.848	926.373	0.807	0.082
30	0.409	789.786	96.171	637.889	459.976	1182.340	733.394	40.903	972.978	0.846	0.046
40	0.612	743.321	94.443	629.071	438.782	1274.839	820.196	37.924	1039.776	0.897	0.086
50	0.807	717.287	67.050	623.280	403.667	1339.349	870.101	31.119	1016.383	0.860	0.030

TABLE LXVI.

10/1 CENTRIFUGAL COMPRESSOR, INDUCER TRAVERSE  
101 PCT SPEED, WOD, -4 DEG IGV TURNING  
BUILD 6

FLOW RATE = 3.214      SPEED = 65934.3

## \*\*\* INLET GUIDE VANE EXIT \*\*\*

MO	VO	ALPHA	VM	VU	U	WU	B	WO	MREL	I	VO/VOMAX
10	0.527	513.572	94.778	571.578	-47.780	978.341	1026.122	29.119	1174.576	1.080	1.780
30	0.527	573.685	93.854	572.387	-38.565	1095.329	1133.895	26.784	1270.176	1.168	4.115
50	0.527	573.685	94.124	572.199	-41.262	1211.126	1252.388	24.553	1376.913	1.266	6.004
70	0.522	567.965	93.419	566.954	-33.870	1326.676	1360.547	22.621	1473.949	1.355	7.047
90	0.200	545.251	93.924	543.973	-37.317	1440.979	1478.296	20.202	1575.204	1.445	7.947

## \*\*\* INDUCER EXIT \*\*\*

INITIAL INTEGRATED FLOW 2.752

MASS AVERAGE TOTAL PRESSURE 24.234  
MASS AVERAGE TOTAL TEMPERATURE 631.609  
INDUCER PRESSURE RATIO 1.649  
INDUCER TEMPERATURE RATIO 1.217  
INDUCER EFFICIENCY 0.705

## INDUCER EXIT VELOCITY TRIANGLES

MO	VO	ALPHA	VM	VU	U	WU	B	WO	MREL	I	VO/VOMAX
10	0.721	334.748	62.465	740.199	385.886	1043.202	657.315	48.394	989.929	0.856	5.305
30	0.654	765.278	59.426	658.951	389.145	1125.683	736.518	41.814	988.289	0.845	7.581
50	0.568	674.934	61.525	593.302	321.798	1208.125	866.326	33.798	1066.575	0.898	11.231
70	0.586	810.987	62.591	719.948	373.327	1290.586	917.258	28.128	1136.037	0.986	2.071
90	0.587	711.554	54.559	580.006	412.190	1373.047	960.856	31.116	1122.343	0.927	4.533

TABLE LXVII.

10/1 CENTRIFUGAL COMPRESSOR, IND AND IMP TRAV  
101 PCT SPEED, NEAR STALL,  $\sim$  DEG IGV TURNING  
BUILD 6

FLOW RATE = 3.209      SPEED = 65987.7

## \*\*\* INLET GUIDE VANE EXIT \*\*\*

MO	VO	ALPHA	VM	VU	U	WU	B	WO	MREL	I	VO/VOMAX
10	0.524	570.826	94.778	568.842	-47.551	979.133	1026.685	28.988	1173.739	1.079	1.911
30	0.522	567.965	93.854	566.680	-38.181	1096.216	1134.397	26.544	1268.063	1.166	4.355
50	0.522	567.965	94.124	566.494	-40.851	1212.106	1232.958	24.328	1375.071	1.264	6.231
70	0.519	565.215	93.419	564.209	-33.706	1327.750	1361.457	22.509	1473.736	1.354	7.160
90	0.497	542.485	93.924	541.213	-37.127	1442.146	1479.274	20.095	1575.171	1.445	8.054

## \*\*\* INDUCER EXIT \*\*\*

INITIAL INTEGRATED FLOW 2.919

MASS AVERAGE TOTAL PRESSURE 25.044  
MASS AVERAGE TOTAL TEMPERATURE 632.864  
INDUCER PRESSURE RATIO 1.704  
INDUCER TEMPERATURE RATIO 1.220  
INDUCER EFFICIENCY 0.746

## INDUCER EXIT VELOCITY TRIANGLES

MO	VO	ALPHA	VM	VU	U	WU	B	WO	MREL	I	VO/VOMAX
10	0.717	631.881	92.785	662.492	503.120	1044.047	540.926	50.768	855.277	0.737	1.000
30	0.713	630.845	92.853	662.262	501.710	1126.575	624.864	46.664	910.520	0.782	2.735
50	0.582	621.634	46.934	505.288	472.272	1209.103	736.830	34.440	893.440	0.752	10.589
70	0.650	772.558	55.676	638.028	435.620	1291.630	856.010	36.699	1067.629	0.699	3.500
90	0.563	684.136	47.931	507.868	458.380	1374.158	915.778	29.011	1047.177	0.862	6.438

TABLE LXVII. (Continued)

* * * IMPELLER EXIT * * *														INITIAL INTEGRATED FLOW 2.678				
PCENT	SPAN	R	MO	VO	VO/VMAX	ALP	VM	VM/VMAX	VU	U	WU	B	WO					
0.0233	0.0055	0.9283	1474.74	0.7245	11.220	277.22	0.4067	1397.51	2028.61	631.10	65.696	304.17						
0.0848	0.0200	1.1484	1707.52	0.8648	15.220	446.43	0.5550	1640.88	2028.61	387.73	76.705	458.72						
0.1697	0.0399	1.3148	1888.65	0.9605	18.470	629.51	0.9237	1780.65	2028.61	247.96	82.072	635.58						
0.2546	0.0600	1.3710	1948.67	0.9910	20.470	681.48	1.0000	1825.62	2028.61	202.99	83.635	685.68						
0.3395	0.0799	1.3816	1959.71	0.9966	19.220	645.13	0.9466	1850.47	2028.61	178.14	84.501	648.11						
0.4264	0.0999	1.3874	1966.25	1.0000	18.220	614.78	0.9021	1867.67	2028.61	160.94	85.074	617.06						
0.5093	0.1200	1.3874	1965.80	0.9997	17.470	590.14	0.8659	1875.13	2028.61	153.48	85.320	592.32						
0.5942	0.1400	1.3617	1939.24	0.9862	15.220	541.68	0.7948	1862.05	2028.61	166.56	84.888	543.84						
0.6791	0.1599	1.3124	1887.34	0.9598	13.970	455.63	0.6685	1831.52	2028.61	197.09	83.858	458.26						
0.7640	0.1800	1.2492	1817.71	0.9244	10.470	330.31	0.4847	1787.45	2028.61	241.16	82.316	333.21						
0.8488	0.2000	1.1883	1725.07	0.8773	6.720	201.86	0.2962	1713.22	2028.61	315.39	77.569	205.25						
0.9125	0.2150	1.1062	1651.35	0.8398	3.220	92.75	0.1361	1648.75	2028.61	379.86	77.025	95.18						
0.9550	0.2250	1.0500	1582.36	0.8047	-0.029	-0.82	-0.0012	1582.36	2028.61	446.25	74.250	-0.85						
0.9868	0.2325	0.8763	1356.32	0.6898	-2.529	-59.87	-0.0878	1355.00	2028.61	673.61	63.566	-56.86						
MASS AVERAGE TOTAL PRESSURE 172.985.																		
M/55 AVERAGE TOTAL TEMPERATURE 1159.000																		
MASS AVG VM 550.241 VU 1808.291 ANGLE 16.924																		
FLOW FACTOR 0.808 SLIP FACTOR INS. STA. 0.891																		
IMP. PRESS. RATIO 6.903 IMP. TEMP. RATIO 1.831																		
IMP. IND. PRESS. RATIO 11.902 IMP. IND. IEMP. RATIO 2.234																		
IMP. IND. IGV PRESS. RATIO 11.772 IMP. IND. IGV TEMP. RATIO 0.812																		
IMP. IND. IGV EFFICIENCY 0.807																		



TABLE LXVIII.

10/1 CENTRIFUGAL COMPRESSOR, IND AND IMP TRAV  
101 PCT SPEED, NS, -4 DEG IGV, WITH COOLANT  
BUILD 6

FLOW RATE = 3.214      SPEED = 65779.6

## \*\*\* INLET GUIDE VANE EXIT \*\*\*

MO	VD	ALPHA	VM	VU	U	WU	B	WO	MREL	I	VO/VOMAX
10	0.926	870.825	94.778	568.842	-47.551	976.046	1023.598	29.062	1171.040	1.077	1.037
20	0.922	847.965	93.854	566.880	-38.181	1092.759	1130.940	26.614	1264.972	1.163	4.285
30	0.922	867.985	94.124	566.494	-40.851	1208.284	1249.135	24.394	1371.589	1.261	6.165
40	0.918	865.215	93.419	564.209	-33.706	1323.563	1357.270	22.572	1469.869	1.351	7.057
50	0.917	842.485	93.924	541.215	-37.127	1437.598	1474.726	20.152	1570.901	1.441	7.997
											0.950

## \*\*\* INDUCER EXIT \*\*\*

INITIAL INTEGRATED FLOW 2.638

MASS AVERAGE TOTAL PRESSURE 24.773  
MASS AVERAGE TOTAL TEMPERATURE 632.556  
INDUCER PRESSURE RATIO 1.685  
INDUCER TEMPERATURE RATIO 1.221  
INDUCER EFFICIENCY 0.725

## INDUCER EXIT VELOCITY TRIANGLES

MO	VD	ALPHA	VM	VU	U	WU	B	WO	MREL	I	VO/VOMAX
10	0.878	991.689	82.661	880.925	455.432	1040.755	585.322	56.398	1057.654	0.933	-2.698
20	0.891	806.208	58.811	689.684	617.501	1123.022	705.521	44.349	986.623	0.846	9.050
30	0.860	669.156	57.408	563.781	360.443	1205.290	844.846	33.715	1015.685	0.820	11.314
40	0.841	760.192	64.248	686.693	330.284	1287.558	957.273	35.574	1176.936	0.952	4.625
50	0.864	662.561	55.541	545.519	377.020	1369.825	992.804	28.778	1132.711	0.929	8.871
											0.868

TABLE LXVIII. (Continued)

TABLE LXVIII. (Continued)									
*** IMPELLER EXIT ***									
PERCENT SPAN	R	MO	VO	VO/VMAX	ALP	VM	VM/VMAX	VU	U
0.0762	0.0179	1.2724	1840.56	0.9369	19.124	403.03	0.8392	1739.07	2022.22
0.1497	0.0400	1.3734	1949.82	0.9819	21.624	718.54	1.0000	1812.59	2022.22
0.2346	0.0860	1.3823	1959.80	0.9969	20.124	674.21	0.9383	1839.97	2022.22
0.3205	0.0799	1.3886	1965.69	1.0000	19.374	652.09	0.9075	1854.38	2022.22
0.4204	0.1000	1.3874	1964.92	0.9996	18.374	619.39	0.8620	1864.74	2022.22
0.5203	0.1199	1.3857	1963.24	0.9896	17.124	572.79	0.7971	1859.10	2022.22
0.6242	0.1399	1.3842	1967.96	0.9659	15.624	511.17	0.7114	1827.83	2022.22
0.6791	0.1599	1.3839	1921.43	0.9266	12.374	390.33	0.5432	1779.12	2022.22
0.7840	0.1800	1.1859	1743.82	0.8871	8.374	253.97	0.3534	1725.23	2022.22
0.8274	0.1999	1.1414	1691.84	0.8604	5.624	165.80	0.2307	1683.69	2022.22
0.8701	0.2090	1.0911	1582.27	0.8049	3.624	100.02	0.1392	1579.10	2022.22
MASS AVERAGE TOTAL PRESSURE 174.934									
MASS AVERAGE TOTAL TEMPERATURE 1195.100									
MASS AVG VM 992.489 VO 1813.782 ANGLE 17.804									
FLOW FACTOR 0.764 SLIP FACTOR INS. STA. 0.896 IMPELLER TIP 0.940									
IMP. PRESS. RATIO 7.062 IMP. TEMP. RATIO 1.824 EFFICIENCY 0.895									
IMP..IND. PRESS. RATIO 12.038 IMP..IND. TEMP. RATIO 2.229 EFFICIENCY 0.821									
IMP..IND..IGV PRESS. RATIO 11.906 IMP..IND..IGV TEMP. RATIO 2.228 EFFICIENCY 0.816									
*** DIFFUSER ***									
CD DIFFUSER THROAT FRONT 0.865 REAR 0.841									
STATIC PRESSURE RISE COEFFICIENT IMPELLER EXIT/DIFFUSER EXIT 0.712									
DIFFUSER THROAT FRONT/DIFFUSER EXIT 0.875 DIFFUSER THROAT REAR/DIFFUSER EXIT 0.846									
DIFFUSER LOSSES TOTAL TO STATIC 0.198 TOTAL TO TOTAL 0.157									
DIFFUSER LOSS COEFFICIENT 0.287									

TABLE LXIX.

10/1 CENTRIFUGAL COMPRESSOR, INDUCER TRAVERSE  
101 PCT SPEED, MGD, 0 DEG IGV TURNING  
BUILD 6

FLOW RATE = 3.192 SPEED = 65834.8

\*\*\* INLET GUIDE VANE EXIT \*\*\*

MGD	VO	ALPHA	VM	VU	U	WU	B	WO	MREL	I	VO/VO MAX
10 0.514	559.486	63.985	559.486	0.147	976.949	976.802	29.802	1125.685	1.034	1.097	1.000
20 0.514	559.486	66.040	559.408	4.372	1093.067	1083.694	27.303	1219.562	1.120	3.596	1.000
50 0.514	559.486	68.370	559.452	6.149	1208.088	1201.938	24.960	1325.761	1.218	5.557	1.000
70 0.508	553.753	68.791	553.630	11.679	1324.231	1312.552	22.869	1424.535	1.308	6.800	0.989
90 0.500	545.251	68.952	545.251	0.449	1438.113	1437.663	20.769	1537.588	1.411	7.380	0.974

\*\*\* INDUCER EXIT \*\*\*

INITIAL INTEGRATED FLOW 2.738

MASS AVERAGE TOTAL PRESSURE 29.687  
MASS AVERAGE TOTAL TEMPERATURE 822.874  
INDUCER PRESSURE RATIO 1.012  
INDUCER TEMPERATURE RATIO 1.200  
INDUCER EFFICIENCY 0.728

INDUCER EXIT VELOCITY TRIANGLES

MGD	VO	ALPHA	VM	VU	U	WU	B	WO	MREL	I	VO/VO MAX
10 0.720	829.239	61.661	729.861	393.624	1041.627	648.002	48.400	976.015	0.848	5.300	1.000
20 0.660	765.596	59.270	658.096	391.210	1123.963	732.752	41.927	984.895	0.849	7.472	0.923
50 0.571	672.354	60.858	587.249	327.412	1206.300	878.088	33.749	1057.027	0.898	11.280	0.810
70 0.658	775.169	63.170	691.721	349.868	1288.636	938.768	36.384	1166.089	0.991	3.815	0.934
90 0.587	707.035	56.115	586.521	394.190	1370.973	976.783	31.001	1139.565	0.947	4.648	0.852

TABLE LXX.

10/1 CENTRIFUGAL COMPRESSOR, IND AND IMP TRAV  
101 PCT SPEED, NEAR STALL, 0 DEG IGV TURNING  
BUILD 6

FLOW RATE = 3.185      SPEED = 65952.6

## \*\*\* INLET GUIDE VANE EXIT \*\*\*

MO	VO	ALPHA	VM	VU	U	WU	B	WO	MREL	I	VO/VOHAX
10	0.511	556.730	89.985	556.730	0.146	978.702	978.555	29.636	1125.841	1.034	1.263
30	0.511	556.730	89.050	556.652	9.326	1095.028	1085.701	27.144	1220.085	1.120	3.759
50	0.511	556.520	89.370	556.586	6.318	1210.254	1204.136	24.807	1326.549	1.218	9.752
70	0.503	550.958	88.791	550.870	11.620	1326.506	1314.985	22.729	1425.705	1.308	6.940
90	0.497	542.485	89.952	542.485	0.446	1440.892	1440.245	20.639	1539.075	1.411	7.510
											1.000

## \*\*\* INDUCER EXIT \*\*\*

INITIAL INTEGRATED FLOW 2.654

MASS AVERAGE TOTAL PRESSURE 23.891  
MASS AVERAGE TOTAL TEMPERATURE 423.890  
INDUCER PRESSURE RATIO 1.525  
INDUCER TEMPERATURE RATIO 1.202  
INDUCER EFFICIENCY 0.734

## INDUCER EXIT VELOCITY TRIANGLES

MO	VO	ALPHA	VM	VU	U	WU	B	WO	MREL	I	VO/VOHAX
10	0.708	817.653	64.302	736.783	354.552	1043.495	688.942	46.921	1008.707	0.873	6.778
30	0.566	771.151	61.066	674.896	379.080	1125.979	752.899	41.873	1011.109	0.871	7.527
50	0.568	670.240	60.157	581.381	333.533	1208.464	874.930	33.603	1050.479	0.891	11.426
70	0.512	724.952	64.928	656.644	307.203	1290.948	953.744	33.722	1182.766	0.999	6.477
90	0.552	666.835	57.991	565.452	353.457	1373.432	1019.974	29.003	1166.227	0.965	6.646
											1.000

TABLE LXX. (Continued)

*** IMPELLER EXIT ***												
PCT	SPAN	R	MD	VO	VO/VMAX	ALP	VM	VM/VMAX	VU	U	WU	WO
0.0233	0.0034	1.0687	1605.56	0.8152	12.934	359.37	0.5193	1564.82	2027.54	462.71	73.527	374.75
0.0636	0.0149	1.2503	1819.42	0.9238	15.934	529.94	0.7659	1740.53	2027.54	287.01	80.636	537.10
0.1273	0.0300	1.3300	1976.36	0.9679	20.184	657.77	0.9506	1789.28	2027.54	238.25	82.415	663.57
0.2122	0.0500	1.3804	1958.92	0.9946	20.684	691.92	1.0000	1832.65	2027.54	194.88	83.929	695.82
0.2971	0.0699	1.3874	1966.25	0.9983	19.684	662.30	0.9571	1851.35	2027.54	176.19	84.563	665.29
0.3820	0.0899	1.3910	1965.45	1.0000	18.684	630.92	0.9118	1865.66	2027.54	161.88	85.041	633.29
0.4688	0.1099	1.3874	1965.36	0.9979	17.684	597.02	0.8628	1872.49	2027.54	155.05	85.266	599.06
0.5537	0.1299	1.3640	1940.84	0.9854	16.434	549.09	0.7935	1861.55	2027.54	165.99	84.504	551.27
0.6366	0.1499	1.3207	1894.98	0.9619	14.184	464.25	0.6709	1836.82	2027.54	190.72	84.072	466.74
0.7215	0.1699	1.2597	1828.00	0.9281	10.434	331.06	0.4784	1797.77	2027.54	229.77	82.716	333.75
0.8064	0.1899	1.1882	1746.54	0.8868	6.434	195.72	0.2828	1735.54	2027.54	292.00	80.449	198.47
0.8701	0.2099	1.1296	1677.53	0.8517	3.934	115.09	0.1663	1673.58	2027.54	353.96	78.057	117.64
0.9123	0.2150	1.0710	1606.54	0.8157	1.934	54.22	0.0783	1603.62	2027.54	421.92	75.276	56.06
0.9350	0.2249	0.7738	1212.51	0.6156	-0.065	-1.39	-0.0020	1212.52	2027.54	815.01	56.092	-1.67

MASS AVERAGE TOTAL PRESSURE 173.578  
 MASS AVERAGE TOTAL TEMPERATURE 1154.000  
 MASS AVG VM 563.468 VU 1821.763 ANGLE 17.244  
 FLOW FACTOR 0.787 SLIP FACTOR INS. STA. 0.898 IMPELLER TIP 0.941  
 IMP. PRESS. RATIO 7.265 IMP. TEMP. RATIO 1.849 EFFICIENCY 0.885  
 IMP..IND. PRESS. RATIO 11.888 IMP..IND. TEMP. RATIO 2.224 EFFICIENCY 0.814  
 IMP..IND..IGV PRESS. RATIO 11.812 IMP..IND..IGV TEMP. RATIO 2.224 EFFICIENCY 0.815

*** DIFFUSER ***									
CD DIFFUSER	THROAT FRONT	0.854	REAR	0.820					
STATIC PRESSURE RISE COEFFICIENT	IMPELLER EXIT/DIFFUSER EXIT	0.737							
DIFFUSER THROAT FRONT/DIFFUSER EXIT	0.695	DIFFUSER THROAT REAR/DIFFUSER EXIT	0.631						
DIFFUSER LOSSES TOTAL TO STATIC	0.182	TOTAL TO TOTAL	0.144						
DIFFUSER LOSS COEFFICIENT	0.262								

TABLE LXXI.

10/1 CENTRIFUGAL COMPRESSOR, INDUCER TRAVERSE  
101 PCT SPEED, WOD, 5 DEG IGW TURNING  
BUILD 6

FLOW RATE = 3.150      SPEED = 65974.5

\*\*\* INLET GUIDE VANE EXIT \*\*\*

MO	VO	ALPHA	VM	VU	U	WU	B	WO	MREL	I	VO/VOMAX
10	0.497	542.485	85.078	540.585	46.543	933.635	30.066	1078.796	0.989	0.833	0.994
30	0.500	545.251	84.757	542.970	49.820	1096.305	27.422	1178.960	1.081	3.477	0.999
50	0.500	545.466	84.743	543.171	49.977	1211.872	25.055	1282.589	1.176	5.504	1.000
70	0.497	542.425	85.240	540.614	45.011	1327.854	22.851	1392.103	1.277	6.818	0.994
90	0.496	531.187	86.867	530.385	29.199	1442.212	20.574	1509.277	1.382	7.575	0.973

\*\*\* INDUCER EXIT \*\*\*      INITIAL INTEGRATED FLOW      2.740

MASS AVERAGE TOTAL PRESSURE      29.178  
MASS AVERAGE TOTAL TEMPERATURE      613.436  
INDUCER PRESSURE RATIO      1.577  
INDUCER TEMPERATURE RATIO      1.182  
INDUCER EFFICIENCY      0.761

INDUCER EXIT VELOCITY TRIANGLES

MO	VO	ALPHA	VM	VU	U	WU	B	WO	MREL	I	VO/VOMAX
10	0.719	826.311	60.936	716.280	407.960	1043.837	635.876	48.403	957.808	0.835	5.296
30	0.683	786.537	59.397	675.267	399.390	1126.346	726.958	42.888	992.197	0.864	6.511
50	0.645	746.344	58.006	632.981	395.428	1208.860	813.431	37.888	1030.697	0.891	7.141
70	0.617	723.861	61.575	636.593	374.563	1291.371	946.808	33.915	1140.919	0.974	6.284
90	0.612	729.147	54.565	594.094	422.737	1373.882	951.145	31.989	1121.439	0.942	3.660

TABLE LXXII.

10/1 CENTRIFUGAL COMPRESSOR, IND AND IMP TRAV  
101 PCT SPEED, NEAR STALL, 5 DEG IGV TURNING  
BUILD 6

FLOW RATE = 3.142      SPEED = 66122.6

## \*\*\* INLET GUIDE VANE EXIT \*\*\*

MD	VO	ALPHA	VM	VU	U	WU	B	WO	MREL	I	VO/VOMAX
10	0.494	539.611	82.981	533.567	65.937	992.067	916.130	30.310	1061.191	0.973	0.989
20	0.497	562.685	82.740	538.136	68.553	1098.767	1030.214	27.500	1162.296	1.066	0.999
30	0.497	562.592	83.342	538.933	62.909	1214.314	1151.405	25.002	1271.292	1.166	1.000
70	0.492	536.735	83.187	532.945	63.670	1330.500	1266.829	22.816	1374.368	1.260	0.989
90	0.481	523.426	83.764	523.921	59.806	1443.229	1406.423	20.433	1500.804	1.374	0.968

## \*\*\* INDUCER EXIT \*\*\*

INITIAL INTEGRATED FLOW 2.716

MASS AVERAGE TOTAL PRESSURE 23.434  
MASS AVERAGE TOTAL TEMPERATURE 614.363  
INDUCER PRESSURE RATIO 1.596  
INDUCER TEMPERATURE RATIO 1.184  
INDUCER EFFICIENCY 0.775

## INDUCER EXIT VELOCITY TRIANGLES

MD	VO	ALPHA	VM	VU	U	WU	B	WO	MREL	I	VO/VOMAX
10	0.713	819.097	59.688	707.084	413.313	1046.161	632.798	48.173	948.896	0.826	0.926
20	0.680	782.780	58.504	687.463	408.947	1128.878	719.931	42.834	981.737	0.853	0.955
30	0.671	775.305	58.839	689.039	424.683	1211.575	787.491	39.494	1020.468	0.883	0.946
70	0.607	713.215	58.865	610.354	368.177	1294.271	925.293	33.410	1108.468	0.943	0.870
90	0.569	659.509	52.578	523.772	400.768	1376.968	976.200	28.215	1107.896	0.923	0.805

TABLE LXXII. (Continued)

** * IMPELLER EXIT ** *		INITIAL INTEGRATED FLOW 2.862									
PERCENT SPAN	R	NO	VO	VC/VMAX	ALP	VM	VM/VMAX	VU	U	WU	W
0.0645	0.0105	1.0045	1628.31	0.8256	20.524	570.19	0.8525	1523.08	2032.76	309.68	71.897
0.1061	0.0250	1.3359	1600.40	0.9647	20.524	666.29	0.9962	1779.77	2032.76	252.99	81.909
0.1697	0.0400	1.3734	1939.30	0.9844	20.174	668.82	1.0000	1820.31	2032.76	212.44	83.943
0.2546	0.0600	1.3921	1959.07	0.9955	19.576	656.34	0.9813	1845.85	2032.76	186.91	84.217
0.3395	0.0799	1.3992	1965.81	0.9979	18.824	634.30	0.9483	1860.66	2032.76	172.10	84.715
0.4244	0.1000	1.4027	1969.84	1.0000	17.924	606.24	0.9064	1874.23	2032.76	138.52	85.165
0.5093	0.1199	1.3984	1955.81	0.9939	16.824	566.11	0.8464	1872.19	2032.76	140.37	85.097
0.5942	0.1399	1.3441	1909.74	0.9695	15.324	504.76	0.7547	1842.03	2032.76	186.73	84.088
0.6791	0.1599	1.2773	1837.99	0.9330	12.876	403.27	0.6029	1793.20	2032.76	239.55	82.390
0.7640	0.1800	1.2070	1760.05	0.8934	8.924	273.03	0.4082	1738.74	2032.76	294.02	80.402
0.8488	0.1999	1.1097	1645.84	0.8335	4.176	119.81	0.1791	1641.57	2032.76	391.18	76.596
0.9125	0.2150	0.9378	1429.91	0.7259	1.424	35.54	0.0531	1429.47	2032.76	603.28	67.118

MASS AVERAGE TOTAL PRESSURE	168.163
MASS AVERAGE TOTAL TEMPERATURE	3145.499
MASS AVG VM	557.524
MASS AVG W	557.524
FLOW FACTOR	0.787
IMP. PRESS. RATIO	7.169
IMP. IND. PRESS. RATIO	11.924
IMP. IND. TEMP. RATIO	11.444
IMP. IND. IGV PRESS. RATIO	11.444
IMP. IND. IGV TEMP. RATIO	2.208
IMP. IND. IGV EFFICIENCY	0.812
IMPELLER TIP	0.928
IMPELLER EFFICIENCY	0.862
IMPELLER EFFICIENCY	0.812



TABLE LXXIII.

10/1 CENTRIFUGAL COMPRESSOR, INDUCER TRAVERSE  
100 PCT SPEED, NEAR STALL, 10 DEG IGV TURNING  
BUILD 6

FLOW RATE • 3.030      SPEED • 63238.1

\*\*\* INLET GUIDE VANE EXIT \*\*\*

WD	VO	ALPHA	VM	VU	U	VU	B	WO	MREL	I	VO/VOHAA
10	6.485	920.580	78.793	929.893	103.193	969.393	866.197	31.019	1010.737	0.926	-0.129
20	6.489	933.993	78.922	926.892	102.899	1083.791	981.291	28.103	1112.449	1.019	2.796
30	6.489	933.993	79.018	926.892	98.937	1198.085	1100.028	25.308	1218.837	1.117	3.031
40	6.489	928.284	79.088	919.870	93.439	1312.859	1219.399	23.090	1323.394	1.214	6.379
50	6.486	908.219	83.191	904.931	81.943	1429.913	1364.869	20.287	1439.136	1.330	7.862
											0.994
											1.000
											1.000
											0.989
											0.991

\*\*\* INDUCER EXIT \*\*\*

INITIAL INTEGRATED FLOW 2.669

MASS AVERAGE TOTAL PRESSURE 23.980  
MASS AVERAGE TOTAL TEMPERATURE 609.348  
INDUCER PRESSURE RATIO 1.805  
INDUCER TEMPERATURE RATIO 1.174  
INDUCER EFFICIENCY 0.829

INDUCER EXIT VELOCITY TRIANGLES

WD	VO	ALPHA	VM	VU	U	VU	B	WO	MREL	I	VO/VOHAA
10	6.506	919.283	92.089	727.028	932.110	1032.187	480.077	36.983	871.732	0.769	-2.883
20	6.516	889.284	92.656	701.894	931.921	1113.778	582.269	30.315	911.807	0.804	-0.915
30	6.521	889.818	92.930	669.940	916.758	1199.368	678.608	44.606	933.164	0.835	0.423
40	6.519	819.969	92.927	669.806	901.128	1276.959	775.892	39.912	1011.312	0.877	0.287
50	6.520	732.883	93.937	918.287	917.594	1358.549	840.955	31.644	987.830	0.837	4.009
											1.000
											0.963
											0.925
											0.897
											0.722

TABLE LXXIV.

AD1 CENTRIFUGAL COMPRESSOR, IND AND IMP TRAY  
101 PCT SPEED, NEAR STALL, -4 DEG IGV TURNING  
BUILD 6

FLOW RATE = 3.209 SPEED = 69987.7

\*\*\* INLET GUIDE VANE CASE \*\*\*

MD	VO	ALPHA	WM	VU	U	VU	W	VO	MREL	I	VO/VOMAX
10 0.924	979.816	99.770	998.862	-47.931	979.133	1026.085	28.988	1173.739	1.079	1.911	1.000
20 0.922	988.965	99.856	999.680	-38.181	1096.216	1134.397	26.344	1268.063	1.166	4.355	0.994
30 0.922	998.965	99.124	999.454	-41.821	1242.104	1252.958	24.328	1375.071	1.264	6.231	0.994
40 0.916	995.215	99.419	999.289	-35.786	1327.750	1361.557	22.559	1473.736	1.354	7.160	0.990
50 0.897	992.465	99.626	999.213	-37.127	1442.146	1479.276	20.095	1575.171	1.445	8.054	0.950

\*\*\* INDUCER CASE \*\*\*

INITIAL INTEGRATED FLOW 3.091

MASS AVERAGE TOTAL PRESSURE 25.034  
MASS AVERAGE TOTAL TEMPERATURE 632.918  
INDUCER PRESSURE RATIO 1.975  
INDUCER TEMPERATURE RATIO 1.220  
INDUCER EFFICIENCY 0.747

INDUCER EXIT VELOCITY TRIANGLES

MD	VO	ALPHA	WM	VU	U	VU	W	VO	MREL	I	VO/VOMAX
10 0.839	992.970	69.827	127.875	614.499	1044.047	429.551	59.453	845.173	0.741	-3.733	1.000
20 0.826	987.390	69.867	109.044	597.153	1126.575	528.021	53.283	886.531	0.749	-3.883	0.973
30 0.838	979.619	69.828	93.820	558.183	1209.103	650.919	39.617	844.999	0.717	5.412	0.814
40 0.894	889.133	62.696	652.364	497.056	1291.630	796.574	39.386	1028.057	0.870	0.814	0.860
50 0.879	882.845	64.956	694.607	497.365	1374.150	876.793	29.526	1007.663	0.831	6.123	0.737

TABLE LXXIV. (Continued)

*** IMPELLER EAST ***														INITIAL INTEGRATED FLOW 2.678													
PCENT	SPAN	R	MD	WC	VD/VMAA	ALP	VM	VM/VMAA	VU	U	WU	S	MO														
0.0233	0.0039	0.0039	0.0233	1424.74	0.7243	11.220	277.22	0.4067	1397.31	2028.61	631.20	65.694	304.17														
0.0248	0.0200	0.0200	1.1484	1700.32	0.8648	13.220	646.43	0.6550	1640.88	2028.61	387.73	76.705	458.72														
0.0297	0.0209	0.0209	1.2168	1288.83	0.9605	19.670	629.51	0.9237	1780.45	2028.61	247.94	62.072	639.38														
0.0346	0.0400	0.0400	1.3710	1948.87	0.9910	20.670	481.48	1.0000	1623.62	2028.61	202.99	83.659	685.48														
0.0353	0.0799	0.0799	1.3814	1859.71	0.9768	19.220	643.13	0.9466	1650.67	2028.61	176.14	84.301	640.11														
0.0404	0.0244	0.0244	1.2874	1964.23	1.0000	18.220	614.78	0.9021	1657.67	2028.61	160.94	85.374	617.06														
0.0403	0.1200	0.1200	1.3874	2549.80	0.9907	17.670	590.14	0.8632	1771.13	2028.61	153.48	84.884	592.12														
0.0442	0.1400	0.1400	1.2417	1939.24	0.9802	16.220	541.68	0.7948	1662.03	2028.61	146.56	84.886	538.26														
0.0401	0.1899	0.1899	1.2184	1887.34	0.9588	13.970	459.63	0.6683	1631.52	2028.61	197.09	83.838	438.26														
0.0440	0.1600	0.1600	1.2492	1817.71	0.9244	10.470	350.31	0.4847	1737.45	2028.61	241.16	82.316	333.31														
0.0486	0.2000	0.2000	1.1683	1725.07	0.8773	6.720	201.66	0.2962	1713.22	2028.61	315.39	79.369	209.23														
0.0415	0.2120	0.2120	1.1682	1651.39	0.8394	3.220	92.75	0.1361	1649.75	2028.61	379.86	77.029	93.18														
0.0510	0.2250	0.2250	1.0900	1582.36	0.8047	-0.029	-0.02	-0.0012	1582.36	2028.61	446.23	74.230	-0.83														
0.0508	0.2323	0.2323	0.8763	1556.32	0.7688	-2.328	-39.87	-0.0873	1355.00	2028.61	673.61	63.366	-66.86														
MASS AVERAGE TOTAL PRESSURE 172.983																											
MASS AVERAGE TOTAL TEMPERATURE 1159.000																											
MASS AVG VM 590.241																											
FLOW FACTOR 0.808																											
IMP. PRESS. RATIO 6.903																											
IMP. IND. PRESS. RATIO 11.922																											
IMP. IND. TO CV PRESS. RATIO 11.772																											
IMP. IND. TO CV TEMP. RATIO 2.234																											
EFFICIENCY 0.812																											
EFFICIENCY 0.807																											

IMPELLER TIP 0.875

14.924

ANGLE

INS. STA.

SLIP FACTOR

IMP. TEMP. RATIO

IMP. IND. TEMP. RATIO

IMP. IND. TO CV TEMP. RATIO

EFFICIENCY

EFFICIENCY

TABLE LXXV.

10/1 CENTRIFUGAL COMPRESSOR, IMPELLER TRAVERSE  
8/1 SPEEDLINE, NEAR STALL, 10 DEG IGV TURNING  
BUILD 6

FLOW RATE = 2.796 SPEED = 61819.2

INITIAL INTEGRATED FLOW 2.518													
PCENT	SPAN	R	MO	VO	VO/VMAX	ALP	VM	VM/VMAX	VU	U	WU	B	WO
0.0443	0.0104	0.9624	1415.37	0.7505	12.782	313.18	0.5110	1380.49	1900.46	519.97	69.360	334.66	
0.1273	0.0300	1.1624	1660.31	0.8802	15.531	444.59	0.7254	1599.88	1900.46	300.78	79.351	452.38	
0.2122	0.0500	1.2961	1812.13	0.9607	17.782	553.41	0.9030	1725.55	1900.46	174.91	84.212	556.25	
0.2971	0.0699	1.3403	1866.56	0.9896	18.782	600.96	0.9808	1767.15	1900.46	133.31	85.685	602.67	
0.3820	0.0899	1.3483	1879.28	0.9963	19.032	612.82	1.0000	1776.25	1900.46	123.90	86.010	614.31	
0.4668	0.1099	1.3545	1886.12	1.0000	19.032	607.27	0.9909	1785.59	1900.46	114.77	86.322	608.52	
0.5517	0.1299	1.3646	1875.14	0.9941	18.032	580.44	0.9471	1783.04	1900.46	117.42	86.232	581.70	
0.6366	0.1499	1.3689	1830.26	0.9703	16.532	520.80	0.8498	1754.80	1900.46	145.86	85.247	522.59	
0.7215	0.1699	1.2374	1753.29	0.9295	14.032	425.10	0.6936	1700.97	1900.46	199.49	83.310	429.02	
0.8064	0.1899	1.1613	1664.49	0.8824	10.032	289.95	0.4731	1639.04	1900.46	261.41	80.938	293.61	
0.8913	0.2099	1.0745	1545.60	0.8194	4.782	128.64	0.2102	1540.22	1900.46	360.24	76.835	132.32	
0.9550	0.2299	0.9893	1394.79	0.7395	1.782	43.37	0.0707	1394.12	1900.46	506.34	70.038	46.14	

MASS AVERAGE TOTAL PRESSURE 141.717				MASS AVERAGE TOTAL TEMPERATURE 1093.729			
MASS AVERAGE VFR 513.392		VU 1712.168		ANGLE 16.691		IMPELLER TIP 0.944	
FLOW FACTOR 0.817		SLIP FACTOR INS. STA. 0.900		EFFICIENCY 0.000		EFFICIENCY 0.000	
IMP. PRESS. RATIO 0.600		IMP. TEMP. RATIO 0.000		IMP. IND. TEMP. RATIO 2.108		EFFICIENCY 0.808	
IMP. IND. PRESS. RATIO 9.702		IMP. IND. TEMP. RATIO 9.644		IMP. IND. EFF. RATIO 2.108		EFFICIENCY 0.805	

MASS AVERAGE TOTAL PRESSURE 141.717

MASS AVERAGE TOTAL TEMPERATURE 1093.729

MASS AVG VR 515.392 VU 1712.168

FLOW FACTOR 0.817 SLIP FACTOR INS. STA. ANGLE 16.691

IMP. PRESS. RATIO 0.600 IMP. TEMP. RATIO 0.900

IMP. IND. PRESS. RATIO 9.702 IMP. IND. IGV TEMP. RATIO 2.108

IMP. IND. IGV PRESS. RATIO 9.644 IMP. IND. IGV TEMP. RATIO 2.108

IMP. IND. IGV PRESS. RATIO 9.644 IMP. IND. IGV TEMP. RATIO 2.108

IMP. IND. IGV PRESS. RATIO 9.644 IMP. IND. IGV TEMP. RATIO 2.108

IMP. IND. IGV PRESS. RATIO 9.644 IMP. IND. IGV TEMP. RATIO 2.108

IMP. IND. IGV PRESS. RATIO 9.644 IMP. IND. IGV TEMP. RATIO 2.108

IMP. IND. IGV PRESS. RATIO 9.644 IMP. IND. IGV TEMP. RATIO 2.108

IMP. IND. IGV PRESS. RATIO 9.644 IMP. IND. IGV TEMP. RATIO 2.108

IMP. IND. IGV PRESS. RATIO 9.644 IMP. IND. IGV TEMP. RATIO 2.108

IMP. IND. IGV PRESS. RATIO 9.644 IMP. IND. IGV TEMP. RATIO 2.108

IMP. IND. IGV PRESS. RATIO 9.644 IMP. IND. IGV TEMP. RATIO 2.108

IMP. IND. IGV PRESS. RATIO 9.644 IMP. IND. IGV TEMP. RATIO 2.108

IMP. IND. IGV PRESS. RATIO 9.644 IMP. IND. IGV TEMP. RATIO 2.108

IMP. IND. IGV PRESS. RATIO 9.644 IMP. IND. IGV TEMP. RATIO 2.108

IMP. IND. IGV PRESS. RATIO 9.644 IMP. IND. IGV TEMP. RATIO 2.108

IMP. IND. IGV PRESS. RATIO 9.644 IMP. IND. IGV TEMP. RATIO 2.108

IMP. IND. IGV PRESS. RATIO 9.644 IMP. IND. IGV TEMP. RATIO 2.108

IMP. IND. IGV PRESS. RATIO 9.644 IMP. IND. IGV TEMP. RATIO 2.108

TABLE LXXVI.

10/1 CENTRIFUGAL COMPRESSOR, IMPELLER TRAVERSE  
 6/1 SPEEDLINE, NEAR STALL, 15 DEG IGV TURNING  
 BUILD 6

FLOW RATE = 2.767 SPEED = 61700.7

INITIAL INTEGRATED FLOW 2.690													
PCENT	SPAN	B	MD	VD	VD/VMAX	ALP	VM	VM/VMAX	VU	U	WU	B	WO
0.0233	0.0056	1.0968	1.0968	1599.58	0.8355	13.275	359.73	0.5843	1524.72	1896.82	372.10	76.285	370.28
0.0626	0.0149	1.2351	1.2351	1725.32	0.9202	16.025	476.29	0.7762	1658.28	1896.82	238.54	81.814	481.19
0.1279	0.0300	1.2843	1.2843	1781.10	0.9499	18.275	558.51	0.9103	1691.26	1896.82	203.56	83.070	562.62
0.2122	0.0500	1.3300	1.3300	1835.74	0.9791	19.525	613.54	1.0000	1730.18	1896.82	166.64	84.498	616.38
0.2671	0.0699	1.3582	1.3582	1851.90	0.9877	19.275	611.32	0.9963	1748.09	1896.82	148.73	85.136	613.53
0.3820	0.0898	1.3433	1.3433	1864.72	0.9945	19.900	604.02	0.9844	1764.16	1896.82	132.44	85.700	605.72
0.4688	0.1099	1.3323	1.3323	1874.91	1.0000	19.650	599.57	0.9772	1776.46	1896.82	120.36	86.123	600.95
0.5317	0.1296	1.3324	1.3324	1852.93	0.9882	17.775	545.47	0.9219	1764.49	1896.82	132.32	85.711	567.26
0.6366	0.1499	1.2867	1.2867	1802.33	0.9613	13.275	474.83	0.7739	1738.68	1896.82	158.14	84.802	476.79
0.7215	0.1699	1.2234	1.2234	1731.02	0.9232	11.525	345.85	0.53637	1696.12	1896.82	200.70	83.231	348.26
0.8034	0.1898	1.1378	1.1378	1632.88	0.8819	7.525	216.46	0.3528	1638.65	1896.82	258.17	81.046	219.13
0.8918	0.2099	1.0921	1.0921	1563.68	0.8340	3.525	96.14	0.1567	1560.72	1896.82	336.10	77.846	98.34
0.9550	0.2249	1.0007	1.0007	1432.18	0.7638	1.025	25.62	0.0417	1431.95	1896.82	464.87	72.014	26.93
MASS AVERAGE TOTAL PRESSURE 141.334													
MASS AVERAGE TOTAL TEMPERATURE 1082.183													
MASS AVG VM 928.194 VU 1723.003													
SLIP FACTOR 0.803 ANGLE 17.041													
IMP. PRESS. RATIO 0.008 INS. STA. 0.908													
IMP.IND. PRESS. RATIO 9.689 IMP. TEMP.IND. 0.000													
IMP.IND. DIV. PRESS. RATIO 9.619 IMP.IND. DIV. TEMP. RATIO 2.088													
IMP.IND. DIV. PRESS. RATIO 0.823 EFFICIENCY 0.922													
IMP.IND. DIV. PRESS. RATIO 0.820 EFFICIENCY 0.820													

MASS AVERAGE TOTAL PRESSURE 141.934  
 MASS AVERAGE TOTAL TEMPERATURE 1083.183  
 MASS AVG VM 928.134 VU 1729.003  
 FLOW FACTOR 0.803 SLIP FACTOR IAS. STA. 17.041  
 IMP. PRESS. RATIO 0.008 IMP. TEMP. RATIO 0.000  
 IMP. IND. PRESS. RATIO 0.008 IMP. IND. TEMP. RATIO 0.000  
 IMP. IND. IGV PRESS. RATIO 9.619 IMP. IND. IGV TEMP. RATIO 2.088  
 IMPELLER TIP EFFICIENCY 0.952  
 IMPELLER TIP EFFICIENCY 0.000  
 IMPELLER TIP EFFICIENCY 0.823  
 IMPELLER TIP EFFICIENCY 0.820

TABLE LXXVII.

10/1 CENTRIFUGAL COMPRESSOR, IMPELLER TRAVERSE  
95 PCT SPEED, MOD. 10 DEG IGV TURNING  
BUILD 6

FLOW RATE = 2.885 SPEED = 62114.1

\*\*\* IMPELLER EXIT \*\*\* INITIAL INTEGRATED FLOW 2.625

PCENT	SPAN	R	WD	WD	VD/VMAX	ALP	VM	VM/VNMAX	VU	U	WU	B	WO
0.0233	0.0054	1.0140	1476.81	0.7866	8.382	215.30	0.3379	1461.04	1909.53	448.49	72.935	225.21	
0.0238	0.0109	1.1315	1622.17	0.8640	12.382	347.86	0.5460	1584.44	1909.53	325.09	78.405	355.11	
0.0273	0.0300	1.2318	1734.40	0.9238	17.382	518.16	0.8134	1655.19	1909.53	254.34	81.264	524.24	
0.0212	0.0300	1.3148	1828.83	0.9741	20.382	637.00	1.0000	1714.42	1909.53	195.11	83.507	641.11	
0.02971	0.0509	1.3371	1859.03	0.9902	19.882	632.25	0.9925	1748.22	1909.53	161.31	96.728	634.94	
0.03820	0.0889	1.3468	1875.33	0.9988	19.132	614.65	0.9645	1771.73	1909.53	137.79	85.552	616.51	
0.0458	0.1089	1.3489	1877.40	1.0000	18.632	599.83	0.9416	1778.99	1909.53	130.53	85.803	601.44	
0.0551	0.1289	1.3335	1858.06	0.9896	17.882	570.55	0.8956	1768.29	1909.53	141.24	85.433	573.37	
0.0636	0.1499	1.2902	1808.94	0.9635	15.882	495.05	0.7771	1739.88	1909.53	169.64	84.438	497.40	
0.0715	0.1699	1.2162	1726.38	0.9195	12.382	370.21	0.5911	1686.22	1909.53	223.30	82.456	373.44	
0.0804	0.1899	1.1484	1609.27	0.8784	8.382	240.44	0.3774	1631.64	1909.53	277.88	80.134	243.90	
0.0913	0.2099	1.0851	1551.45	0.8317	4.632	126.11	0.1579	1556.35	1909.53	353.16	77.214	128.32	
0.0950	0.2249	0.9488	1376.75	0.7322	2.382	57.15	0.0497	1373.56	1909.53	535.97	68.683	61.35	
MASS AVERAGE TOTAL PRESSURE 143.894													
MASS AVERAGE TOTAL TEMPERATURE 1089.031													
MASS AVG VM 927.324 VM 1714.098 ANGLE 17.087													
FLOW FACTOR 0.6205 SLIP FACTOR INS. STA. 0.898													
IMP. PRESS. RATIO 0.000 IMP. TEMP. RATIO 0.000													
IMP.IND. PRESS. RATIO 9.988 IMP.IND. TEMP. RATIO 0.000													
IMP.IND.IGV PRESS. RATIO 9.928 IMP.IND.IGV TEMP. RATIO 0.026													
IMP.IND.IGV PRESS. RATIO 2.101 EFFICIENCY 0.826													
IMP.IND.IGV PRESS. RATIO 2.101 EFFICIENCY 0.826													

MASS AVERAGE TOTAL PRESSURE 143.894

MASS AVERAGE TOTAL TEMPERATURE 1099.831

MASS AVG VM 927.924 VS 1718.098 ANGLE 17.087

FLOW FACTOR 0.806 SLIP FACTOR INS. STA. 0.898

IMP. PRESS. RATIO 0.600 IMP. TEMP. RATIO 0.000

IMP. IND. PRESS. RATIO 9.988 IMP. IND. IGV TEMP. RATIO 2.101

IMP. IND. IGV PRESS. RATIO 9.928 IMP. IND. IGV TEMP. RATIO 2.101

IMP. IND. IGV PRESS. RATIO 9.928 IMP. IND. IGV TEMP. RATIO 2.101

IMP. IND. IGV PRESS. RATIO 9.928 IMP. IND. IGV TEMP. RATIO 2.101

IMP. IND. IGV PRESS. RATIO 9.928 IMP. IND. IGV TEMP. RATIO 2.101

IMP. IND. IGV PRESS. RATIO 9.928 IMP. IND. IGV TEMP. RATIO 2.101

IMP. IND. IGV PRESS. RATIO 9.928 IMP. IND. IGV TEMP. RATIO 2.101

IMP. IND. IGV PRESS. RATIO 9.928 IMP. IND. IGV TEMP. RATIO 2.101

IMP. IND. IGV PRESS. RATIO 9.928 IMP. IND. IGV TEMP. RATIO 2.101

IMP. IND. IGV PRESS. RATIO 9.928 IMP. IND. IGV TEMP. RATIO 2.101

IMP. IND. IGV PRESS. RATIO 9.928 IMP. IND. IGV TEMP. RATIO 2.101

IMP. IND. IGV PRESS. RATIO 9.928 IMP. IND. IGV TEMP. RATIO 2.101

TABLE LXXVIII.

10/1 CENTRIFUGAL COMPRESSOR, IMPELLER TRAVERSE  
95 PCT SPEED, NEAR STALL, 10 DEG IGV TURNING  
BUILD 6

FLOW RATE = 2.877 SPEED = 62138.8

*** IMPELLER EXIT ***		INITIAL INTEGRATED FLOW 2-621									
PERCENT SPAN	R	MD	VO	VD/VMAX	ALP	VM	VM/VMAX	VU	U	WU	W
0-0536	0-0149	1-0886	1968-89	0-8328	14-994	409-92	0-8103	1515-47	1910-29	394-82	75-397
0-1273	0-0300	1-2679	1774-63	0-9419	18-994	577-55	0-8684	1677-82	1910-29	232-46	82-111
0-2122	0-0520	1-3218	1835-24	0-9742	21-244	653-01	1-0003	1710-54	1910-29	199-75	83-339
0-2971	0-0899	1-3394	1860-98	0-9879	20-244	653-95	0-9883	1740-51	1910-29	164-27	84-625
0-3820	0-1099	1-3476	1876-33	0-9950	19-2-4	618-44	0-9299	1771-48	1910-29	138-80	85-519
0-4660	0-1299	1-3523	1883-74	1-0000	18-994	613-12	0-9219	1761-17	1910-29	129-12	85-853
0-5517	0-1499	1-3512	1861-28	0-9880	18-244	582-72	0-8762	1767-71	1910-29	142-58	85-388
0-6366	0-1699	1-2808	1809-29	0-9523	15-994	497-44	0-7480	1735-40	1910-29	174-89	84-243
0-7219	0-1899	1-2117	1727-16	0-9168	12-494	373-67	0-5619	1686-25	1910-29	224-04	82-431
0-8064	0-2099	1-1390	1640-44	0-8708	8-494	242-32	0-3643	1622-44	1910-29	287-84	79-939
0-8913	0-2299	1-0558	1532-77	0-8136	4-744	126-78	0-1906	1527-52	1910-29	382-77	75-932

MASS AVERAGE TOTAL PRESSURE 143.845  
 MASS AVERAGE TOTAL TEMPERATURE 1094-412  
 MASS AVG VM 53-898 YU 178-142 ANGLE 17-858  
 FLOW FACTOR 0-375 SLIP FACTOR INS. STA. 0-899 IMPELLER TIP 0-943  
 IMP. PRESS. RATIO 0-000 IMP. TEMP. RATIO 0-000 EFFICIENCY 0-000  
 IMP. IND. PRESS. RATIO 0-985 IMP. IND. IGV TEMP. RATIO 2-109 EFFICIENCY 0-821  
 IMP. IND. IGV PRESS. RATIO 9-925 IMP. IND. IGV TEMP. RATIO 2-109 EFFICIENCY 0-816

TABLE LXXIX.

10/1 CENTRIFUGAL COMPRESSOR, IMPELLER TRAVERSE  
101 ACT SPEED, NEAR STALL, -4 DEG IGV TURNING  
BUILD 6

FLOW RATE = 1.209 SPEED = 65987.7

*** IMPELLER EXIT ***			INITIAL INTEGRATED FLOW 2.635										
P-CENT	SPAN	R	MO	VO	VO/VMAX	ALP	VM	VM/VMAX	VU	U	WU	W	MO
0.0233	0.0055	0.0283	1428.75	0.7131	0.7131	11.431	283.17	0.4033	1400.40	2028.61	428.21	65.839	310.36
0.0248	0.0200	1.1484	1713.64	0.8253	0.8253	15.431	455.96	0.6927	1651.66	2028.61	376.75	77.132	467.69
0.1607	0.0339	1.2148	1608.73	0.8237	0.8237	19.681	642.85	0.9262	1797.22	2028.61	231.39	82.663	648.15
0.2546	0.0600	1.3722	1978.01	0.8873	0.8873	20.681	698.52	1.0000	1950.54	2028.61	178.07	84.503	701.81
0.3395	0.0799	1.5828	1995.37	0.9939	0.9939	19.431	663.82	0.9502	1881.71	2028.61	144.90	85.536	665.84
0.4244	0.0999	1.7874	2002.57	0.9995	0.9995	18.431	633.16	0.9063	1899.84	2028.61	128.77	86.122	634.61
0.5093	0.1200	1.9874	2003.63	1.0000	1.0000	17.431	608.50	0.8710	1908.78	2028.61	119.82	86.407	609.70
0.5942	0.1400	1.9817	1975.51	0.9940	0.9940	16.431	558.92	0.7999	1894.83	2028.61	133.78	85.981	560.21
0.6791	0.1599	1.9124	1919.89	0.9923	0.9923	14.181	470.37	0.6733	1861.38	2028.61	167.23	84.864	472.26
0.7640	0.1800	1.2503	1847.33	0.9240	0.9240	10.681	342.41	0.4901	1815.32	2028.61	213.29	83.298	344.76
0.8488	0.2000	1.1683	1744.62	0.8707	0.8707	6.931	210.52	0.3013	1731.67	2028.61	296.94	80.269	213.60
0.9125	0.2150	1.1062	1647.38	0.8222	0.8222	3.431	95.51	0.1411	1644.42	2028.61	384.18	76.849	101.26
0.9950	0.2250	1.0500	1557.30	0.7773	0.7773	0.181	4.94	0.0070	1557.29	2028.61	471.32	73.161	9.16
0.9988	0.2325	0.8769	1326.10	0.6619	0.6619	-2.318	-53.64	-0.0767	1325.02	2028.61	703.59	62.031	-60.73

MASS AVERAGE TOTAL PRESSURE 172.835

MASS AVERAGE TOTAL TEMPERATURE 1194.597

MASS AVG VM 584.387 VU 1833.551

FLOW FACTOR 0.800 SLIP FACTOR INS. STA. 17.108

IMP. PRESS. RATIO 0.800 IMP. TEMP. RATIO 0.903

IMP. IND. PRESS. RATIO 11.892 IMP. IND. TEMP. RATIO 0.000

IMP. IND. IGV PRESS. RATIO 11.762 IMP. IND. IGV TEMP. RATIO 0.000

IMP. IND. IGV PRESS. RATIO 2.303 IMP. IND. IGV TEMP. RATIO 0.748

IMP. IND. IGV PRESS. RATIO 0.763



TABLE LXXX.

10/1 CENTRIFUGAL COMPRESSOR, IMPELLER TRAVERSE  
101 PCT SPEED, NS, -4 DEG IG, WITH COOLANT  
BUILD 6

FLOW RATE = 3.216 SPEED = 65779.6

INITIAL INTEGRATED FLOW 2.657

IMPELLER EXIT

PCENT	SPAN	R	MO	VD	VD/VMAX	ALP	VM	VM/VMAX	VU	U	WU	S	MO
0.0742	0.0179	1.2714	1855.99	0.9256	19.395	616.36	0.8368	1750.45	2022.22	271.56	81.182	623.73	
0.1897	0.0600	1.3748	1974.93	0.9849	21.895	736.49	1.0000	1832.47	2022.22	189.73	84.088	740.43	
0.2546	0.0800	1.3839	1994.03	0.9944	20.395	694.92	0.9435	1869.02	2022.22	153.19	85.314	897.26	
0.3195	0.0789	1.3884	2002.12	0.9999	19.443	674.13	0.9153	1888.40	2022.22	133.81	85.946	875.82	
0.4244	0.1000	1.3874	2005.16	1.0000	18.443	641.08	0.8704	1899.91	2022.22	122.30	86.316	842.41	
0.5093	0.1199	1.3887	1986.44	0.9996	17.395	593.29	0.8055	1893.68	2022.22	128.54	86.116	594.43	
0.5942	0.1398	1.3833	1935.90	0.9634	15.895	530.22	0.7199	1881.87	2022.22	160.34	85.077	532.18	
0.6701	0.1599	1.2530	1855.40	0.9253	12.443	406.19	0.5515	1810.39	2022.22	211.83	83.326	408.96	
0.7460	0.1800	1.1871	1774.54	0.8848	8.443	246.76	0.3622	1754.37	2022.22	267.84	81.319	269.85	
0.8276	0.1949	1.1425	1716.47	0.8360	5.895	176.31	0.2393	1707.39	2022.22	314.82	79.532	179.28	
0.8701	0.2050	1.0911	1590.94	0.7934	3.895	108.09	0.1457	1587.27	2022.22	434.95	74.675	112.07	

MASS AVERAGE TOTAL PRESSURE 174.860

MASS AVERAGE TOTAL TEMPERATURE 1194.437

MASS AVG VM 600.004 VU 1861.002 ANGLE 18.052

FLOW FACTOR 0.795 SLIP FACTOR INS. STA. 0.910

IMP. PRESS. RATIO 0.000 IMP. TEMP. RATIO 0.000

IMP. IND. PRESS. RATIO 12.031 IMP. IND. TEMP. RATIO 0.000

IMP. IND. PRESS. RATIO 11.900 IMP. IND. TEMP. RATIO 0.000

IMP. IND. PRESS. RATIO 11.900 IMP. IND. TEMP. RATIO 0.000

IMP. IND. PRESS. RATIO 11.900 IMP. IND. TEMP. RATIO 0.000

IMP. IND. PRESS. RATIO 11.900 IMP. IND. TEMP. RATIO 0.000

IMP. IND. PRESS. RATIO 11.900 IMP. IND. TEMP. RATIO 0.000

IMP. IND. PRESS. RATIO 11.900 IMP. IND. TEMP. RATIO 0.000

IMP. IND. PRESS. RATIO 11.900 IMP. IND. TEMP. RATIO 0.000

IMP. IND. PRESS. RATIO 11.900 IMP. IND. TEMP. RATIO 0.000

IMP. IND. PRESS. RATIO 11.900 IMP. IND. TEMP. RATIO 0.000

IMP. IND. PRESS. RATIO 11.900 IMP. IND. TEMP. RATIO 0.000

IMP. IND. PRESS. RATIO 11.900 IMP. IND. TEMP. RATIO 0.000

IMP. IND. PRESS. RATIO 11.900 IMP. IND. TEMP. RATIO 0.000

IMP. IND. PRESS. RATIO 11.900 IMP. IND. TEMP. RATIO 0.000

IMP. IND. PRESS. RATIO 11.900 IMP. IND. TEMP. RATIO 0.000

IMP. IND. PRESS. RATIO 11.900 IMP. IND. TEMP. RATIO 0.000

IMP. IND. PRESS. RATIO 11.900 IMP. IND. TEMP. RATIO 0.000

IMP. IND. PRESS. RATIO 11.900 IMP. IND. TEMP. RATIO 0.000

IMP. IND. PRESS. RATIO 11.900 IMP. IND. TEMP. RATIO 0.000

IMP. IND. PRESS. RATIO 11.900 IMP. IND. TEMP. RATIO 0.000

TABLE LXXXI.

10/1 CENTRIFUGAL COMPRESSOR. IMPELLER TRAVERSE  
101 PCT SPEED. NEAR STALL. 0 DEG IGV TURNING  
BUILD 6

FLOW RATE = 3.185 SPEED = 65952.0

* * * IMPELLER EXIT * * *										INITIAL INTEGRATED FLOW 2.679									
SCENT	SPAN	R	MD	VO	VO/VMAX	ALP	VM	VM/VMAX	VU	U	WU	B	MO						
0.0233	0.0034		1.0687	1613.46	0.8022	13.192	368.22	0.2189	1570.88	2027.54	456.66	73.790	383.47						
0.0236	0.0168		1.2315	1836.50	0.9131	17.192	562.83	0.7650	1756.44	2027.54	273.10	81.152	549.37						
0.0273	0.0500		1.3312	1927.39	0.9584	20.442	573.24	0.9488	1806.20	2027.54	221.34	83.013	678.27						
0.0282	0.0500		1.3816	1983.03	0.9870	20.942	709.50	1.0000	1853.90	2027.54	173.63	84.649	712.61						
0.02971	0.0699		1.3874	1998.23	0.9936	19.942	681.54	0.9605	1878.41	2027.54	149.13	85.480	683.69						
0.0320	0.0888		1.3921	2011.07	1.0000	18.942	652.82	0.9201	1902.16	2027.54	125.38	86.228	654.24						
0.0368	0.1099		1.3886	2009.88	0.9994	17.642	619.16	0.8726	1912.13	2027.54	115.41	86.545	620.29						
0.0317	0.1299		1.3852	1986.84	0.9869	16.692	570.11	0.8035	1901.20	2027.54	126.34	86.198	571.36						
0.0366	0.1499		1.3218	1936.44	0.9628	14.442	482.95	0.6806	1875.24	2027.54	152.29	85.356	484.55						
0.0219	0.1899		1.2597	1864.23	0.9269	10.692	345.88	0.4874	1831.86	2027.54	195.67	83.902	367.84						
0.0364	0.2099		1.1882	1779.12	0.8846	6.692	207.33	0.2922	1767.00	2027.54	260.54	81.612	209.57						
0.0701	0.2069		1.1296	1706.69	0.8483	4.192	124.75	0.1758	1701.89	2027.54	325.65	79.167	127.01						
0.0829	0.2330		1.0710	1631.73	0.8113	2.192	62.42	0.0879	1630.53	2027.54	396.98	76.316	64.24						
0.0950	0.2548		0.7738	1221.61	0.6074	0.192	4.10	0.0057	1221.60	2027.54	805.94	56.585	4.91						

MASS AVERAGE TOTAL PRESSURE 173.429

MASS AVERAGE TOTAL TEMPERATURE 1193.339

MASS AVG VM 982.282 YU 1850.259 ANGLE 17.488

FLOW FACTOR 0.778 SLIP FACTOR INS. STA. 0.912

IMP. PRESS. RATIO 0.200 IMP. TEMP. RATIO 0.000

IMP.IND. PRESS. RATIO 11.877 IMP.IND. TEMP. RATIO 0.000

IMP.IND.IGV PRESS. RATIO 11.802 IMP.IND.IGV TEMP. RATIO 0.000

IMP.IND.IGV PRESS. RATIO 2.300 EFFICIENCY 0.768

IMP.IND.IGV PRESS. RATIO 2.300 EFFICIENCY 0.768

IMP.IND.IGV PRESS. RATIO 2.300 EFFICIENCY 0.768

IMP.IND.IGV PRESS. RATIO 2.300 EFFICIENCY 0.768

IMP.IND.IGV PRESS. RATIO 2.300 EFFICIENCY 0.768

IMP.IND.IGV PRESS. RATIO 2.300 EFFICIENCY 0.768

IMP.IND.IGV PRESS. RATIO 2.300 EFFICIENCY 0.768

IMP.IND.IGV PRESS. RATIO 2.300 EFFICIENCY 0.768

IMP.IND.IGV PRESS. RATIO 2.300 EFFICIENCY 0.768

IMP.IND.IGV PRESS. RATIO 2.300 EFFICIENCY 0.768

IMP.IND.IGV PRESS. RATIO 2.300 EFFICIENCY 0.768

IMP.IND.IGV PRESS. RATIO 2.300 EFFICIENCY 0.768

IMP.IND.IGV PRESS. RATIO 2.300 EFFICIENCY 0.768

IMP.IND.IGV PRESS. RATIO 2.300 EFFICIENCY 0.768

IMP.IND.IGV PRESS. RATIO 2.300 EFFICIENCY 0.768

TABLE LXXXII.

10/1 CENTRIFUGAL COMPRESSOR, IMPELLER TRAVERSE  
101 PCT SPEED, NEAR STALL, 5 DEG IGV TURNING  
BUILD 6

FLOW RATE • 3.142 SPEED • 66122.6

*** IMPELLER EXIT ***										INITIAL INTEGRATED FLOW 2.791									
PCT	SPAN	R	MD	VO	VO/VMAX	ALP	VM	VM/VMAX	VU	U	MU	B	MO						
0.0445	0.0105	1.0957	1.3339	1.3746	1.3921	1.4003	1.4039	1.4039	1.4039	1.4039	1.4039	1.4039	1.4039	1.4039	1.4039	1.4039	1.4039	1.4039	1.4039
0.1051	0.0250	1.3339	1.3746	1.3921	1.4003	1.4039	1.4039	1.4039	1.4039	1.4039	1.4039	1.4039	1.4039	1.4039	1.4039	1.4039	1.4039	1.4039	1.4039
0.1697	0.0400	1.3746	1.3921	1.4003	1.4039	1.4039	1.4039	1.4039	1.4039	1.4039	1.4039	1.4039	1.4039	1.4039	1.4039	1.4039	1.4039	1.4039	1.4039
0.2546	0.0600	1.3921	1.4003	1.4039	1.4039	1.4039	1.4039	1.4039	1.4039	1.4039	1.4039	1.4039	1.4039	1.4039	1.4039	1.4039	1.4039	1.4039	1.4039
0.3395	0.0799	1.4003	1.4039	1.4039	1.4039	1.4039	1.4039	1.4039	1.4039	1.4039	1.4039	1.4039	1.4039	1.4039	1.4039	1.4039	1.4039	1.4039	1.4039
0.4244	0.1000	1.4039	1.4039	1.4039	1.4039	1.4039	1.4039	1.4039	1.4039	1.4039	1.4039	1.4039	1.4039	1.4039	1.4039	1.4039	1.4039	1.4039	1.4039
0.5093	0.1199	1.3898	1.3441	1.2705	1.2070	1.1109	0.9378	0.7081	0.4589	0.2032	0.0658	0.0000	0.0000	0.0000	0.0000	0.0000	0.0000	0.0000	0.0000
0.5942	0.1399	1.3441	1.2705	1.2070	1.1109	0.9378	0.7081	0.4589	0.2032	0.0658	0.0000	0.0000	0.0000	0.0000	0.0000	0.0000	0.0000	0.0000	0.0000
0.6791	0.1599	1.2705	1.2070	1.1109	0.9378	0.7081	0.4589	0.2032	0.0658	0.0000	0.0000	0.0000	0.0000	0.0000	0.0000	0.0000	0.0000	0.0000	0.0000
0.7640	0.1800	1.2070	1.1109	0.9378	0.7081	0.4589	0.2032	0.0658	0.0000	0.0000	0.0000	0.0000	0.0000	0.0000	0.0000	0.0000	0.0000	0.0000	0.0000
0.8488	0.1999	1.1109	0.9378	0.7081	0.4589	0.2032	0.0658	0.0000	0.0000	0.0000	0.0000	0.0000	0.0000	0.0000	0.0000	0.0000	0.0000	0.0000	0.0000
0.9325	0.2150	0.9378	0.7081	0.4589	0.2032	0.0658	0.0000	0.0000	0.0000	0.0000	0.0000	0.0000	0.0000	0.0000	0.0000	0.0000	0.0000	0.0000	0.0000

MASS AVERAGE TOTAL PRESSURE 187.975

MASS AVERAGE TOTAL TEMPERATURE 1201.692

MASS AVG VM 592.968 VU 1861.167

FLOW FACTOR 0.772 SLIP FACTOR INS. STA. 17.851

IMP. PRESS. RATIO 0.000 IMP. TEMP. RATIO 0.000

IMP. IND. PRESS. RATIO 11.911 IMP. IND. TEMP. RATIO 2.316

IMP. IND. IGV PRESS. RATIO 11.631 IMP. IND. IGV TEMP. RATIO 0.743

IMPELLER TIP

EFFICIENCY 0.949

EFFICIENCY 0.000

EFFICIENCY 0.746

EFFICIENCY 0.743

### STATIC PRESSURE DISTRIBUTIONS

This section consists of static pressures along the entire flow path of the rig for Builds No. 3 and 6. Figures 220 through 229 consist of static pressure profiles along the inlet flow path; Figures 230 through 239 of static pressure variations along the impeller shroud; and Figures 240 and 241 of diffuser static pressure profiles.

Figures 220 through 225 are Build No. 3 data, which had a straight axial inlet, shroud, and hub static pressure taps from the inlet guide vane leading edge to the impeller. Figures 226 through 229 consist of Build No. 6 static pressures with the converging inlet, which had only shroud static taps. These taps range from the inlet guide vane trailing edge through the inducer. Figures 230 through 235 show Build No. 3 shroud static pressures along the impeller shroud and Figures 236 through 239 show the pressures for Build No. 6. Figure 240 is a Build No. 3 diffuser static pressure profile for 95% speed and inlet guide vanes of 0, 10, and 20 deg. Figure 241 is a Build No. 3 diffuser static pressure profile for a 10-deg inlet guide vane at speeds of 30, 70, 95, and 100%.

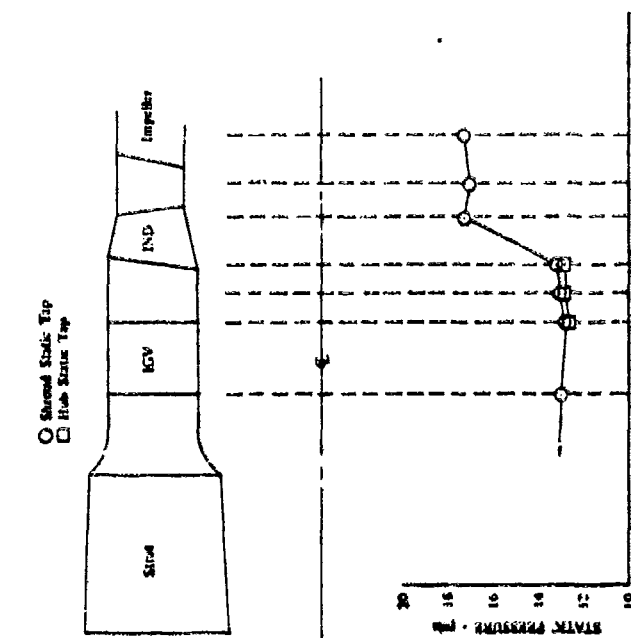


Figure 220. Static Pressure Profile Along Flow Path, Build No. 3, 109% Speed, 10-deg IGV, Near Stall.

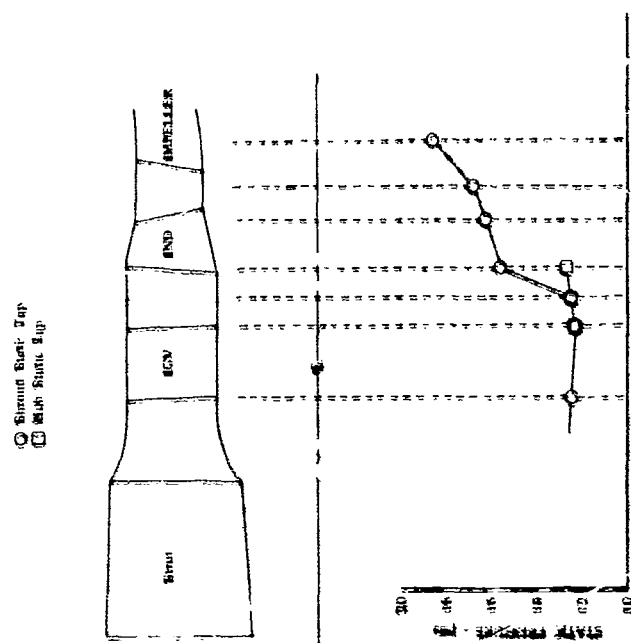


Figure 221. Static Pressure Profile Along Flow Path, Build No. 3, 95% Speed, 20-deg IGV, Near Stall.

○ Shroud Static Tap  
□ Hub Static Tap

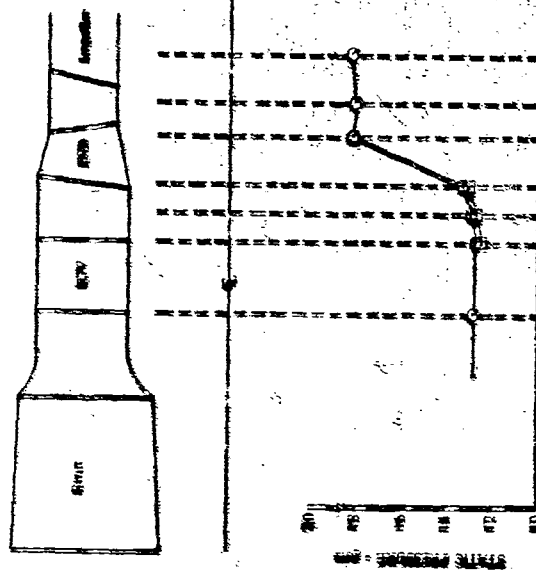


Figure 222. Static Pressure Profile Along Flow Path, Build No. 3, 95% Speed, 10-deg IGV, Wide Open Discharge.

○ Shroud Static Tap  
□ Hub Static Tap

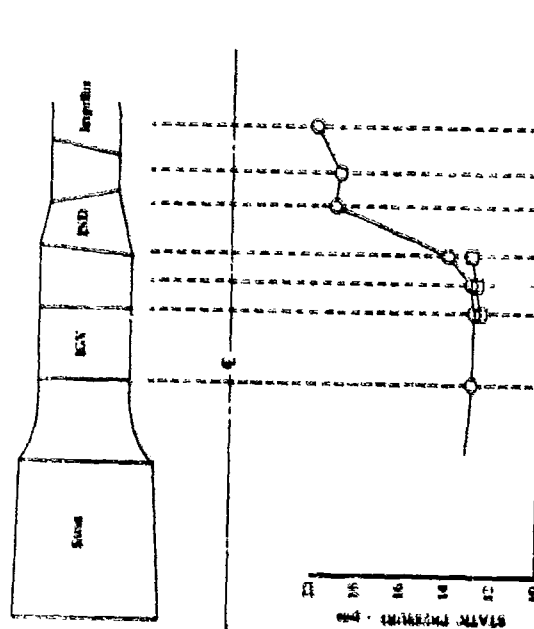


Figure 223. Static Pressure Profile Along Flow Path, Build No. 3, 95% Speed, 10-deg IGV, Near Stall.

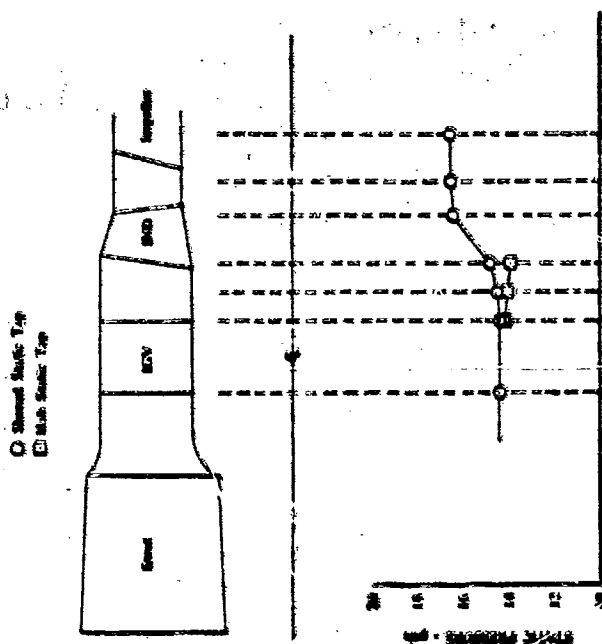


Figure 225. Static Pressure Profile Along Flow Path, Build No. 3, 70% Speed, 10-deg IGV, Near Stall.

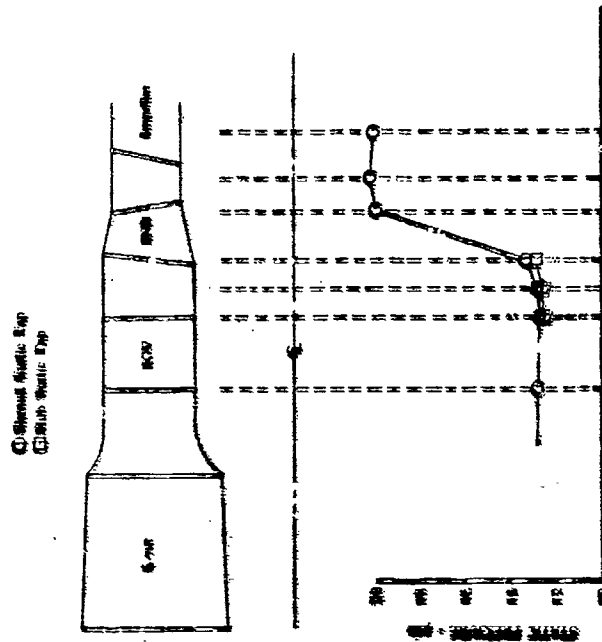


Figure 224. Static Pressure Profile Along Flow Path, Build No. 3, 95% Speed, 0-deg IGV, Near Stall.

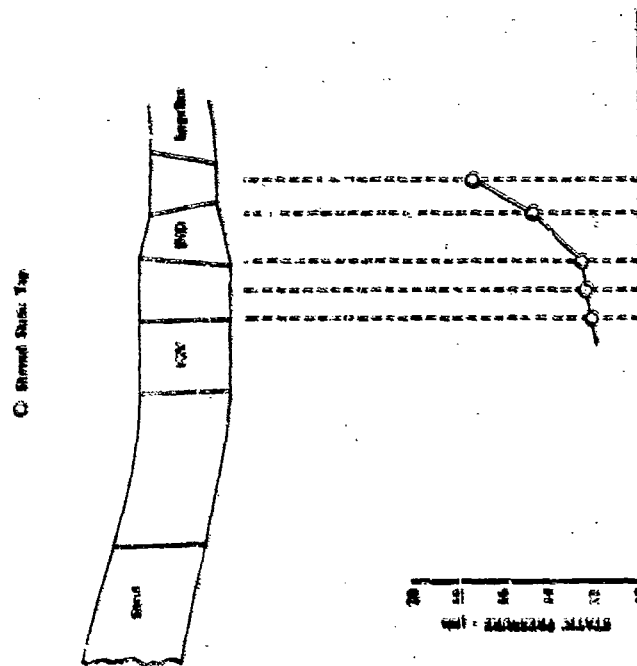


Figure 227. Static Pressure Profile Along Flow Path, Build No. 6, 100% Speed, 10-deg IGV, Near Stall.

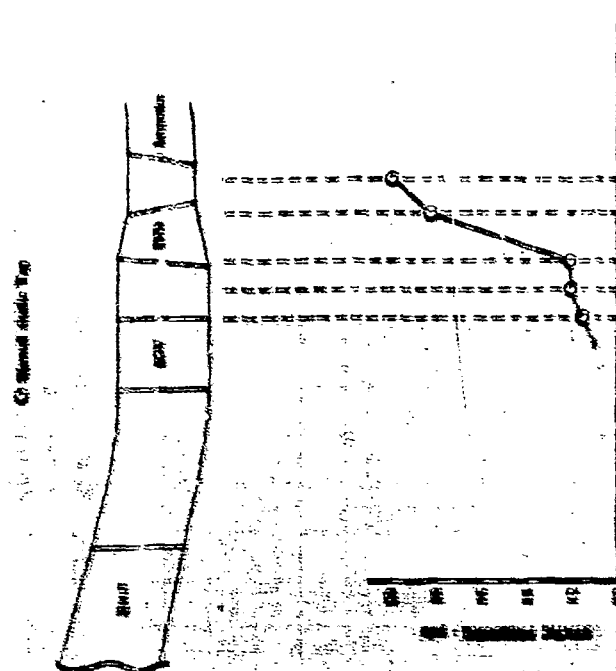


Figure 226. Static Pressure Profile Along Flow Path, Build No. 6, 101% Speed, -4-deg IGV, Wide Open Discharge.



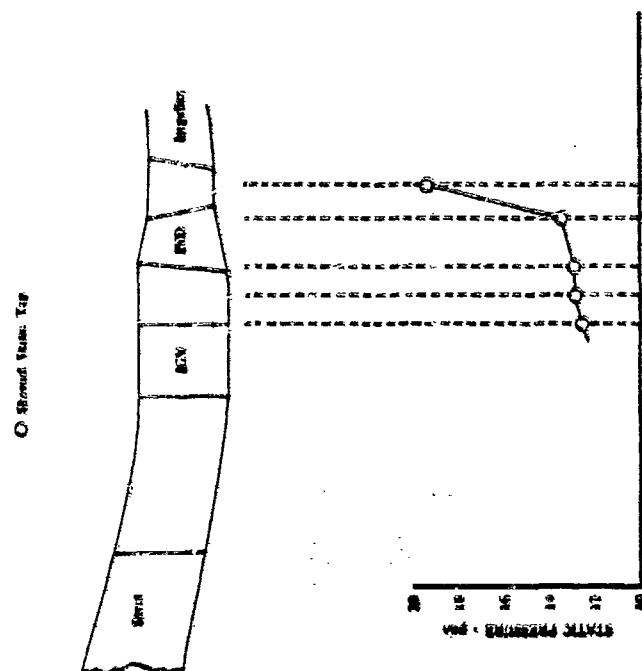


Figure 229. Static Pressure Profile Along Flow Path, Build No. 6, 95% Speed, 10-deg IGV, Near Stall.

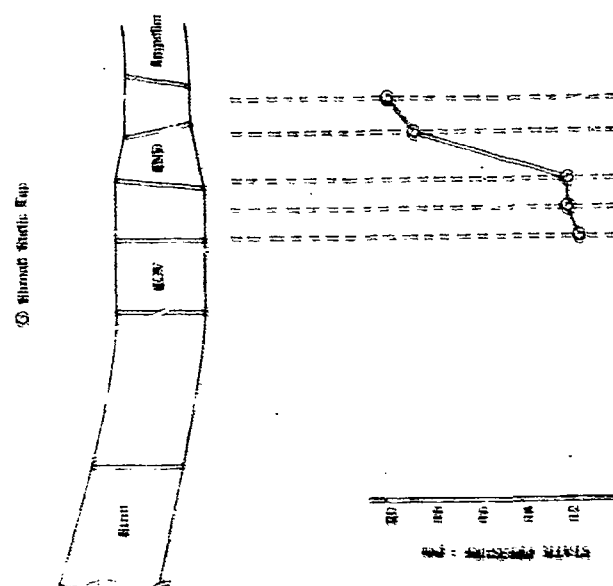


Figure 228. Static Pressure Profile Along Flow Path, Build No. 6, 101% Speed, -4-deg IGV, Near Stall.

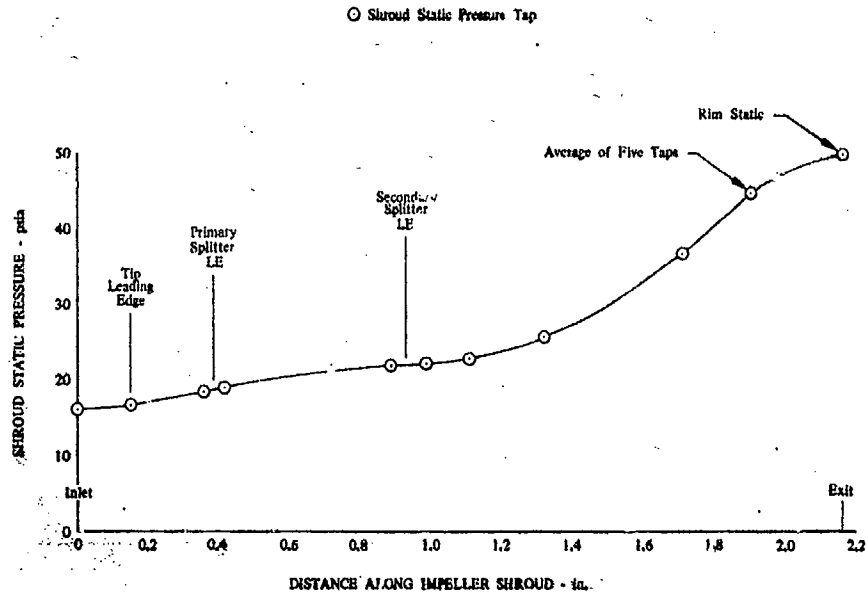


Figure 230. Static Pressure Variation Along Impeller Shroud, Build No. 3, 100% Speed, 10-deg IGV, Near Stall.

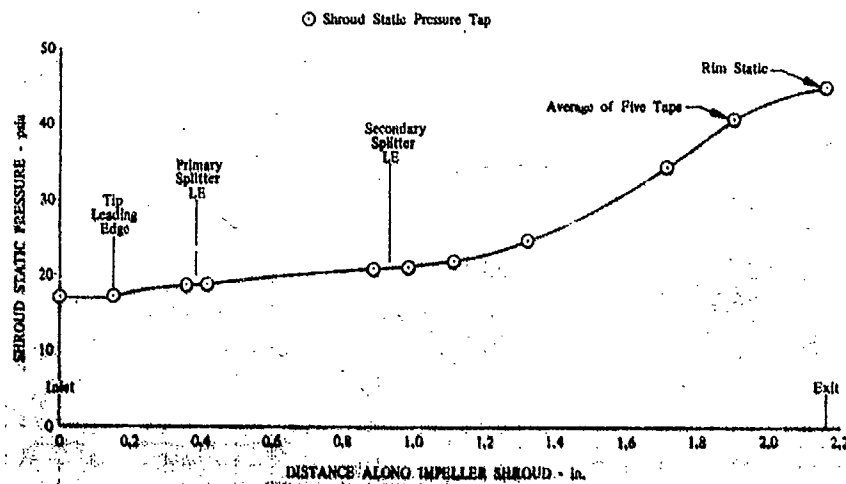


Figure 231. Static Pressure Variation Along Impeller Shroud, Build No. 3, 95% Speed, 20-deg IGV, Near Stall.

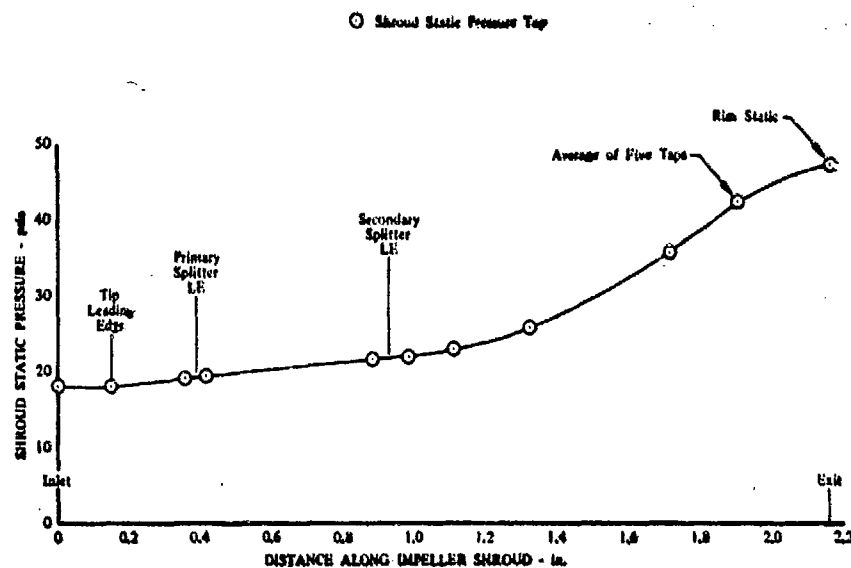


Figure 232. Static Pressure Variation Along Impeller Shroud, Build No. 3, 95% Speed, 10-deg IGV, Wide Open Discharge.

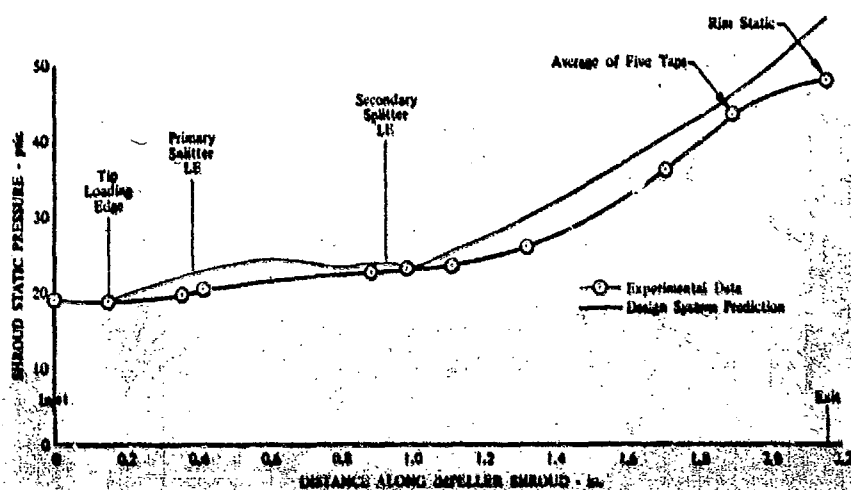


Figure 233. Static Pressure Variation Along Impeller Shroud, Build No. 3, 95% Speed, 10-deg IGV, Near Stall.

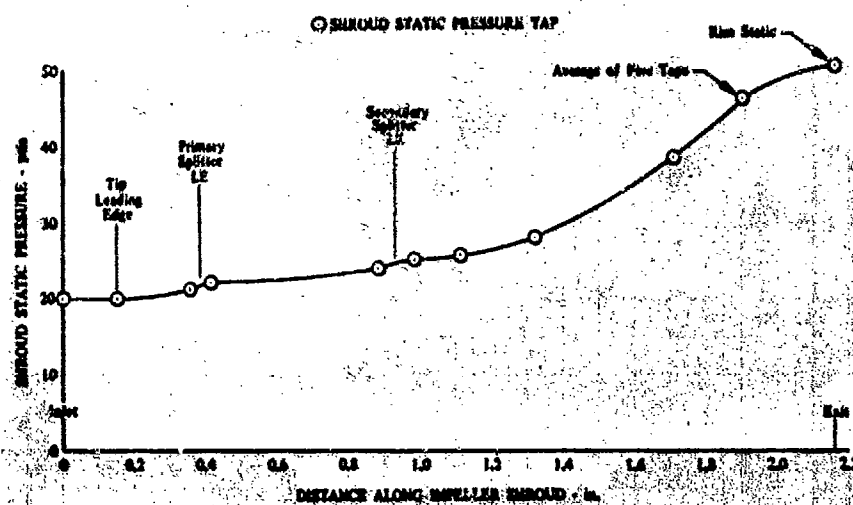


Figure 234. Static Pressure Variation Along Impeller Shroud, Build No. 3, 95% Speed, 0-deg IGV, Near Stall.

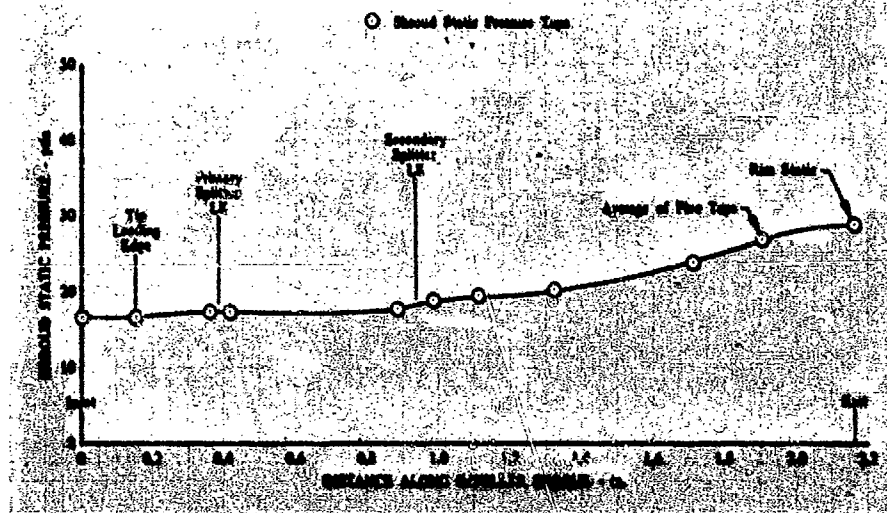


Figure 235. Static Pressure Variation Along Impeller Shroud, Build No. 3, 70% Speed, 10-deg IGV, Near Stall.

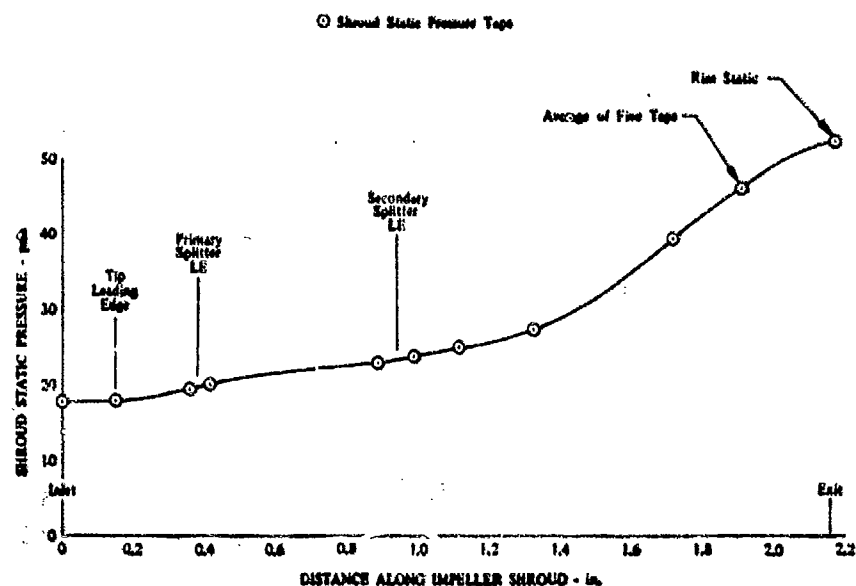


Figure 236. Static Pressure Variation Along Impeller Shroud, Build No. 6, 101% Speed, -4-deg IGV, Wide Open Discharge.

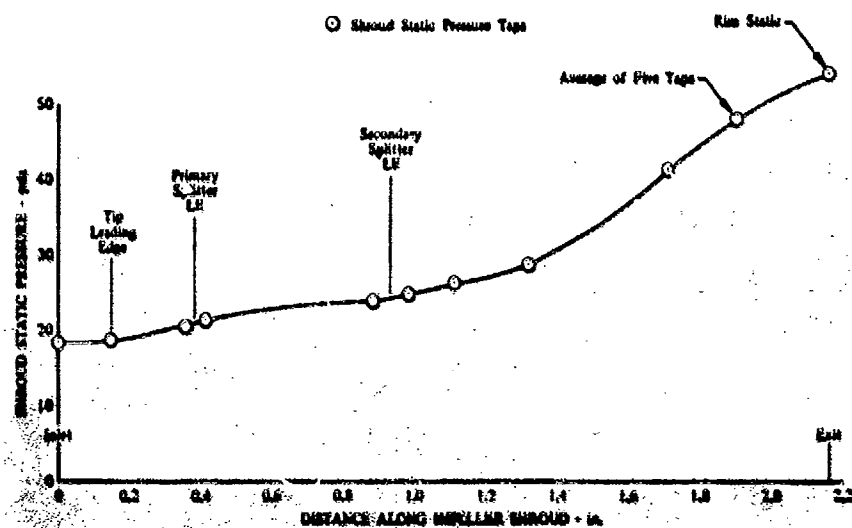


Figure 237. Static Pressure Variation Along Impeller Shroud, Build No. 6, 101% Speed, -4-deg IGV, Near Stall.

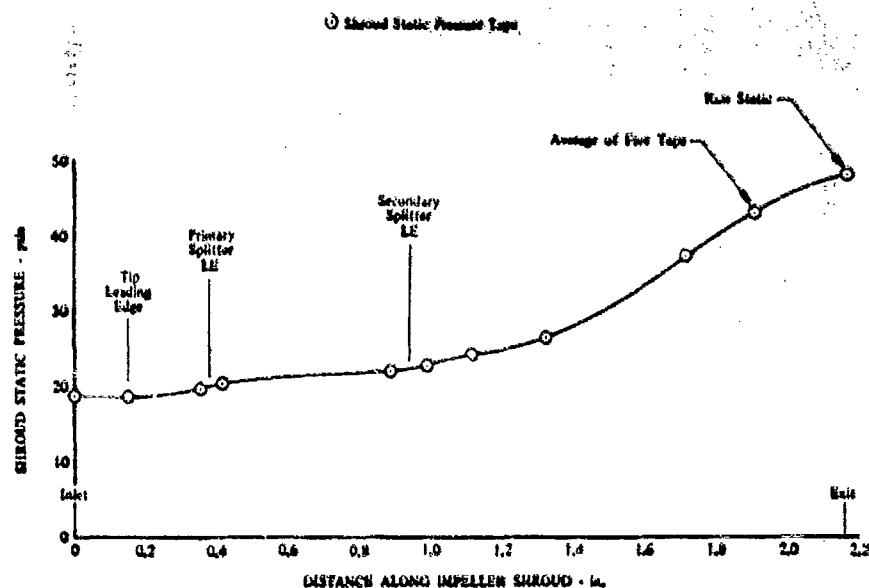


Figure 238. Static Pressure Variation Along Impeller Shroud, Build No. 6, 100% Speed, 10-deg IGV, Near Stall.

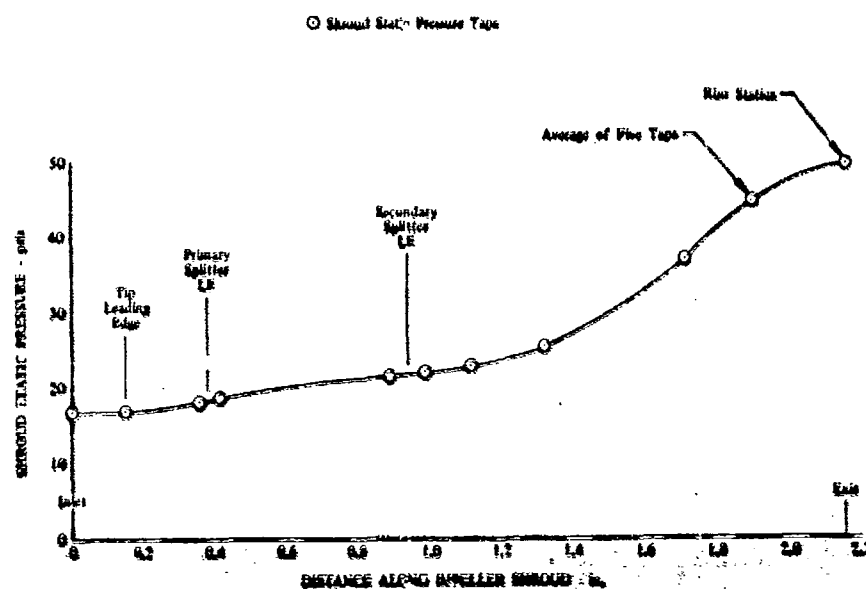


Figure 239. Static Pressure Variation Along Impeller Shroud, Build No. 6, 95% Speed, 10-deg IGV, Near Stall.

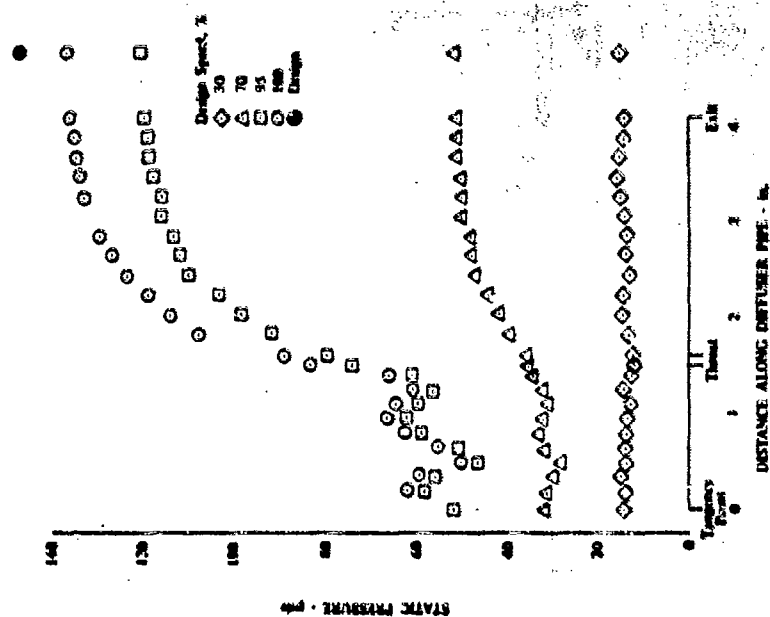


Figure 240. Diffuser Static Pressure Profile, Build No. 3, 95% Speed, Near Stall.

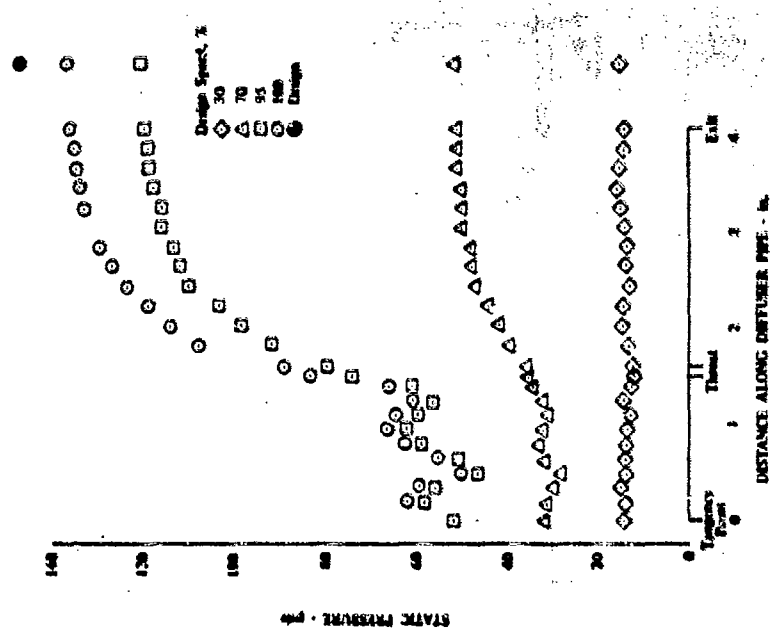


Figure 241. Diffuser Static Pressure Profile, Build No. 3, 10-deg IGV, Near Stall.

### HIGH-FREQUENCY RESPONSE INSTRUMENTATION DATA PLOTS

High-response (Kulite) data were obtained during Build No. 6 testing at a near-stall, steady-state point and during a stall transient for both 70 and 78% design speeds. Data were recorded from one total pressure probe at the impeller exit (header PTIDK1), two static pressure probes in the diffuser vaneless space (PSDVK1 and PSDVK2), and one static pressure probe at the diffuser exit (PSDEK1).

Plots produced from the data are shown in Figures 242 through 296. Each figure includes a plot of pressure vs time, peak-to-peak pressure vs frequency, and a cross correlation. The cross correlation was generated to determine the commonality of the signals. It was accomplished as follows: Time samples of the two waveforms to be correlated were divided into a number of segments. The corresponding segments of the two waveforms were multiplied together and the resulting products were summed to obtain a value that was representative of the similarity of the two waveforms at time delay zero. The segments of one of the waveforms were shifted in time by a chosen amount. The corresponding segments of the first waveform and the time shifted segments of the second waveform were multiplied together and their products summed to obtain a value that was representative of the similarities of the first waveform and a time shifted version of the second waveform. The shift in time, multiplication, and summation were repeated for all time delays of interest. The cross-correlation plot is a plot of these similarities vs their corresponding time delays. Plots produced at a near-stall, steady-state point at 70% speed for each parameter are shown in Figures 242 through 245. Figures 246 through 251 show the plots produced from the total pressure Kulite data at successive time increments proceeding into stall at 70% speed. The time statement on each plot refers to the day of the year, hour of day, minute, second, and fraction of second. The fraction of second code is included in the title of each plot to aid in identification. Transient plots at the same successive time increments for PSDVK1, PSDVK2, and PSDEK1 are shown in Figures 252 through 257, Figures 258 through 263, and Figures 264 through 269, respectively. Near-stall, steady-state plots at 78% speed for each parameter are shown in Figures 270 through 273. The transient plots into stall for each parameter at 78% speed are as follows: PTIDK1, Figures 274 through 279; PSDVK1, Figures 280 through 285; PSDVK2, Figures 286 through 291; and PSDEK1, Figures 292 through 297.



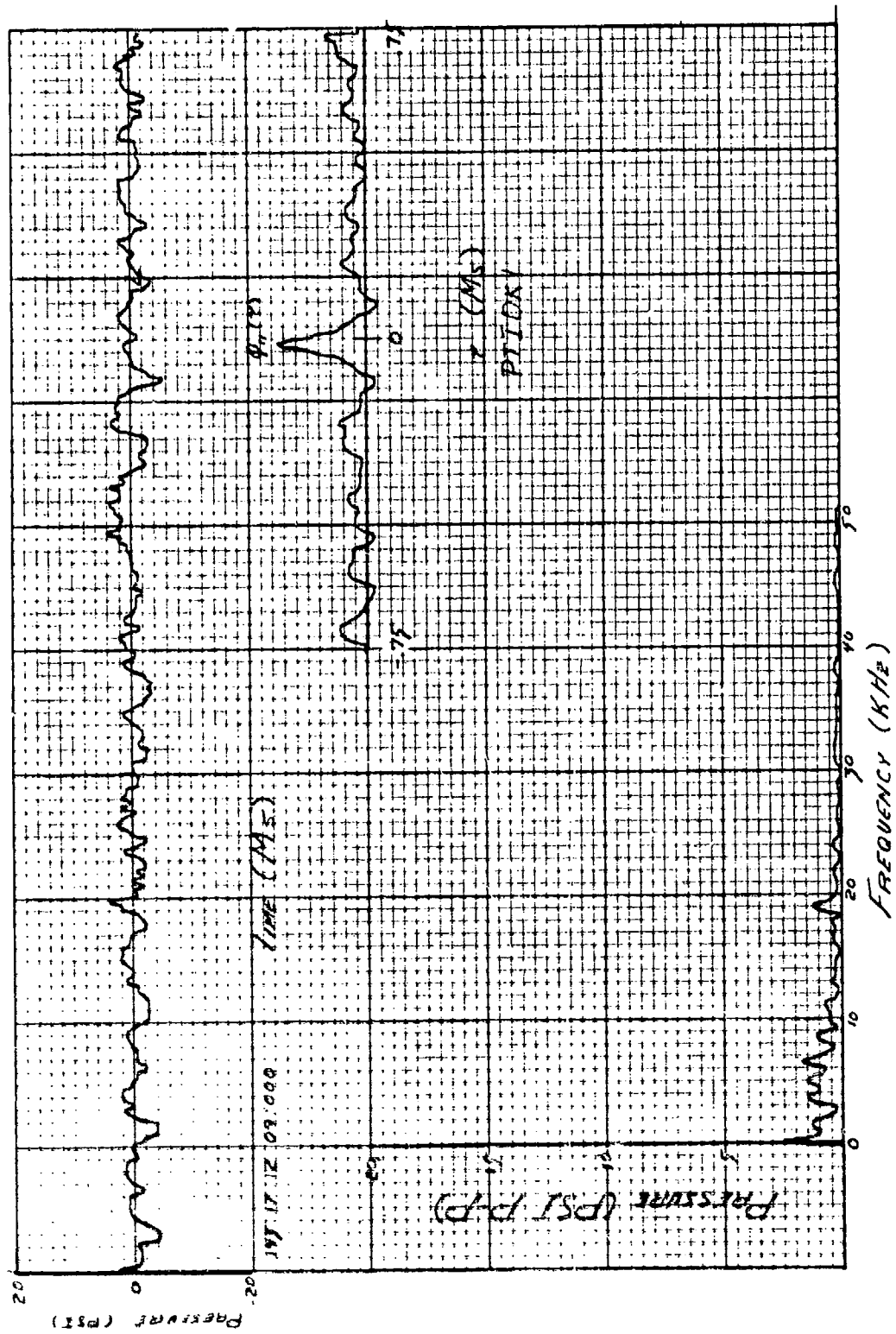


Figure 2-2. High-Frequency Response Data, 70% Speed, Steady-State, PTIDK1.

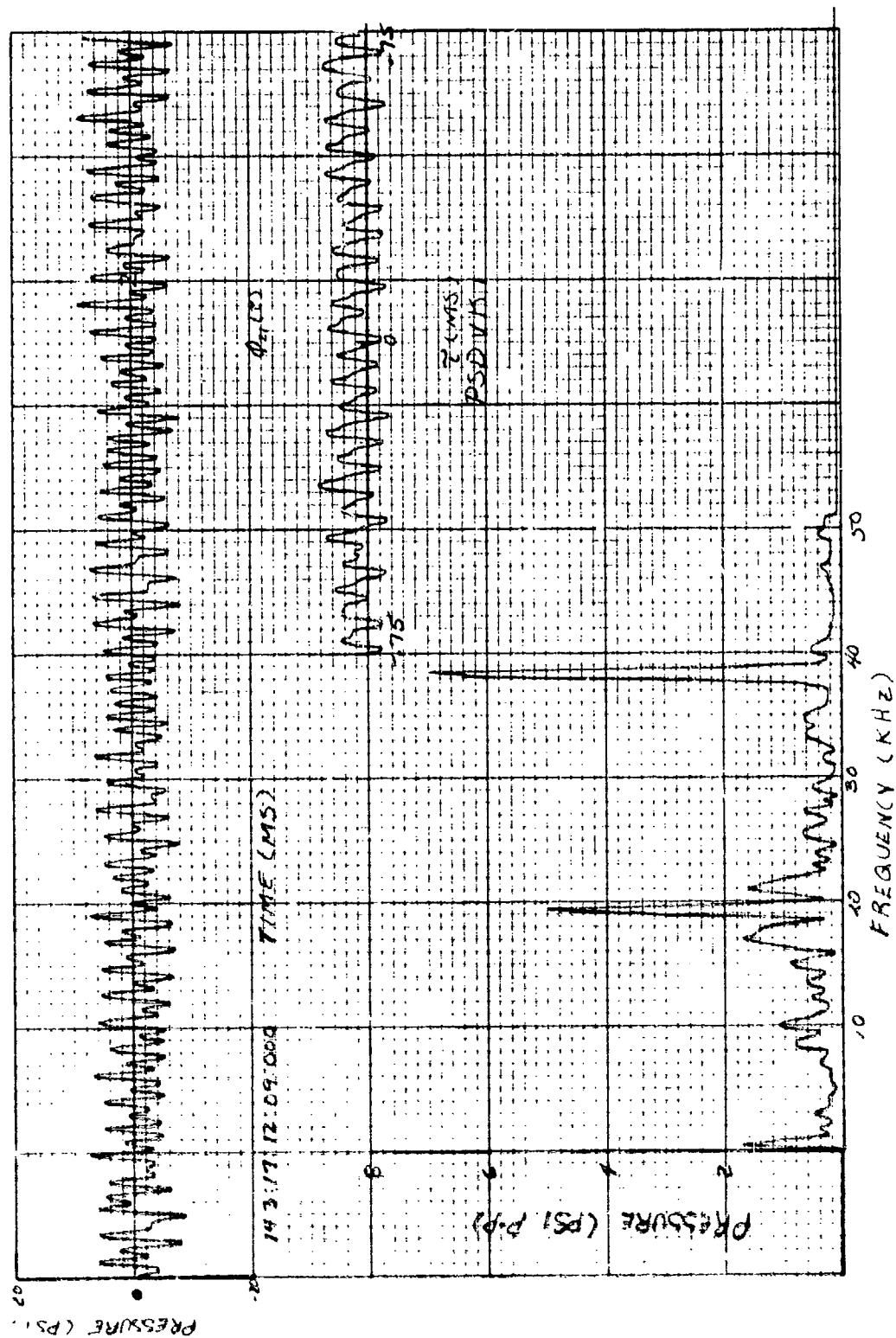


Figure 243. High-Frequency Response Data, 70% Speed, Steady-State, PSDVK1.

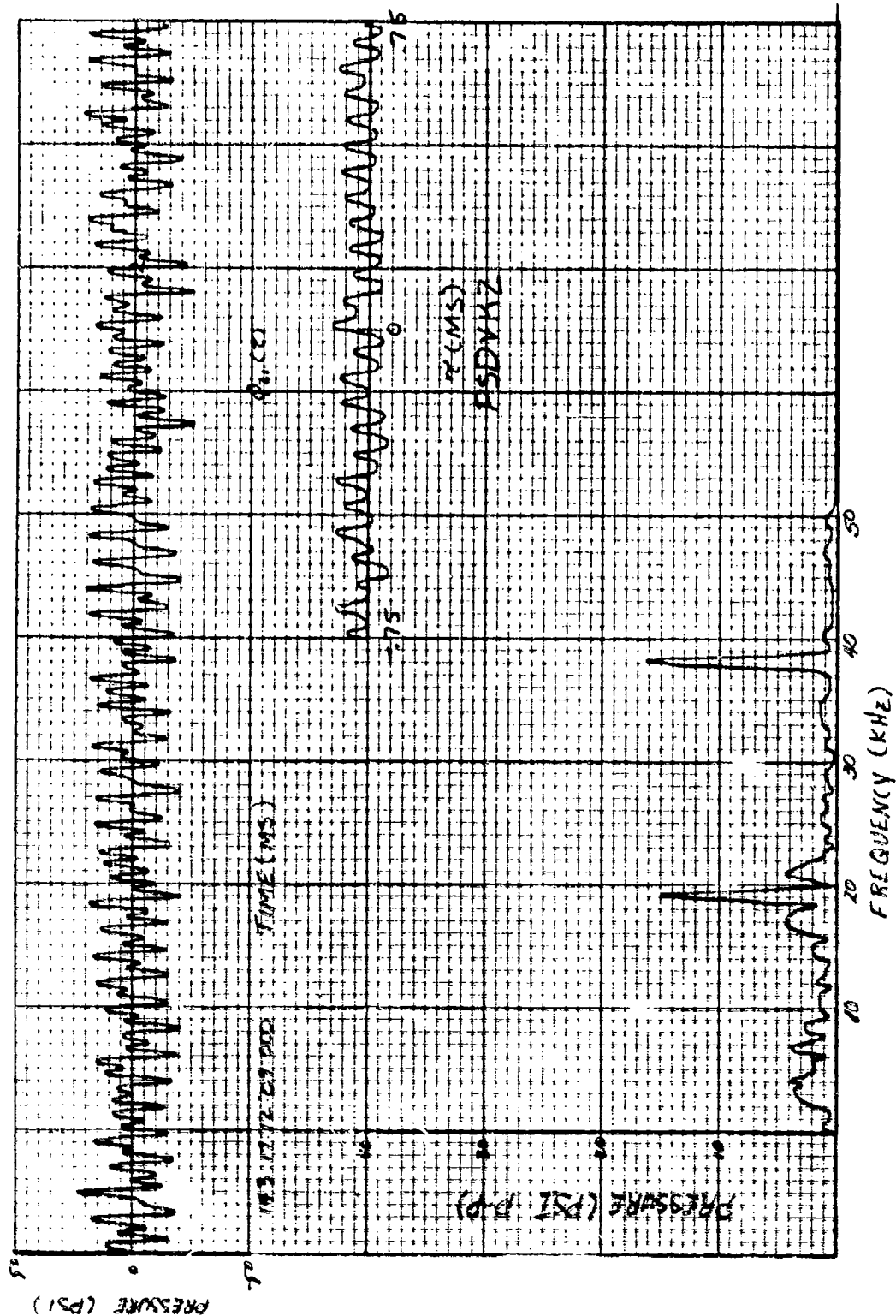


Figure 244. High-Frequency Response Data, 70% Speed, Steady-State, PSDVK2.

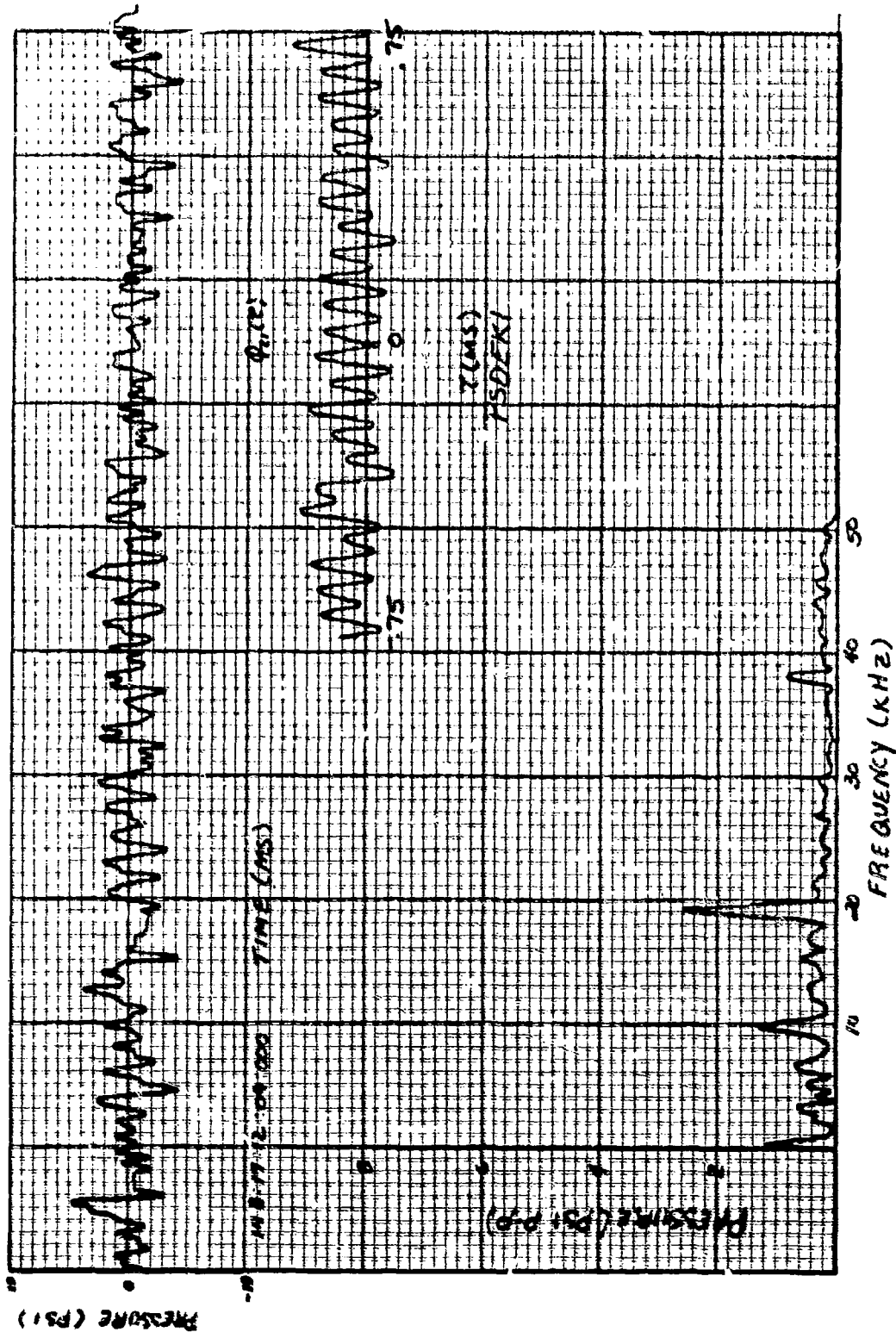


Figure 245. High-Frequency Response Data, 70% Speed, Steady-State, PSEDEK1.

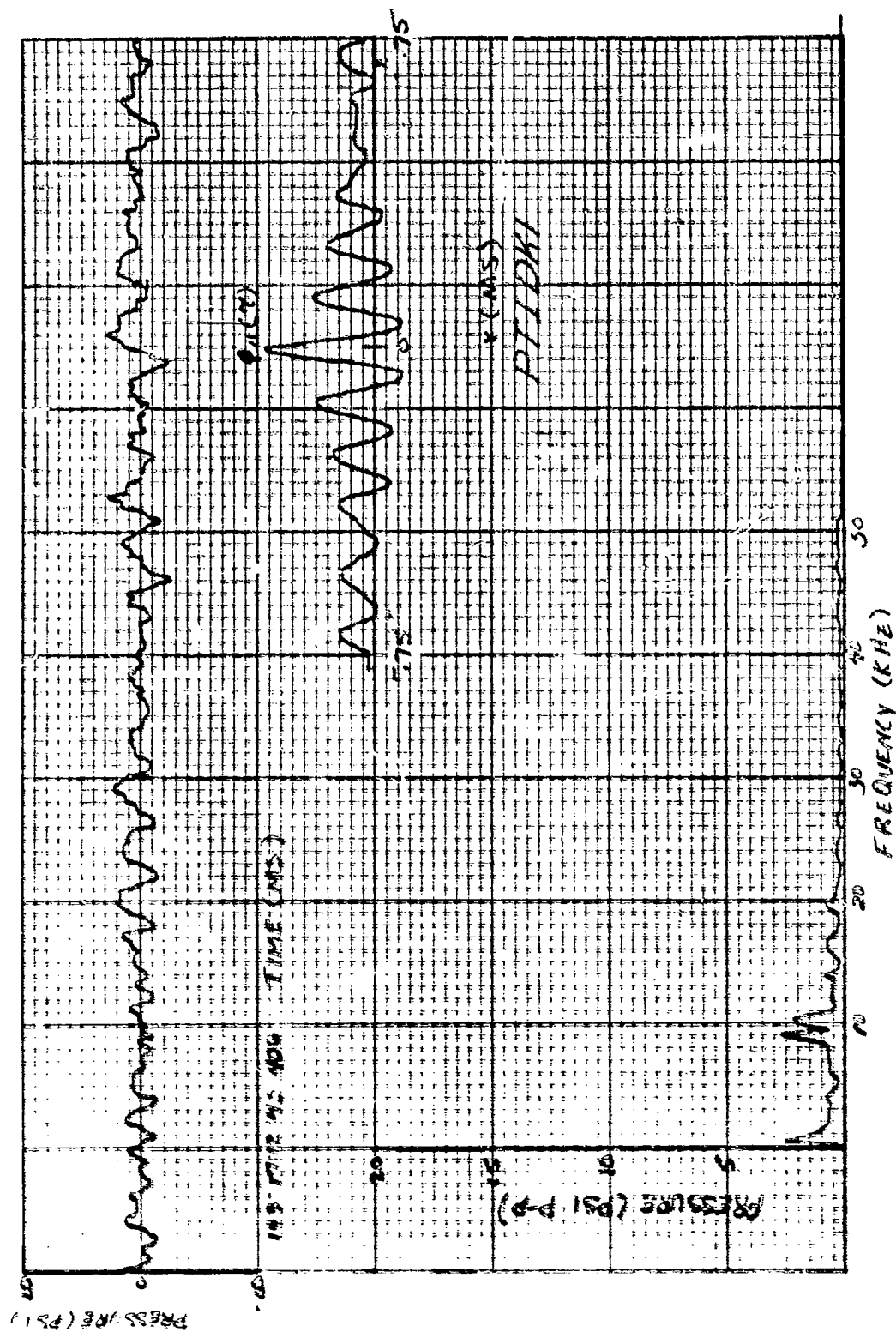


Figure 246. High-Frequency Response Data, 70° Speed, Stall Transient, Time 406, PTIDK1.

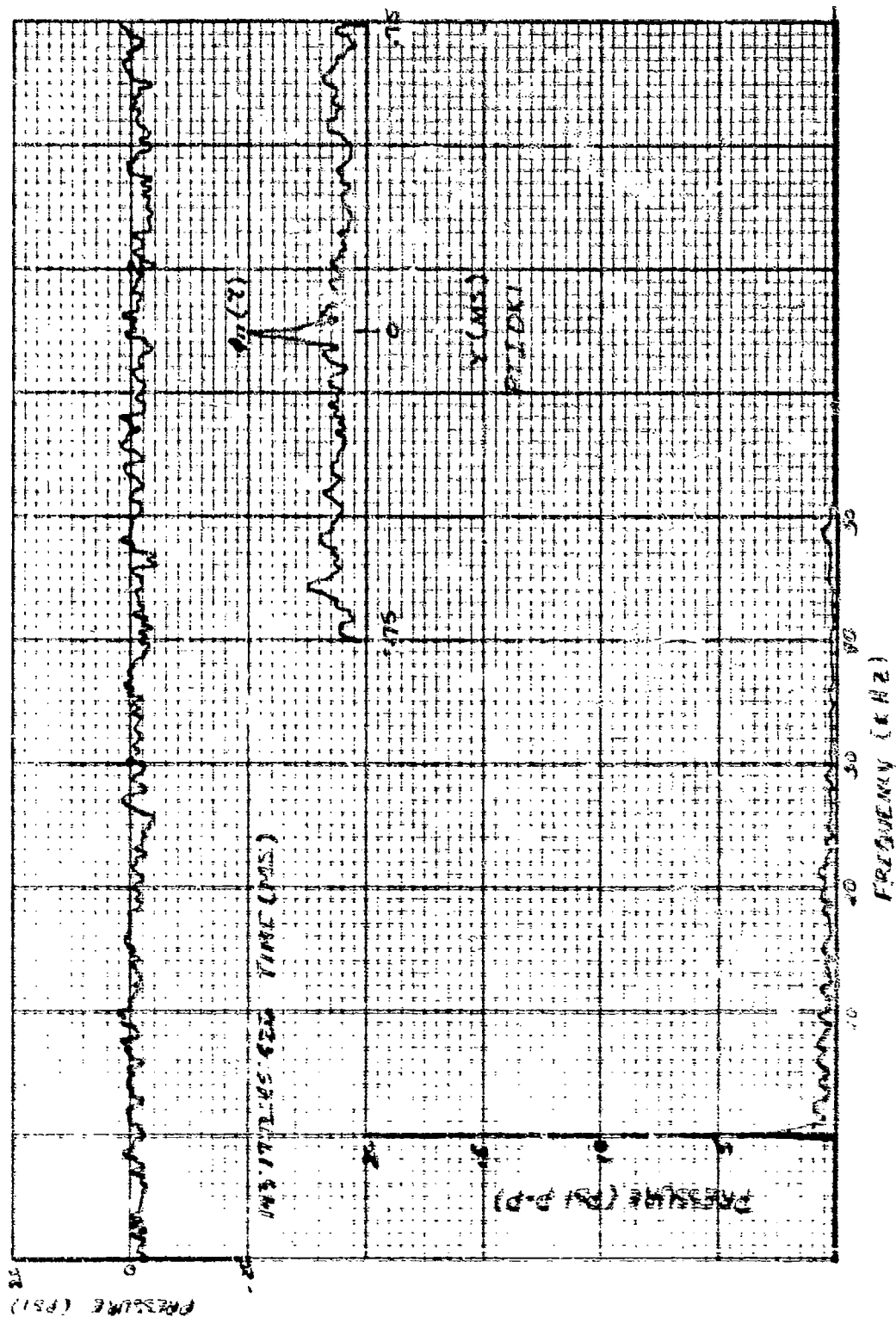


Figure 247. High-Frequency Response Data, 70% Speed, Stall Transient, Time 426, PTIDK1.

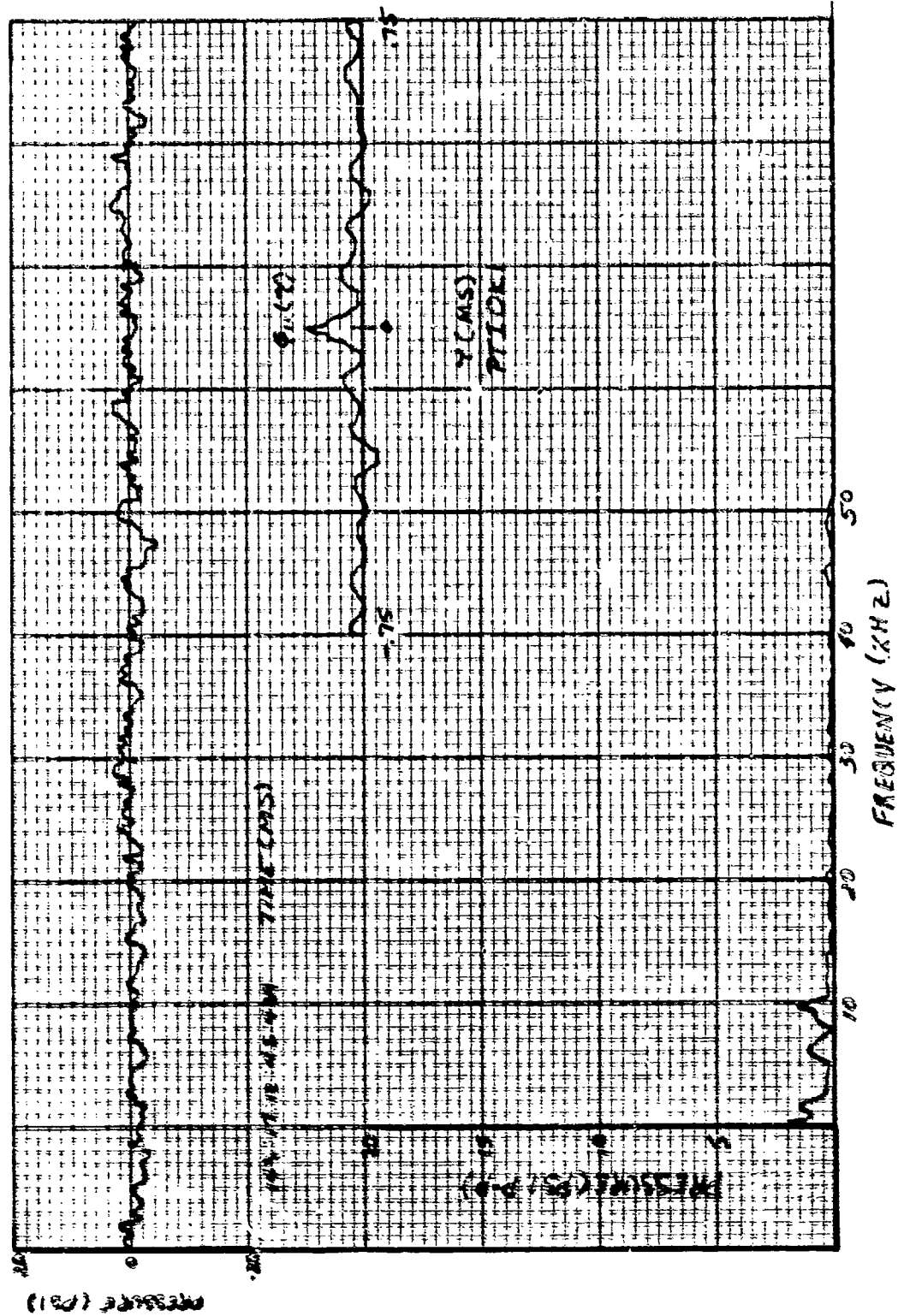


Figure 248. High-Frequency Response Data, 70° Speed, Stall Transient, Time 434 PTIDK1.

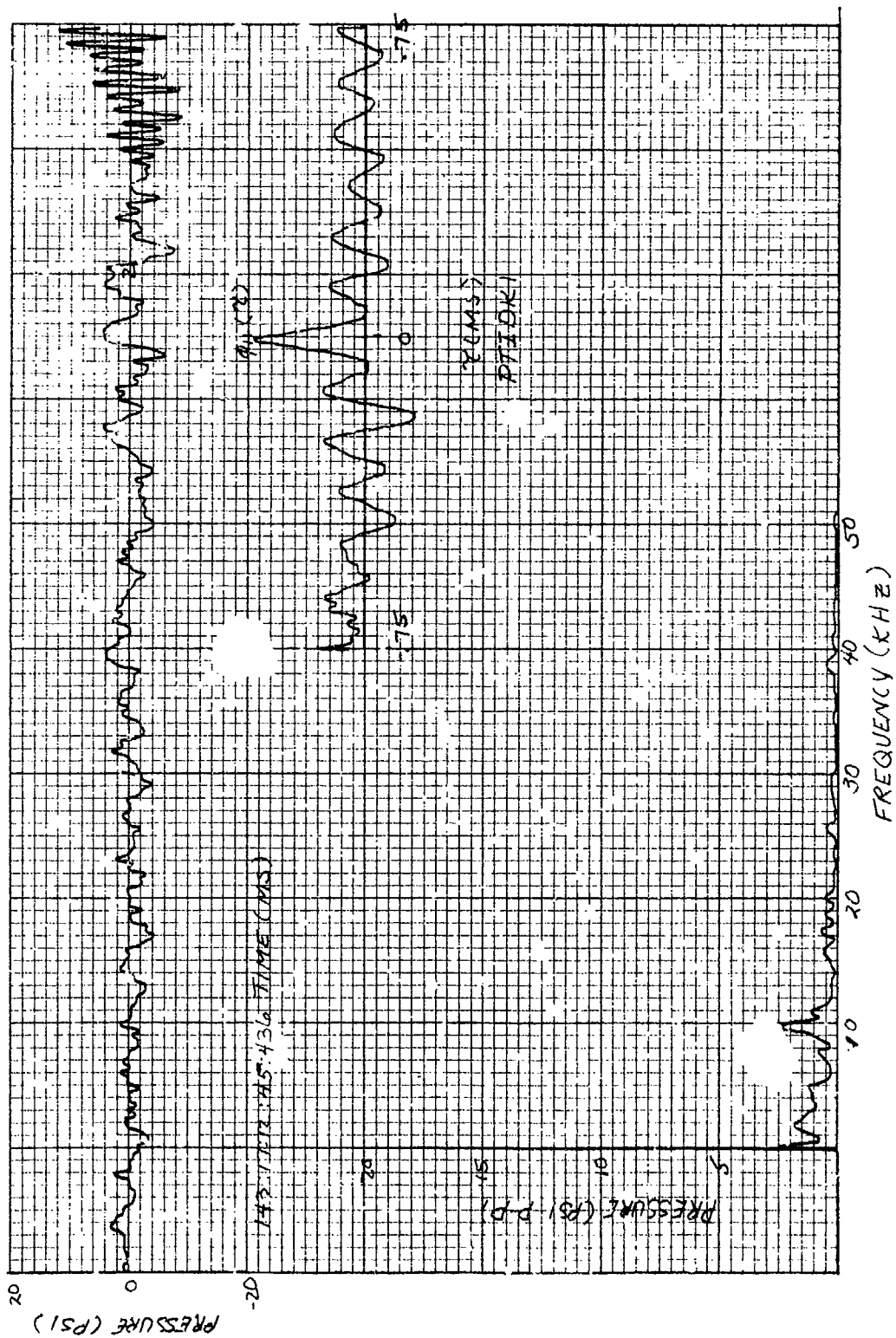


Figure 249. High-Frequency Response Data, 70% Speed, Stall Transient, Time 436, PTIDK1.



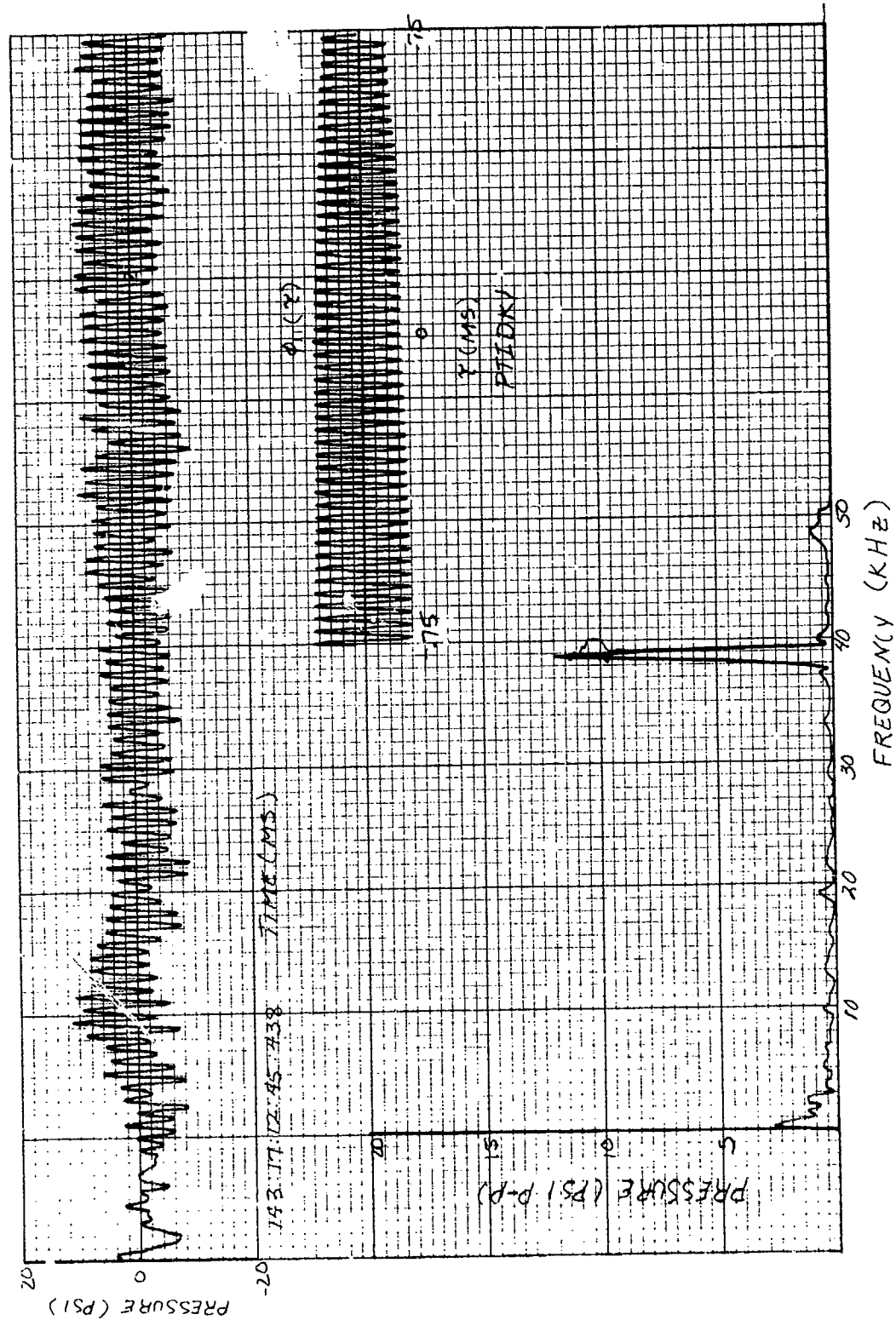


Figure 250. High-Frequency Response Data, 70% Speed, Stalled, Time 438, PTIDK1.

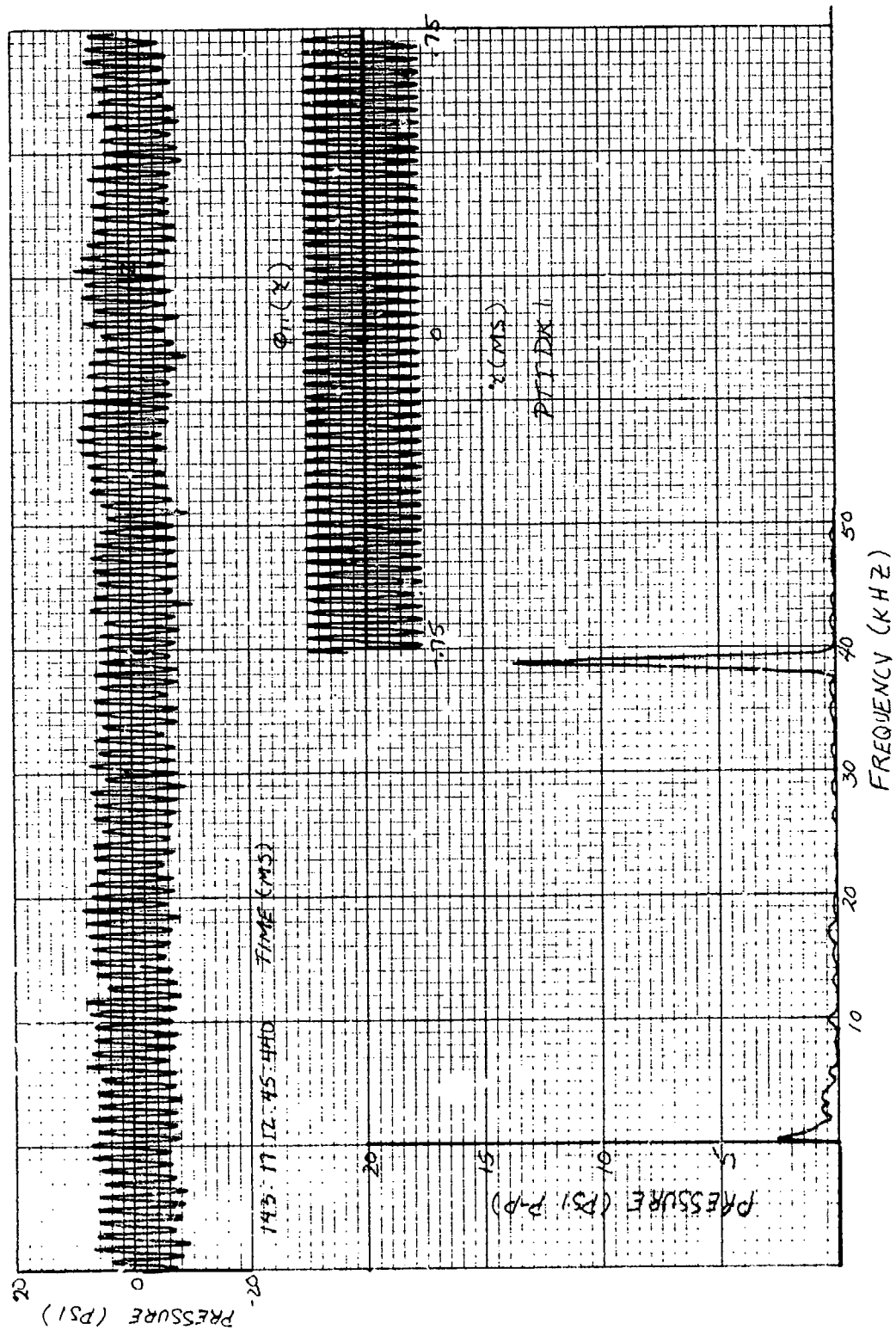


Figure 251. High-Frequency Response Data, 70% Speed, Stalled, Time 440, PTIDK1.

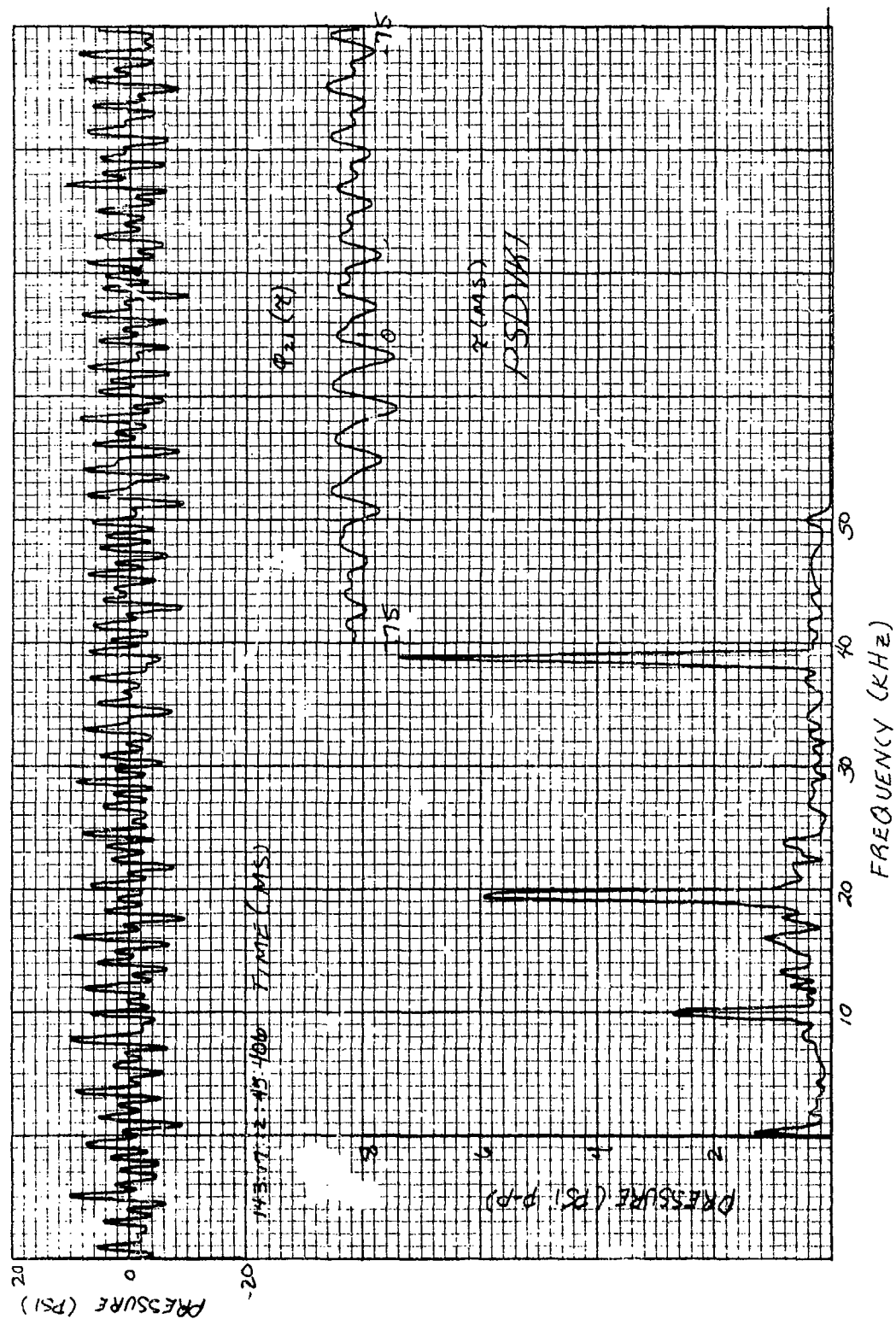


Figure 252. High-Frequency Response Data, 70% Speed, Stall Transient, Time 406, PSDVK1.

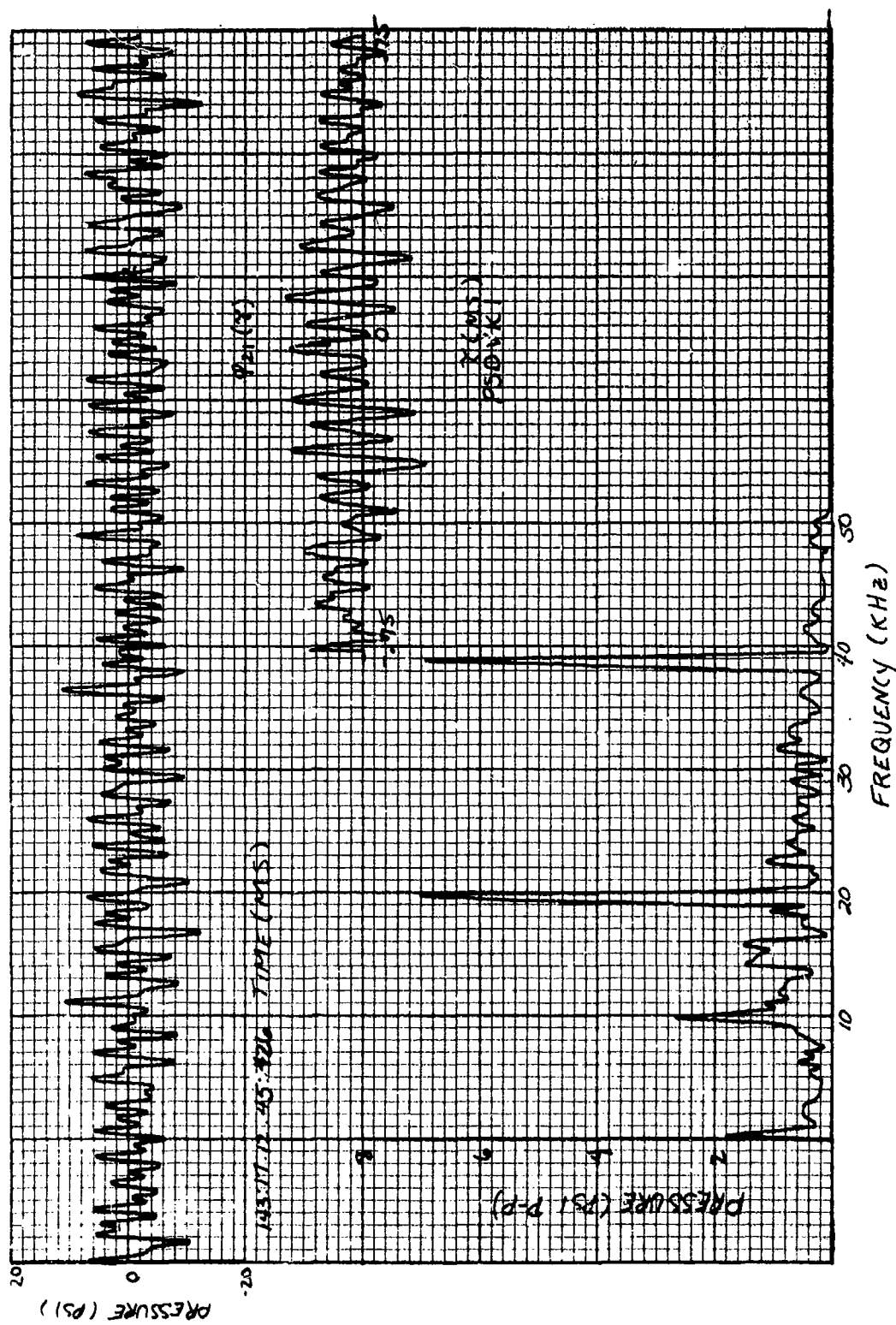


Figure 253. High-Frequency Response Data, 70% Speed, Stall Transient, Time 426, PSDVK1.

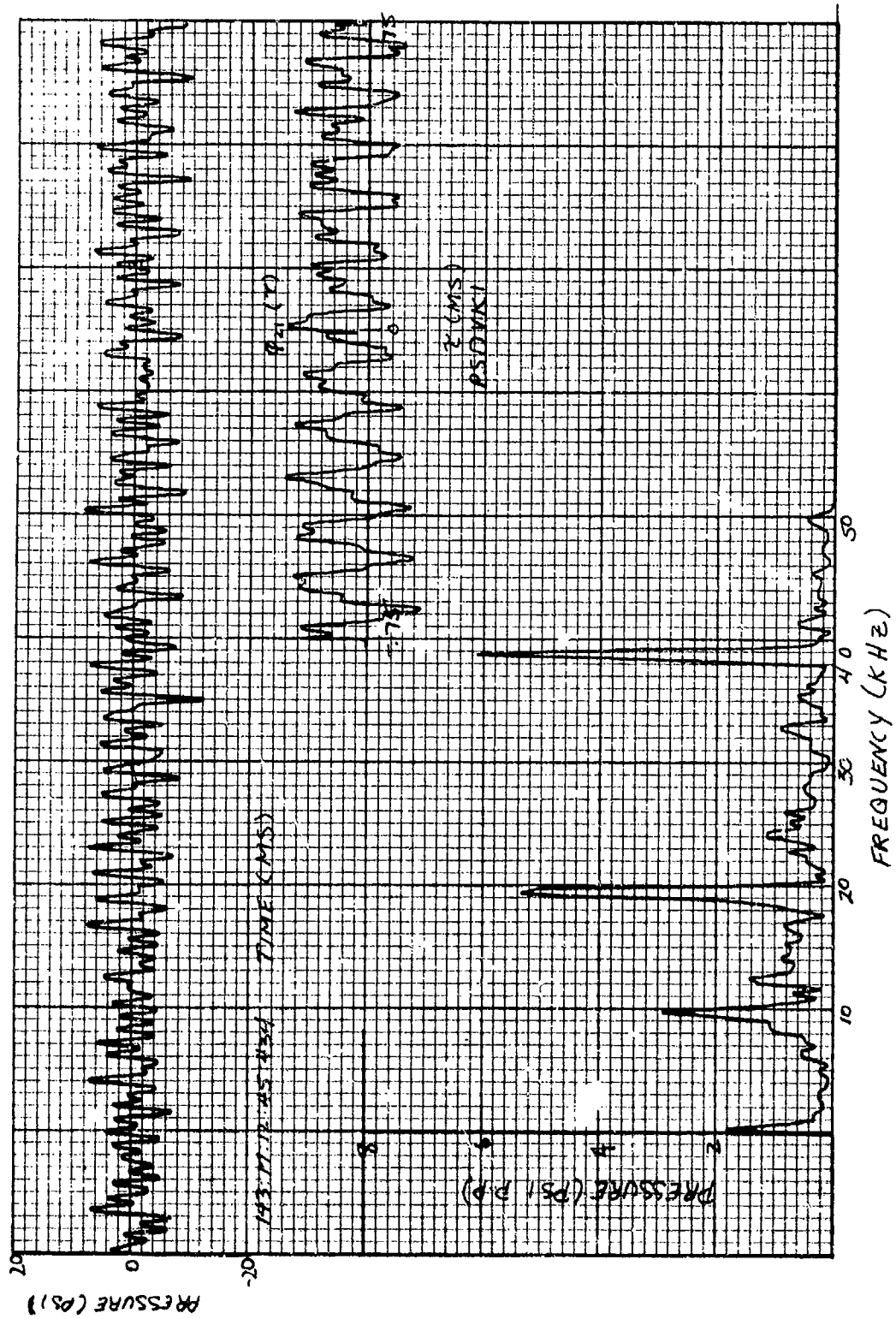


Figure 254. High-Frequency Response Data, 70% Speed, Stall Transient, Time 434, PSDVK1.

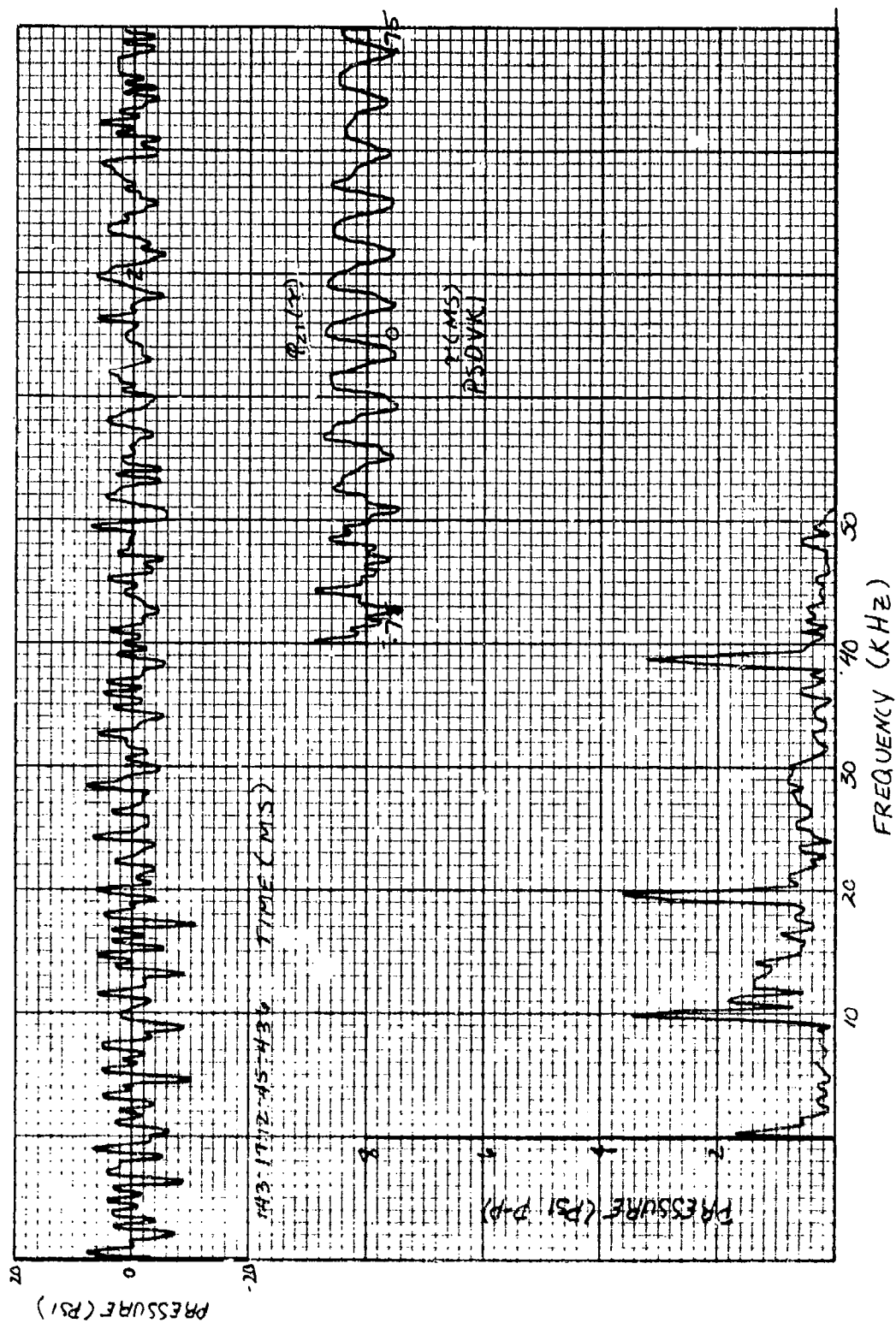


Figure 255. High-Frequency Response Data, 70% Speed, Stall Transient, Time 43<sup>s</sup> PSDVK1.

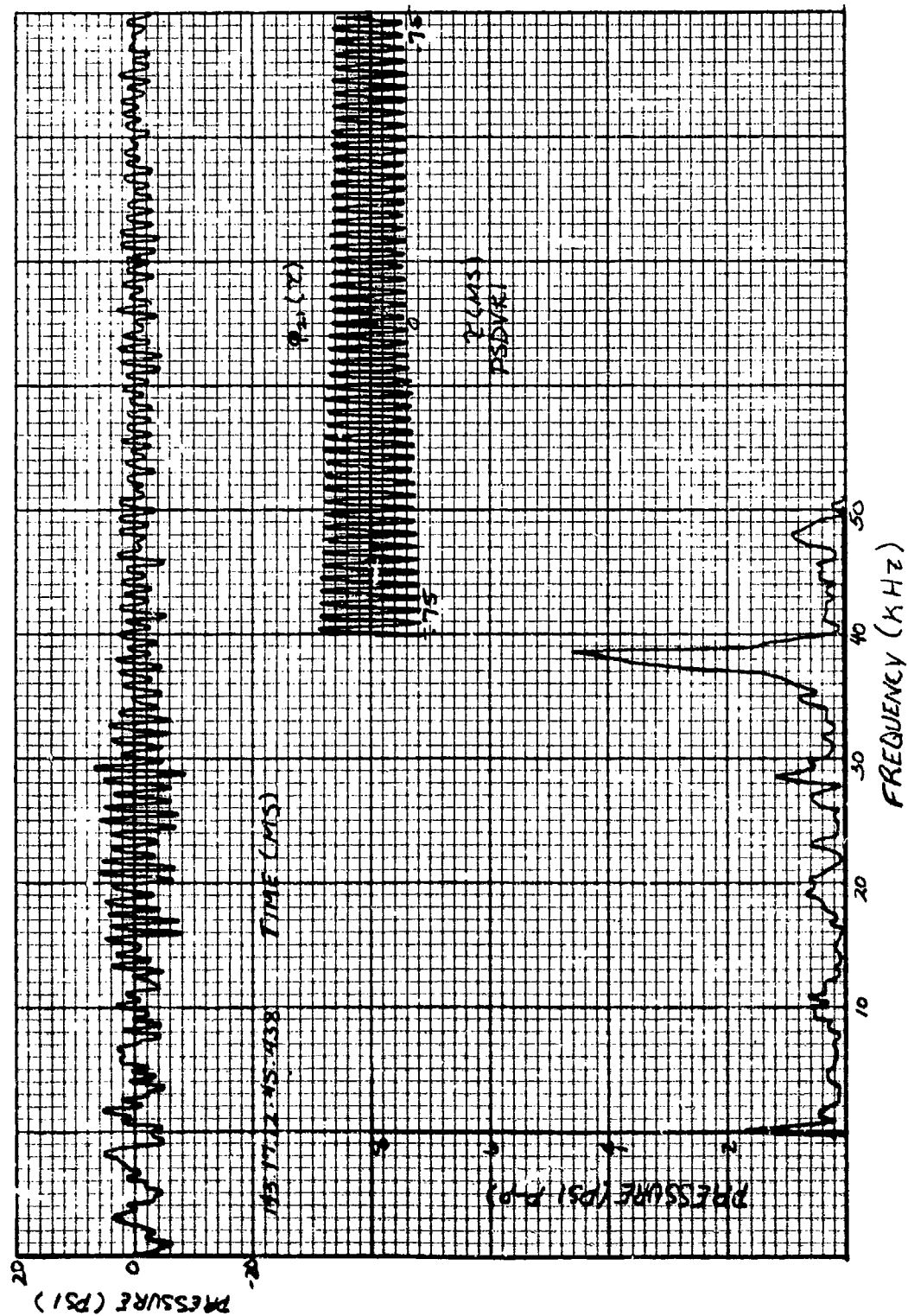


Figure 256. High-Frequency Response Data, 70% Speed, Stalled, Time 438, PSDVK1.



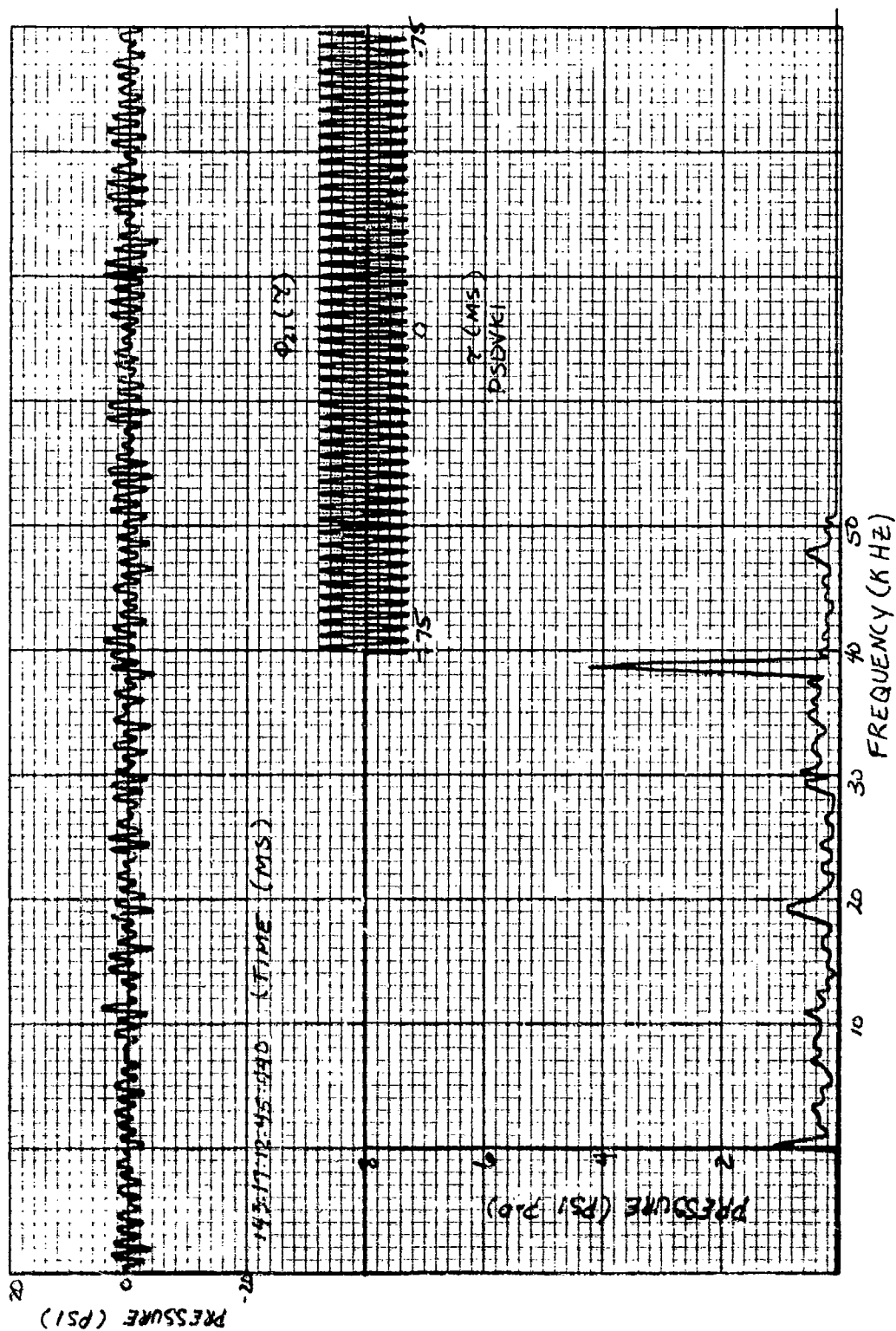


Figure 257. High-Frequency Response Data, 70% Speed, Stalled, Time 440, PSDVK1.



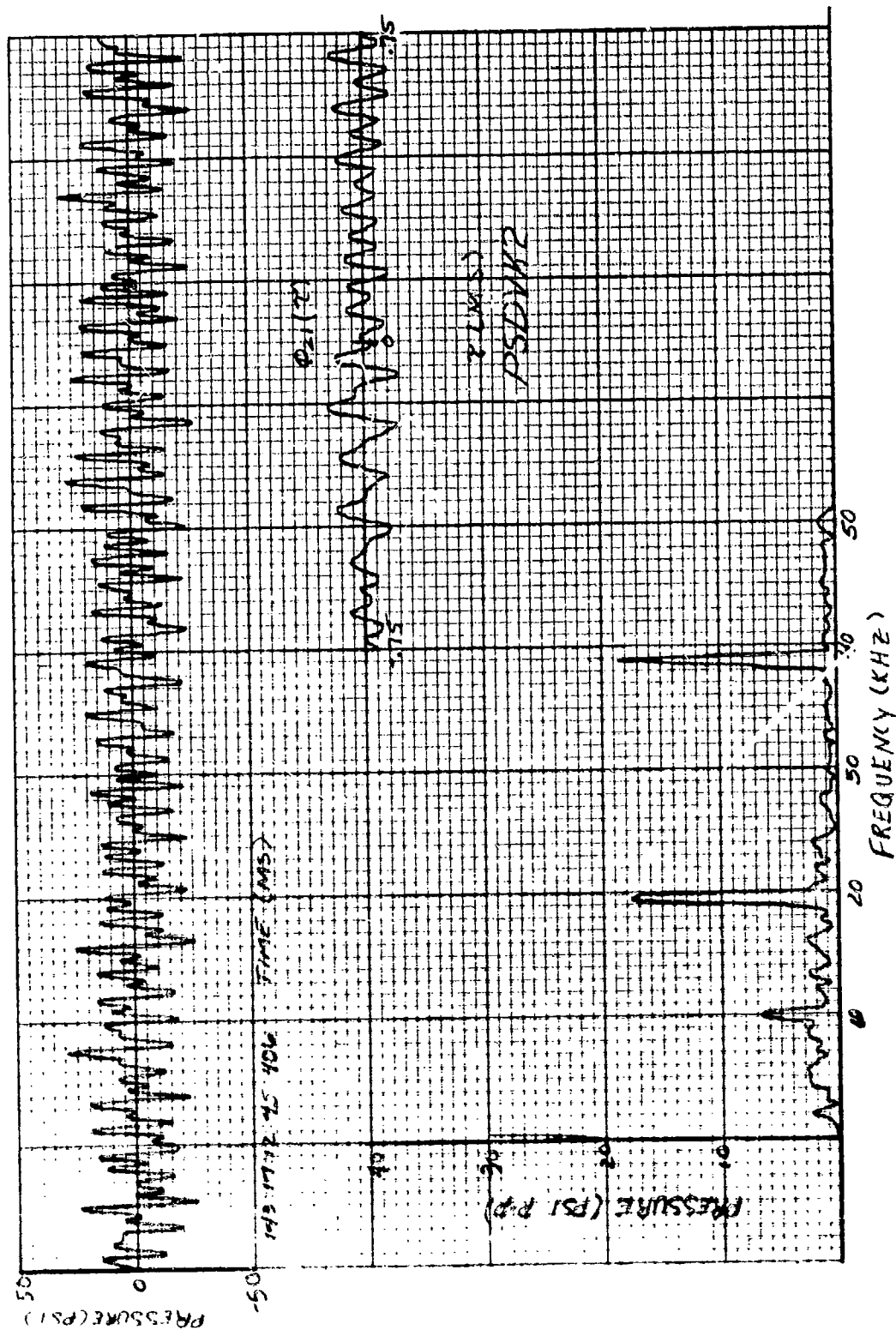


Figure 258. High-Frequency Response Data, 70<sup>th</sup> Speed, Stall Transient, Time 406, PSD K2.

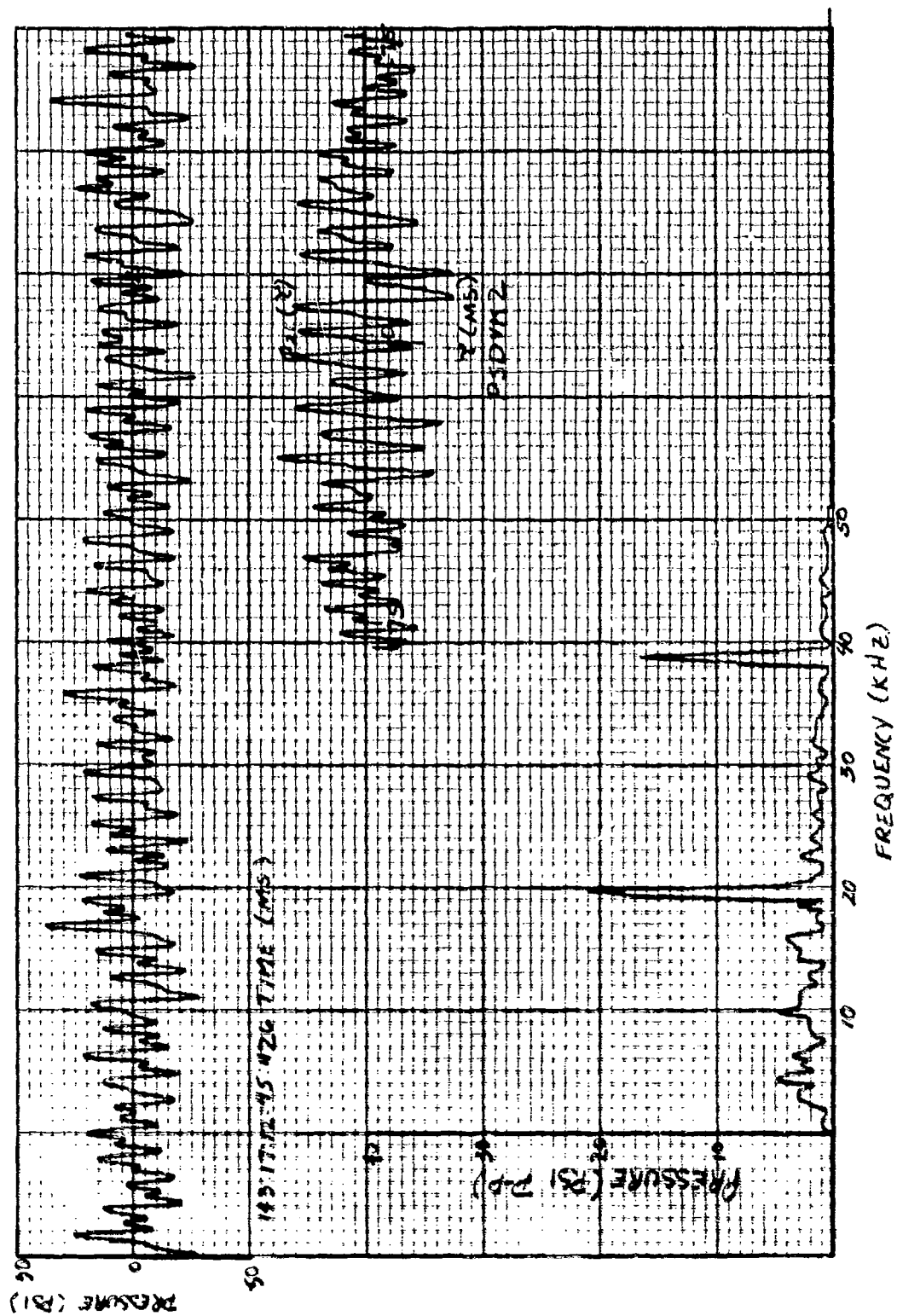


Figure 259. High-Frequency Response Data, 70% Speed, Stall Transient, Time 426, PSDVK2.

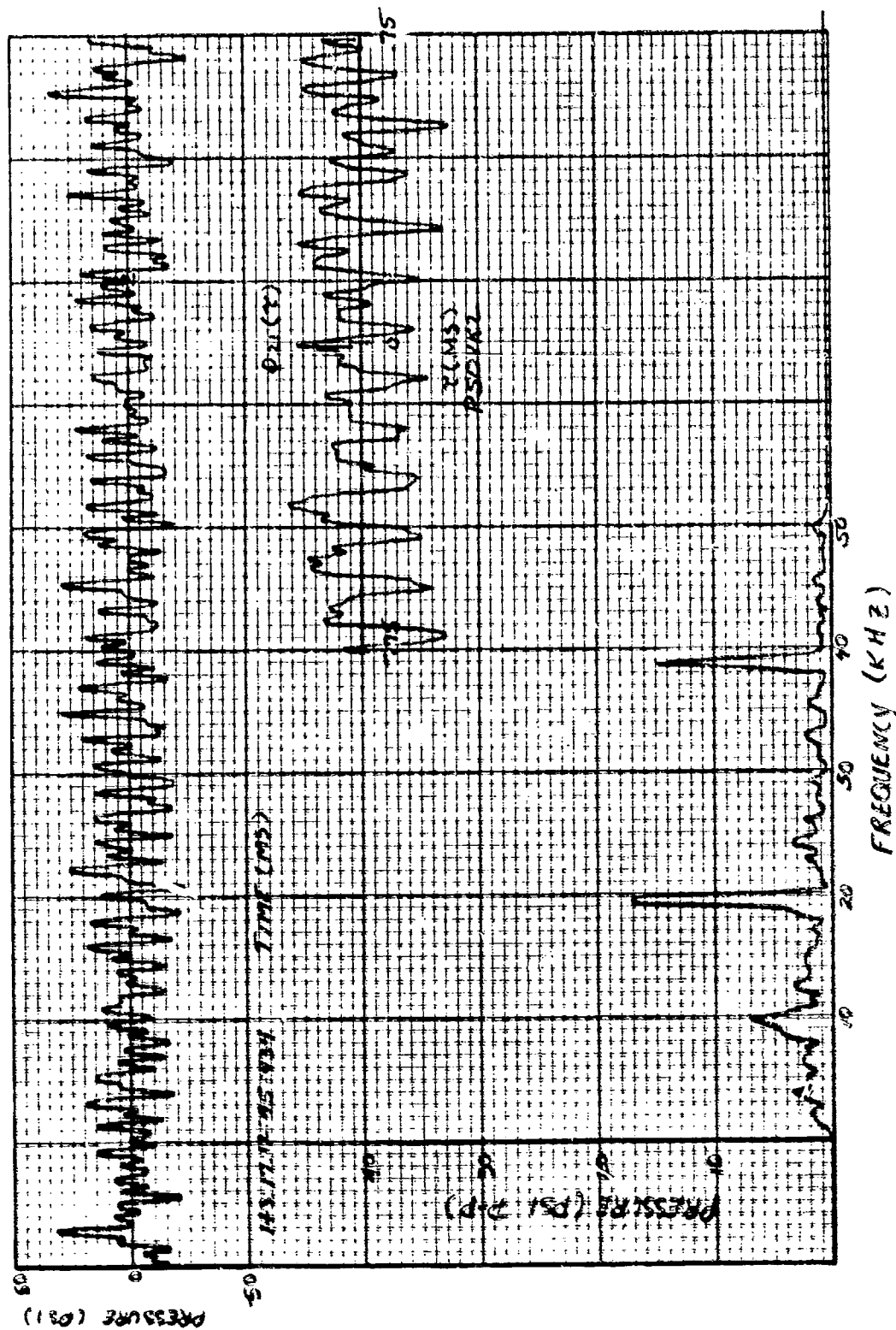


Figure 266. High-Frequency Response Data, 70% Speed, Stall Transient, Time 434, PSDVK2.

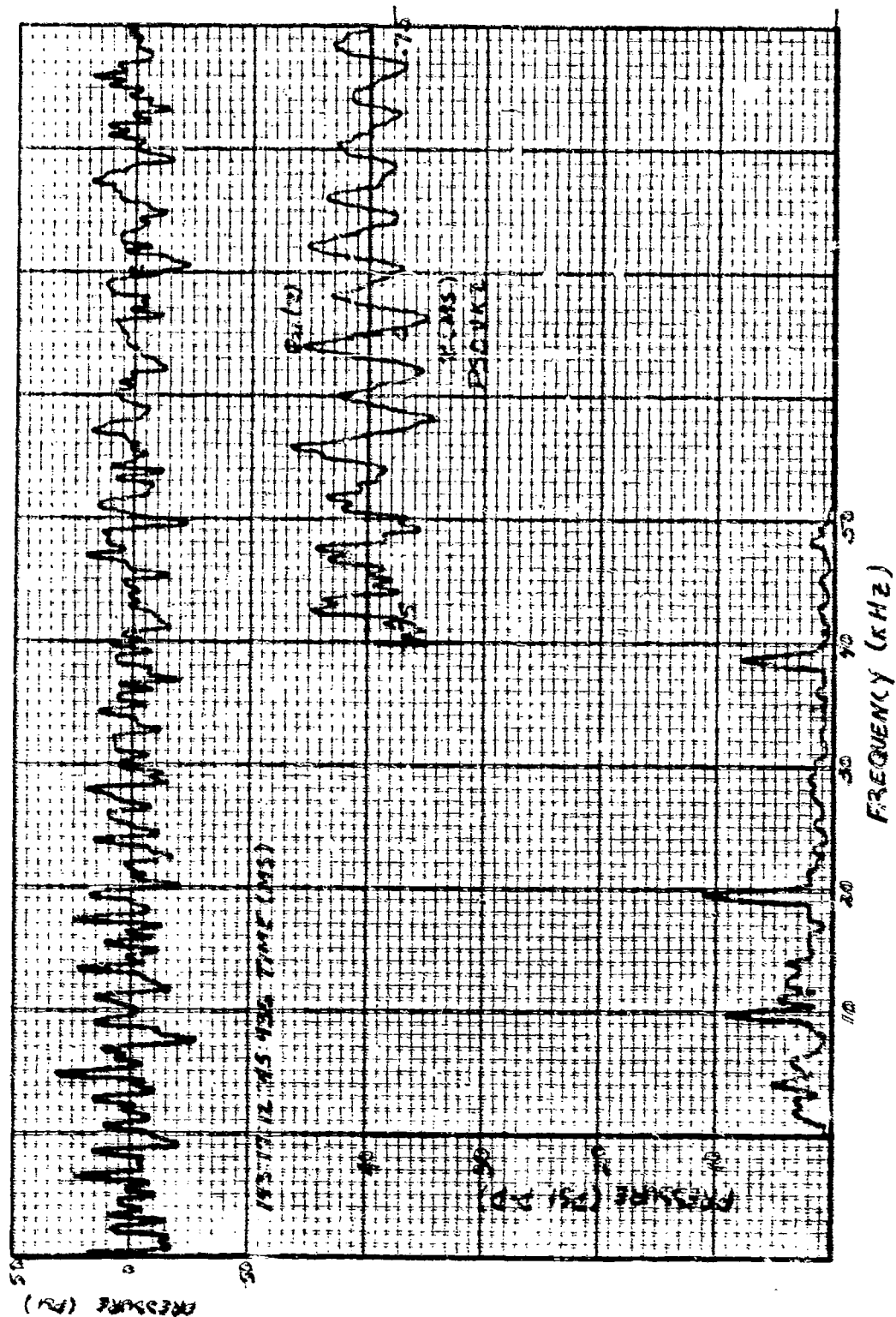


Figure 261. High-Frequency Response Data, 70% Speed, Stall Transient, Time 436, PSDVK2.

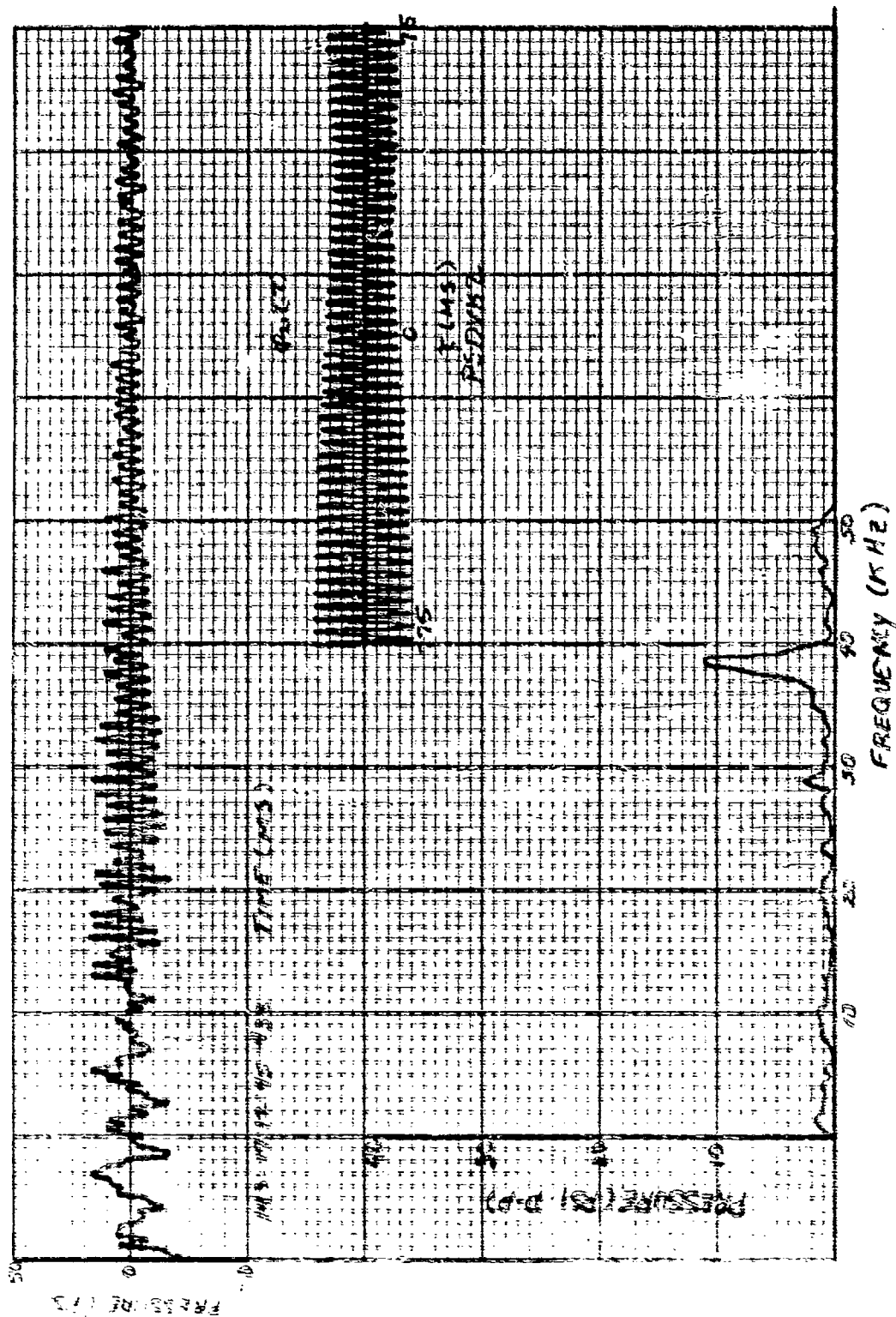


Figure 262. High-Frequency Response Data, 70% Speed, Stalled, Time 43%, PSD/K2.

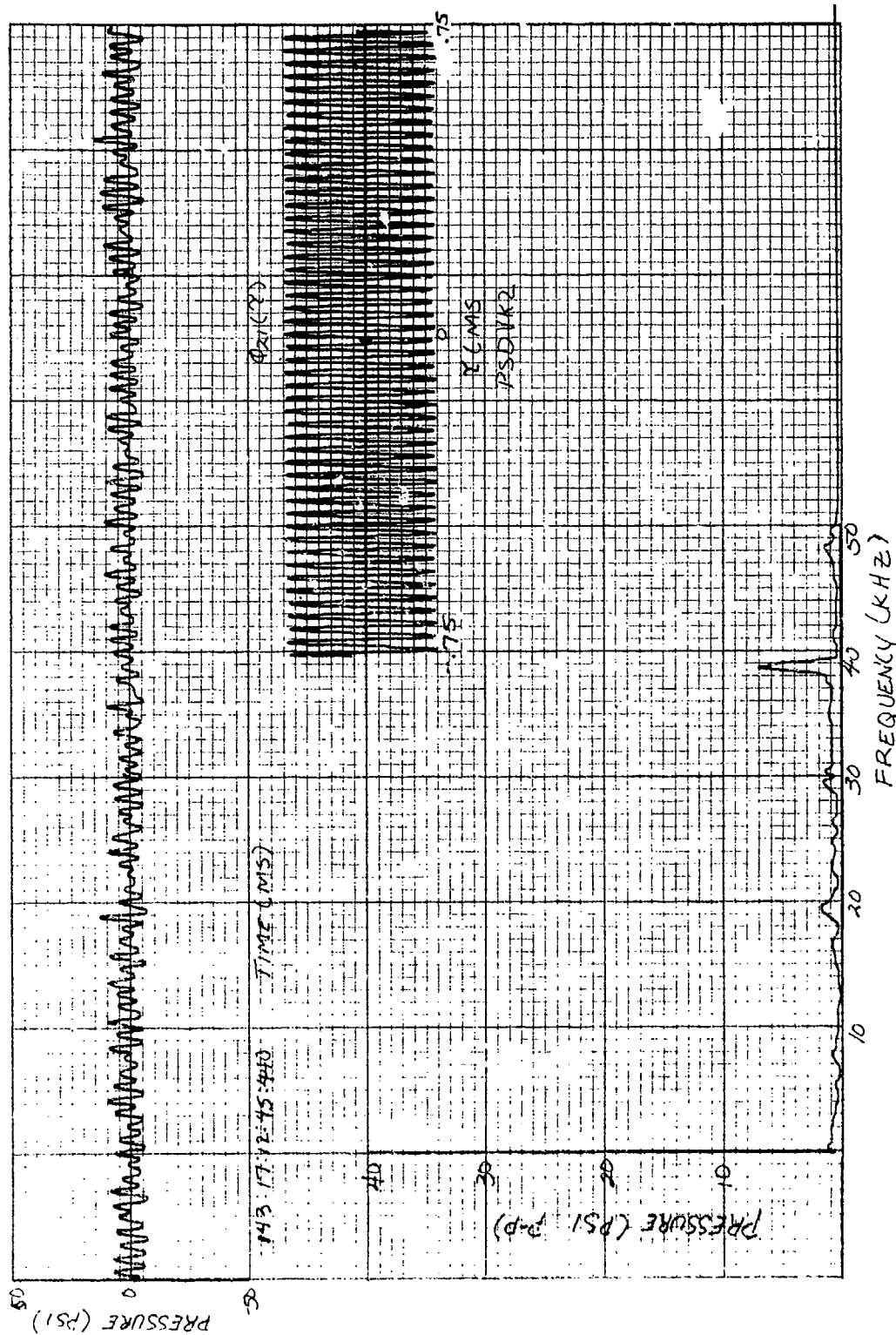


Figure 263. High-Frequency Response Data, 70% Speed, Stalled,  
Time 440, PSDVK2.

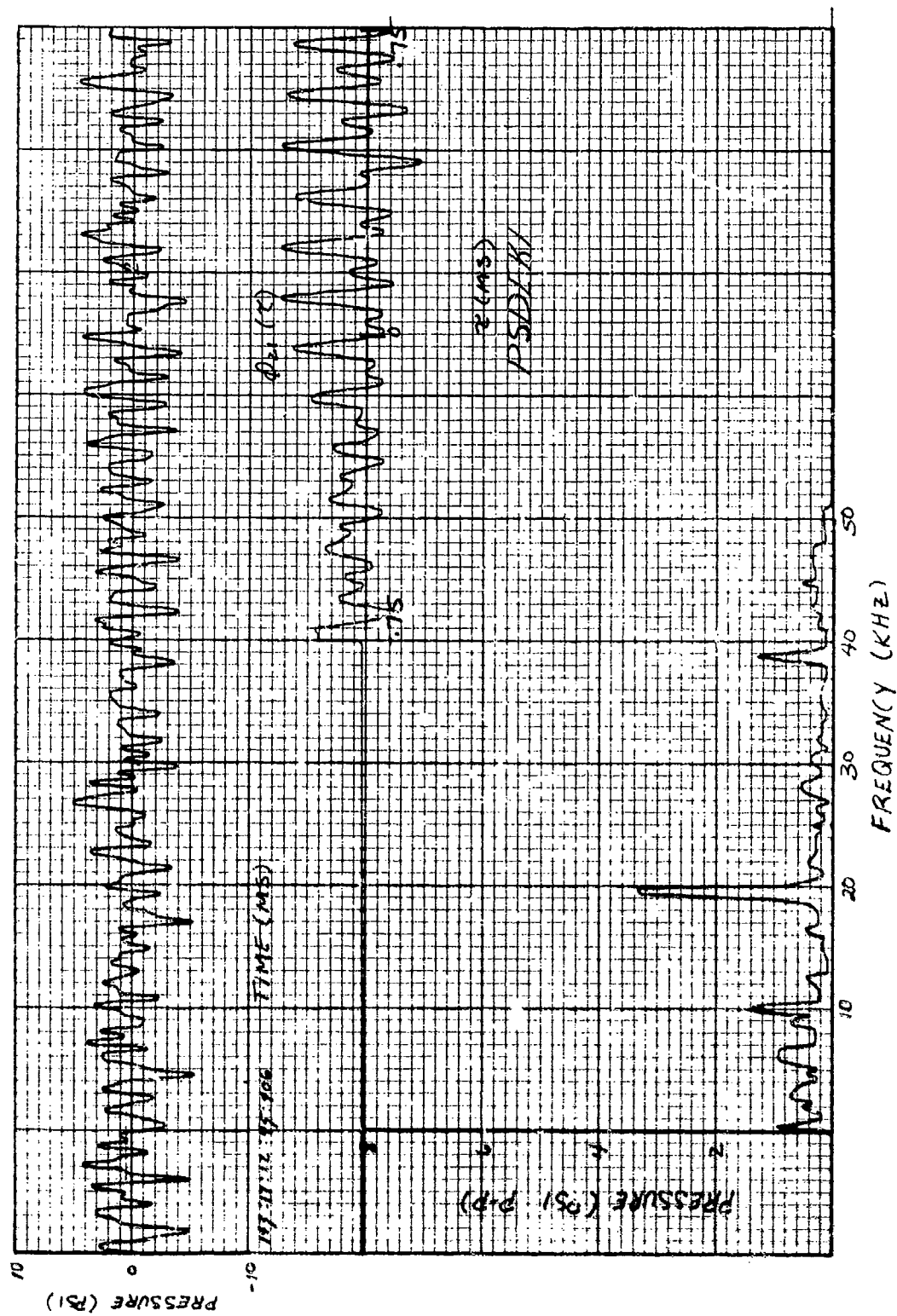


Figure 264. High-Frequency Response Data, 70% Speed, Stall Transient, Time 406, PSDEK1.



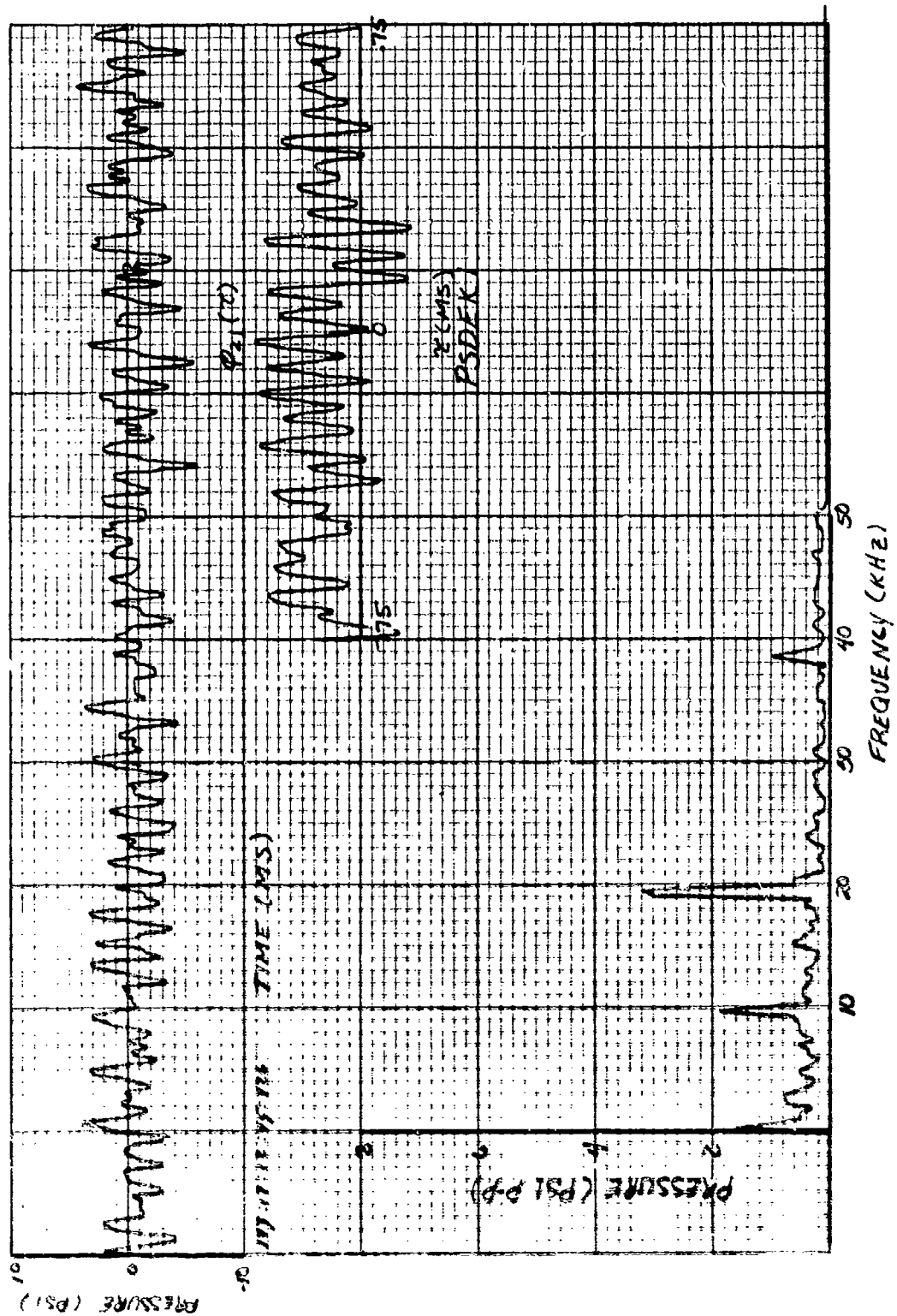


Figure 265. High-Frequency Response Data, 70% Speed, Stall Transient, Time 426, PSDEK1.



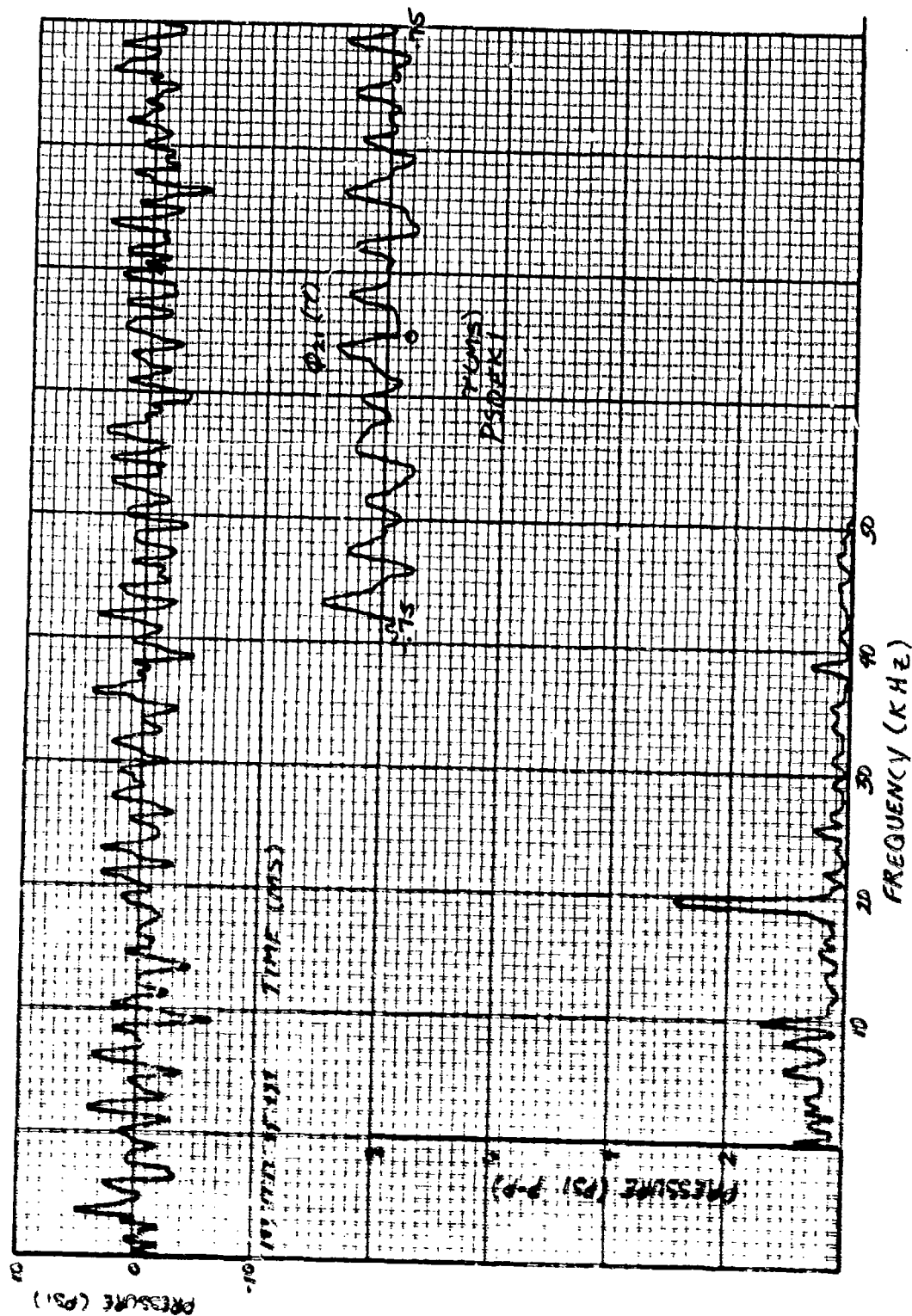


Figure 266. High-Frequency Response Data, 70% Speed, Stall Transient, Time 434, PSDEK1.

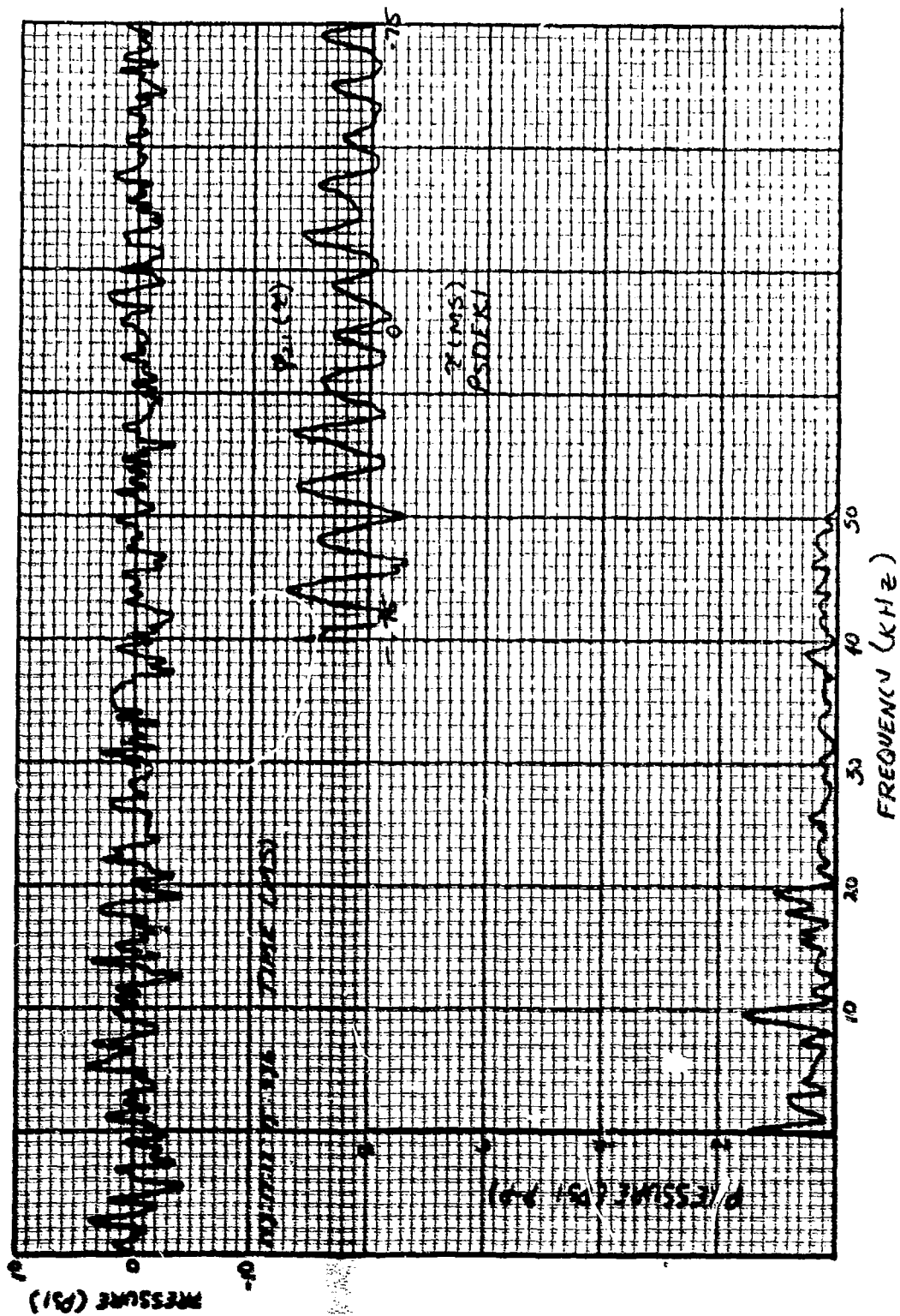


Figure 267. High-Frequency Response Data, 70% Speed, Stall Transient, Time 436, PSDEK1.

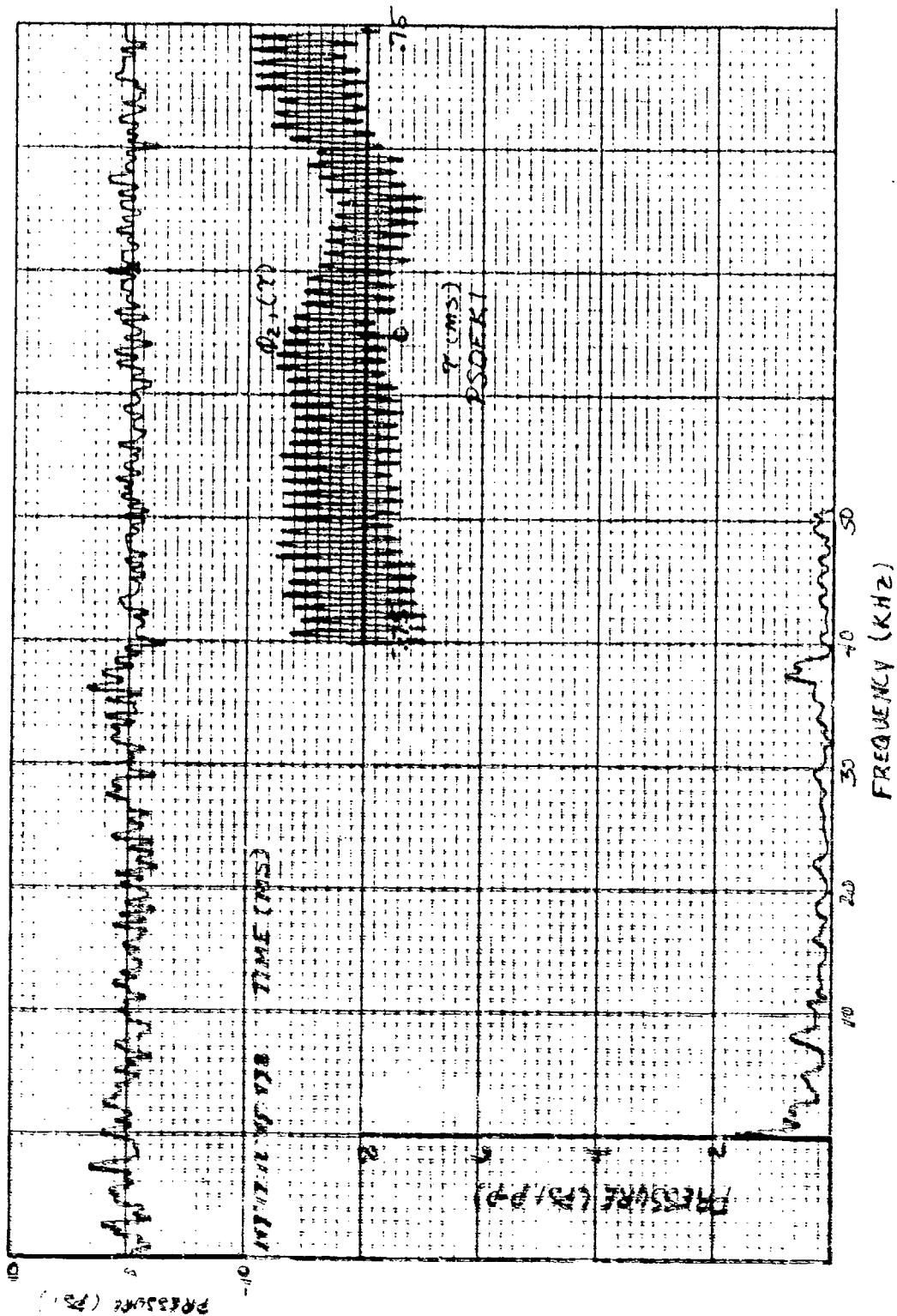


Figure 265. High-Frequency Response Data, 70% Speed, Stalled, Time 438, PSDEK1.

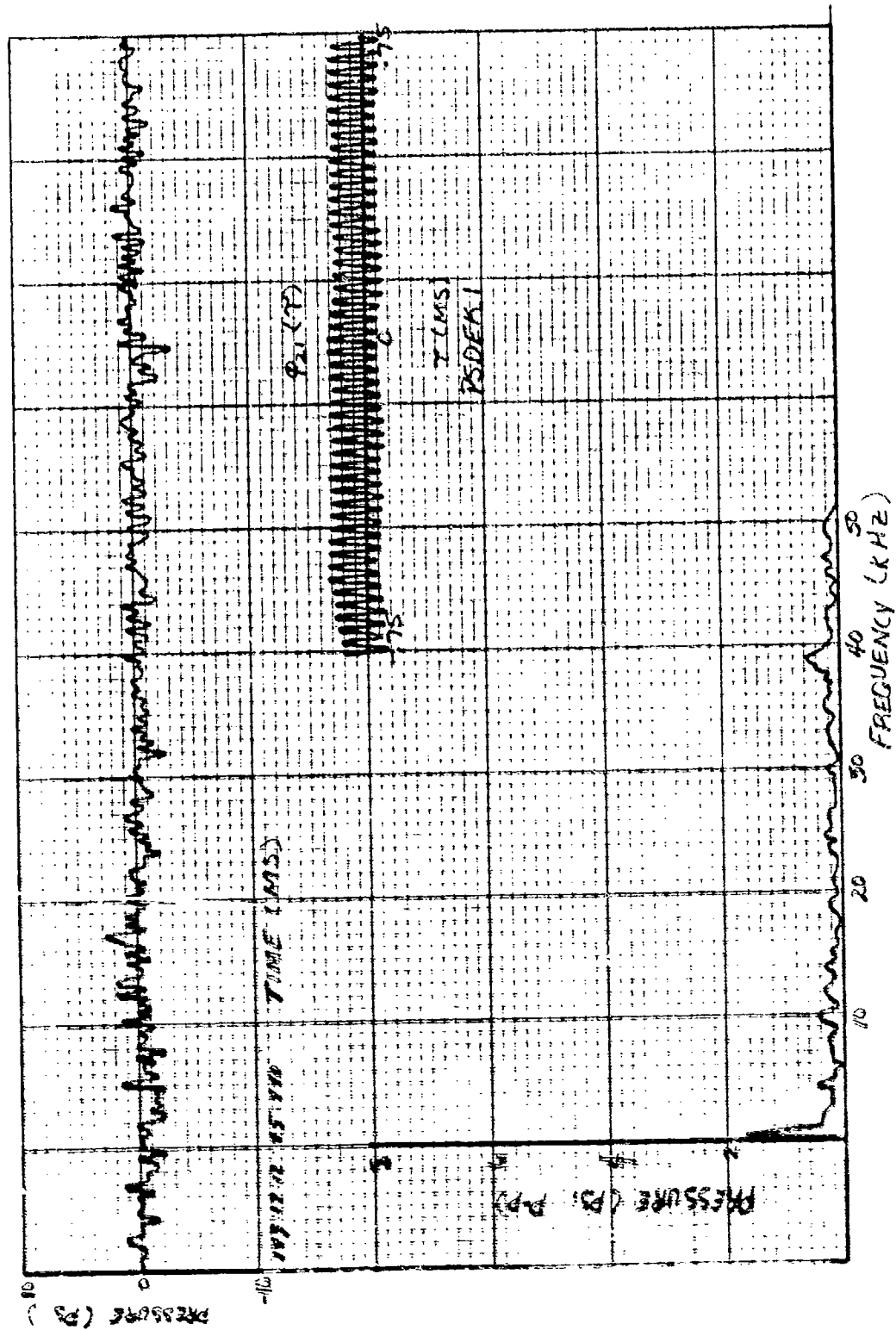


Figure 269. High-Frequency Response Data, 70% Speed, Stalled, Time 440, PSDEK1.

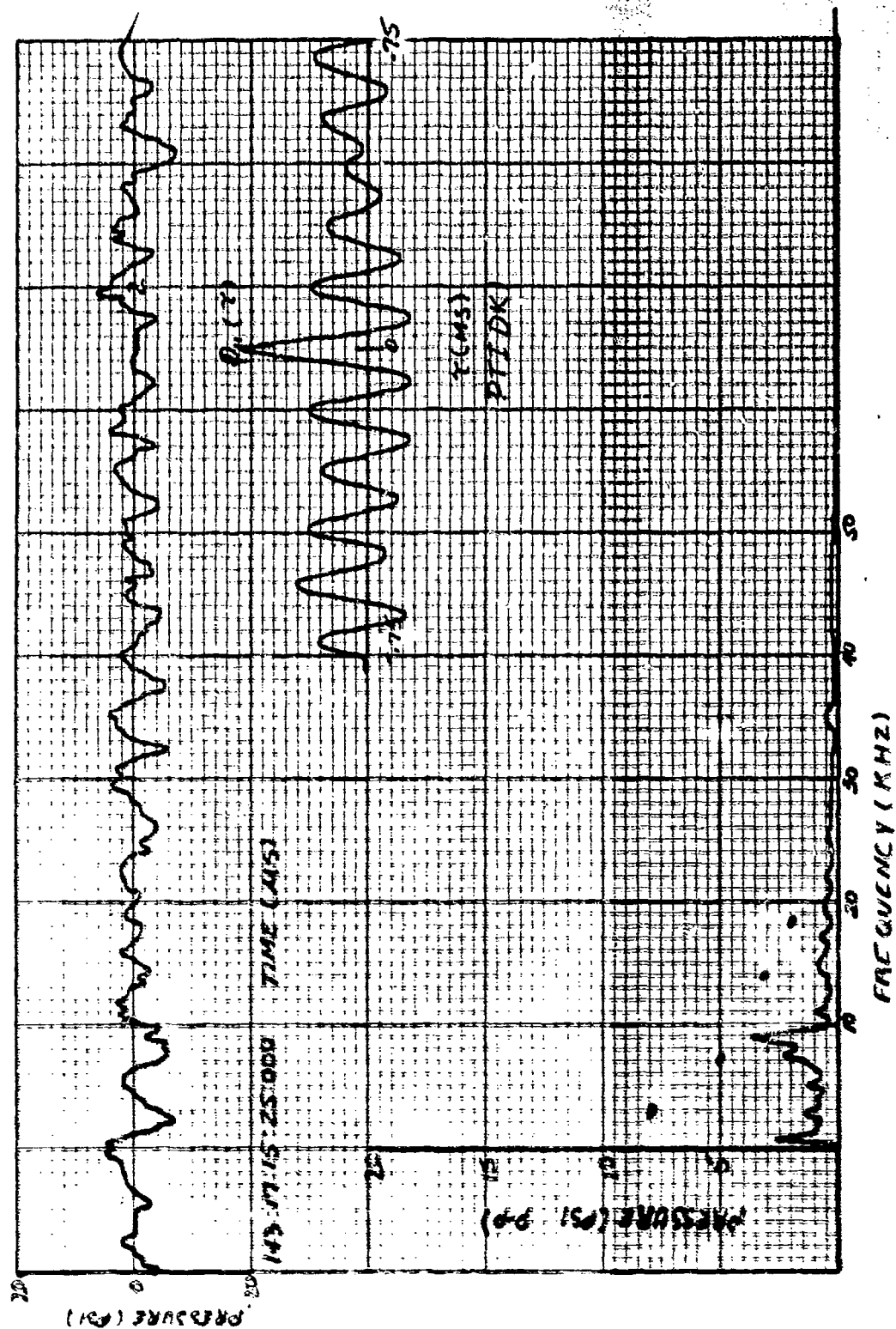


Figure 270. High-Frequency Response Data, 78% Speed, Steady-State, PTIDK1.

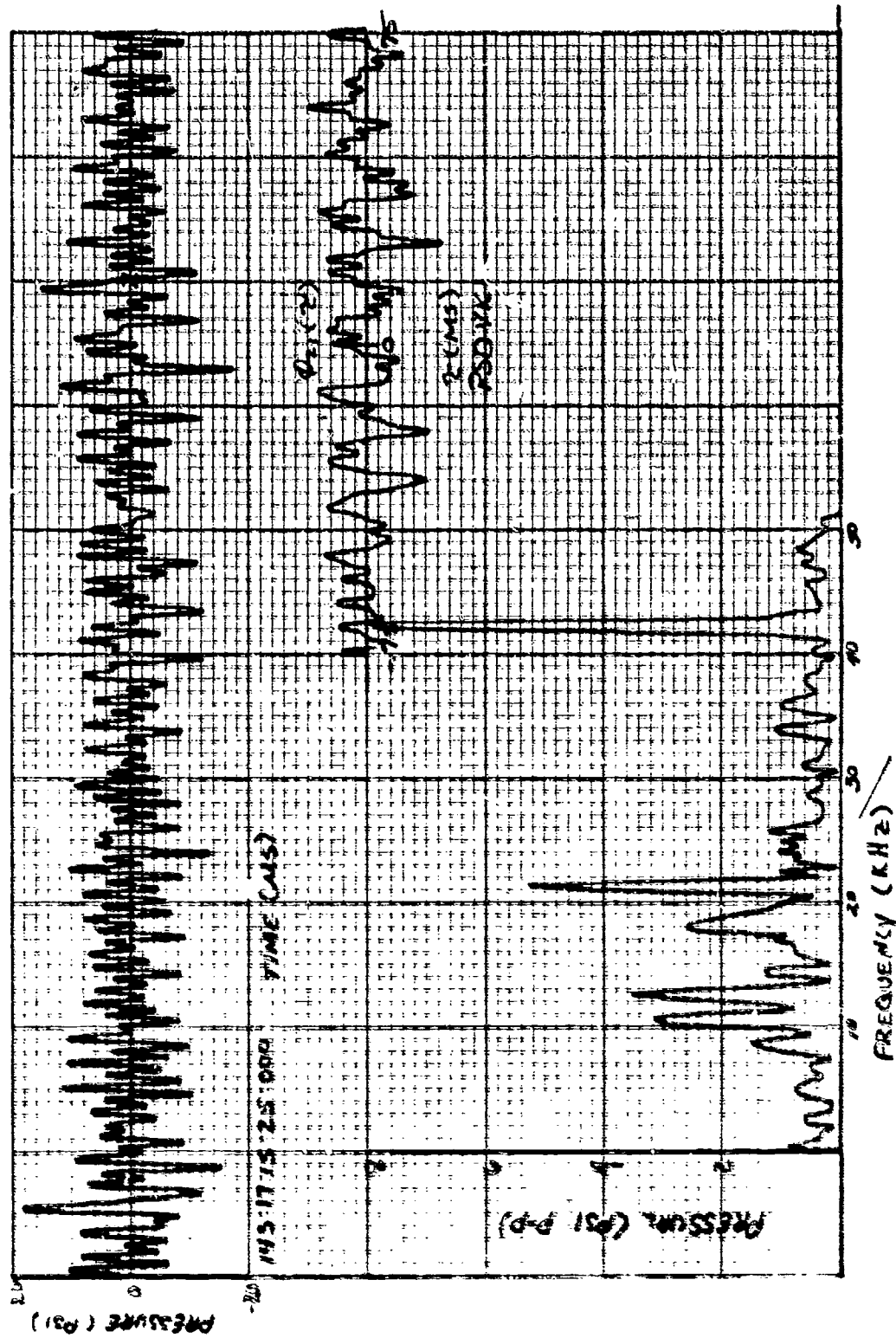


Figure 271. High-Frequency Response Data, 78% Speed, Steady-State, PSDVK1.

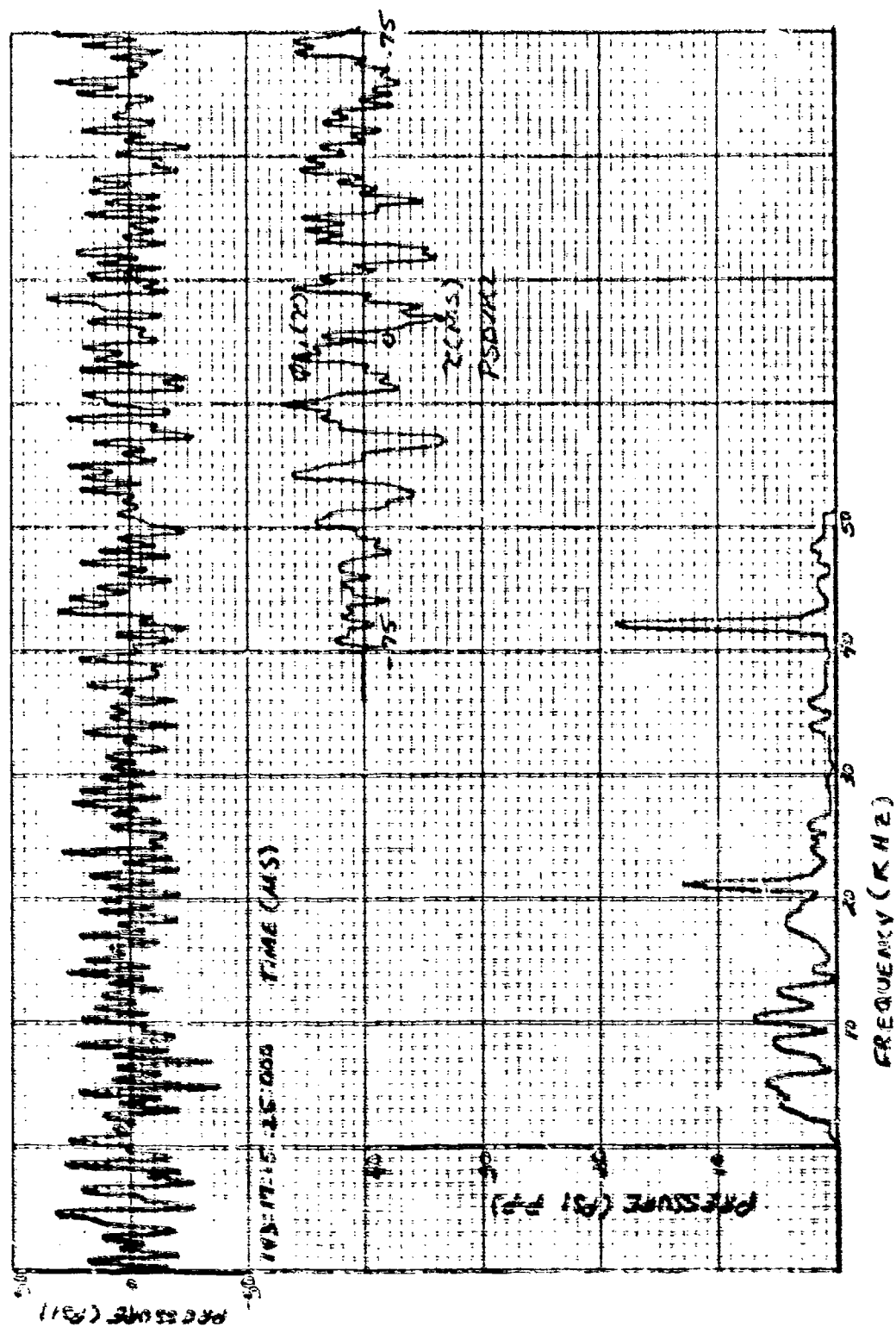


Figure 272. High-Frequency Response Data, 75% Speed, Steady-State, PSDVK2.

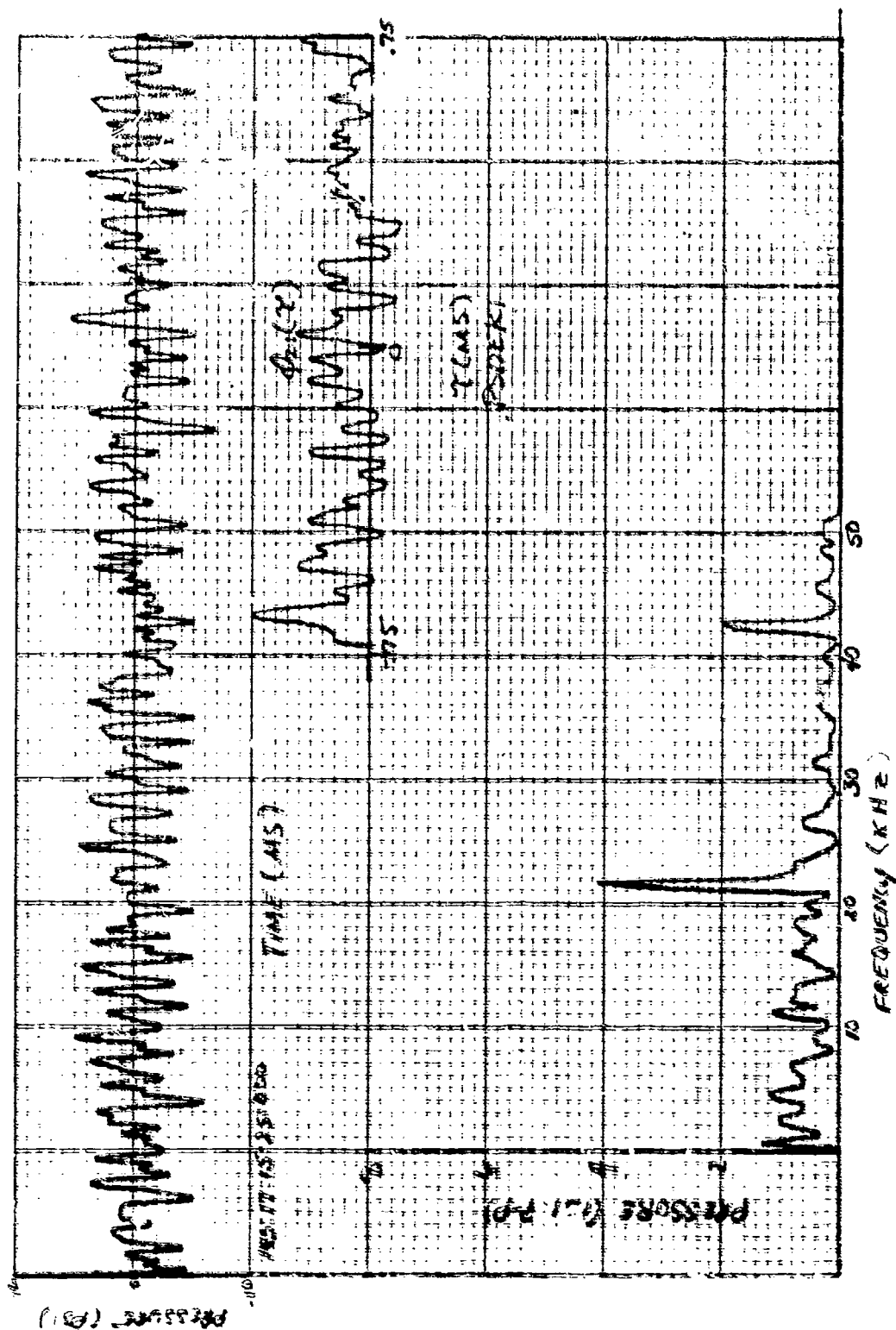


Figure 273, High-Frequency Response Data, 78% Speed, Steady-State, PSDEN1.





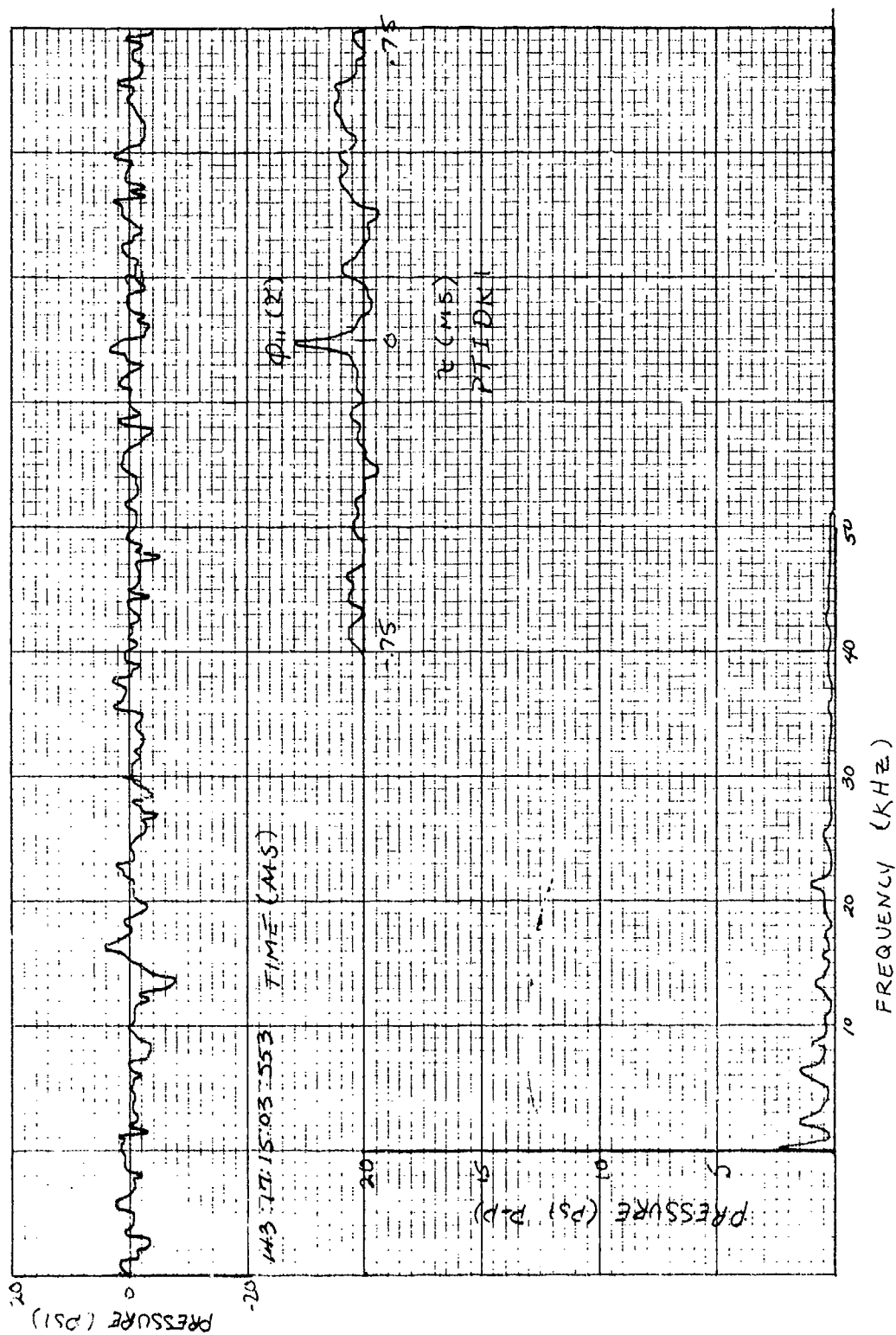


Figure 275. High-Frequency Response Data, 78% Speed, Stall Transient, Time 553, PTIDK1.



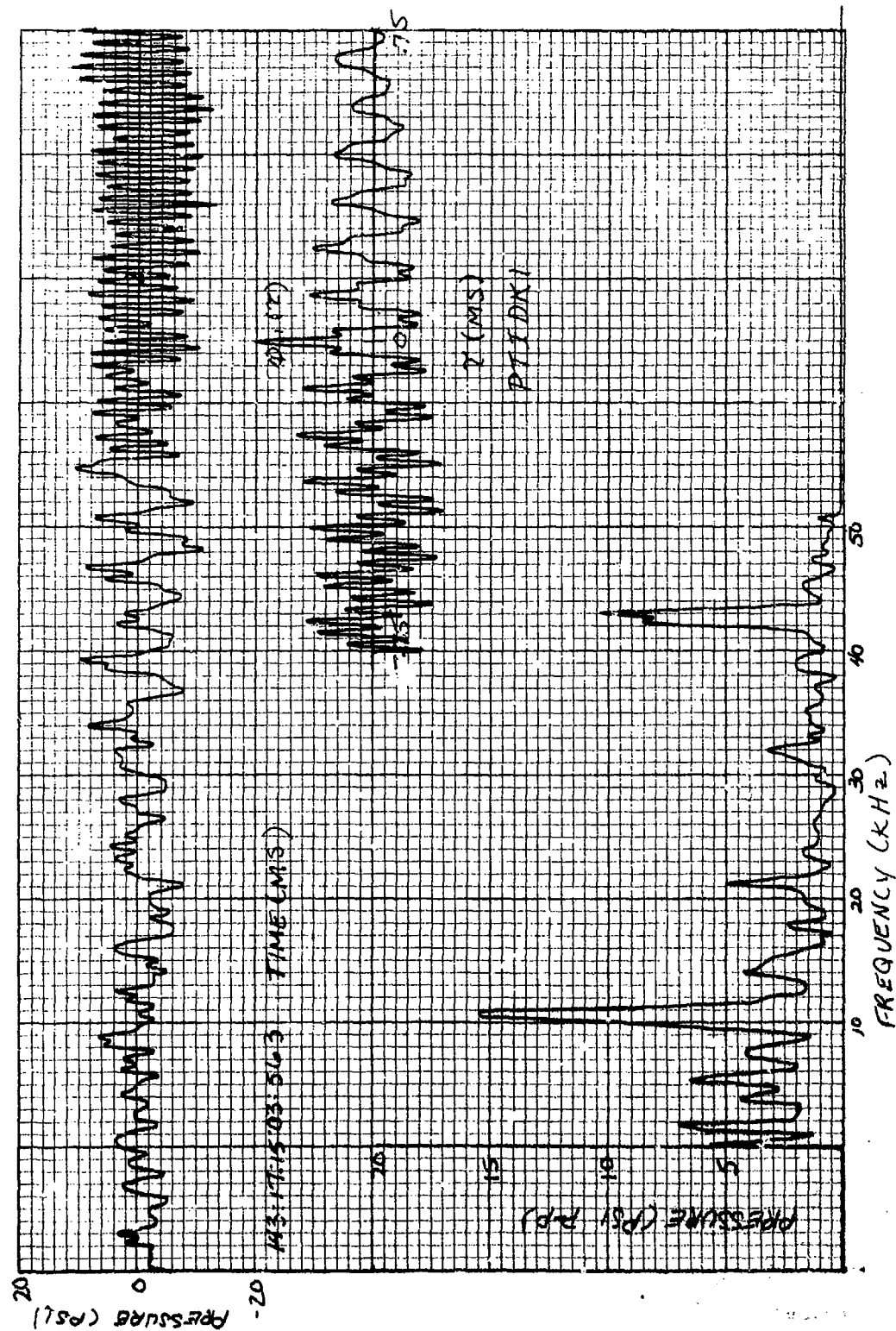


Figure 277. High-Frequency Response Data, 78% Speed, Stall Transient, Time 563, PTIDK1.

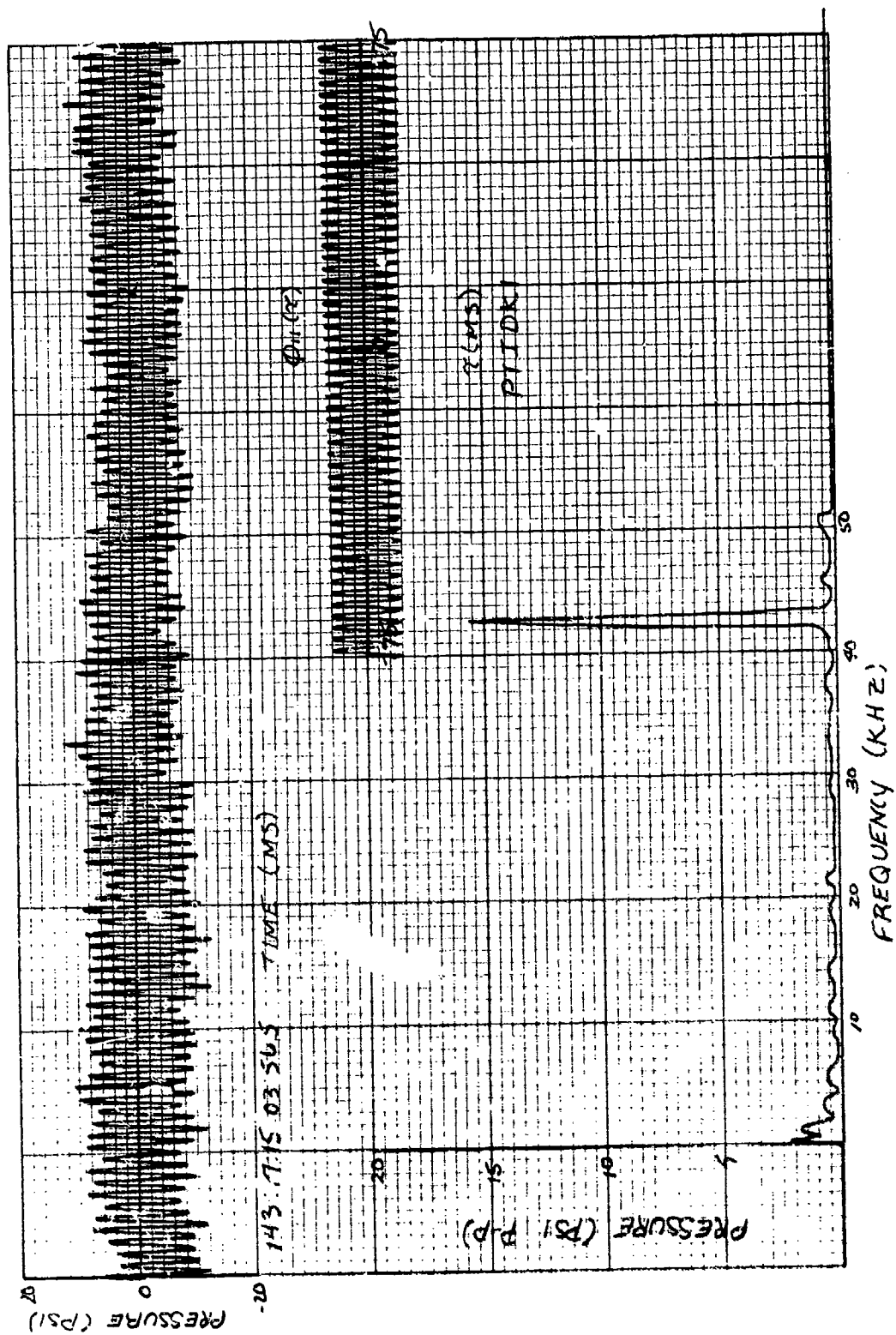


Figure 278. High-Frequency Response Data, 78% Speed, Stalled, Time 565, PTIDK1.

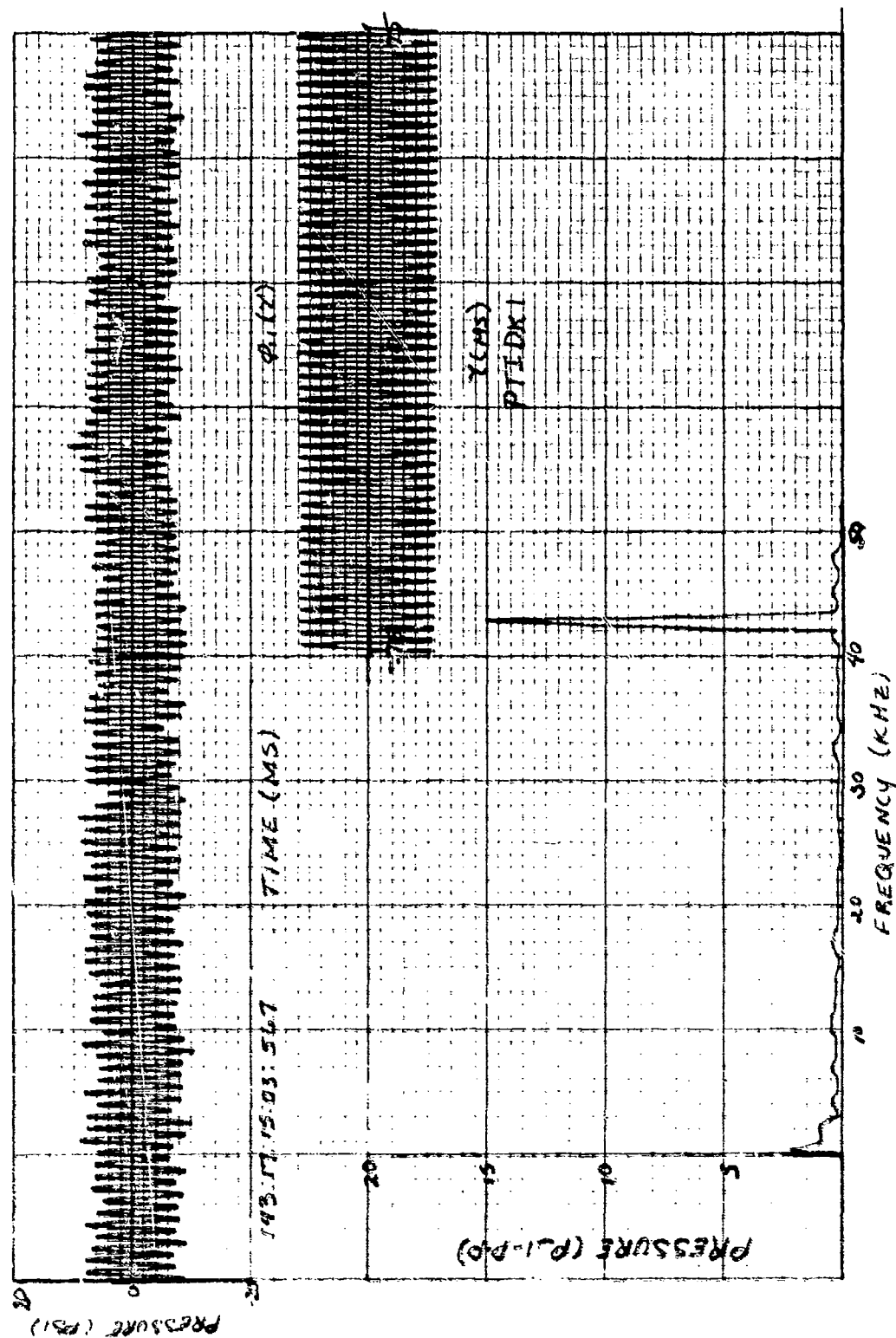


Figure 279. High-Frequency Response Data, 78% Speed, Stalled, Time 567, PTIDK1.

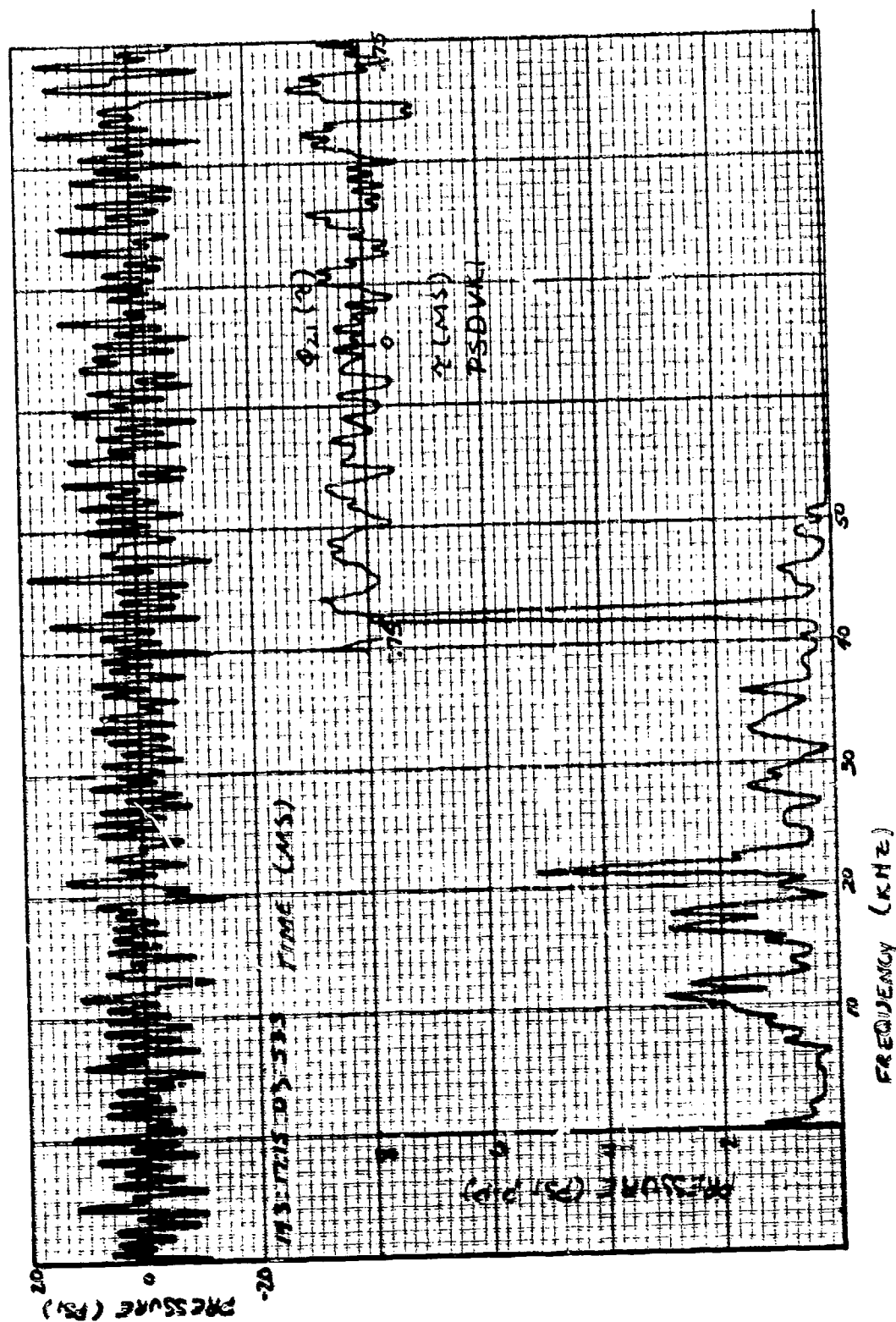


Figure 250. High-Frequency Response Data, 78% Speed, Stall Transient, Time 533, PSDVK1.



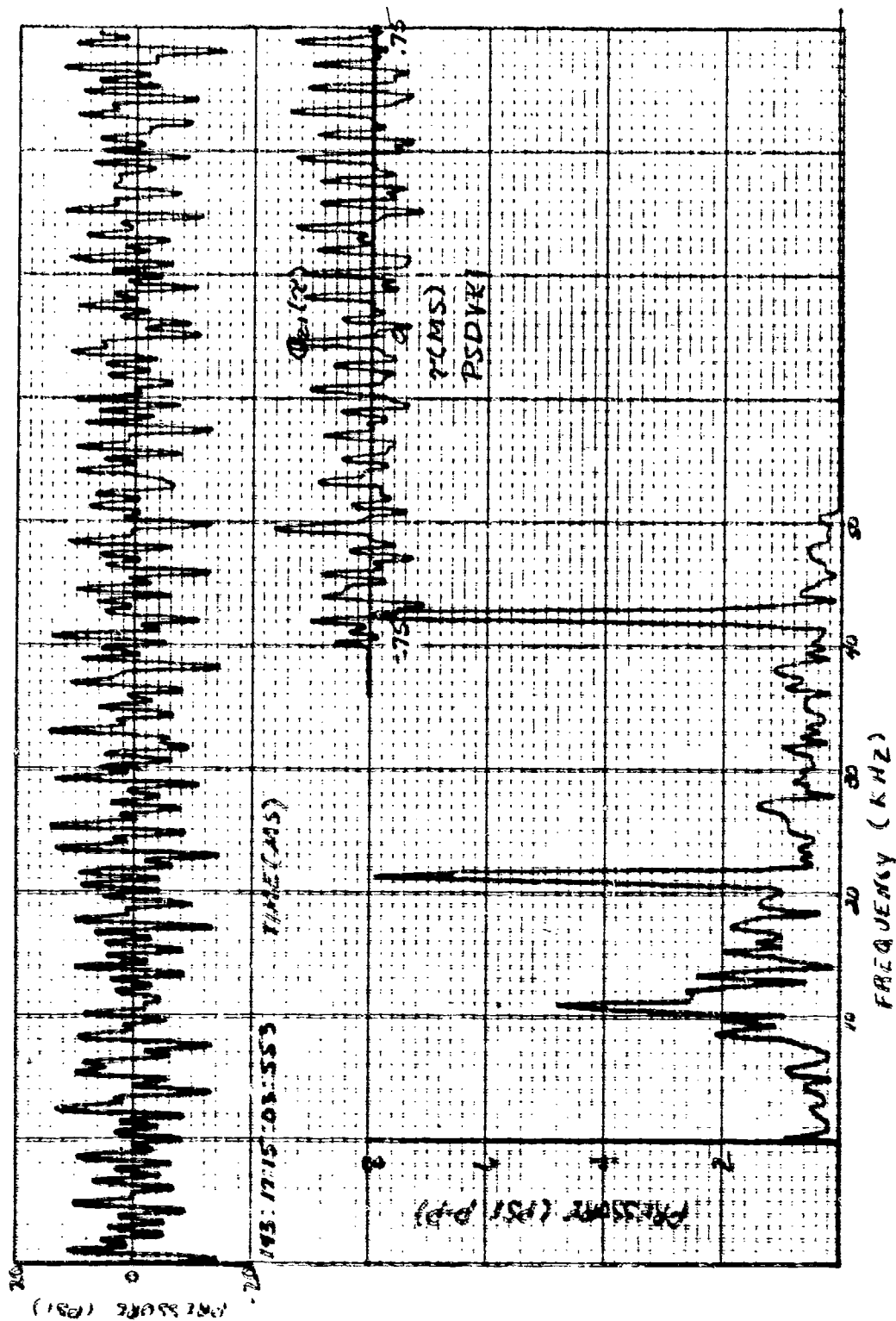


Figure 281. High-Frequency Response Data, 78% Speed, Stall Transient, Time 553, PSDVK1.



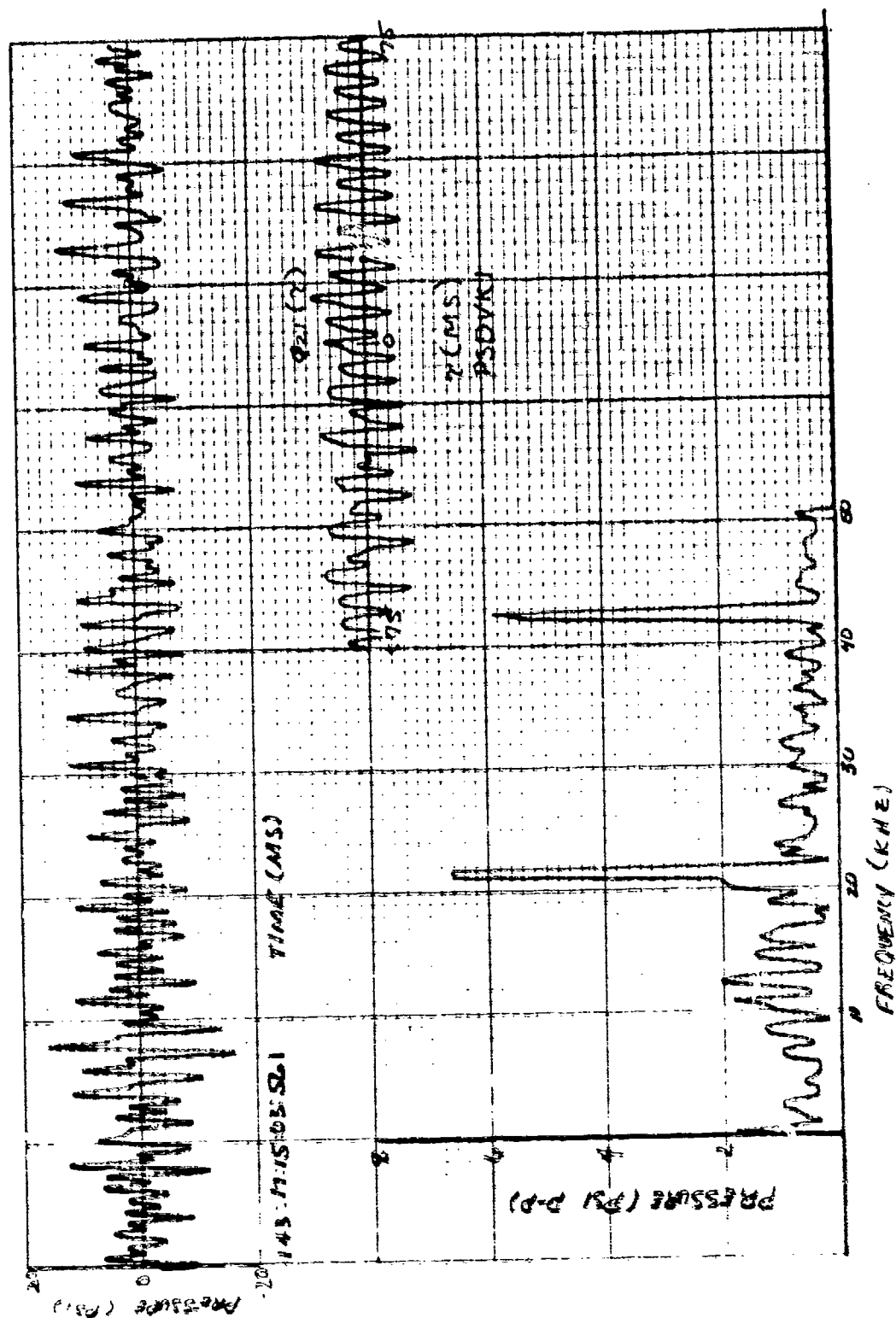


Figure 282. High-Frequency Response Data, 78% Speed, Stall Transient, Time 561, PSDV K1.

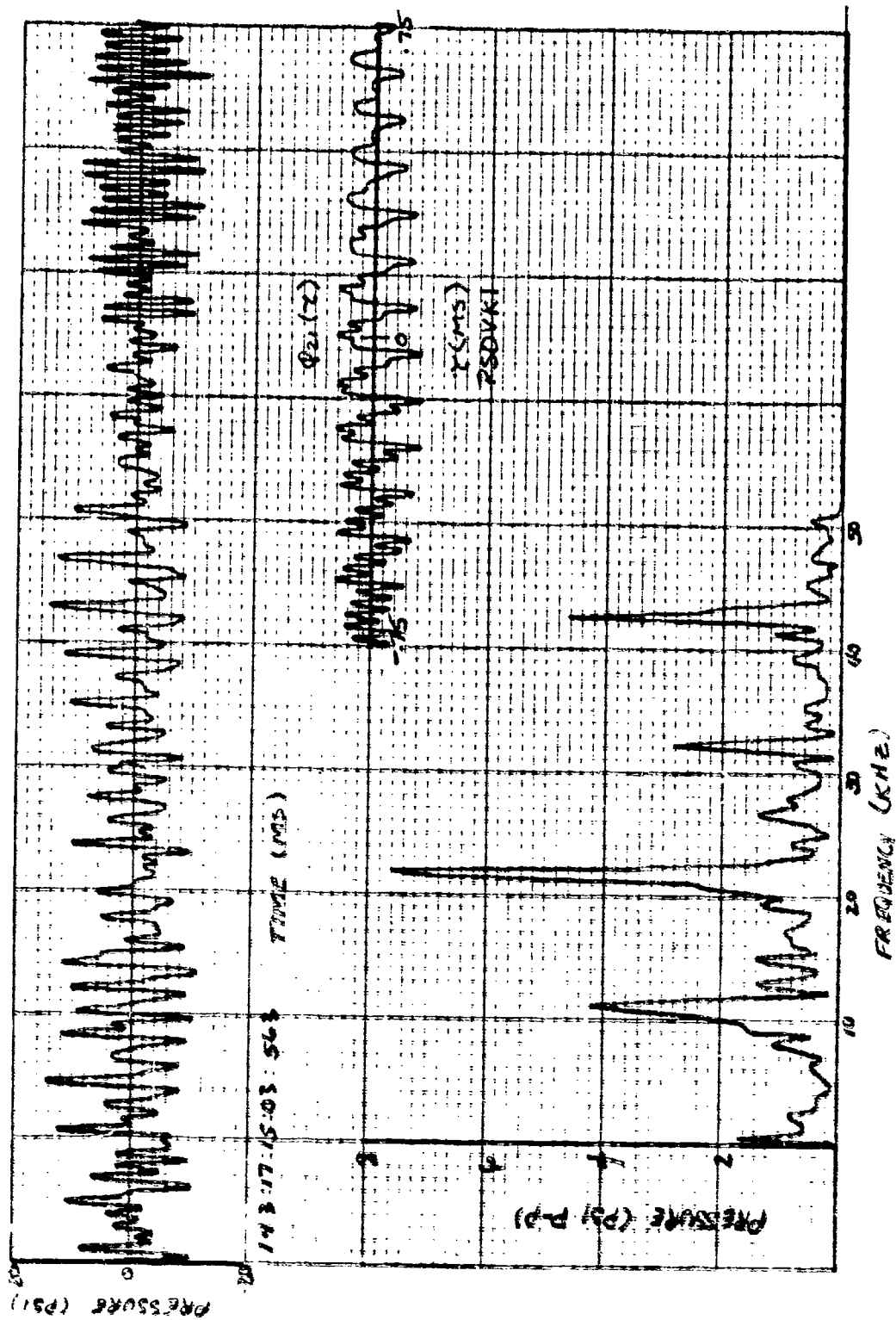


Figure 283. High-Frequency Response Data, 78% Speed, Stall Transient, Time 563, PSDVK1.

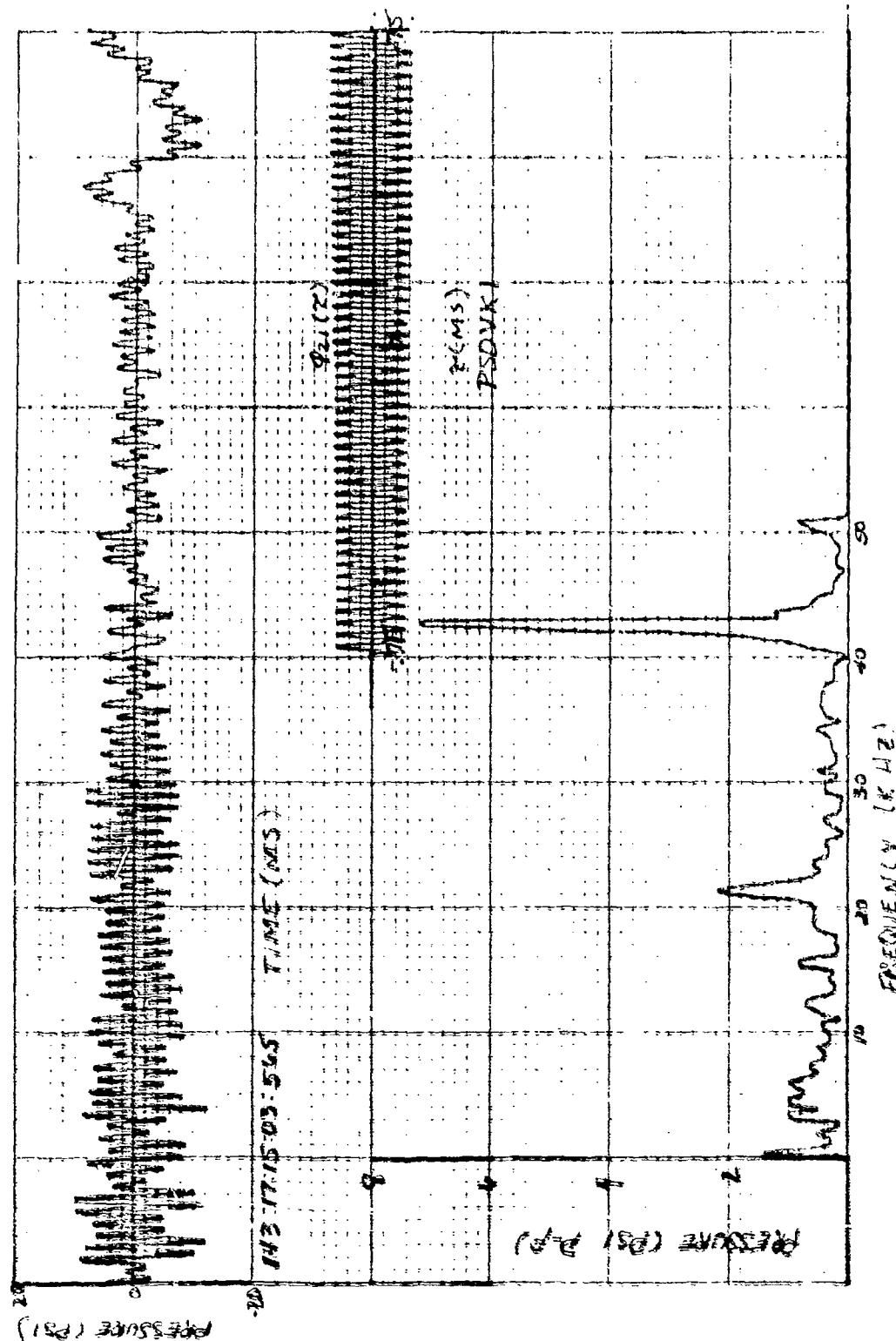


Figure 224. High-Frequency Response Data, 78% Speed, Stalled, Time 565, PSDVK1.

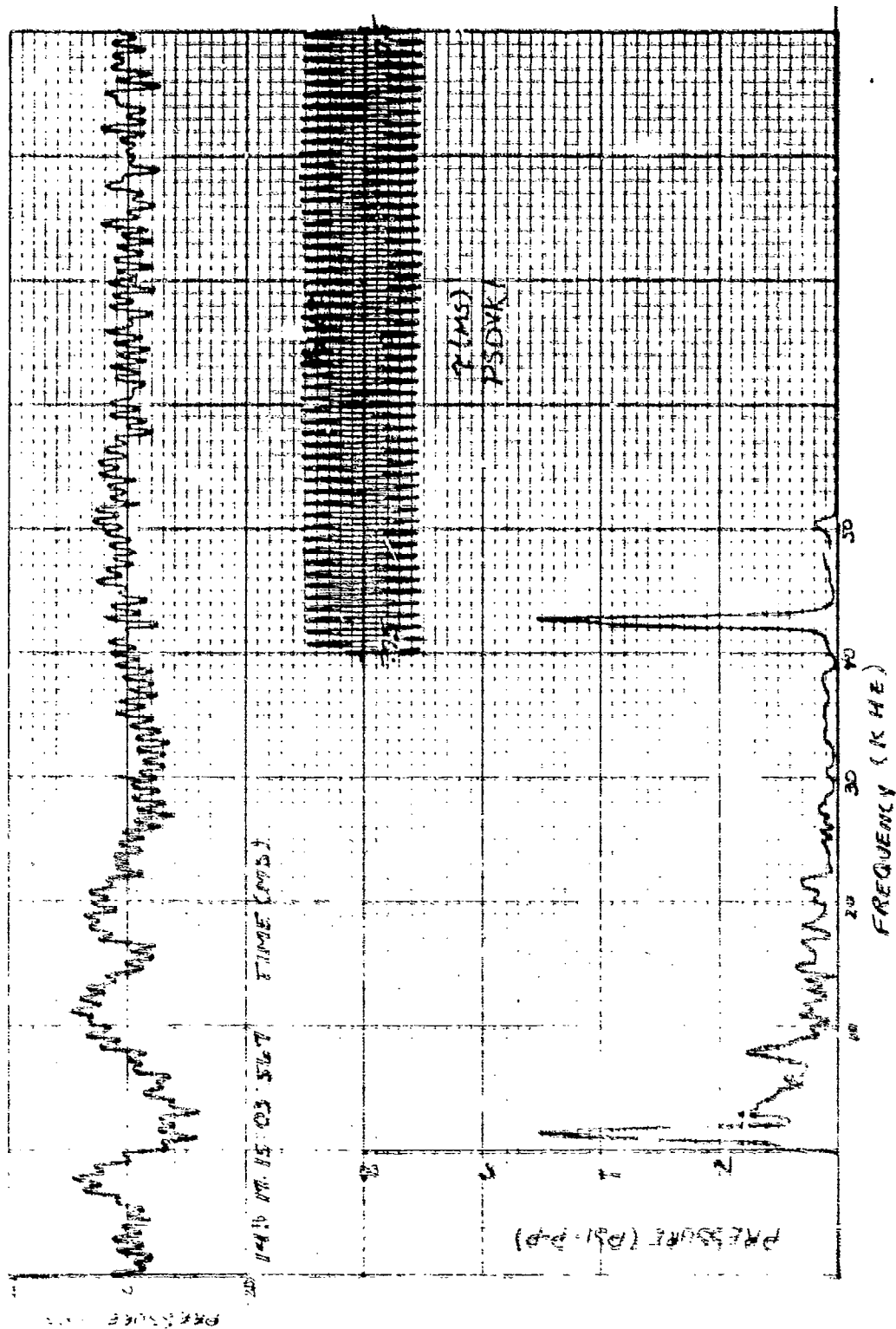


Figure 285. High-Frequency Response Data, 787 Speed, Stalled, Time 557, PSDWKL.

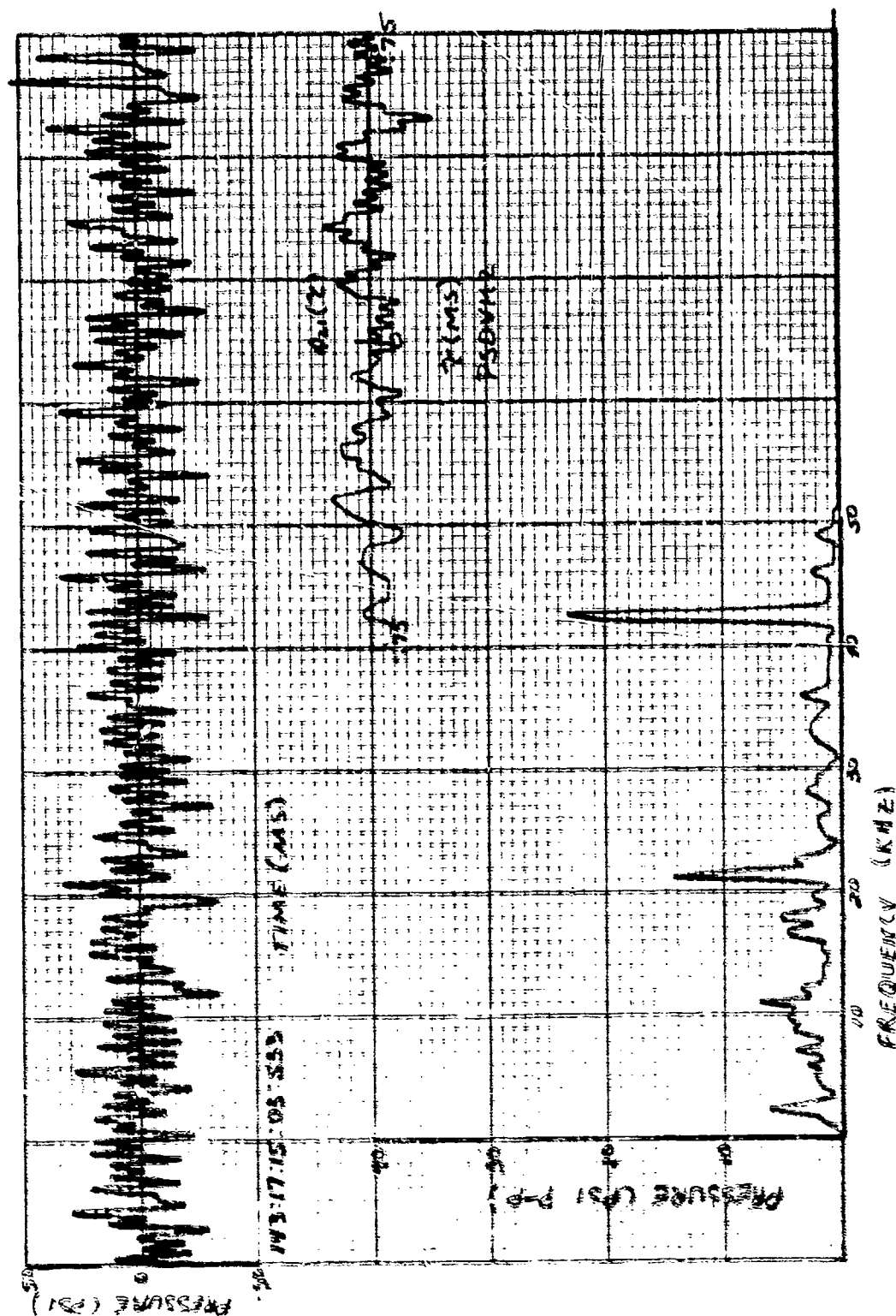


Figure 286. High-Frequency Response Data, 78% Speed, Stall Transient, Time 533, PSDVK2.

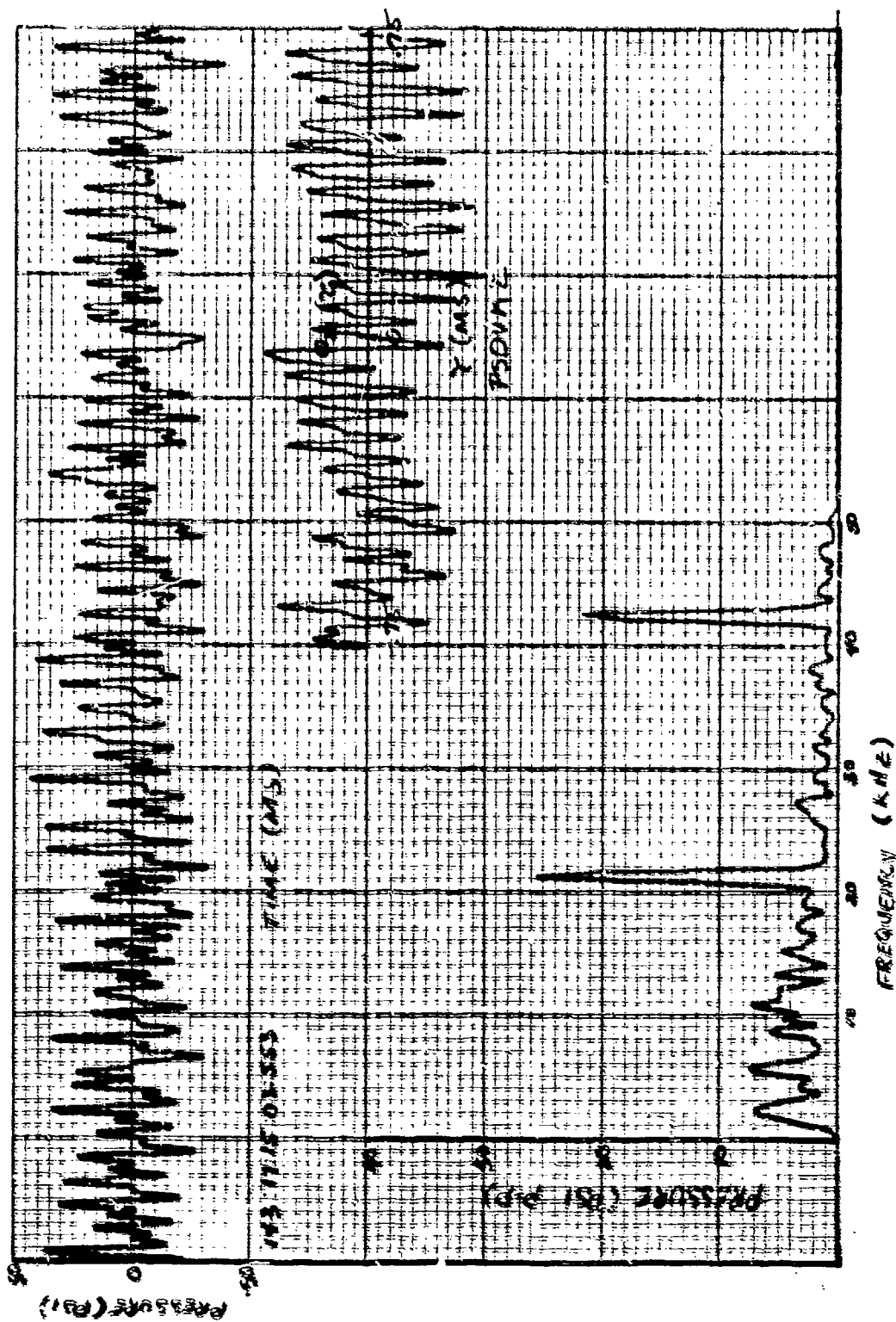


Figure 25: High-Frequency Response Data, 75% Speed, Stall Transient, Time 553, PSDVK2.



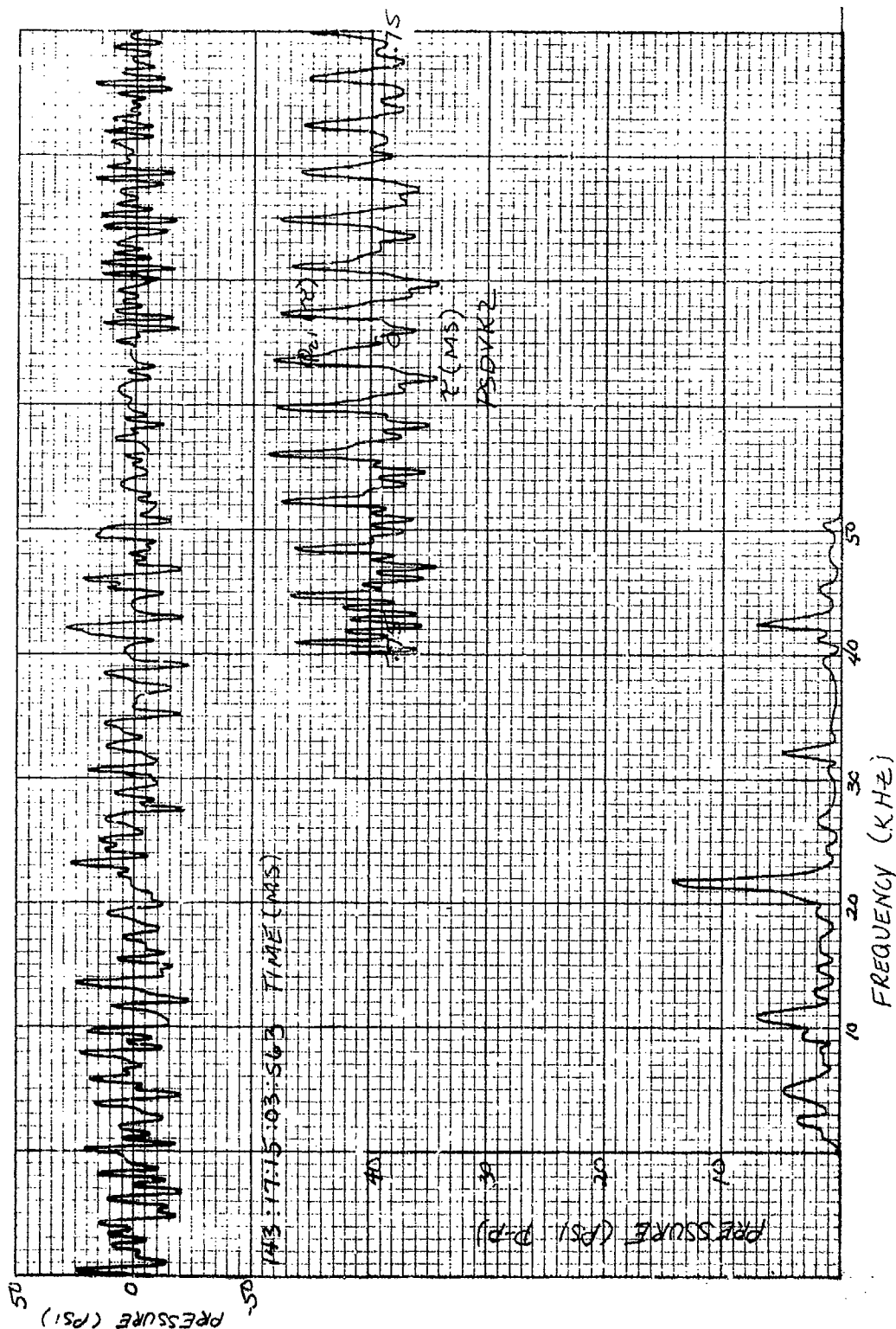


Figure 289. High-Frequency Response Data, 78% Speed, Stall Transient,  
Time 563, PSDVK2.



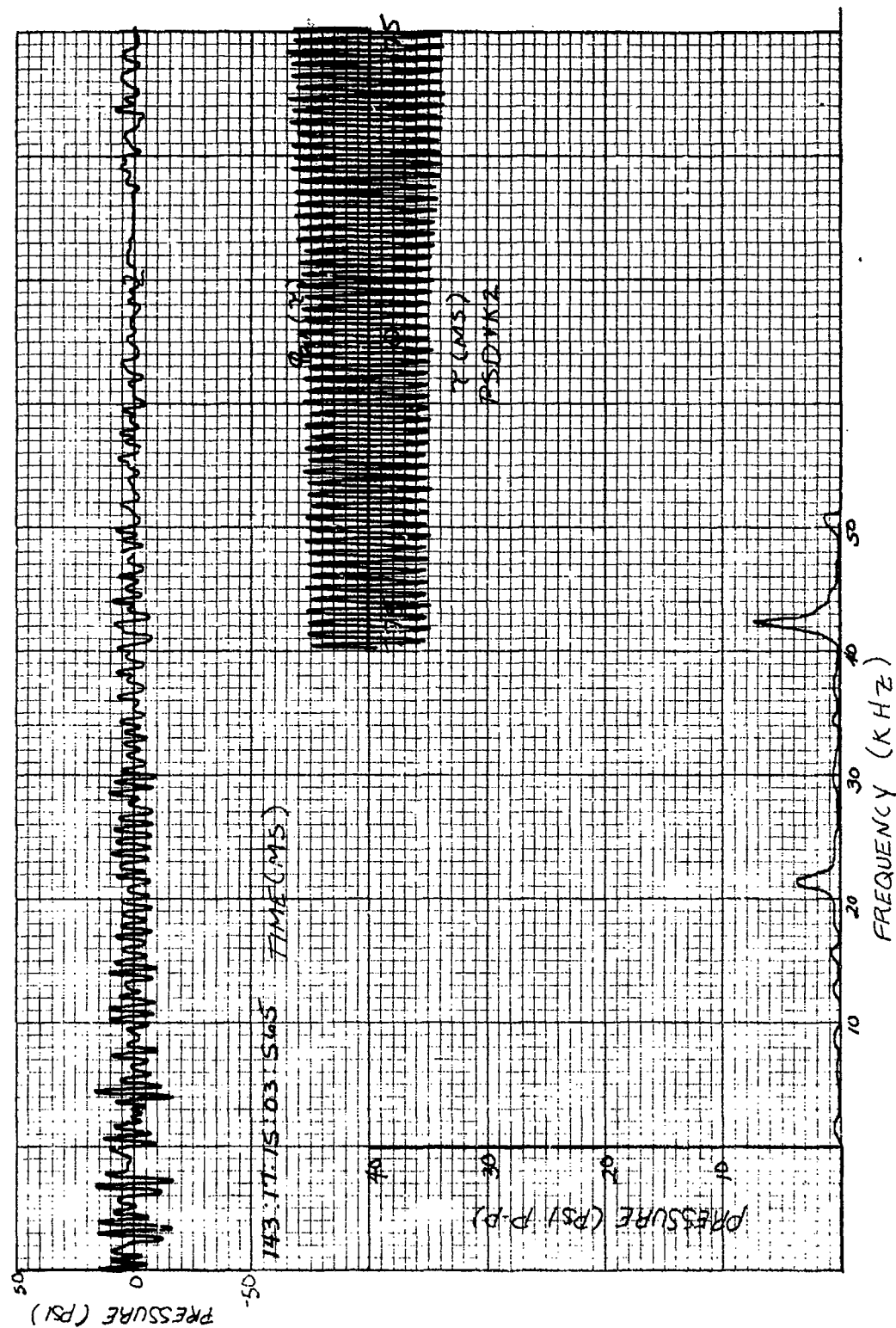


Figure 290. High-Frequency Response Data, 78% Speed, Stalled, Time 565, PSDVK2.

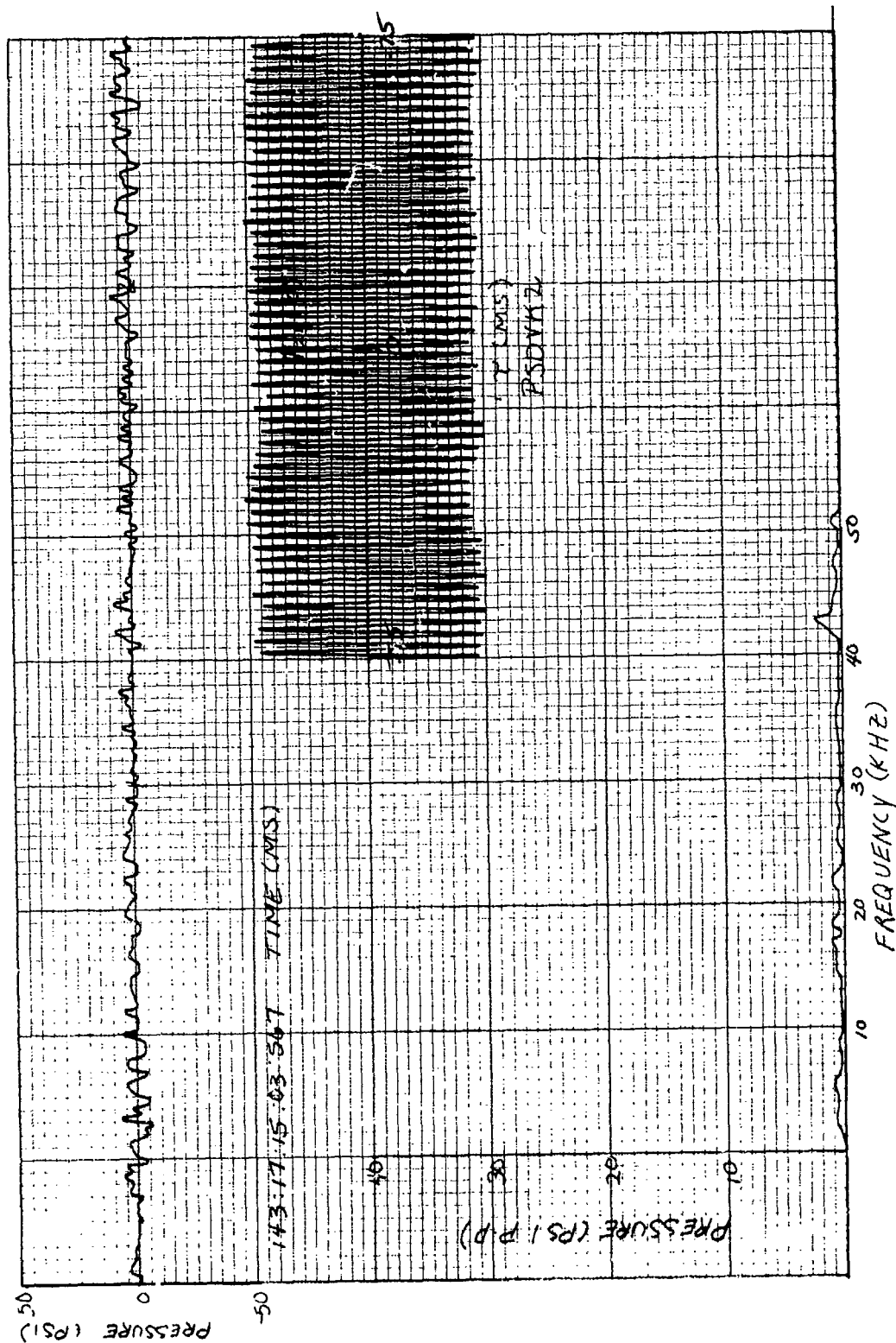


Figure 291. High-Frequency Response Data, 78% Speed, Stalled, Time 567, PSDVK2.

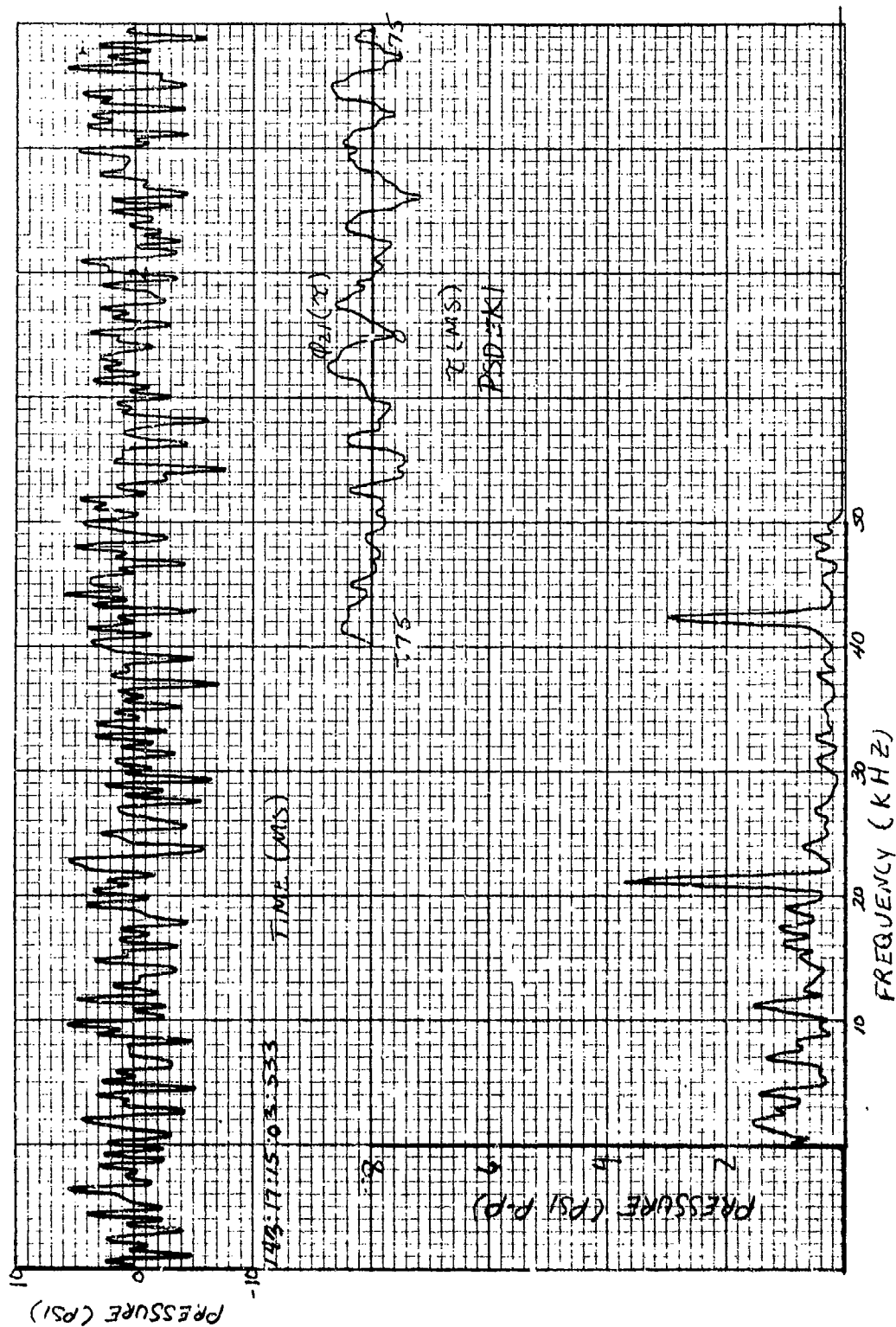


Figure 292. High-Frequency Response Data, 78% Speed, Stall Transient, Time 533, PSDEK1.

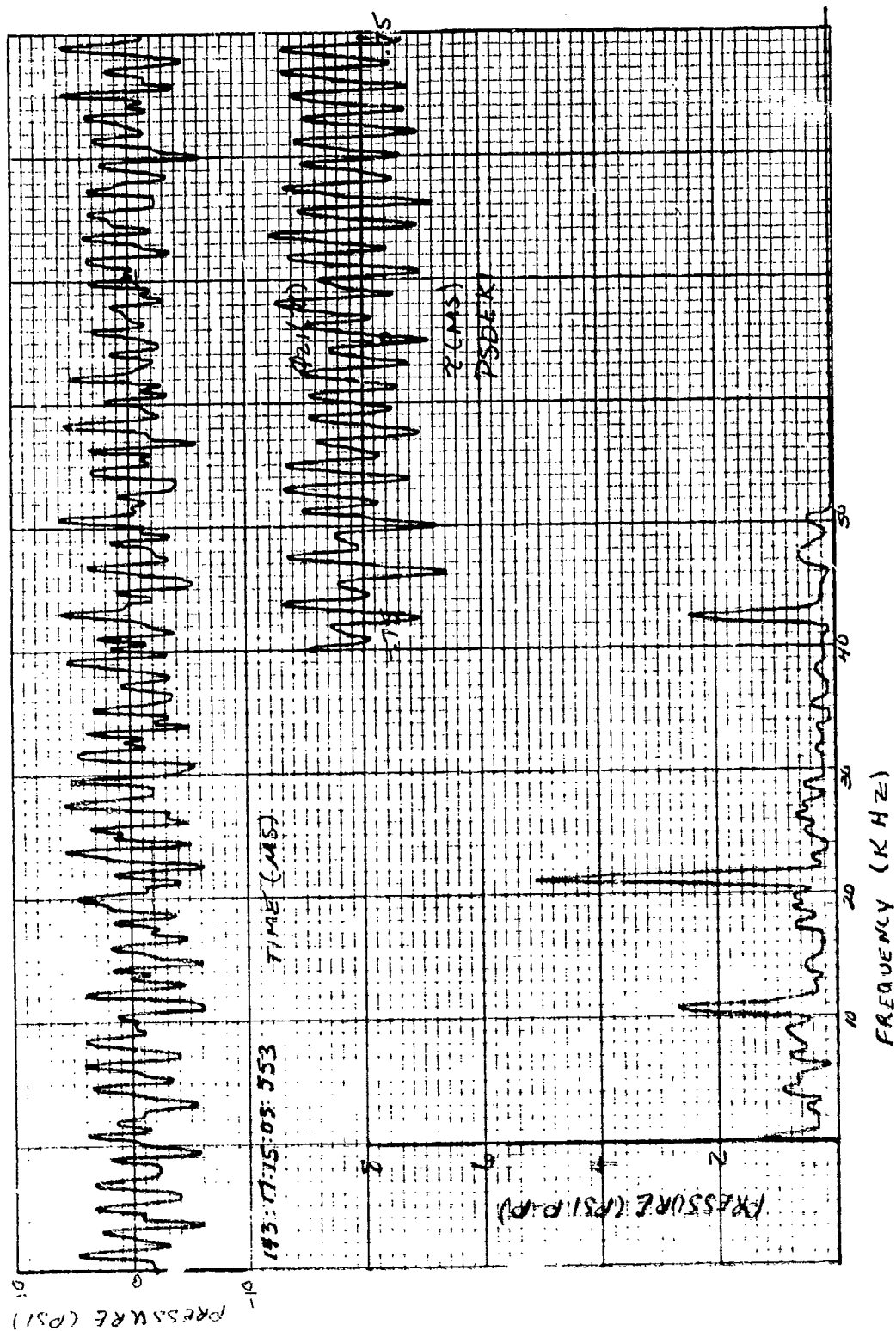


Figure 293. High-Frequency Response Data, 78% Speed, Stall Transient, Time 553, PSDEK1.

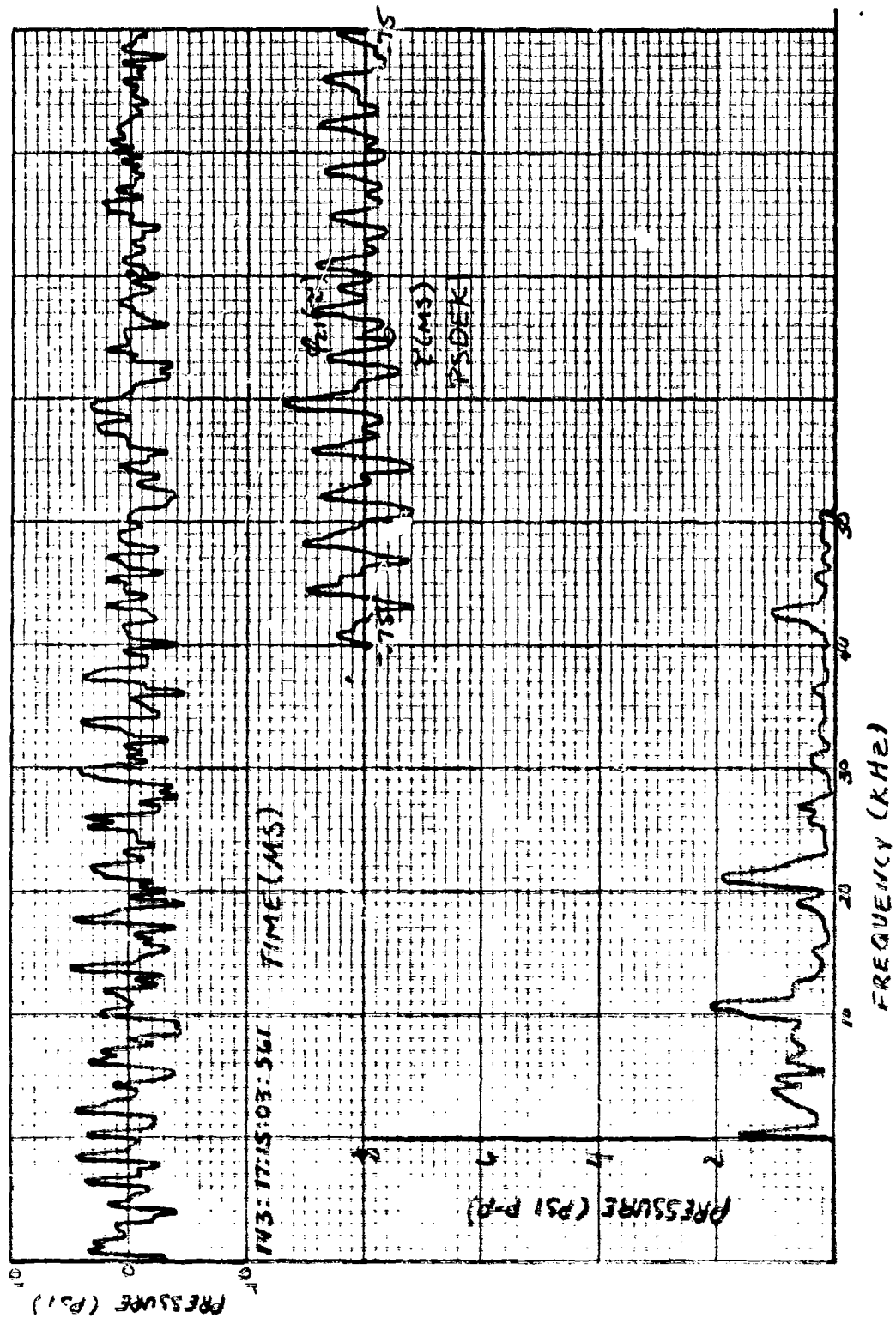


Figure 294. High-Frequency Response Data, 78% Speed, Stall Transient, Time 561, PSDEK1.

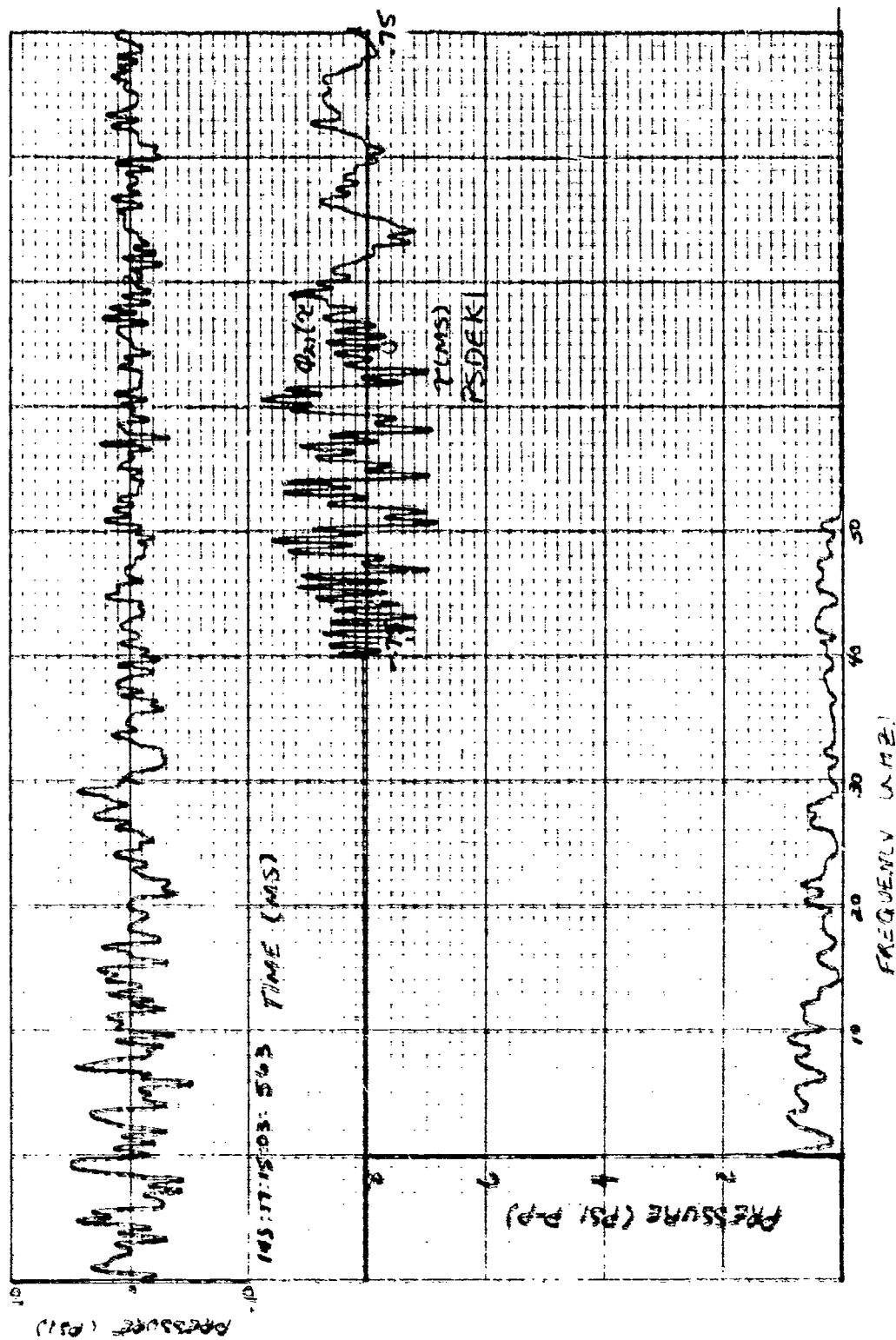


Figure 295. High-Frequency Response Data, 78% Speed, Stall Transient, Time 563, PSDEK1.

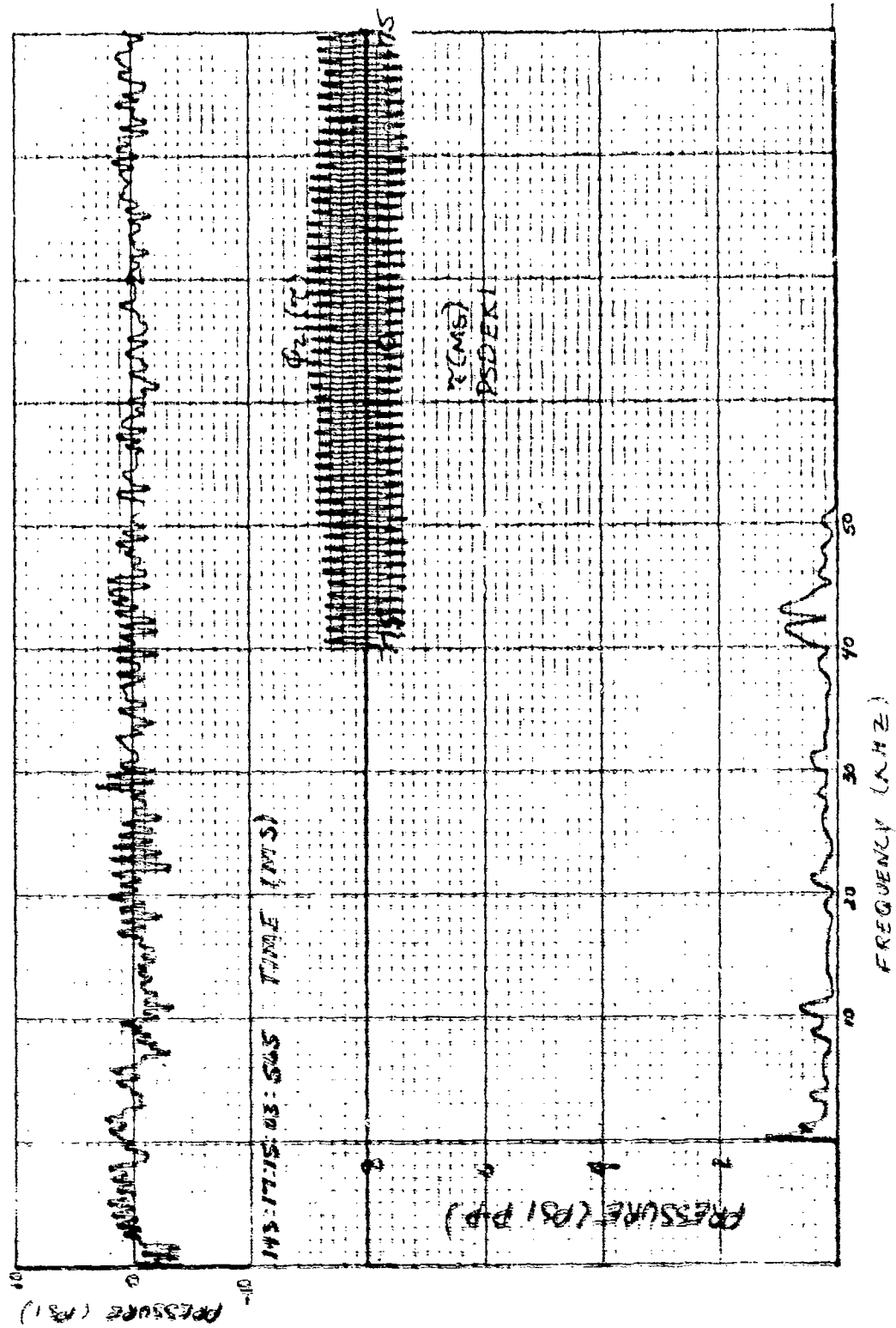


Figure 296. High-Frequency Response Data, 78<sup>o</sup> Speed, Stall Transient, Time 565, PSDEKI.

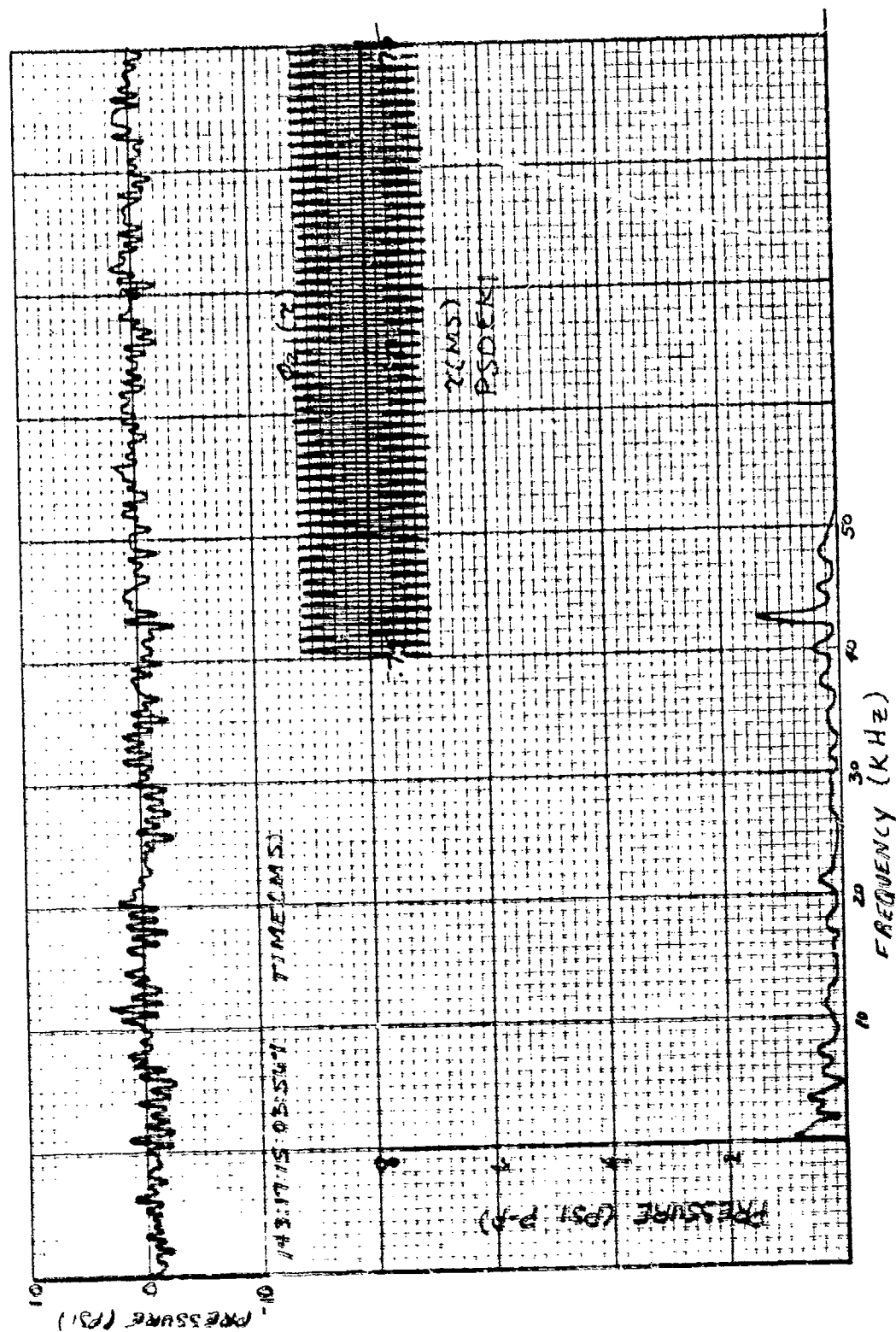


Figure 297. High-Frequency Response Data, 78% Speed, Stalled, Time 567, PSDEK1.



### IMPELLER EXIT 17% STALL TRANSIENT DATA

This section contains stall transient data obtained with the impeller exit (Station 2) cobra probe sensor positioned 17% of the flow path width from the shroud wall. The cobra probe and recording equipment were identical to that used in regular traverses. Frequency response of this system should be considered poor for transient characteristics. Impeller exit air angle and total pressure and collector static pressure are presented vs time. The pressures were ratioed to standard day conditions. The key denotes the proper symbol to the scales from right to left in ascending order. Each condition was recorded at two scanning rates, one scan/sec and maximum (approximately 6 scans/sec). Conditions for Figures 298 and 299 were 101% speed, 5-deg IGV; Figures 300 and 301 were 101% speed, 0-deg IGV; Figures 302 and 303 were 101% speed, -4-deg IGV; Figures 304 and 305 were 94.5% speed, 15-deg IGV; and Figures 306 and 307 were 95% speed and 10-deg IGV.

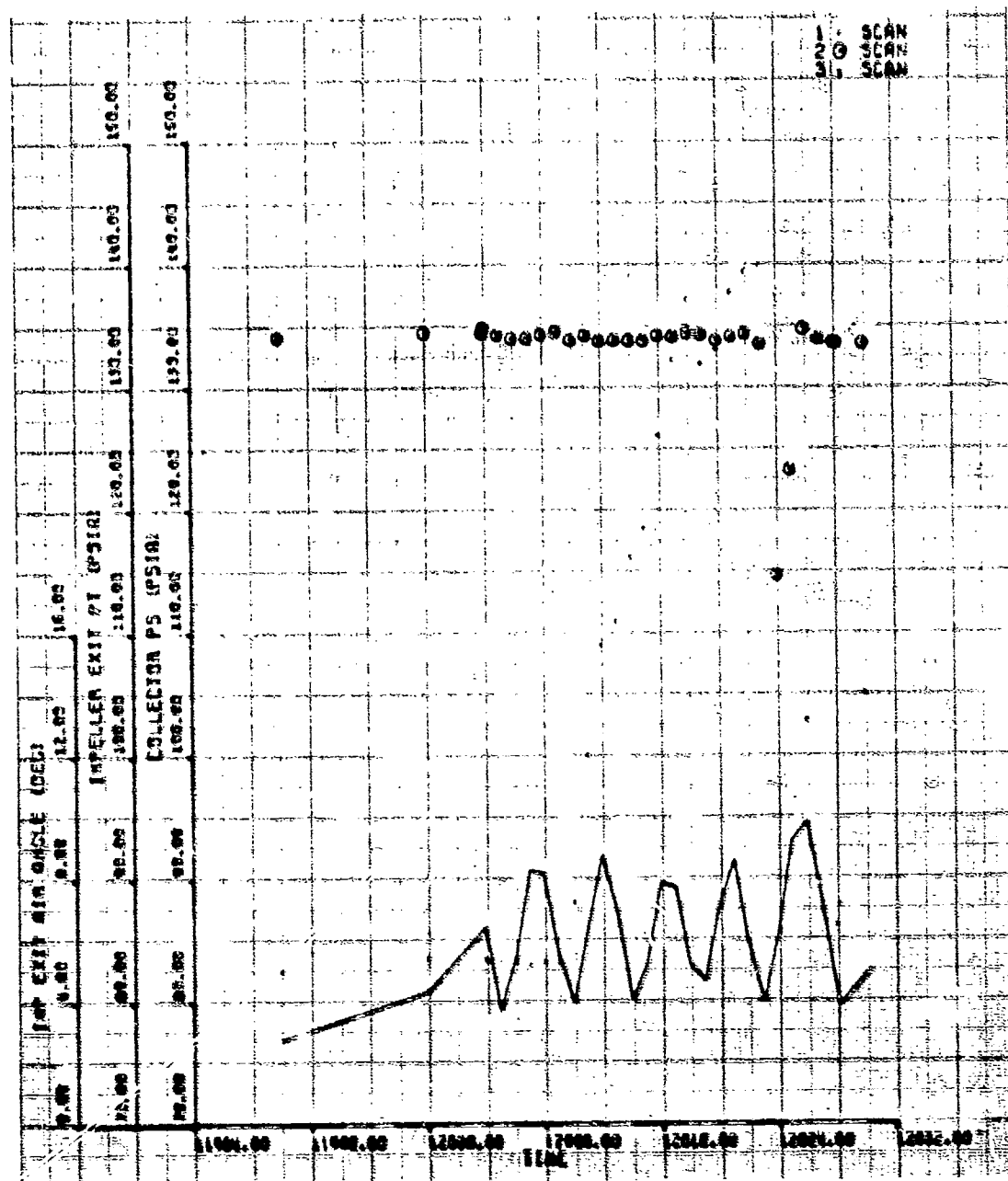


Figure 298. Stall Transient Data, 101% Speed, 5-deg IGV, ISPS Rate.

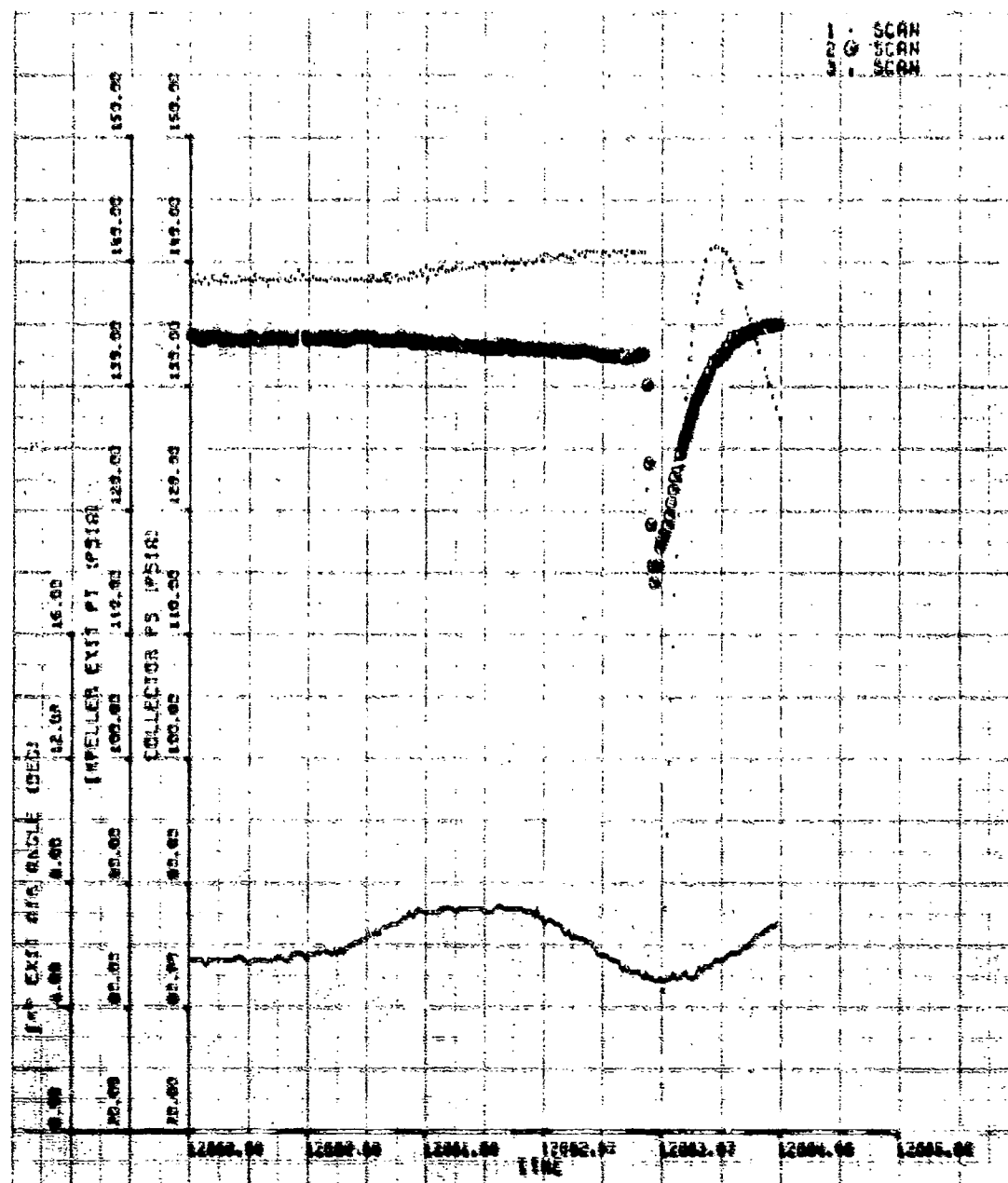


Figure 299. Stall Transient Data, 101% Speed, 5-deg IGV, Maximum Rate.

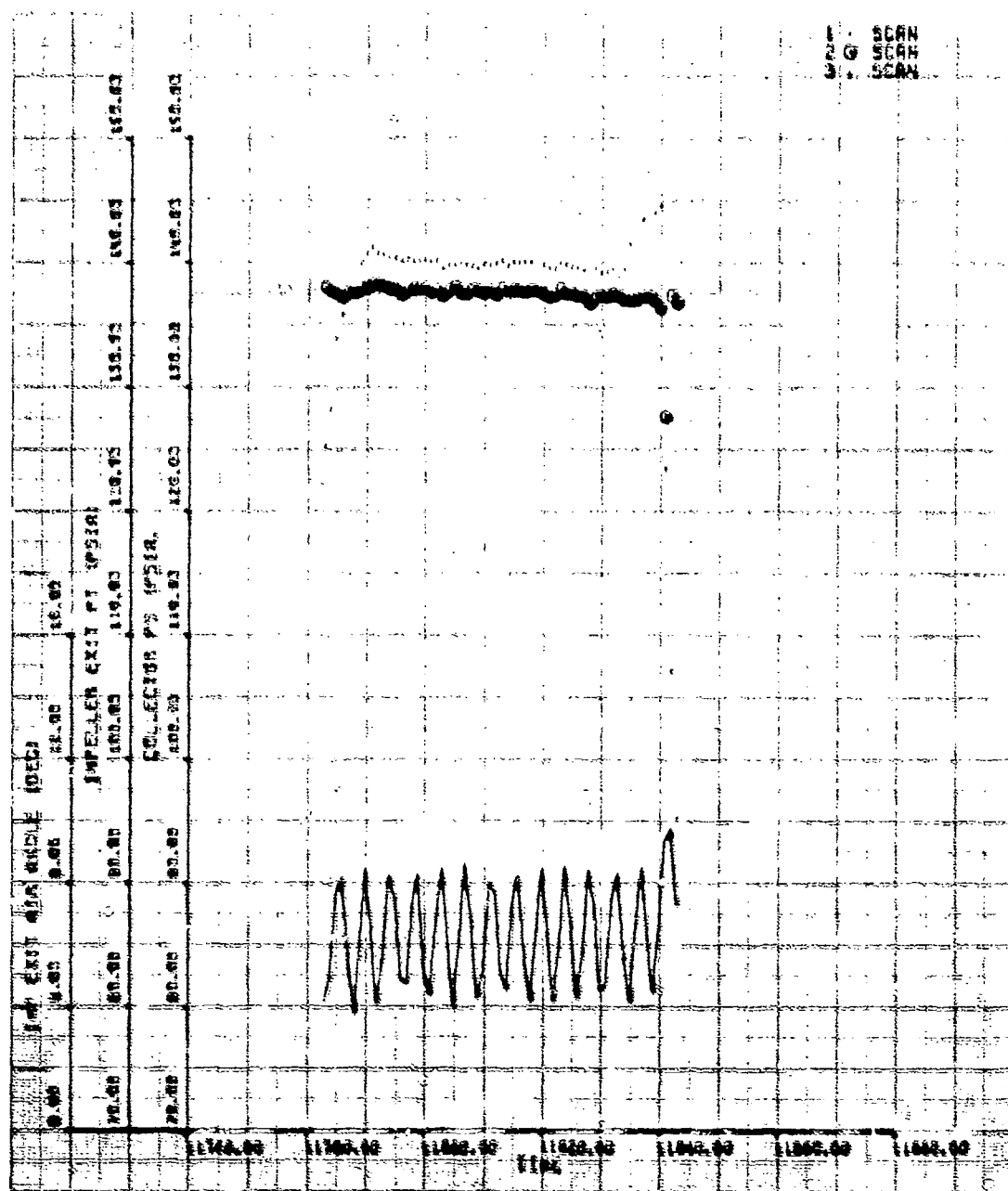


Figure 306. Stall Transient Data, 101% Speed, 0-deg IGV, ISPS Rate.

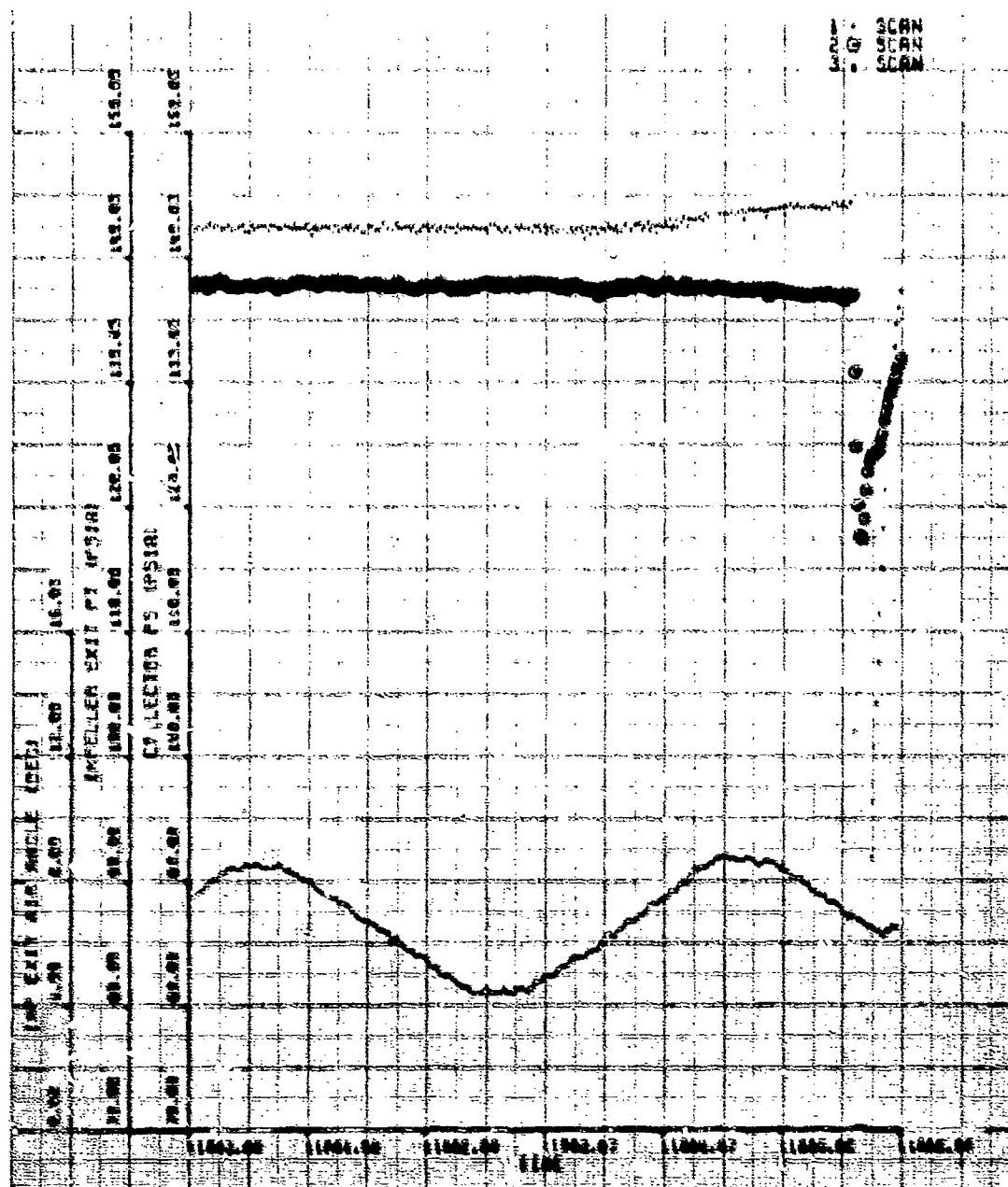


Figure 301. Stall Transient Data, 101% Speed, 0-deg IGV  
Maximum Rate.

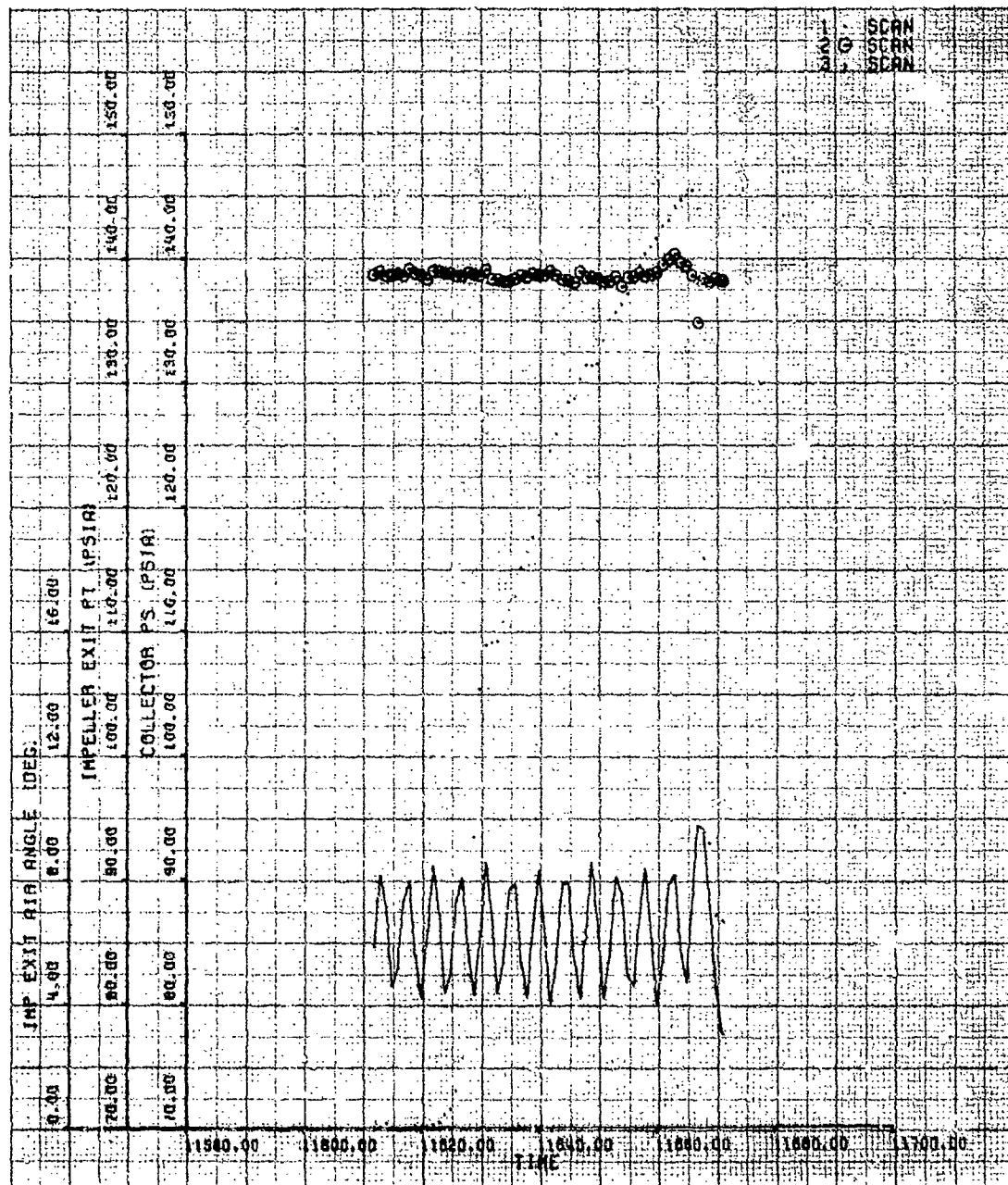


Figure 302. Stall Transient Data, 101% Speed, -4-deg IGV, ISPS Rate.

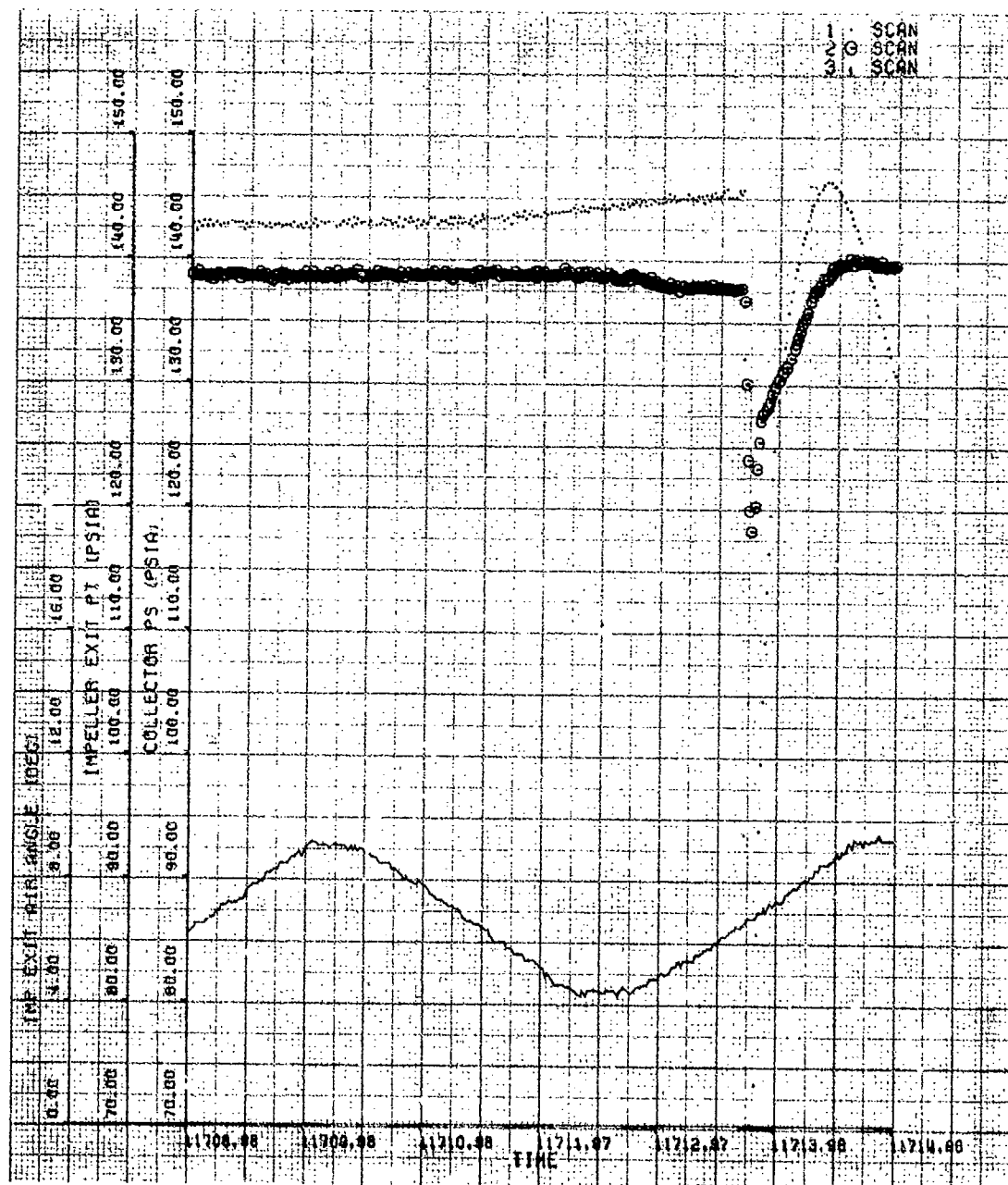


Figure 303. Stall Transient Data, 101% Speed, -4-deg IGV, Maximum Rate.

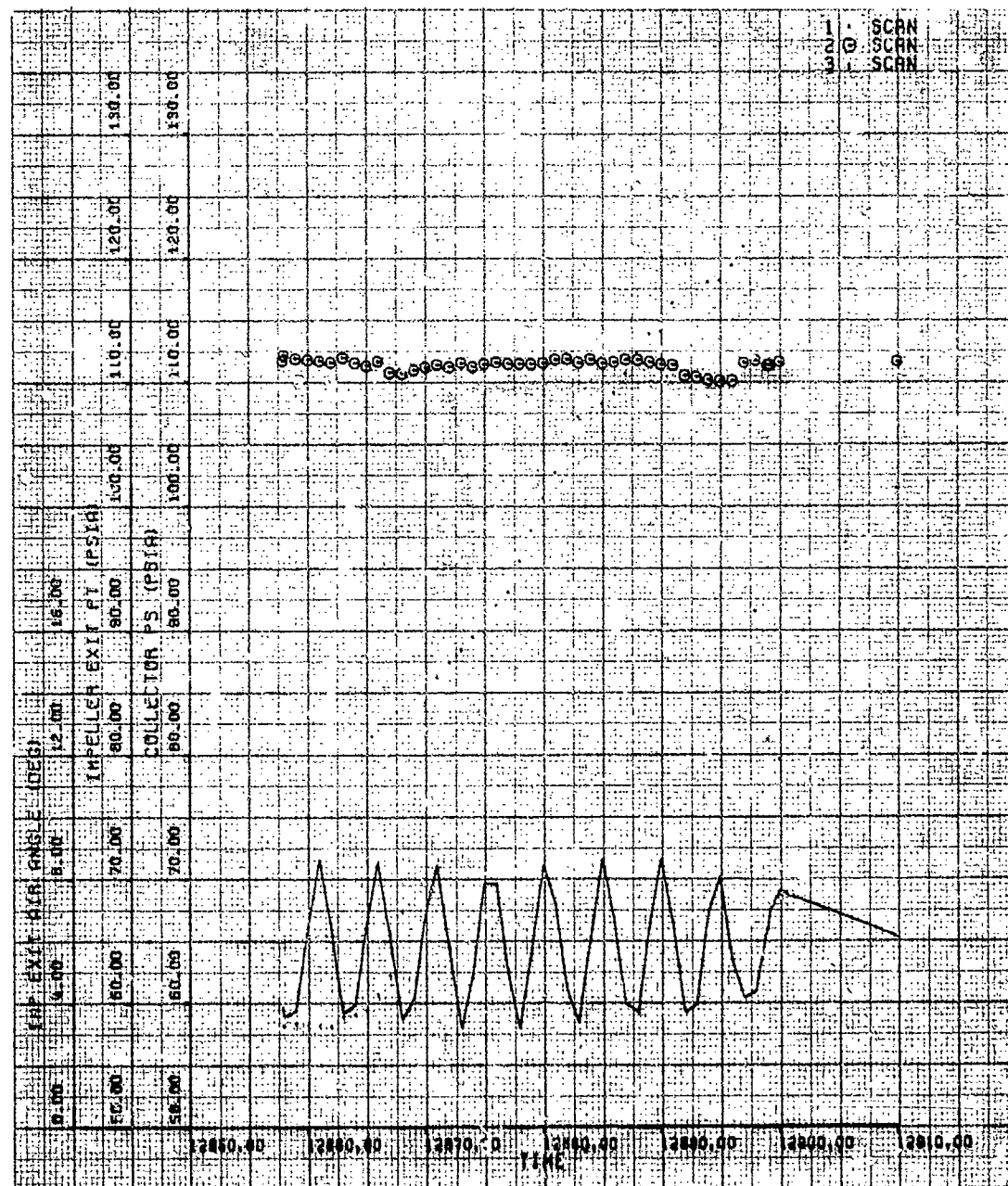
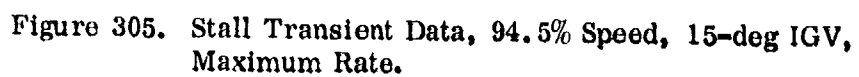


Figure 304. Stall Transient Data, 94.5% Speed, 15-deg IGV, 1SPS Rate.





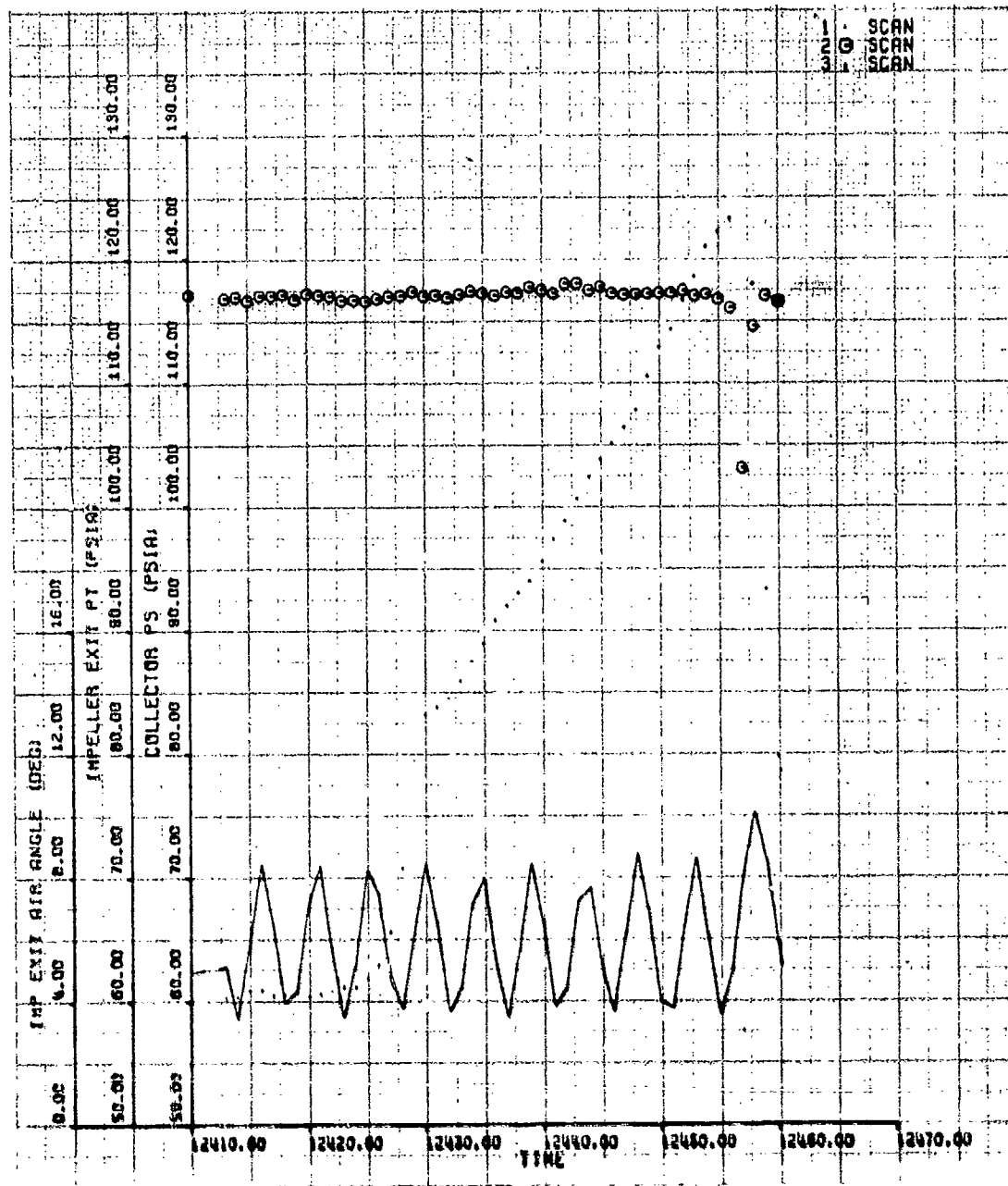


Figure 306. Stall Transient Data, 95% Speed, 10-deg IGV, ISPS Rate.

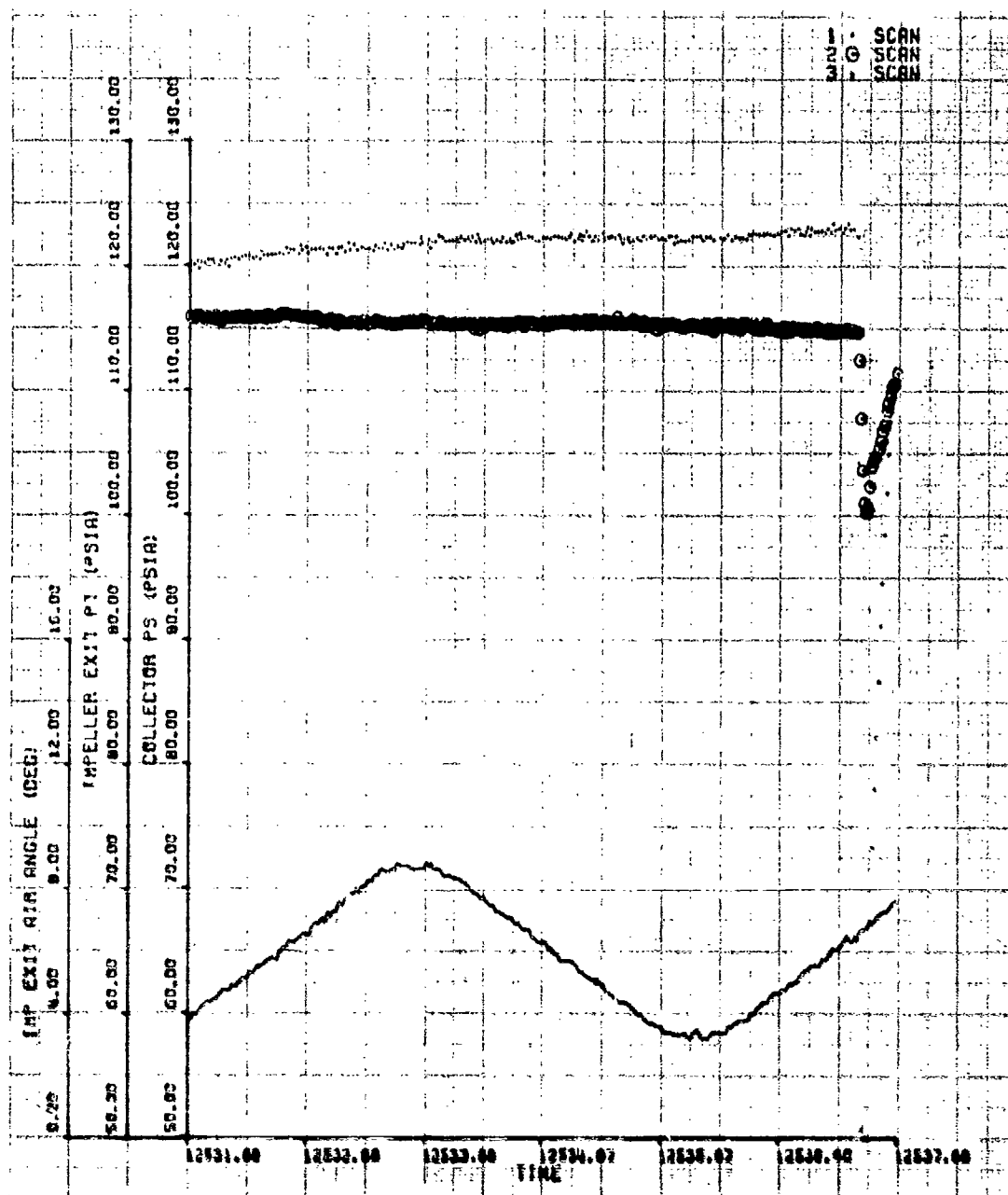


Figure 307. Stall Transient Data, 95% Speed, 10-deg IGV, Maximum Rate.

## DISTRIBUTION

Director of Defense Research & Engineering	2
Assistant Secretary of the Army (R&D)	1
Deputy Chief of Staff for Logistics, DA	1
Chief of R&D, DA	1
Army Materiel Command	3
Army Aviation Systems Command	2
Hq, Army Air Mobility R&D Laboratory	2
Systems Research Integration Office, AMRDL	1
Ames Directorate, Army Air Mobility R&D Laboratory	1
Eustis Directorate, Army Air Mobility R&D Laboratory	20
Langley Directorate, Army Air Mobility R&D Laboratory	2
Lewis Directorate, Army Air Mobility R&D Laboratory	2
Army Aviation Systems Test Activity	2
Army R&D Group (Europe)	2
Army STINFO Team (Europe)	1
Army Aeromedical Research Laboratory	1
Army Coating & Chemical Laboratory	1
Harry Diamond Laboratories	1
Army Ballistic Research Laboratories	1
Army Research Office	1
Army Materials & Mechanics Research Center	5
Army Test & Evaluation Command	1
Army Materiel Systems Analysis Agency	1
Army Missile Command	1
USACDC Aviation Agency	3
Army Transportation School	1
Army Arctic Test Center	1
Army Field Office, AFSC	1
Air Force Aero Propulsion Laboratory	2
Air Force Flight Dynamics Laboratory	2
Aeronautical Systems Division, AFSC	2
Naval Air Systems Command	9
Chief of Naval Research	2
Naval Air Development Center	1
Naval Air Propulsion Test Center	2
Naval Ship R&D Center	3
Marine Corps Liaison Officer, Army Transportation School	1
Ames Research Center, NASA	4
Langley Research Center, NASA	2
Lewis Research Center, NASA	1
Goddard Space Flight Center, NASA	1
STINFO Facility, NASA	2
National Aviation Facilities Experimental Center, FAA	1
Department of Transportation Library	1
Eastern Region Library, FAA	1
Federal Aviation Administration, Washington	2
Government Printing Office	1
Defense Documentation Center	2

Unclassified

Security Classification

## DOCUMENT CONTROL DATA - R &amp; D

(Security classification of title, body of abstract and indexing annotation must be entered when the overall report is classified)

1. ORIGINATING ACTIVITY (Corporate author) Pratt & Whitney Aircraft Division United Aircraft Corporation Florida Research and Development Center West Palm Beach, Florida		20. REPORT SECURITY CLASSIFICATION Unclassified	
3. REPORT TITLE 10:1 PRESSURE RATIO SINGLE-STAGE CENTRIFUGAL COMPRESSOR PROGRAM		21. GROUP	
4. DESCRIPTIVE NOTES (Type of report and inclusive dates) Final Report			
5. AUTHOR(S) (First name, middle initial, last name) William J. McAnally, III			
6. REPORT DATE April 1974	7a. TOTAL NO. OF PAGES 429	7b. NO. OF REFS	
8a. CONTRACT OR GRANT NO. DAAJ02-70-C-0006	8b. ORIGINATOR'S REPORT NUMBER(S) USAAMRDL Technical Report 74-15		
9. PROJECT NO. a. Task 1G162203D14413 b.	9b. OTHER REPORT NO(S) (Any other numbers that may be assigned this report) FR-6086		
10. DISTRIBUTION STATEMENT Distribution limited to U. S. Government agencies only; test and evaluation; April 1974. Other requests for this document must be referred to the Eustis Directorate, U. S. Army Air Mobility Research and Development Laboratory, Fort Eustis, Virginia 23604.			
11. SUPPLEMENTARY NOTES		12. SPONSORING MILITARY ACTIVITY Eustis Directorate, U. S. Army Air Mobility Research and Development Laboratory Fort Eustis, Virginia	
13. ABSTRACT The objective of this program was to design, fabricate and test a 3.1-lb/sec airflow single-stage centrifugal compressor that could be incorporated in a future Army advanced technology gas turbine engine. The design performance goals were to exceed 75% efficiency at 10:1 pressure ratio. Since gas turbine engines for Army aircraft applications operate under part-power conditions a majority of the time, an off-design performance goal of 80% efficiency at 8:1 pressure ratio was established.  In the design of the compressor, parametric studies were conducted to select an overall design consistent with optimum compressor performance at both performance goals. These studies defined the compressor inlet corrected flow rate, impeller inlet hub and tip radii, corrected impeller rotational speed, and inlet prewhirl. Airflow selection and the selection of the hub radius were influenced by the decision to design a compressor that could be used in a small turboshaft engine with a concentric shaft front drive.  The tip radius was selected after determining the effect on axial Mach number, inducer tip relative Mach number, and inlet choke flow margin. The effect of inlet guide vane losses, inlet shock losses, diffuser losses, and shroud friction heating were parametrically evaluated before selecting an IGW prewhirl and rotor speed to provide optimum overall compressor performance. A remote inducer design was selected over an integral inducer-impeller configuration so that the inducer could be designed using transonic axial-flow compressor technology. The work split between the inducer and impeller was selected so that the relative Mach number into the impeller would be subsonic. A pipe diffuser was selected over vane island and cascade diffusers, because it has the lowest demonstrated losses over the largest range of Mach number and because P&WA <sup>®</sup> had substantial experience in designing and fabricating this type of diffuser.  Demonstrated total-to-static performance was as high as 79.6% efficiency at 8.192:1 pressure ratio and 73.8% efficiency at 10.03:1 pressure ratio. Performance adjusted for increased losses from a damaged diffuser (10.15:1 pressure ratio and 75.9% efficiency) indicates that the basic compressor design would surpass the 10:1 pressure ratio program goal. Evaluation of component performance data revealed that excessive losses occurred in the inducer above 95% of design speed and that a redesign of this component could produce an additional performance improvement at 10:1 pressure ratio.			

DD FORM 1473

REPLACES DD FORM 1473, 1 JAN 62, WHICH IS OBSOLETE FOR ARMY USE.

Unclassified

Security Classification

Unclassified  
Security Classification

14. KEY WORDS	LINK A		LINK B		LINK C	
	ROLE	WT	ROLE	WT	ROLE	WT
Compressors Fabrication Pressure Ratio Engines Turbines Performance (Engineering)						

Unclassified

Security Classification